

Karl Kent Benedict

Candidate

Anthropology

Department

This dissertation is approved, and it is acceptable in quality
and form for publication on microfilm:

Approved by the Dissertation Committee:

Bruce Huckell

, Co-Chairperson

James Boone

, Co-Chairperson

Wirt Wills

Louis Scuderi

Accepted:

Dean, Graduate School

Date

Settlement and Subsistence in the Western Anasazi Core Area: Development and
Assessment of a Risk Response Model

By

Karl Kent Benedict

B.A., Anthropology, University of California, Berkeley, 1986
M.A., Anthropology, University of New Mexico, 1995

DISSERTATION

Submitted in Partial Fulfillment of the
Requirements for the Degree of

Doctor of Philosophy
Department of Anthropology

The University of New Mexico
Albuquerque, New Mexico

July, 2004

Acknowledgements

As is the case in any undertaking of this magnitude, this project could have not been accomplished without the hard work, dedication, and assistance of many individuals and organizations. First, the many researchers, field workers, and support staff that participated in the Long House Valley and Black Mesa Archaeological Projects and the Southwest Paleoclimate Project deserve recognition for their hard work in planning, executing, documenting, and publishing the results of these large projects. The products of their efforts have and will continue to provide valuable data and analytic results for years to come. George Gumerman, Jeff Dean, Sylvia Gaines, and Lee Ann Newsom deserve special recognition for their encouragement and the data they provided in support of this project.

My dissertation committee has provided key support and direction in the development and execution of this project. Chip Wills provided valuable insights into the Black Mesa Archaeological Project as a result of his work on it, Louis Scuderi provided the geospatial analysis and modeling foundation that underlies all of the analyses performed, Jim Boone provided my introduction to and continued refinement of the behavioral ecological modelling framework used, and Bruce Huckell made sure that I remained grounded within the empirical record while pursuing 'virtual archaeology'. Without these contributions (and more), this project would never have been successfully completed.

Financial support for this project was provided by a variety of organizations, including: the University of New Mexico Department of Anthropology, UNM Office of Graduate Studies, UNM Graduate and Professional Student Association, UNM Anthropology Graduate Student Union, and a UNM Regents Endowed Fellowship. Additional support was provided by the National Science Foundation through a Dissertation Improvement Grant (Award number 0305103).

My colleagues at the Earth Data Analysis Center at the University of New Mexico have provided valuable inspiration throughout this project through their continued development and refinement of cutting-edge geospatial technologies while never losing sight of a need to generate actual products at the end of the day. In particular, I would like to thank Stan Morain, Mike Inglis and Rick Watson for their patience and logistical support as I worked on this project while also working full time for EDAC.

My family and friends have all exhibited unending patience throughout this project and I must thank all of them for not giving up on me and providing me accommodations when visiting far-flung archives and museums. Special thanks go to Bill and Peg Kruse and Bob and Nancy Butterly for housing me during my visits to the Arizona State Museum and the Museum of Northern Arizona.

Finally, to my wife Cynthia, I can only express my deep appreciation for her unending support, patience, understanding, and more patience. Needless to say, I could not have finished this project without her.

**Settlement and Subsistence in the Western Anasazi Core Area: Development and
Assessment of a Risk Response Model**

By

Karl Kent Benedict

ABSTRACT OF DISSERTATION

Submitted in Partial Fulfillment of the
Requirements for the Degree of

Doctor of Philosophy
Department of Anthropology

The University of New Mexico
Albuquerque, New Mexico

July, 2004

Settlement and Subsistence in the Western Anasazi Core Area: Development and Assessment of a Risk Response Model

By

Karl Kent Benedict

B.A., Anthropology, University of California, Berkeley, 1986

M.A., Anthropology, University of New Mexico, 1995

Ph.D., Anthropology, University of New Mexico, 2004

ABSTRACT

This research project focuses on the general question of human response to subsistence risk in the context of the mixed farmer-forager economy of the Western Anasazi of Northeastern Arizona. The time period for the analysis is A.D. 600-1150, while the specific area of study is the portion of northern Black Mesa researched by the Black Mesa Archaeological Project and the adjacent Long House Valley survey area examined by the Long House Valley Archaeological Project. Potential localized productivity is estimated through the use of interpolated paleoclimate data. Subsistence risk is estimated through reference to the absolute variance in localized productivity. Sensitivity to risk, and therefore likelihood of response to risk, is estimated through local population indices that increase as estimated relative population for the study area increases.

The analytic methods employed include spatial interpolation methods, geographic information system (GIS) enabled spatial data processing, analysis and visualization, and simulation-based statistical methods for hypothesis testing. In combination, these methods facilitate the integration and analysis of multiple large datasets in a unified, spatially enabled, analysis environment.

The results obtained in the analysis are consistent with hypotheses related to the z-score model, a model of risk-response based upon variance estimation and location of mean harvest rates to requirements. Under conditions of population decline on northern Black Mesa, high-variance locations are selected. In contrast, during conditions of population growth, low-variance locations are selected. Detailed diachronic models of locational response to other environmental variables have also been produced and interpreted in the course of the analysis, addressing relationships between vegetation community, elevation, and water availability.

The use of recently developed spatial analytic methods, large extant archaeological datasets, and detailed environmental data allow for the development and testing of archaeological hypotheses that are based upon evolutionary ecological theory - ultimately providing an illustration of one approach to the application of evolutionary ecology models to the archaeological record.

Contents

List of Figures	ix
List of Tables	xiii
1 Introduction	1
1.1 Research Background	4
1.1.1 Regional Analyses	4
1.1.2 Models of Subsistence Change	5
1.1.3 Project Location and Environment	7
1.1.4 Culture History	15
1.2 Research Problem and Research Methodology	19
1.3 Hypotheses and Archaeological Correlates	21
1.4 Data Requirements and Analysis Steps	24
1.4.1 Spatial Distribution of Activity Locations	24
1.4.2 Resource Distribution Model Development	24
1.4.3 Subsistence Risk	25
1.4.4 Hypothesis Testing	26
2 Modern and Historic Environment	28
2.1 Physical Environment	29
2.1.1 Geology	30
2.1.2 Topography and Characterization	40
2.1.3 Soils	51
2.1.4 Hydrology	59
2.2 Biotic Environment	60
2.2.1 Plant Communities	60
2.2.2 Animal Distribution	69
2.3 Climate and Weather	78
2.3.1 Historic Climate Trends	79
2.4 Summary and Relevance of Modern Environmental Conditions for the Analysis	92
3 Paleoenvironmental Research	95
3.1 Paleoenvironmental Overview	96
3.2 Vegetation Distribution Data	98

3.3	Drainage System Behavior	102
3.4	Dendroclimate	104
3.4.1	Regional Dendroclimate Reconstructions	106
3.4.2	Precipitation Reconstruction	109
3.4.3	Temperature Reconstruction	112
3.4.4	Integration of Precipitation and Temperature Reconstructions . .	115
3.4.5	Regional Dendroclimate Discussion	116
3.5	Paleoclimate Data Used in the Analysis	117
3.6	Significance of Paleoenvironmental Variation and Conditions for the Analysis	124
4	Archaeological Background	125
4.1	Notes on Chronology	126
4.2	Paleoindian Period	126
4.3	Archaic Period	128
4.4	Basketmaker II	130
4.4.1	White Dog Phase	136
4.4.2	Lolomai Phase	137
4.4.3	Basketmaker II Summary	139
4.5	Basketmaker III	139
4.6	Pueblo I	143
4.7	Pueblo II	146
4.8	Pueblo III	148
4.9	Demography	150
4.10	Sites Used in the Analysis	154
5	Analysis	162
5.1	Outline of Procedures	162
5.2	Input and Process Source Data	164
5.2.1	Archaeological Site Data	165
5.2.2	Historic and Prehistoric Climate Data	167
5.2.3	Environmental Data	168
5.3	Generate Derived Data	170
5.3.1	Archaeological Site Data	170
5.3.2	Generation of Extrapolated/Interpolated Paleoclimate Parameters	173
5.4	Characterization and Extraction of Data for Analysis	191
5.4.1	Selection of the Archaeological Data Subset Used in the Analysis	193
5.4.2	Calculation of Moving Mean and Variance for Climate Parameters	194
5.4.3	Extraction of Environmental Parameters for Site Locations	196
5.5	Hypothesis Testing	200

6 Results and Conclusions	204
6.1 Interpretive Framework - the Z-score Model	207
6.2 Analysis Results	210
6.2.1 Analyses of Temporally Aggregated Climate Data	210
6.2.2 Analyses of Environmental Data Treated as Temporally Invariate	229
6.3 Relationship of Analysis Methods and Results to Previous Analyses . . .	243
6.4 Analysis Summary and Conclusions	246
Appendices	251
A USGS Quads Used in the Analyses	252
A.1 7.5 Minute: 1:24,000	252
A.2 1x2 Degree: 1:250,000	254
B Project Area - Colorado Plateau Physiographic Values Comparison	255
C Plant Species Associated With Mapped Biotic Communities	257
D Summary Statistics for USHCN Monthly Climate Values	266
D.1 Precipitation Data (hundredths of an inch)	267
D.2 Daily Minimum Temperature (°F)	277
D.3 Maximum Daily Temperature (°F)	288
E Climate Parameter Regression Models	302
F Merged Master Site List Used in the Analysis	306
G SQL Expression for Merging Black Mesa and Long House Valley Archaeological Data Tables	364
H Result Plots for All 42 Archaeological – Environmental Analyses	367
H.1 All Sites	367
H.2 Pithouse Sites	373
H.3 Masonry Sites	379
H.4 Kiva Sites	385
H.5 Sites with Storage	391
H.6 Lithic Sites	397
H.7 Groundstone Sites	403
I Mean Precipitation Plots	409
J Precipitation Variance Plots	414
References Cited	419

List of Figures

1.1	Project Location	3
1.2	Vegetation Community Distribution within the Project Area	9
1.3	Historic Climate and Paleoclimate Data Locations Relative to the Project Area	10
1.4	Mean Daily Precipitation for Betatakin and Lukachukai, Arizona, 1961-1990	12
1.5	Daily Mean Minimum and Maximum Temperature (°F) for Betatakin and Lukachukai, Arizona, 1961-1990	12
1.6	Probability of Various Freeze Levels for Betatakin, Arizona	13
1.7	Regional Chronology	16
1.8	Kayenta Population Trends	18
2.1	Colorado Plateau Physiographic Province	31
2.2	Geologic Formations Within and Surrounding the Project Area	33
2.3	Geologic Strata and Elevations Along a Profile Through the Long House Valley and Black Mesa Project Areas	34
2.4	Latitude and Longitude Ranges for the Project Area and the Colorado Plateau	43
2.5	Elevation Values for the Project Area and Colorado Plateau	45
2.6	Interpolated Lapse Rates over the Project Area	47
2.7	Slope (°) for the Project Area and Colorado Plateau	48
2.8	Aspect (°) for the Project Area and the Colorado Plateau	49
2.9	Percent-Distribution Values of Elevation (m), Aspect (°), Lapse Rate (°C), and Slope (°) for the Colorado Plateau and Project Area	51
2.10	Colorado Plateau Regions with Elevation Values within the Range Represented by the Project Area	52
2.11	Colorado Plateau Regions with Lapse Rate Values within the Range Represented by the Project Area	53
2.12	Soil Thickness (in.) for the Project Area and Surrounding Region	55
2.13	Available Water Capacity (in. of water per in. of soil) for the Project Area and Surrounding Region	56
2.14	Soil Permeability (in inches per hour) for Soils Within and Surrounding the Project Area	57
2.15	Organic Content (% by weight) of Soils Within and Surrounding the Project Area	58

2.16	Drainage Networks Within and Surrounding the Project Area	61
2.17	Biotic Communities	62
2.18	Proportional Distribution of Plant Associations Within the Project Area .	70
2.19	Mammalian Species Richness for the Project Area and Surrounding Region	74
2.20	Distribution of NWS/NOAA Cooperative Network and U.S. Historical Cli- matology Network Station Locations	81
2.21	Year Ranges for Precipitation Records from Meteorological Stations Within 250 km of the Project Area	82
2.22	Year Ranges for Temperature Records from Meteorological Stations Within 250 km of the Project Area	83
2.23	Average Monthly Precipitation Profiles for 18 USHCN Stations within 250 km of the Project Area	87
2.24	Average Monthly Minimum Temperature Profiles for 18 USHCN Stations within 250 km of the Project Area	89
2.25	Average Monthly Maximum Temperature Profiles for 18 USHCN Stations within 250 km of the Project Area	90
2.26	Relationship Between Monthly Precipitation and Interannual Variation .	93
2.27	Relationship Between Monthly Average Daily Minimum Temperature (°F) and Interannual Variation	93
2.28	Relationship Between Monthly Average Daily Maximum Temperature (°F) and Interannual Variation	94
3.1	Paleoclimate Parameters and Reference Demographic Trend for the Project Area and Surrounding Region	100
3.2	Reconstructed Precipitation and Temperature Extremes for the San Fran- cisco Peaks Area of Northeastern Arizona	110
3.3	Annual and 10-Year Precipitation Reconstructions for Six Stations Sur- rounding the Project Area	118
3.4	Meteorological Station at Fort Valley Experimental Station, Arizona . .	123
3.5	Annual and 21-year Smoothed Temperature Trends for San Francisco Peaks, Arizona	123
4.1	Regional and Local Population/Site Frequency Curves	151
4.2	Location of Eastern Lease Area	153
5.1	Top Level Analysis Flowchart	163
5.2	Data Input and Processing Process	166
5.3	Generation of Derived Data Process	171
5.4	Elevation Data, USHCN Station, and Prehistoric Climate Locations .	177
5.5	Calculated Total Annual Solar Radiation for the USHCN Station Locations and Study Area	178
5.6	Project Area Temperature Reconstruction: A.D. 1070	181
5.7	Sample Gaussian Weighting Surfaces	186
5.8	Regional Precipitation Interpolation: A.D. 1070	189
5.9	Project Area Precipitation Interpolation: A.D. 1070	190

5.10	Data Characterization and Extraction Process	192
5.11	Archaeological Sites, Sites and Areas Excluded from Analysis	195
5.12	Illustration of the Process of Calculating Summary Statistics for Rasters, and the Extraction of Values from Those Rasters	197
5.13	30-Year Moving Average of Annual Mean Maximum Daily Temperature .	197
5.14	Smoothed 30-Year Moving Average of Annual Mean Maximum Daily Temperature (480m IDW Smoothing Filter)	198
6.1	Analysis Sample Sizes.	206
6.2	z-score Model Characteristics	209
6.3	Analysis Results: Precipitation Mean and Variance, A.D. 600-1150 . . .	213
6.4	Analysis Results: Precipitation Mean and Variance, Site Distribution, and Result Plot, A.D. 600	215
6.5	Analysis Results: Precipitation Mean and Variance, Site Distribution, and Result Plot, A.D. 700	216
6.6	Analysis Results: Precipitation Mean and Variance, Site Distribution, and Result Plot, A.D. 800	217
6.7	Analysis Results: Precipitation Mean and Variance, Site Distribution, and Result Plot, A.D. 900	218
6.8	Analysis Results: Precipitation Mean and Variance, Site Distribution, and Result Plot, A.D. 1000	220
6.9	Analysis Results: Precipitation Mean and Variance, Site Distribution, and Result Plot, A.D. 1080	221
6.10	Analysis Results: Precipitation Mean and Variance, Site Distribution, and Result Plot, A.D. 1150	223
6.11	Analysis Results: Mean Annual Mean Daily Maximum Temperature, A.D. 600-1150	227
6.12	Analysis Results: Vegetation Community Proportion P-Values, A.D. 600-1150	231
6.13	Analysis Results: Elevation Distribution of Activity Locations, A.D. 600-1150	236
6.14	Analysis Results: Maximum Flow Accumulation for Activity Locations, A.D. 600-1150	240
A.1	7.5' USGS Quads	253
D.1	Interannual Variation in Precipitation for 18 USHCN Stations Within 250 km of the Project Area	299
D.2	Interannual Variation in Average Minimum Daily Temperature for 18 USHCN Stations Within 250 km of the Project Area	300
D.3	Interannual Variation in Average Maximum Daily Temperature for 18 USHCN Stations Within 250 km of the Project Area	301
H.1	Elevation Data Analysis for All Sites	368
H.2	Flow Accumulation Data Analysis for All Sites	369
H.3	Precipitation Data Analysis for All Sites	370

H.4	Temperature Data Analysis for All Sites	371
H.5	Vegetation Data Analysis for All Sites	372
H.6	Elevation Data Analysis for Pithouse Sites	374
H.7	Flow Accumulation Data Analysis for Pithouse Sites	375
H.8	Precipitation Data Analysis for Pithouse Sites	376
H.9	Temperature Data Analysis for Pithouse Sites	377
H.10	Vegetation Data Analysis for Pithouse Sites	378
H.11	Elevation Data Analysis for Masonry Sites	380
H.12	Flow Accumulation Data Analysis for Masonry Sites	381
H.13	Precipitation Data Analysis for Masonry Sites	382
H.14	Temperature Data Analysis for Masonry Sites	383
H.15	Vegetation Data Analysis for Masonry Sites	384
H.16	Elevation Data Analysis for Kiva Sites	386
H.17	Flow Accumulation Data Analysis for Kiva Sites	387
H.18	Precipitation Data Analysis for Kiva Sites	388
H.19	Temperature Data Analysis for Kiva Sites	389
H.20	Vegetation Data Analysis for Kiva Sites	390
H.21	Elevation Data Analysis for Storage Sites	392
H.22	Flow Accumulation Data Analysis for Storage Sites	393
H.23	Precipitation Data Analysis for Storage Sites	394
H.24	Temperature Data Analysis for Storage Sites	395
H.25	Vegetation Data Analysis for Storage Sites	396
H.26	Elevation Data Analysis for Lithic Sites	398
H.27	Flow Accumulation Data Analysis for Lithic Sites	399
H.28	Precipitation Data Analysis for Lithic Sites	400
H.29	Temperature Data Analysis for Lithic Sites	401
H.30	Vegetation Data Analysis for Lithic Sites	402
H.31	Elevation Data Analysis for Groundstone Sites	404
H.32	Flow Accumulation Data Analysis for Groundstone Sites	405
H.33	Precipitation Data Analysis for Groundstone Sites	406
H.34	Temperature Data Analysis for Groundstone Sites	407
H.35	Vegetation Data Analysis for Groundstone Sites	408
I.1	Analysis Area Mean Precipitation: A.D. 600 – 749	410
I.2	Analysis Area Mean Precipitation: A.D. 750 – 899	411
I.3	Analysis Area Mean Precipitation: A.D. 900 – 1049	412
I.4	Analysis Area Mean Precipitation: A.D. 1050 – 1150	413
J.1	Analysis Area Precipitation Variance: A.D. 600 – 749	415
J.2	Analysis Area Precipitation Variance: A.D. 750 – 899	416
J.3	Analysis Area Precipitation Variance: A.D. 900 – 1049	417
J.4	Analysis Area Precipitation Variance: A.D. 1050 – 1150	418

List of Tables

2.1	Biotic Community Hierarchy for the Project Area	65
2.2	Total, Percentage, Minimum, and Maximum Polygon Area, and Number of Polygons for Each Habitat Type Identified by the Arizona GAP Project	70
2.3	Mammals Found Within or Near the Project Area	71
2.4	USHCN Stations Used in the Analysis	85
3.1	Precipitation Reconstruction Locations and Date Ranges	117
3.2	Paleoclimate Precipitation Quantiles (inches)	118
4.1	Plant Taxa from Black Mesa Subsurface Contexts	130
4.2	Animal Taxa from Black Mesa Subsurface Contexts	133
4.3	Archaeological Site Database Field Names/Descriptions	154
4.4	Analysis Site Frequencies by Period/Phase	157
4.5	Analysis Site Frequencies by Artifact/Feature Presence	158
4.6	Analysis Lithic Site Frequencies by Period/Phase	158
4.7	Analysis Ceramic Site Frequencies by Period/Phase	159
4.8	Analysis Groundstone Site Frequencies by Period/Phase	159
4.9	Analysis Pithouse Site Frequencies by Period/Phase	159
4.10	Analysis Masonry Site Frequencies by Period/Phase	160
4.11	Analysis Kiva Site Frequencies by Period/Phase	160
4.12	Analysis Storage Site Frequencies by Period/Phase	161
5.1	Analysis Map Projection Parameters	169
5.1	Analysis Map Projection Parameters (<i>Continued</i>)	170
5.2	USHCN Station Smoothed Radiation (W/m^2) and Elevation (m)	179
5.3	Temperature Regression Model Coefficients	180
5.4	Temperature Regression ANOVA Table	181
6.1	Basketmaker III Vegetation Association P-Value Trends	232
6.2	Pueblo I Vegetation Association P-Value Trends	233
6.3	Pueblo II Vegetation Association P-Value Trends	234
A.1	7.5' USGS Quads	252
A.2	1:250000 USGS Quads	254
B.1	Physiographic Attributes Sample Sizes	255

C.1	Great Basin Conifer Woodland	257
C.2	Great Basin Desertsrub	260
C.3	Plains and Great Basin Grassland	263
D.1	Station 2432 Precipitation	267
D.2	Station 2592 Precipitation	267
D.3	Station 3160 Precipitation	268
D.4	Station 3611 Precipitation	268
D.5	Station 4089 Precipitation	269
D.6	Station 4508 Precipitation	270
D.7	Station 4849 Precipitation	270
D.8	Station 5148 Precipitation	271
D.9	Station 5733 Precipitation	271
D.10	Station 6601 Precipitation	272
D.11	Station 6686 Precipitation	272
D.12	Station 692 Precipitation	273
D.13	Station 738 Precipitation	274
D.14	Station 7435 Precipitation	274
D.15	Station 788 Precipitation	275
D.16	Station 86 Precipitation	275
D.17	Station 9359 Precipitation	276
D.18	Station 9717 Precipitation	276
D.19	Station 2432 Min. Temp.	277
D.20	Station 2592 Min. Temp.	278
D.21	Station 3160 Min. Temp.	278
D.22	Station 3611 Min. Temp.	279
D.23	Station 4089 Min. Temp.	280
D.24	Station 4508 Min. Temp.	280
D.25	Station 4849 Min. Temp.	281
D.26	Station 5148 Min. Temp.	281
D.27	Station 5733 Min. Temp.	282
D.28	Station 6601 Min. Temp.	282
D.29	Station 6686 Min. Temp.	283
D.30	Station 692 Min. Temp.	284
D.31	Station 738 Min. Temp.	284
D.32	Station 7435 Min. Temp.	285
D.33	Station 788 Min. Temp.	285
D.34	Station 86 Min. Temp.	286
D.35	Station 9359 Min. Temp.	286
D.36	Station 9717 Min. Temp.	287
D.37	Station 2432 Max. Temp.	288
D.38	Station 2592 Max. Temp.	288
D.39	Station 3160 Max. Temp.	289
D.40	Station 3611 Max. Temp.	289
D.41	Station 4089 Max. Temp.	290

D.42 Station 4508 Max. Temp.	291
D.43 Station 4849 Max. Temp.	291
D.44 Station 5148 Max. Temp.	292
D.45 Station 5733 Max. Temp.	292
D.46 Station 6601 Max. Temp.	293
D.47 Station 6686 Max. Temp.	293
D.48 Station 692 Max. Temp.	294
D.49 Station 738 Max. Temp.	295
D.50 Station 7435 Max. Temp.	295
D.51 Station 788 Max. Temp.	296
D.52 Station 86 Max. Temp.	296
D.53 Station 9359 Max. Temp.	297
D.54 Station 9717 Max. Temp.	297
E.1 Monthly Precipitation Regression Models	303
E.2 Average Daily Minimum Temperature Regression Models	304
E.3 Average Daily Maximum Temperature Regression Models	304
F.1 Analysis Site List	306

Chapter 1

Introduction

The question of the influence of ecological factors in the development of specific subsistence and settlement patterns is a long-standing archaeological problem. As early as the mid-19th century European prehistorians recognized the importance of looking at the paleoenvironmental context for archaeological sites. In the late 1930's, following the influence of Julian Steward, American archaeologists and ethnologists began to explicitly examine human behavior in an ecological context. With this increasing interest in the behavior-ecology relationship came the recognition that the analysis of settlement patterns was one means for examining these relationships (Trigger 1989; Willey and Sabloff 1974). The utility of settlement pattern analyses based upon large-scale regional surveys continues today through the existence of numerous large-scale survey reports resulting both from long-term research programs and from cultural resources management (CRM) projects (e.g. the research programs presented in Fish and Kowalewski 1990). Survey data, in conjunction with increasingly sophisticated models of subsistence behavior, and tools for managing and analyzing complex geographic data sets (i.e. geographic information systems [GIS]), provide a rich environment for the development and testing of explicitly spatial models of settlement and subsistence.

The research program presented here represents just such a confluence of extant regional datasets, models of subsistence behavior and settlement location, and technical analyses utilizing GIS and statistical methods. Specifically, this research project addresses the relationship between human activity location and plant resource distribution and

productivity. Archaeological data from northeastern Arizona, specifically northern Black Mesa and Long House Valley (Figure 1.1), for the period from A.D. 600 to 1150 are used in the evaluation of settlement and subsistence hypotheses derived from evolutionary ecological models relating resource productivity and the concept of subsistence 'risk'. These areas lie within the region identified as the 'heartland' of the Kayenta Anasazi subtradition (Euler 1988) and were chosen primarily because there have been large-scale research programs in both areas that have documented thousands of sites within large areas of contiguous surface reconnaissance (Dean 1990; Dean, et al. 1978; Euler 1988). The analysis focuses on specific activity locations within the larger region as defined through the presence of diagnostic features and artifactual materials (e.g. habitations as indicated by masonry and pit structures, storage through cists and pits, etc.).

The activity locations are superimposed upon a diachronic, high-resolution, resource productivity model for the 550-year period in question. This model of resource productivity is generated from a combination of high-resolution modern vegetation distribution maps (GAP vegetation maps: Graham 1995), detailed dendroclimatic (i.e. Dean 1988a; Dean and Robinson 1977; H. C. Fritts 1991) and paleohydrological (i.e. Thor N. V. Karlstrom 1988) data, and models that allow for the interpolation of climatic data across complex terrain (Collins and Bolstad 1996; Hungerford, et al. 1989; Thornton, et al. 1997).

With activity locations identified and localized resource productivity modeled, hypotheses relating human behavior (specifically in terms of locational behavior) and localized resource productivity may be tested. While this goal is not new, particularly for this research area (Dean 1988a, b, 1990; Dean, et al. 1985; Dean, et al. 1978; Euler, et al. 1979; F. Plog, et al. 1988; S. Plog and Hantman 1990), the approach proposed here builds upon previous research through the explicit use of 'risk' as an explanatory variable. In the context of this proposal, risk is defined in terms of the "effects of stochastic variation in the outcome associated with some decision" (E. A. Smith 1991:231). Furthermore, the decisions considered in the analysis relate to the specific locations selected for subsistence activities (i.e. procurement, processing, storage, consumption).

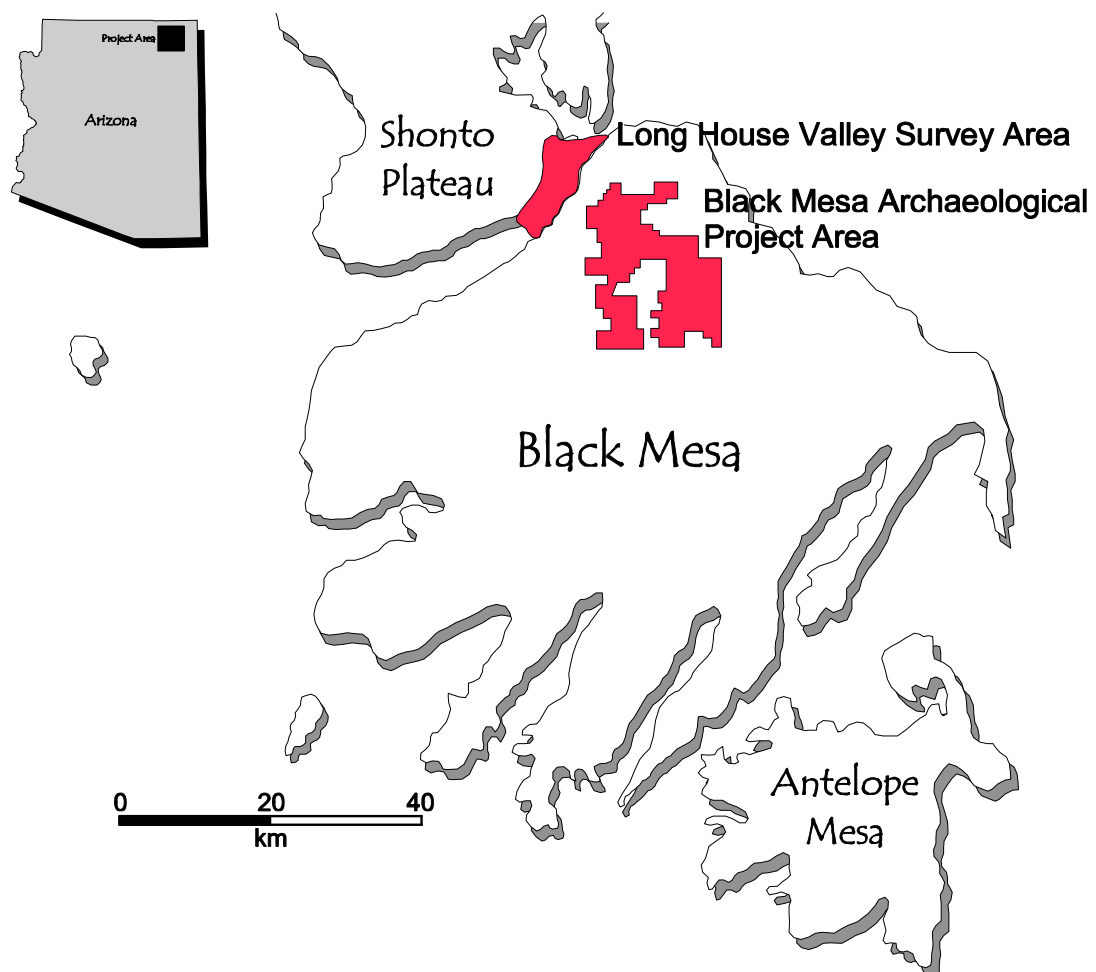


Figure 1.1: Project Location

1.1 Research Background

The problem addressed in this project consists of two components: 1) characterization of locational behavior within the study area relative to subsistence risk estimates from high-resolution diachronic resource distribution models and, 2) development of a general set of methods appropriate for the use of risk-response models. The first component builds upon a large body of research for the Kayenta Anasazi that has identified correlations between environmental conditions and patterns of regional cultural development. The second component addresses a general need to develop and evaluate evolutionary ecological models in a prehistoric context.

1.1.1 Regional Analyses

Extensive research in the northern Southwest has suggested a relationship between environmental conditions and patterns in regional prehistory. These inferred relationships include correlations between colonization, range expansion, abandonment, upland and lowland movement and climatic variables including spatial variation in precipitation, aggradation, and effective moisture (Dean 1990; Dean, et al. 1985; Dean, et al. 1978; Euler, et al. 1979; T. N. V. Karlstrom, et al. 1976; F. Plog, et al. 1988). While the argued relationships between climate and regional patterns in prehistory have been challenged by some researchers (e.g. S. Plog 1986b; S. Plog and Hantman 1990), this analysis follows the lead of Larson et al. in acknowledging that "Although Plog's analyses drive home the valid point that humans do not respond just to changes in the weather, we suggest that it is a mistake to ignore or underestimate the effects of rainfall patterns among arid land agriculturalists." (1996:218).

Implicit in the relationships proposed by Plog et al. (1988) are assumptions about how humans behave under variable environmental and population conditions. In particular, Plog et al. employ a mixture of mean-maximization and risk-minimization arguments in their development and interpretation of environment-behavior relationships. In their analyses, population and environment are treated as independent variables, while behavior is treated as a dependent variable. The analysis proposed here is consistent with their perspective, generally treating the environment as independent, regional population as

independent (though expecting localized variation), and expecting subsistence behaviors to vary in response to these variables. The major difference between the work conducted by Plog and others and this analysis is the explicit utilization of risk-minimization as a 'goal' of prehistoric decision-makers as manifested through household-level behaviors.

The utility of the household as a minimum level of analysis has its basis in three considerations. At the practical level, when considering prehistoric behavior in an archaeological context, it is difficult to identify and measure individual behaviors, and more tractable to utilize the household as a meaningful unit of archaeological observation. In a historical context, there is a long tradition in Southwestern archaeology for defining households as the basic unit of decision-making and behavior. This tradition is reflected in a number of recent simulation studies within the northern Southwest in which household decisions are modeled using agent-based methods, yielding specific locational behaviors relative to maize productivity (G. Gumerman 1998; Hegmon 1989; Kohler and Van West 1996; Kohler, et al. 1996a). Finally, at the theoretical level, the abstraction of individual decisions to the level of the household is consistent with the concept of methodological individualism, in which decisions made by individuals contribute to observable patterns at the supra-individual level. The concept of methodological individualism is the key to bridging the logical gap between individual decision makers and their more visible households (E. A. Smith 1991). This logical linkage between the individual person and the household allows one to speak of individuals making decisions while developing hypotheses related to the locations of households and their associated activities.

1.1.2 Models of Subsistence Change

Economic and evolutionary models of subsistence change have converged over the last 15 years, making similar predictions about the results of subsistence decision-making, but relying upon different theoretical bases (Christenson 1980, 1983; E. A. Smith 1983, 1987; E. A. Smith and Winterhalder 1992). Both modeling paradigms make similar assumptions about the behavior of humans, specifically, that humans are 'rational actors', and 'utility maximizers' (Schneider 1974; E. A. Smith 1983).

Evolutionary ecological models have neo-Darwinian evolutionary theory as their the-

oretical foundation. This allows for the consideration of survival value and long-term reproductive success in addition to proximate cause (Krebs and Davies 1993; E. A. Smith and Winterhalder 1992). Fundamental preferences and the ability to decide among alternatives are assumed to be derived from underlying cognitive capacities that are and have been subject to natural selection (E. A. Smith 1987, 1991; E. A. Smith and Winterhalder 1992). In economic terms, the 'rationality' of the actor is assumed to be the result of natural selection, while 'utility maximization' is defined in terms of fitness or proxy measures of fitness such as net energy capture per unit of foraging time (E. A. Smith 1983), or the probability of a subsistence shortfall (E. A. Smith 1991; Stephens and Krebs 1986; Winterhalder 1986).

Numerous models of subsistence choice utilize mean-maximization as a criterion for the definition of optimal subsistence solutions. These models do not consider the variation in return rates over time, but instead concentrate on the long-term mean return rate in the evaluation of alternative strategies, potentially yielding inaccurate results in cases where stochastic variation in production can have a significant impact on individual survival and reproductive success. In risk-minimization modeling, stochastic variation is built into models of subsistence choice through consideration of both the mean and variance of production (Winterhalder 1986, 1990; Winterhalder and Goland 1997).

The 'z-score' model has been proposed for integrating production mean and variance into models of subsistence choice. This model quantifies the degree of risk to an individual by calculating the probability of experiencing a significant resource availability shortfall. Probability is determined through the calculation of the mean and variance of production for a given subsistence strategy, and use of the resulting probability distribution in estimating the probability of obtaining less than a required minimum value (Stephens and Krebs 1986; Winterhalder 1986, 1990; Winterhalder and Goland 1997). An implication of this model is that response to subsistence risk is dependent upon the relationship between the mean rate of return and the 'minimum' threshold value. When the mean rate of return is above the threshold, an individual is expected to invest in decreasing the variance in the rate of return. When the mean rate of return is less than the threshold, an individual is expected to invest in increasing the variance in the rate of return (Stephens and Krebs 1986). These expectations result from an overall goal of

minimizing the probability of a shortfall. An alternative strategy for decreasing risk may involve investment in increased mean production rates, but in many cases it has been demonstrated that increasing mean rates of return also increase the variance for that return, offsetting any benefits of the increased mean (Winterhalder and Goland 1997). A risk-minimization model may entail both variance and mean modification in attempting to minimize the probability of a shortfall.

Risk-based behavioral models for Southwestern populations have been proposed by a number of authors (e.g. Braun and Plog 1982; Hegmon 1989; Kohler and Van West 1996; Minnis 1985; Wills 1992), with many utilizing an implicit or explicit hierarchy of response model (c.f. Minnis 1985). Minnis (Minnis 1985:20-25) outlines the hierarchical character of human response to risk in terms of increasingly more extensive social integration as risk increases. This model proposes that as stress increases, a greater number of individuals will become involved; the process starts at the household level, continues through kin group integration, and eventually leads to extracommunity integration. The benefits of pooling and sharing (particularly limited pooling as a means of providing greater economic integration) are demonstrated in the historic maize productivity simulations developed by Hegmon (1989; 1996). A simple assumption embedded within the models proposed above, and shared with this analysis, is that risk-reduction strategies follow a sequence from least expensive to most expensive in terms of labor investment.

1.1.3 Project Location and Environment

The project area is located in the northern Southwest, within the southern portion of the larger Colorado Plateau region. The Colorado Plateau is a diverse environment that exhibits marked vertical zonation in the distribution of biotic communities due to observed relationships between temperature, precipitation, and elevation (Hack 1942; Richard H. Hevly 1988; Lowe and Brown 1994; S. Plog 1986b). The combination of these elevationally-influenced temperature and precipitation gradients yields a pattern of vegetation distribution that is primarily defined by the cold-tolerance (for the upper elevation limit) and the drought-tolerance (for the lower elevation limit) of plant communities (Richard H. Hevly 1988) and their constituent species.

The environmental conditions that contribute to the vertical zonation in biotic communities also contribute to their horizontal distribution and reflect potential for change in their productivity through time under different climatic conditions (Jones 1992; Woodward 1987). Localized edaphic conditions can moderate or accentuate regional climatic trends through the creation of microclimatic variation (c.f. Barry 1992; Yoshino 1975).

The project area is located on the northern portion of Black Mesa and within the adjacent Long House Valley area (Figure 1.1), which represent a range of physiographic microenvironments offering the potential for differentiation across portions of the study area along microclimatic gradients. The biotic communities are a small, but important, subset of the full range of communities within the Colorado Plateau. These include several associations within the Great Basin Conifer Woodland and Great Basin Desertsrub communities identified by Brown and Lowe (D. E. Brown 1994b) (Figure 1.2), both of which contain economically important wild species (Cummings 1995; Dunmire and Tierney 1997; Martin, et al. 1991: Table 3-1; Whiting 1939), and which, in some locations, may also support agricultural production.

Modern Climate

Modern climate for the study area may be approximated from the weather stations that contribute to the United States Historical Climatology Network (USHCN Easterling, et al. 1999) with supplemental data provided by additional local weather stations (data available from the Utah Climate Data Center) when available (Figure 1.3).

While daily and monthly measurements provide a detailed view of the data derived from instrumental records, seasonal measurements may be more appropriate for estimating pre-instrumental climatic conditions and calibrating dendroclimatic data. Seasonal measurements may reasonably represent dominant atmospheric flows (i.e. sea-surface air pressure) that in turn influence localized precipitation and temperature patterns (H. C. Fritts 1991). Seasonal measurements also correspond with periods of relative internal consistency (i.e. similar conditions within seasons) allowing for simplified comparisons. Seasonality in climatic conditions correlates with seasonality in plant growth and development, facilitating consideration of dominant conditions during different stages of plant development. Consistent with the recommendations of Fritts, the following seasons are

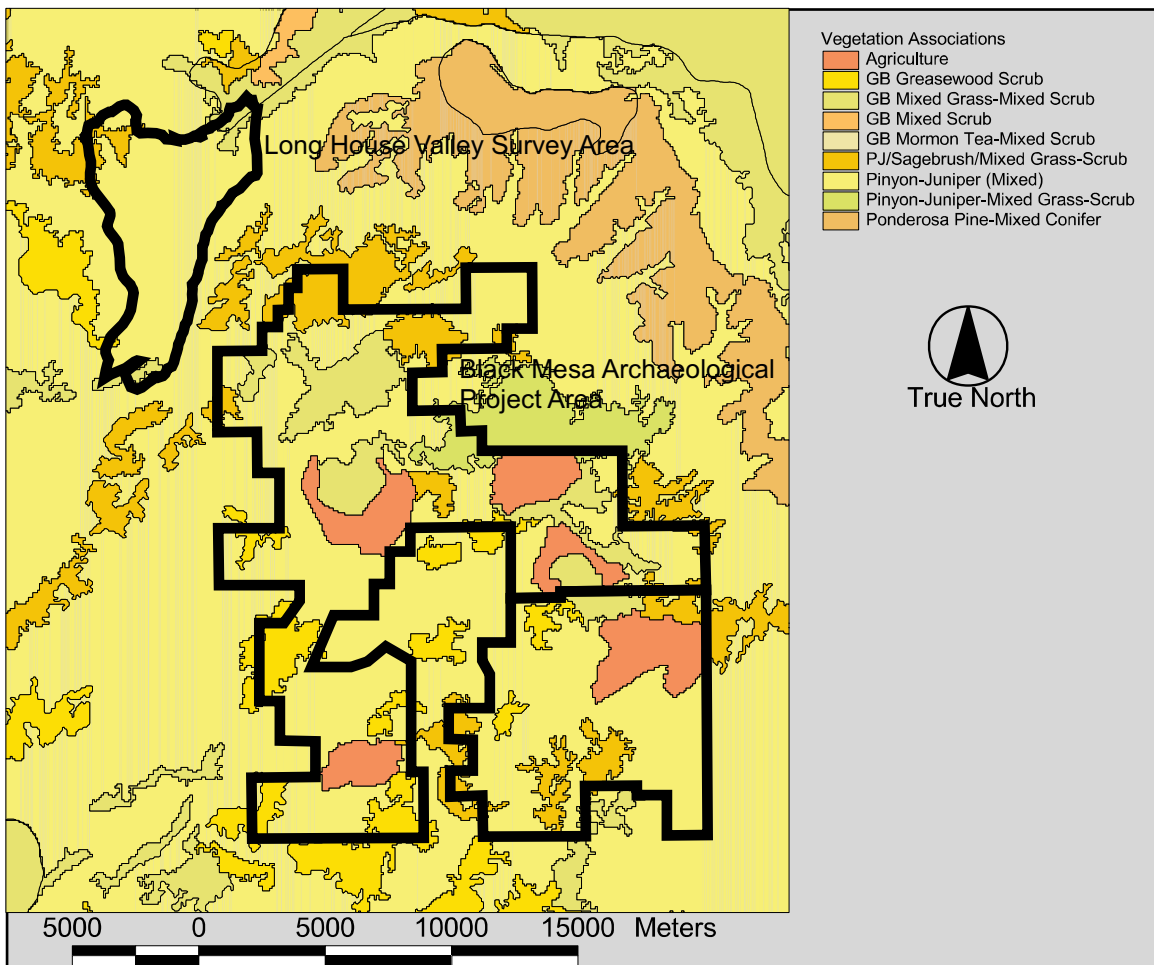


Figure 1.2: Vegetation Community Distribution within the Project Area

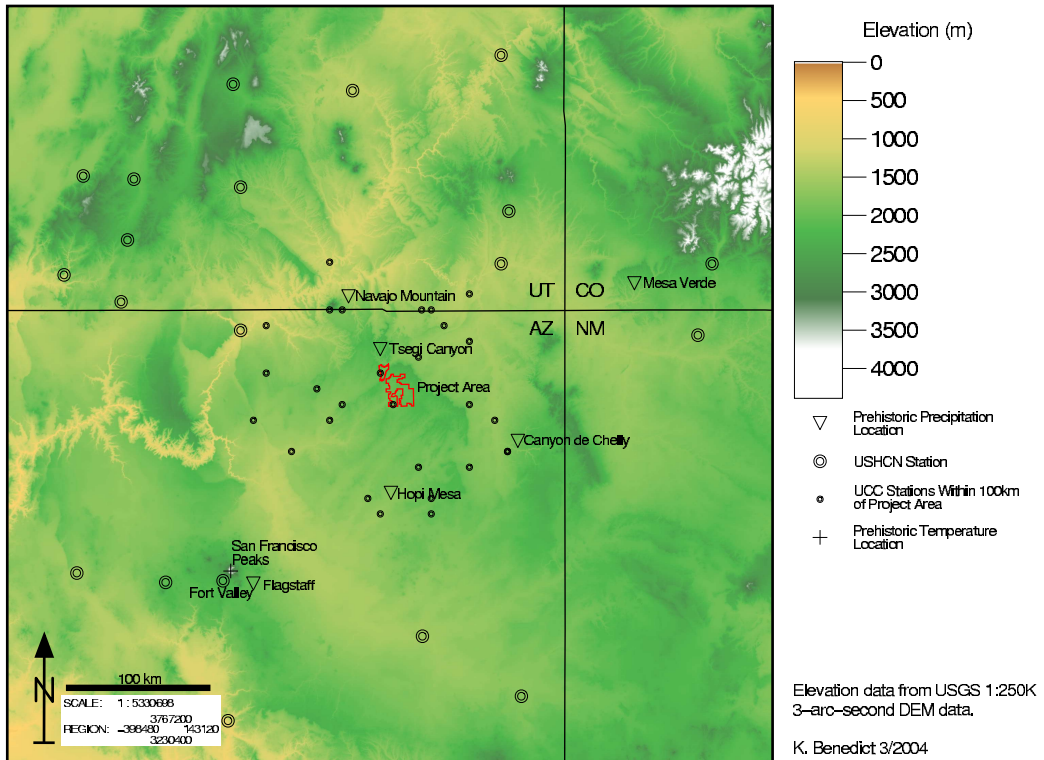


Figure 1.3: Historic Climate and Paleoclimate Data Locations Relative to the Project Area

defined for consideration in the analysis: Winter (December - February), Spring (March - June), Summer (July - August), Fall (September - November) (H. C. Fritts 1991:32). These seasons correspond well with observed precipitation and temperature trends near the study area, and allow for specific consideration of seasonally differentiated conditions relative to plant growth and productivity (e.g. "Spring Drought" Dean 1988a:123).

Historic records indicate that precipitation reaches its maximum during the Summer 'Monsoon' season, maintains an intermediate level throughout the Fall and Winter months, and declines significantly in the mid to late spring (Figure 1.4). These climatic characteristics contribute to a dependence upon Winter-precipitation-derived soil moisture and runoff to support Spring growth and development of critical plant species, both wild and domestic. Likewise, rainfall during the summer months is critical for plant growth and survival following the Spring dry period. A shortfall during either the Winter or Summer may contribute to a seasonal drought(s) within a year with overall non-drought conditions. Without sufficient soil moisture during the Spring and Summer (dependent upon winter and summer precipitation), annual drought conditions prevail. Either set of drought conditions may result in a reduction in the productivity of wild and cultivated species.

Seasonal temperature changes (Figure 1.5) play an important role in the growth and development of economically important plant species including maize. The sensitivity of maize to length of growing season is both well documented and variable. Depending upon the maize cultivar employed, growing season requirements range from as short as 75 days to as many as 120 days for short-season Southwestern maize cultivars and modern hybrid maize varieties, respectively (Muенchrath and Salvador 1995:311). Through reference to instrumental temperature data it is possible to estimate the probability of a catastrophic freeze (Figure 1.6), with catastrophic freeze defined in terms of the low temperature below which plant survival is impaired. In the case of maize, that temperature is approximately -4 °C (24.8 °F) (Muенchrath and Salvador 1995:311).

Finally, extra-regional climatic variations also influence local climates within the Southwestern US. Recently documented impacts from the El Nino/Southern Oscillation (ENSO) demonstrate a strong linkage between Southwestern precipitation and the Southern Oscillation Index (SOI), a measurement of the severity of the El Nino and La Nina climate

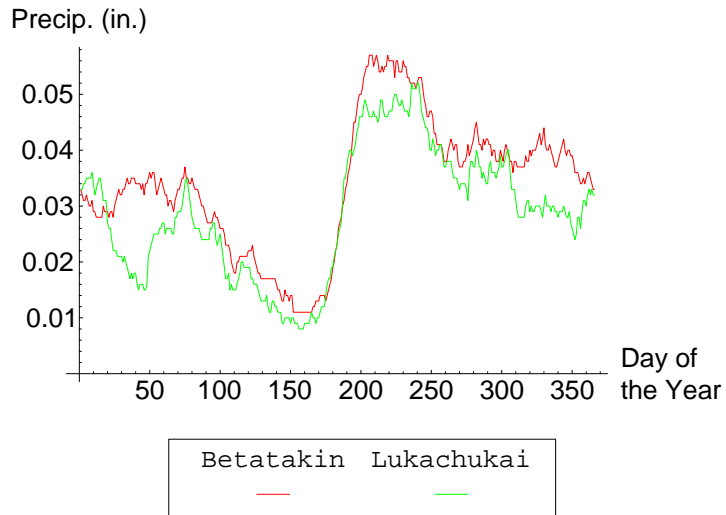


Figure 1.4: Mean Daily Precipitation for Betatakin and Lukachukai, Arizona, 1961-1990
(Western Regional Climate Center 2003a, b)

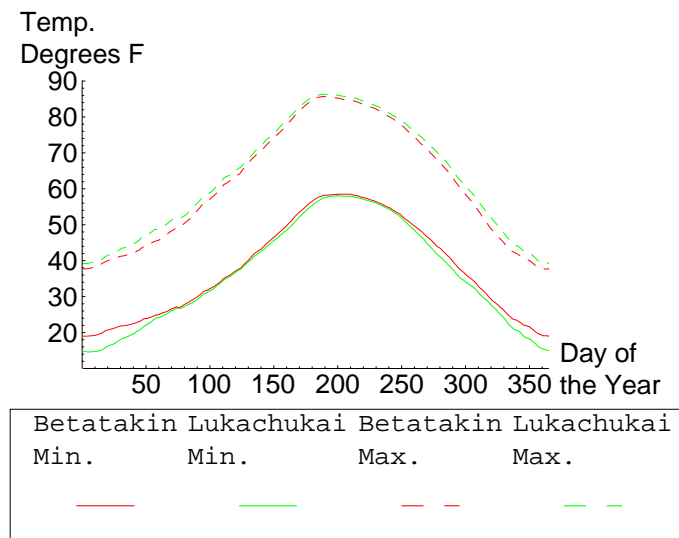


Figure 1.5: Daily Mean Minimum and Maximum Temperature ($^{\circ}$ F) for Betatakin and Lukachukai, Arizona, 1961-1990 (Western Regional Climate Center 2003a, b)

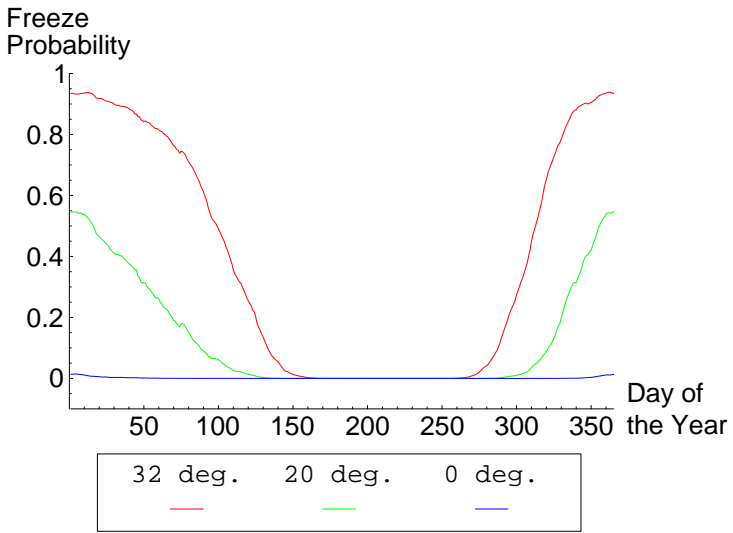


Figure 1.6: Probability of Various Freeze Levels ($^{\circ}\text{F}$) for Betatakin, Arizona (Western Regional Climate Center 2003a)

phenomena. Instrumental data related to Southwest climate teleconnections with ENSO events suggest that there are significant precipitation increases during the September, October, and November following the spring appearance of an El Nino event (Diaz and Kiladis 1992). Snow water content and streamflow are higher than normal in the Southwest during the northern hemisphere winter phase of El Nino, and lower than normal during La Nina events. Frequency and amount of precipitation in February, March, and April of El Nino vs. La Nina years show an increase in El Nino years (Cayan and Webb 1992). The conclusions reached by both Diaz and Kiladis (1992) and Cayan and Webb (1992) are consistent with the presence of a relationship between ENSO events and climatic variations in the Southwest, particularly in relation to the negative correlation between the SOI and winter precipitation, and the weaker negative correlation between southern Pacific sea-surface-temperatures and Southwest temperature.

In this analysis historic climate data are used in the development and testing of climate interpolation models that may be applicable to the interpolation of paleoclimate data across the study region.

Paleoclimate

Paleoclimatic reconstructions for Black Mesa, and by extension the southern Colorado Plateau (Dean 1999; Thor N. V. Karlstrom 1988; T. N. V. Karlstrom, et al. 1976), include several datasets important in modelling resource productivity within the project area. Hydrologic reconstructions suggest that periods of aggradation occurred between A.D. 600 and A.D. 775, and A.D. 1000 and 1150. Periods of stream entrenchment are found in the intermediate period of A.D. 775 to A.D. 1000. Dendroclimatic data for this region suggest that spatial and temporal variation in climate (Dean 1988a; Dean and Robinson 1977) as well as changes in the absolute values of temperature and precipitation exist throughout the period of analysis. The period of A.D. 750 through A.D. 1000 represents a period of high temporal variation while A.D. 600 through A.D. 750 and A.D. 1000 through A.D. 1150 represent periods of relatively low temporal variation (Dean 1999; Euler, et al. 1979; Plog, et al. 1988). Spatial variation, in contrast, is linked to whether tree growth is rapid or slow; with lower spatial variation associated with periods of limited tree growth (Dean 1988a).

The response of vegetation to climatic variation is dependent upon both the degree of variation, the speed of onset and duration of change (Levitt 1980). Spatial variation in climatic conditions has an impact on the degree of confidence one can have in the interpolation of climatic variables between measurement locations (i.e. weather stations or tree-ring sites), with periods of greater spatial variation resulting in diminished confidence in interpolated values.

Critical in the analyses conducted here is the relationship between plant productivity and climate, both for wild and domesticated plant species. This relationship is key for providing the bridging argument for linking mean and variation in climate parameters to mean and variation in wild and domesticated plant productivity, ultimately allowing for the use of climate parameters as proxy measures of relative plant productivity. Webb found that there exists a significant ($\alpha = 0.10$) correlation between perennial plant "above ground net primary production (ANPP) and actual evapotranspiration (AET)" for the current year's AET ($R^2 = 0.64$), the previous year's AET ($R^2 = 0.62$), and the combination of both the current and previous year's AET ($R^2 = 0.69$). Webb also

found that annual plant productivity (also measured at ANPP) had a poor correlation with annual precipitation ($R^2 = 0.08$), with the ANPP of annuals exhibiting a greater dependence on the seasonal distribution of rainfall (Webb, et al. 1983:1243).

Burns found similar trends, but with lower correlation coefficients (Burns 1983: Table 4-3), in his preliminary examination of the relationship between dendroclimatological precipitation estimates from several record locations and regional corn and dry bean yields in southwestern Colorado. These results led him to pursue the development regression models for predicting crop yield from multiple precipitation reconstructions, ultimately succeeding in producing statistically significant predictive models (Burns 1983: Tables 4-4 – 4-7) for corn and dry bean yields.

Both sets of analyses cited above demonstrate the positive correlation between precipitation and plant productivity. This relationship provides the foundation for treating precipitation estimates derived from dendroclimate reconstructions as a proxy for potential yields from wild and domesticated plant resources.

1.1.4 Culture History

The period of time analyzed by this research project (A.D. 600 - A.D. 1150, Figure 1.7) corresponds to the Basketmaker III (BMIII), Pueblo I (PI) and Pueblo II (PII) periods outlined in the Pecos classification system (F. Plog 1979). It also corresponds with the entire Black Mesa phase sequence with the exception of the Basketmaker II (BMII) Lolomai phase (S. Plog 1986a; Francis E. Smiley and Ahlstrom 1998a), and corresponds with and predates the earliest period analyzed by Dean and his collaborators (Dean 1990; Dean, et al. 1978) in their analyses of Long House Valley archaeological patterning.

The general pattern of BMII settlement and subsistence within the larger Kayenta region was one of reliance upon a variable mix of agricultural and wild food resources as indicated by archaeobotanical, skeletal, and site locational data (Chisholm and Matson 1994; Leonard 1989; Martin, et al. 1991; Matson 1994; Matson and Chisholm 1991; S. Plog 1986a). Basketmaker III cultural developments within the study region reflect continuity of the trends begun during the BMII period. Population densities were low but increasing from their BMII levels throughout this period. Subsistence consisted of a

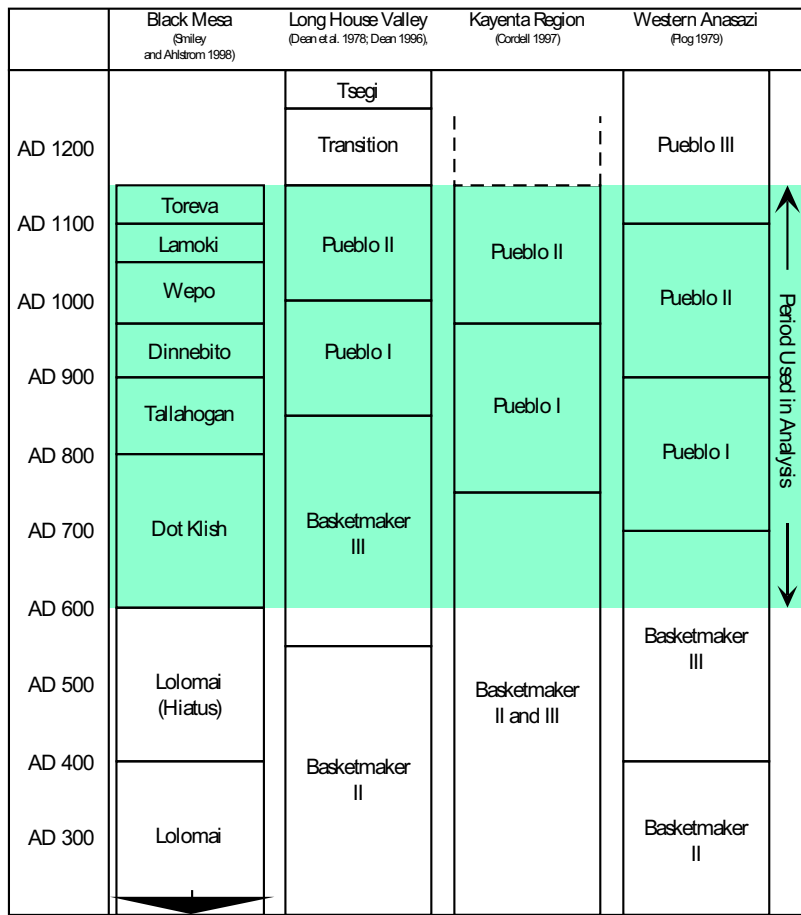


Figure 1.7: Regional Chronology

mixture of agricultural production and seasonal wild resource utilization, with habitation site placement emphasizing locations of high agricultural productivity and limited activity sites concentrating on locations of high wild resource density. The spatial patterning of these complimentary activities has often been presented in terms of upland versus lowland resource utilization (Euler 1988; S. Plog 1986a; Powell 1983). The appearance of ceramics at this time provides an improved level of chronological control. The recorded BMIII sites on Black Mesa appear to represent short-term seasonal occupations related to the collection of wild resources, while more stable settlements appear to be found in lowland areas associated with potential agricultural land (S. Plog 1986a). Other technological changes also differentiate this period from the BMII period. These changes include increased use of two-hand manos in trough metates, changes in storage feature characteristics, and the use of beans in addition to maize (M. F. Smith 1994a).

During the PI period, habitation site locations continued to focus on lowland locations but the numbers of habitation and limited activity sites increased along major upland drainages, indicating more intensive use of upland wild resources and increased agricultural activity in these locations (Braun and Plog 1982; G. J. Gumerman and Dean 1989; M. F. Smith 1994b). Structural features observed at PI sites include larger and more substantial pithouses, slab-lined cists, and in some cases, roomblock-kiva-midden complexes supplemented with pithouses and jacal dwellings. This is a more formalized layout than observed previously (S. Plog 1986a; M. F. Smith 1994b). Population trends for Black Mesa during PI are characterized by punctuated population growth while maintaining generally low population densities (S. Plog 1986b). Long House Valley population trends are more poorly defined, though the population of the valley during PI times appears to be very low compared to later levels (see Figure 1.8 for the general Kayenta population trends for the period of analysis).

Pueblo II and early Pueblo III developments represent a continuation of formalized site plans, variable population trends, and expansion of settlement locations. This period on Black Mesa is characterized by initial population decline followed by rapid population growth, reaching a maximum population by roughly A.D. 1100. Population then declined rapidly, leading to effective abandonment of northern Black Mesa by A.D. 1150. In Long House Valley, population increased continuously throughout the PII-PIII periods (Dean

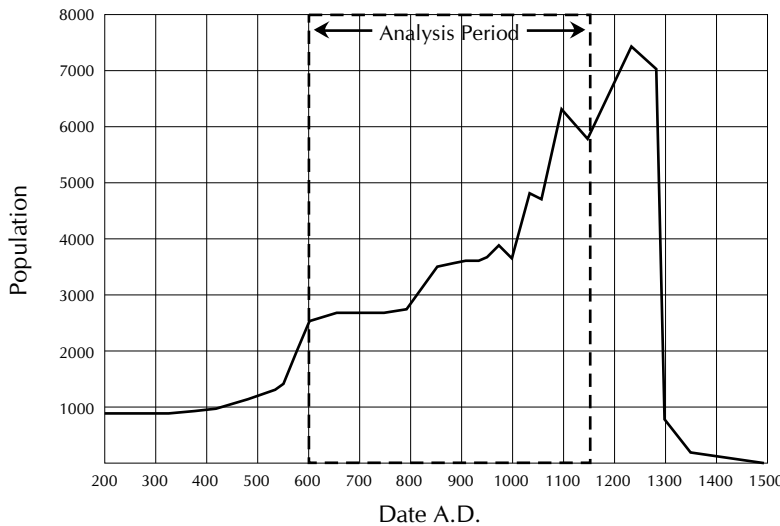


Figure 1.8: Kayenta Population Trends (based upon Dean, et al. 1994: Fig. 4.2, pg. 61)

1996b). Settlement locations appear in all ‘habitable’ upland and lowland locations, suggesting that population density was relatively high, particularly in northern Black Mesa. There was an increase in the number of small ‘homestead’ sites relative to larger nucleated village sites (Dean, et al. 1978; G. J. Gumerman and Dean 1989; S. Plog 1986a).

Following the abandonment of northern Black Mesa (and postdating the period addressed in this analysis), population continued to increase in Long House Valley through A.D. 1300, when the Kayenta region was effectively abandoned (Figure 1.8). In conjunction with this population increase was the development of large aggregated villages in the northern regions of Long House Valley (Dean 1996b; Dean, et al. 1978). While this has been explained in reference to hydrologic shifts entailing stream entrenchment in the southern portion of the valley (Dean 1996b; Dean, et al. 1978; G. Gumerman 1998), the placement of some of these sites in defensible locations suggests that conflict with nearby settlements may have also played a role in the observed aggregation (Haas and Creamer 1996).

Overall, the cultural developments within the study area represent a dynamic process of activity location modification through expansion and shift in environmental focus. This process is overlain upon a variable environment and dynamic population structure, reflecting potentially complex interactions between activity location, environment, and

population level (Braun and Plog 1982). This analysis examines the nature of these interactions through the development of detailed, diachronic productivity maps that allow for a detailed assessment of localized productive potential relative to inferred relative population levels and activity locations.

1.2 Research Problem and Research Methodology

The specific research problem addressed in this analysis is:

How does the spatial distribution of human activity relate to the degree of subsistence risk as estimated from a high-resolution, diachronic resource productivity model?

Included within this problem statement are several terms and concepts requiring specific definition and expansion. These items include:

Spatial distribution of human activity. In the context of this analysis, human activities of interest include those that are directly related to subsistence, including food acquisition, processing, storage, and consumption. Although not solely related to subsistence, habitation location is another activity with locational characteristics that are examined relative to resource distribution and risk. The spatial distribution of the activities outlined above is determined through the identification of feature and artifact locations that are thought to be diagnostic of those activities. For example, habitation locations are defined through the presence of non-storage masonry or pit structures, and food processing locations are identified through the presence of food-processing artifacts (e.g. groundstone) and features.

Subsistence risk. Subsistence risk is specifically defined in terms of the probability of a significant shortfall in subsistence resources. This definition entails three components: mean regional productivity (as represented by current regional productivity), productivity variance (as represented by temporal variation in regional productivity), and regional population. As outlined previously, when mean regional productivity is greater than the minimum productivity requirement for the current population, risk is minimal. Risk increases when mean productivity declines or productivity variance increases. Likewise, if mean productivity increases or productivity variance decreases, risk declines. Most often both variables change simultaneously, yielding potentially mixed effects. For example, if

mean productivity and variance increase (as is often the case in instances where mean productivity is obtained through intensification in the production of a limited number of resources (Rindos 1980; 1984:272-284; Winterhalder 1990; Winterhalder and Goland 1993, 1997)), risk reduction would only be possible if additional variance reduction strategies are employed. Finally, if population increases and mean productivity and variance remain stable, risk also increases, potentially requiring the adoption of risk reduction strategies. Overall, it is the interaction of all three components that defines the degree of subsistence risk at a given time.

In the context of this analysis, a base level of risk ("base risk") for each year in the analysis is evaluated through simulation-based estimation of distribution of thirty-year precipitation variance values for randomly selected locations within the analysis area. This simulated distribution of precipitation variance provides a null hypothesis against which observed variance values calculated at site locations may be compared. A three decade time 'window' has been chosen for this analysis since it represents a period of time slightly longer than the median age of individuals within the Black Mesa skeletal population study area (Martin, et al. 1991), providing for individual perception of risk (E. A. Smith 1991) based upon personal experience and information provided by an individual's parents. While there exist mechanisms for storage and communication of information over longer periods of time than proposed here (c.f. Gunn 1994), the relatively conservative length of time utilized allows for an assumption of more direct knowledge of the range of environmental variation, and thus more complete knowledge on the part of decision makers.

While critical, risk minimization is only one of several factors that potentially influence activity location. For this reason, it is assumed that as risk increases, the utilization of risk-minimization strategies will also increase. This assumption is consistent with the economic and evolutionary ecological assumptions outlined above, in particular the existence of finite resources in addressing multiple, competing needs. As a result of this assumption, population is expected to influence the degree of risk-response, with the expectation that low relative population levels will be associated with weak risk-response patterning while high relative population levels will be associated with increased risk-response patterning.

High resolution, diachronic resource productivity model. The resource productivity model employed in this analysis uses several variables, yielding mapped qualitative proxy measures of plant resource productivity at an annual time-scale for the 550 years in the analysis. These potential productivity proxies are based upon the following input variables:

- Interpolated (Collins and Bolstad 1996; Hungerford, et al. 1989; Thornton, et al. 1997) temperature and precipitation estimates from dendroclimatic data sources (i.e. Laboratory of Tree Ring Research [LTRR] and the International Tree Ring Data Bank [ITRDB]) and historic climate (i.e. the US Historic Climate Network and the Utah Climate Center) data sources.
- Base vegetation association maps derived from satellite imagery (GAP vegetation GIS coverages, Graham 1995)
- Localized plant species distribution data derived from vegetation transect records (Moore 1979) and site-specific vegetation information.
- Hydrologic conditions related to drainage aggradation or incision. This attribute is used in the assessment of overall agricultural potential, with periods of incision having relatively lower agricultural potential than periods of aggrading or stable surfaces.
- Generalized soil data. These data provide an overview of alluvial soils within the study area, helping to identify potential agricultural locations.

1.3 Hypotheses and Archaeological Correlates

In order to test the applicability of the proposed risk-response model, archaeological correlates of theoretical expectations must be identified and evaluated. Following are three general theoretical expectations and corresponding archaeological patterning that should be observed if the expectations find support.

During periods of low risk, risk reduction strategies may be employed, but not as consistently as during periods of relatively high risk.

When total risk is relatively low during a given analysis period, the reduction in risk associated with behavior modification yields only a small benefit, leading to the expectation that risk reduction strategies including mean-enhancement and variance reduction might be employed. Generally, since the benefits of risk reduction tend to be small in low-risk situations, only those behaviors that further reduce risk without a significant cost will be widely employed. Expected archaeological patterns related to this hypothesis include:

1. Habitation locations (as indicated by habitation features such as pithouses and non-storage masonry rooms) will be consistently associated with locations that balance access to areas of highest wild resource productivity and agricultural potential, while also recognizing the critical importance of water availability. Habitation locations will be relatively stable, changing primarily in response to localized wild-resource depletion.
2. Specialized habitation locations including field houses (as indicated by low artifact diversity and density, absence of storage features, small number of habitation features) will be closely associated with specific locations of high agricultural potential (resulting in minimal variation between activity locations).
3. Resource collection locations (as indicated by low artifact diversity and density and an absence of habitation features) will be associated with locations of high wild resource productivity (again resulting in minimal variation between these activity locations).
4. Storage features (as indicated by storage-related masonry structures and storage features such as pits and cists) will be relatively frequent (relative to the estimated population) because interannual fluctuations in productivity are expected to be relatively low during periods of low risk, allowing for consistent subsistence levels through time-averaging.

These patterns are expected to be most strongly exhibited during times of low risk in conjunction with low population density, because the potential disparity between population and the available resource base is minimized. During periods of low BRI but

intermediate or high population levels, higher levels of total risk are expected, weakening the patterning outlined above and instead yielding patterning closer to the high risk patterns presented below (Kohler and Van West 1996).

During times of high risk, variance reduction strategies will become prevalent.

When total risk is high, there will be greater incentives to employ variance reduction strategies since variance reduction yields reductions in total risk (in cases where the mean level of production is above the minimum threshold), particularly under conditions of high temporal and spatial variation in productivity. This expectation should manifest itself archaeologically in the following ways:

1. Habitation locations will maintain a balance between wild resource and agricultural production areas, but display a weaker correlation with prime agricultural field locations than observed under low total risk conditions (because of field dispersal to reduce production variance) (Winterhalder 1990; Winterhalder and Goland 1993, 1997). Habitation locations may become more concentrated spatially as extra-household pooling and sharing comes into play (Hegmon 1989; Kohler and Van West 1996).
2. Specialized habitation locations such as field houses will be closely associated with locations of agricultural potential, but with a greater diversity of agricultural locations than observed under low total risk conditions. This pattern is expected because of increasing utilization of field dispersal strategies in conjunction with field development in more marginal locations.
3. Resource collection activities will be associated with productive wild resource locations, though in a greater diversity of locations than observed under conditions of low total risk.
4. Storage features will be less frequent (in proportion to the estimated population) because temporal fluctuations in productivity are expected to be more severe, reducing the efficacy of storage as a risk-minimization strategy.

In summary, the expectations outlined above present two extremes along the expected continuum of BRI-population configurations. At both of these extremes, the following

general patterns are expected. Under conditions of low total risk, it is expected that activity locations will be relatively homogeneous in terms of the localized productivity diversity, with locations focusing on high-productivity positions on the landscape. Conversely, under conditions of high total risk, it is expected that activities will take place over a greater range of locations on the landscape, yielding a more heterogeneous distribution of activities relative to localized productivity, ultimately producing a pattern of site locations in association with low variance (risk-reducing) locations.

1.4 Data Requirements and Analysis Steps

1.4.1 Spatial Distribution of Activity Locations

Assessment of the spatial distribution of activity locations requires the following data:

1. Chronological data of sufficient resolution to determine the probability of a specific feature or artifact assemblage dating to a particular decade. A combination of radiocarbon, dendrochronological, and ceramic dating methods is employed to determine the probability of an activity taking place during a specified analysis year.
2. Consistent definition of activity indicators. For example, habitation is indicated by non-storage structures (pit or masonry), storage by storage features (cists, storage rooms, pits), processing by artifactual materials (groundstone), and consumption by remains (burned botanical remains, faunal remains, and coprolites).

1.4.2 Resource Distribution Model Development

Development of the resource distribution and productivity model requires the following:

1. Source of high-resolution modern vegetation data from which to work back. In this analysis, the GAP vegetation maps produced as a part of the National GAP Program provide the baseline vegetation distribution data (Graham 1995).
2. Ground observations of species distributions within remotely sensed polygons represented in the GAP vegetation coverage. The data employed in this analysis consist

of the original vegetation data collected as a part of the Black Mesa Archaeological Project, both for archaeological sites and for vegetation transects.

3. Detailed dendroclimatic records for several locations within and near the project area. Data from six primary measurement locations (Dean 1999) archived by the Laboratory for Tree-Ring Research at the University of Arizona, in addition to other datasets available from the International Tree-Ring Database, provide the paleoclimatic foundation for this analysis.
4. Historic and modern instrumental climate records for developing a transfer function for dendroclimatic record. Data from the US Historic Climate Network (USHCN, Easterling, et al. 1999) in addition to data from the Utah Climate Center provide the collection of historic climate data employed in this analysis.
5. Application of interpolation routines to determine local climatic estimates for points on the landscape remote from dendroclimate stations. Input variables include slope, aspect, elevation, remote temperature, remote precipitation, and remote physiographic context (Collins and Bolstad 1996; Hungerford, et al. 1989; Thornton, et al. 1997).
6. Application of local climate estimates to model relative local productivity within the project area.

1.4.3 Subsistence Risk

Subsistence risk is defined utilizing the following dimensions:

1. Spatial variation in climate interpolation as estimated from the degree of variation across the entire spatial field for dendroclimatic observations.
2. Temporal variation in resource productivity (as estimated from time-lag deviations).
3. Areal extent of productivity changes (indexed according to estimated localized species composition and impacts of climatic factors, particularly drought)

4. Measurable impacts of climatic/hydrologic events (i.e. degradation index and its potential impact on localized agricultural production)

1.4.4 Hypothesis Testing

The evaluation of the specific archaeological correlates outlined above requires the development of spatial models for hypothesized and null-hypothesis activity distributions. The null-hypotheses generally take the form of spatial simulation models in which random locations are simulated and compared to observed patterning. When the observed patterns are significantly different from those observed using simulated random activity locations, the corresponding null-hypotheses are rejected. In those cases where the null-hypothesis of random distribution of activity locations is rejected, a further analysis of the correlation between spatial patterns derived from the above defined hypotheses and those observed yields a test of the specific hypotheses that are derived from the risk-response model proposed here.

In summary, the research presented herein entails the evaluation of a set of hypotheses relating the locations of subsistence and habitation activities to vegetal resource distribution. Underlying the tested hypotheses is an assumption that individual decision-makers (cooperating within households) seek to minimize the probability of a subsistence shortfall through adoption of variance reduction strategies, particularly when relative population levels are high. This assumption is based upon a body of evolutionary ecological and anthropological research that suggests that risk-minimization strategies may be more effective than mean-maximization strategies in highly variable environments like those encountered in the Southwestern U.S.

The particular area and time period selected for the research has been intensively investigated over the past 30 years, providing a large number of sites in a variety of topographic settings for hypothesis testing. Likewise, the paleoclimate of the northern Southwest has also been intensively studied, providing a rich source of data for reconstructing past climatic conditions influencing vegetal resource productivity. Finally, detailed vegetation data are available for the research area both in the form of remotely-sensed vegetation map data and ground-based vegetation assessments. The combination

of these three components allows for the testing of activity-resource location hypotheses using detailed diachronic resource productivity models.

Chapter 2

Modern and Historic Environment

The topography, climate, vegetation, and agricultural potential of any square mile area of the Black Mesa coal lease is a study in contrast and variability. Standing on the edge of an entrenched drainage, one can view an adjacent terrace of saltbush and greasewood vegetation with an occasional saltcedar, a Eurasian tree which is spreading rapidly on the mesa at the expense of native vegetation. Beyond this is a terrace covered by a mosaic of sagebrush, snakeweed, rabbitbrush, and scattered clumps of saltbush. The walls between tributaries of the major drainages are filled with deep colluvium which supports a dense growth of big sagebrush and an understory of herbs and grasses. The more distant eroded sandstone hills have a shallow mantle of soil covered with a pygmy pinyon and juniper forest, isolated shrubs, herbs, and grasses and forbs in disturbed openings. This mosaic reflects differences in soil chemistry, soil depth, and climatic variation in local temperature and annual moisture (Ford, et al. 1983).

Characterization of the environment for the study area and the surrounding region is critical for a successful identification and definition of any relationships between subsistence-related locational behavior and subsistence risk. Multiple dimensions of environmental variability are embedded within this analysis. These dimensions include physical variables such as geology and soils; topographic characteristics including slope, aspect, and elevation; and hydrologic conditions consisting of stream course locations and catchment areas. The analysis also utilizes biotic data representing modern and historic plant and animal distribution data. Finally, historic climate records (presented in this chapter) and prehistoric climate records (presented in Chapter 3) provide a critical data source for estimating variation in landscape productivity, allowing for an estimation of subsistence risk both through time and across space. This final model of subsistence risk provides

the foundation for testing hypotheses relating locational behavior to subsistence risk.

This chapter summarizes the historic and modern environmental data employed in the analysis at two scales, first at the scale of the southern Colorado Plateau and second for the area directly surrounding and including the study. Environmental data at these different scales are essential to the research problem for several reasons. Regional environmental data provide the baseline conditions from which local conditions vary based upon location-specific attributes. For example, regional paleoclimate conditions estimated from multiple dendroclimate datasets provide a baseline condition which, when combined with local physiographic conditions, contributes to localized microclimatic variation. Likewise, regional vegetation community data provide a picture of the broad-scale distribution of numerous plant and animal species (e.g. D. E. Brown 1994b), while identified plant associations within those communities (e.g. Graham 1995) provide for more detailed characterization of local plant and animal species distribution. Local environmental data play a critical role in both calibrating regional data and providing location-specific data for validation of interpolated or extrapolated data for the study region. Localized vegetation transect data were collected as part of the Black Mesa Archaeological Project (Black Mesa Archaeological Project 1977, 1978, 1980, 1981, 1982, 1983). Data characterizing vegetation and animal species within the Black Mesa leasehold were collected by Espey, Huston, and Associates, Inc. (1980) for the Peabody Coal Company. These provide a comparison dataset for the GAP vegetation data (derived from satellite imagery and aerial videography, Graham 1995) and illustrate the use of local data for validation and calibration of a regional dataset. Finally, in some cases, the local data for specific locations provide the only appropriate scale of data for the analysis. The necessity of detailed localized physiographic data including slope, aspect, and elevation is easily recognized when considering the data most appropriate for making local adjustments to regional trends in climate.

2.1 Physical Environment

Black Mesa and Long House Valley are situated in the southern portion of the Colorado Plateau Physiographic Province (Figure 2.1) in Northern Arizona (Figure 1.1). The

Colorado Plateau is a region of the Western United States that includes portions of Utah, Colorado, Arizona, and New Mexico and is characterized by its relatively high elevation, diverse landscape, and aridity (S. Plog 1986b).

2.1.1 Geology

While distinguishable geologically from the physiographic provinces surrounding it, the salient geologic characteristics of the Colorado Plateau are those that are manifest in the exposed geology of the study area. Local and regional geologic features pertinent to this analysis include those that influence raw material availability, soil characteristics, and water availability. Each of these factors directly or indirectly contributes to the suitability of specific locations on the landscape for different activities. Raw material availability directly impacts the range of locations where needed materials for flaked and groundstone tool production, ceramic manufacture, and habitation construction may be found (Bradfield 1971; Garrett 1986; Green 1985, 1986). Soil characteristics significantly contribute to the locations, types and characteristics of natural plant communities, while also determining the agricultural potential for specific landscape locations (Bradfield 1971; Dean, et al. 1978; Hack 1942). Water availability (as defined by the presence of springs, conditions conducive to shallow well excavation, or surface accumulation, i.e. Gregory 1916; Hack 1942) is critical for most human activities, and in an arid region such as the study area plays a key role in determining where moisture-dependent activities may take place. The underlying geology of the study area plays a significant role in determining all of these characteristics.

The underlying geologic structure for the Black Mesa and Long House Valley project areas and surrounding area expose a wide range of formations. These formations include Triassic age Navajo Sandstone elements of the Glen Canyon group in the areas west of Long House Valley, Jurassic San Rafael group in Long House Valley, Cretaceous Dakota Sandstone and Mancos Shale formations along the escarpment between Long House Valley and Black Mesa, and the Upper Cretaceous Mesa Verde group deposits exposed on the top of Black Mesa (Figure 2.2, Figure 2.3) (Beaumont and Dixon 1965; Gregory 1916). These formations (listed in ascending order from deep to shallow in the complete

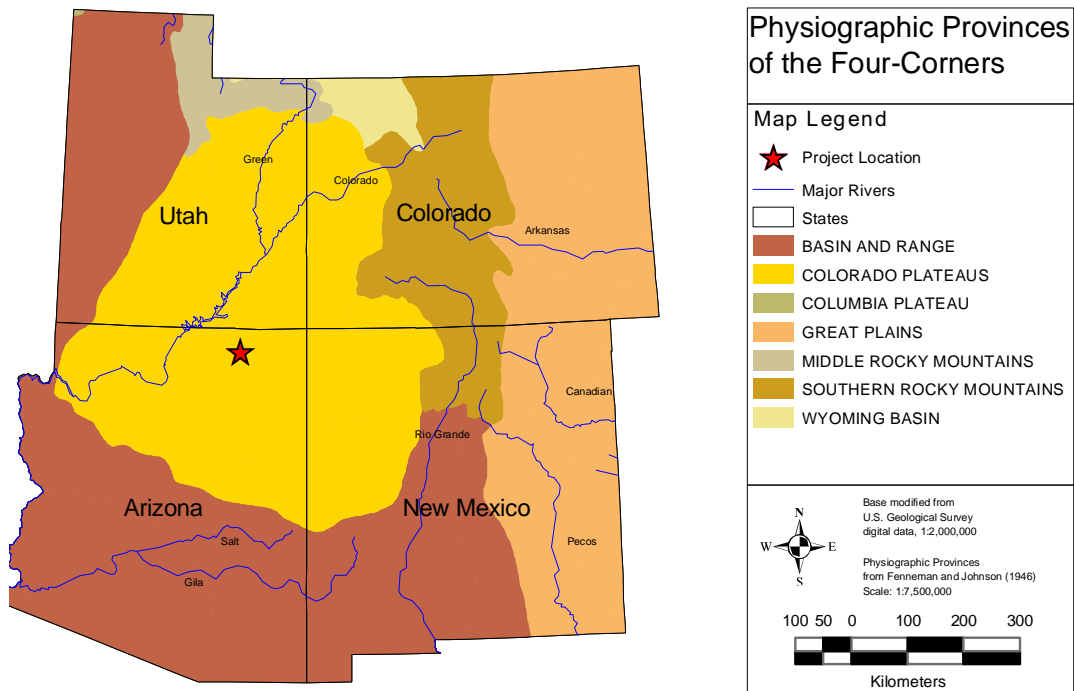


Figure 2.1: Colorado Plateau Physiographic Province

geologic profile) are described in the following sections, with an emphasis on their general characteristics and associated raw material, hydrologic, physiographic influences.

Chinle Formation

The Triassic Chilne Formation represents the oldest exposed geologic strata in the vicinity of the study area and consists of three members (from oldest to youngest): Petrified Forest, Owl Rock, and Church Rock (Beaumont and Dixon 1965:A5). Outcrops of the Petrified Forest member are found in several locations north of the Tsegi Trading Post (within Marsh Pass, at the north end of Long House Valley) and north of Kayenta, while the Owl Rock member is exposed along Tsegi Canyon, within several of its tributary drainages, and in several drainage basins draining into Laguna Creek (Beaumont and Dixon 1965:Plate 1).

Archaeologically, the petrified wood available from the Petrified Forest member resembles the coarse-grained gray and black petrified wood found in the Wepo formation (see below), and generally appears in Black Mesa archaeological sites at relatively low frequencies (Green 1985:73; 1986:155). The higher quality petrified wood associated with these deposits within the Petrified Forest National Monument is not found at the locations proximate to the study area (William J. Parry 1987:27). Two principal varieties of chert have been observed in association with the Owl Rock stratum: a silicified limestone including small deposits of red or purple and green chert that may contain fossils, and a "purplish white or smoky white translucent chalcedony that sometimes grades into a more purple chert" (Green 1986:154-155). Various assessments (i.e. Garrett 1986; Green 1985, 1986; Hill 1994; William J. Parry 1987) suggest that there are no known specific uses of lithic or ceramic raw materials from the Church Rock member.

Geib and Callahan's (1987) assessment of Tusayan white ware clay sources makes a general reference to clays derived from the Chinle Formation, suggesting that there exists a possibility that clays derived from any of the three Chinle Formation members discussed above may have been useful in ceramic production, particularly in the production of ceramics that fire to a reddish-yellow to reddish-brown color (Geib and Callahan 1987:103; Hill 1994:37).

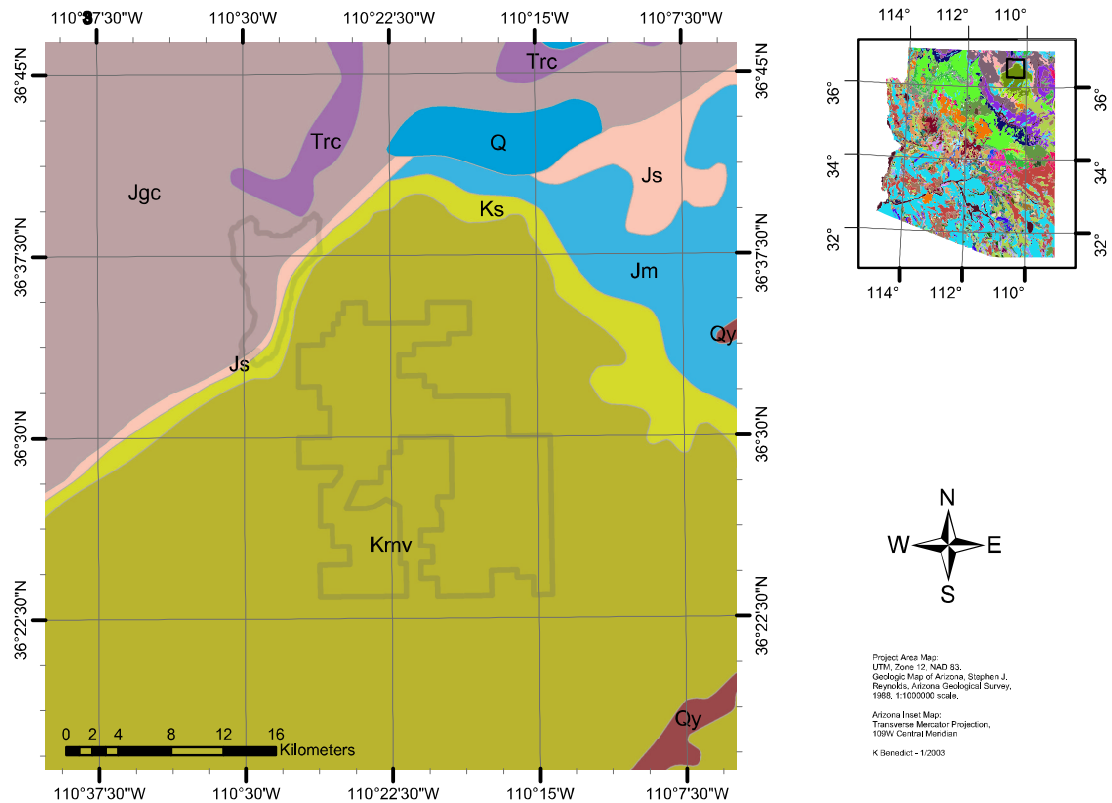
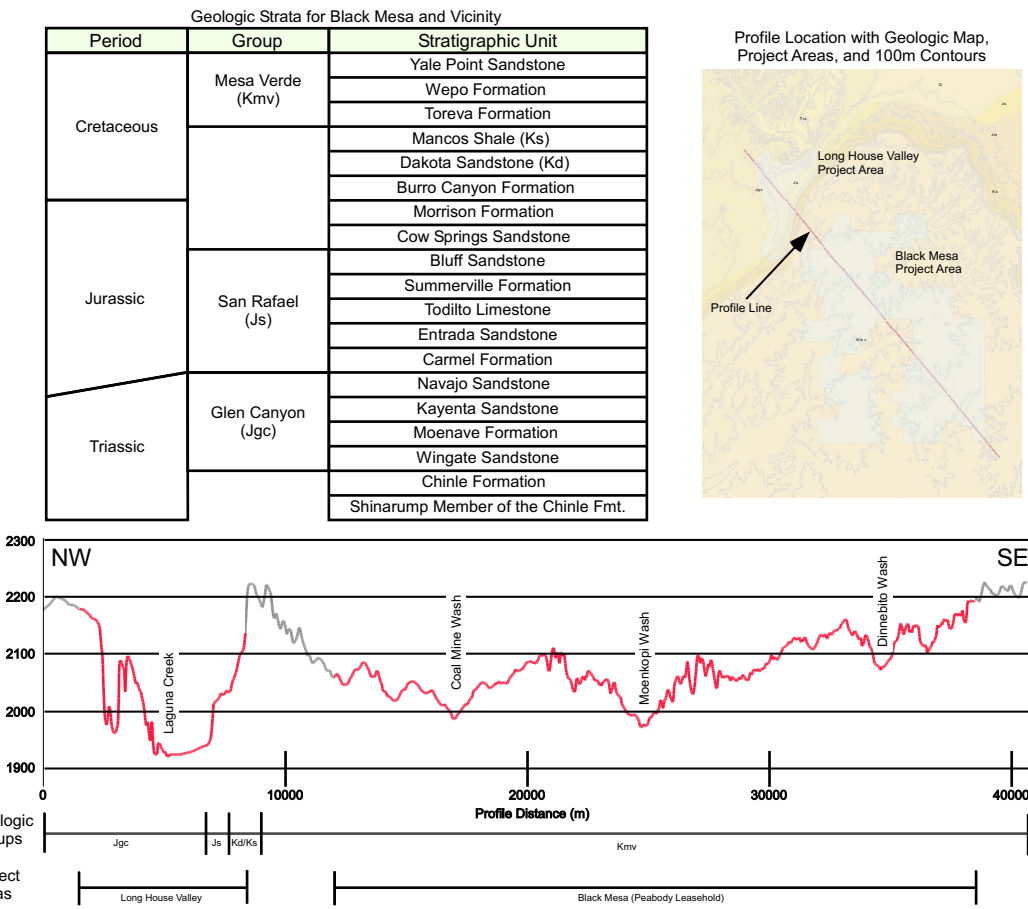


Figure 2.2: Geologic Formations Within and Surrounding the Project Area (see Figure 2.3 for explanation of symbols, Reynolds 1988)

Figure 2.3: Geologic Strata and Elevations Along a Profile Through the Long House Valley and Black Mesa Project Areas.(Green 1985:Fig. 4.2, 4.3; Reynolds 1988)



Glen Canyon Group

The Triassic/Jurassic age Glen Canyon Group consists of several formations, including the Kayenta, Wingate, and Navajo Sandstone formations (listed from oldest to youngest) (Beaumont and Dixon 1965:A7). Elements of the Kayenta and Wingate formations have been observed north of Marsh Pass and near Kayenta (profiles 8, 13, and 15 in Beaumont and Dixon 1965: Plate 2).

The Wingate Sandstone formation is known for its porosity and contribution to springs and seeps where it contacts the underlying Chinle formation (Gregory 1916:138). The Navajo sandstone formation dates to the Jurassic/Triassic boundary and is a light-orange to brown cross-bedded sandstone with lenticular cherty limestone deposits (Beaumont and Dixon 1965:A6; Green 1985:66). Erosion of this formation creates large sheltering overhangs (Green 1985:66), alcoves, bridges, windows (Gregory 1916:79), deeply incised drainages, and small to large basins that catch and hold water (Dean, et al. 1978:27). Due to the high porosity of this sandstone, there is little appreciable runoff during normal precipitation events (Gregory 1916:145). Hydrologically, the Navajo Sandstone formation acts as an efficient aquifer, absorbing large volumes of precipitation and providing source water for a number of springs and seeps located along the western edge of Long House Valley (Dean, et al. 1978:27; Gregory 1916:138), and producing artesian water flow in localities where the overlying strata are broken by faulting or excavated wells (Gregory 1916:131-132; McGavock and Levings 1974).

A review of the various assessments (i.e. Garrett 1986; Green 1985, 1986; Hill 1994; William J. Parry 1987) of local lithic raw material utilization and ceramic raw material procurement suggests that there are currently no known specific uses of lithic or ceramic raw materials from the Kayenta and Wingate formations, in spite of the fact that occasional outcrops of a red silty clay may be obtained from the Kayenta formation. (Geib and Callahan 1987:102). Green (1985:72-73; 1986:154) has noted the presence of variable quality cherts within the limestone deposits of the Navajo sandstone, with some identified sources possibly providing tool-quality raw materials. Parry (1987:29-30) argues that, with the exception the 'Starling Site', a known high-quality locality 8 km east of Kayenta, the quality of chert within the Navajo sandstone formation is so low as

to be "seldom an important source of raw materials for the Anasazi and that most of the archaeological specimens classified as 'Navajo chert' are materials derived from gravel deposits" (William J. Parry 1987:29).

San Rafael Group

The Jurassic age San Rafael Group consists of several formations including the Carmel, Entrada Sandstone, Todilto Limestone, Summerville, Bluff Sandstone, and Cow Springs formations (from oldest to youngest). Some members of the San Rafael group have limited exposure within and near the project area. In particular, the Carmel and Entrada Sandstone formations appear on southern Black Mesa (Beaumont and Dixon 1965:A8-A10; Wilson 1974:201), the Entrada Sandstone and Summerville formations appear near Kayenta (Beaumont and Dixon 1965:A9-A10), and the Cow Springs formation appears in a rounded cliff in Long House Valley (Beaumont and Dixon 1965:A11). The Todilto Limestone and Bluff Sandstone formations are not observed within or near the study area.

No prehistoric utilization of raw materials from these formations have been noted for the production of lithic tools (Green 1985, 1986; William J. Parry 1987) or ceramics (Garrett 1986; Hill 1994). Two instances of potential utilization, unrealized in the locally recovered archaeological materials, include Geib's (1987:102) observation that there are occasional outcrops of the Carmel formation that provide red-silty clay usable for ceramic production, and non-local use of cherts from the Carmel and Entrada formations for lithic tool production noted by Green (1985:72; 1986:153).

Morrison Formation

The Morrison Formation is the uppermost Jurassic age geologic unit and in northeastern Arizona consists of four members (in ascending order): Salt Wash, Recapture, Westwater Canyon, and Brushy Basin (Wilson 1974:203). Beaumont and Dixon (1965:A11-A12) identified three of the four members (excluding the Brushy Basin member) in their analysis area (extending well beyond the northern and northeastern escarpment of Black Mesa), while Green (Green 1985:71; 1986:153) notes only two members (the Westwater Canyon and Recapture members) in the immediate vicinity of the Black Mesa Archaeological

Project area, neither of which are known to provide lithic raw material (Green 1985:71; 1986:153).

The Brushy Basin member is known as a source for a silicified claystone (referred to as 'chert' by Parry, William J. Parry 1987) commonly used as a lithic raw material that appears as a part of lithic assemblages throughout the four-corners region, including a small number of specimens discovered on Black Mesa (Green 1985:71; 1986:153). There may be an exposure of the Brushy Basin member (and therefore the silicified claystone lithic material) along the northeastern escarpment of Black Mesa (Harshbarger, et al. 1957), but the specific location was not verified by Beaumont and Dixon (1965:A12) or Green (1985:71; 1986:153). Local members of the Morrison formation are not known to have provided materials used in the manufacture of ceramics (Garrett 1986; Hill 1994). Slightly more distant from the project area, the Chilchinbito locality of the Morrison formation is known to yield high quality clays (Geib and Callahan 1987:101-102).

Burro Canyon Formation

The Burro Canyon formation is the earliest of the Cretaceous period geologic strata consisting primarily of sandstones similar to those belonging to the underlying Morrison formation, and is presented here only for completeness, since it has completely eroded away within the study area and therefore is not evident in any discussions of local geology (Baars 1983:190-191). The absence of Burro Canyon formation strata within the study area precludes any contribution to the local availability of raw materials for either lithic tool or ceramic production.

Dakota Sandstone

Within the study area, the Dakota Sandstone represents the earliest Cretaceous Period stratum and within "the Black Mesa basin, the Dakota overlies the Jurassic Cow Springs Sandstone in the south and west, and the Morrison formation to the north and east." (Wilson 1974:204). This stratum is the first of the substantially exposed Cretaceous Period strata that provide the foundation and constituent rocks for Black Mesa.

In the four-corners region this stratum is known for containing small chert cobbles that are associated with lithic tools found at Mesa Verde and occasionally at Black Mesa,

but the local manifestation of this stratum appears to yield cobbles of insufficient size to be useful for lithic tool production (Green 1985:71; 1986:153). This stratum appears to have not contributed clays or temper materials to ceramic production on Black Mesa (Garrett 1986; Hill 1994).

Mancos Shale

The Mancos Shale formation grades into the underlying Dakota Sandstone and overlying Mesa Verde Group (Beaumont and Dixon 1965:A14-A15; Wilson 1974:205) and ranges in thickness from 145 m at the southern end of Black Mesa to over 215 m along Black Mesa's northern escarpment (Wilson 1974:205). In spite of the fact that Mancos Shale in the Mesa Verde region is known for providing silicified siltstone material appropriate for producing stone tools, the local Mancos Shale sediments are not known to yield raw materials useful for producing stone tools (Green 1985:71; 1986:152). The Mancos Shale formation is known for providing clay-bearing sediments accessible along the flanks of Black Mesa (Geib and Callahan 1987:102; Hill 1994:37).

Mesa Verde Group

The Mesa Verde Group includes three formations, all of which are exposed in Black Mesa's escarpment, providing surface rock for the upland areas of Black Mesa, or are exposed in the deeply incised drainages of Black Mesa. These formations are, in ascending order, the Toreva, Wepo, and Yale Point formations (Beaumont and Dixon 1965; Wilson 1974).

Local raw materials derived from the Toreva formation include quartzite and vein quartz cobbles laying directly on top of the Toreva formation. Within the gravel deposit were also found pebbles of chert, though these are thought to be of insufficient size to be useful for stone tool production. A purple conglomerate sandstone, often used in groundstone manufacture, has been found in landslide deposits thought to originate in the Toreva formation (Green 1985:70-71; 1986:152). Both light-firing and red-firing clays are available in the Toreva formation (Geib and Callahan 1987:102-103; Hill 1994:37), as are the tempering materials observed within locally manufactured ceramics found on Black Mesa (Garrett 1986:137; Hill 1994:36).

The presence of coal beds within the Wepo formation contributes to the presence of the most frequently recovered lithic raw material on Black Mesa archaeological sites, white baked siltstone (William J. Parry 1987:Table 2-1). The relationship between coal and baked siltstone is a simple one of naturally occurring coal fires heating adjacent siltstone, creating a metamorphic stone suitable for use as a lithic raw material (William J. Parry 1987:25). Other lithic raw materials available within the Wepo formation include: coarse-grained petrified wood, siderite, and iron concretions (Green 1985:69-70; 1986:149-152; William J. Parry 1987:25-27). Like the Toreva formation below it, the Wepo formation also provides light-firing and red-firing clays (Geib and Callahan 1987:102-103; Hill 1994:37), in addition to tempering materials observed within locally manufactured ceramics (Garrett 1986:137; Hill 1994:36).

The Yale Point formation, unlike the other two members of the Mesa Verde group, is not known for the lithic or ceramic raw materials available from its strata. In particular, it is not known to have contributed raw materials for either locally produced stone tools or ceramics (Garrett 1986; Green 1985, 1986; Hill 1994; William J. Parry 1987).

Summary of Relevant Geological Information

The area within and surrounding the Long House Valley study area and the Black Mesa Leasehold presents a diversity of geologic formations important in shaping the landscape, collecting and providing water, and providing raw materials needed for the production of stone tools and ceramics. Of particular note are the hydrologic capabilities of the Navajo Sandstone formation, and the wealth of lithic and ceramic raw materials provided by the Mesa Verde Group exposed by the Black Mesa escarpment, surface, and drainages. While the foregoing discussion has emphasized the contribution that the geologic formations make to human activity, the following sections in this chapter build upon the geologic foundation by fleshing out other environmental characteristics critical for successful human use of the landscape.

2.1.2 Topography and Characterization

The shape of the land within and surrounding the project area has a direct effect upon localized conditions experienced by plant, animal, and human inhabitants of the area. It also aids in the application of landscape characterizations to regions beyond the analysis area (e.g. to the larger Kayenta Anasazi region, Colorado Plateau in general, or the greater Southwest).

Mountain meteorology is significantly influenced by four fundamental landscape characteristics: latitude, continentality, altitude/elevation, and topography (Barry 1992:18). Recent meteorological interpolation efforts (Glassy and Running 1994; Hungerford, et al. 1989; Kimball, et al. 1995; Running and Coughlan 1988; Running, et al. 1987; Thornton, et al. 1997) employ latitude, elevation, slope, and aspect in estimating temperature, humidity, and precipitation values for locations remote from observation stations for which minimum temperature, maximum temperature, and precipitation data are available (Thornton, et al. 1997:216). These interpolation methods integrate all four of the influential characteristics presented by Barry (1992:18): latitude, altitude, topography (as represented by slope and aspect), and continentality (as represented by the observed temperature ranges for individual stations, which if necessary, could be summarized as the annual range of mean monthly temperatures, Barry 1992:21). The following discussion presents the characteristics and their significance for the project area for latitude, elevation, slope, and aspect. These values are compared to value ranges derived from a 10m Digital Elevation Model (DEM) for the local area and a 3-arc second DEM for the Colorado Plateau.

Incident solar radiation is an important factor in local climate that is directly affected by the landscape characteristics presented above. Actual incident radiation may be calculated through the application of formulas (e.g. Oke 1978:Appendix A1) representing sun-earth geometry, solar geometry and atmosphere, slope geometry, and shape factors.

Sun-Earth Geometry: Sun-earth geometry defines the relationship between the sun and the earth in terms of the seasonally variable orientation of the earth to the sun. Variables important in characterizing Sun-Earth Geometry include: latitude of the location of interest, solar declination (the angle between the sun's rays and a plane crossing

the equatorial), solar zenith angle (the angle between the sun's rays and a line passing through the location of interest and the center of the earth), hour angle (the angle of rotation required to bring the longitude of interest directly in-line with the sun's rays), solar azimuth angle (the horizontal angle [measured clockwise from 0° to 360°] between true north and the sun position), and julian day (the number of the day of the year). Calculations using these variables yield an estimate of the solar radiation entering the top of the atmosphere in transit to the location of interest.

Solar Geometry and the Atmosphere: Solar geometry and atmospheric effects reduce (from the baseline radiation entering the top of the atmosphere) the radiation that actually strikes the earth's surface. The incidence angle for the sun's rays influences the atmospheric distance to the ground (path length), with increasing distance reducing the radiation striking the earth's surface. Likewise, atmospheric constituents including gasses, droplets, or particulates reduce vertical atmospheric transmissivity by scattering, reflecting, or absorbing solar radiation (Oke 1978:345).

Slope Geometry: Slope geometry describes the relationship between the orientation of the earth's surface and the incidence angle of the sun. Important variables in defining slope geometry include slope angle (the deviation of a slope from horizontal, expressed in degrees), and slope azimuth angle (also known as aspect, the orientation, in degrees clockwise from true north, of a downward slope). These variables interact with sun-earth geometry, solar-geometry, and transmissivity to yield estimates of solar radiation incident at ground level for locations not obstructed by objects or landforms (Oke 1978:346-348).

Shape Factors: Shape factors represent the shape of objects and the effects of shape upon the amount of solar radiation to which an object is exposed. Shape factors also represent the influence of adjacent objects or landscape components (e.g. trees and other vegetation, structures, adjacent hillslopes) on incoming radiation, primarily through shading. Both the shape of objects and their orientation to the sun affect the radiation contacting those objects and the radiation blocked by those objects (Oke 1978:346-348).

All of these factors combine to determine the amount of solar radiation impinging upon a specific point on the landscape. In the context of the meteorological interpolation approach employed here, incoming solar radiation is critical in estimating local temperature and humidity from regional averages. As outlined above, the meteorolog-

ical interpolation model developed by Thornton and others (Glassy and Running 1994; Hungerford, et al. 1989; Kimball, et al. 1995; Running and Coughlan 1988; Running, et al. 1987; 1997) embodies these characteristics, and depends upon reasonable estimates for specific parameters for the project area. These parameters include latitude, elevation, slope, aspect, and climatic attributes calculated from these values. The following discussion outlines the specific climatic influences of these attributes and their general characteristics within the project area and the surrounding Colorado Plateau.

Latitude

Latitude influences local climate directly and indirectly in three ways. First, solar radiation, and temperature are closely related to latitude, with higher latitude areas receiving less solar radiation and exhibiting lower temperatures when compared to similar locales at more equatorial locations. Second, higher latitudes exhibit greater seasonal variation in temperature than is observed at equatorial locations. Finally, latitude influences dominant airflow characteristics, which in turn impacts precipitation patterns and amounts (Barry 1992:18-19).

Though the latitude range represented by the project area is insignificant, the larger latitude range for local instrumental meteorological data increases the likelihood of latitudinal variation in climate. Specifically, the latitude range for the project area is from 36.39°N to 36.65°N, a range of only 0.26° of latitude. In comparison, the latitude range for the entire Colorado Plateau is 7.69°, ranging from 33.15°N to 40.84°N. Though representing only a small portion of the latitudinal range of the Colorado Plateau, the project area is located near the midpoint of the latitudinal range for the Plateau, facilitating extrapolation of climatic interpretations from the study area to other parts of the Colorado Plateau. For comparison, Figure 2.4 illustrates the latitude range for both the project area and the Colorado Plateau.

Elevation

Elevation plays a critical role in several aspects of local climate, including air pressure and density, vapor pressure, solar radiation, cloud cover, temperature, and wind patterns. The elevation range for the project area is from 1834 m to 2270 m (as calculated from a digital

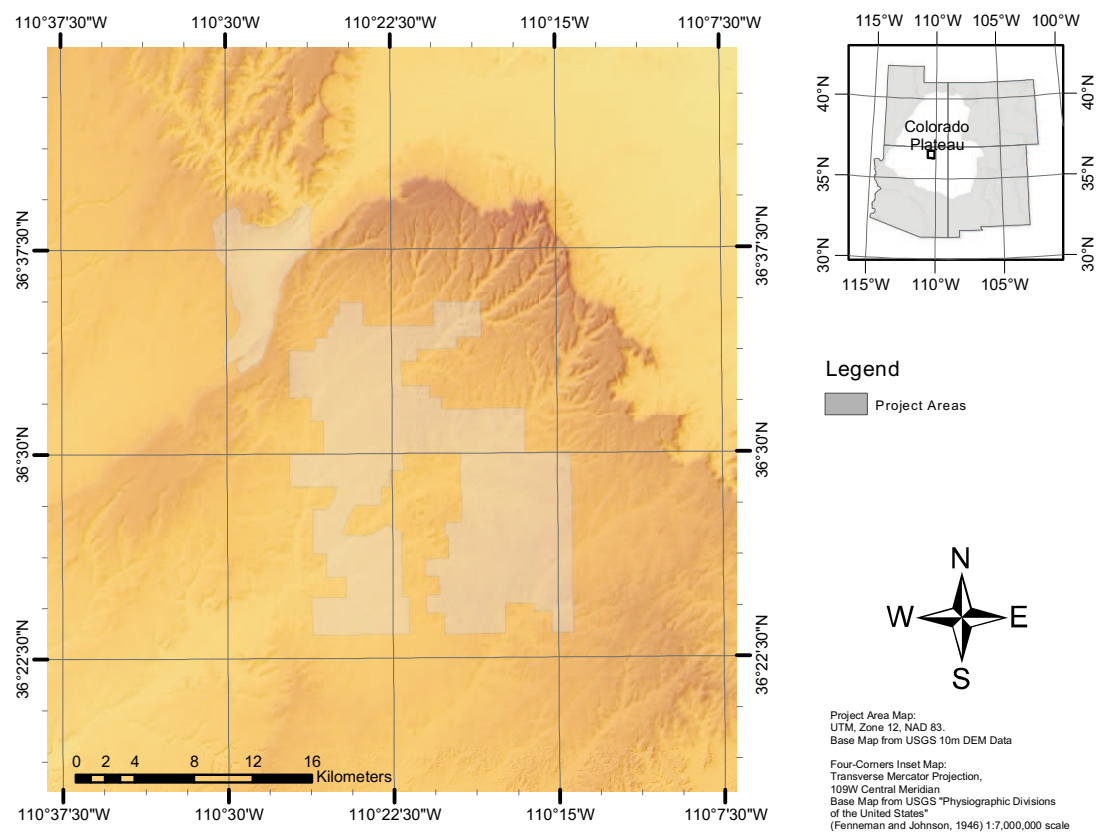


Figure 2.4: Latitude and Longitude Ranges for the Project Area and the Colorado Plateau

elevation model derived from the 10 m USGS DEMs overlapping the project area), with a mean of 2055 m. This elevation range represents 10.8 percent of the elevation range for the Colorado Plateau, which ranges from 293 m to 4023 m (as estimated from a digital elevation model derived from the 3-arc-second 1:250,000 USGS DEMs overlapping the four-corners states), with a mean elevation of 1949 m (Figure 2.5). The elevation range for the project area places it approximately in the middle of the full range for the Colorado Plateau as a whole, suggesting that elevationally derived environmental patterns observed within the project area may be extended to large regions of the Colorado Plateau.

Air pressure, density, and solar radiation are related through their dependence upon the thickness of the column of air above a given observation point. As elevation increases the thickness of the air column decreases, producing lower air pressure and density, and increasing the transmissivity of the atmosphere, yielding greater solar radiation energy values (Barry 1992:26-27, 29-41).

Temperature generally decreases with increasing elevation with the rate of decrease (the lapse rate, generally presented in $^{\circ}\text{C}/\text{km}$) varying both spatially and temporally. Theoretically, the rate of temperature change for a dry parcel of air, moving vertically through the atmosphere and exchanging no heat with the surrounding atmosphere, will be $9.8\text{ }^{\circ}\text{C}/\text{km}$ (Barry 1992:45; Oke 1978:51). This value, known as the dry adiabatic lapse rate (DALR), provides a point of reference for observed lapse rates under conditions other than those defined for dry adiabatic conditions. Terrestrial lapse rates observed in the Western United States illustrate departures from DALR conditions and tend to "decrease with decreasing latitude for a given altitude and decrease with decreasing altitude for a given latitude" (Wolfe 1992:1). This trend is illustrated in Figure 2.6, an interpolation (using an inverse squared distance weighting [IDW]) of observed annual terrestrial lapse rates calculated by Wolfe in his analysis for the western United States (1992). The variation observed in the small inset figure results from localized topographic variation (i.e. the deep canyon of the Colorado River), latitudinal variation, and elevational effects. These interpolated annual lapse rates over the project area range from $1.32\text{ }^{\circ}\text{C}/\text{km}$ to $1.69\text{ }^{\circ}\text{C}/\text{km}$. These rates represent 17.2% of the observed range for the entire Colorado Plateau, with lapse rates for the Colorado Plateau ranging from $-5.6\text{ }^{\circ}\text{C}/\text{km}$ to $3.89\text{ }^{\circ}\text{C}/\text{km}$, and having a mean lapse rate of $1.83\text{ }^{\circ}\text{C}/\text{km}$ ($\pm 1.08\text{ }^{\circ}\text{C}$). The position of the

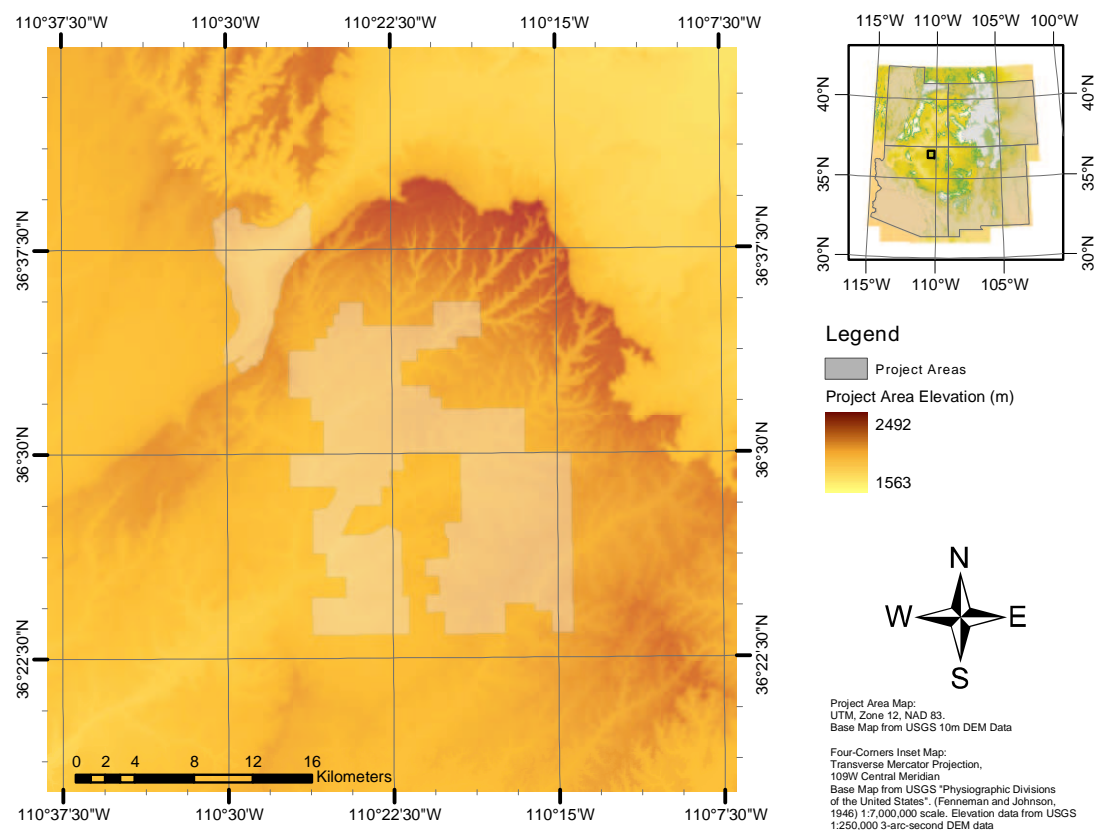


Figure 2.5: Elevation Values for the Project Area and Colorado Plateau

lapse rates for the project area within the ± 1 SD range for the Colorado Plateau suggests that lapse rate characteristics for the study area are not substantially different from those calculated for large portions of the Colorado Plateau.

Slope and Aspect

Slope, defined as the deviation of the ground surface from horizontal (Barry 1992:76; Oke 1978:171), and aspect, defined as downslope orientation of a slope (Barry 1992:76; Oke 1978:172), significantly influence the amount of solar radiation incident upon a given location through interaction with sun position at different times of day and different days of the year. Maximum solar radiation at a given location is achieved when the ground surface is perpendicular to the rays of sunlight incident upon that location. Deviations from perpendicular result in reduced solar radiation per unit area, as do conditions that reduce the transmissivity of the atmosphere (Oke 1978:342-346). Slope values within the project area range from 0° to 77.5° while slope values for the Colorado Plateau as a whole range from 0° to 74.2° (Figure 2.7). The upper value for these estimates differs because the larger pixel resolution of the digital elevation model for the Colorado Plateau (80 m per pixel) tends to smooth the differences between adjacent pixels when compared to the higher-resolution (10m) digital elevation model used for the project area. Overall, the range of slope values observed for the project area is similar to that observed for the Colorado Plateau as a whole. Aspect values for the project area cover the entire range from 0° to 360° , the same range observed for the Colorado Plateau as a whole (Figure 2.8).

Summary of Landscape Characteristics in the Context of the Colorado Plateau

The preceding discussion of landscape characteristics within the project area has emphasized the characteristics within the project area and their relationship with local climatic conditions. If the methods employed and results obtained in this analysis are to have broader applicability, a more detailed comparison of the values for these characteristics to candidate regions of interest is necessary. For comparative purposes, the Colorado Plateau is an appropriate larger-scale region to which the analysis procedures may be applied.

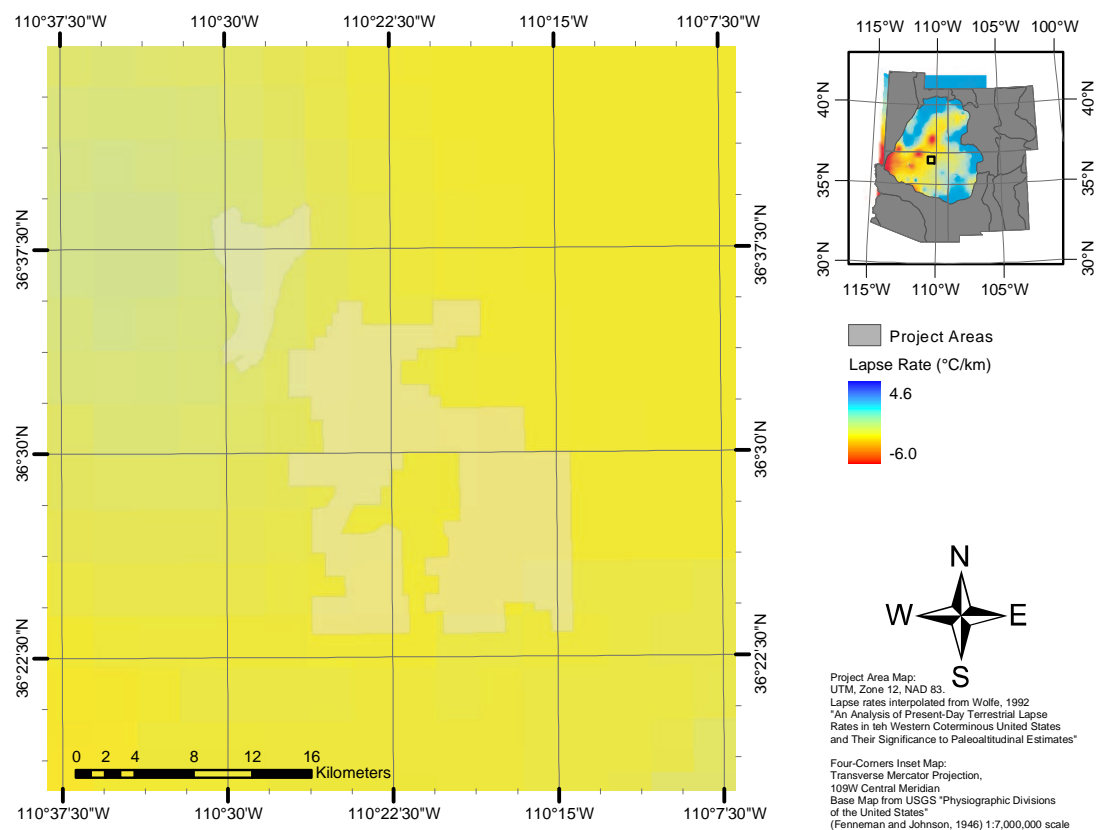


Figure 2.6: Interpolated Lapse Rates over the Project Area (from Wolfe 1992: Plate I)

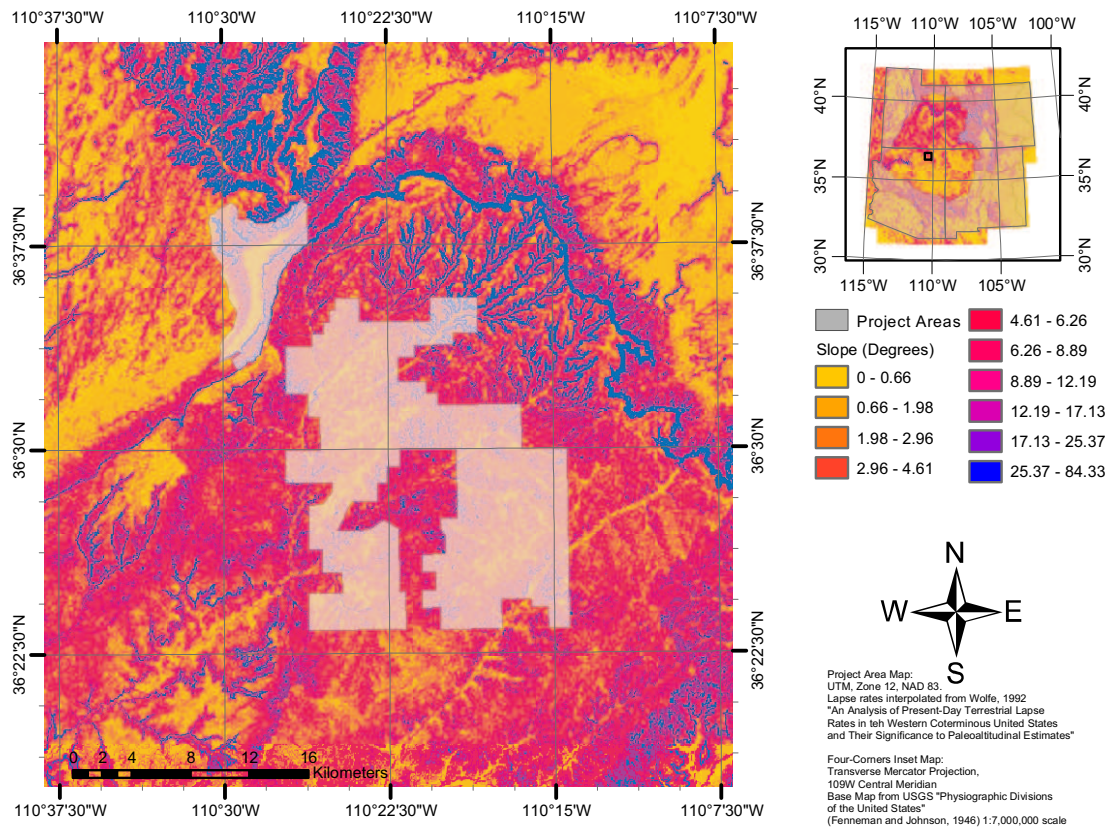


Figure 2.7: Slope ($^{\circ}$) for the Project Area and Colorado Plateau

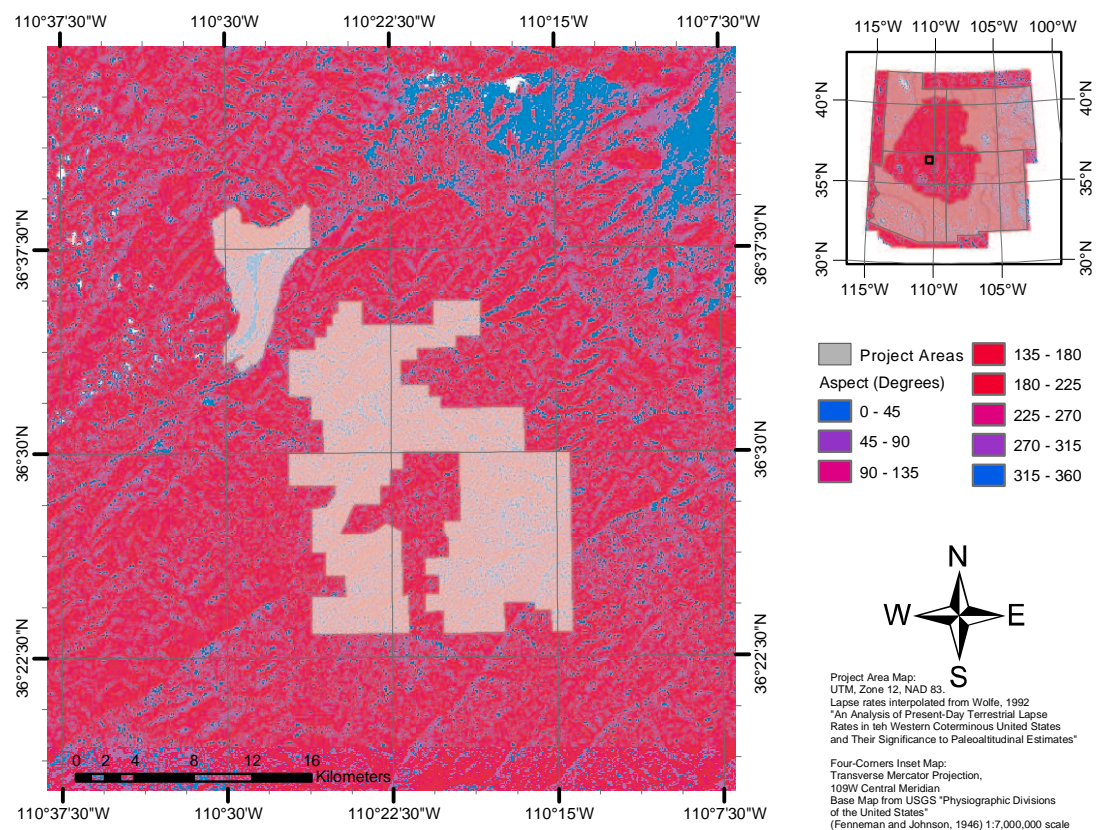


Figure 2.8: Aspect ($^{\circ}$) for the Project Area and the Colorado Plateau

In all landscape characteristic categories the project area falls well within the midrange of values for the Colorado Plateau (Figure 2.9) while also being significantly different from the Colorado Plateau as a whole (Kolmogorov-Smirnov, $p=0.000$ for all four comparisons [elevation, lapse-rate, slope, aspect] - Appendix B). Visual inspection of the percentage distributions in Figure 2.9 suggests slope and aspect values (Figure 2.9 d, and b respectively) for the study area cover the entire range of values for the Colorado Plateau, with the difference between the project area and the Colorado Plateau manifesting itself as differences in the distribution of slope and aspect values across the range of observed values. Elevation and lapse rate (Figure 2.9 a, and c respectively) values may be conceptualized as a subset of the full range of Colorado Plateau values, appropriately visualized through the identification of regions of the Colorado Plateau that have elevation and interpolated lapse-rate values that fall within the range represented by the study area.

These regions are depicted in Figure 2.10 and Figure 2.11.

The regions highlighted in Figures 2.10 and 2.11 represent a subset of the Colorado Plateau where the elevations and lapse-rates are comparable to those observed within the project area, suggesting that these areas are most closely related to the project area in terms of the climatic processes that are influenced by elevation and lapse rate - temperature in particular. The meteorological interpolation procedures outlined and employed in Chapter 5 have been validated over a variety of spatial, temporal, and physiographic domains (Glassy and Running 1994; Hungerford, et al. 1989; Running and Gower 1991; Running and Jr. 1993; Running, et al. 1987; Thornton, et al. 1997), making this analytic approach applicable to regions of the Colorado Plateau (and beyond) that do not match the range of values for the study area.

The values for slope, aspect, and elevation presented above form the foundation of the meteorological interpolation methods employed in estimating local climate conditions. While presented here for summary purposes, lapse rates for the analysis will be calculated from local temperature estimates when possible, with the interpolated values presented above being used only when locally calculated values are unavailable. In summary, landscape characteristics important in determining local climate vary both within the project area and across the larger Colorado Plateau, potentially contributing to localized variation in temperature, moisture, and incident solar radiation.

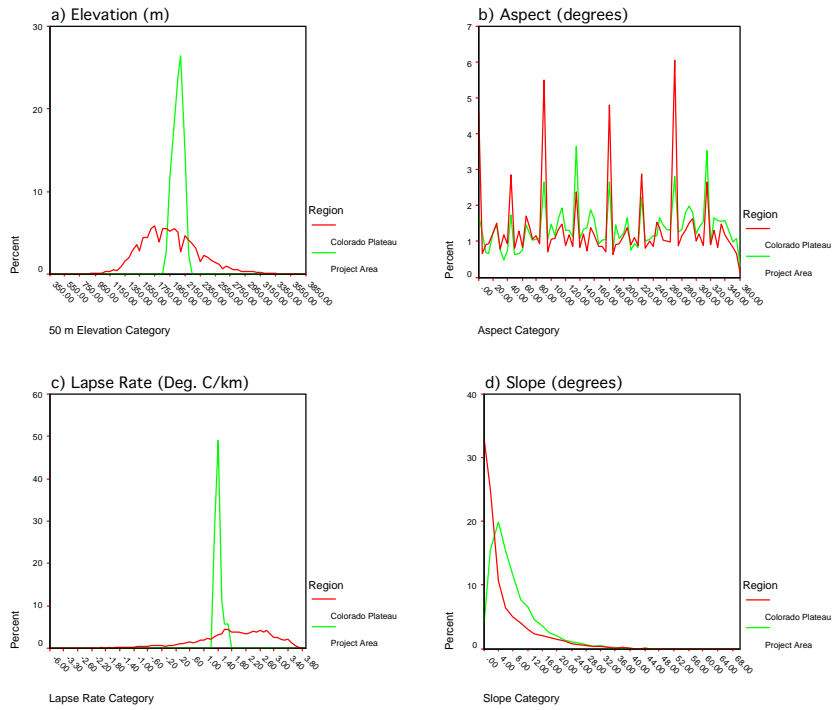


Figure 2.9: Percent-Distribution Values of Elevation (m), Aspect ($^{\circ}$), Lapse Rate ($^{\circ}\text{C}/\text{km}$), and Slope ($^{\circ}$) for the Colorado Plateau and Project Area

2.1.3 Soils

Detailed published soil maps for the study area are not available, but general soil data collected as part of the State Soil Geographic (STATSGO) Data Base are available for all of North America, including the project area. While these data were "designed to support regional, multistate, State, and river basin resource planning, management, and monitoring" (Schwarz and Alexander 1995), they describe general soil characteristics including soil thickness, available water holding capacity, clay and organic content, permeability, annual frequency of flooding, liquid limit, and other characteristics. While not reflecting localized soil variation associated with drainages passing through the study area, these characteristics provide a useful context for general comparisons between two subsets of the project area: Long House Valley and the northern portion of Black Mesa.

The contrast between northern Black Mesa and Long House Valley is fundamentally related to the thickness of the sediments, the sources of those sediments, and their associated hydrologic properties. While the sediments on northern Black Mesa tend to

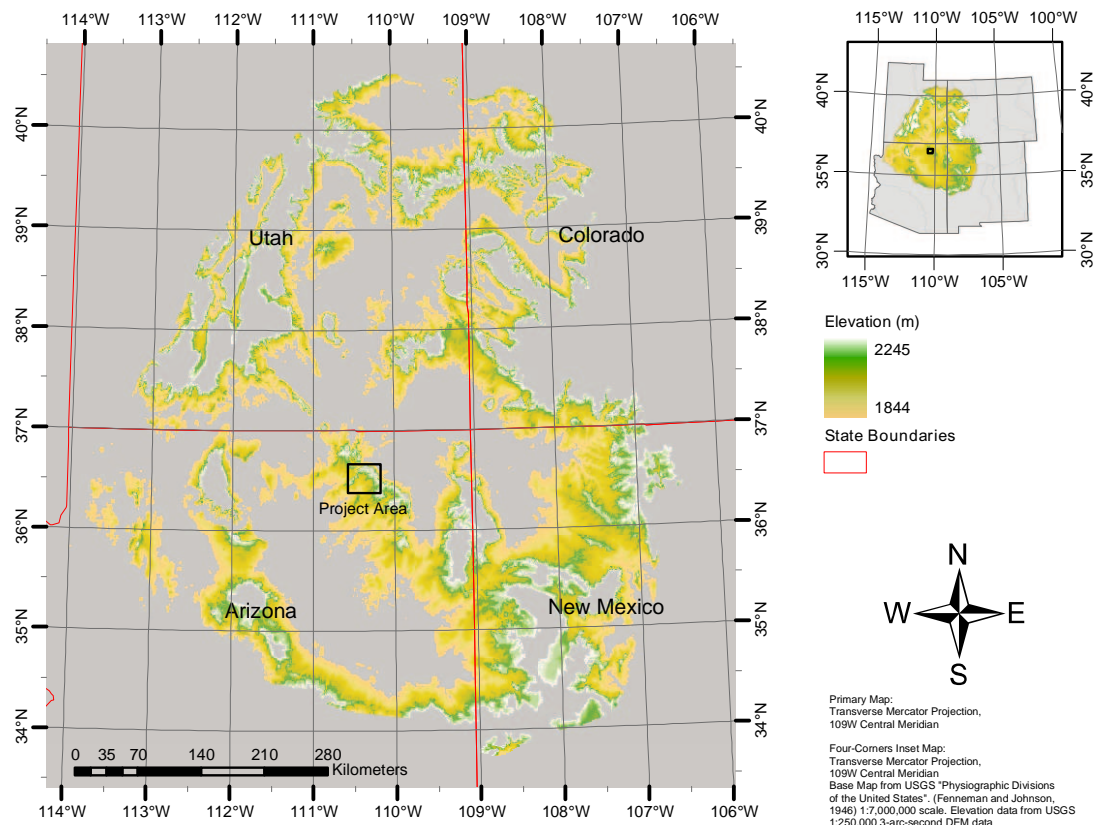


Figure 2.10: Colorado Plateau Regions with Elevation Values within the Range Represented by the Project Area

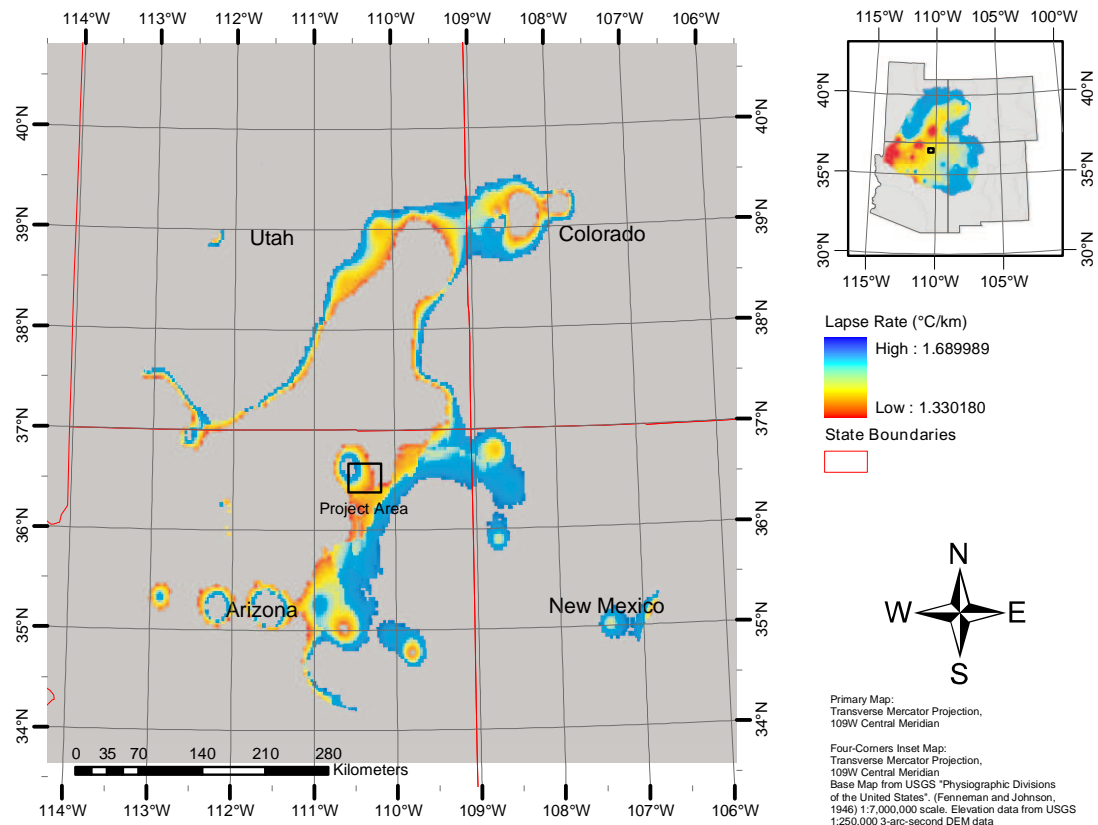


Figure 2.11: Colorado Plateau Regions with Lapse Rate Values within the Range Represented by the Project Area

range from 51 to 76 cm in depth, the sediments of Long House Valley (particularly in the western two-thirds of the valley) range from 102 to 178 cm in depth (Figure 2.12). Long House Valley sediments have a marginally higher Available Water Capacity (AWC, specified in inches of water per inch of sediment) than the sediments of northern Black Mesa, with most Long House Valley soils having AWC values of 0.09 in./in. while Black Mesa soils have an AWC of 0.07 (Figure 2.13).

Soil permeability also differs between the northern Black Mesa portion of the study area and the Long House Valley area. Soil permeability, measured in terms of inches of water absorbed into the soil column per hour, on northern Black Mesa averages 1.89 in./hr. for the entire Peabody Leasehold, while the average permeability for most of the Long House Valley is 4.54 in./hr., with extreme values of 0.1 in./hr. and 9.97 in./hr. at the extreme northern and southern ends of Long House Valley (Figure 2.14). This difference in permeability is a likely result of differences in the parent material contributing to the sediments in both areas. The clay content of sediments derived from the Mesa Verde formation strata that are exposed on Black Mesa is higher than for those derived from the Glen Canyon formation sandstone deposits west of Long House Valley. These differences are reflected in the clay content percentages mapped in the STATSGO Data Base, with the soils on and adjacent to Black Mesa having clay percentage values of 28.4%, greater than twice the value of 11% assigned to most of the Long House Valley area (Schwarz and Alexander 1995). These quantitative estimates are consistent with the observations made by Dean et al. (1978) in which they note that "Alluvium derived from Black Mesa is a dense black clay that is nearly impervious to water, while that derived from the Navajo sandstone is a light tan sand of high permeability and porosity." (1978:27).

All of the preceding soil characteristics contribute to a greater potential plant productivity for Long House Valley when compared to the adjacent upland Black Mesa area. This potential translates into higher soil organic content, measured as the percentage of organic material by weight in soil, in the Long House Valley areas when compared to Black Mesa. The average organic percentage for Black Mesa sediments is 0.2% while Long House Valley has an organic percentage 2.5 times greater than that for Black Mesa, 0.5% (Figure 2.15).

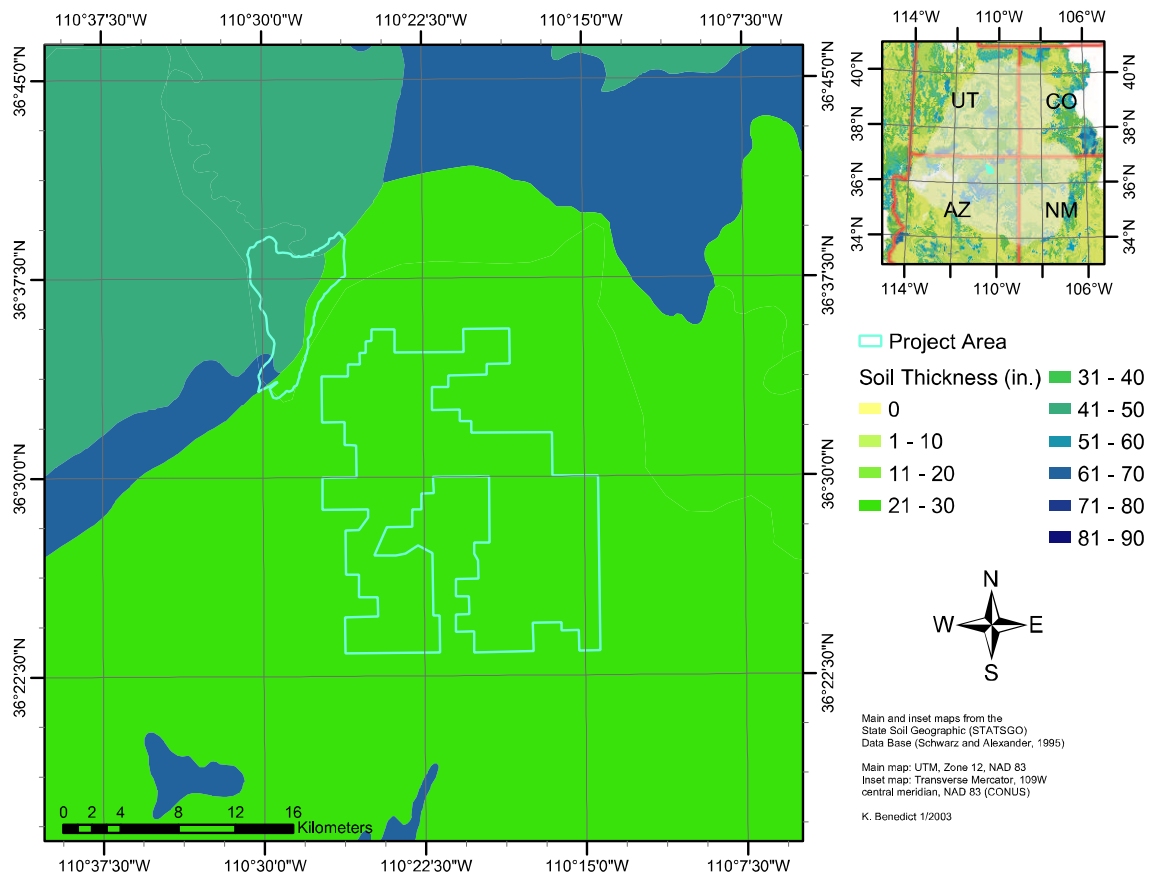


Figure 2.12: Soil Thickness (in.) for the Project Area and Surrounding Region (Schwarz and Alexander 1995)

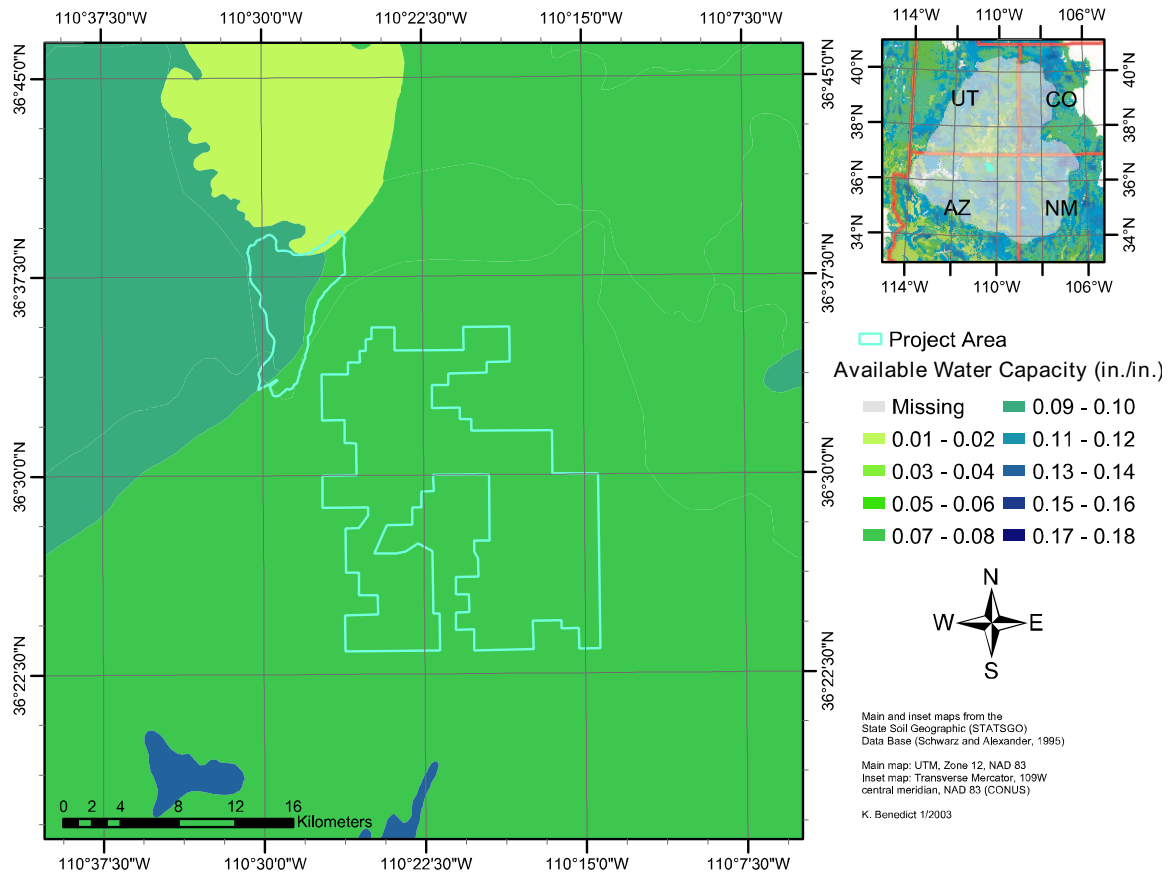


Figure 2.13: Available Water Capacity (in. of water per in. of soil) for the Project Area and Surrounding Region (Schwarz and Alexander 1995)

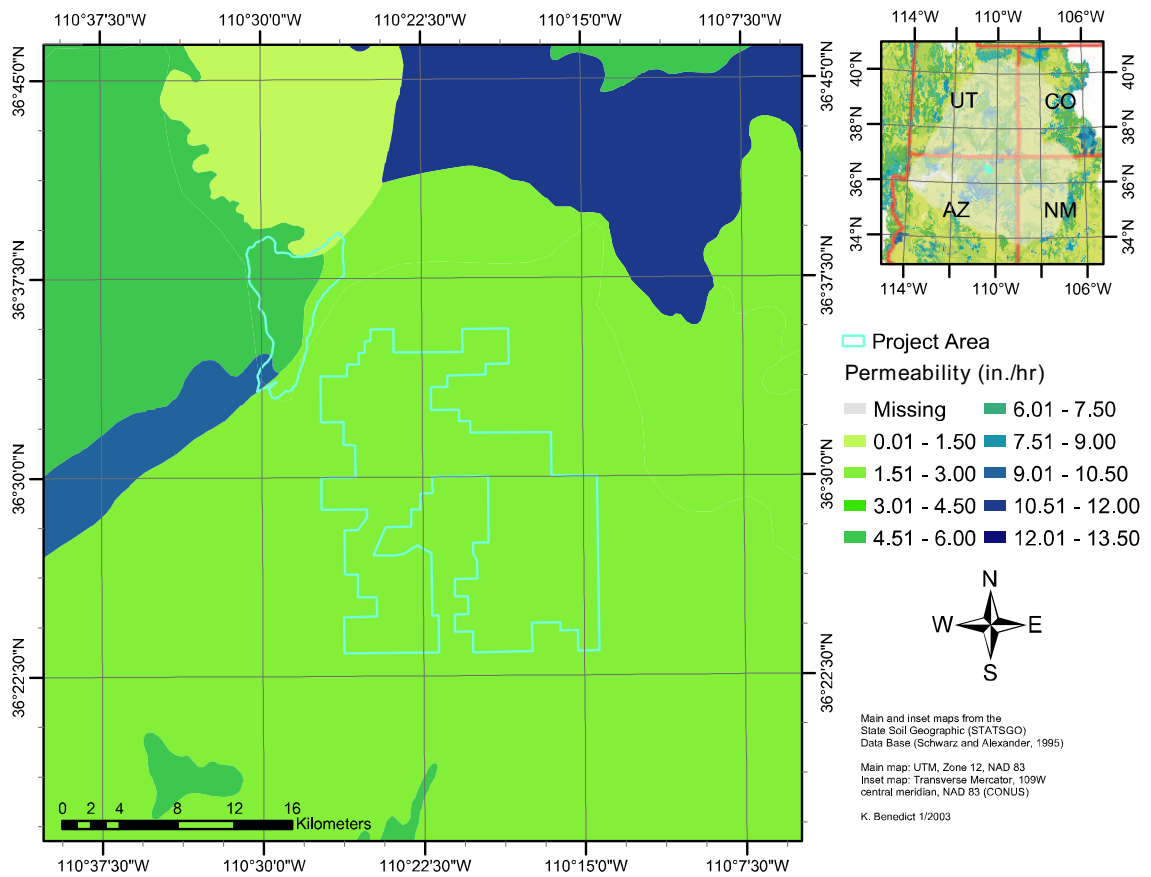


Figure 2.14: Soil Permeability (in inches per hour) for Soils Within and Surrounding the Project Area (Schwarz and Alexander 1995)

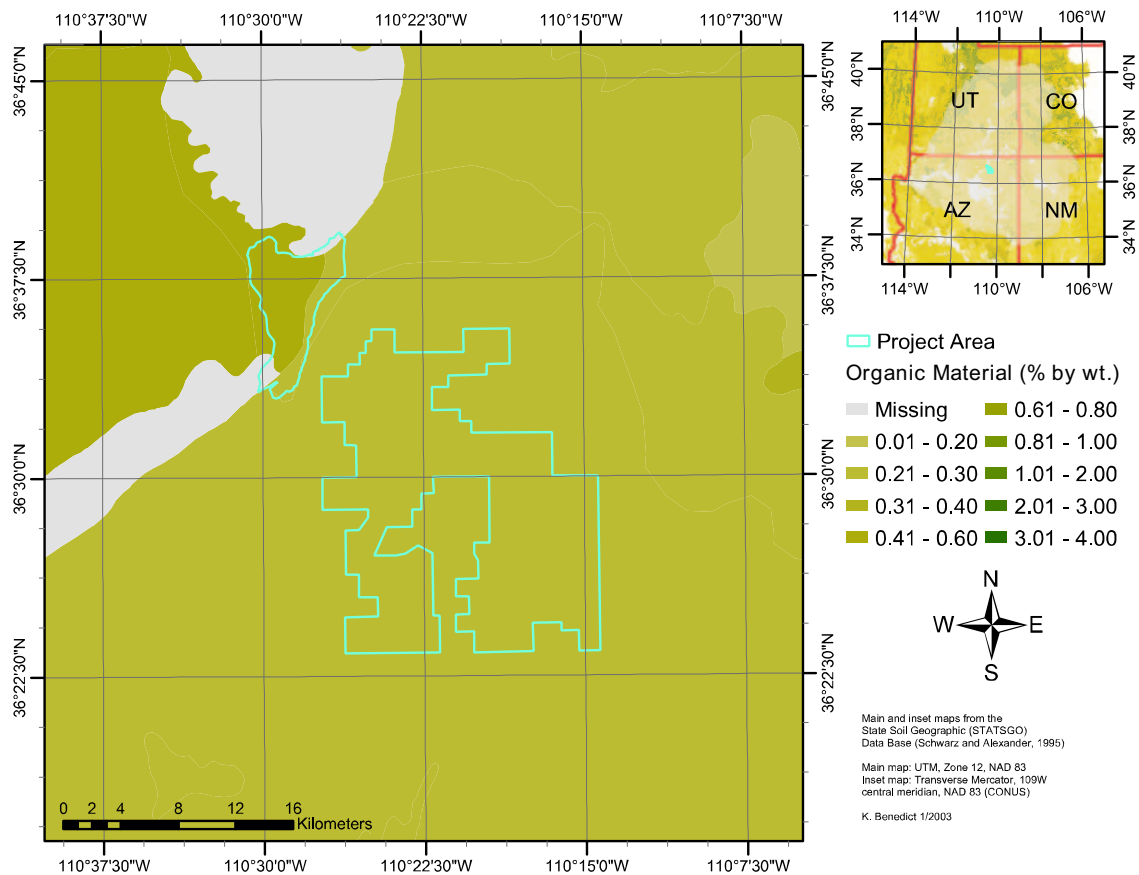


Figure 2.15: Organic Content (% by weight) of Soils Within and Surrounding the Project Area (Schwarz and Alexander 1995)

2.1.4 Hydrology

Surface hydrology for the study area consists primarily of water moving through the ephemeral drainage systems that dissect the Black Mesa portion of the project area, the ephemeral drainages that feed into Long House Valley from the west and northwest, and drain into perennial Laguna Creek at the north end of Long House Valley. These drainages, in combination with the springs and seeps found along the western edge of Long House Valley, soils in the bottom of drainages, dunes in Long House Valley, temporary catchment pools, and direct precipitation, provide the locally available moisture within the project area. The hydrologic characteristics of underlying geologic formations and overlying sediments have been discussed in previous sections, while this section provides a brief discussion of drainage patterns within the project area.

Four named drainages cross the project area: Laguna Creek at the north end of Long House Valley and Coal Mine, Moenkopi and Dinnebito Washes on Black Mesa. With the exception of Laguna Creek (Dean, et al. 1978:26), these drainages and their tributaries are ephemeral in nature, and flow only seasonally or during and following precipitation events. Water is absent from these drainages during much of the year (Espey Huston and Associates Inc. 1980: 3-13). As illustrated in Figure 2.16, the drainage network for the study area may be represented by a variety of data sources, two of which are used in the figure. The dark-blue lines represent USGS data for drainages in the area while the light-blue areas represent areas within the project area that drain more than $500,000\text{ m}^2$, as determined from the 10-meter digital elevation model for the project area.

The drainage network was derived from the mosaic of 10-m DEMs for the project area by first filling all sinks in the model, calculation of flow-direction for the entire model, and calculating flow-accumulation from the flow-direction data. These steps result in a model of water flow through the region that quantifies the number of 10-meter pixels contributing flow to each pixel in the model. The flow-accumulation model was then filtered to only retain pixels that have accumulated flow above 5000 pixels, or $500,000\text{ m}^2$.

The resulting flow-accumulation model provides a baseline for modeling water availability throughout the project area based upon assumptions about the timing and loca-

tion of precipitation over northern Black Mesa. Similarly, precipitation over the Shonto Plateau west of Long House Valley may be integrated into localized hydrologic models through use of the same flow-accumulation data represented in the figure.

2.2 Biotic Environment

The preceding section has outlined the abiotic characteristics of the study area to define the underlying landscape variables to which plants and animals must respond. This section summarizes the pertinent compositional and distributional characteristics for the plants and animals available within and around the study area. This discussion begins with a presentation of the general biotic communities that exist within and around the project area, then proceeds to summarize the identified plant associations within those communities. This section concludes with a presentation of animal distribution.

2.2.1 Plant Communities

The distribution of plant communities has been mapped at the 1:1,000,000 scale by Brown and Lowe (1994a), with this map providing the background distributional information presented in the inset map in Figure 2.17. The level of detail in this map is limited by its broad geographic scale, which includes portions of California, Nevada, Utah, Colorado, Texas, and Northwestern Mexico, and the entirety of Arizona and New Mexico.

The small scale of the Southwest Biotic Communities map resulted in the omission of "relict conifer sites and many small discontinuous outlier stands in all of the biomes" (Lowe and Brown 1994:16). Additionally, it also omitted "wetland formations, most of which are small in extent even when shown; generally, therefore, wetlands are not further differentiated on the map" (Lowe and Brown 1994:16). The plant and animal species identified with these biomes provide a baseline of information for the project area, with information from more detailed statewide and local vegetation documentation projects providing greater differentiation of community, series, and association (*sensu* Lowe and Brown 1994) distribution within the project area.

More detailed identification of vegetation and animal distributions for the state of Arizona was completed during the 1990s as part of the National Biological Survey's

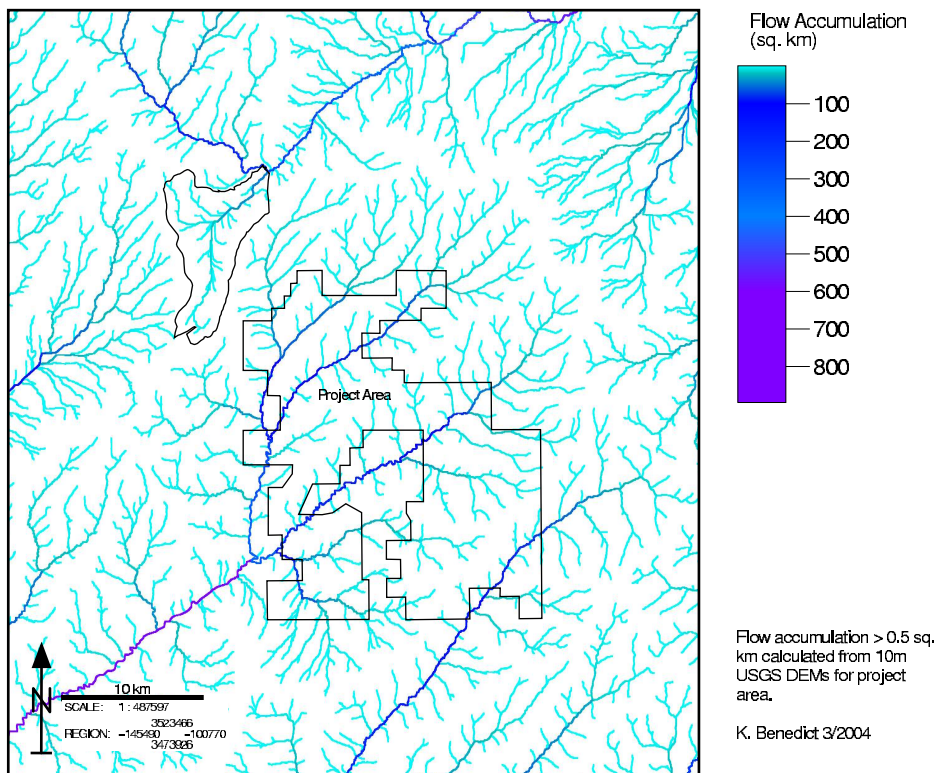


Figure 2.16: Drainage Networks Within and Surrounding the Project Area

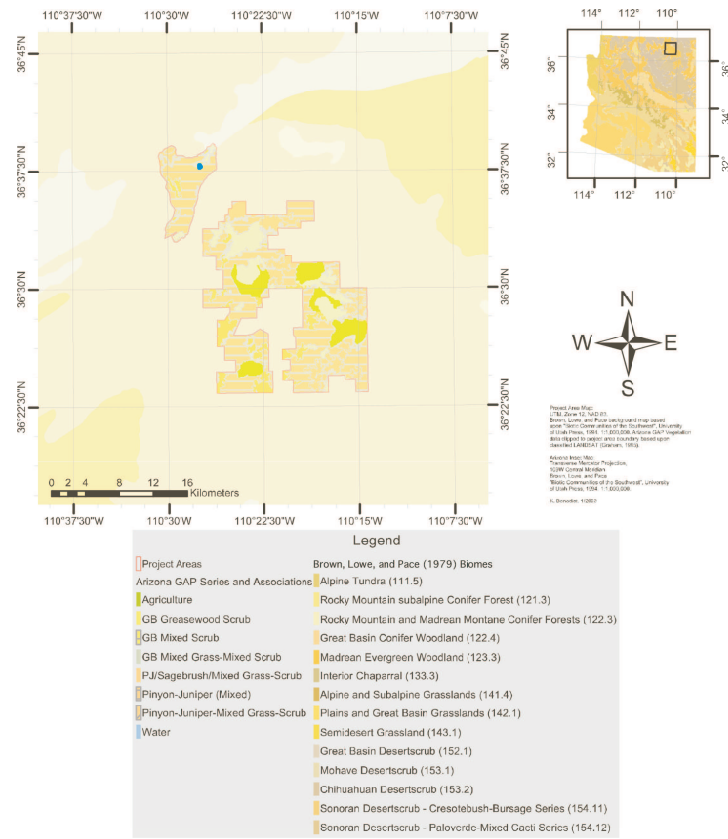


Figure 2.17: Vegetation Distribution Data - Biotic Communities for the State of Arizona and the Area Surrounding the Project Area, and GAP Vegetation Data for the Project Area

Arizona GAP Analysis Program (Graham 1995), resulting in a more detailed definition of biome, community, and plant association distributions. In contrast to the large mapped regions presented on the Southwest Biotic Communities map (median polygon area = 2950 ha), the Arizona GAP program produced a more detailed map of plant distribution, both in terms of spatial resolution (median polygon area = 4.86 ha) and community characterization (Figure 2.17, project area map).

The Arizona Gap Analysis Program employed 30m resolution LANDSAT Thematic Mapper imagery (collected primarily in 1991, with some imagery dating from 1990 and 1992) in the unsupervised classification of vegetation associations. These associations were then combined with GPS-referenced airborne video sample points to assign the satellite-derived polygons to the associations identified using videography. The resulting image was edited manually to resolve classification errors, and a polygon GIS coverage was generated (Graham 1995). A follow-up verification process was then undertaken in which randomly selected 1 ha plots were examined for dominant and co-dominant species (Thomas 1997). These identifications were compared with and contributed to corrections and revisions to the original GAP dataset, producing the final 1999 version of the GAP dataset employed in this analysis.

The plant association polygons produced by the GAP project are defined using a modified Brown, Lowe and Pase (1979) classification scheme. This classification scheme consists of a hierarchical numerical system in which the numeric values to the left of the decimal place represent natural ecosystems ranging in size (and generality) from Biogeographic (continental), through Vegetation, Formation Type, and Climatic Zone. To the right of the decimal point (in increasing levels of specificity and decreasing spatial extent) are Regional Formation (Biome - the level of detail mapped in Brown and Lowe 1994a), Series (community of generic dominants), Association (community of specific dominants - the level of detail mapped by the GAP vegetation project Graham 1995), and finally, Composition-structure-phase (D. E. Brown, et al. 1979).

The full hierarchy for the project area, starting at the Formation level and including biotic communities and association information, is presented in Table 2.1. This table presents the articulation between the more general classification provided in Brown (D. E. Brown 1994b) and the more specific classification provided by the Arizona GAP project.

Two levels within each hierarchy (a series of levels starting with a given formation) are of particular importance in this analysis. First, the lowest level from the Brown, Lowe, and Pase classification (1979), labelled BLP in Table 2.1, provides species composition data for each biotic community. Second, the lowest level(s) in the GAP classification, labeled GAP in Table 2.1, provide more detailed information about dominant and co-dominant species within subregions of the biotic communities mapped by Brown and Lowe (D. E. Brown and Lowe 1994a).

The biotic communities mapped as associations by the Arizona GAP project correspond with the national Gap Analysis Program's Community Alliance level of community mapping in which "Community Alliances are a uniform group of plant association that share one or more diagnostic species. The diagnostic species is primarily the dominant or co-dominant species of the uppermost vegetation canopy" (Jennings 1996:76). This level of detail in the definition of community composition and mapping allows the general species information provided in the broader biotic community specifications provided by Brown and Lowe (D. E. Brown and Lowe 1994a) to be enhanced with additional information about relative frequencies (i.e. dominance) of species, within the otherwise undifferentiated biotic communities.

The three biotic communities identified within the project area are Great Basin Conifer Woodland, Great Basin Desertsrub, and Plains Grassland. The species compositions for these communities are provided in Appendix C, with the following discussion providing a general overview of their characteristics, including a discussion of the GAP plant associations identified within the project area for each community.

Great Basin Conifer Woodland

The Great Basin Conifer Woodland is widely distributed throughout Colorado, Utah, Nevada, southeastern California, northern Baja California Norte, northern and central Arizona, New Mexico, and mountainous areas in Trans-pecos Texas at elevations ranging between 1,500 and 2,300 m. It often appears upslope of the Great Basin Desertsrub community in areas of thin, rocky soils. This community typically consists of a combination of juniper (*Juniperus* sp.) and pinyon (*Pinus edulis*) in an open woodland overstory with the understory typically including grasses (e.g. blue grama [*Bouteloua gracilis*], Indian rice-

Table 2.1: Biotic Community Hierarchy for the Project Area from Brown, Lowe, and Pase (Labeled as BLP in the left column, 1979) and the Arizona GAP Program (Labeled as GAP in the left column, Graham 1995)

BLP	1,120 Forest and Woodland Formation
	1,122 Cold Temperate Forests and Woodlands
	1,122.4 Great Basin Conifer Woodland!GAP
GAP	1,122.l0a0 Pinyon-Juniper
	—Pinyon-Juniper (Mixed)
	—Pinyon-Juniper-Mixed Grass-Scrub
	—Pinyon-Juniper/Sagebrush/Mixed Grass-Scrub
BLP	1,150 Desertland Formation
	1,152 Cold Temperate Desertlands
	1,152.1 Great Basin Desertsrub
GAP	1,152.l0a5 Mixed Scrub
	—Great Basin Mixed Scrub
	1,152.l0a6 Saltbush
	—Great Basin Greasewood Scrub
BLP	1,140 Grassland Formation
	1,142 Cold Temperate Grasslands
	1,142.1 Plains Grassland
GAP	1,142.j0a4 Shrub-Grass Disclimax
	—Great Basin Mixed Grass - Mixed Scrub

grass [*Oryzopsis hymenoides*], and western wheatgrass [*Agropyron smithii*]), shrubs (e.g. snakeweed [*Gutierrezia sarothrae*], cliffrose [*Cowania mexicana*], Mormon-tea [*Ephedra viridis*], sagebrush [*Artemisia* spp.], and fourwing saltbush [*Atriplex canescens*])), and a variety of cacti (e.g. prickly-pear [*Opuntia* spp.], and hedgehog [*Echinocereus* spp.]) (D. E. Brown 1994d).

The Arizona GAP project identified three associations of the Great Basin Conifer Woodlands within the project area: Pinyon-Juniper (mixed), Pinyon-Juniper-Mixed Grass-Scrub (PJGS), and Pinyon-Juniper / Sagebrush / Mixed Grass-Scrub (PJSGS, Graham 1995). Each association represents variation in the co-dominant species within the more generally defined biotic community. The species represented by the dominant and co-dominant associations within the GAP vegetation map are based upon the designations provided by Graham (1995) and the regional species lists for the Great Basin Conifer Woodland provided by Brown (1994d). The Pinyon-Juniper (mixed) association consists of a mixed community dominated by pinyon (*Pinus* spp., particularly *P. edulis* within the project area) and juniper (*Juniperus* spp., particularly *J. osteosperma* within the project area), with other species taking on a sub-dominant role. The PJGS and PJSGS associations represent vegetation communities with a greater number of co-dominant species. The Pinyon-Juniper-Mixed Grass-Scrub association adds mixed grasses and a variety of scrub species (examples of which are listed above and in greater detail in Appendix C) to the combination of pinyon and juniper species that are make up the dominant species of the Pinyon-Juniper (mixed) association. The Pinyon-Juniper/Sagebrush/Mixed Grass-Scrub extends the PJGS association further by adding sagebrush (*Artemisia* spp.) to the collection of co-dominant species for this community.

Great Basin Desertscrub

The Great Basin Desertscrub biotic community consists of a combination of warm- and cold-temperature vegetation and is widely distributed in regions north of 36° north latitude that range in elevation from 1,200 to 2,200 m and generally receive less than 250 mm of annual precipitation. This low diversity community is generally dominated by various sagebrush (*Artemisia*) or shadscale (*Atriplex confertifolia*) species, though occasionally (as is the case in the Great Basin Greaswood Scrub association found within the

project area) other woody species are found in association with these dominants. Most commonly these additional species are soft wood, aromatic, evergreen species such as blackbrush (*Coleogyne ramosissima*), winterfat (*Ceratoides lanata*), greasewood (*Sarcobatus vermiculatus*), and rabbitbrush (*Chrysothamnus* sp.). While few, the occasional cacti found within this community include cholla and prickly pears (*Opuntia* sp.), hedgehog cacti (*Echincereus* ssp.), and other small cacti. Grasses are occasionally found as a minority understory component in this community, but overall appear at very low frequencies when present. Grass species, when found, include gramas (*Bouteloua* spp.), galleta (*Hilaria jamesii*), desert needlegrass (*Stipa speciosa*), and Indian ricegrass (*Oryzopsis hymenoides*) (Turner 1994:141-148).

The Arizona GAP project identified two associations within the Great Basin Desertscrub community - Great Basin Mixed Scrub and Great Basin Greaswood Scrub. As with the general characteristics for the Great Basin Desertsrub, the Great Basin Mixed Scrub association consists of a combination of dominant scrub species consisting primarily of sagebrush (*Artemisia* spp.), but also including other shrub species such as fourwing saltbush (*Atriplex canescens*), Mormon tea (*Ephedra* spp.), and rabbitbrush (*Chrysothamnus* spp.). The Great Basin Greasewood association is defined as having greasewood (*Sarcobatus vermiculatus*) as the dominant shrub species, with a variety of subdominant species including fourwing saltbush (*Atriplex canescens*), fivehook bassia (*Bassia hyssopifolia*), inland saltgrass (*Distichlis spicata* var. *stricta*), and seepweeds (*Suaeda* spp.) (Graham 1995; Turner 1994).

Plains Grassland

The Plains Grassland biotic community, though much modified by grazing, generally consists of mixed- or short-grass communities within the project area. This community represents the Great Basin-affiliated grasslands found north and west of the project area that grade into the Plains grasslands encountered east of the project area. It gives way to woodland communities at its upper boundary, and Great Basin Desertsrub at its lower boundary. In general, this community tends to occur at elevations ranging from 1,200 m to 2,300 m in locations that are relatively dry (180-300 mm mean annual precipitation) and colder (mean annual growing season of 125-200 days) than other areas of the Plains

Grassland community (D. E. Brown 1994c:115-116). The Arizona GAP project identified a single association within the Plains Grassland community, the Great Basin Mixed Grass - Mixed Scrub association. This association is characterized by a combination of co-dominant species including a variety of perennial grasses and shrubs (D. E. Brown 1994c; Graham 1995). Specifically, grass species common in this association include a variety of grama grasses (*Bouteloua* spp.), buffalograss (*Buchloe dactyloides*), Indian rice grass (*Oryzopsis hymenoides*), galleta grass (*Hilaria jamesii*), prairie junegrass (*Koeleria cristata*), Plains lovegrass (*Eragrostis intermedia*), vine mesquite grass (*Panicum obtusum*), and alkali sacaton (*Sporobolus airoides*). Co-dominant shrub species present in this association include four-wing saltbush (*Atriplex canescens*), sagebrush (*Artemisia* spp.), winterfat (*Ceratoides lanata*), wild rose (*Rosa* spp.), cholla (*Opuntia* spp.), soapweed yucca (*Yucca glauca*), prairie sumac (*Rhus copallina* var. *lanceolata*), rabbitbrush (*Chrysothamnus* spp.), and snakeweed (*Gutierrezia* spp.) (D. E. Brown 1994c:117).

Land Use Categories Not Considered Under the Arizona GAP Project

The Arizona GAP project analyzed only those vegetation communities that could be assigned to the “naturally vegetated or scarcely vegetated” land use category (Jennings 1996:74). This approach differs from that employed by the contributors to Biotic Communities Southwestern United States and Northwestern Mexico (Biotic Communities, D. E. Brown 1994b). In *Biotic Communities*, the authors defined the boundaries of biotic communities based upon potential natural vegetation (Lowe and Brown 1994:13) while the Arizona GAP project followed the general classification criteria for the National GAP program - employing classification criteria that demonstrate “an ability to distinguish areas of different *actual dominant vegetation* at multiple scales” (emphasis added, Jennings 1996:73).

The difference between the two systems of community classification resulted in the identification of two land-use categories in the Arizona GAP project that did not correspond with the mapped biotic communities provided by Brown et. al. (D. E. Brown 1994b). These land-use categories were water and agriculture. The mapped water regions are all less than 6 ha in area, making them smaller than the minimum mapping unit size of 15 ha found for the Southwest Biotic Communities map (D. E. Brown and

Lowe 1994a), as calculated from the minimum polygon size presented in the GIS coverage representing the communities created by the Arizona Game and Fish Department (D. E. Brown and Lowe 1994b).

Summary of Plant Community Attributes

In total, 162 separate plant community polygons were mapped by the Arizona GAP project for areas within the project area. These polygons represent six categories of plant association, one human-modified agricultural category, and a water category. The Pinyon-Juniper (mixed) association encompasses a majority (58.3%) of the study area, with the Agriculture, Great Basin - Mixed Grass - Mixed Scrub, Pinyon-Juniper/Sagebrush/Mixed Grass/Scrub, and Great Basin - Greasewood Scrub each representing roughly 7.5% to 11% of the project area. The remaining three mapped habitats (Great Basin - Mixed Scrub, Pinyon-Juniper-Mixed Grass-Scrub, and Water) total less than 3% of the project area. These data are summarized in Table 2.2 and Figure 2.18.

2.2.2 Animal Distribution

Animal species distribution data are commonly presented in two ways - either as species lists reflecting the presence of animal species within given areas (often biotic communities) or as summary statistics representing some measure of biodiversity such as the number of species found within a given area (richness). The list-based approach provides important information about the presence of specific (economically or otherwise) important species while richness may be used as a proxy for the variety of ecological niches available within an area (Boughey 1973; J. H. Brown 1995). The species lists provided by Brown (1994a) for the three biotic communities identified within the project area provide a starting point from which a more refined list may be developed using additional resources such as the vertebrate survey performed by Espey, Huston, and Associates (1980) for the Peabody Leasehold and adjacent areas, and the vertebrate habitat and species richness models developed as part of the Arizona GAP project (Graham 1995; McCarthy, et al. 1998). Reference to these four sources of mammalian distribution data indicate that 93 different mammalian species (Table 2.3) inhabit biotic communities similar to those

Table 2.2: Total, Percentage, Minimum, and Maximum Polygon Area, and Number of Polygons for Each Habitat Type Identified by the Arizona GAP Project

Habitat Type	Polygon Area (m ²)				
	Sum	Percentage	Minimum	Maximum	N
Agriculture	33,223,074	10.9%	8,100	10,024,241	7
Great Basin - Greasewood Scrub	22,388,702	7.4%	3,002	4,996,598	27
Great Basin - Mixed Grass - Mixed Scrub	32,997,477	10.9%	3,052	10,740,331	19
Great Basin - Mixed Scrub	3,867,063	1.3%	83	934,784	8
Pinyon-Juniper-Mixed Grass-Scrub	3,856,056	1.3%	256	729,000	15
Pinyon-Juniper (mixed)	177,085,171	58.3%	175	46,907,826	38
Pinyon-Juniper / Sagebrush / Mixed Grass / Scrub	30,023,703	9.9%	190	4,225,463	36
Water	210,739	0.1%	1,419	56,704	12
Total	303,651,985				162

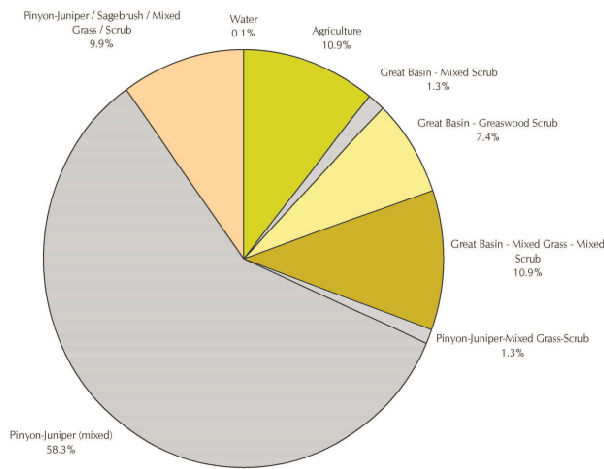


Figure 2.18: Proportional Distribution of Plant Associations Within the Project Area

found within the project area (D. E. Brown 1994a), are known to be present within the larger surrounding area (Leonard 1989), have been observed within the project area (Espey Huston and Associates Inc. 1980), or have specifically defined habitat boundaries that overlap the project area (Graham 1995; McCarthy, et al. 1998).

Table 2.3: Mammals Found Within or Near the Project Area

Scientific Name	Common Name	Scientific Name	Common Name
<i>Ammospermophilus leucurus</i> ^{βγδ}	White-tailed Squirrel	<i>Antilocapra americana</i> ^{αβδ}	Pronghorn
<i>Antrozous pallidus</i> ^{βδ}	Pallid Bat	<i>Neotoma mexicana</i> ^{βδ}	<i>Neotoma stephensi</i> ^{βγδ}
<i>Bassariscus astutus</i> ^{βδ}	Ring-tailed Cat	<i>Notiosorex crawfordi</i> ^δ	Desert Shrew
<i>Bison bison</i> ^α	Bison, Buffalo	<i>Nyctinomops macrotis</i> ^δ (<i>Tadarida macrotis</i> ^β)	Big Free-tailed Bat
<i>Canis latrans</i> ^{αβγ}	Coyote	<i>Odocoileus hemionus</i> ^{αβγδ}	Mule Deer
<i>Canis lupus</i> ^β	Gray Wolf	<i>Ondatra zibethicus</i> ^β	Muskrat
<i>Cervus elaphus</i> ^{αβ}	Elk, Wapiti	<i>Onychomys leucogaster</i> ^{βδ}	Northern Grasshopper Mouse
<i>Cynomys gunnisoni</i> ^{αβγδ}	Gunnison's Prairie Dog	<i>Ovis canadensis</i> ^{βδ}	Mountain Sheep
<i>Cynomys ludovicianus</i> ^α	Plains Prairie Dog	<i>Perognathus amplus</i> ^β	Arizona Pocket Mouse
<i>Dipodomys microps</i> ^α	Chisel-toothed Kangaroo Rat	<i>Perognathus apache</i> ^{βδ}	Apache Pocket Mouse
<i>Dipodomys ordii</i> ^{βαδ}	Ord's Kangaroo Rat	<i>Perognathus flavus</i> ^{βγδ}	Silky Pocket Mouse
<i>Eptesicus fuscus</i> ^{βδ}	Big Brown Bat	<i>Perognathus intermedius</i> ^β	Rock Pocket Mouse
<i>Erethizon dorsatum</i> ^{βδ}	Porcupine	<i>Perognathus parvus</i> ^α	Great Basin Pocket Mouse
<i>Euderma maculatum</i> ^{βδ}	Spotted Bat	<i>Peromyscus boylii</i> ^{βδ}	Brush Mouse
<i>Eutamias dorsalis</i> ^β	Cliff Chipmunk	<i>Peromyscus crinitus</i> ^{βδ}	Canyon Mouse
<i>Eutamias minimus</i> ^β	Least Chipmunk	<i>Peromyscus difficilis</i> ^β	Rock Mouse
<i>Eutamias quadrivittatus</i> ^{βγ}	Colorado Chipmunk	<i>Peromyscus leucopus</i> ^β	White-footed Mouse
<i>Felis concolor</i> ^{βδ}	Mountain Lion	<i>Peromyscus maniculatus</i> ^{βγδ}	Deer Mouse
<i>Geomys bursarius</i> ^α	Plains Pocket Gopher	<i>Peromyscus truei</i> ^{αβγδ}	Pinyon Deer Mouse
<i>Idionycteris phyllotis</i> ^δ	Allen's Big-eared Bat	<i>Pipistrellus hesperus</i> ^{βδ}	Western Pipistrelle
<i>Lagurus curtatus</i> ^α	Sagebrush Vole	<i>Plecotus townsendii</i> ^{βδ}	Townsend's Big-eared Bat
<i>Lasionycteris noctivagans</i> ^β	Silver-haired Bat	<i>Procyon lotor</i> ^β	Raccoon
<i>Lasiurus borealis</i> ^{βδ}	Red Bat	<i>Rattus norvegicus</i> ^δ (non-native)	Norway Rat (Brown Rat)
<i>Lasiurus cinereus</i> ^β	Hoary Bat	<i>Reithrodontomys megalotis</i> ^{βγδ}	Western Harvest Mouse
<i>Lepus californicus</i> ^{αβγδ}	Black-tailed Jackrabbit	<i>Reithrodontomys montanus</i> ^α	Plains Harvest Mouse
<i>Lutra canadensis</i> ^β	River Otter	<i>Sciurus aberti</i> ^β	Abert's Squirrel
		<i>Sorex merriami</i> ^α	Merriam's Shrew

continued on next page

Table 2.3: Mammals Found In the Plant Communities Within the Project Area, or Within and Around the Project Area (*continued*)

Scientific Name	Common Name	Scientific Name	Common Name
<i>Lynx rufus</i> ^{βγδ}	Bobcat	<i>Spermophilus lateralis</i> ^β	Colden-mantled Ground Squirrel
<i>Mephitis mephitis</i> ^{βδ}	Striped Skunk	<i>Spermophilus soma</i> ^{βδ}	spilo- Spotted Ground Squirrel
<i>Microdipodops megalcephalus</i> ^α	Dark Kangaroo Mouse	<i>Spermophilus townsendi</i> ^α	Townsend's Ground Squirrel
<i>Microdipodops pallidus</i> ^α	Pallid Kangaroo Mouse	<i>Spermophilus tridecemlineatus</i> ^α	Thirteen-lined Ground Squirrel
<i>Microtus longicaudus</i> ^β	Long-tailed Vole	<i>Spermophilus variegatus</i> ^δ	Rock Squirrel
<i>Microtus mexicanus</i> ^β	Mexican Vole	<i>Spilogale putorius</i> ^{βδ}	Spotted Skunk
<i>Mocrotis montanus</i> ^α	Montane Vole	<i>Sylvilagus audubonii</i> ^{βγδ}	Desert Cottontail
<i>Mus musculus</i> ^{βδ}	House Mouse	<i>Sylvilagus nuttallii</i> ^{βδ}	Nuttall's Cottontail
<i>Mustela nigripes</i> ^β	Black-footed Ferret	<i>Tadarida brasiliensis</i> ^{βδ}	Brazilian Free-tailed Bat
<i>Myotis californicus</i> ^{βδ}	California Myotis	<i>Tamias quadrivittatus</i> ^δ	Colorado Chipmonk
<i>Myotis evotis</i> ^{βδ}	Long-eared Myotis	<i>Tamiasciurus hudsonicus</i> ^β	Red Squirrel
<i>Myotis leibii</i> ^{βδ}	Small-footed Myotis	<i>Taxidea taxus</i> ^{βδ}	Badger
<i>Myotis thysanodes</i> ^δ	Fringed myotis	<i>Tayassu tajacu</i> ^δ	Collared Peccary
<i>Myotis velifer</i> ^β	Cave Myotis	<i>Thomomys bottae</i> ^{βγ}	Botta's Pocket Gopher
<i>Myotis volans</i> ^β	Long-legged Myotis	<i>Thomomys talpoides</i> ^β	Northern Pocket Gopher
<i>Myotis yumanensis</i> ^{βδ}	Yuma Myotis	<i>Urocyon cinereoargenteus</i> ^{βγδ}	Gray Fox
<i>Neotoma albigenula</i> ^{βγδ}	White-throated Woodrat	<i>Ursus americanus</i> ^β	Black Bear
<i>Neotoma cinerea</i> ^{βδ} (<i>arizonae</i> ^α)	Bushy-tailed Woodrat (Arizona Bushy-Tailed Woodrat)	<i>Vulpes velox</i> ^α	Swift Fox
<i>Vulpes vulpes</i> ^{βδ}	Red Fox		

^α(D. E. Brown and Lowe 1994a), ^β(Leonard 1989), ^γ(Espey Huston and Associates Inc. 1980), ^δ(McCarthy, et al. 1998)

The vertebrate species lists provided by Brown (1994a) yield the most general information about the species that are found in the biotic communities overlapping the project area. The vertebrate species lists provided in Appendix II of Brown (1994a: 316) list 22 distinct mammalian species (designated with a superscript-^α in Table 2.3) that are associated with the three biotic communities found within the project area. Of these 22 species, 14 are not listed in the other three more specific species lists for the region surrounding the project area or the project area itself. This fact suggests that while these species lists may be useful for representing general mammalian presence in the biotic communities throughout the southwest, they are insufficient for providing necessarily detailed lists used in local landscape resource characterization.

Though more detailed in terms of local composition, Leonard's mammalian species list (with species from this list designated with superscript- β in Table 2.3) is, for the most part, a general list, as it includes those species "whose geographic range includes northern Navajo County, Arizona" (Leonard 1989:8). The more specific information that it provides is through reference to 16 mammalian species that were documented within the project area by Espey, Huston and Associates (identified with a superscript-* in Table 2.3), though Leonard notes that:

It should be cautioned, however, that this modern census may not be fully reflective of prehistoric vertebrate populations. The researchers conducting the census believe that Black Mesa today exhibits less species diversity than would be expected. While the taxa present are expected given the semiarid setting, the individuals present are few. Investigators suggest that this phenomenon may be due, at least in part, to overgrazing of lands in historic times, particularly near homesteads. (Leonard 1989:7)

This skepticism regarding the observed diversity within the Black Mesa portion of the project area is supported by the mammalian habitat and species diversity models produced by the Arizona GAP project. Specifically, the Arizona GAP project identified 51 mammalian species habitats within and immediately surrounding the project area (identified with superscript- δ in Table 2.3) with local diversity categories ranging from fewer than 8 to between 36 and 42. Nearly 80 percent of the project area (24,259 ha, 79.9% of the project area) exhibits mammalian diversity values of 22 or more species (Figure 2.19, Graham 1995; McCarthy, et al. 1998).

The differences between these sources of animal distribution data for the project area highlight the hazards of applying a single line of evidence to the problem of characterizing the prehistoric distribution of animals. General sources, such as the species lists and associated mapped community polygons provided by Brown (1994a), provide a valuable context for examining the spatial distribution of important species across a large region such as the entire Southwest, but provide an inadequate level of detail when attempting to develop an environmental context for a localized analysis like this one. In contrast, localized lists of species like those provided by Leonard (1989) provide a more detailed picture of the species within and near the study area, but does not provide detailed spatial data needed to characterize variation in the distribution of species across the study area.

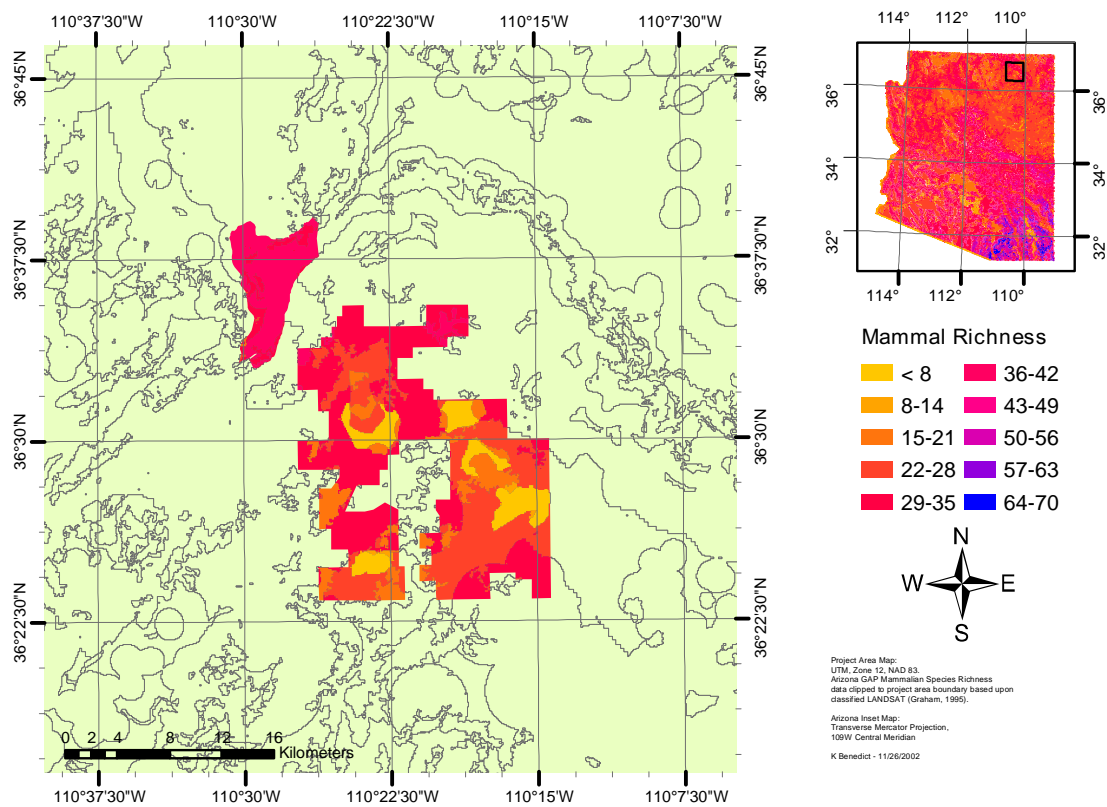


Figure 2.19: Mammalian Species Richness for the Project Area and Surrounding Region

The inventory performed by Espey, Huston and Associates (1980) provides a local analog to the regional biotic community species lists provided by Brown (D. E. Brown and Lowe 1994a). Specifically, mammalian and other vertebrates species lists are provided for vegetation community areas mapped within the Black Mesa project area (Espey Huston and Associates Inc. 1980: Exhibit 2-1, Sheets 1-6). This type of inventory differs from that provided as part of the Arizona GAP project by employing vegetation community boundaries as the defining boundaries for the distribution habitats for vertebrate species. It is this characteristic that suggests that the Arizona GAP Analysis vertebrate habitat models provide the most appropriate source of information regarding the potential distribution of species within the project area.

Characteristics of the Arizona Gap Analysis Vertebrate Habitat Models

While the Arizona GAP program used vegetation community boundaries as an input into the delineation of habitat boundaries for individual species, additional data sources and criteria contributed to the final habitat boundaries defined for the National GAP program. In particular, the National GAP Analysis Program employs two lines of evidence in generating the GIS representation of vertebrate habitat localities: "Predicted Presence in a Vegetation Cover Type" and "Predicted Presence in a Geographic Unit" (Csuti 1996:Figure 1). Separate bodies of data contribute to these two components in the determination of habitat boundaries.

Predicted presence of a given species within a specific vegetation cover type is based upon documented relationships between species and particular habitat characteristics including "elevation, soil type, temperature, rainfall, aspect, hydrologic networks, lakes, and wetlands" (Csuti 1996:136, 138-139) in addition to vegetation type and distribution. These relationships are generally derived from analyses and databases that include habitat characteristics and preferences for each species of interest. In general, the prediction of species presence from habitat characteristics depends upon abstract associations between habitat and locality, independent of whether or not the species has actually been observed within a given locality.

In contrast to the prediction of species presence within a given vegetation cover type, the prediction of the presence of a given species within a geographic unit depends upon

documented observations of that species. Typical data sources employed in the determination of geographic unit presence include existing mapped ranges, locality records from museum collections, literature, and other confirmed observations (Csuti 1996:136-138). These point and area data are then merged into generalized regional-scale geographic units that are classified into categories representing the likely presence or absence of a given species.

The final species distribution maps produced by projects working under the National GAP program are generated through intersecting the vegetation cover and geographic unit maps.

This overlay in a geographic information system starts with the predicted presence in a geographic unit, then filters out all polygons of vegetation types in that geographic unit that are inappropriate for that species... To prevent runaway extrapolation of species distributional areas, the species is predicted to be present only in vegetation polygons adjacent to geographic units in which the species is predicted to be present, not in all geographic units through which a polygon may pass (Csuti 1996:139).

The resulting species habitat GIS coverage represents a merging of knowledge about the types of habitats that individual species prefer and the observed distribution of that species within specified geographic regions (such as counties, townships, or other logical subdivisions of space).

Assessment of the accuracy of the resulting species habitat GIS maps entails several assumptions about the distribution of species within the mapped polygons and may be accomplished through several methods. Assumptions regarding the distribution of species within mapped habitat areas significantly influence the interpretation of observational assessment and expert evaluation of the identified habitat polygons. These assumptions include:

1. Species are assumed to occur within a polygon representing potential habitat but are not predicted to occur at any particular point within that polygon.
2. Species are assumed to be present within a polygon, but no assumptions are made about the abundance of the species in the polygon.

3. Species are assumed to be present in a polygon at least once in the last 10 years but need not be present every year in the last decade.
4. Species are assumed to be present during some portion of their life history, not necessarily during the entire year(Csuti and Crist n.d.:2).

Given these assumptions, three assessment methods (in addition to expert review of resulting habitat boundaries) are suggested for use by participants in the National GAP program: 1) comparison with species checklists, 2) comparison with species occurrence records, and 3) field surveys. Common to all three methods is a requirement that the data used in the accuracy assessment be independent of the data used to develop the habitat distribution maps. This may be accomplished in two ways. First, existing data may be withheld from the habitat definition process, or, second, new data may be collected and applied to the accuracy assessment (Csuti 1996; Csuti and Crist n.d.). To date, available accuracy assessments primarily employ the first and second methods using existing checklist and museum records (Csuti 1996; Csuti and Crist n.d.; Krohn 1996; McCarthy, et al. 1998), and in some cases, recently collected point data from forestry and utility projects (Csuti and Crist n.d.).

Vertebrate habitat model assessments accomplished under the National GAP program have yielded estimated omission and/or commission error rates for a variety of taxa, for each of several states. The vertebrate habitat mapping assessment performed as part of the Wyoming GAP project yielded mean omission error rates (the percentage of species that are on a given site list but not predicted by the GAP analysis) ranging from 3.40 to 16.37 percent for four groups of species: amphibians, birds, mammals, and reptiles. Mean commission error rates (the percentage of species that are predicted by a GAP Analysis but not included in the site list) for these groups ranged from 7.05 to 21.02 percent. Overall accuracy rates (the percentage of all species where the taxon appears in both the site list and the GAP Analysis) for these groups ranged from 74.60 to 80.71 percent, meaning that from just under 75 percent to over 80 percent of species observed were correctly included in the mapped habitat polygons (Merrill, et al. 1996: Table 3.5).

Vertebrate model assessments for Utah and Idaho yielded values similar to those obtained for the groups defined for the Wyoming GAP analysis. Specifically, omission

error rates for the Idaho GAP project range from 2.1 to 10.7 percent and from 1.9 to 16.1 percent for the Utah GAP project. Commission error rates for the Idaho and Utah GAP projects range from 11.6 to 42.9 percent and 7.5 to 14.5 percent, respectively (Edwards, et al. 1996:Table 1; Krohn 1996:Table 3). Overall accuracy rates for the Utah GAP project range from 69.42 to 90.63 percent (Edwards, et al. 1996:Table 1).

Thompson's (Thompson, et al. 1996) assessment of vertebrate species habitat maps from the New Mexico GAP project (cited in Csuti and Crist n.d.) found that overall habitat accuracy rates ranged from 53.8 to 77.1 percent for amphibians, reptiles and birds within the White Sands Missile Range, and 88.6 percent for birds in San Juan County (Csuti and Crist n.d.).

The least comprehensive, but most pertinent vertebrate habitat model assessment is the one performed as part of the Arizona GAP Analysis project. Though the final report for the Arizona GAP project has not yet been published, preliminary assessments of herpetofauna, mammals, and birds presented by McCarthy (McCarthy, et al. 1998) indicate omission error rates ranging from 0 to 7.7 percent for a portion of the Chiricahua Mountains for which museum datasets were available. Similarly, omission error rates of 6.7 and 12.1 percent were obtained for herpetofauna and mammals respectively (McCarthy, et al. 1998: Table 1).

The overall results of these systematic GAP vertebrate habitat mapping assessment activities indicate that, while variable, the overall accuracy rates for the integrated habitat maps are reasonable and present useful representations of the general range for each species. These results suggest that the habitat polygons generated by the Arizona GAP project provide an appropriate proxy for the distribution of economically important animal species prehistorically.

2.3 Climate and Weather

The animal and plant distribution data presented above only reflect one component of the environment of the project areas - the anticipated distribution of animal and plant species without reference to variation in their frequency or character through time and across space. Weather and climate contribute significantly to variation in plant community

health and productivity which in turn influences the local carrying capacity for animals, including humans.

This section provides a summary of historically documented meteorological conditions for a number of locations surrounding the project area. These historic data are important for two reasons. First, they provide a context for the characterization of general climatic condition for the region surrounding the project area. Second, they provide essential calibration data for two key modeling efforts undertaken as part of this project.

The first modeling effort entails the development and testing of local (i.e. project-area specific) meteorological interpolation methods that provide detailed temperature and precipitation values for locations for which direct meteorological data are not available. Once tested, these meteorological interpolation methods may be applied to the second modeling effort - the use of these models on analogous paleoclimate records for locations surrounding the project area.

While the details of the modeling procedures are presented in subsequent chapters, the purpose of the following discussion is to summarize the available historic data for the region surrounding the project area. This discussion will examine two aspects of the historic climate dataset - temporal and spatial variation.

2.3.1 Historic Climate Trends

Historic meteorological station data provide an important source of raw data from which local and regional climate trends may be determined. Two sources of information are available for these meteorological data: the data compilations for all National Weather Service Cooperative Station Network affiliates (NOAA 2002) available through the National Climate Data Center (<http://lwf.ncdc.noaa.gov/oa/ncdc.html>) and affiliated distribution centers (e.g. the Utah Climate Center [<http://climate.usu.edu>] and the Western Regional Climate Center [<http://www.wrcc.dri.edu/>]), and quality controlled and standardized long-term records compiled as part of the National Climate Data Center's U.S. Historical Climatology Network (<http://lwf.ncdc.noaa.gov/oa/climate/research/ushcn/-ushcn.html>, USHCN) (Easterling, et al. 1999). Electronic collections of data and documentation from both sources are available for download and use via the Internet.

Both data sources have strengths and weaknesses for use in characterizing the climatic characteristics within and surrounding the project area. The density of Cooperative Network Stations is much greater than that of the USHCN (Figure 2.20), with 396 Cooperative Network Stations located within 250 km of the project area, 44 Cooperative Network Stations located within 100 km of the project area (NOAA 2002), and only 18 USHCN stations within 250 km (Easterling, et al. 1999). Though lower in station density, the length of record and the follow-on quality control applied to stations used in the USHCN make these stations more useful for longer-term climate characterization and calibration of paleoclimate data. In reference to the temporal coverage for USHCN data, the significantly longer time of coverage for many USHCN stations when compared to Cooperative Network stations is illustrated in Figures 2.21 and 2.22. Overall, 228 Cooperative Network stations have temperature records and 217 Cooperative Network stations have precipitation records. Eighteen USHCN stations within a 250 km radius have both precipitation and temperature records. The mean record lengths for the precipitation and temperature from Cooperative Network stations are 22.4 ($s = 13.3$) and 25.1 ($s = 16.7$) years respectively (NOAA 2002), while the mean record lengths for the USHCN Stations are 75.3 ($s = 21.5$) and 75 ($s = 21.5$) years respectively (Easterling, et al. 1999). These summary statistics for record duration for the two collections of stations support the following observations that may be made from Figures 2.21 and 2.22:

- On average, the record length for the USHCN stations is roughly three times the length of the Cooperative Network Stations.
- For the USHCN stations, the lengths of records for precipitation and temperature are very similar.
- For the Cooperative Network stations, the length of the temperature record is longer for several stations, resulting in the longer average record length for the temperature records when compared to the precipitation records.
- The estimates of record lengths for the USHCN and Cooperative Network stations probably underestimate the actual length of record, since the datasets used in this analysis end in 1997 and 1999, respectively, in spite of the fact that data continue

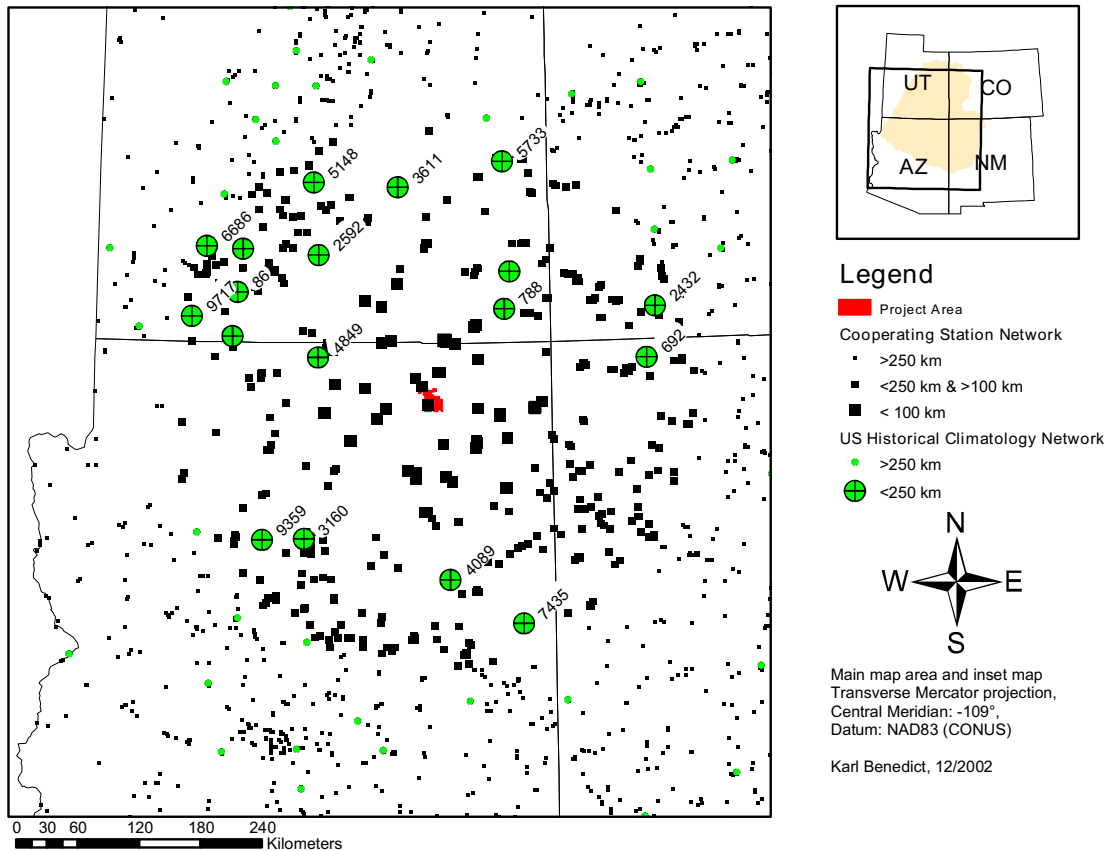


Figure 2.20: Distribution of NWS/NOAA Cooperative Network and U.S. Historical Climatology Network Station Locations

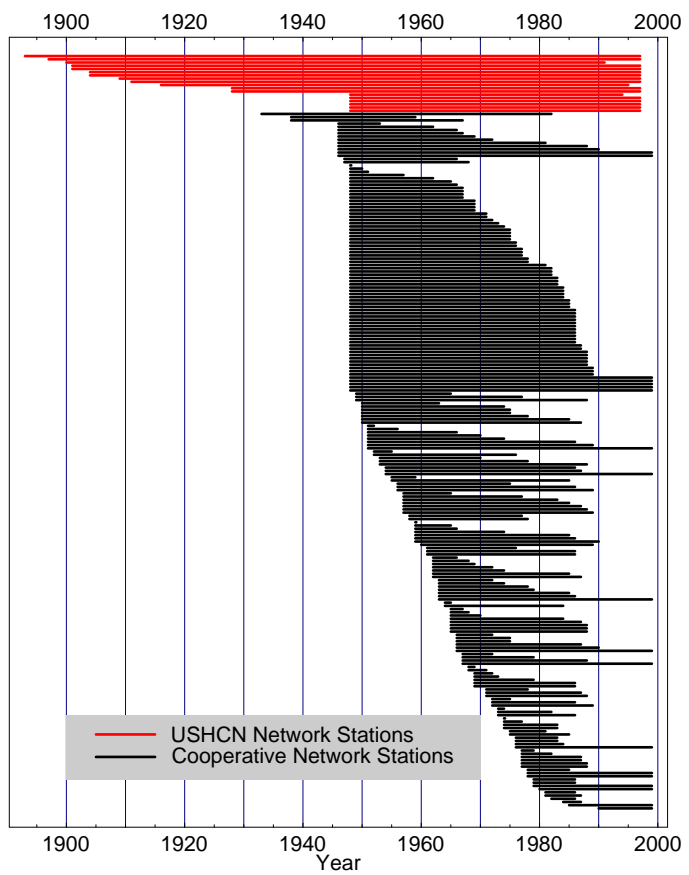


Figure 2.21: Year Ranges for Precipitation Records from Meteorological Stations Within 250 km of the Project Area

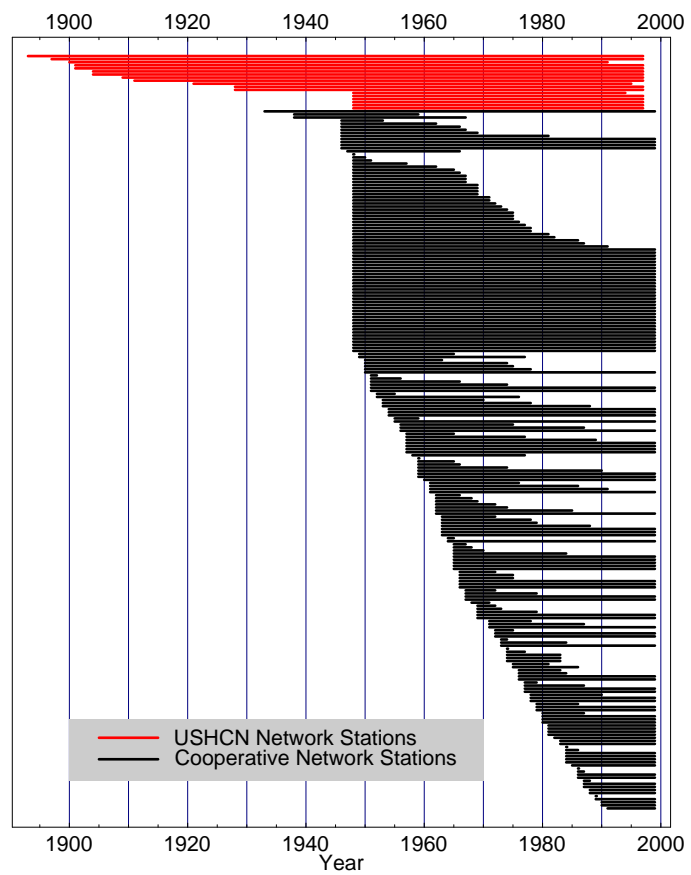


Figure 2.22: Year Ranges for Temperature Records from Meteorological Stations Within 250 km of the Project Area

to be collected at many of these record locations.

These record characteristics suggest that the two datasets may play complementary roles in the climate modeling activities employed in this analysis. Specifically, the USHCN station records provide needed data to develop a localized meteorological interpolation model that will provide meteorological estimates for use in calibrating dendroclimatic data and interpolating local conditions from those calibrated paleoclimate records. The numerous short-term records available from the Cooperative Network stations have the potential to provide independent observations against which the USHCN-derived interpolated meteorological data can be compared. The following discussions characterizing the temporal and spatial variation in the historic climate data are based upon the 18 long-term records of the USHCN (Easterling, et al. 1999) because these provide the most spatially and temporally stable record for the historic period

Temporal and Spatial Variation in Historic Climate Data

Descriptions of temporal and spatial variation in climatic data are typically presented in two forms: summaries of monthly observations (often based upon daily observations) from a long period of data collection, and longitudinal presentation of monthly or annual values over a long period of observation. Both methods of description are employed in the following summary of regional climatic conditions.

Spatial Variation. As noted by Dean (Dean 1988a: 122-126), precipitation patterns in the Southwest are largely determined by the flow of atmospheric moisture from the Gulf of Mexico and the Pacific Ocean. The movement of Northern Pacific frontal storms through the Southwest dominates the winter precipitation patterns over the entire region, producing greater precipitation in the western portion of the Southwest than in the eastern. Atmospheric moisture originating in the Gulf of Mexico and Pacific Ocean contributes to summertime convectional thunderstorms common in the southern Southwest (Dean 1988a:123). Additionally, hurricanes originating in low-pressure zones off the west coast of Mexico produce extremely high precipitation in the late Summer and Fall in some areas of the Southwest. These large-scale meteorological forces combine to produce precipitation patterns throughout the Four-Corners region that vary both from

Table 2.4: USHCN Stations Used in the Analysis

Station ID	Station Name	N Latitude	W Longitude	Elevation (m)
7435	SAINT JOHNS	34.52°	109.39°	1765
4089	HOLBROOK	34.91°	110.17°	1545
9359	WILLIAMS	35.26°	112.19°	2057
3160	FORT VALLEY	35.27°	111.74°	2239
692	AZTEC RUINS NATL MONUMENT	36.84°	108.00°	1720
4849	LEES FERRY	36.87°	111.60°	978
4508	KANAB	37.05°	112.54°	1509
9717	ZION NATIONAL PARK	37.22°	112.99°	1234
2432	DURANGO	37.29°	107.89°	2012
788	BLUFF	37.29°	109.55°	1315
86	ALTON	37.44°	112.49°	2146
738	BLANDING	37.62°	109.49°	1841
2592	ESCALANTE	37.77°	111.60°	1771
6601	PANGUITCH	37.82°	112.44°	2015
6686	PAROWAN POWER PLANT	37.84°	112.84°	1829
3611	HANKSVILLE	38.37°	110.72°	1313
5148	LOA	38.41°	111.66°	2155
5733	MOAB	38.59°	109.55°	1226

south to north and west to east. The localized manifestations of these combined forces are summarized in Figure 2.23. This figure depicts the monthly average precipitation for each of the 18 USHCN stations, with each plot located at the approximate location of the station relative to the project area. Each plot represents 12 monthly values ranging from January through December, with the vertical axis of each plot representing 3 inches of average monthly precipitation, with the USHCN station ID at the end of each vertical axis.

One feature common to all 18 stations is a period of relatively low average precipitation in the Spring. This is apparent in each of the plots in Figure 2.23 as a low point in the distribution just to the left of the plot midpoint. This portion of the plot corresponds with April, May, and June, and reflects the pan-Southwestern "Spring Drought" described by Dean (1988a:123). Winter precipitation exhibits marked spatial variation, with notable peaks in Winter precipitation being found in stations within the southwestern quadrant (with the exception of station 2432 in southwestern Colorado) of the region surrounding the project area. Other areas of the region display much lower Winter precipitation values, both in absolute terms and relative to the overall precipitation trend for each station. Peaks in Summer precipitation also exhibit spatial variation, but with different characteristics. Specifically, noticeable peaks in Summer precipitation are visible in the records for stations located within the southern two-thirds of the study region, with stations in the northern third exhibiting only minor increases in Summer precipitation relative to the remainder of the calendar year. These general trends in average monthly precipitation (which tend to underemphasize the occasional high-precipitation events associated with late-Summer and Fall hurricanes) yield the bi-modal precipitation patterns noted by Dean (1988a:123, Fig. 5.1) for most of Arizona and portions of New Mexico. On the other hand, stations north and east of the project area (again, with the exception of station 2432) tend to exhibit less definitive peaks in their distributions.

Spatial variation in observed mean monthly minimum and mean monthly maximum temperatures is less obvious from figures depicting the annual trends in these variables. Figure 2.24 depicts average minimum monthly temperatures for the 18 USHCN stations surrounding the project area, and shows no obvious trends other than higher average minimum temperatures for several stations along the western end of the Utah - Arizona

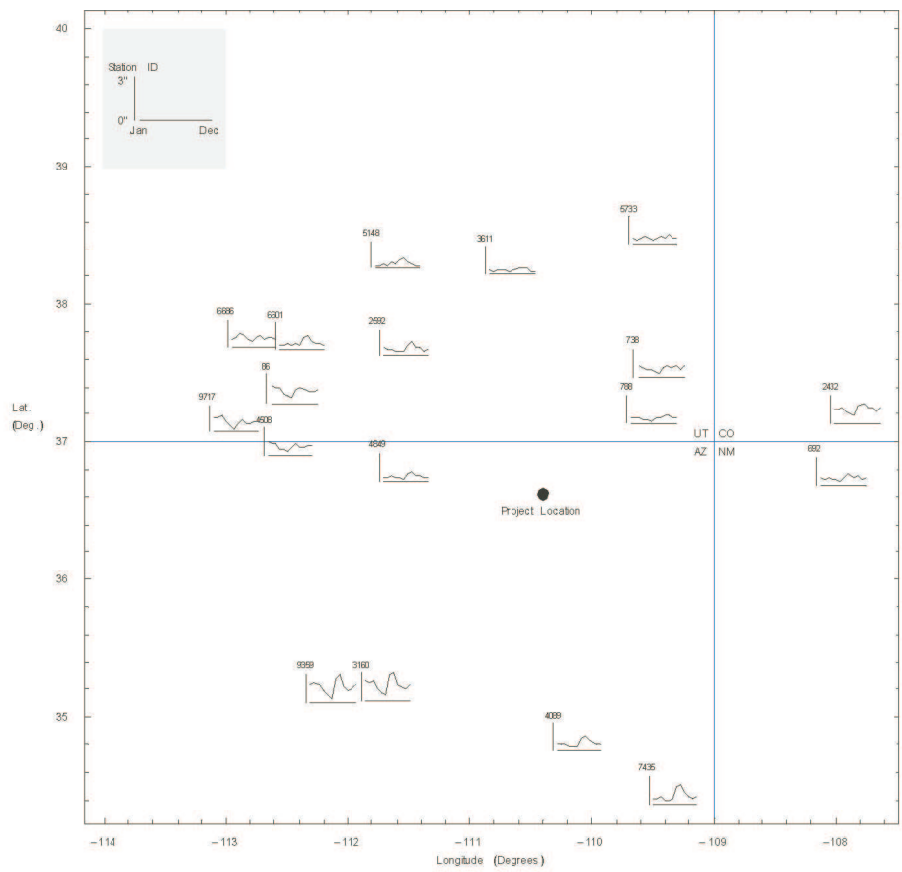


Figure 2.23: Average Monthly Precipitation Profiles for 18 USHCN Stations within 250 km of the Project Area (Easterling, et al. 1999)

border, and a general trend of decreasing minimum temperatures as latitude increases, particularly for the colder months of the year. Similarly, average monthly maximum temperature for the 18 USHCN stations, depicted in Figure 2.25, exhibit decreasing temperatures with increasing latitudes, again, particularly for the cooler months of the year, and higher average maximum temperatures for the three western stations along the Utah - Arizona border. Overall, these trends are consistent with the well-established latitudinal trends and elevational influences on temperature noted above.

Details of these patterns may be resolved through the development of regression models that quantify the relationship between precipitation and temperature and latitude and elevation. The detailed regression models that result from these analyses are presented in Appendix E, with the following discussion being based upon those results.

Average monthly precipitation is found to vary in response to elevation or latitude, depending upon the season. Elevation is a significant parameter in predicting precipitation in the months of June, July and August, with significant ($\alpha = 0.05$) R^2 values ranging from 0.52 to 0.67. In each month, the weighting parameter for elevation is positive, indicating a positive predictive relationship between elevation and precipitation - increasing elevation is predictive of increased precipitation for these months. In contrast, latitude is found to be a significant predictor of precipitation for the months of November and December, with significant R^2 values of 0.71 and 0.83 for November and December, respectively. The weighting parameters for latitude for these months are negative, suggesting an inverse relationship between precipitation and latitude for the regional USHCN stations - increasing latitude is predictive of decreasing precipitation. Both of these patterns are consistent with the general climate trends for the region presented above: spatial variation in precipitation during the winter months is largely determined by the movement of large fronts through the greater Southwest, with the paths of those fronts following large-scale atmospheric flow patterns; and summer precipitation amounts determined by the convective cooling of moisture-laden air over areas of high elevation.

The regression analyses conducted to determine the predictability of temperature from elevation and latitude resulted in a significant contribution of elevation to mean daily temperature for all months and a mixed contribution of latitude to temperature. In particular, latitude significantly contributes to the prediction of temperature in the

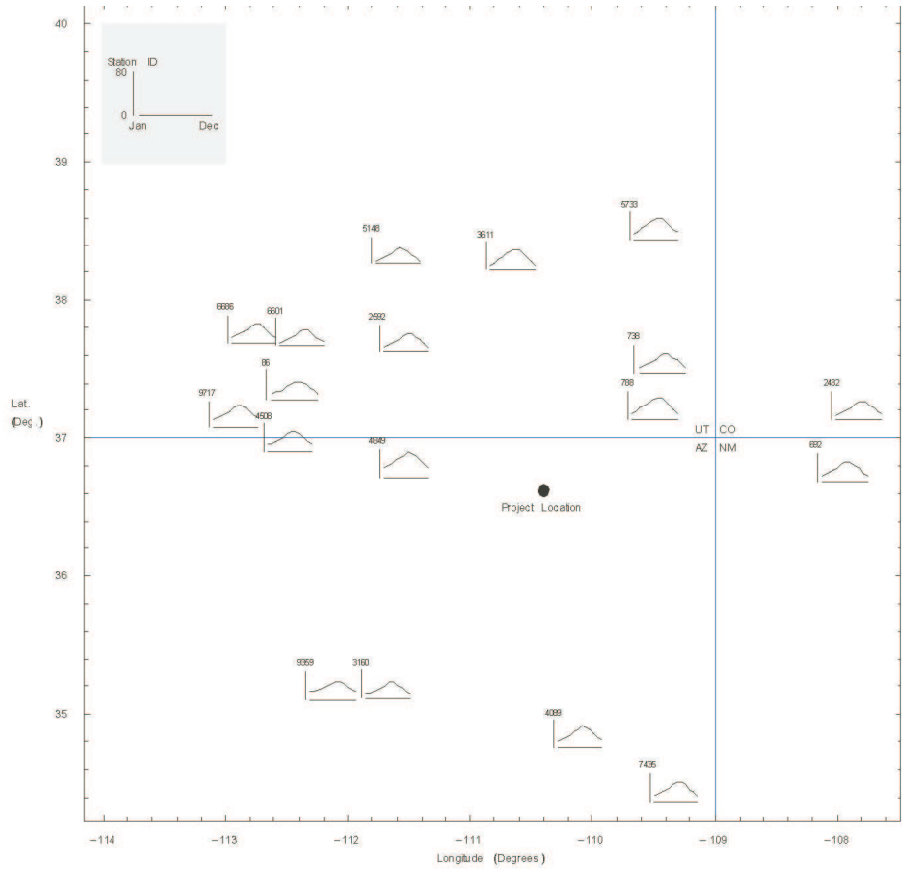


Figure 2.24: Average Monthly Minimum Temperature Profiles for 18 USHCN Stations within 250 km of the Project Area (Easterling, et al. 1999)

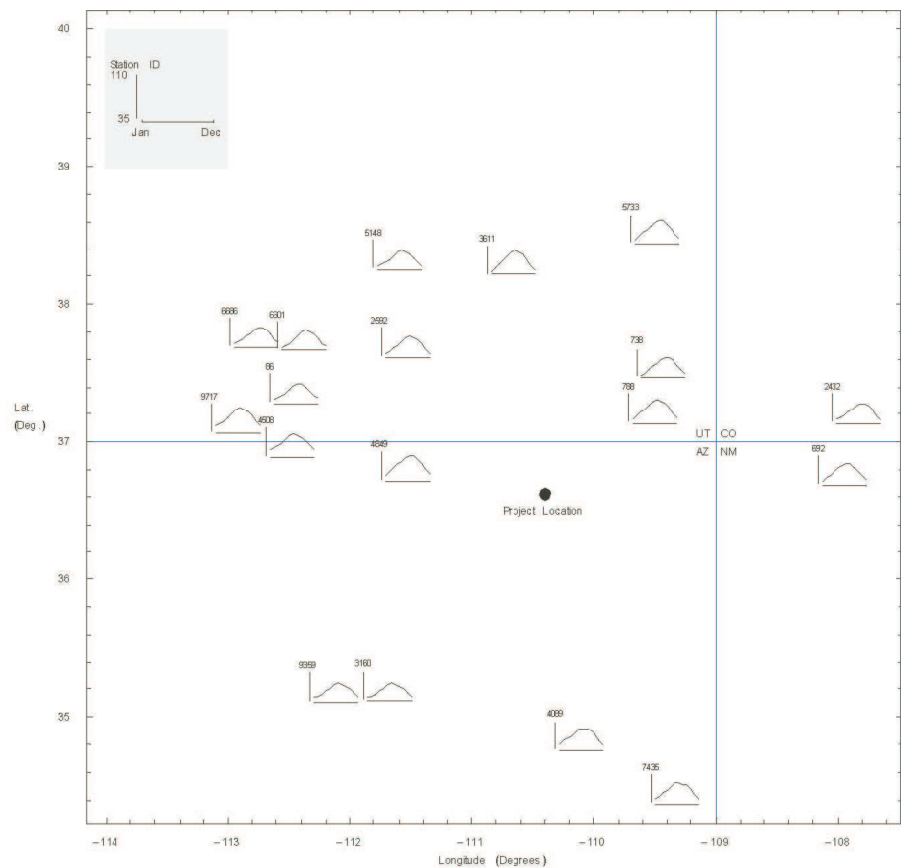


Figure 2.25: Average Monthly Maximum Temperature Profiles for 18 USHCN Stations within 250 km of the Project Area (Easterling, et al. 1999)

colder months of the year (January, February, and November in the case of average daily minimum temperature; November - April in the case of average daily maximum temperature). In all cases, the regression models for both average minimum and maximum daily temperature produced statistically significant ($\alpha = 0.05$) predictive models with R^2 values ranging from 0.62-0.91 (with 10 months having R^2 values above 0.80) for average daily minimum temperature and from 0.69-0.99 (with 10 months having R^2 values above 0.90) for average daily maximum temperature. The elevation parameter weights for all models are negative, supporting the general inverse relationship between elevation and temperature outlined above. Similarly, when making a significant contribution to the regression model, the weighting parameters for latitude are also negative, reinforcing the inverse relationship between latitude and temperature described above. The high R^2 values in conjunction with the significance of the models employing elevation and latitude reinforce the strong influence that these spatial attributes have on local and regional climate throughout the study area.

Interannual Variation. One aspect of temporal variation has already been presented - variation from month to month when monthly values are averaged over a long period of time. This variation is represented in the individual plots presented in Figures 2.23, 2.24, and 2.25 for monthly precipitation, average daily minimum temperature, and average daily maximum temperature, respectively. Another aspect of temporal variation in climate variables is interannual variation in the monthly values. Interannual variation is easily summarized through the calculation of variance or standard deviation values for the monthly values for the range of available years. Interannual variation is critical in characterizing the range of variation around the mean for each month at each station. The detailed results of the analyses are presented in Appendix D , while the results are summarized and presented graphically below.

Interannual variation in precipitation shows a strong relationship between mean monthly values and the range of variation around the mean (Figure 2.26). While not surprising, this characteristic does have a significant impact on the predictability of monthly precipitation values based purely upon previously observed monthly precipitation values. In particular, this relationship reflects a general situation in which months with low average precipitation will vary little from year to year while months with high average precipitation

will vary substantially from year to year in the actual precipitation that occurs.

Interannual variation in average daily minimum and maximum temperature exhibits a different pattern than that observed for precipitation. Specifically, average minimum daily temperature displays a minor negative trend in variation with increasing temperature (Figure 2.27), while average maximum daily temperature shows a clear negative trend in variation with increasing temperature (Figure 2.28). Both of these trends reflect a situation in which months with low temperatures have the highest variation in temperature while months with high temperatures have comparably lower variation. These characteristics in temperature variation reflect a lower degree of predictability (based upon observed variation) for low daily temperatures than that observed for higher temperatures. This relationship between temperature and predictability has a direct effect upon the predictability of spring freezes, a significant factor in determining the growth and productivity of both wild and agricultural plant species.

2.4 Summary and Relevance of Modern Environmental Conditions for the Analysis

The preceding discussion of the geologic, physiographic, biologic, and climatic conditions for the project area and the surrounding region provides critical baseline information from which inferences about prehistoric conditions may be derived. In the case of geologic and physiographic conditions, the uniformitarian assumption of direct comparability of modern to prehistoric conditions is easily made, considering the stability of those attributes over the time span covered by this study. Biologic and climatic conditions, on the other hand, may be subject to significant variation, within the period of time studied for this analysis, between the beginning of the period of study and the onset of the historic period, and during the historic period. Fortunately, these variations can be quantified through the use of proxy records such as tree-ring records, pack-rat middens and other paleobotanical data for the prehistoric period and calibrated and compared with observations and measurements from the historic period, like those summarized above.

The geologic summary presented above provides information needed for considering

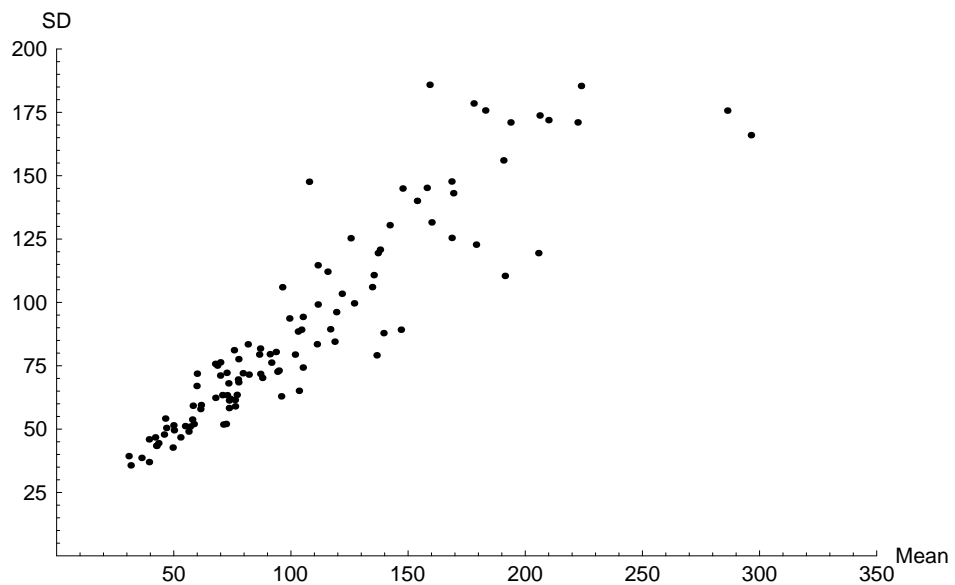


Figure 2.26: Relationship Between Monthly Precipitation and Interannual Variation (represented by the Standard Deviation)

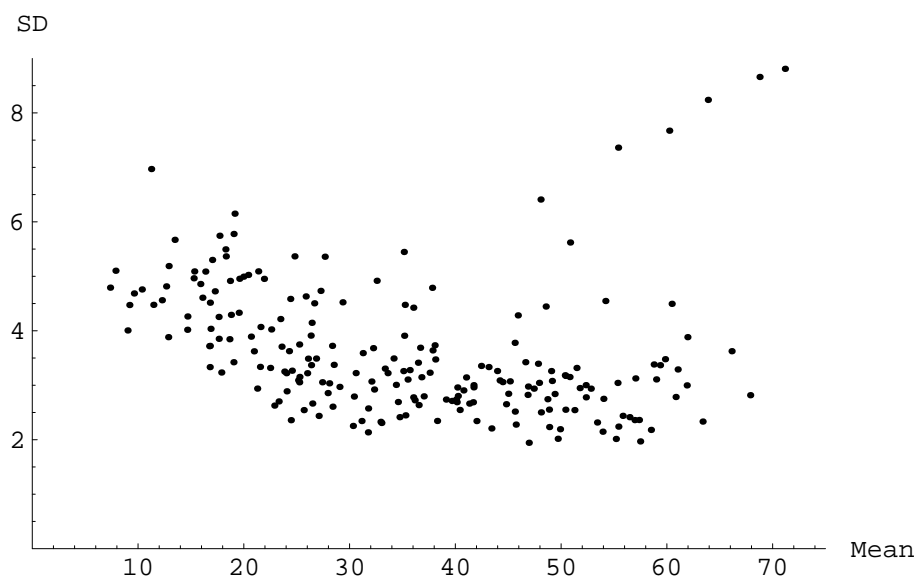


Figure 2.27: Relationship Between Monthly Average Daily Minimum Temperature ($^{\circ}\text{F}$) and Interannual Variation (represented by the Standard Deviation)

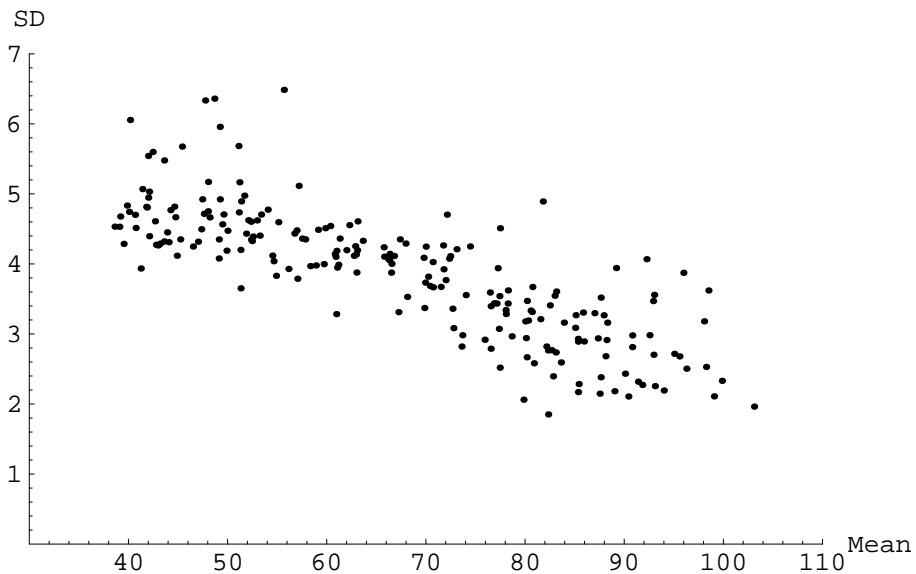


Figure 2.28: Relationship Between Monthly Average Daily Maximum Temperature (°F) and Interannual Variation (represented by the Standard Deviation)

the distribution of mineral raw materials in locational decision-making. While not the primary focus of this analysis, these factors contribute to the final interpretation of the spatial patterning observed in the analysis. More directly related to the analysis are the physiographic data for the project area. These data provide necessary quantifiable attributes of the landscape that have demonstrable effects upon local climate, a key attribute in this analysis.

The biological data presented above are key in defining the modern spatial distribution of economically important plant and animal species. When combined with localized climate data (derived from historic and modern instrumental observations and interpolated across the study area), the biological data allow for the quantification of the climatic tolerances of those species, ultimately allowing for a qualitative assessment of prehistoric variation in localized productivity in response to climatic variation. Critical for integrating these modern data into a study of prehistoric environmental conditions that may have influenced locational decision-making is an examination of proxy measures for prehistoric conditions and their relationship with historic and modern conditions. The next chapter presents these data in the context of the larger program of research that has been conducted for the study area and surrounding region.

Chapter 3

Paleoenvironmental Research

The history of paleoenvironmental research within and surrounding the project area is a long and distinguished one, producing detailed environmental and climatic reconstructions from a range of data sources including dendroclimatic reconstructions from regional long-term records, local and regional alluvial chronological reconstructions, site-specific pollen records, localized macrobotanical records, both from archaeological and non-archaeological contexts, and faunal analyses (Cordell 1997:51-65; Dean 1988a; Dean and Robinson 1977; Eckles 1984; Euler, et al. 1979; Ford 1984; Richard H. Hevly 1988; Thor N. V. Karlstrom 1988; T. N. V. Karlstrom, et al. 1976; S. Plog 1986b; Rupp 1985; Sem 1984; Trigg 1985). While estimates of paleoenvironmental conditions from prehistoric records provide a relatively detailed record of conditions during the period of study, the use of modern and historic data as a proxy for conditions that cannot be reconstructed in detail from prehistoric data sources necessitates a consideration of historic and prehistoric factors that may have produced modern conditions that differ significantly from those present prehistorically. These factors may include anthropogenic processes such as historic grazing impacts, landscape modification through conversion to agricultural production, localized reduction in fuelwood availability, and localized depletion of wild plant and animal resources. They may also include natural processes such as stream channel aggradation and entrenchment, wildfire impacts, and changing water table levels.

This chapter addresses paleoenvironmental and paleoclimatic conditions within and surrounding the project area based upon studies of materials extant during the period of

study and based upon analogous conditions observed in the historic and modern era with explicit consideration of prehistoric, historic and modern modifications of analogous data. The first section of this chapter provides a general overview of the paleoenvironmental data available for the project area and its surroundings while the second section of this chapter details the dendroclimatic data employed in the analysis.

3.1 Paleoenvironmental Overview

Paleoenvironmental data available for the project area and its environs include a variety of data that were collected in support of the Black Mesa Archaeological Project, local and regional alluvial chronological analyses, and regional paleoclimatic reconstructions produced as part of the Southwest Paleoclimate Project of the Laboratory of Tree-Ring Research at the University of Arizona. These datasets combine to provide a multi-faceted description of local and regional environmental conditions for the period of study that includes localized vegetation characterization based upon palynological and macrobotanical data, local and regional aggradation and entrenchment records for major drainage systems, regional precipitation, drought severity, and temperature conditions from dendroclimatic data.

Previous examinations of human response to climatic variation have concentrated on the identification and characterization of high- and low-frequency processes across the southern Colorado Plateau and the local region. These processes have been defined in terms of their period, direction, amplitude, and spatial variation.

Processes with periodicities greater than 25 years (e.g. cycles of deposition and erosion, long-term shifts in plant community composition) have been defined as low-frequency processes (LFP), and processes with periodicities of less than 25 years (e.g seasonal and annual climate variation, variation in wild plant productivity) have been defined as high-frequency processes (HFP). Patterns of variation in LFP are generally inferred from alluvial chronostratigraphy and long-term palynological records, while HFP are identified and characterized through palynological, macrobotanical, faunal, and dendroclimatic studies (Dean 1988b, 1996a; Dean, et al. 1994; Dean, et al. 1985; Euler, et al. 1979; F. Plog, et al. 1988).

Both direction and amplitude of deviations are frequently defined from the long-term mean for the proxy record being considered, generally in terms of standard deviation (SD) units above or below the mean deviation (e.g. Dean 1988a; Richard H. Hevly 1988), with values above or below a specified SD threshold interpreted as representing conditions that would result in potential adaptive consequences for plant, animal, and human populations (Dean and Robinson 1977:7). Different analyses have employed varying thresholds, including a ± 2.0 SD unit threshold in the qualitative reconstructions developed by Dean and Robinson (Dean and Robinson 1977:7) and the quantitative reconstructions developed by Rose, Dean and Robinson (Rose, et al. 1981:92), and, more recently ± 1.1 SD unit threshold in the case of the quantitative reconstructions developed by Salzer (2000), and the qualitative reconstructions by Dean et al. (Dean 1988a, 1996a; Dean, et al. 1994).

Typically, the measured deviations are for one of two values: 1) reconstructed climate parameters such as temperature or precipitation (e.g. H. C. Fritts 1976, 1991; Kohler and Van West 1996; Rose, et al. 1981; Salzer 2000; Van West 1994); or, 2) proxy measures of climate that have well-demonstrated correlations with climate (e.g. Dean, et al. 1985; Euler 1988; Euler and Gummerman 1974; Euler, et al. 1979; Richard H. Hevly 1988; R. H. Hevly and Karlstrom 1974; T. N. V. Karlstrom, et al. 1976; Thor N. V. Karlstrom, et al. 1974). Significantly, the primary difference between these two approaches to paleoclimate interpretation rests on the specificity of the reconstruction of climate parameters through the development and testing of statistical models of the relationship between particular proxy data and historic climate observations. This quantitative approach to climate parameter estimation yields information about the strength, direction, and associated error for the modeled association between the proxy record and the climate parameters of interest (H. C. Fritts 1976, 1991; Rose, et al. 1981; Van West 1994). In contrast, directionality and amplitude inferred from proxy records depend upon established, but non-quantified, relationships between climate parameters and the proxy record.

This distinction between reconstructed climate parameters and the proxy data from which those data are derived relates to the three hierarchical components of a given paleoenvironmental discipline identified by Dean (1988a:120):

1. The Data. For example, standardized tree-ring index values, arboreal- and non-

arboreal pollen abundance values, stratigraphic and chronological data from alluvial contexts

2. The Reconstructions. For example, temperature or precipitation, general moisture conditions, water-table levels.
3. The Model. The specification of the "interrelationships among variables that provide the basis for the inferences that convert the raw data of the first level into the paleoenvironmental reconstructions of the second" (Dean 1988a:120).

In the case of the reconstructed climate parameters, the model defining the relationship between the data and the reconstruction yields parameter values that are in meteorological units such as mm or inches of precipitation or °C or °F. The model for inference of climate trends from proxy data produces reconstructions that treat deviations in proxy measurements as direct representations of direction and amplitude for climate parameter trends. The use of reconstructed values (in units commonly employed), when available, allows for the use of recently developed meteorological interpolation methods and physical models for landscape processes in prehistoric contexts, as is the case in the analysis that follows.

3.2 Vegetation Distribution Data

In the context of the analysis performed herein, the modern plant communities presented in the previous chapter provide a baseline for the distribution of economically important species. While the use of modern community data yields a more detailed and synoptic perspective over the entire analysis area, the uniformitarian assumption of similarity between observed modern plant communities and prehistoric communities must be explicitly acknowledged and evaluated. Two primary lines of evidence provide data necessary for assessing the match between modern environmental conditions and those within which the prehistoric inhabitants of the southern Colorado Plateau lived: palynological, and macrobotanical.

Palynological analyses presented by Hevly (1988) and Ruppé (1985) reflect a general similarity between the prehistoric and modern vegetation conditions, with variation

within the analysis period being ascribed to climatic variation, the development of anthropogenic environments in the vicinity of archaeological sites, and localized fuelwood collection. These trends and relationships were illustrated by Hevly, and have been reproduced with modifications in Figure 3.1. The trends noted by Hevly for northern Black Mesa include reduced arboreal pollen (AP) ratios for samples from archaeological contexts, when compared with samples from alluvial contexts, particularly when population levels are high. Hevly observes that this trend could result from two possible causes: localized reduction in pollen-producing trees as a result of firewood and construction material collection in close proximity to sites and/or the invasion of disturbed areas associated with sites by non-arboreal weedy species, yielding an increased local abundance of non-arboreal pollen (NAP), producing an overall reduction in the proportion of AP in samples collected from archaeological contexts (Richard H. Hevly 1988:113). Trends in non-archaeological AP departures track closely with both the large-scale tree-ring departure and depositional trend data presented in Figure 3.1. Specifically, visual inspection of the depositional, tree-ring departure, and AP departure values shows general positive AP departures with positive tree-ring departures, negative AP departures with negative tree-ring departures, and reversals of long-term trends with transitions from depositional to non-depositional (and reverse) conditions.

Ruppé's (1985) site-specific analysis of the long-term pollen record from Tsosie Shelter (D:7:2085), a rockshelter and associated open-air Archaic occupation site near the northwestern edge of the Black Mesa Project area, also indicates the presence of high abundance NAP for much of the Tsosie Shelter record. Ruppé argues that this might also reflect a high degree of disturbance in the area surrounding the site as opposed to the more traditional interpretation of high NAP proportions being indicative of dry conditions. In particular, the conditions observed in the Tsosie Shelter pollen record are argued by Ruppé to represent a combination of climatic and cultural factors, with the cultural contribution leading to reduced certainty when inferring climate conditions from the archaeological pollen assemblage from Tsosie Shelter (Ruppé 1985:521).

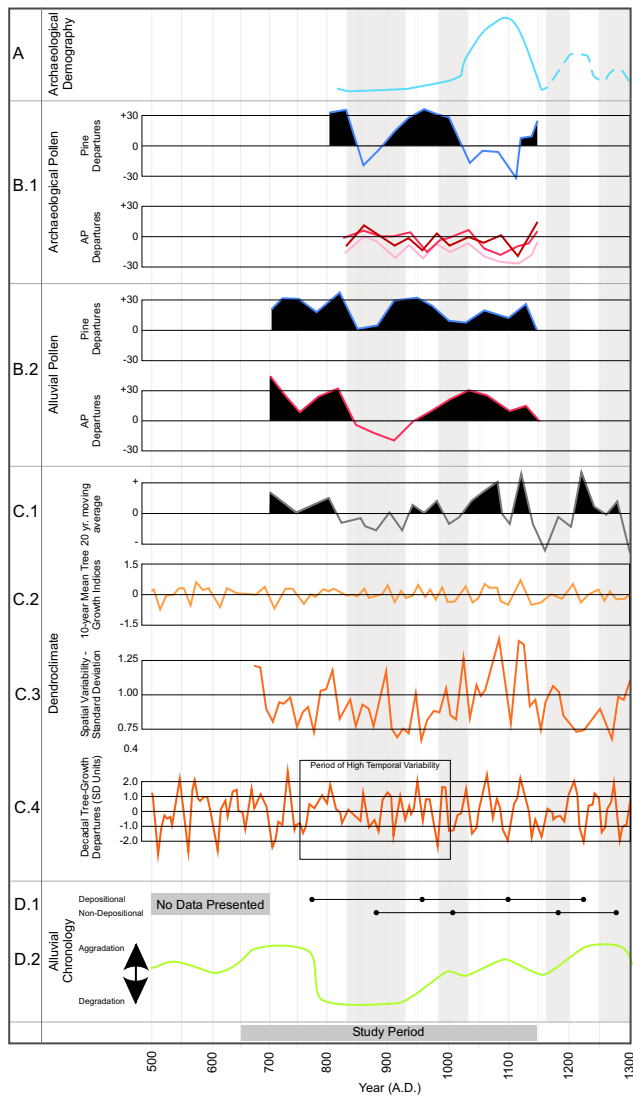


Figure 3.1: Paleoclimatic Parameters and Reference Demographic Trend for the Project Area and Surrounding Region. A. General Population Trends for Northern Black Mesa (solid) and Local Area (Dashed). B. Alluvial and Archaeological Pollen Trends for Northern Black Mesa. C.1. 20-Year Moving Average Tree-Ring Departures for Navajo National Monument. C.2 Southern Colorado Plateau 10-Year Mean Tree Growth Indices. C.3 Spatial Variability in Decadal Tree-Ring Departures, Represented by the Standard Deviation of the Tree-Ring Departures for Network of Tree Ring Records from the Southern Colorado Plateau. C.4 Decadal Tree-Growth Departures, Overlapped Five Years. D.1 Black Mesa Alluvial Characteristics, Presented as Depositional or Non-Depositional Periods, Gray Bands on Figure Represent These Periods. D.2 Floodplain Aggradation Curve for the Southern Colorado Plateau (A, B, C.1, D.1 based upon Richard H. Hevly 1988: Fig. 4.9).(C.2, C.3, C.4 based upon Dean 1988a: Fig. 5.7-C, -G, -A) (D.2 based upon F. Plog, et al. 1988: Fig. 8.1-A).

In total, the archaeological and non-archaeological pollen records presented by Hevly and Ruppé provide complimentary views of natural and anthropogenic influences on regional and local vegetation characteristics, both of which reflect variation within compositionally stable larger vegetation communities. Furthermore, both authors suggest that variation observed in the pollen record may be ascribed to a combination of natural and cultural factors, both of which need to be considered in any discussion of localized variation in community productivity and composition in the context of natural and cultural landscape modification.

Trigg's (1985) analysis of the long-term macrobotanical record from Tsosie Shelter and Ford's (1984) summary of BMII Lolomai macrobotanical remains lend support to Hevly's and Ruppé's palynological analyses. Data from Tsosie Shelter indicate decreasing percentages of conifer as opposed to shrub species in charcoal samples (Trigg 1985: Fig. G.1, pg. 496), a condition consistent with Hevly's and Ruppé's suggestions regarding localized conifer fuelwood depletion, with shrub species wood increasing in use as conifer fuelwood decreased in availability. Trigg's second potential explanation for an increase in shrub charcoal representation - that shrubs cleared from agricultural fields were used as fuel - is also consistent with the general concept of the development of anthropogenic environments near occupation sites, expanded agricultural fields in the case of this alternative explanation for the increasing prominence of shrub species in charcoal samples from the later occupation layers in Tsosie Shelter. Ford's analysis (1984), in which seeds recovered from BMII Lolomai archaeological contexts on northern Black Mesa suggest increased frequencies of disturbed-ground annuals (e.g. *Chenopodium* and *Portulaca*, Ford 1984:136) in the vicinity of analyzed sites, also argues for the development of anthropogenic environments, again in the form of nearby agricultural fields.

In sum, the palynological and paleobotanical data outlined above support the conclusion that the modern distribution of vegetation communities may serve as a reasonable proxy for the prehistoric distribution of those communities for the period of study. These data also indicate that while broad community composition and distribution remain constant from before the beginning of the study period, there are anthropogenic and natural processes that contribute to variation in the localized concentration and productivity of plant community members within the larger general distribution. Anthropogenic pro-

cesses are argued to include the localized depletion of fuelwood and the development of agricultural fields near archaeological sites. Natural processes related to water availability and associated depositional and erosional regimes are also correlated with long-term trends in the localized productivity and distribution of economically important fuelwood and wild food species. This observed variation in productivity and distribution of economic species, particularly food species, is key in demonstrating the potential for spatial variation and therefore differential preference for locations based upon the predictability of resource availability at those locations, a key component of the analysis undertaken herein.

3.3 Drainage System Behavior

One manifestation of the environmental variability for the study region is the well-documented variation in depositional patterns within the major drainage systems of northern Black Mesa, Long House Valley, Tsegi Canyon (northwest of Long House Valley), and the drainages separating the Hopi Mesas at the southern end of Black Mesa. While the causes of the aggradational and erosional processes documented for these drainage systems are debated (Cordell 1997:51; Thor N. V. Karlstrom 1988), the depositional and erosional trends embodied in these records and their potential effects on agricultural productivity are well documented by several researchers, including Bryan (1925; 1929; 1941), Hack (1942), Bradfield (1971), and Karlstrom (Euler, et al. 1979; Thor N. V. Karlstrom 1988; T. N. V. Karlstrom, et al. 1976; Thor N. V. Karlstrom, et al. 1974). Karlstrom's summary of the chronostratigraphy for Black Mesa is the most recent and complete record for the study area and provides the basis for the summary presented below.

As discussed previously, and outlined in Figure 3.1, there are several periods of alternating deposition and erosion embodied in the alluvial stratigraphy of northern Black Mesa and the surrounding region. Karlstrom's analyses (Euler, et al. 1979; Thor N. V. Karlstrom 1988; T. N. V. Karlstrom, et al. 1976; Thor N. V. Karlstrom, et al. 1974) of tree germination and growth, and non-depositional soil horizons (point boundaries) with associated radiocarbon/ceramic/tree-ring dates, suggests synchronous primary and

secondary regional depositional cycles with periodicities of 550 and 275 years respectively.

The specific trends in depositional conditions reconstructed by Karlstrom are summarized in Figure 3.1, and the following discussion highlights potentially important inflection points and trends in the data that contribute to the environmental picture for the study area and region. The reconstructed depositional patterns for the time interval prior to the study period indicate a period of aggradation from A.D. 1 through the early part of the 3rd century A.D., followed by a rapid transition to erosional conditions that persist through the middle of the 4th century A.D.. Beginning in the middle of the 4th century A.D., and continuing through the early 6th century A.D., depositional conditions slowly transition to an intermediate aggradational state that, following a century-long dip toward erosional conditions, stabilizes with aggradational conditions from the middle of the 7th century through the middle of the 8th century A.D.. The middle of the 8th century exhibits another rapid decline to erosional conditions that persist into the early 10th century before beginning an uneven upward trend towards aggradational conditions that briefly stabilize in the mid-13th century before rapidly declining to erosional conditions in the late 13th/early 14th centuries. These erosional conditions persisted through the beginning of the 16th century when an upward trend towards aggradational conditions began, culminating in aggradational conditions in the late 18th through the mid-19th century. The late 19th century witnessed another rapid transition to erosional conditions which continue to dominate the depositional environment throughout much of the Southwest.

The depositional sequence outlined above exhibits a record of variation that, with the exception of early historic accounts (e.g., those cited in Kirk Bryan 1925), greatly exceeds recently observed variation. The dominance of the recent record by erosional conditions has the potential to have significantly influenced plant community composition and productivity within the narrow alluvial environments dissecting the project area. This variation is documented in the alluvial pollen record summarized above and contributes to the broader interpretive context for the results of the following analysis.

3.4 Dendroclimate

Dendroclimatic data derived from a variety of locations surrounding the project area provide the foundation for the localized climate reconstructions developed in the analysis and provide a detailed record of climate variation for the entire period of study. This section summarizes the climatic trends for the region as derived from tree-ring data, while the following section details the specific datasets employed in the generation of the localized climate reconstructions used in the analysis.

The preceding discussion of vegetation composition trends and alluvial chronology provides insights into the response of alluvial systems and vegetation to variations in climate, with the timing of changes for those records inferred from radiocarbon dates, datable ceramics, and tree-ring dates. While useful for painting a general picture of localized climate conditions, the annual resolution of climate reconstructions based upon tree rings provides a more detailed record (in terms of the frequency of annual observation) than that which can be obtained from the pollen and macrobotanical records. This characteristic compliments the ability of pollen records and alluvial chronological records to provide records of long term variation that is suppressed in the standardization process of dendroclimatological record construction (Dean 1988a: 134-135).

Beginning with the compilation and re-evaluation of tree-ring records from throughout the Southwest starting in the early 1960s (e.g. Bannister, et al. 1966, 1968, 1969), and continuing with the development of the first regional paleoclimate reconstructions in the late 1960's and 1970's (Dean and Robinson 1969; 1977; 1978; cited in Salzer 2000), the researchers at the Laboratory of Tree-Ring Research at the University of Arizona have taken the lead in developing precipitation, temperature, meterological drought [PDSI; !Palmer, 1965 *3491], and other climate parameter reconstructions from those records (e.g. Dean 1982, 1986, 1988a; Dean 1999; Dean and Robinson 1969; Dean and Robinson 1977; 1978; H. C. Fritts 1965, 1976, 1991; H. C. Fritts, et al. 1979; Rose, et al. 1981).

Tree-ring records from the southern Colorado Plateau have yielded long-term annual reconstructions of precipitation from a network of locations in the region (Dean 1999; Salzer 2000), temperature from the San Francisco Peaks (Salzer 2000), and qualitative reconstructions of past climate that infer changes in temperature and precipitation

without actually estimating those climate parameters (Dean 1988a; Dean and Robinson 1977). The qualitative reconstructions for this region have been characterized in terms of temporal (Figure 3.1, C.4) and spatial variation (Figure 3.1, C.3) in standardized tree-ring index values, both in absolute terms (Figure 3.1, C.2) and as deviations from the long-term average value (Figure 3.1, C.1). Quantitative reconstructions frequently concentrate on the actual climate parameters (i.e. precipitation, temperature), temporal variation within single and averaged records, and deviation of those records from the long-term average record (e.g. Rose, et al. 1981; Salzer 2000).

Both qualitative and quantitative reconstructions have been used to identify individual years or periods of significantly higher or lower temperature or precipitation, with different threshold values being used in different analyses. For example, Dean and Robinson's (1977) summary of southwestern dendroclimatic variability suggests 2 standard deviations (SD) as a reasonable threshold for identifying variation that is considered to be significant in the sense that such departures are sufficiently rare to have had potential adaptive consequences for plant, animal, and human populations (Dean and Robinson 1977:8). Likewise, Rose, Dean and Robinson (1981) recommend a 2 SD threshold for identifying periods of significant climatic departures. More recently, Dean (1988a) recommended a 1.1 SD threshold

because variation in tree growth underestimates the full range of climatic variability ... a particular tree-growth departure is equivalent to a greater climatic deviation. Although exact correspondences cannot be given, it is likely that departures exceeding ± 2.0 standard deviation units represent climatic extremes beyond ± 3.0 standard deviations (Charles W. Stockton, personal communication). Therefore, a lower level of potential significance is warranted, and a limit that specifies 25 per cent of tree-growth variation (the extreme 12.5 per cent of the variability above the mean and the 12.5 per cent below the mean) is used here. Thus, tree-growth departures that exceed 1.1 standard deviation units in either direction are considered potentially significant. (Dean 1988a:137-138)

A combination of these criteria were used in Salzer's recent (Salzer 2000) development and analysis of dendroclimatic reconstructions for the region surrounding Flagstaff, Arizona. Salzer's analysis of the precipitation record for A.D. 570-1988 uses the extreme 2.5 percent of values in the identification of individual wet or dry years (Salzer 2000:36-39), with a more inclusive threshold of 1.1 SD used for the identification of intervals of

greater than 5 years that exhibit wet or dry conditions from a 10-year smoothing spline representation of the annual precipitation data, with the starting and ending points of each interval being defined by the occurrence of an individual annual value greater than ± 0.5 SD from the mean (Salzer 2000:39-42). Salzer used the same criteria for identifying cold and warm years and periods for 663 B.C. - A. D. 1997. Specifically, 2.5 percent is used as a criterion for the identification of individual years with extreme hot or cold conditions and 1.1 SD units are used as a criterion for the identification of hot or cold periods. In his analysis of the temporal variance in both the precipitation (Salzer 2000:45-51) and temperature records (Salzer 2000:73-77), Salzer also used a 1.1 SD threshold, this time for 25-year overlapped moving variances.

The annual precipitation estimates produced in a given reconstruction represent the period of precipitation that influences each growing-season's ring development. This period is called the tree-year, and, depending upon the specific reconstruction, starts in June (Dean 1988a; G. J. Gumerman 1988; Rose, et al. 1981), August (in the case of the annual precipitation reconstructions provided by Jeff Dean for use in this analysis, 1999) or October (in Salzer's precipitation reconstructions, 2000) of the previous year and extends through July of the current year. Similarly, the period for which temperature is reconstructed also varies by analysis. In particular the temperature reconstruction developed, tested, and ultimately rejected by Rose, et al. (1981:49-78) represents June through July of the current year, and October through November of the prior year. In contrast, Salzer's (2000:57) mean-maximum temperature reconstructions for the San Francisco Peaks area cover the standard calendar year (January through December) for the year preceding the growing season.

3.4.1 Regional Dendroclimate Reconstructions

Regional dendroclimate reconstructions for northeastern Arizona have been developed using statistical models that combine historic and prehistoric standardized tree-ring measurements. Qualitative dendroclimate reconstructions that infer prehistoric climate trends directly from standardized tree-ring values (the calculation of which is described in Dean and Robinson 1977:7; H. C. Fritts 1976) identify temperature and precipitation trends

through reference to a positive correlation between tree-ring width and precipitation and a negative correlation between tree-ring width and temperature for different portions of the year, depending upon the growth characteristics of the tree species contributing to the reconstruction (Dean and Robinson 1977:7-8). Quantitative reconstructions based upon statistical models yield estimated precipitation and temperature values for dendroclimate locations with demonstrable sensitivity to variation in those parameters. That sensitivity is quantified through the development and testing of first, a response function that estimates tree-growth from historic climate variables, and second, a transfer function that estimates prehistoric climate variables from tree-ring widths (H. C. Fritts 1976; Rose, et al. 1981:7-10).

Qualitative dendroclimate reconstructions applicable to the project area include those developed by Dean and Robinson (1977) and Dean (1988a) for the Southwest and southern Colorado Plateau, respectively. Both reconstructions employ deviations from long-term mean conditions, either at the level of the individual reconstruction, in the case of Dean and Robinson's (1977) analysis of spatial variation throughout the Southwest; or at the level of a regional composite, in the case of the analysis of decadal variance and tree-ring deviations presented by Dean (1988a). Both analyses are based upon the same network of 25 long-term Southwest dendroclimate stations, with all 25 records used in the case of Dean and Robinson's analysis, and 21 of the 25 records (those that are located on the Colorado Plateau) used in Dean's analysis.

The qualitative dendroclimate trends for the southern Colorado Plateau are summarized in Figure 3.1 (C.1-C.4), with the following characteristics observable within the regional record:

- As the period of time over which tree-ring data are averaged increases, there is an increased ability to identify periods of above- or below-average climate conditions (compare Figure 3.1: C.1 and C.2)
- Even when averaged over a relatively brief 20-year time span, both above- and below-average climate conditions are observable within the period of analysis, with the periods of A.D. 700-800, 930-990, 1020-1090, and 1110-1130 representing periods of above-average tree-ring growth; and A.D. 800-930, 990-1020, 1090-

1110, and 1130-1150 representing periods of below-average tree-growth. (Figure 3.1: C.1)

- Spatial and temporal variation vary throughout the analysis period, with spatial variation defined in terms of the variance in standardized tree-ring index values for the network of dendroclimate records for the southern Colorado Plateau, and temporal variation defined in terms the frequency of changes from positive to negative (and vice-versa) tree-ring growth departures.
- Spatial variation was higher than average from A.D. 680-690, 790-810, 890-910, and 1110-1130 (with short periods of intervening low variation). Spatial variation was lower than average from A.D. 690-790, 810-890, 910-1110, and 1130-1150.
- Periods of high temporal variation have been identified by Dean (1988a:Figure 5.7), with A.D. 750-1000 identified as a period of high temporal variation.

Given these identified trends, and the temperature and precipitation conditions that may be inferred from them, the following general climate conditions are implied:

- Higher precipitation and lower temperature values are generally associated with wider tree-rings (Dean 1988a:133; H. Fritts 1974), suggesting that these conditions were dominant during the periods of above average tree-ring growth: A.D. 700-800, 930-990, 1020-1090, and 1110-1130.
- Lower precipitation and higher temperatures are associated with narrower tree-rings (Dean 1988a:133; H. Fritts 1974), suggesting that these conditions prevailed during the periods of: A.D. 800-930, 990-1020, 1090-1110, and 1130-1150.

The periods of above average and below average climate conditions discussed above provide a general picture of the climate trends, but do not provide actual climate parameter estimates that are typically used in quantitative archaeological hypothesis testing (e.g. Euler, et al. 1979; Larson, et al. 1996; F. Plog, et al. 1988). In contrast, Salzer's (2000) quantitative models for northeastern Arizona precipitation and San Francisco Peaks temperature provide a foundation for the implementation of meteorological interpolation models employed in the analysis. They also provide a valuable point of

reference for the paleoclimate reconstructions developed, tested, and employed in the analysis.

Salzer's (2000) temperature and precipitation reconstructions are a quantitative record for these parameters that provides adequate spatial and temporal coverage for quantitatively summarizing the paleoclimate conditions for the region surrounding the project area and the time period under analysis (Figure 3.2).

3.4.2 Precipitation Reconstruction

Salzer's precipitation reconstruction combines historic climate data from seven meteorological stations (including the Williams, Grand Canyon, and Fort Valley USHCN stations; and the shorter duration Burrus Ranch, Flagstaff, Walnut Canyon, and Sunset Crater Cooperative Network stations) and three tree-ring chronologies (Flagstaff, Navajo Mountain, and Canyon de Chelly) to produce tree-year (prior October through current July) precipitation estimates. These estimates were produced using a linear regression model (Equation 3.1) that predicts tree-year precipitation (the log-transformed average precipitation for the seven meteorological stations) from four variables: the current year's ring width for all three tree-ring chronologies and the next year's tree-ring width for Navajo Mountain, with the regression model represented by the following formula:

$$\Pi = \eta + \alpha\mathcal{A} + \beta\mathcal{B} + \gamma\Gamma + \phi\Phi \quad (3.1)$$

where,

- Π = tree-year precipitation value
- η = Regression model intercept constant
- $\alpha, \beta, \gamma, \phi$ = regression model weighting parameters
- $\mathcal{A}, \mathcal{B}, \Gamma$ = tree-ring width for the current year, for each of the three stations
- Φ = tree-ring width for the current year + 1 for Navajo Mountain

with the resulting model explaining 64 percent of the variance in the calibration period of 1897-1988 (Salzer 2000:30-34).

The result of Salzer's precipitation reconstruction was the identification of extreme individual years (Salzer 2000:Table 3), time intervals (Salzer 2000:Table 4), and intervals

of high and low variability (Salzer 2000:Table 5). Different methods and criteria were used in the identification of each of these characterizations of the precipitation record.

Individual years were categorized as extremely wet or dry if they fell into the lower or upper 2.5 percent of values for the entire record. For the period of analysis, nine low-precipitation (represented by the red circles in Figure 3.2-a, A.D. 660, 664, 704, 809, 954, 972, 981, 1067, 1121), and twelve high-precipitation (represented by the blue circles in Figure 3.2-a, A.D. 731, 804, 805, 822, 899, 928, 942, 960, 988, 989, 1047, 1080) years were identified using this criterion.

The systematic identification of short-term (≥ 5 years and ≤ 50 years) extreme wet or dry intervals was an additional goal in Salzer's analysis of precipitation trends in the San Francisco Peaks region. In order to control for high interannual variation in the precipitation record, a 10-year smoothing spline (a low-pass filter that maintains short-term trends) was applied to the annual values, creating a new smoothed annual series, with each year's value representing the values from the preceding and following five years. The start and end points of each interval were defined using the unsmoothed values, while the smoothed data were used in identifying the intervening years.

The minimum length for periods was established at five years. The beginning year for an extreme period was determined as that point when the original reconstructed value first substantially deviated from mean conditions (< -0.5 or > 0.5 SD). The ending year for periods was defined as that point when average conditions (> -0.5 and < 0.5 SD) returned for more than two consecutive years or when conditions substantially deviated in the other direction for more than a single year. During each extreme period, the smoothed reconstructed values deviate from the long-term average by at least ± 1.1 sd

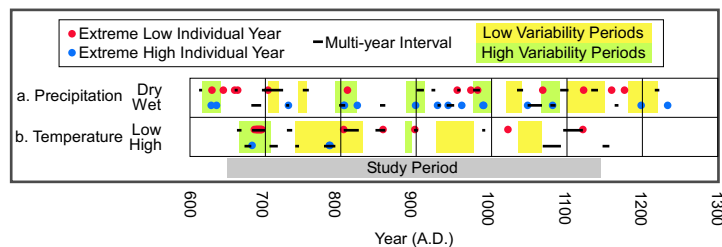


Figure 3.2: Reconstructed Precipitation and Temperature Extremes for the San Francisco Peaks Area of Northeastern Arizona (data from, Salzer 2000:Tables 3-8)

for at least one year (Salzer 2000:40).

This procedure resulted in 10 dry intervals (nine of which correspond with dry intervals identified by Grissino-Mayer (1995) for west-central New Mexico) and eight wet intervals (three of which correspond with wet intervals identified by Grissino-Mayer (1995) for west-central New Mexico) within the period of analysis (the horizontal bars in Figure 3.2.a). The lengths of the identified dry intervals range from 5 to 29 years while the lengths of the wet intervals range from 5 to 20 years.

The third component of Salzer's analysis of precipitation trends for the region consists of an analysis of changes in variability in precipitation through time. The importance of precipitation variability (a key variable in the current analysis) was stated by Salzer as follows:

Annual rainfall in the region is highly variable and the recognition of what to expect must have been of great importance to prehistoric farming communities. In local Anasazi populations, HV [high variability] periods could favor behavior aimed at guarding against the variability, such as long-term food storage (Dean et al. 1994). Alternatively, HV periods could encourage adaptability and change. Populations might benefit from being less specialized or less "adapted" to a particular economy dependent upon reliable climatic conditions. HV periods could also favor mobility and other strategies that increase adaptability rather than adaptedness. LV [low variability] periods, on the other hand, would encourage populations to demonstrate a strong adaptation and specialization to current climatic conditions because current conditions would not substantially change from year to year. (Salzer 2000:46)

Precipitation variability was defined by Salzer using a 25-year moving variance with the resulting value being assigned to the year in the center of the 25-year range for which the variance was calculated. The variance values were then converted to z-score values, with the z-score values providing the basis for the identification of high and low variability intervals. The same criteria were used for the identification of periods of high and low variability as were used in the definition of periods of high or low precipitation: individual years with moving variance values > 0.5 or < -0.5 standard deviation units from the mean long-term variance marking the beginning and two consecutive years with moving variance values < 0.5 and > -0.5 marking the end of each interval. Each identified interval must also contain at least one year with a deviation of ± 1.1 or greater standard

deviation units from the long-term mean variance. These criteria resulted in the definition of five low variability intervals (highlighted in yellow in Figure 3.2.a) ranging in length from 12 to 50 years, and five high variability intervals (highlighted in green in Figure 3.2.a) ranging in length from 24 to 30 years.

Examination of the three aspects of the precipitation reconstruction presented in Figure 3.2.a provides several insights into the general characteristics of regional precipitation. First, the association between individual extreme years and extreme intervals within the analysis period is only partial, with only five out of nine (55.6%) dry years lying within identified dry intervals and seven out of 12 (58.3%) wet years lying within wet intervals. Second, neither individual extreme years nor extreme intervals are associated with specific climate conditions (Salzer 2000:46), with two out of nine (22.2%) dry years falling into high variance, and two out of nine dry years (22.2%) falling into low variance intervals within the analysis period. Seven out of 12 (58.3%) wet years within the analysis period fall within high variability periods, with the remaining five extreme wet years falling into neither high nor low variance intervals. The pattern of association between extreme intervals is similar to that for individual years, with four of 10 (40%), and two of 10 (20%) extremely dry intervals falling into low variability and high variability intervals respectively, with the remaining four dry intervals falling into neither. Two of eight (25%) of extremely wet intervals fall into high variability periods, with the remaining six falling into neither high nor low variability intervals.

3.4.3 Temperature Reconstruction

Salzer's temperature reconstruction for the San Francisco Peaks area is the first reconstruction of this parameter that covers the time period for this analysis (Salzer 2000:53) and in total extends from 650 B.C. to A.D. 1996 (Salzer 2000:Figure 8). The reconstruction was developed using a single-predictor linear regression model (Equation 3.2) in which the previous calendar year's mean maximum temperature is predicted from the current year's tree-ring width from the long-term bristlecone pine (*Pinus aristata*) tree-ring record recovered from near treeline on Agassiz and Humphreys peaks within the San Francisco Peaks area north of Flagstaff, Arizona. The regression model accounted for 46

percent of the variation in the calibration temperature record from 1909-1994, a result that Salzer argues "compares favorably with other tree-ring based temperature reconstruction" (Salzer 2000:57). The historic climate record used in the development of the temperature reconstruction was that of the Fort Valley Experimental Research Station, one of the USHCN stations employed in the summary of modern climate presented in Chapter 2 (Salzer 2000:53-60).

$$\Pi = \eta + \beta \mathcal{B} \quad (3.2)$$

where,

Π = Annual mean maximum temperature for Year - 1 °C

η = Regression model intercept constant

β = regression model weighting parameter

\mathcal{B} = tree-ring width for the current year

The analysis of the temperature reconstruction mirrors that outlined above for precipitation, with three attributes of the temperature reconstruction receiving detailed discussion: extreme annual values, extreme intervals, and high and low variability intervals, with the emphasis in Salzer's analysis on interval-based summaries.

The identification of extreme years within the analysis period found 18 years that were below the 2.5th percentile or above the 97.5th percentile for the long-term reconstruction. Fifteen years were defined as extremely cool years (the red circles in Figure 3.2.b, A.D. 686, 688-696, 804, 856, 898, 1021, 1120), while three years were identified as extremely warm years (the blue circles in Figure 3.2.b, A.D. 678, 880, 881).

Salzer's identification of extremely cold or warm intervals followed the same procedure as that employed in the precipitation data, with the primary difference being that the temperature analysis employed a 25-year smoothing spline as opposed to the 10-year smoothing spline used in the precipitation analysis. Using the same criteria for defining extreme intervals (starting year marked by one individual year > 0.5 or < -0.5 standard deviation units from the long term mean; the ending year marked by two consecutive individual years > -0.5 and < 0.5 standard deviation units from the long-term mean; at least one intervening year with a smoothed value > 1.1 or < -1.1 standard deviation

units from the mean), Salzer identified eight extremely cool intervals and six extremely warm intervals within the analysis period (the solid bars in Figure 3.2.b). The cool intervals range in length from 7 to 27 years while the warm intervals range in length from 6 to 25 years.

Following the same approach employed in his analysis of the variance in precipitation through time, Salzer employed a 25-year moving variance and the same criteria for identifying intervals of high and low variance in temperature. This procedure defined three low variability intervals (highlighted in yellow in Figure 3.2.b, A.D. 740-829, 926-976, and 1034-1065) and two high variability intervals (highlighted in green in Figure 3.2.b, A.D. 666-708, 886-894), with their lengths ranging from 32 to 90 years and 9 to 43 years respectively.

In contrast to the precipitation reconstruction, there is a much greater overlap between identified extreme years and intervals of extreme temperatures. All but one of the 15 (93.3%) extreme cool years overlap the identified cool intervals, while all three (100%) extreme warm years overlap the identified warm intervals.

The patterns of association between extreme years and intervals and periods of low and high variation are not dominated by specific associations between climate extremes and variation. In particular, while a large number (10 of 15, 66.7%) of extreme cool years are associated with periods of high variability, the fact that all 10 years occur during a single 11 year period lessens the potential impact of this association, particularly with the absence of any association between the other extreme cool years and periods of high variability. Extreme warm years show no clear association with intervals of a particular level of variation, with one of the three extreme warm years occurring during an interval of high variability and the other two extreme warm years occurring during neither high nor low variability periods. A similar lack of clear association is found when comparing defined intervals of extreme temperature to intervals of high and low variability. Specifically, two of eight (25%) cool intervals are associated with high variability intervals, one of eight (12.5%) with low variability intervals, with the remaining five (62.5%) overlapping neither high nor low variability intervals. Similarly, two of six (33.3%) warm intervals overlap high variability intervals, two (33.3%) overlap low variability intervals, and two (33.3%) overlapping neither high nor low variability intervals.

3.4.4 Integration of Precipitation and Temperature Reconstructions

After development and analysis of the regional temperature and precipitation reconstructions, Salzer (2000:81-84) discussed the intersection of the identified extreme temperature and precipitation intervals, and patterns of overlap between the high and low variability intervals for both datasets (Salzer 2000:86-88). This follow-up analysis resulted in the identification of intervals that were cool/dry, cool/wet, warm/dry, and warm/wet, as well as intervals of high variability for both temperature and precipitation, low variability for both, high variability-temperature/low variability-precipitation, and high variability-precipitation/low variability-temperature.

Visual inspection of Figure 3.2 provides a point of reference for the intersection of the extreme intervals and variability characteristics from both datasets, but in summary the following general characteristics hold:

- Thirteen intervals within the analysis period were identified which represent the intersection of extreme intervals in both the precipitation and temperature records. Four represent cool/dry intervals, four cool/wet, two warm/dry, and one warm/wet interval. The duration of these intervals is short, ranging from 2 to 12 years (Salzer 2000:Table 9).
- Six intervals within the analysis period were identified which represent the intersection of intervals of extreme variability. Two intervals represent high variability in both the precipitation and temperature records, two intervals represent low variability in both records, one interval represents high variability temperature and low variability precipitation conditions, and one interval represents high variability precipitation and low variability temperature. With the exception of the high variability precipitation/low variability temperature interval with a duration of 30 years, the other identified intervals have relatively short durations ranging from 5 to 14 years (Salzer 2000:Table 10).

3.4.5 Regional Dendroclimate Discussion

In summary, the preceding discussion of qualitative and quantitative dendroclimate reconstructions brings out several important general characteristics of previous paleoclimate reconstructions while also demonstrating important methodological issues in the construction and interpretation of these reconstructions.

Whether qualitative or quantitative, both classes of dendroclimatic reconstruction illustrate significant year-to-year variability, both in standardized tree-ring index values and in climate parameter estimates based upon those tree-ring values. This variability tends to mask short-term trends in the data, making more difficult the task of identifying and displaying trends. The smoothing methods employed in both types of reconstruction greatly facilitate the systematic identification of periods that deviate from the long-term average (e.g. identifying all periods that deviate by more than 1.1 standard deviation units from the long term mean) while also yielding graphic representations of the climate trends that are easily interpreted visually. Unfortunately, the partitioning of variation into "normal" /"extreme" categories (a condition inherent in the definition of a well-defined, but arbitrary threshold for deviations from "normal") collapses a continuum of variation into a binary (or trinary if extremely low, extremely high, and "normal" are the classes of climate conditions employed) set of categories that makes more difficult the evaluation of hypotheses regarding human response to those conditions, especially if the selected threshold for defining "extreme" conditions does not match a level at which humans decide that current conditions deviate sufficiently from a "normal" condition to produce an archaeologically observable response.

Another critical characteristic of the smoothed reconstructions is the compression of observed variation for a specified period of time into a value assigned to a given year in the reconstruction. For example, when Salzer employs a 25-year running variance in his assessment of temporal variability in the temperature and precipitation records for the San Francisco Peaks region (Salzer 2000:Figures 4,9), the value for a given 25-year variance is assigned to the middle year of the 25-year range (e.g. the variance for A.D. 570-594 was plotted at A.D. 582, Salzer 2000:Table 10). This mapping of multi-year values to a single year must be considered when linking smoothed, or otherwise modified

climate parameters to archaeologically observable trends in settlement, subsistence, or environmental response, and is a key consideration in the definition and use of climate reconstructions in the following analysis.

3.5 Paleoclimate Data Used in the Analysis

The actual dendroclimatic data used in this analysis are derived from two sources: first, an assemblage of six annual precipitation reconstructions provided by Jeff Dean and produced by the Southwest Paleoclimate Project at the University of Arizona, Laboratory of Tree Ring Research (Dean); and second, Salzer's temperature reconstruction described above (Salzer 2000).

The six precipitation reconstructions employed in the following analysis provide tree-year (August of the prior year through July of the current year) precipitation measurements (in inches) for the period overlapping the analysis period (Table 3.1).

The data from these stations illustrate similarities and differences between records, both in terms of synchronous and asynchronous trends (Figure 3.3). While the analysis presented in subsequent chapters performs a detailed interpolation based upon these data, the following discussion provides a brief sketch of the general characteristics of the six records.

The data presented in Figure 3.3 represent the annual precipitation values, a 21-year weighted moving average, with the data points centered within each 21-year range, and percentile values for the 2.5, 12.5, 50, 87.5, and 97.5th percentiles for the entire record for

Table 3.1: Precipitation Reconstruction Locations and Date Ranges

Location	Latitude	Longitude	Elevation (m)	Date Range
Canyon de Chelly	36°10'N	109°25'W	1829	A.D. 2-1988
Flagstaff	35°15'N	111°30'W	2134	A.D. 571-1988
Hopi Mesas	35°50'N	110°25'W	1829	A.D. 501-1988
Mesa Verde	37°10'N	108°30'W	2072	A.D. 481-1989
Navajo Mountain	37°05'N	110°45'W	1829	A.D. 343-1988
Tsegi Canyon	36°45'N	110°30'W	1981	A.D. 382-1988

Locations from (Dean and Robinson 1978), date ranges derived from data, with geographic locations in original cited units

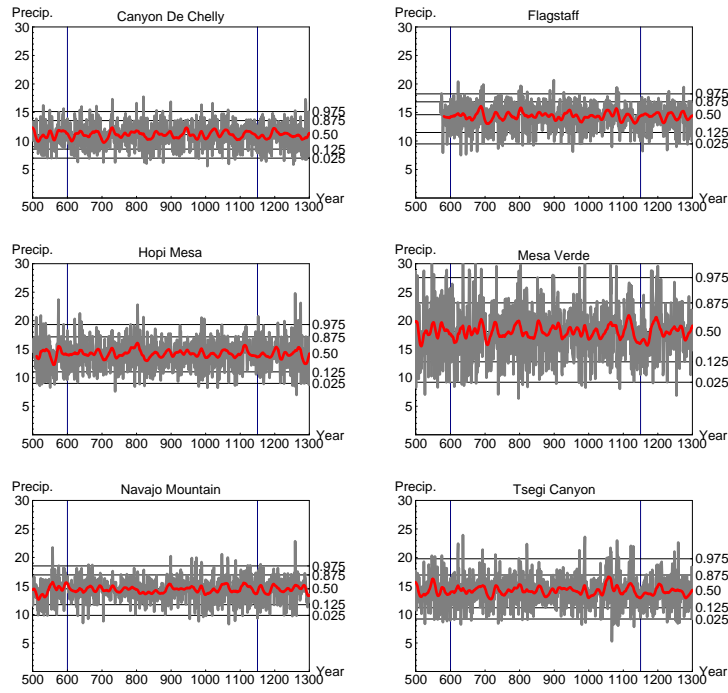


Figure 3.3: Annual and 10-Year Precipitation Reconstructions for Six Stations Surrounding the Project Area. Including 2.5, 12.5, 50, 87.5, and 97.5th percentiles for each long term record. (Dean 1999; Southwest Paleoclimate Project of the Laboratory of Tree-Ring Research 1999a, b, c, d, e, f)

Table 3.2: Paleoclimate Precipitation Quantiles (inches) for the Period of Record for Each Location

Location	2.5%	12.5%	50%	87.5%	97.5%
Canyon de Chelly	6.99	8.58	11.12	13.58	15.16
Flagstaff	9.49	11.49	14.61	16.87	18.26
Hopi Mesas	9.01	11.03	14.35	17.17	19.33
Mesa Verde	9.21	12.79	18.12	23.13	27.56
Navajo Mountain	9.84	11.72	14.5	16.94	18.52
Tsegi Canyon	9.21	11.17	14.18	16.93	19.77

each station (the "Date Range" column in Table 3.1). The axes for the individual stations represent the same ranges of time and precipitation values, and aid in the comparison of the trends for each of the six stations. Table 3.2 also presents the actual quantile values presented graphically in the plots in Figure 3.3.

Inspection of the trends represented in Figure 3.3 and Table 3.2 leads to the following observations:

- Five (Flagstaff, Hopi Mesas, Mesa Verde, Navajo Mountain, and Tsegi Canyon) of the six paleoclimate locations have roughly similar lower precipitation values, with those five having 2.5 percent quantile values within the 9-10 inch range. Canyon de Chelly has a value of 6.99 inches, over 2 inches lower than the next lowest record (Hopi Mesas).
- Four (Flagstaff, Hopi Mesas, Navajo Mountain, and Tsegi Canyon) paleoclimate locations also share similar upper quantile (97.5% quantile) values for precipitation, with those values ranging from 18.26 to 19.75 inches, a range of just under 1.5 inches. Canyon de Chelly exhibits a much lower upper quantile value, over 2 inches below the lowest value (Flagstaff) for the four stations listed above. Mesa Verde, on the other hand, has a much higher upper quantile value of 27.56 inches, nearly 8 inches higher than the highest value (Tsegi Canyon) observed for the four stations listed above.
- The trends noted in the preceding two points suggest that four stations (Flagstaff, Hopi Mesas, Navajo Mountain, and Tsegi Canyon) exhibit similar overall ranges and value for precipitation, while Canyon de Chelly exhibits a smaller range and lower precipitation, and Mesa Verde exhibits a wider range and greater precipitation.
- The 21-year smoothed trends in Figure 3.3 (the red lines in each reconstruction's plot) indicate differences between reconstructions in the interannual variation, even between reconstructions exhibiting similar ranges and values. Specifically, Navajo Mountain exhibits lower interannual variation than the other similarly ranged reconstructions — Flagstaff, Hopi Mesas, and Tsegi Canyon — while showing slightly lower interannual variation than that observed for Canyon de Chelly, a record that

has a smaller range of variation than Navajo Mountain.

- As might be expected from Mesa Verde's high range of variation, the 21-year smoothed trend plot for Mesa Verde exhibits a greater interannual variation than that observed for the other five reconstructions.
- There are particular events visible in the smoothed reconstructions that are not uniformly represented across the entire study region. For example, the distinctive peak in precipitation observable in the Hopi Mesas, Mesa Verde, and to a lesser extent Flagstaff reconstructions around A.D. 800, is nearly absent in the Canyon de Chelly, Navajo Mountain reconstructions, and shows only a minor peak in the Tsegi Canyon reconstruction.

Overall, the preceding discussion highlights some characteristics of the regional precipitation record that bear directly upon the applicability of these reconstructions to the analysis performed herein. Specifically, they demonstrate that there is variation across the region both in terms of the amount and variability of precipitation. This spatial and asynchronous temporal variability suggests that the use of several precipitation records in an interpolation of precipitation across the study area might better represent local precipitation as an alternative to the use of only the closest record, since the use of a single record does not allow for the consideration of regional patterns of variation.

Salzer's annual mean-maximum temperature reconstruction (Salzer 2000) for San Francisco Peaks (see Section 3.4.3 for a discussion of the general characteristics of this reconstruction) provides the most recent and complete regional temperature reconstruction for the area. It is based upon 234 bristlecone pine (*Pinus aristata*) tree-ring series collected from 130 trees near treeline (3535m) on Agassiz Peak (35°19'33" N, 111°40'38" W, 3766 m msl) and Humphreys Peak (35°20'47" N, 111°40'40" W, 3850 m msl) (GNIS, U.S. Geological Survey 2003) within the San Francisco Peaks north of Flagstaff, Arizona (Salzer 2000:53). This reconstruction has been subjected to the standard suite of verification and validation tests (Salzer 2000:54) and has been found to reasonably reconstruct the temperature trends for the nearby Fort Valley Experimental Research Station (4.5 km from the locations from which the tree-ring samples were collected, and lying at an elevation of 2239 m), the USHCN Station (see Table 2.4) used by Salzer in the development

of the calibration and response functions for the temperature reconstruction. Furthermore, because the Fort Valley Experimental Station temperature record was used in the calibration and response analysis for the reconstruction, the effective elevation for the derived temperature record is 2239 m, the elevation of the station.

In his analysis, Salzer found a significant positive correlation between tree-ring width and monthly mean-maximum temperatures while finding a negative correlation between tree-ring width and monthly mean-minimum temperature, and no correlation between ring width and monthly mean temperature. Furthermore, Salzer found that the strongest correlation between ring width and monthly mean-maximum temperature was found when temperature data from the prior year were used in the correlation analysis, indicating that

the period from January through December prior to the growth year is the interval when mean-maximum temperatures (daytime highs) had the most significant effect upon tree growth. Monthly mean-maximum values for this period were averaged for the years 1909 to 1994 [from the Fort Valley Experimental Station] to create the final climate series used in the reconstruction. Consequently, the variable being reconstructed is annual mean-maximum temperature. This variable can be considered a general measure of how warm it gets during the daytimes of a given year. (Salzer 2000:57)

Since local topographic effects can influence local climate (see Section 2.1.2 on page 40 for a detailed discussion of those characteristics), the tree-ring data used by Salzer in his reconstruction were derived from three loci in an effort to minimize the influence of local (i.e. local to the tree stands from which the samples were drawn) conditions on the reconstruction (Salzer 2000:54). Similarly, local conditions may adversely influence the historic climate data used in the reconstruction of temperature trends. In particular, Davey and Pielke (n.d.) found that some National Weather Service Cooperative Network weather stations in eastern Colorado, including some stations in the U.S. Historic Climate Network, are placed in locations that do not meet current World Meteorological Organization standards for instrument placement, therefore introducing the potential for non-representative temperature measurements from these stations.

This problem is unlikely for the Fort Valley Experimental Station climate record. In her paper discussing the history of the station, Olberding (2000) notes that

In January 1909, Pearson initiated a project to determine the effect of weather on ponderosa pine seed regeneration. He established six meteorological observation stations in a chain across the open park of Fort Valley, of which, three

stations were checked daily, and the others weekly. The stations monitored temperature, precipitation, relative humidity, and wind movement within the park area. (Olberding 2000:13)

This description of the distribution of the meteorological stations at the Experimental Station, in conjunction with the photo of one of the stations provided in Olberding's paper (Figure 3.4), provides evidence that the types of problems identified by Davey and Pielke, such as placement adjacent to buildings or over materials unrepresentative of general regional conditions (e.g. a gravel lot outside a building), are not present in the Fort Valley Experimental Station record.

Visual inspection of the annual and 21-year smoothed temperature reconstruction (Figure 3.5) leads to several observations regarding the specifics of the record within the period of study for this analysis. Specifically:

- The study period includes individual years and longer intervals in which temperature significantly deviates, both positively and negatively, from the long-term median value (the 50th percentile reference line in the figure)
- Following an extreme cold event in the late 7th century A.D., subsequent warm and cold events, particularly as indicated by the smoothed reconstruction, tend to vary within the range encompassing 75 percent of the variation for the entire reconstruction.
- Fluctuations in the smoothed temperature reconstruction are more extreme between A.D. 680 and A.D. 910, and after A.D. 1050, with the remainder of the analysis period representing less extreme variation.

These observations are consistent with the general trends observed by Salzer (see Section 3.4.3) and also consistent with an environment in which there is temporal variation in temperature, both in terms of temperature values and variation in temperature.



Figure 3.4: 1910 Photograph of One of the Meteorological Stations at Fort Valley Experimental Station, Arizona. (U.S. FOREST SERVICE PHOTO #90949)

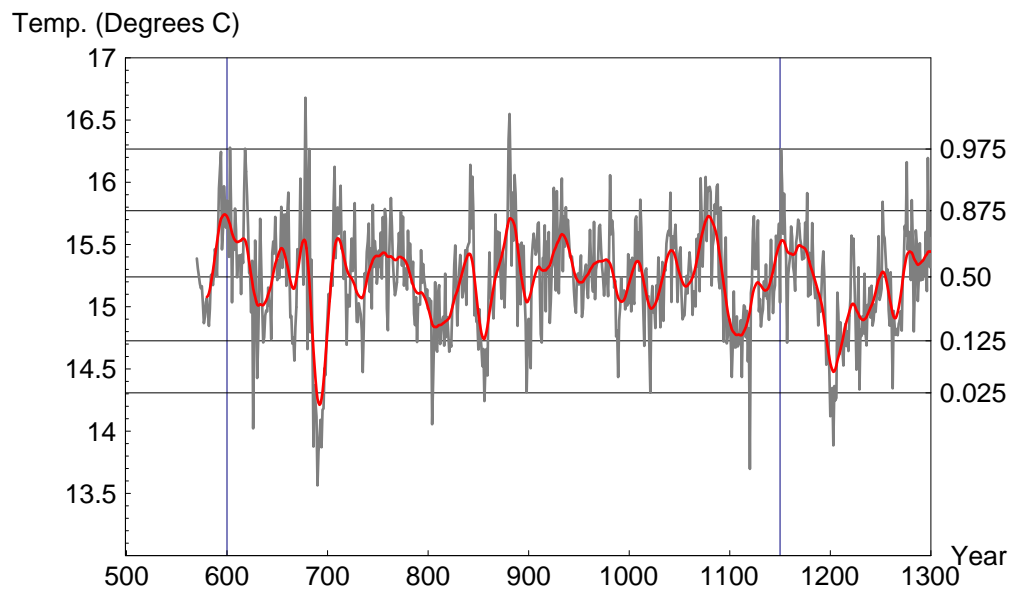


Figure 3.5: Annual and 21-year Smoothed Temperature Trends (Mean Maximum Daily Temperature °C) for San Francisco Peaks, Arizona. Including 2.5, 12.5, 50, 87.5, and 97.5th percentiles for the long term record. (data from, Salzer 2000)

3.6 Significance of Paleoenvironmental Variation and Conditions for the Analysis

This chapter has summarized the significant aspects of the environment with which the prehistoric inhabitants of the project area had to contend. These aspects include both the biotic environment from which food, fuel, and shelter must be obtained, and the climatic conditions which influence the productivity of the landscape. In both cases, the paleoenvironmental record documents variation in both the biotic and climatic realms, variation that plays a critical role in the hypotheses regarding human response to risk tested in this analysis. Without variation, uncertainty in the productive conditions from year to year and from place to place would not exist, therefore making the concept of risk defined in Chapter 1 a non-existent factor in decision making.

Chapter 4

Archaeological Background

The prehistory of the research area and surrounding region was extensively and intensively researched in the late 1960s through mid-1980s under the auspices of the Long House Valley Archaeological Project and the Black Mesa Archaeological Project. Prior to the research conducted by these projects, archaeological knowledge of the local area was based upon the pioneering work of early archaeological expeditions, including those of Wetherill in 1895 (Lebo 1991:73); Kidder and Guernsey (cited in Lebo 1991:73) in 1914-1915 (Kidder and Guernsey 1919), 1916-1917 (Guernsey and Kidder 1921), and 1920-1923 (Guernsey 1931; Kidder and Guernsey 1921); Colton in 1916, 1919, 1921, 1923, 1925 and 1926 (Brannon, et al. 1927:333); Cummings' 1920-1921 survey and excavation work in Tsegi (spelled "Segi" by Cummings) and Nitsi Canyons, and "some cave pueblos on Black Mesa near Kayenta" (National Research Council Committee on State Archaeological Surveys 1922:234-235); and Noel Morss in 1925 (cited in Lebo 1991:73; Morss 1927).

Because they provide the archaeological site data for this analysis, the emphasis in the following discussion of the archaeological background for the project areas is on data derived from the archaeological survey of Long House Valley and northern Black Mesa and the excavations on northern Black Mesa conducted under the auspices of the Long House Valley and Black Mesa Archaeological Projects.

The culture history of the region within which the study area is located consists of evidence of human occupation spanning the Paleoindian, Archaic, Anasazi, and historic periods. The following sections provide a general outline of these components of the re-

gional occupation history, with particular attention to observed patterns of site structure, land use, and subsistence that relate to the period of study and the specific patterns observed within and surrounding the study area. The final two sections of this chapter provide a synthesis of regional and local demographic patterns and a specific discussion of the site database used in the analysis.

4.1 Notes on Chronology

A variety of chronological frameworks have been developed for the study area and surrounding region over the past century of archaeological work (Figure 1.7). These frameworks include regional chronologies like those used by Cordell (1997) and Plog (1979) in their regional syntheses. At the other end of the spectrum lie the local chronologies developed for use in particular project areas and their environs. Included in this class of chronologies are the local frameworks developed for and from the Long House Valley Archaeological Project (Dean, et al. 1978) and the Black Mesa Archaeological Project (Smiley and Ahlstrom 1998b).

In the discussion that follows, the chronological framework employed in the organization of the discussion utilizes the generalized regional chronology based upon the standard Pecos Classification period designations like those employed by Cordell (1997) and Plog (1979). Within this general organizational structure, reference will be made to aspects of local chronological frameworks that articulate with the broad regional framework.

4.2 Paleoindian Period

The general sequence of southwestern Paleoindian complexes begins with Clovis (though disputed pre-Clovis remains are argued to have been discovered at Sandia and Pendejo caves), for which radiocarbon dates ranging from 11,650 to 11,000 BP have been obtained (Cordell 1997:81). Clovis assemblages typically consist of characteristic large, lanceolate, fluted, concave-based projectile points; and other tools including large bifaces, bone and ivory tools (when preservation conditions permit their survival), end- and side-scrappers, gravers, and other tools made on flakes, and blades. Lithic raw materials used in the man-

ufacture of Clovis artifacts are commonly high-quality, bedrock-derived, cryptocrystalline materials, often collected from locations distant (up to 300 km) from the locations of artifact recovery (Cordell 1997:80; Meltzer 1995). Clovis settlement and subsistence has been commonly described as a highly mobile hunting and gathering strategy that specialized in the hunting of Pleistocene megafauna, with other mammalian and plant species also playing an important subsistence role (Cordell 1997:91; Meltzer 1995; Wagstaff and Surovell 2003). In both regions, the transition to the late Paleoindian from the early Paleoindian Clovis complex is marked by the extinction of nearly 35 mammalian genera (Kelly and Todd 1988:232), and the adoption of subsistence resources more localized in their distribution than the broadly distributed megafauna exploited during the Clovis period.

Subsequent Paleoindian complexes exhibit diverse artifact assemblages and subsistence strategies, generally dividing the Southwest into eastern and western regions. The Paleoindian complex of the western Southwest consists of the Western Stemmed Point Tradition of the Great Basin and southern California, dating from 11,200 to 7,500 B.P., and was manifested in the Southwest as the San Dieguito complex; while the Paleoindian traditions of the eastern Southwest include the broadly distributed Folsom complex, and elements of the Plainview, Agate Basin, Firstview, Cody, and Jay Complexes, all defined by diagnostic projectile points (Cordell 1997:83-93).

Paleoindian utilization of northeastern Arizona and the greater Four Corners area of the Southwestern U.S. is represented by Clovis, Folsom, and late Paleoindian Plainview, Midland, and Agate Basin point finds, such as those cited by Parry and Smiley (1990), Matson (1991), and by Nichols (Nichols and Smiley 1985:52) for northeastern Arizona (e.g. Ayres 1966; Danson 1961; G. J. Gumerman 1966; B. Huckell 1982; Woodbury 1954) and southern Utah (e.g. Davis 1985, 1986; Davis and Brown 1986a, b; Hunt and Tanner 1960; Schroedl 1977), including finds near Kayenta, Arizona (north of the study area), the Hopi Mesas (at the southern end of Black Mesa), and the Shonto Canyon rim (west of the project area). In spite of these nearby finds, no definitive Paleoindian remains were encountered during the survey and excavation work undertaken as part of the Black Mesa Archaeological Project (Nichols and Smiley 1985:52; Smiley 2002a) or the survey accomplished as part of the Long House Valley Project (Dean, et al. 1978;

Gaines 1978, n.d.).

4.3 Archaic Period

Between 9000 and 8000 B.P. post-Pleistocene climatic conditions and vegetation distributions emerged (Smiley 2002a:25). In association with these changes, human populations, generally operating in small groups, adopted a more generalized hunting-and-gathering settlement and subsistence pattern that used a combination of wild plant and animal resources in a highly mobile pattern of land use over large territories. This general description holds for both the study area (W. J. Parry, et al. 1994; Smiley 2002a) and the Central Colorado Plateau in general (Matson 1991:202).

The oldest evidence for human occupation of northern Black Mesa is found in the deepest dated stratum (Stratum 14) of Tsosie Shelter, with a calibrated radiocarbon date of 8900 B.P.. While this date and the calibrated radiocarbon dates for two other coeval sites (another BMAP site, D:11:3063, and the Hastqin site, B. B. Huckell 1977; cited in Smiley 2002a) fall within the date range for the late Paleoindian, the few projectile points from these sites are consistent with those associated with the Early Archaic period, and include no points diagnostic of the Paleoindian period (Smiley 2002a).

The Four Corners Archaic is represented by sites found throughout the region, including several on northern Black Mesa and Long House Valley that were documented as part of the Black Mesa Archaeological and Long House Valley projects. Many early Archaic sites in the region consist of Pinto or similar appearing Bajada and San Jose points found in surface contexts lacking associated ceramic materials. While the exact dates of these sites are difficult to determine, they arguably may date from as early as 8000 B.P. through 3750 B.P. (W. J. Parry and Smiley 1990:51-53). Contemporaneous with early Archaic sites containing Pinto/San Jose/Bajada points are Desha Complex strata (dating from 8000-7000 B.P.) identified in two sheltered sites on Navajo Mountain in southeastern Utah: Sand Dune Cave and Dust Devil Cave. Both of these sites have yielded rich collections of organic materials, both artifactual and subsistence-related. Subsistence data from these deposits consist of

Numerous wild plant foods ... with an emphasis on dropseed (*Sporobolus*),

goosefoot (*Chenopodium*), and prickly pear (*Opuntia*). Faunal remains are overwhelmingly dominated by cottontail rabbit (*Sylvilagus*), with much less exploitation of large mammals (such as mountain sheep) than in later Basketmaker and Puebloan occupations (W. J. Parry and Smiley 1990:53-54)

Middle and late Archaic occupation data from the Four Corners are sparse, but do indicate that hunter-gatherer populations were present, though at low population levels. Evidence for middle and late Archaic utilization of the Four Corners region include numerous split-twig figurine finds in the area around the Grand Canyon in Arizona and the Green River in Utah, with the figurines dating from roughly 3000-4000 B.P. (uncalibrated radiocarbon years) (W. J. Parry and Smiley 1990:54-55).

The evidence of Archaic hunter-gatherer utilization of the study area is sparse and is comprised of a combination of radiocarbon dates and artifactual materials. The radiocarbon evidence includes nine dates obtained from two sites within the Black Mesa survey area (D:7:2085 [Tsosie Shelter] and D:11:3063) with the obtained dates ranging from 9000 B.P. to 5500 B.P.. Artifactual evidence for Archaic use of the study area consists largely of isolated projectile points and small assemblages of lithic debitage, with a large number of Archaic projectile points appearing in securely dated subsequent early agricultural preceramic and Puebloan sites (Smiley 2002a:30).

In total, the Paleoindian and Archaic record from northeastern Arizona and the greater Four Corners region represents a sparse but persistent record of resource exploitation and occupation throughout the region from the earliest Clovis occupation through the end of the pre-agricultural Archaic Period. While Berry and Berry (1986) propose a model of regional abandonment and reoccupation for portions of the Southwest, Parry and Smiley (1990:54-55) propose that the record from the Four Corners region argues against this possibility. Available Archaic subsistence data suggest the utilization of weedy annual plant species, prickly pear, and small mammals, with a less utilization of larger mammalian species than in subsequent early agricultural Basketmaker occupations. The sparse Archaic occupation of northern Black Mesa is consistent with Ford's argument that Black Mesa lacks sufficient wild plant and animal resources to provide subsistence resources for more than a handful of hunter-gatherers (Ford, et al. 1983:464).

4.4 Basketmaker II

The adoption of cultigens and the associated changes to northern Southwestern settlement and subsistence patterns marks the beginning of the Basketmaker II period and correspondingly the initiation of the Western Anasazi cultural tradition (G. J. Gumerman and Dean 1989; F. Plog 1979). The adoption of domesticates marks the end of the Archaic hunter-gatherer settlement and subsistence lifestyle, with direct radiocarbon dating of maize having great potential for identifying the timing of agricultural adoption (e.g. Smiley 1994). Some implications of agricultural adoption were noted by Ford (1983:464) for the Black Mesa region:

The critical Basketmaker II sequence indicates the continuous importance of maize agriculture for understanding Black Mesa prehistory. Without corn as a caloric source, this region would never have supported more than a few individuals for a day or two. But corn by itself was not a solution to foraging from biotic communities with low and unpredictable yields. The ecological consequence of open fields enabled edible wild plants to grow in abundance during the farming season and when old fields were left fallow. Basketmaker sites reveal the antiquity of a process that continued and expanded until Anasazi abandonment in the twelfth century.

This statement emphasizes direct and secondary subsistence effects of the adoption of cultigens. The Black Mesa Lolomai Phase Basketmaker II subsistence pattern, as defined through the recovery of botanical (Table 4.1) and animal (Table 4.2) remains from excavated Lolomai phase sites, reflects the local use of a variety of wild plant and animal species in addition to domesticated plants. The presence of maize in all but one of the dated Black Mesa Lolomai sites and all of the Marsh Pass Basketmaker II rockshelters indicates the importance of this domesticate in the local diet, though the degree of dependence remains unclear (cf. Chisholm and Matson 1994; Matson 1991:92-105).

Table 4.1: Plant Taxa from Black Mesa Subsurface Contexts

TAXON	LOLOMAI	PI ^N	PII ^N
Wood/Charcoal			
<i>Pinus</i> sp.	•	•	•
<i>Pinus edulis</i>	•	•	•
<i>Pinus ponderosa</i>	•	•	
<i>Juniperus</i> spp.	•	•	•
<i>Atriplex</i> spp.	•	•	•

(continued on next page)

Table 4.1: Plant Taxa from Black Mesa Subsurface Contexts (*continued*)

TAXON	LOLOMAI	PI ^η	PII ^η
<i>Artemisia</i> spp.	•	•	•
<i>Salix</i> sp.		•	•
<i>Populus</i> sp.		•	
<i>Salix / Populus</i>	•	•	•
<i>Quercus</i> sp.	•	•	•
<i>Chrysothamnus</i> sp.	•	•	•
Compositae	•	•	•
<i>Pseudotsuga menziesii</i>		•	•
<i>Cowania mexicana</i>	•	•	•
Compositae		•	
<i>Gutierrezia</i> sp.	•	•	
<i>Phragmites communis</i>		•	•
<i>Sarcobatus vermiculatus</i> ^β	•	•	
<i>Ephedra</i> sp.		• ^δ	•
<i>Yucca</i> sp.			•
<i>Celtis</i> sp.			• ^δ
<i>Wild Seeds/Nuts</i>			
<i>Juniperus osteosperma</i>	•	•	•
<i>Pinus edulis</i>	•	•	•
Chenopodiaceae	•	•	•
<i>Atriplex</i> sp.	•	•	•
<i>Chenopodium</i> spp.	•	•	•
<i>Portulaca</i> sp.	•	•	•
<i>Lepidium</i> ^α sp.	•	•	•
<i>Mentzelia</i> ^α sp.	•	•	•
<i>Amaranthus</i> spp.	•	•	•
<i>Cleome</i> sp.	•	• ^δ	•
Graminae	•	•	•
<i>Oryzopsis hymenoides</i>	•	•	•
<i>Bouteloua</i> sp.	•	•	•
Compositae	•		•
<i>Helianthus</i> spp.	•	•	•
<i>Sphaeralcea</i> spp.	•		• ^γ
Polygonaceae	•		
<i>Eriogonum</i> spp.	•	•	
<i>Astragalus</i> spp.	•	•	
Cactacea	•	•	•
<i>Opuntia</i> spp.	•	•	•
<i>Echinocactus</i> sp.	•	•(• ^δ)	
<i>Mamillaria</i> sp.	•		•
Malvaceae	•		
<i>Descurainia</i> sp.	•	• ^ε (• ^δ)	• ^ε
<i>Yucca</i> sp.		•	•
<i>Celtis</i> sp.			• ^δ
<i>Cultigens</i>			
<i>Zea mays</i>	•	•	•
<i>Phaseolus lunatus</i>		•	
<i>Phaseolus vulgaris</i>		•	• ^δ
<i>Cucurbita pepo</i>	• ^γ		• ^γ

(continued on next page)

Table 4.1: Plant Taxa from Black Mesa Subsurface Contexts (*continued*)

Taxon	Lolomai	PI ⁿ	PII ⁿ
●= Specifically identified taxon, * = element in a multi-taxon ID			
ⁿ All Basketmaker III materials were jointly assigned by the analysts to Basketmaker II and an additional period (e.g. BMIII/P1). Likewise, all Pueblo III materials were jointly assigned (e.g. PII/PIII). In all cases these materials were included under either PI or PII, as appropriate.			
^a Ford notes (Ford, et al. 1985) that <i>Kochia</i> identifications prior to the 1983 field season are in error and that the collections were to be reanalyzed and determined to be either <i>Lepidium</i> or <i>Mentzelia</i> . When there are not specific taxon identifications for either <i>Lepidium</i> or <i>Mentzelia</i> , <i>Kochia</i> identifications are recorded as multi-taxon IDs.			
^b Listed as <i>Sarcobatus vermiculatus</i> by Wagner (Wagner, et al. 1984)			
^c Sample from D:7:2085 assigned to Basketmaker II/Pueblo II - Pueblo III by Wagner (Wagner, et al. 1984)			
^d Sample from D:11:2068 assigned to Basketmaker III/Pueblo II by Ford (Ford, et al. 1983)			
^e Sample from D:7:2094 assigned to Pueblo I / Pueblo II-III by Ford (Ford, et al. 1983) (n=9, Cowan 1978; n=12, but overlaps with some preceding analyses, Ford 1984; n=17, Ford, et al. 1983; n=12, Ford, et al. 1985; n=23, Wagner, et al. 1984)			

Evidence for the vegetal taxa used for subsistence includes charred and uncharred plant macrofossils recovered from archaeological contexts like those on Cedar Mesa (e.g. Matson 1991), the Chinle Valley (Gilpin 1994), and Northern Black Mesa (Table 4.1 presents summary presence/absence data for 61 excavated sites from the Black Mesa Archaeological Project). These data point to an assemblage of wild plant species including goosefoot (*Cheonpodium* sp.), *Amaranthus* sp., sunflower (*Helianthus* sp.), pine nuts (*Pinus edulis*), Indian ricegrass (*Oryzopsis hymenoides*), and yucca (*Yucca bacata*). These wild species complement the widely distributed domesticate, maize (*Zea mays*), and the much less frequently encountered (at least in terms of recovered macrofossils) squash (*Cucurbita pepo*) and common bean (*Phaseolus* spp.).

Coprolite analyses from Turkey Cave on Cedar Mesa provide additional information about both the wild and domesticated plants included in the Basketmaker II diet. Twenty-eight analyzed coprolites yielded macrofossils of pinyon nuts, chenopod leaves, amaranth seeds, Indian rice grass seeds, prickly pear (*Opuntia* sp.) seeds, squash seeds, beeweed (*Cleome* sp.), bur-sage (*Franseria* sp.). A followup pollen analysis of the coprolites provided additional information regarding the presence of sagebrush (*Artemisia*), high counts of chenopod and amaranth pollen, Ambrosia (a subclass of the Compositae family), and moderate pollen frequencies for squash, beeweed, and Mormon tea (*Ephedra* sp.) (Matson 1991:92-94).

A key difference between the regional picture presented above, and the data obtained from the Black Mesa Basketmaker II sites, is the absence of a clear presence of squash

and beans during the Basketmaker II period. Macrobotanical remains of squash were recovered from one site (D:7:2085) that was assigned to the Basketmaker II / Pueblo II-III periods (Wagner, et al. 1984), while evidence for beans does not appear until Pueblo I on northern Black Mesa (see Table 4.1).

Regarding Basketmaker II use of animal resources, Leonard's (1989) analysis of faunal evidence from 64 excavated sites within the Black Mesa Archaeological Project area provides a summary of local faunal exploitation throughout the study period. An examination of Table 4.2 (a summary of the observed presence or absence of each observed taxon within each of the three periods in Leonard's analysis) indicates that a large number of taxa were recovered from archaeological contexts on northern Black Mesa, and that most of those taxa were recovered from all three temporal periods that Leonard examined. Of the 53 taxa in Table 4.2, Leonard focused his analysis on three, based upon their observed abundance: cottontail rabbits (*Sylvilagus* spp.), hares and jackrabbits (*Lepus* spp.), and members of the Order Artiodactyla.

The abundance of specimens representing *Sylvilagus*, *Lepus*, and Artiodactyla suggests the potential economic importance of these animals to the site inhabitants. To consider these three taxa separately as taxa with potential economic significance does not suggest that other taxa were not procured and/or affected by the prehistoric peoples of Black Mesa. Nor does it suggest that the only agents contributing specimens of these taxa to site deposits were human ones. This consideration only suggests that humans were a significant agent of deposition for specimens of these animals in these cultural open-site deposits (Leonard 1989:45).

While the other species listed in Table 4.2 play a role in Basketmaker II subsistence, these three taxa provide the foundation for faunal exploitation for northern Black Mesa.

Table 4.2: Animal Taxa from Black Mesa Subsurface Contexts

Taxon	Lolomai	Early-Middle Puebloan	Late Puebloan
<i>Mammalia</i>			
Leporidae	•	•	•
<i>Sylvilagus</i> sp.	•	•	•
<i>Lepus</i> sp.	•	•	•
Rodentia	•	•	•
<i>Reithrodontomys megalotis</i> ^β		•	
Sciuridae	•	•	•
<i>Cynomys</i> sp.	•	•	•

(continued on next page)

•= Specifically identified taxon, ·= element in a multi-taxon ID

Table 4.2: Animal Taxa from Black Mesa Subsurface Contexts (*continued*)

Taxon	Lolomai	Early-Middle Puebloan	Late Puebloan
<i>Ammospermophilus</i> sp.	•	•	•
<i>Spermophilus spilosoma</i>	•	•	•
<i>Spermophilus variegatus</i>		•	•
<i>Eutamias</i> sp.	•		•
<i>Thomomys</i> sp.	•	•	•
<i>Perognathus</i> sp.	•	•	•
<i>Dipodomys</i> sp.	•	•	•
Cricetinae	•		•
<i>Peromyscus</i> sp.	•	•	•
<i>Neotoma</i> sp.	•	•	•
<i>Microtus</i> sp.			•
<i>Erethizon dorsatum</i>		•	
<i>Onychomys</i> sp.	•		•
Carnivora	•		
<i>Canis</i> sp.	•	•	•
<i>Urocyon cinereoargenteus</i>	•	•	
<i>Mustela frenata</i>			•
<i>Taxidea taxus</i>	•	•	•
<i>Felis concolor</i>	•		
<i>Lynx rufus</i>	•	•	•
<i>Vulpes</i> sp.	•	•	
<i>Equus</i> ^α sp.		•	
<i>Odocoileus</i> sp.	•	•	•
<i>Antilocapra americana</i>	•	•	•
<i>Bos taurus</i> ^α	•	•	
<i>Ovis</i> sp.	•	•	•
Artiodactyla	•	•	•
<i>Capra hircus</i> ^α	•	·	•
Aves			
Passeriformes	•	•	•
<i>Accipiter cooperii</i>	•		
<i>Meleagris gallopavo</i>	•	•	•
<i>Eremophilia alpestris</i>	•		
<i>Apelocoma coerulescens</i>	•		
<i>Gymnophinus cyancephala</i>	•		
<i>Falco sparverius</i>		•	
<i>Bubo virginianus</i>		•	
<i>Aquila chryseatos</i> ^γ / <i>Haliaeetus leucocephalus</i>		•	•
<i>Buteo</i> sp.		•	
<i>Speotyto cunicularia</i>		•	
<i>Callipepla</i> sp.		·	
<i>Lophortyx</i> sp.		·	
Reptilia/Amphibia			
<i>Crotaphytus collaris</i>		•	
Serpentes	•		•
<i>Phrynosoma</i> sp.	•		•
Anura		•	
Invertebrates			
(continued on next page)			
● = Specifically identified taxon, · = element in a multi-taxon ID			

Table 4.2: Animal Taxa from Black Mesa Subsurface Contexts (*continued*)

Taxon	Lolomai	Early-Middle Puebloan	Late Puebloan
Succineidae		●	
● = Specifically identified taxon, · = element in a multi-taxon ID			
Data from Leonard (1989:Table A-1)			
Lolomai: A.D. 100-300, Early Puebloan: A.D. 800-900, Middle Puebloan: A.D. 900-1030, Late Puebloan: A.D. 1070-1150			
^α Intrusive Historic Species			
^β Listed by Leonard as <i>Reithmodontomys megalotis</i>			
^γ Listed by Leonard as <i>Acquila chryseatos</i>			
Note: Only those sites excavated as part of the Black Mesa Archaeological Project between 1975 and 1983 were included in Leonard's (1989) faunal exploitation analysis, therefore only specimens from those sites are included in this table.			

In total these data point to a local and regional Basketmaker II subsistence pattern that provides the basis for the subsequent Puebloan diet, with that diet consisting of a foundation of domesticated plants (maize, squash, and beans). Building upon the foundation of domesticates, wild plant and animals make a significant contribution to the overall diet through the provision of supplemental protein, vegetables, and storable seed and nut crops.

The development of a “gathering-hunting-horticulture subsistence economy”, as the Basketmaker II subsistence system has been described by Gumerman and Dean (1989:112), also required organizational changes in response to changing “scheduling, labor input, settlement, and demographic possibilities and constraints” resulting from the inclusion of maize into the subsistence system (Nichols and Smiley 1985:58). Among these organizational changes are modifications to the settlement system, both in terms of seasonality and stability. Specifically, the highly mobile Archaic subsistence system was replaced with a pattern of relatively permanent lowland winter occupations and summer upland occupations associated with agricultural locales (G. J. Gumerman and Dean 1989:112).

Chronologically, sites associated with the preceramic Basketmaker II period have been dated using radiocarbon dates on both charred wood and cultivated annuals (maize). Based upon these data, Smiley (1998a; 2002b) argues for the division of the Basketmaker II into early and late phases, the White Dog and Lolomai phases, respectively.

The White Dog phase of the Basketmaker II manifestation consists mainly of rock shelter sites used for storage, burial, and habitation. The Lolomai

phase consists of open-air habitation and campsites. (Smiley 2002b:39)

In combination, both phases of the Basketmaker II period span the period of roughly 4000 B.P. to 1500 B.P., immediately preceding the period of study for this analysis.

This 2500 year time span is much longer than the 500 year period (A.D. 1 - A.D. 500) to which the Basketmaker II had been previously been assigned (Euler, et al. 1979; c.f. F. Plog 1979; Smiley 1985; Smiley 2002b). Two factors contribute to Smiley's extension and refinement of Basketmaker II chronology. First, radiocarbon dates as old as 4000 B.P. have been obtained for cultigens recovered from rockshelter contexts in the northern Southwest (Smiley 1994) in addition to dates on Basketmaker II maize from the Marsh Pass area (Kidder and Guernsey 1921) that range from 3000 B.P. to 2000 B.P. (Smiley 1998a:18-19). Second, Smiley's reanalysis of the radiocarbon dates (in light of the potential effects of old wood) from open-air early agricultural sites from northern Black Mesa narrows the likely span of time for those sites to 250 years beginning roughly 2000 B.P. (Smiley 1985). These combined factors led Smiley to split the Basketmaker II period into the two phases outlined below.

4.4.1 White Dog Phase

The White Dog phase represents the earliest integration of maize into the subsistence patterns of the study area and surrounding region. Based upon direct radiocarbon dates on maize, Smiley (Smiley 1998a:19; Smiley 2002b:42) places the beginning of the White Dog phase some time between 4000 B.P. and 3000 B.P., with this initial date range derived from the earliest dates obtained from Bat Cave (3740 ± 70 B.P., 4090 cal. B.P.) (A-4187, a date that Wills finds unreliable because of potential contamination, Wills 1988:Table 18, 126) and Three Fir Shelter (3610 ± 170) (Beta-26275, Smiley 1994:Table 1), a rock shelter located on the north rim of Black Mesa. The end of the White Dog phase is marked by the appearance, by approximately 2000 B.P., of the numerous open-air settlements that characterize the Lolomai phase (Smiley 1994; Smiley 2002b:49).

Recent radiocarbon dates (Smiley 1985) obtained from cultigens recovered by Kidder and Guernsey (1921) in their Marsh Pass excavations place these materials within the White Dog Phase, as defined chronologically by Smiley (1998a:19; 2002b:42). These

materials, excavated in the early 20th century, and contributing to the definition of the pattern of Basketmaker II occupation of the northern Southwest, generally characterize the White Dog phase. Sites of this phase often contain “human burials in storage facilities and storage facilities with associated corn” and appear in sheltered locations which demonstrate remarkable similarities of artifacts from “southern Utah to the Four Corners region and from Marsh Pass to Canyon de Chelly” (Smiley 2002b:43). Three Fir Shelter is a recently excavated Basketmaker II White Dog phase site, lacking only the recovery of burial remains from the relatively small sample of the rock shelter floor area excavated (Smiley 2002b:43).

Another possible manifestation of the White Dog phase settlement pattern is found in the small number of short-occupation, open-air campsites excavated on northern Black Mesa that yielded uncalibrated radiocarbon dates clustering around 3000 B.P.. While these dates were originally interpreted as representing a late Archaic (Hisatsinom) use of northern Black Mesa (Nichols and Smiley 1985:53-57; W. J. Parry and Smiley 1990:54-55), the early dates for other Basketmaker II components now place the sites well within the time range for the White Dog phase and they potentially “comprise a component of the White Dog Phase settlement system” (Smiley 2002b:31). Similarly, two sites (SARG 2072 and 2087) within the Long House Valley survey area have assigned date ranges of 3500-1950 B.P. (Gaines 1978, n.d.), also potentially placing them within the White Dog phase. More distant non-rockshelter sites arguably associated with the White Dog phase include site HS-2 from Cedar Mesa reported by Matson (1994:234) and the Lukachukai and Salina Springs sites, of the Chinle Valley, reported by Gilpin (1994).

4.4.2 Lolomai Phase

The Lolomai phase begins by roughly 2000 B.P., and is marked on northern Black Mesa by the appearance of widespread open-air habitation sites ranging in size and occupation intensity from small camps to larger “proto-villages” of six to twelve pit structures (Smiley 2002b:49). Originally dated to a 1200 year period ranging from 600 B.C. to A.D. 600 (Andrews 1982:42), the Lolomai occupation of Black Mesa is now thought to span the period from 1900 B.P. to 1600 B.P. (e.g. Smiley 1998a:19; Smiley 2002b:50). The 1600

B.P. termination for Lolomai occupation of northern Black Mesa predates the end of the regional Basketmaker II period, which is marked by the appearance of ceramics and is generally dated to 1490 B.P. to 1320 B.P. (Nichols 2002:66).

Smiley's reassessment of Black Mesa Lolomai chronology is based upon a simulation of the effects of wood age on radiocarbon dates obtained from the open-air Lolomai sites of northern Black Mesa. This effect was modeled using ethnographically documented Navajo wood use and associated dendrochronological measurements, providing data used in the simulation of actual occupation dates from observed wood dates. The simulation suggests that an assemblage of wood-based radiocarbon dates spanning 1200 years (as is the case for the Lolomai wood dates) may be the product of a 200-300 year occupation (Smiley 1985; Smiley 1998b, c; Smiley 2002b:51-52). This resulting 200-300 year occupation, ranging from 1900 B.P. to 1600 B.P., corresponds well with all but one of the Black Mesa Lolomai maize dates (Smiley 1998d; Smiley 2002b). The northern Black Mesa Lolomai occupation corresponds with a period of regional climatic amelioration and low-frequency variation in precipitation that ended by 1700 B.P. with the appearance of higher-frequency variation in precipitation and lowering of water tables marked by floodplain degradation (Smiley 2002b:51-52).

Black Mesa Lolomai phase sites typically consist of shallow deposits (< 20 cm deep); frequent structural, intra- and extramural storage (bell-shaped pits and slab-lined cists), and cooking features (hearths and roasting pits); a variety of artifactual materials including flaked and ground stone tools and debitage, with much of the flaked stone being made from locally available white baked siltstone; and small animal bones and carbonized plant remains recovered through excavation, screening and flotation. Smiley (2002b: 53) defines four classes of Lolomai sites within the Black Mesa assemblage:

- (1) proto-villages or settlements with from six to twelve structures; (2) habitation sites with earthen storage pits and a few small subterranean and surface structures as well as external storage pits; (3) non-storage habitation sites with a few surface or shallow pit structures; and (4) campsites consisting of small clusters of hearths surrounded by lithic scatter

In general, the Lolomai sites on northern Black Mesa lie along the major drainages, at locations that also provide ready access to wild plant and animal resources, water, fuel, and arable land. Smiley (2002b: 59) concluded that

The site locations, thus, appear not to be particularly sensitive to elevational or resource locational criteria within the pinyon and juniper zones of the study area.

The various site classes occur in a variety of landform settings and vegetational contexts. Furthermore, Lolomai sites tend to be positioned on relatively flat locations or locations that are topographically oriented away from the direction of the local prevailing winds (west or southwest) (Smiley 2002b:59).

Basketmaker II sites in Long House Valley include rockshelter habitation, storage, and burial sites in the narrow Kin Biko canyon. Hunting and gathering camps are found throughout the western portions of the valley and on the adjacent Shonto Plateau, particularly in the vicinity of the Kin Biko rockshelter sites. This pattern of sites is interpreted to represent a seasonal round of gathering, hunting, and farming activities undertaken from “semi-permanent base camps” (Dean, et al. 1978:32-33).

4.4.3 Basketmaker II Summary

In total, the Basketmaker II period represents the first appearance of a lifestyle predicated on the use of cultigens and a reduction in mobility that appears at the beginning of Basketmaker II. The adoption of cultigens allowed highly mobile Archaic populations to occupy locations that had not previously been available for regular utilization due to their low wild resource productivity (Ford, et al. 1983; Matson 1991:92). With this change in mobility came modifications in the structure and configuration of the settlement and subsistence system that were manifest in new forms of habitation sites, modified seasonal dynamics of land use, increased use of storage features to mitigate uncertainty in food productivity, and changes in artifact assemblage characteristics.

4.5 Basketmaker III

The Basketmaker III (BMIII) period in the northern Southwest is marked by the first appearance of ceramics, the replacement of the atlatl with the bow and arrow, broad evidence for bean agriculture (Nichols 2002; P. F. Reed 2000), increased sedentism, an inferred increased dependence upon agriculture, and the development of larger and

more highly structured villages of slab-lined pithouses in association with lowland alluvial floodplains amenable to groundwater farming (G. J. Gumeran and Dean 1989:113-115).

Chronologically, the BMIII is variously assigned to A.D. 400/450 to 700/750 (P. F. Reed 2000:7), A.D. 550 to 825 (G. J. Gumeran and Dean 1989:113), and A.D. 600 to 850 (Nichols 2002:66). The early start date provided by Reed (2000:7) is based upon early radiocarbon dates for brown ware ceramics, beans, and arrow points from Rainbow Plateau (Geib and Spurr 2000) and sparsely distributed brown ware ceramics elsewhere on the Colorado Plateau (L. S. Reed, et al. 2000). Diagnostic BMIII ceramics include plain gray wares, Lino Gray, Lino Fugitive Red, and small amounts of plain redwares and Lino Black-on-gray (Nichols 2002; Nichols and Smiley 1985). Locally, the Dot Klish phase in the Black Mesa chronology correlates with the BMIII, with the primary difference being the use of the later initiation date of A.D. 600 as opposed to the more broadly applicable early dates used by Reed.

In spite of upland abandonments, the onset of the BMIII settlement pattern is associated with a rapid regional population increase followed by a period of slowly increasing population between A.D. 600 and 800 (Dean, et al. 1994:Figure 4.2, 60). Basketmaker III settlement patterns reflect a general trend towards the development of large pithouse village settlements in lowlands adjacent to alluvial floodplains with access to groundwater, and a virtual abandonment of uplands for habitations.

BMIII is fairly well represented in the sample of excavated sites, and survey reveals such sites to be abundant. Canyon and valley sites in the Red Rock (Morris 1980), Chinle (Bannister et al. 1968:67-68), Laguna Creek (Haury 1928), and Klethla (Ambler and Olson 1977) Valleys, in Canyons del Muerto (Morris 1925, 1936) and de Chelly, in Tsegi and Navajo Canyons, along middle reaches of the Tusayan Washes on Black Mesa (Klessert 1982a, Linford 1982; Ward 1976), and on Antelope (Daifuku 1961) and Second Mesas (Sebastian 1985) provide information on Western Anasazi BMIII. (G. J. Gumeran and Dean 1989:113-114)

Dean et al. (1978) in their discussion of BMIII occupations in Long House Valley noted small habitation sites along the valley margins, and the development of "special use sites" (e.g. field houses) on the edge of the floodplain and on the Shonto Plateau. The Black Mesa side of Long House Valley appears to have been little used, and the rockshelters that were occupied during BMII were abandoned and little used during BMIII.

In conjunction with the establishment of larger pithouse villages in well-watered lowland locations, many upland locations that have evidence for BMII occupation have little to none for BMIII until nearly the end of the period. These locations include northern Black Mesa, the Red Rock Plateau, Cedar Mesa, and several locations north of Navajo Mountain (Nichols 2002:70).

This change in settlement pattern is ascribed to the establishment of year-round residences at lowland locations where agricultural production had the greatest probability of success while also providing access to nearby wild plant and animal resources. Local characteristics argued to contribute to the selection of particular locations include “deeper alluvium, longer growing seasons, and higher water tables” (G. J. Gumerman and Dean 1989:114). The absence of visible upland occupations during most of the BMIII has been attributed to a variety of causes (Nichols 2002:72), including:

- Actual abandonment in the face of deteriorating hydrologic conditions in upland areas
- Low population levels, contributing to differential occupation of locations that best meet the criteria listed above
- Changing patterns of land use in which decreased mobility contributes to a more “logistical” (Binford 1980:10-12) organization of settlement and resource procurement (G. J. Gumerman and Dean 1989:114).

All three of these factors likely contribute to the observed changes in the site distribution pattern between BMII and BMIII. Under low population conditions, deteriorating hydrologic conditions might lead to a shift in agricultural activities to available lowland locations with more dependable water resources. The predictability of agricultural production at these locations may well have led to the establishment of the larger year-round residential occupations observed at the preferred lowland locations. Upland wild resources may still have been used, but because of their dispersed nature and low productivity in many upland areas (Ford, et al. 1983; Matson 1991:92), logistical activity locations (i.e. field camps, stations, and caches, Binford 1980:10-12) might be of such low visibility that they have not been identified as part of the BMIII settlement system.

Alternatively, Plog (1986a:54-58, 78) and Powell (1983:22) have argued that the relative absence of Black Mesa BMIII (Dot Klish) sites may be an artifact of the low frequency of diagnostic ceramics on Black Mesa sites for this period. Finally, Gumerman and Euler (G. J. Gumerman and Dean 1989:114; 1976:165) argue that the BMIII preference for low knolls, sand dune areas and low river terraces and the potential for substantial alluviation in these areas, would contribute to a visibility problem for many Dot Klish sites within the BMAP project area.

The observed shift in settlement focus to locations of high agricultural potential has led many researchers to infer an increased reliance on cultigens during BMIII in contrast to BMII (e.g. G. J. Gumerman and Dean 1989:114; T. N. V. Karlstrom, et al. 1976:153; Nichols 2002:67; S. Plog 1986a:79), though the degree of reliance and the consistency of broad regional changes continue to be debated (Nichols 2002:67). The appearance of domesticated beans (*Phaseolus* spp.) within the regional subsistence system is one of the defining characteristics of BMIII, and occurs as early as A.D. 425-660 (2-sigma, calibrated radiocarbon date) on the Rainbow Plateau, with the recovery of a single whole bean from Atlatl Rock Cave . Evidence for turkey (*Meleagris gallopavo*) husbandry is found in Atlatl Rock Cave in the same deposits from which the bean was recovered (Geib and Spurr 2000:197-198).

Within the BMAP project area, domesticated common beans (*Phaseolus vulgaris*) were recovered in large quantities from a burned store room on site D:11:2068 that was dated to BMIII/PII-III (Ford, et al. 1983:Table 157), pointing to the potential availability of this domesticate on northern Black Mesa by the end of BMIII. The paucity of material recovered from definitive BMIII (Dot Klish) contexts within the project area (Leonard 1989:11) prevents a detailed assessment of the wild resources potentially used during BMIII, but the relative consistency of taxa across the Lolomai, PI, and PII periods in Table 4.1, and across the Lolomai, Early-Middle Puebloan, and Late Puebloan periods in Table 4.2 suggests that while emphasis on particular taxa might have varied, it is likely that the full range of wild and domesticated taxa enumerated in these tables were employed throughout the BMIII period.

With the advent of the BMIII period, site structure and composition changed relative to the patterns observed during BMII. Specifically, pithouse village sites containing rel-

atively standardized slab-lined pit structures appeared, replacing smaller BMII pithouse sites containing more variable pit structures. Basketmaker III pit structures possess

a fairly standard set of floor features including fire and ash pits, low clay ridges delineating functionally specific areas of the floor, small intramural storage pits, and sometimes grinding equipment. Commonly, one to three circular slab-lined storage cists were set into the ground behind each pithouse. (G. J. Gumerman and Dean 1989:114)

In addition to these more standardized characteristics for individual pithouses, the layout of larger pithouse villages reflects increasing formalization. In particular, the larger sites exhibit a site layout in which individual pithouses are “laid out according to topographic features or arranged in parallel rows” (G. J. Gumerman and Dean 1989:114). Communal architecture, as represented by a possible “great kiva” at the large Juniper Cove site, also first appears in the northern Southwest for the first time during the BMIII period (Nichols 2002:73-74; Powell 2002:97).

In summary, while the BMIII period represents continuity of development from the BMII agricultural economy, there were changes in technology, land-use, settlement structure, and subsistence economy that differentiate BMIII from BMII. Technologically, BMIII is defined by the first appearance of ceramics and the bow and arrow, both of which appeared on the Rainbow Plateau as early as A.D. 175 (Geib and Spurr 2000). Basketmaker III land-use patterns shifted from an upland/lowland residential pattern evident in many areas of the northern Southwest during the BMII period, to one with larger pithouse villages located in agriculturally productive, well-watered lowland locales. Settlement structural changes in BMIII include the adoption of more standardized pithouse structure forms and the development of more formalized site layouts in the larger pithouse villages that developed during this period. Finally, in spite of evidence for the availability of beans in some BMII sites (see 4.4 above), BMIII is also defined by the broad appearance of beans as part of the suite of cultigens within the subsistence system.

4.6 Pueblo I

The Pueblo I (PI) period in the northern Southwest represents a “continuation and elaboration of the BMIII pattern” (G. J. Gumerman and Dean 1989:116) of settlement and

subsistence. In particular, people maintained a commitment to cultigens while continuing to use a broad range of wild plant and animal resources. The locations of residential sites expanded to include previously abandoned upland areas on northern Black Mesa, particularly those adjacent to major drainages, and floodplain areas avoided during the BMIII period. Pithouses remain the standard residential structure, though with the elimination of the antechamber component observed in BMIII pithouses. Pueblo I artifact assemblages are similar to those of BMIII, only exhibiting stylistic changes and modifications in manufacturing processes (G. J. Gumeran and Dean 1989).

Chronologically, the PI period begins early in the 9th century A.D., and ends by A.D. 1000 (G. J. Gumeran and Dean 1989:115), with the majority of sites assigned to this, and other, Puebloan periods, via ceramic dating (Powell 2002:85). Ceramics of this period are dominated by graywares, with Black Mesa ceramics predating A.D. 1025 including plain (Lino Gray), neck-banded (Kana-a Gray), and Lino Tradition graywares, in addition to Kana-a Black and White (Nichols and Smiley 1985; Powell 2002:85). The regionally defined PI period overlaps several phases of the Black Mesa chronological framework, including the end of the Dot Klish (A.D. 600-800), Tallahogan (A.D. 800-900), Dinnebito (A.D. 900-975), and Wepo (A.D. 975-1050) (Smiley and Ahlstrom 1998b).

Pueblo I settlement patterns reflect a continuation of those established in BMIII times, with expansion to new locations in some areas. In Long House Valley, the pattern of sites remains the same as observed during BMIII, with no use of Kin Biko canyon, continued use of the floodplain areas for agriculture, limited use of the Black Mesa side of the valley, pithouse occupations along the margins of the valley, and special use sites located on the Shonto Plateau (Dean, et al. 1978:33). Regionally, territorial expansion is observed through the establishment of a widespread distribution of new settlements in floodplain regions that had previously been avoided, and upland areas, including northern Black Mesa, that had been abandoned during BMIII (G. J. Gumeran and Dean 1989:115-16; Powell 2002:104). Powell (2002:106) notes that

Much simplified, Pueblo I and Pueblo II regional settlement patterns suggest expansion out from low-lying Basketmaker III occupation zones into highlands and to the west. Many of the new sites are small, lacking ceremonial structures, storage facilities, trash accumulations, and burials, suggesting that the people occupying them maintained social and ceremonial ties to more

established villages that had these facilities and capabilities.

This statement regarding the dispersal of sites into floodplain and upland locations highlights the importance of the presence or absence of particular feature classes for differentiating between inferred site activities.

Site structure during Pueblo I represents continuity and modification of form for pithouse structures, continuity of surface storage facilities, the disappearance of "great kivas", and the development of below-ground ceremonial chambers (kivas) (Dean 1996b; G. J. Gumerman and Dean 1989; Powell 2002). Pithouse structures maintain the same suite of ventilator and floor features observed during the BMIII, but lack the antechamber present in previous pithouses. Pueblo I pithouses are associated with a variety of external surface features, including storage (slab-lined cists, jacal, slab-lined, and masonry), and work areas (G. J. Gumerman and Dean 1989:116). With PI, the large pit structures called "great kivas" disappear, and smaller pit structures with features infrequently found in habitation structures appear. Some of these structural features include ventilators, partial or full benches, numerous floor features, and in many instances have earthen walls and plastered floors (Powell 2002:97-98).

In a situation similar to that seen at the beginning of the BMIII period, the beginning of the PI period is associated with a brief but rapid regional population increase between A.D. 800 and 850. Following A.D. 850, regional population increases slowly until A.D. 950, when a period of uneven but rapid population increase begins (Dean, et al. 1994:Figure 4.2, 60)

Pueblo I subsistence also represents continuity from the BMIII pattern of mixed farming and wild resource hunting and gathering. As illustrated in Tables 4.1 and 4.2, recovered plant and animal remains represent a wide range of wild animal and plant taxa in addition to the three major cultigens (maize, squash, and beans) (Powell 2002:90-94).

In summary, the PI period may be characterized as a time when settlements expanded into areas unoccupied during BMIII while continuing to pursue a mixed subsistence system that includes both wild and domesticated food resources. Site features expanded to include subsurface non-habitation chambers and an expanded suite of above surface storage and non-storage features.

4.7 Pueblo II

The Pueblo II (PII) period reflects a time of changing patterns of population aggregation, the appearance of standardized unit pueblo homesteads throughout the Kayenta Anasazi region, and the development of more clearly defined and identifiable kiva structures (Dean 1996b; G. J. Gumeran and Dean 1989; Powell 2002).

Chronologically, the PII period begins at A.D. 1000 and lasts until A.D. 1150 (G. J. Gumeran and Dean 1989:117), and overlaps the following Black Mesa Chronology phases: Wepo (A.D. 975-1050), Lamoki (A.D. 1050-1100), and Toreva (A.D. 1100-1150) (Smiley and Ahlstrom 1998b). On northern Black Mesa, beginning between A.D. 1025 and 1050, the plain-bodied graywares that characterized PI were replaced with corrugated graywares, often of the Tusayan Corrugated type (Powell 2002:95). Polychrome ceramics appear after A.D. 1050. Whitewares consisting of Dogoszhi Black-on-white, Sosi Black-on-white, and lower frequencies of Flagstaff Black-on-white appear during the Toreva (A.D. 1100-1150) phase within the northern Black Mesa Peabody leasehold (Nichols and Smiley 1985:75).

The pattern of population dispersal initiated during PI continued with the establishment of numerous homesteads and a reduction in size of the large villages found during the BMIII and PI periods. These homesteads were eventually distributed throughout the region, with Gumeran and Dean (1989:118) noting that:

In the Kayenta nuclear area, PII habitations occupied virtually every conceivable spot. Only the aggrading surfaces of the floodplains were shunned, although even brief interruptions of sediment accumulation induced habitation construction on the floodplains.

This broad expansion of sites throughout the region (including Long House Valley and northern Black Mesa) is interpreted as reflecting population growth and territorial expansion (Dean, et al. 1994:60; G. J. Gumeran and Dean 1989:117), with some of the large-scale patterns of population change correlated with low- and high-frequency climate fluctuations. Growth between A.D. 950 and 1100 correlates with a period of climatic conditions conducive to floodwater farming, while a dip in regional population between A.D. 1100 and 1200 correlates with a period of stream degradation and a brief but severe drought (Dean, et al. 1994:60). Related to this regional population increase

and drop are local population changes that include first rapid population growth between A.D. 1000 and 1100 and the abandonment of northern Black Mesa between A.D. 1100 and 1150 (e.g. Dean, et al. 1985; G. Gumerman and Powell 1981; G. J. Gumerman 1988; G. J. Gumerman and Dean 1989; T. N. V. Karlstrom, et al. 1976). Long House Valley exhibits rapid population growth throughout the PI period that continues until the late 12th century (Dean 1996b:Figure 3.3; Dean, et al. 1978:33).

Architecturally, the widespread PII habitation sites reflect an increasingly standardized layout of masonry storage roomblocks, above-ground jacal habitation structures abutting each end of the roomblock, a kiva, and midden. The general orientation of this assemblage of settlement features is along a northwest to southeast axis. Referred to as unit pueblos, these sites represent a frequently observed, if not ubiquitous, residential site (Powell 2002:96-97).

While the broad distribution of sites throughout all habitable regions is argued to have “curtailed gathering and hunting as humans appropriated habitats formerly occupied by wild plants and animals” (G. J. Gumerman and Dean 1989:117), there is ample evidence for continued use of a mixture of wild and domesticated food resources. Specifically, palynological and macrobotanical analyses of materials recovered from the BMAP area indicate that the range of wild and domesticated plant species employed during PII times changed little when compared to the preceding periods (Table 4.1 and Powell 2002:91). Leonard’s (1989) analysis of BMAP faunal materials is also consistent with continued use of a wide range of animal resources, with a continued emphasis on *Lepus*, *Sylvilagus*, and artiodactyls (Table 4.2).

Non-ceramic artifact assemblages for the PII period differ little from preceding periods with the exception of reductions in the quantity and quality of lithic projectile points (G. J. Gumerman and Dean 1989:119) and an increase in the proportion of two-handed manos (Nichols and Smiley 1985:77). In spite of the relative consistency of artifact assemblage composition, PI lithic raw materials and ceramic styles begin to exhibit a localization of artifact traditions, with use of local raw material sources and stylistic distributions shrinking in geographic extent (G. J. Gumerman and Dean 1989:119).

In total, PII represents continuity in subsistence, continued territorial expansion and population growth, and the development of widely distributed smaller sites throughout all

habitable areas of the Kayenta region. Both domesticated and wild resources continued to play important roles in the overall subsistence system. The widespread distribution of habitation sites during PII is inferred to reflect a period of rapid population growth that is correlated with a period of climatic conditions amenable to floodwater farming, with the only population shrinkage occurring during a period of drought and falling water tables.

4.8 Pueblo III

The Pueblo III (PIII) period represents the final period of the Puebloan sequence in the Kayenta region, the development of large aggregated settlements, and the eventual abandonment of the region by A.D. 1300. While this period post-dates the period of analysis, this brief discussion is provided to complete the descriptive archaeological context for the broader region.

For the purposes of this discussion, PIII is defined as covering the period from A.D. 1150 through 1300. This date range is a combination of the Transition Period (A.D. 1150-1250) and Tsegi phase (A.D. 1250-1300) defined by Dean (1996b) for the Kayenta region, and the Transition (A.D. 1150-1250) and Pueblo III (A.D. 1250-1300) periods defined by Gumerman and Dean (1989) for the Western Anasazi area.

The common identification of a Transition period in the chronological PIII chronological frameworks referenced above highlights the different characters of the two phases. The Transition period represents a period over which the widely distributed assemblage of relatively small unit pueblos was replaced by a small number of large aggregated sites. This period also represents a continuation of the pattern established on northern Black Mesa at the end of the previous period, an abandonment of upland locations and a general contraction of settlements into central areas with access to arable land and water. This trend towards population aggregation culminates in the settlement pattern of the Tsegi period (Dean 2002), in which clusters of habitation sites form large pueblos in Long House Valley and other well-watered locales in the region (Dean 1996b; Dean, et al. 1978; G. J. Gumerman and Dean 1989).

Architecturally, PIII is marked by significant changes in architectural organization. During the Transition period unit pueblos increased in size and large pueblos organized

around central plazas appeared for the first time (Dean, et al. 1978). Gumerman and Dean (1989:121) recognize two Transition Period site types: “randomly scattered pithouses associated with masonry-lined kivas”, and “a more traditional pueblo configuration with a masonry roomblock facing and open or enclosed plaza containing one or more kivas”. The size of these sites ranges from fairly small for the pithouse-kiva sites, to moderately large (as many as 50 rooms) for the pueblos. In contrast, three site types are identified for the Tsegi phase:

Plaza-oriented sites consist of masonry roomblocks situated on one to four sides of an open or enclosed plaza that contains one or more kivas. Most large open sites and nearly all central pueblos are of the plaza type...*Room Cluster* sites lack central plazas. Instead, the room clusters are grouped around single or multiple courtyards, or are oriented along formal walkways or “streets.” ...*Pithouse* sites, consisting of loose agglomerations of rather informal subterranean habitation structures often grouped around a central pueblo, are fairly abundant in the Klethla Valley (Haas and Creamer 1985), less so elsewhere. (G. J. Gumerman and Dean 1989:125)

Increased investment in agricultural production is evident during the Transition period, with the first appearance within the area of soil and water control and storage features. This increased investment is interpreted as representing agricultural intensification and an increased reliance on cultigens (Dean 2002:127). A large number of special use sites on the Shonto Plateau and Kin Biko suggest a continued importance of wild resources for the Long House Valley population during both the Transition and Tsegi periods (Dean, et al. 1978; G. J. Gumerman and Dean 1989:125).

The changes seen between the pre-PIII settlement system and the Tsegi phase pattern have been ascribed by Dean (Dean 2002) to environmental deterioration and population response to that change. In particular, population aggregation is seen as a response to the reduction in arable land due to arroyo cutting while the development of a multi-tiered settlement hierarchy within Long House Valley is seen as an organizational response to a combination of high population, decreasing landscape productivity, and increasing labor requirements for maintaining agricultural productivity. By A.D. 1300, the Kayenta area was abandoned, indicating that the adaptive system that developed within the late 14th century cultural and physical environment ultimately failed to sustain the local and regional population (Dean 2002:157).

4.9 Demography

There are three aspects of regional demography that are important for the analysis: 1) the total regional population trend, 2) the local population trend for Long House Valley, and 3) the local population trend for the BMAP study area (Figure 4.1).

The regional population trend (Figure 1.8, based upon Dean, et al. 1994:Figure 4.2) is important because it defines the larger demographic context within which the local populations lived. It also provides a regional synthesis of multiple population curves that, while probably underestimating actual regional population, “probably accurately portrays the trajectory of population variability” (Dean, et al. 1994:60).

The Long House Valley site frequency curve presented in Figure 1.8 is based upon a count of sites in the Long House Valley SARG database (Gaines n.d.) that have assigned date ranges that overlap each year in the plot, with years with changes in the number of sites connected with straight lines. This procedure for generating the demographic curve results in a more smoothed trend line than would be obtained by plotting each year's site count, since the annual site counts display a stepped line that abruptly changes at the phase boundaries used by the Long House Valley project. While not representing actual population (population aggregation into large pueblos after A.D. 1150 skews the estimation of population from site frequency), the frequency of sites within limited periods of time will provide a reasonable proxy for use in the analysis for weighting sites for subsegments of their occupation span in the analysis.

The Black Mesa population curve presented in Figure 1.8 is based upon the population reconstruction developed by Plog (1986b: Figure 43, Table 68). Plog's estimate is based upon five-year interval occupied structure counts, using an assumption of 25-year occupation duration within each site. Plog developed this reconstruction using a combination of excavation and survey data from the 1975 field season in which 796 prehistoric loci representing 820 occupations (S. Plog 1986a:63; 1986d:49) were documented within the 120.4 km^2 eastern lease area of the Black Mesa Archaeological Project study area (Figure 4.2). The number of rooms for each survey site are estimated using a regression equation derived from room counts, site area, and artifact density from twelve excavated habitation sites within the eastern lease area (S. Plog 1986b:232). The dates for each

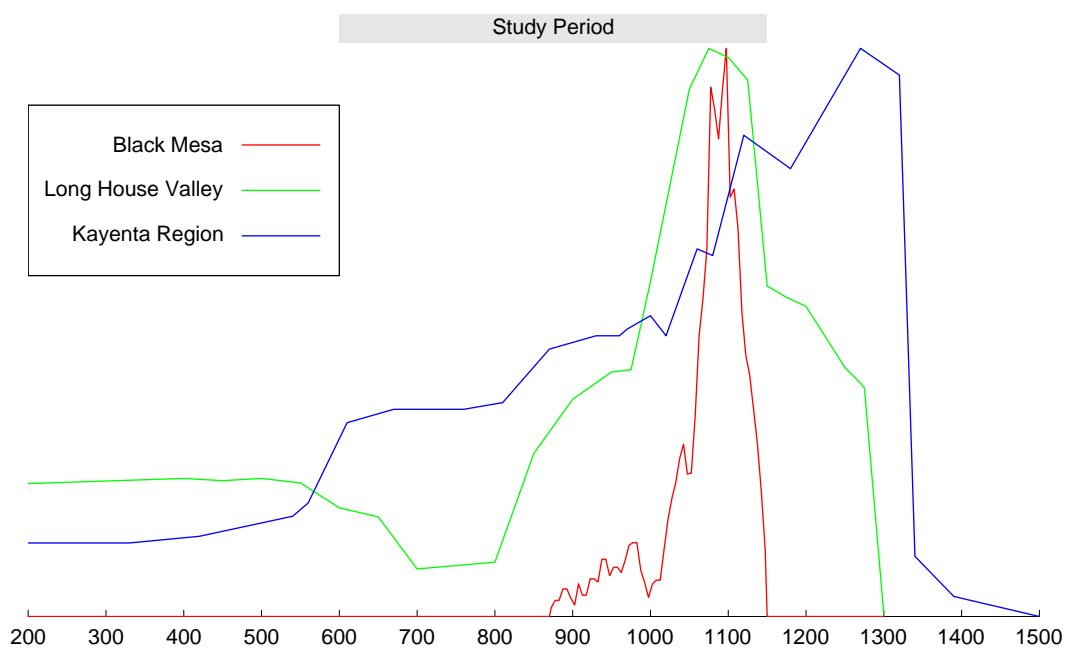


Figure 4.1: Population Curves for the Kayenta Region, Long House Valley, and Black Mesa Archaeological Project Area (see text for a description of how these curves were generated)

survey site in the eastern lease area are calculated based upon a ceramic attribute multiple regression model that is based upon dendrochronological data and ceramic attributes from 22 excavated sites (S. Plog and Hantman 1986:Table 19) from both the eastern and western lease areas of the Black Mesa Archaeological Project study area. Because it is based upon a large proportion of the Black Mesa Archaeological Project site sample, and a reasonable spatial sample of the analysis area, the resulting high-resolution demographic reconstruction provides a reasonable model for relative population trends throughout the Black Mesa study area.

All three population curves in Figure 1.8 have standardized to a scale ranging from 0 to 1, with 0 representing a population/site/structure count of 0 and 1 representing the maximum number of people/sites/structures for the entire analysis period. This standardization process allows for the depiction of reconstructions based upon different observation units, while maintaining internal consistency within each plot line. The standardized demographic curve for the Kayenta region provides the population scale that is used as the population component in hypothesis tests relating risk response to population. The standardized demographic curves for Long House Valley and Black Mesa provide the weighting factors for the sites in each portion of the study area (see the analysis chapter for a description of the weighting algorithm employed in the analysis).

In total, these demographic reconstructions reflect the population trends noted in the archaeological period descriptions. In particular, all three curves depict relatively low population levels both locally and regionally prior to A.D. 550. Following A.D. 550 the regional population curve begins a stair step period of growth that exhibits periods of relatively rapid growth at the onset of each period followed by periods of slow growth until the beginning of the next period. In spite of the regional trend, Long House Valley exhibits a reduction in population between A.D. 600 and 850, while northern Black Mesa maintains a low or non-existent level of population until A.D. 850, when population began to grow. Both Long House Valley and northern Black Mesa exhibit population growth between A.D. 850 and 1100, at which point Long House Valley site counts begin to decline (more a result of population aggregation than population decline (Dean 2002; Dean, et al. 1978) and the rapid abandonment of northern Black Mesa begins. Both of these declines correlate with a period of regional population decline at about A.D. 1150.

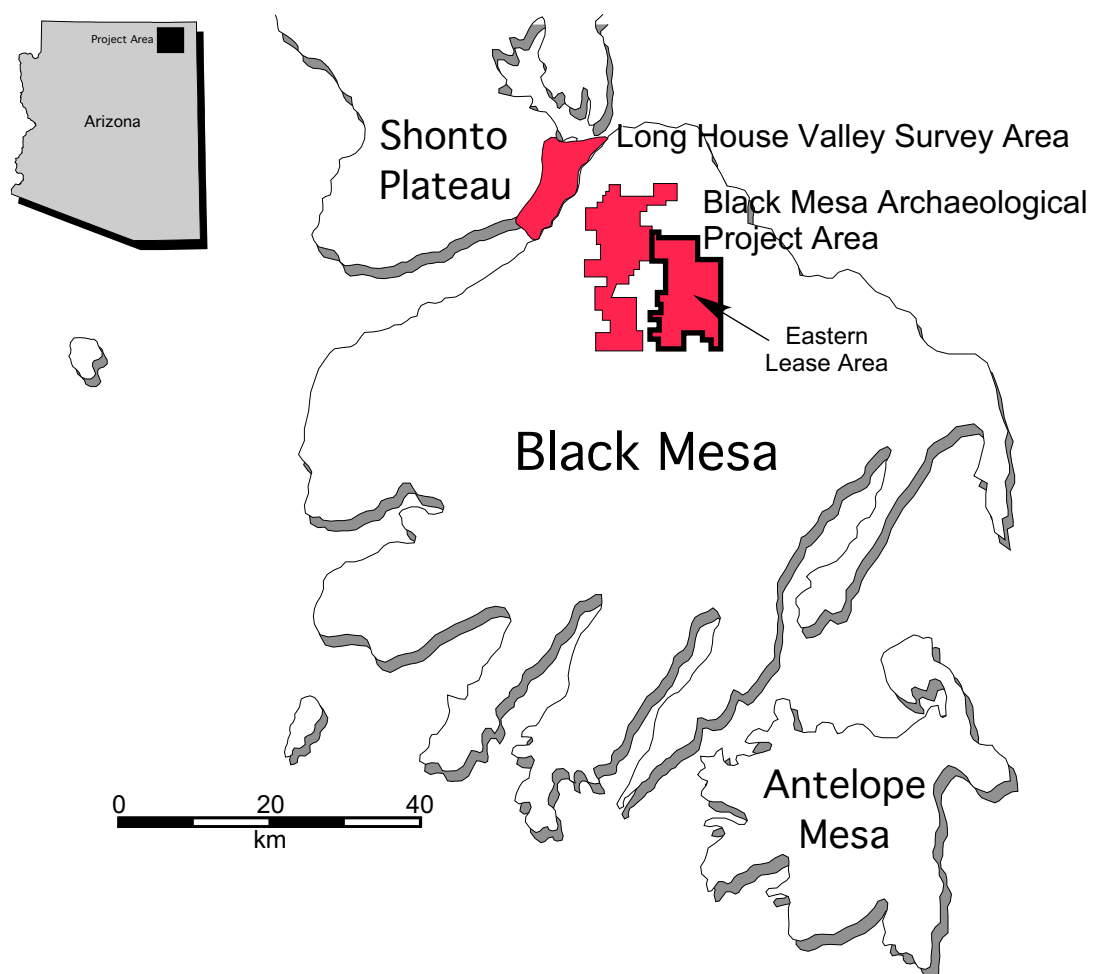


Figure 4.2: Location of Eastern Lease Area Within the Black Mesa Archaeological Project Area (S. Plog 1986c: Figure 2, pg. 6)

Following the abandonment of northern Black Mesa by A.D. 1150, the rate of decline in Long House Valley site counts slows and regional population rebounds and grows through A.D. 1250, at which point both regional and Long House Valley population declines, ultimately reflecting regional abandonment by A.D. 1300.

4.10 Sites Used in the Analysis

The above summary of regional culture history provides the archaeological context for the analysis including the overarching chronological framework within which patterns of settlement variation are evaluated. The database of archaeological sites used in the analysis consists of two separate tabulations of site data, one for each of the archaeological projects. The tabulated data for the Black Mesa Archaeological Project study area are based upon the archaeological site compliance summary for the project (Robison 1984), while the data for the Long House Valley Archaeological Project are based upon the SARG database compiled from the survey data (Gaines 1978, n.d.).

Both tabulations encode site attributes that include location (in UTM coordinates), project site number, chronological assignment (either as a phase assignment [Black Mesa], or as a date range [Long House Valley]), and frequency or presence/absence data for a variety of artifact classes and features (Table 4.3). Section 5.3.1 outlines the method used to merge these separate tables while Appendix F provides a listing of all sites in the combined database with the merged site attributes used in the analysis.

Table 4.3: Archaeological Site Database Field Names/Descriptions

Long House Valley Fieldnames	Black Mesa Fieldnames
SARG SITE NUMBER	SITE NUMBER (BMAP)
UTM ZONE	UTM ZONE
METERS NORTH	EASTING
METERS EAST	NORTHING
INITIAL DATE	PHASE
TERMINAL DATE	RUBBLE MOUNDS
MEDIAN DATE	SLAB LINED
PROJECT AREA SIZE	STAINS
SITE TYPE	MIDDENS
SITE SIZE	KIVA DEPRESSIONS

(continued on next page)

Table 4.3: Archaeological Site Database Fieldnames (*Continued*)

Long House Valley Fieldnames	Black Mesa Fieldnames
DEGREE OF NATURAL SHELTER	PITHOUSE DEPRESSIONS
SUMMARY DESCRIPTION	RED WARE
ROOM COUNT	WHITE WARE
CERAMICS	LITHICS
CHIPPED STONE	NUMBER OF MANOS
GROUND STONE	NUMBER OF METATES
KIVA	
GREAT KIVA	
PITHOUSE	
SURFACE ROOMS - MASONRY	
SURFACE ROOMS - PERISHABLE	
WALL	
MIDDEN	
SURFICIAL ARTIFACT SCATTER	
HEARTH - FIREPIT	
STORAGE CIST	
ROASTING PIT	
COURT - PLAZA	
BALL COURT	
PLATFORM MOUND	
TOWER	
CHECK DAM	
TERRACE	
BORDER	
DITCH OR CANAL	
WAFFLE GARDEN	
RESERVOIR	
OTHER WATER SOIL	
ROCK ART	
BEDROCK MORTAR	
ABRADING GROOVES	
PECKED STEPS	
SHRINE	
ROAD - TRAIL	
ON-SITE PLANT COMMUNITY	
PRIMARY PLANT COMMUNITY-1 KM	
SECONDARY PLANT COMMUNITY-1KM	
TERTIARY PLANT COMMUNITY-1KM	
PRIMARY PLANT COMMUNITY-5KM	
SECONDARY PLANT COMMUNITY-5KM	
TERTIARY PLANT COMMUNITY-5KM	

(continued on next page)

Table 4.3: Archaeological Site Database Fieldnames (*Continued*)

Long House Valley Fieldnames	Black Mesa Fieldnames
VERTICAL DISTANCE-HIGHEST TO LOWEST,100M	
VERTICAL DISTANCE-HIGHEST TO LOWEST,1KM	
VERTICAL DIST-LOWEST POINT TO SITE,100M	
VERTICAL DIST-LOWEST POINT TO SITE,1KM	
ELEVATION	
LOCAL LANDFORM CHARACTERIZATION	
LANDFORM PROFILE - 100M	
LANDFORM PROFILE - 1KM	
PERCENTAGE OF ARABLE LAND	
DISTANCE TO FARMING	
RAINFALL	
DRAINAGE RANK - CLOSEST STREAM	
AVERAGE DRAINAGE RANK	
PERMANENCE OF NEAREST STREAM	
PRIMARY DOMESTIC WATER TYPE	
DISTANCE - PERMANENCE	
SECONDARY DOMESTIC WATER TYPE	
DISTANCE - PERMANENCE	
TERTIARY DOMESTIC WATER TYPE	
DISTANCE - PERMANENCE	
AGRICULTURAL TYPE	
NUMBER OF PERMANENT WATER SOURCES IN 1KM	
NUMBER OF IMPERM WATER SOURCES IN 1KM.	

In total, the combined site database from the Long House Valley and Black Mesa Archaeological projects contains 2139 records, each representing a specific site location. Of those 2139 records 1886 have chronological data that may be converted to the start and end-date ranges applicable to the analysis. Sites lacking start and end-date ranges are typically from the Black Mesa Archaeological Project area and are classified in the site tabulation (Robison 1984) as one of the following:

- “Early Pueblo”
- “Late Pueblo”
- “Lithic Scatter, non-white based siltstone”
- “Dual occupation, not listed above” (i.e. in the chronological classes listed in Table 4.4)

- “Unknown Anasazi”
- “Unknown Pueblo”
- “Archaic”

The mapping of individual sites into the phase system outlined above results in the tabulation presented in Table 4.4. This summary represents the number of sites that *overlap* the date range defined for each period/phase. This method for counting sites within each period/phase results in the assignment of sites to multiple periods/phases when the start or end-dates for a site overlap multiple periods/phases. Because of this pattern of multiple period overlapping, the sum of the total column is much greater than the 1886 sites for which date ranges are defined.

Table 4.4: Analysis Site Frequencies by Period/Phase

Period/Phase	Date (A.D.)	Range	Black Mesa	Long Valley	House	Total
BMII (Lolomai)	50–350	125	57		182	
BMIII/BMIII (Lolomai-Dot Klish)	50–800	175	99		274	
BMIII (Dot Klish)	600–800	56	48		104	
BMIII/PI (Dot Klish-Dinnebito)	600–975	202	152		354	
BMIII/PI (Tallahogan)	800–900	41	80		121	
PI (Dinnebito)	900–975	187	113		300	
PI/PI-II (Dinnebito-Wepo)	900–1050	353	197		550	
PI/PII (Wepo)	975–1050	189	192		381	
PI-II/PII (Wepo-Lamoki)	975–1100	667	325		992	
PII (Lamoki)	1050–1100	502	259		761	
PII/PII-PIII (Lamoki-Toreva)	1050–1150	872	284		1156	
PII/PIII (Toreva)	1100–1150	483	247		730	
Early PIII [Transition]	1150–1250	0	189		189	
Late PIII [Tsegi]	1250–1300	0	110		110	

The analysis employs three artifact classes and four feature classes in evaluating the relationship between mapped subsistence risk and spatial patterning of archaeological phenomena. The presence or absence of these feature classes is encoded for the analysis based upon the attributes listed in Table 4.3. The number of sites for which the presence of these artifact and feature classes varies both by class and time period. The total number of sites for each study area for which each artifact and feature class is documented

is presented in Table 4.6. The number of sites overlapping each defined period/phase which contain each artifact or feature class is summarized in Tables 4.6 (lithics), 4.7 (ceramics), 4.8 (groundstone), 4.9 (pithouses), 4.10 (masonry), 4.11 (kivas), and 4.12 (storage). In total, the archaeological database used in this analysis provides a large sample of sites with which to test hypotheses relating activity location with subsistence risk.

Table 4.5: Analysis Site Frequencies by Artifact/Feature Presence

Artifact/Feature Class	Black Mesa	Long Valley	House	Total
Lithics	853	455		1308
Ceramics	1235	484		1719
Groundstone	441	107		548
Pithouses	64	49		113
Masonry	490	225		715
Kivas	200	63		263
Storage	373	72		445

Table 4.6: Analysis Lithic Site Frequencies by Period/Phase

Period/Phase	Date (A.D.)	Range	Black Mesa	Long Valley	House	Total
BMII (Lolomai)	50–350	119	51		170	
BMII/BMIII (Lolomai-Dot Klish)	50–800	150	83		233	
BMIII (Dot Klish)	600–800	36	36		72	
BMIII/PI (Dot Klish-Dinnebito)	600–975	139	123		262	
BMIII/PI (Tallahogan)	800–900	25	58		83	
PI (Dinnebito)	900–975	128	89		217	
PI/PI-II (Dinnebito-Wepo)	900–1050	239	157		396	
PI/PII (Wepo)	975–1050	125	154		279	
PI-II/PII (Wepo-Lamoki)	975–1100	396	261		657	
PII (Lamoki)	1050–1100	287	205		492	
PII/PII-PIII (Lomoki-Toreva)	1050–1150	505	221		726	
PII/PIII (Toreva)	1100–1150	275	192		467	
Early PIII [Transition]	1150–1250	0	149		149	
Late PIII [Tsegí]	1250–1300	0	82		82	

Table 4.7: Analysis Ceramic Site Frequencies by Period/Phase

Period/Phase	Date (A.D.)	Range	Black Mesa	Long Valley	House	Total
BMII (Lolomai)	50–350	33	6		39	
BMII/BMIII (Lolomai-Dot Klish)	50–800	80	41		121	
BMIII (Dot Klish)	600–800	51	36		87	
BMIII/PI (Dot Klish-Dinnebito)	600–975	196	138		334	
BMIII/PI (Tallahogan)	800–900	41	72		113	
PI (Dinnebito)	900–975	186	104		290	
PI/PI-II (Dinnebito-Wepo)	900–1050	351	187		538	
PI/PII (Wepo)	975–1050	188	182		370	
PI-II/PII (Wepo-Lamoki)	975–1100	666	312		978	
PII (Lamoki)	1050–1100	502	249		751	
PII/PII-PIII (Lamoki-Toreva)	1050–1150	869	272		1141	
PII/PIII (Toreva)	1100–1150	480	235		715	
Early PIII [Transition]	1150–1250	0	178		178	
Late PIII [Tsegí]	1250–1300	0	99		99	

Table 4.8: Analysis Groundstone Site Frequencies by Period/Phase

Period/Phase	Date (A.D.)	Range	Black Mesa	Long Valley	House	Total
BMII (Lolomai)	50–350	37	11		48	
BMII/BMIII (Lolomai-Dot Klish)	50–800	53	14		67	
BMIII (Dot Klish)	600–800	16	4		20	
BMIII/PI (Dot Klish-Dinnebito)	600–975	72	25		97	
BMIII/PI (Tallahogan)	800–900	12	15		27	
PI (Dinnebito)	900–975	68	21		89	
PI/PI-II (Dinnebito-Wepo)	900–1050	132	37		169	
PI/PII (Wepo)	975–1050	73	37		110	
PI-II/PII (Wepo-Lamoki)	975–1100	220	55		275	
PII (Lamoki)	1050–1100	156	44		200	
PII/PII-PIII (Lamoki-Toreva)	1050–1150	277	54		331	
PII/PIII (Toreva)	1100–1150	161	46		207	
Early PIII [Transition]	1150–1250	0	46		46	
Late PIII [Tsegí]	1250–1300	0	29		29	

Table 4.9: Analysis Pithouse Site Frequencies by Period/Phase

Period/Phase	Date (A.D.)	Range	Black Mesa	Long Valley	House	Total
BMII (Lolomai)	50–350	5	3		8	
BMII/BMIII (Lolomai-Dot Klish)	50–800	7	9		16	

(continued on next page)

Table 4.9: Analysis Pithouse Site Frequencies by Period/Phase (*Continued*)

Period/Phase	Date (A.D.)	Range	Black Mesa	Long Valley	House	Total
BMIII (Dot Klish)	600–800	2	5		7	
BMIII/PI (Dot Klish-Dinnebito)	600–975	16	32		48	
BMIII/PI (Tallahogan)	800–900	1	20		21	
PI (Dinnebito)	900–975	15	27		42	
PI/PI-II (Dinnebito-Wepo)	900–1050	24	32		56	
PI/PII (Wepo)	975–1050	11	31		42	
PI-II/PII (Wepo-Lamoki)	975–1100	29	36		65	
PII (Lamoki)	1050–1100	18	14		32	
PII/PII-PIII (Lomoki-Toreva)	1050–1150	34	15		49	
PII/PIII (Toreva)	1100–1150	19	11		30	
Early PIII [Transition]	1150–1250	0	5		5	
Late PIII [Tsegí]	1250–1300	0	1		1	

Table 4.10: Analysis Masonry Site Frequencies by Period/Phase

Period/Phase	Date (A.D.)	Range	Black Mesa	Long Valley	House	Total
BMII (Lolomai)	50–350	6	0		6	
BMII/BMIII (Lolomai-Dot Klish)	50–800	20	1		21	
BMIII (Dot Klish)	600–800	14	1		15	
BMIII/PI (Dot Klish-Dinnebito)	600–975	77	28		105	
BMIII/PI (Tallahogan)	800–900	12	12		24	
PI (Dinnebito)	900–975	75	27		102	
PI/PI-II (Dinnebito-Wepo)	900–1050	149	67		216	
PI/PII (Wepo)	975–1050	84	66		150	
PI-II/PII (Wepo-Lamoki)	975–1100	262	140		402	
PII (Lamoki)	1050–1100	188	129		317	
PII/PII-PIII (Lomoki-Toreva)	1050–1150	343	141		484	
PII/PIII (Toreva)	1100–1150	200	124		324	
Early PIII [Transition]	1150–1250	0	103		103	
Late PIII [Tsegí]	1250–1300	0	59		59	

Table 4.11: Analysis Kiva Site Frequencies by Period/Phase

Period/Phase	Date (A.D.)	Range	Black Mesa	Long Valley	House	Total
BMII (Lolomai)	50–350	1	0		1	
BMII/BMIII (Lolomai-Dot Klish)	50–800	3	0		3	
BMIII (Dot Klish)	600–800	2	0		2	
BMIII/PI (Dot Klish-Dinnebito)	600–975	23	6		29	

(continued on next page)

Table 4.11: Analysis Kiva Site Frequencies by Period/Phase (*Continued*)

Period/Phase	Date (A.D.)	Range	Black Mesa	Long Valley	House	Total
BMIII/PI (Tallahogan)	800–900	1	2		3	
PI (Dinnebito)	900–975	22	6		28	
PI/PI-II (Dinnebito-Wepo)	900–1050	51	21		72	
PI/PII (Wepo)	975–1050	32	21		53	
PI-II/PII (Wepo-Lamoki)	975–1100	105	36		141	
PII (Lamoki)	1050–1100	78	35		113	
PII/PIII (Lomoki-Toreva)	1050–1150	152	38		190	
PII/PIII (Toreva)	1100–1150	95	32		127	
Early PIII [Transition]	1150–1250	0	35		35	
Late PIII [Tsegi]	1250–1300	0	25		25	

Table 4.12: Analysis Storage Site Frequencies by Period/Phase

Period/Phase	Date (A.D.)	Range	Black Mesa	Long Valley	House	Total
BMII (Lolomai)	50–350	26	23		49	
BMII/BMIII (Lolomai-Dot Klish)	50–800	40	35		75	
BMIII (Dot Klish)	600–800	15	14		29	
BMIII/PI (Dot Klish-Dinnebito)	600–975	70	31		101	
BMIII/PI (Tallahogan)	800–900	14	11		25	
PI (Dinnebito)	900–975	69	18		87	
PI/PI-II (Dinnebito-Wepo)	900–1050	119	23		142	
PI/PII (Wepo)	975–1050	59	23		82	
PI-II/PII (Wepo-Lamoki)	975–1100	187	31		218	
PII (Lamoki)	1050–1100	138	18		156	
PII/PIII (Lomoki-Toreva)	1050–1150	238	20		258	
PII/PIII (Toreva)	1100–1150	136	16		152	
Early PIII [Transition]	1150–1250	0	9		9	
Late PIII [Tsegi]	1250–1300	0	4		4	

Chapter 5

Analysis

As outlined in Chapter 1, the goal of this analysis is to apply geospatial and statistical analytic methods to the problem of assessing the locational response of the prehistoric occupants of northern Black Mesa and Long House Valley to subsistence risk. The analysis entails several phases, each of which contributes to the conversion of bulk data to useful information and moves the analysis closer to the end point at which hypotheses relating to risk-response may be tested. The following sections describe the data used, the processing steps in the distillation of information from data, the derivation of diachronic models of site location and climate parameters, the development of null-hypotheses against which observed data may be compared, and finally, the visualization and quantification of the relationships between observations and null-hypotheses.

5.1 Outline of Procedures

The analysis described in this chapter represents a long sequence of data acquisition and processing, model development and evaluation, and hypothesis testing steps, each of which are detailed in the sections below. This section provides an overview of the analysis steps in order to provide a high-level road map for the more detailed discussions that follow. The overall flow of the analysis is presented in Figure 5.1, with subsequent sections providing more detailed versions of this figure for each of the outlined steps.

The first step in the analysis consists of the acquisition and initial processing of the data to be used. These data include archaeological site data from the Long House

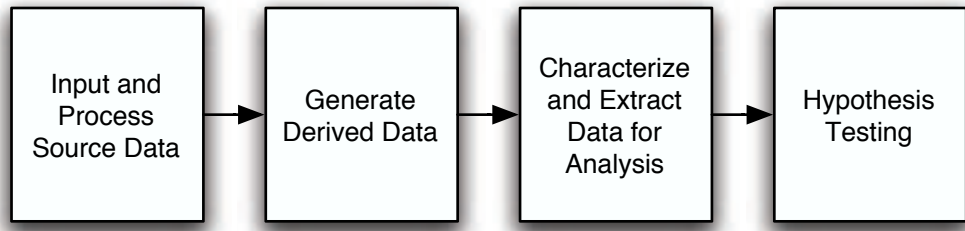


Figure 5.1: Top Level Analysis Flowchart

Valley and Black Mesa Archaeological Projects, demographic reconstructions for the local area and region, historic climate data, prehistoric climate proxy data, digital elevation data, vegetation community data, and other environmental data useful in providing an interpretive context for the analysis. These data provide the primary source information for the previous chapters that summarize the modern environment (Chapter 2), prehistoric environment (Chapter 3), and archaeological background (Chapter 4, Section 4.10). These data also provide the raw material from which the derived data used in the analysis are generated.

The second step in the analysis consists of the generation of derived data from the minimally processed data described above. The processing involved in this step varies by dataset, but includes merging data into a single aggregated dataset (i.e. the archaeological data from Long House Valley and Black Mesa), calculation of new data from source data (i.e. the interpolation and extrapolation of historic and prehistoric climate data based upon statistical models), spatial resampling of data to provide data at resolutions that differ from those they were originally in (i.e. smoothing of elevation data, rescaling of demographic curves), and temporal smoothing of data (i.e. calculation of moving mean and variance values for interpolated prehistoric climate data). These derived data provide the inputs into the next step in the analysis, the characterization and extraction of data for the analysis.

In many respects, the characterization and extraction of data for the analysis represents a continuation of the previous derived data generation step, with the exception that this step results in data that represent subsets of the derived data. Specifically, the data subsets that result from this step include: a subset of archaeological sites for which

environmental parameters will be extracted, spatial subsets of environmental parameter values that are limited to site locations included in the analysis, and spatial subsets of environmental parameters for randomly located points within the analysis area. These data provide the final data that are input into the hypothesis testing step in the analysis.

Hypothesis testing is the final step, and provides the information needed to assess the relationships between risk (as modeled using paleoclimate data) and locational decision-making. The assessment is facilitated through simulation-based climate parameter estimation for randomly located points within the study area, and the assessment of the relationship between parameter values for site locations and the simulated parameter distribution.

5.2 Input and Process Source Data

The acquisition and processing of data for the analysis is the critical first step that defines the potential for success for the analysis; it represents a significant undertaking, both in terms of logistics and processing. The data used in the analysis are derived from sources including printed documents, digital tabular data in a variety of formats, and GIS coverages in a variety of formats and spatial frameworks. This chapter briefly describes the source and initial processing steps for each of the datasets employed in the analysis. The primary data used in the analysis include:

- Archaeological site data from the Long House Valley and Black Mesa Archaeological Projects
- Historic climate data appropriate for the development and testing of climate parameter interpolation and extrapolation algorithms
- Prehistoric climate proxy data to provide the basis for interpolated and extrapolated climate reconstructions for the study area
- Digital elevation data appropriate for use in the development of climate parameter interpolation and extrapolation algorithms
- Modern vegetation community data for the study area

- Other environmental data for use in developing an interpretive context for the analysis results.

The relationship of these data processing steps to the overall analysis is graphically depicted in Figure 5.2.

5.2.1 Archaeological Site Data

The archaeological site data used in the analysis were obtained from two primary resources; a digital data file for the Long House Valley Archaeological Project data and a hard copy manuscript for the Black Mesa Archaeological Project data. Additional published and archival data were used as necessary to resolve questions regarding the data in the database or manuscript.

The Long House Valley Archaeological Project site data were obtained from Sylvia Gaines (Gaines n.d.) as an SPSS data file and associated SPSS data import program. These data were converted within SPSS to a dBase file for general access via a variety of software applications, and were ultimately converted to an ASCII text file for import into PostgreSQL, the relational database environment used to store all tabular data for the analysis. The site data are consistent with the field definitions defined for the SARG project (Gaines 1978), and are listed in the first column of Table 4.3.

While Sylvia Gaines also provided a copy of the SARG data for northern Black Mesa, the data were not complete and ultimately not used in the analysis. The source for the Black Mesa archaeological data is a manuscript on file at the Center for Archaeological Investigations at Southern Illinois University, Carbondale entitled “Summary of Archaeological and Compliance Information on Archaeological Sites in the Peabody Coal Company’s Leasehold on Black Mesa, Navajo County, Arizona” (Robison 1984). This manuscript contains tabular data for both Anasazi and Navajo sites within and adjacent to the Peabody Leasehold. Data used in this analysis are derived from Part 1 (Site Numbers and UTM coordinates) and Part 3 (site numbers, phase, structure and feature designations, artifact designations) of the Anasazi site information section of the manuscript. These data were manually entered into PostgreSQL, hard copy output generated, and double-checked for data entry errors. Descriptions of the database fields coded for the

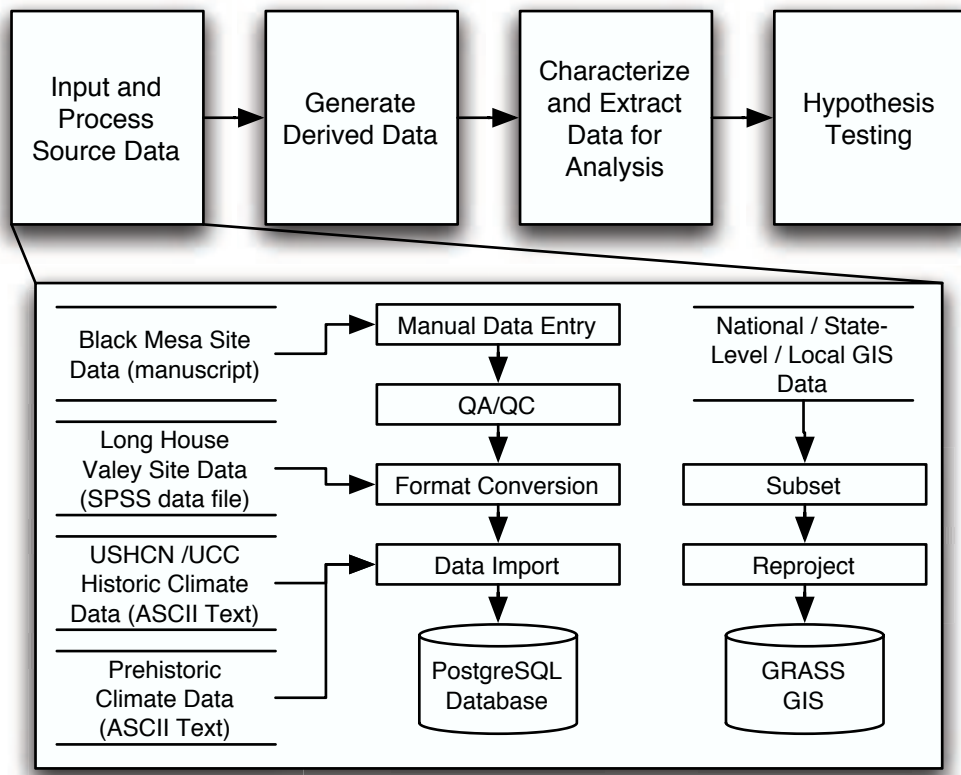


Figure 5.2: Data Input and Processing Process

analysis are provided in the second column of Table 4.3.

The entry of both sets of data into PostgreSQL allows for simplified data management, and manipulation. These data are more easily merged with other data and efficiently queried within the database than would be possible in alternative tabular environments like spreadsheets or text files. When necessary, the database may be used to export custom “snapshots” of data in a wide variety of formats suitable for ingestion into other applications.

5.2.2 Historic and Prehistoric Climate Data

Historic and prehistoric climate data used in the analysis are derived from four sources, two for historic data, and two for prehistoric data. The long-term historic climate data derived from the U.S. Historical Climatology Network (USHCN, Easterling, et al. 1999) are available for download from the National Climate Data Center USHCN web page (<http://www.ncdc.noaa.gov/oa/climate/research/ushcn/ushcn.html>). The much more limited short term historic climatological data available for download from the Western Regional Climate Center (<http://www.wrcc.dri.edu/>) and the Utah Climate Center (UCC, <http://climate.usu.edu/>) were considered to have potential utility and were downloaded and processed as well. In both cases (the USHCN and UCC), the downloaded data came in the form of ASCII text files that were first processed into a format compatible with efficient import into the PostgreSQL database, and then imported into the database for storage and management.

The prehistoric climate proxy data used in the analysis were similarly treated. After the data were obtained from the researchers responsible for the generation and management for the data – Jeff Dean in the case of the prehistoric precipitation data (Dean 1999), and Mathew Salzer in the case of the prehistoric temperature reconstruction (Salzer 2000) – the ASCII text files were reformatted and imported into the database for storage and processing.

5.2.3 Environmental Data

The environmental data used in the analysis and interpretation of results are inherently spatial, and as such, were obtained and have been maintained as GIS coverages throughout the project. Both raster (representing continuous fields of data: e.g. elevation, aerial photography, satellite imagery) and vector (representing discontinuous data symbolized by points, lines or polygons) data were obtained in support of the analysis. These data include:

- *Vegetation Data*
 - Vector GIS coverage representing the GAP vegetation data (Graham 1995) for the state of Arizona available for download from the Southern Arizona Data Services Program (<http://sdfsnet.srnr.arizona.edu/index.php>)
 - Vector GIS coverage representing the biotic communities mapped by Brown, and Lowe (1994b), described in Brown, Lowe and others (D. E. Brown and Lowe 1994a), and available for download from the Arizona Land Resource Information System (ALRIS, <http://www.land.state.az.us/alris/index.html>)
- *Elevation Data*
 - Digital elevation data for both the immediate study area and the greater region. These data were obtained at two spatial scales, 10m resolution over the project area (ordered from USGS and delivered on CD) and 3-arc-second resolution (approximately 80 m over the project area) over the entire four-states region. Both sets of data are available for download from the EROS Data Center USGS Geographic Data Download web site (<http://edc.usgs.gov/geodata/>)
- *Soil Data*
 - Vector soil data based upon the STATSGO database (Schwarz and Alexander 1995), available for download from the Natural Resources Conservation Service National Cartography and Geospatial Data Center (<http://www.ncgc.nrcs.usda.gov/branch/ssb/products/statsgo/data/az.html>).

- *Aerial Photography, Satellite Imagery, and Scanned Maps*
 - LANDSAT ETM data from the Arizona Regional Image Archive (ARIA, <http://aria.arizona.edu/>)
 - USGS Digital Orthophoto Quads (DOQQ) from ARIA
 - USGS Digital Raster Graphics files (DRG, scanned USGS topographic maps) from ARIA

In all cases, these geospatial data were obtained in resolutions and geographic projections that differ from those selected for use in this analysis. All of the above mentioned datasets were reprojected and, when appropriate and necessary, resampled to new resolutions for use in the analysis. The projection selected for the analysis is a Transverse Mercator projection with the specific parameters (as defined for the PROJ projection library/utility, Evenden 1995a; Evenden 1995b) provided in Table 5.1. This projection was selected over the more traditionally used UTM, Zone 12, NAD83 projection primarily because of the regional nature of the analysis and the fact that the study region changes UTM zones near the Arizona/New Mexico, Utah/Colorado borders (Zone 12 for Arizona and Utah, Zone 13 for New Mexico and Colorado), needlessly complicating many cartographic and analysis activities. Additionally, this projection closely resembles the familiar depiction of the four-corners states with the vertical axis of the projection oriented along the eastern and western state borders for Utah, Colorado, Arizona, and New Mexico. Unless otherwise specified in a given analysis step, the spatial resolution at which analysis steps are undertaken is 80m, the approximate resolution of the regional 3-arc-second digital elevation model. Finally, some of the datasets were subsetted to provide more manageable data within the analysis. For example, the GAP vegetation coverage is quite large and slow to process when working with the entire statewide coverage, so it was subsetted to a much smaller area immediately surrounding the analysis area.

Table 5.1: Analysis Map Projection Parameters

Parameter Name	Parameter Description	Value
name	Projection Name	Mercator
datum	Horizontal Datum	nad83
dx	East/West Offset	0.000000

(continued on next page)

Table 5.1: Analysis Map Projection Parameters (*Continued*)

Parameter Name	Parameter Description	Value
dy	North/South Offset	0.000000
dz	Vertical Offset	0.000000
proj	Projection Code	merc
ellps	Ellipsoid	grs80
a	Semimajor Ellipsoid Axis	6378137.0000000000
es	Eccentricity Squared	0.0066943800
f	Flattening	298.2572221010
lat_ts	Latitude of True Scale	36.5000000000
lon_0	Central Meridian	-109.0000000000
k_0	Scale Factor at Central Meridian	1.0000000000
unit	Projected Units	meter

In total, these data, some of which are described in great detail in the previous chapters, provide the empirical foundation upon which the following analysis is built. These data are the raw material from which the data products described in the next section may be derived.

5.3 Generate Derived Data

Though important for the analysis, the data described in the previous section do not meet all analysis requirements. In some cases the data must be restructured to allow for combination with other data. Other required datasets must be generated through mathematical transformations. Finally, several required datasets must be generated through more complex procedures that employ statistical and physical models to derive new datasets from those listed above. This section provides an outline of the methods used for, and the products of, these data manipulation and generation activities. Figure 5.3 illustrates the general processing flow for this portion of the analysis sequence.

5.3.1 Archaeological Site Data

The archaeological data used in the analysis, by virtue of having been collected under two different archaeological projects, use different encoding schemes for similar data. In order to successfully complete the analysis, the separately encoded site databases need to be

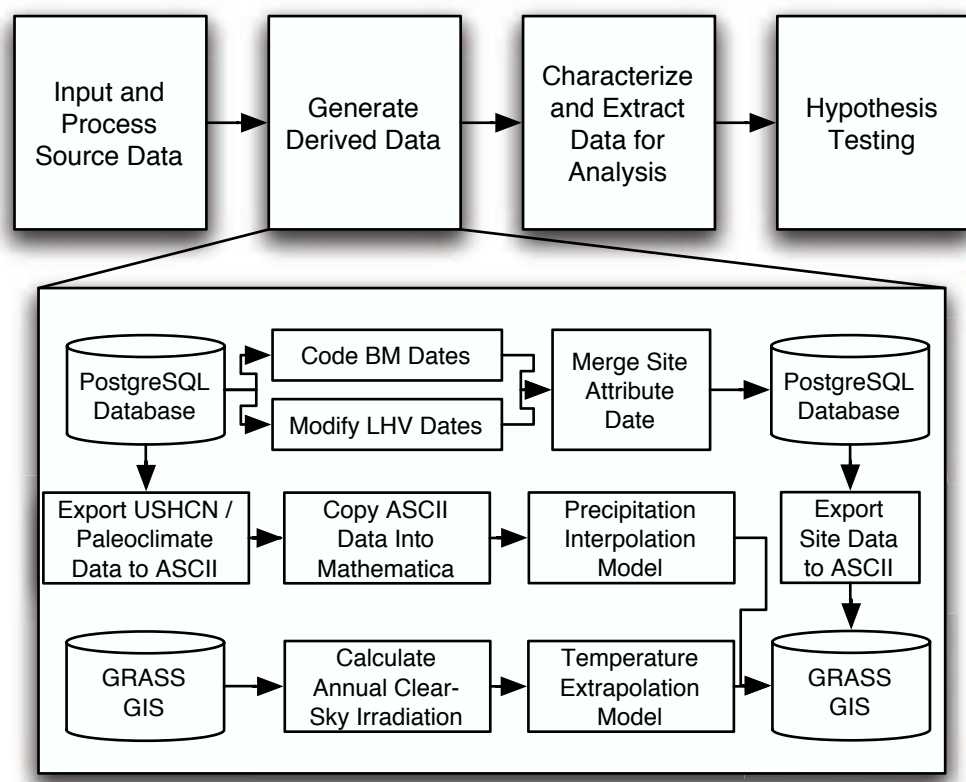


Figure 5.3: Generation of Derived Data Process

reconciled into a single consistent representation for use in the analysis. Fortunately, while encoded differently, there is sufficient overlap in the data represented in each database to allow this reconciliation.

The first step in the data reconciliation process consists of internal conversion of data within the table of Black Mesa sites to convert the phase designations used in the source manuscript into time spans comparable to those encoded in the Long House Valley database: initial and terminal dates for each site. This was accomplished by creating a view of the Black Mesa site data table that included initial and terminal dates based upon the period/phase dates presented in Table 4.4. The date ranges from the Long House Valley site database also required modification. In the case of Long House Valley, the initial and terminal dates were encoded as years before present. For comparability with the years A.D. dates associated with the Black Mesa sites, 1950 was subtracted from each Long House Valley data to obtain the equivalent years A.D. date.

Once both tables had comparable date ranges, the problem of merging their attributes into a usable composite was addressed. This was accomplished through the use of a temporary database table which was first loaded with recoded attributes from the Black Mesa tables and then appended with recoded attribute values from Long House Valley. Because the Long House Valley data are encoded using a greater number of more general feature and artifact classes, the recoding process yielded a composite data set that assigns each of the retained artifact or feature classes a 0 (absent) or 1 (present) with -999 representing missing data. The fields retained in the output table consist of: siteid, utm zone, utm easting, initial date (Years A.D.), terminal date (Years A.D.), lithics (present or absent), ceramics (present or absent), groundstone (present or absent), pithouses (present or absent), masonry (present or absent), kivas (present or absent), and storage (present or absent). These retained fields are based directly upon their corresponding fields in the original Long House Valley table (column 1 in Table 4.3). The fields encoded in the Black Mesa site table correspond with those in the output table as follows: lithics → lithics, manos and/or metates → groundstone, redware and/or grayware → ceramics, pithouse depressions → pithouses, rubble mounds → masonry, kiva depressions → kivas, and slab-lined features → storage (the SQL expression that created the temporary table containing the combined data is presented in Appendix G). The resulting temporary table

was then exported to an ASCII file and imported into the GIS as a GRASS sites file for use in the environmental data extraction activities outlined below.

5.3.2 Generation of Extrapolated/Interpolated Paleoclimate Parameters

The key goal of the analysis is to explore the relationship between subsistence risk and locational response by the prehistoric population occupying the study area. Given the relationship between climate and plant productivity, and the dependence of the regional population upon both cultivated and wild plant resources, the development of local, high-spatial-resolution, climate reconstructions for the project area is a prerequisite for any examination of risk-responsive locational behavior within the study area. The methods employed here for generating those reconstructions are based upon recently developed meteorological and climatological extrapolation and interpolation methods that take into effect local topographic factors in the modeling of local conditions from remote measurement locations (Thornton, et al. 1997). Due to differences in the available paleoclimate data, two different climate modeling approaches were employed. Because there is only a single temperature reconstruction available for the analysis, a regression-based extrapolation model employing measured temperature at the San Francisco Peaks reconstruction location, elevation, and calculated annual clear-sky irradiation was developed for predicting local temperatures within the study area. The availability of six precipitation reconstructions within the region surrounding the study area led to an attempted application of a more sophisticated interpolation/extrapolation method that combines spatial interpolation of values from multiple points with extrapolation based upon annual regression models for elevational effects on local precipitation.

Preparation for both climate modeling efforts began with the migration of the historic (USHCN) and prehistoric climate (temperature and precipitation) data from the database within which they are stored into Mathematica, the mathematical programming environment used for all statistical modeling activities. For the temperature analysis this was a trivial activity because the prehistoric mean daily maximum (MDM) temperature data are based upon the calendar year (Salzer 2000). The historic MDM temperature data

for each of the 18 USHCN stations within the project area were generated for each year of record for the stations and converted into a format easily used within Mathematica. Similarly, the MDM temperature data for the San Francisco Peaks reconstruction were exported from the database and inserted into Mathematica for the analysis.

Migration of the precipitation data into Mathematica required additional processing of the historic climate data because the prehistoric precipitation data (annual total precipitation) are based upon a tree-year that extends from August of the previous year through July of the current year (Dean 1999). In order to develop and test an annual precipitation model that is comparable to the prehistoric precipitation data, the historic data were aggregated using the tree-year specification instead of a calendar year. This yielded tree-year total annual precipitation values for each of the USHCN stations used in the analysis. The prehistoric precipitation data were simply exported to Mathematica without modification.

Once the data for each of the modeling efforts were exported to Mathematica, each climate parameter was separately modeled.

Temperature Extrapolation

Extrapolation of MDM temperature from the single San Francisco Peaks reconstruction requires the development of a reasonable model for temperature prediction at locations remote from the point of measurement. Frequently temperature estimates for remote locations are calculated based upon known or measured lapse rates that represent the change in temperature as elevation increases. Commonly, remote temperature is estimated using the simple formula (e.g. Salzer 2000, both in the development and application of the San Francisco Peaks temperature reconstruction):

$$T_p = T_o + \frac{(E_o - E_p)}{1000} * L \quad (5.1)$$

where

- T_p = Predicted Temperature ($^{\circ}\text{C}$)
 T_o = Temperature at Observation Location ($^{\circ}\text{C}$)
 E_o = Elevation of Observation Location (m)
 E_p = Elevation of Prediction Location (m)
 L = Lapse Rate ($^{\circ}\text{C}/\text{km}$)

While lapse rates are an important element in estimating temperature for remote locations, there are other factors that play a role in local temperature variation (refer to Section 2.1.2 for a detailed discussion of these factors), with many of those factors relating to the amount of incoming solar radiation incident upon a given location. Because of this, it was decided to evaluate the potential for incident radiation to enhance a regression model for local temperature that includes both elevation and solar radiation in addition to temperature at a single point location: the Fort Valley USHCN Station (Station 3160, the USHCN station used in the generation of the prehistoric temperature reconstruction).

Prior to the development of the regression model, local incoming solar radiation values needed to be calculated for each of the 17 USHCN stations for which temperature was to be predicted. Total annual solar radiation (including direct, diffuse, and reflected radiation) was calculated for a 10km region surrounding each USHCN station and the combined Black Mesa and Long House Valley study areas. The analysis region was limited in this way to allow for more efficient computation – the calculation still required over 200 cpu-hours to complete). This was accomplished using the GRASS GIS r.sun program, a program that uses local elevation, slope, and aspect data to calculate instantaneous or cumulative daily radiation. The implemented algorithm within r.sun accounts for Sun-Earth position, date, time, latitude, and shadowing from local topography in the radiation calculations. While the program is capable of modifying the radiation calculations to account for cloud cover, this analysis is limited to the calculation of clear-sky radiation at a daily time step for each site. These daily values were summed for the calendar year to yield the final values used in the regression analysis. The elevation data used in the analysis are derived from USGS 3-arc-second Digital Elevation Model data for the region

(resampled to an 80m nominal ground resolution). The slope and aspect data used in the calculate were generated from the DEM using the GRASS GIS r.slope.aspect command. The input elevation data and resulting total annual solar radiation maps are presented in Figures 5.4 and 5.5 respectively. Because the positional data for the USHCN stations are provided only to the nearest 1/100th of a degree, the generated 80m resolution radiation data were smoothed using a 15-pixel average value filter, with the dimension of the filter selected to approximate the potential $\pm 0.005^\circ$ positional uncertainty in the station locations.

The resulting solar radiation data were used in conjunction with elevation and the Annual MDM temperature at Fort Valley to develop a regression model for predicting temperature at the other 17 USHCN stations within the study region. Two regression models were considered, one including all three predictors (Equation 5.2), and one including only Fort Valley temperature and elevation (Equation 5.3). The elevation and smoothed radiation values are provided in Table 5.2.

$$T_p = \beta_0 + \beta_1 T_{FV} + \beta_2 E_p + \beta_3 R_p \quad (5.2)$$

$$T_p = \beta_0 + \beta_1 T_{FV} + \beta_2 E_p \quad (5.3)$$

where

T_p = Predicted Temperature ($^{\circ}\text{C}$)

T_{FV} = Temperature at Fort Valley ($^{\circ}\text{C}$)

E_p = Elevation of Prediction Location (m)

R_p = Total Annual Solar Radiation at the Prediction Location ($\frac{W}{m^2}$)

$\beta_0, \beta_1, \beta_2, \beta_3$ = Regression Coefficients

A comparison of the results of the two regression analyses indicates that solar radiation is a statistically significant model parameter, and improves the total model in its ability to predict temperature. Specifically, the p-value obtained for the statistical test that the coefficient β_3 in Equation 5.2 is equal to 0 is < 0.0001 , suggesting that solar radiation is

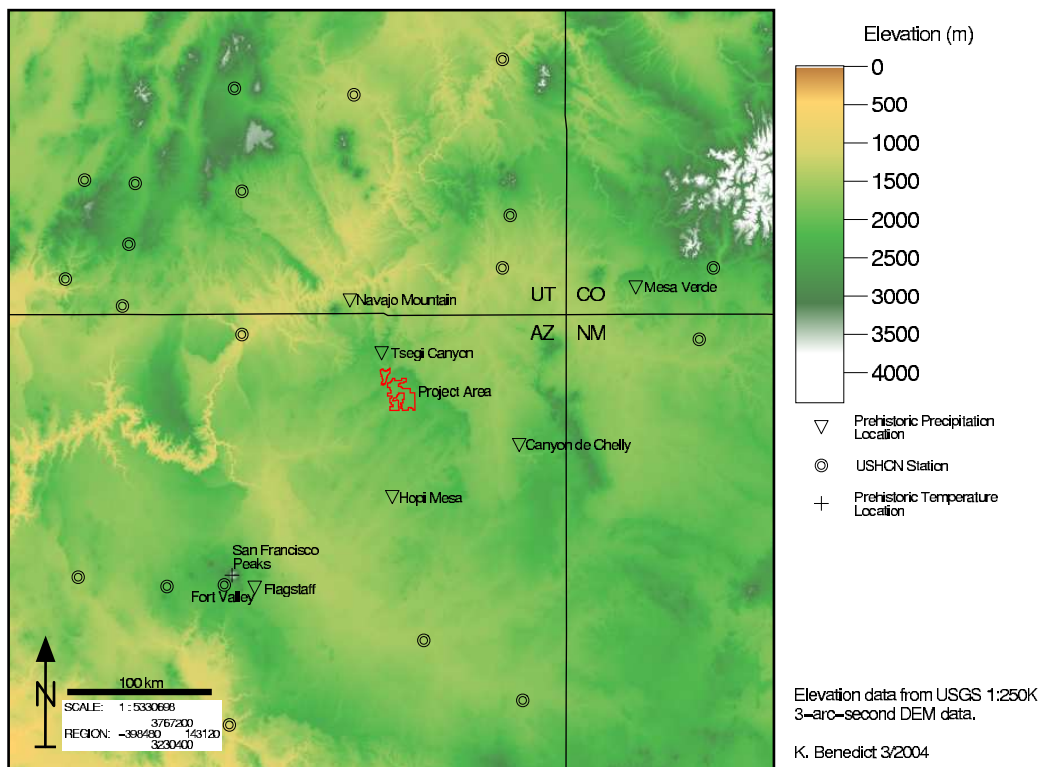


Figure 5.4: Elevation Data, USHCN Station, and Prehistoric Climate Locations

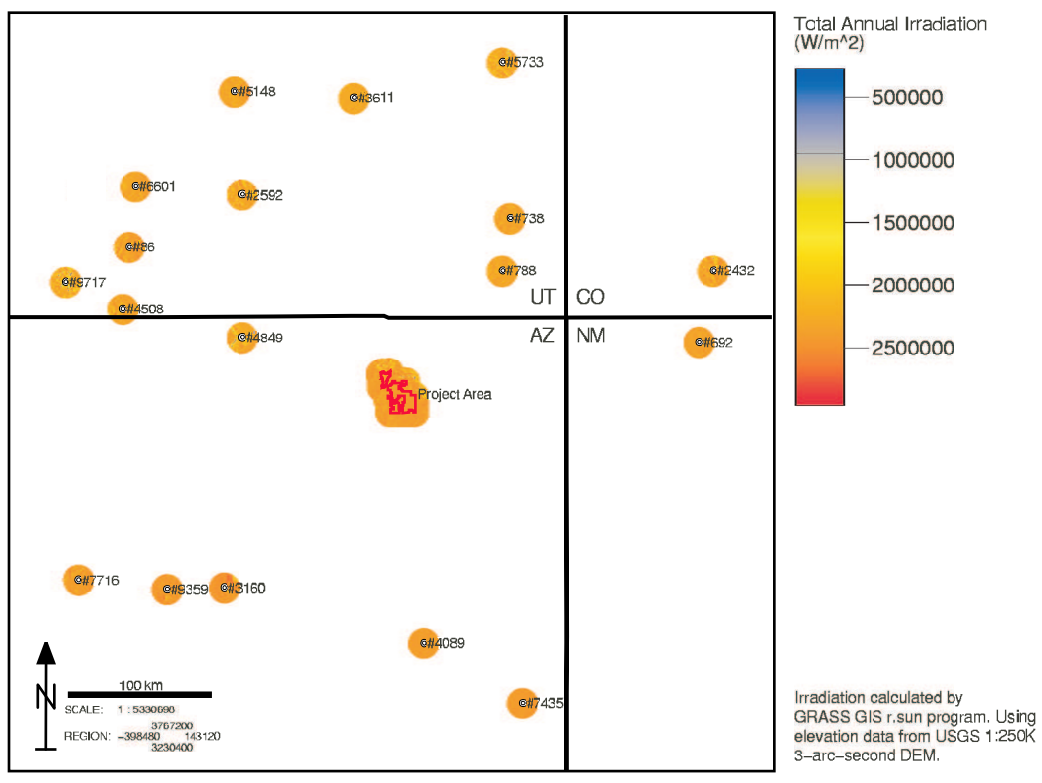


Figure 5.5: Calculated Total Annual Solar Radiation for the USHCN Station Locations and Study Area

Table 5.2: USHCN Station Smoothed Radiation (W/m^2) and Elevation (m)

Station ID	Station Name	Smoothed Radiation (W/m^2)	Elevation (m)
7435	SAINT JOHNS	2411988.5	1765
4089	HOLBROOK	2397114.75	1545
9359	WILLIAMS	2421062.75	2057
3160	FORT VALLEY	2424129	2239
692	AZTEC RUINS NATL MONU- MENT	2297536	1720
4849	LEES FERRY	2346021.25	978
4508	KANAB	2280279.75	1509
9717	ZION NATIONAL PARK	2072218.625	1234
2432	DURANGO	2167101.5	2012
788	BLUFF	2250619.25	1315
86	ALTON	2283977	2146
738	BLANDING	2348148.25	1841
2592	ESCALANTE	2314841	1771
6601	PANGUITCH	2324290.25	2015
6686	PAROWAN POWER PLANT	2350555	1829
3611	HANKSVILLE	2252451	1313
5148	LOA	2315893	2155
5733	MOAB	2353856.5	1226

a significant model parameter. The inclusion of solar radiation in the model also results in an increase in the adjusted R^2 value from 0.581 for the two parameter model, to 0.700 for the three parameter model. The resulting three-parameter model coefficients are listed in Table 5.3, and the model ANOVA table is provided in Table 5.4.

The final step in the generation of extrapolated temperature values for the project area is the application of the above described regression model to the area. The regression model employed in the extrapolation is represented by Equation 5.2 and the regression coefficients are presented in Table 5.3. The input parameters T_{FV} , E_p , and R_p for the prehistoric temperature reconstruction are provided by Salzer's San Francisco Peaks temperature reconstruction (4km from the Fort Valley USHCN station, Salzer 2000), the 80m resolution 3-arc-second DEM for the study area, and the calculated solar radiation for each 80m pixel in the analysis area, respectively. The regression model was run for each year from A.D. 570 to 1150, producing 580 annual temperature reconstruction rasters for the analysis area. A sample of one of the produced rasters is provided in Figure 5.6, the reconstructed temperatures for the project areas for the year A.D. 1070. These rasters provide the data, exported as ASCII text files for import into Mathematica, used in the calculation (described in Section 5.4.2) of 30-year moving means for the study period of A.D. 600 - 1150.

Precipitation Interpolation

The availability of six prehistoric precipitation reconstructions within the larger region surrounding the project area provides the *potential* for the application of recent meteorological interpolation methods to the problem of predicting local precipitation from a network of remote precipitation measurement locations. While this potential was not realized in this analysis, the process of model development and evaluation is presented below in an effort to highlight the continuing potential for these methods in paleoclimatic

Table 5.3: Temperature Regression Model Coefficients

Coefficient	Value	Standard Error	t-statistic	P-value
β_0 Constant	8.35232	1.04105	8.02297	$2.44249 * 10^{-15}$
β_1 Fort Valley Temp.	0.484693	0.0513093	9.44648	0
β_2 Prediction Location Elevation	-0.00758795	0.000145608	-52.1122	$6.93818 * 10^{-311}$
β_3 Solar Radiation	$7.11515 * 10^{-6}$	$3.25995 * 10^{-7}$	21.826	0

Table 5.4: Temperature Regression ANOVA Table

	DF	Sum of Squares	Mean Square	F-Ratio	P-value
Model	3	8248.24	2749.41	938.825	$1.34131 * 10^{-311}$
Error	1204	3526.	2.92857		
Total	1207	11774.2			

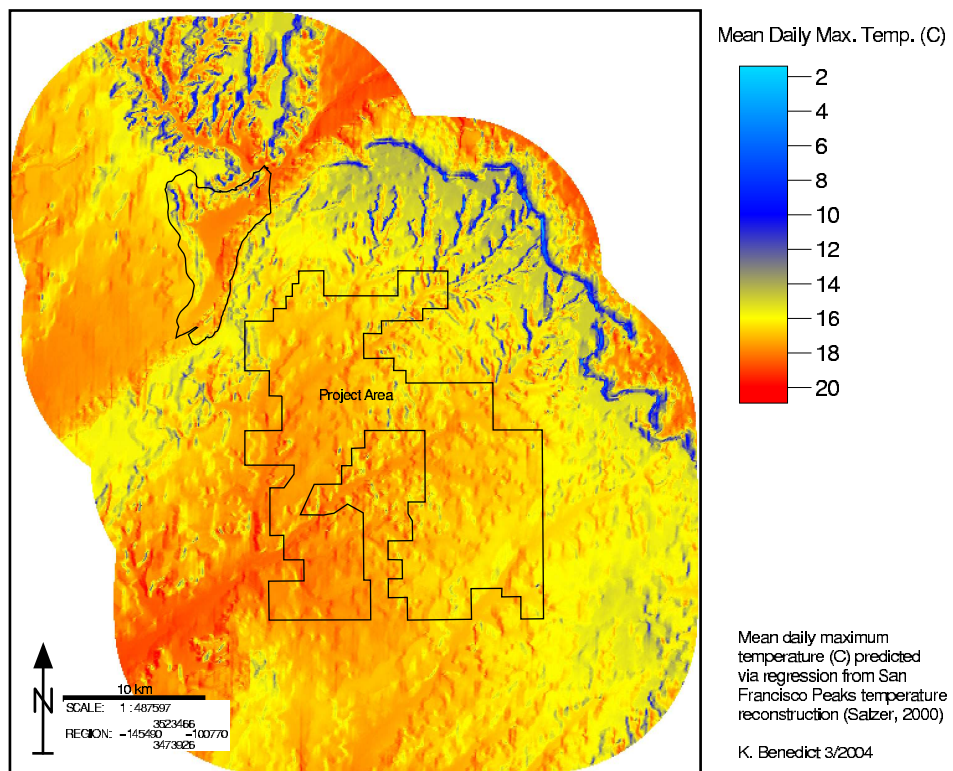


Figure 5.6: Project Area Temperature Reconstruction: A.D. 1070

reconstruction. Ultimately, a simplified interpolation method based upon the more complex meterological interpolation approach is used in the estimation of precipitation over the study area.

Thornton and others (Glassy and Running 1994; Hungerford, et al. 1989; Kimball, et al. 1995; Running, et al. 1987; Thornton, et al. 1997) have developed models for the interpolation and extrapolation of meteorological and climatological parameters over heterogeneous terrain that have been extensively validated (e.g. Thornton, et al. 1997) and broadly implemented (e.g. the DAYMET [Daily Surface Weather and Climatological Summaries] web site: <http://daymet.org>). These methods have been developed specifically to generate

large interpolated surfaces for a suite of daily meteorological variables, with simulations typically of 1–5 years, grids on the order of 500 × 500 cells, and incorporating hundreds of observation sites. (Thornton, et al. 1997:218)

These design criteria, and the optimization of the interpolation algorithms to achieve high levels of computational efficiency, suggest that these algorithms might have direct applicability to the problem of interpolating prehistoric climate parameters across large regions from a network of observation locations.

In the case of total annual precipitation interpolation, the model developed by Thornton, Running and White (Thornton, et al. 1997:221-222) generates predicted precipitation values for a grid of locations for which elevation data are available from a network of point precipitation records. Mathematically, the model is represented in Equations 5.4, 5.5, 5.6, and 5.7.

$$P_p = \frac{\sum_{i=1}^n W_i (\frac{1+f}{1-f})}{\sum_{i=1}^n W_i} \quad (5.4)$$

$$f = \beta_0 + \beta_1(z_p - z_i) \quad (5.5)$$

$$W(r) = \begin{cases} 0; & r > R_p \\ e^{(\frac{r}{R_p})^2 \alpha} - e^{-\alpha}; & r \leq R_p \end{cases} \quad (5.6)$$

and

$$\left(\frac{P_1 - P_2}{P_1 + P_2} \right) = \beta_0 + \beta_1(z_1 - z_2) \quad (5.7)$$

The above equations represent the following components of the model:

- *Precipitation Prediction Formula*: Equation 5.4 provides the overall precipitation prediction based upon weighted average predictions from n observation locations obtained from a weighted regression model (f , Equation 5.5). The weights (W_i) for each regression prediction are based upon a truncated Gaussian filter (Equation 5.6)
- *Annual Regression Model*: Equation 5.5 represents a specific annual realization of the general regression model represented by Equation 5.7. This equation produces a normalized difference of precipitation based upon a linear regression model that includes a constant (β_0) and regression coefficient (β_1) for the difference between the prediction location elevation (z_p) and the observation location elevation (z_i).
- *Observation Location Weighting Formula*: Equation 5.6 calculates the weight applied to a given observation in the calculation of the weighted average precipitation for each location in the prediction grid. The size and shape of the Gaussian filter is defined by the radius (r) and shape parameter (α). To limit the number of stations included in a given calculation, a truncation distance (R_p) is defined that sets the weight to 0 if r is greater than R_p . Thornton et al. (1997:219) use an iterative process to locally optimize R_p to produce both a smooth interpolation surface and achieve a specified average number of stations contributing to each point in the prediction region.
- *Normalized Difference Precipitation Regression Model*: Equation 5.7 represents the general model used for the calculation of precipitation for each year for a given prediction location and observation location. It predicts the normalized difference for precipitation ($\frac{P_1 - P_2}{P_1 + P_2}$) using a weighted regression in which the elevation difference ($z_1 - z_2$) for each unique pair of observation locations (i.e. station 1: station 2, station 1:station 3, ..., station n-1:station n) is used as the predictor variable. When all 18 USHCN stations are used in the generation of a model, the number of data points (i.e. paired stations) is 153. The weighting factors for the regression are the product of the weights calculated using Equation 5.6, with r equal to the distance between the paired stations, and α set to the same value as used elsewhere in the analysis. This weighted regression model has the effect of assigning greater weight

in the regression model to station pairs that are close together than to those that are far apart. The model also uses transformed data in the development of the model. When run at a daily time step, observations are smoothed both spatially and temporally. Temporally, a five-day smoothing filter is used to reduce day-to-day variance, while spatial smoothing of the elevation data to a resolution of 2-8 km was found to reduce prediction errors (Thornton, et al. 1997:229).

Prior to application to the prehistoric precipitation data, a slightly simplified version of the above described model was implemented using the historic precipitation record (tree-year total precipitation) for the 18 USHCN stations within the larger analysis area (Figure 5.4). Model simplification primarily consists of the use of an untruncated Gaussian filter for calculating weighting surfaces for each site. The equation for the simplified Gaussian weighting filter is presented in Equation 5.8. Sample weighting surfaces for two USHCN stations are presented in Figure 5.7. These sample surfaces are based upon three different values of r , set at 50, 100, and 150km, illustrating the influence of this parameter upon the shape of the weighting surface. Higher areas of the weighting surface have a greater influence upon points at that location while lower areas have correspondingly lower influence upon corresponding points. The Gaussian model employed in this analysis was simplified because the number of available stations, both for the historic period and for the prehistoric analysis, is substantially smaller than that typically used in larger regional runs. Because one of the primary purposes of using the truncated Gaussian filter is to reduce the number of low-weighted stations contributing to the calculation of a climate parameter at any location (Thornton, et al. 1997:219), the simplified continuous Gaussian distribution was used instead. This choice vastly simplified model development, and is not likely to have had any significant impact of the performance of the model.

$$W(r) = e^{-\frac{r^2}{2\sigma^2}} \quad (5.8)$$

where

$W(r)$ = Gaussian Weight for distance r

σ = Width of Kernel in Map Units

The implementation of the model for the USHCN stations serves two purposes: 1) to develop the necessary program logic to properly implement the model, and 2) to quantify the effectiveness of the model for the specific area under study. Model implementation was accomplished in Mathematica using the previously exported historic and prehistoric precipitation data, and a value of 130km for σ . The specific σ value selected for the historic climate analysis was chosen because it yields meaningful weights for all stations while maintaining the influence of nearby stations when available. The main concern when selecting a value for σ is that it not be so large that all locations for which climate parameters are to be estimated are closer than 1σ to all stations. This situation leads to less variable weighting between stations, with estimated values closely matching the regional average. Similarly, as the tails of the Gaussian distribution asymptotically approach 0, the selection of a small value for σ , such as the case when all prediction locations are more than 2σ from all record locations, the predicted values also approach the regional average. In both cases, obtaining a value that increasingly approximates the regional average defeats the purpose of the interpolation approach.

The model was run for the years 1907 through 1997 and yielded statistically significant regression models for most years ($\alpha = 0.05$). The ability of each year's model to explain regional variation in precipitation, as reflected in the adjusted R^2 values for each regression, covered the range from less than 0 to 1, with many values greater than 0.6 obtained.

Evaluation of the ability of the model to predict precipitation at locations not included in the development of the model was accomplished through the prediction of precipitation at each of the six paleoprecipitation record locations used in the analysis for the period of overlap between the USHCN record and the dendroclimate record. In spite of an association between the predicted and observed precipitation values, the model appears to be biased towards overestimation of precipitation, as indicated by a mean error of -13.77 ± 4.06 (percent of observed annual total precipitation, 95% confidence limits).

In spite of this apparent bias and the presence of a few non-significant regression models in the reconstruction, the fact that many years produce a combination of statistical significance and relatively high R^2 suggests that the model might provide useful for interpolating prehistoric precipitation, at least for some years. Keeping these problems

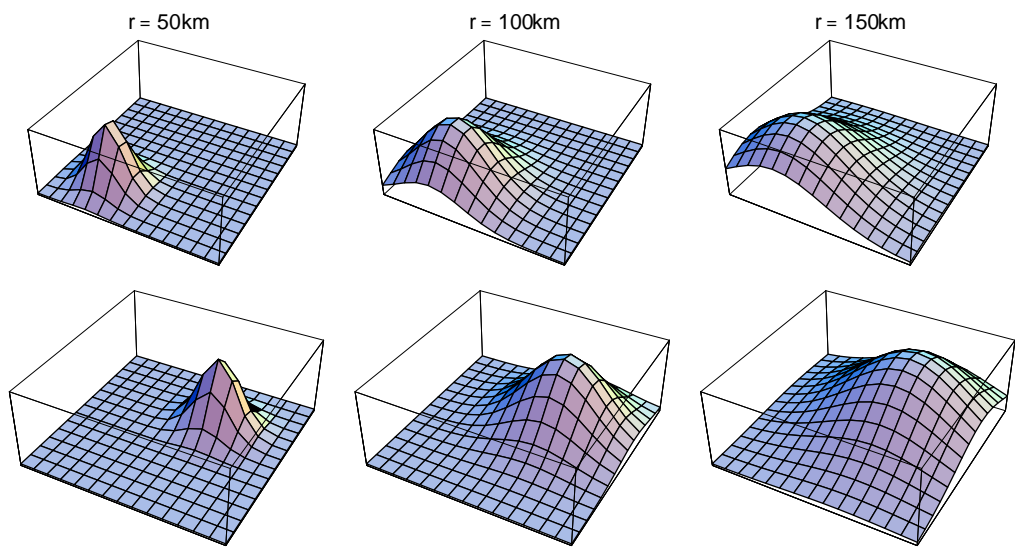


Figure 5.7: Sample Gaussian Weighting Surfaces for USHCN Stations 3160 (top row) and 788 (bottom row) for Three Kernel Widths ($r = 50\text{km}$, $r = 100\text{km}$, $r = 150\text{km}$)

in mind, the model was run for the analysis period using the six prehistoric precipitation reconstructions provided by Dean (1999), and exported from the database for analysis in Mathematica.

In spite of the potential noted above, the application of the model to the prehistoric precipitation record failed to produce significant regression models for most analysis years, and produced relatively small adjusted R^2 values (primarily ranging from -.1 to 0.4). This result can be explained by three significant differences between the historic application and the prehistoric application. First, the number of "stations" available for the prehistoric analysis is only 1/3 the number available for the historic analysis, reducing the maximum number of station pairs from 153 for the historic analysis to 15 for the prehistoric reconstruction. This reduction in sample size for each annual regression makes the development of a statistically significant model more difficult. Second, in spite of the smaller number of "stations", the distance between stations of the prehistoric precipitation record is similar to, if not larger than that of the USHCN stations (Figure 5.4). This broad spatial distribution reduces the degree of commonality between records, therefore again reducing the likelihood of generating a significant regression model. Third, the elevation range for the prehistoric model (1829m – 2134m, Table 3.1) is much smaller than that represented by the stations in the USHCN network (978m – 2239m, Table 2.4), with this reduction in elevation range reducing the likelihood of identifying a significant elevation-based regression model for any year. Overall, this result indicates that the statistical interpolation/extrapolation model demonstrated for the historic period is unable, given the currently available data, to provide a reasonable reconstruction of prehistoric precipitation.

As an alternative to the more sophisticated statistical model described above, the basic Gaussian interpolation algorithm (Equation 5.8) described above was used as an inverse distance weighting filter for the network of six prehistoric precipitation record locations. This simple smoothing interpolator is represented by Equation 5.9. This approach is similar to the daily precipitation estimation procedure proposed by Running et al. (1987) for estimating precipitation for locations remote from a single weather station. Both methods employ an interpolated surface as the reference for remote precipitation estimation: annual regional precipitation isohyets in the case of the application by Running,

and Gaussian interpolated values in the case of this analysis.

$$P_p = \frac{\sum_{i=1}^n W_i P_i}{\sum_{i=1}^n W_i} \quad (5.9)$$

where

W_i = Weighting for Station i from Eqn. 5.8

P_p = Predicted Precipitation

P_i = Observed Precipitation at Station i

This interpolation approach was run at an annual time-step for the years A.D. 570 - 1150, producing 580 interpolated precipitation surfaces. The value of r used for the Gaussian filter is 40km, a smaller value than that used in the statistical approach used above, because of a desire to more heavily weight local values while maintaining an influence from more distant observation locations. The ability of this filter to reflect local variation while maintaining the influence of more distant measurement locations is illustrated in Figure 5.8, a mapped representation of the interpolated precipitation values for the year A.D. 1070. While not obvious from the regional map of the interpolated values, variation exists within and across the project area shown in the center of Figure 5.8. This variation is illustrated in Figure 5.9, a more localized map of the project area, with the interpolated precipitation rescaled to more closely match the range of values observed within the project area. The resulting interpolated precipitation values were exported to an ASCII text file for import into the GIS for visualization while also being retained within Mathematica for the calculation of running means and variances, as is described in the next section.

Overall, this section summarizes the derivation of modified or derived data from the less processed data products presented in the previous section. Among the derived data described in this section are:

- A combined archaeological dataset that merges the independently collected and encoded databases from Long House Valley and Black Mesa.

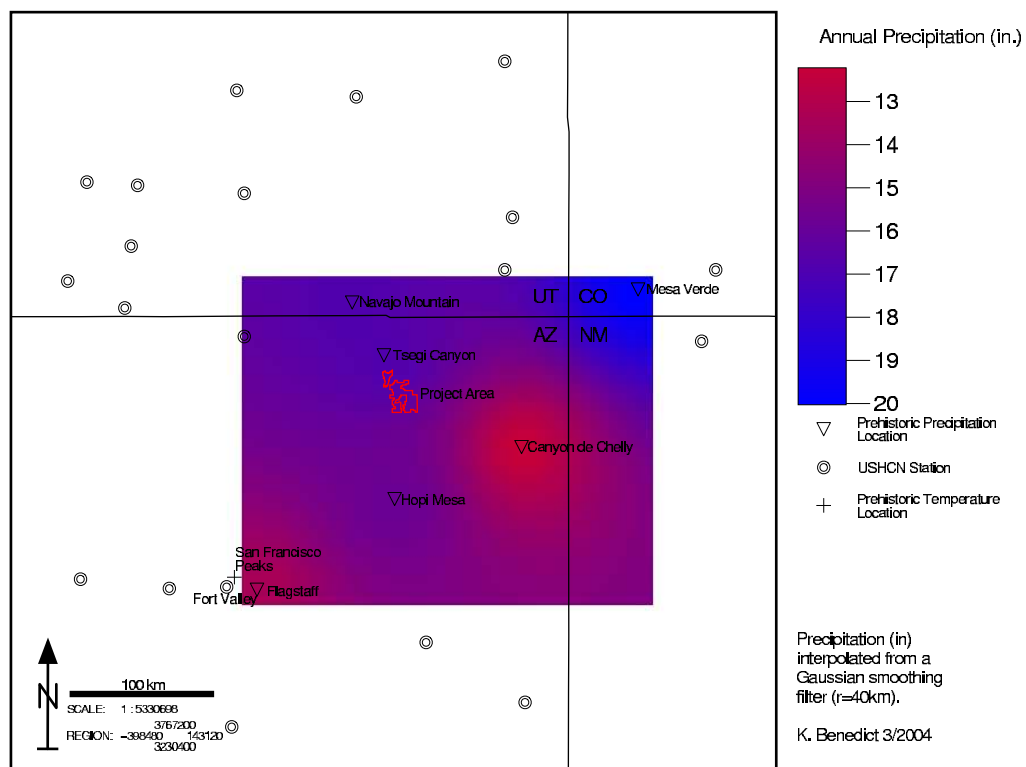


Figure 5.8: Regional Precipitation Interpolation: A.D. 1070

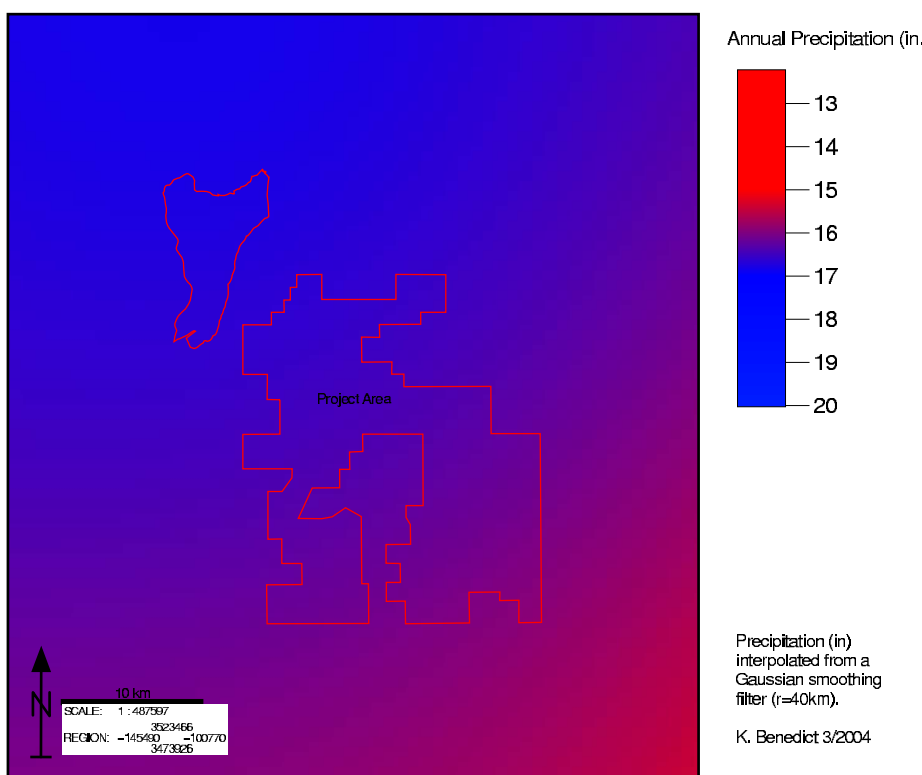


Figure 5.9: Project Area Precipitation Interpolation: A.D. 1070

- A continuous field, for each of the years A.D. 570-1150, of mean daily maximum temperatures for the project area based upon a regression model that includes local solar radiation, elevation, and the observed temperature for the San Francisco Peaks temperature reconstruction developed by Salzer (2000).
- A continuous field, for each of the years A.D. 570-1150, of total annual (tree-year, previous August - current July) precipitation for the region encompassed by the six prehistoric precipitation record locations provided by Dean (1999).

These data, in combination with the unmodified data from the previous section, provide the larger collection of data from which data collections for use in the final analysis will be distilled. This distillation process is described in the next section.

5.4 Characterization and Extraction of Data for Analysis

The previous two sections described the collection, preliminary processing, and generation of derived datasets that form the total collection of data available for analysis. This section outlines the summarization and extraction of data to produce final data products for use in the hypothesis testing phase of the analysis. These summarization and extraction processes include:

- The development of a subset of archaeological sites for use in the analysis.
- The generation of 30-year moving mean rasters for precipitation and temperature, and 30-year moving variance rasters for precipitation.
- The extraction of moving mean and variance values for each site location, for each year from A.D. 600-1150
- The extraction of other environmental attributes for site locations for the entire study period.

Each of these processing steps is described below and are depicted in Figure 5.10.

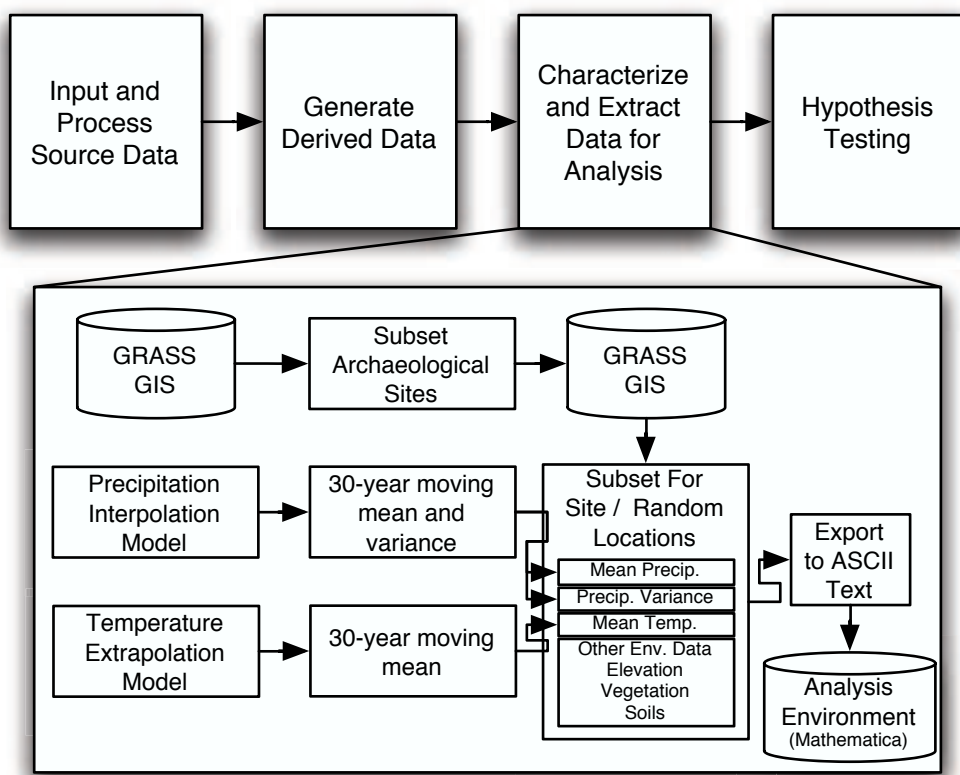


Figure 5.10: Data Characterization and Extraction Process

5.4.1 Selection of the Archaeological Data Subset Used in the Analysis

Sites available for the analysis includes 2139 sites from the combined databases from Long House Valley and Black Mesa. Not all of these sites fall within the boundaries of the GIS polygons that represent the surveyed areas for both projects. Both GIS boundaries were screen digitized from scanned maps for each project: the maps published in the SARG 1976 proceedings volume for Long House Valley (Dean, et al. 1978: Fig. 1), and the original mylar base map for the Black Mesa Archaeological Project depicting the locations of excavated sites and archaeological compliance areas (Black Mesa compliance map, Sink, et al. 1985). While it is likely that the digitized boundaries differ slightly from the actual boundaries for each project, a conservative approach to selecting sites for the analysis was taken in which only sites falling within the digitized boundaries were included in the analysis. This selection process resulted in the exclusion of 227 sites from the analysis, almost all of which fall within areas designated as outside the leasehold by the BMAP compliance map between the eastern and western leasehold areas. The rationale for the exclusion of these sites is that without boundaries that clearly define the region under analysis (as is the case for sites that fall outside the digitized project area boundaries), subsequent analysis and hypothesis testing cannot be accomplished. The distribution of sites included and excluded from the analysis is presented in Figure 5.11.

The exclusion of these sites from the analysis is not likely to have a negative impact on the outcome of the analysis for three reasons. First, the excluded sites represent only 10.6 percent of the total site sample, a relatively small proportion of the sites available for the analysis. Second, all of the sites lie within environmental settings well represented within the analysis area (i.e. locations directly adjacent to the study area boundaries, segments of Moenkopi Wash that are both upstream and downstream from the excluded region in the center of the Black Mesa Archaeological Project study area). Third, the simulation-based approach to hypothesis testing employed in the analysis limits consideration of environmental factors to the same region used to limit the sites used in the analysis, producing comparability in the sampling methods used both for the archaeological and environmental data. The final sample of 1912 sites retained for use in the analysis provide

the point locations used for testing locational hypotheses relating activity location with mapped climate variation and other environmental data.

Also identified in Figure 5.11 is an area of the Peabody Leasehold near the northeastern corner of the project area that is excluded from the analysis. It is excluded because, in spite of the fact that it is part of the leasehold, it is not identified on the Black Mesa compliance map as having been inventoried archaeologically, a characteristic that is reinforced by the absence of any sites within this area. Finally, regarding the established boundaries for the analysis, the Black Mesa compliance map identifies an area within the central opening in the leasehold where a compliance survey was completed in spite of the fact that it lies outside the leasehold boundary. Although this area was mapped as having received compliance coverage, it is excluded from the analysis because it lies outside the defined leasehold boundary.

5.4.2 Calculation of Moving Mean and Variance for Climate Parameters

To facilitate the analysis of locational response to subsistence risk, represented in this analysis by variation in climate, a measure of variation must be defined. Previous studies have characterized trends in climatic variation in reference to deviations from the entire record, interpreting human response to those deviations (e.g. F. Plog, et al. 1988). This analysis differs from previous studies by explicitly defining the period of time contributing to estimated variation in terms of the period over which individuals or their parents would have experienced the variation: 30 years. The mean and variance values that are tested for association with prehistoric locational response are calculated using a 30-year moving window, with the climatic record of the past 30 years providing the raster of values for the current year. For example, in computing the precipitation mean and variance for A.D. 600, the mean for years A.D. 570-599 is calculated. Similarly, the variance of the values from A.D. 570-599 yield the variance assigned to A.D. 600.

The other major difference between this analysis and previous ones is the explicit spatial modeling of climate variation. This contrasts with the general characterization of periods of high and low spatial variation without reference to the localized manifestations

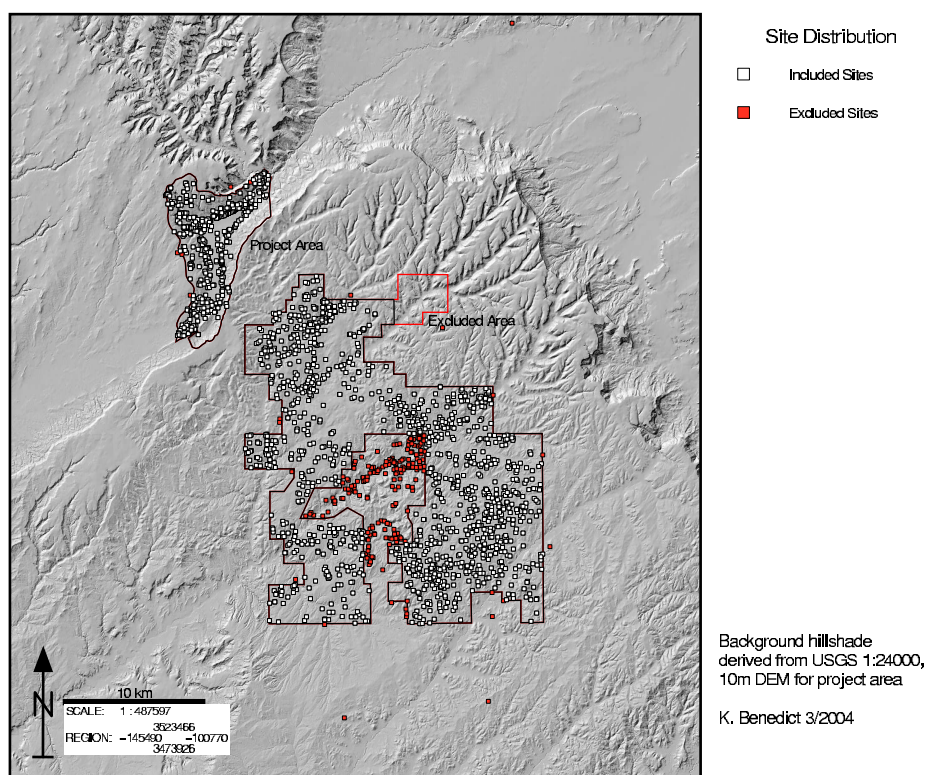


Figure 5.11: Archaeological Sites, Sites and Areas Excluded from Analysis

of this variation (e.g. Dean 1988a). Spatial modeling of variation is accomplished through the use of rasters to represent variable climate parameter values, and the calculation of mean and variance from those rasters. The results of the calculations are new rasters that represent continuous variation in these climatic statistics across space. The left half of Figure 5.12 illustrates this calculation process. The right half of the figure is explained in the following section. In total, the process of calculating moving mean and variance values for the climate parameters yields 1675 rasters: annual 30-year means for temperature and precipitation for the years A.D. 600-1150, and 30-year variances for precipitation for the same years. The spatial resolutions of these rasters are 2km for precipitation and 80m for temperature.

The relatively high spatial resolution of the temperature rasters necessitates an additional processing step prior to the extraction of values for site locations: the calculation of neighborhood-based summary values to account for location selection for an area and not just the point where the site is located. This is analogous to selecting a location for a fieldhouse because it is *adjacent* to a promising field location. Because this study focus is upon localized spatial decision-making, a relatively small neighborhood of 480m (6x80m pixels in a square configuration) surrounding each pixel was used to calculate a weighted average for the neighborhood. The weighting factor for each pixel is based upon proximity to the central pixel, with the outermost pixels receiving a weight of 1, the next pixels in from the exterior receiving weights of 2, continuing in this fashion until the central pixel receives a weight of 7. This calculation has the effect of smoothing the temperature reconstruction, as can be seen when Figure 5.14 (the smoothed version) is compared to Figure 5.13 (the original, unsmoothed version). Following the calculation of the 30-year moving mean and variances and the smoothing of the temperature data, the climate data are prepared for value extraction for site locations and randomly selected locations within the analysis region.

5.4.3 Extraction of Environmental Parameters for Site Locations

The extraction of environmental data, including the previously generated annual 30-year moving mean and variance values for temperature and precipitation, for specific

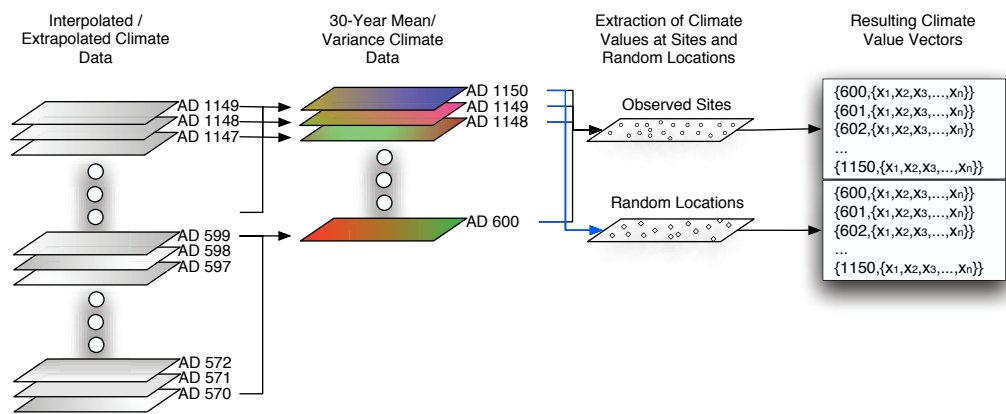


Figure 5.12: Illustration of the Process of Calculating Summary Statistics for Rasters, and the Extraction of Values from Those Rasters

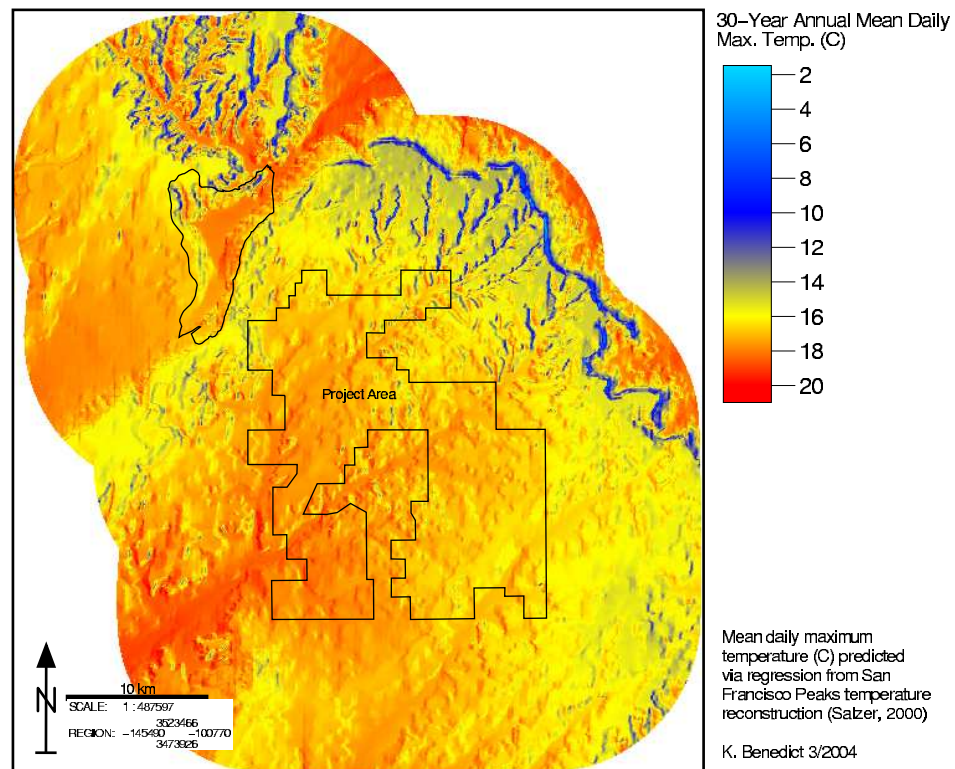


Figure 5.13: 30-Year Moving Average of Annual Mean Maximum Daily Temperature

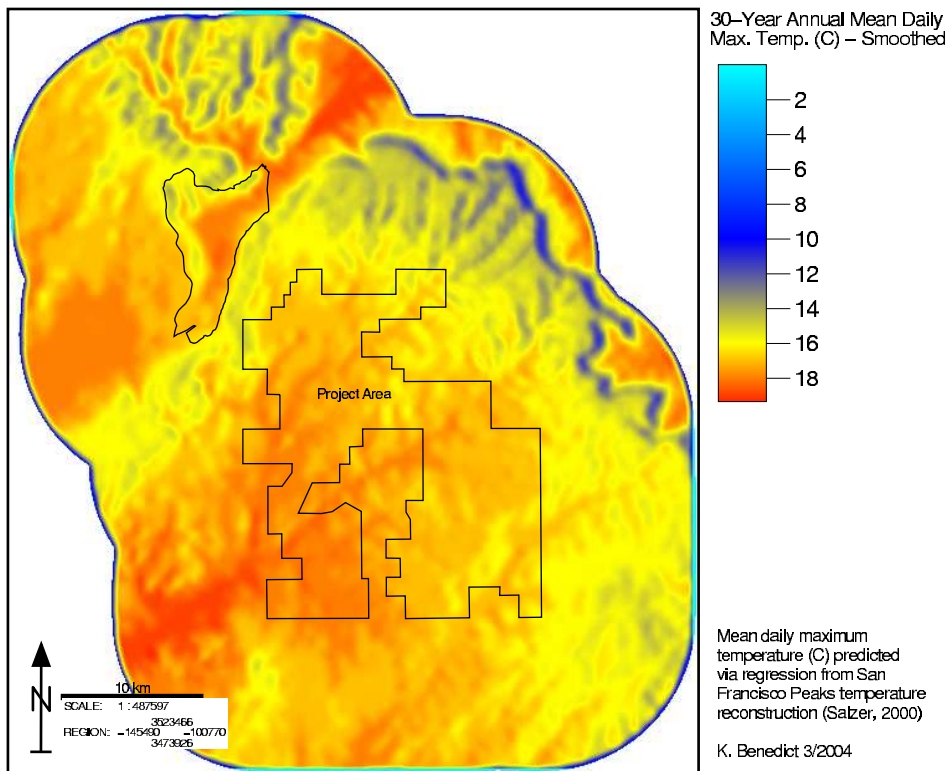


Figure 5.14: Smoothed 30-Year Moving Average of Annual Mean Maximum Daily Temperature (480m IDW Smoothing Filter)

locations within the analysis region is the final data processing step prior to the hypothesis testing phase of the analysis. Value extraction is performed for two classes of locations: recorded site locations and randomly selected points within the analysis region. The data extracted from these classes of locations provide the values used in the hypothesis tests of association between activity locations and environmental parameters.

Prior to value extraction a collection of random locations was generated to facilitate hypothesis testing. The random locations were generated using the GRASS GIS “v.random” command, resulting in 30,000 random locations within a rectangular region encompassing the analysis area. A subset of locations falling within the analysis area was selected using the GRASS GIS “s.mask” command. This subsetting process resulted in a sample of 12,195 random points within the analysis area.

To facilitate hypothesis testing, environmental attributes were extracted from the rasters for point locations corresponding to all site locations and each of the 12,195 random locations. In the case of the annual 30-year mean and variance rasters, data were extracted for each year of the reconstruction. Environmental variables assumed to be constant throughout the analysis period were extracted once for each site and random location. Extracted data were exported to ASCII text files for reading by Mathematica during the hypothesis testing analysis phase (the right half of Figure 5.12). Extracted data include:

- Annual 30-year moving mean and variance for annual (tree-year) accumulated precipitation (in.) for years A.D. 600-1150
- Annual 30-year moving mean annual (calendar year) mean daily maximum temperature ($^{\circ}\text{C}$)
- GAP vegetation community (Figure 2.17)
- Flow accumulation derived from the USGS 1:24000 DEM (Figure 2.16)
- Elevation (Figure 2.5)

5.5 Hypothesis Testing

The testing of hypotheses regarding the relationship between activity location and subsistence risk is the final, and most important, step in the analysis. This section outlines the process of developing the quantitative approach used to develop null-hypotheses against which observed data may be compared. As the analysis is fundamentally an analysis of spatial association, null-hypotheses of no association between environmental attributes and activity locations are based upon the concept of Complete Spatial Randomness (CSR, Bailey and Gatrell 1995:96-104) in which

The standard model for CSR is that events follow a *homogeneous Poisson process* over the study region. In terms of our earlier representation of a spatial point process as the set of random variables $\{Y(A), A \in R\}$, this would imply that $Y(A_i)$ and $Y(A_j)$ are independent for any choices of A_i and A_j and further, that the probability distribution of $Y(A)$ is a Poisson distribution with mean value λA , where A is the area of A ...

Intuitively, this amounts to saying firstly, that any event has an equal probability of occurring at any position in R ; and secondly, that the position of any event is independent of the position of any other — events do not interact with one another.

One could simulate n events from such a process by enclosing R in a rectangle $\{(x, y) : x_1 \leq x \leq x_2, y_1 \leq y \leq y_2\}$ then generating events with x coordinates from a uniform distribution on (x_1, x_2) and y coordinates from a uniform distribution on (y_1, Y_2) and then 'rejecting' any that do not lie in R .(Bailey and Gatrell 1995:96)

This model of CSR has been implemented through the generation of random points described above. The extraction of environmental attributes for each of the randomly generated locations yields a random sample of the each environmental parameter for use in a bootstrap approach to statistical evaluation.

The bootstrap approach applied in the statistical assessment of whether there are significant associations between environmental parameters and activity location is based upon repeated sampling from randomly selected points to generate a distribution of simulated summary values against which the observed summary value may be compared (Davison and Hinkley 1997:422). In this analysis two summary statistics are employed: weighted averages are calculated for numerical data (e.g. mean and variance values for

precipitation and temperature, elevation, flow accumulation), and weighted frequencies for categorical data (GAP vegetation communities). If the observed summary statistic differs significantly from the simulated distribution, the null-hypothesis of no association may be rejected. Following the rule-of-thumb suggested by Efron (Efron and Tibshirani 1993:52), 200 replicated samples for each test were run to define the distribution of summary statistics for each test.

The calculation of weighted average values for site and random locations is necessary to conduct the analysis at a temporal resolution that differs from the chronological frameworks used in both the Long House Valley and Black Mesa Archaeological Projects. The chosen temporal resolution of the analysis is one year – the temporal resolution of the available climate data. The integration of the archaeological site data, data assigned to much longer time spans, with the annual time-step of the analysis was accomplished through the development of a weighting method for site locations that reflects the likelihood of occupation for each site location for each year of analysis.

The likelihood of occupation is estimated from the following values:

- The period to which the site is assigned.
- The shape of the local population curve (the Long House Valley and Black Mesa curves presented in Figure 4.1) corresponding to the site time span
- The year for which the likelihood is to be calculated.

The weighting formula is represented mathematically by Equation 5.10.

$$W_y = \frac{f_p(y)}{\int_{y_{min}}^{y_{max}} f_p} \quad (5.10)$$

where

- W_y = Site weight for year y
 y = Year for which weight is to be calculated
 f_p = A function describing the total population curve
 y_{min} = Site date range, minimum value
 y_{max} = Site date range, maximum value

After calculation of the annual weights for each site, the weighted average environmental attribute value is calculated for each year according to Equation 5.11.

$$\bar{Y}_w = \frac{\sum_{i=1}^n W_i x_i}{\sum_{i=1}^n W_i} \quad (5.11)$$

where

- \bar{Y}_w = Weighted average attribute value
 W_i = The weight associated with a specific site
 x_i = The value associated with a specific site

The resulting weighted average value for each year is compared to the distribution of weighted average values generated through repeated sampling, with replacement, from the 12,195 random locations and their associated attribute values. The calculation of the weighted average for each sample of random locations follows the procedure outlined above, using the vector of weights calculated for the site locations as the weights for the random locations. This process yields a comparable number of random locations that are weighted in the same way as the site locations, and a similarly derived weighted average. The process is repeated 200 times for each year, yielding a distribution of weighted averages against which the observed weighted average may be compared. If the observed weighted average is beyond the upper or lower 2.5% point of the distribution a statistically significant ($\alpha = 0.05$) deviation from the null-hypothesis of no association may be inferred.

Because of the large number of individual analyses performed – 550 for each examined variable, detailed examination of each result is both impractical and unnecessary. Instead, efficient visualization methods have been developed for summarizing the results of numerous analyses into single figures that display trends in several attributes simultaneously, allowing for efficient identification of trends and patterns of association that would otherwise be difficult to assess. These visualizations provide the core interpretive tool for the discussions of analysis results presented in the next chapter.

Chapter 6

Results and Conclusions

This chapter presents the results and conclusions resulting from the data preparation and hypothesis testing methods described in the previous chapter. Overall, the results presented below summarize 23,100 individual simulation-based hypothesis tests, one for each of 550 years (A.D. 600-1150), for each environmental variable, and for each archaeological feature and artifact class. Environmental variables considered in the analysis include:

- Temporally aggregated (30-year moving mean and variance) Gaussian interpolated precipitation data at a spatial resolution of 2km over the analysis area.
- Temporally aggregated (30-year moving mean), spatially smoothed (13-pixel IDW weighted average filter) temperature data at a spatial resolution of 80m over the analysis area.
- Vegetation community data derived from the Arizona GAP analysis program (Graham 1995).
- Elevation, as extracted from a mosaic of USGS 10m 1:24,000 Digital Elevation Models (DEMs, see Appendix A for a list of the quads covering the analysis area) for the analysis area.
- Upslope flow accumulation, as calculated from the mosaic of 10m USGS DEMs for the study area.

The distribution of sites containing each of four feature and two artifact classes is analyzed relative to the distribution of each of these environmental attributes. Only those years for each feature and artifact class with a sample size (Figure 6.1) of more than ten sites are considered in the discussion. The feature classes considered in the analysis, and any years excluded from the analysis due to small sample sizes are:

- Pithouses (excluding A.D. 600–849, 1150)
- Masonry
- Kivas (excluding A.D. 600–899)
- Storage (excluding A.D. 800–849)

The artifact classes included in the analysis include:

- Lithics
- Groundstone (excluding A.D. 800–849)

Additionally, all sites, regardless of feature or artifact composition, are analyzed relative to each of the above listed environmental variables. Plots summarizing all 42 analyses are presented in Appendix H while select plots are provided within this chapter to illustrate discussed trends.

Overall, the presentation of the results of the analysis is broken into two major sections. First, the results of the analysis of activity locations relative to the diachronic reconstructions for temperature and precipitation are presented. The precipitation data play a particularly important role in this analysis because they provide a record of both mean and variance for precipitation across the study area through time. The temperature reconstruction, while providing a highly detailed diachronic record of mean temperature across the study area, does not provide a model of variance across the analysis area. This is because variance is constant across the analysis area for each year of the reconstruction because of the linear model used in reconstructing temperature. Fortunately, since plant growth (both wild and cultivated) within this region is limited by water availability in addition to frost sensitivity (Richard H. Hevly 1988:95), the precipitation reconstruction

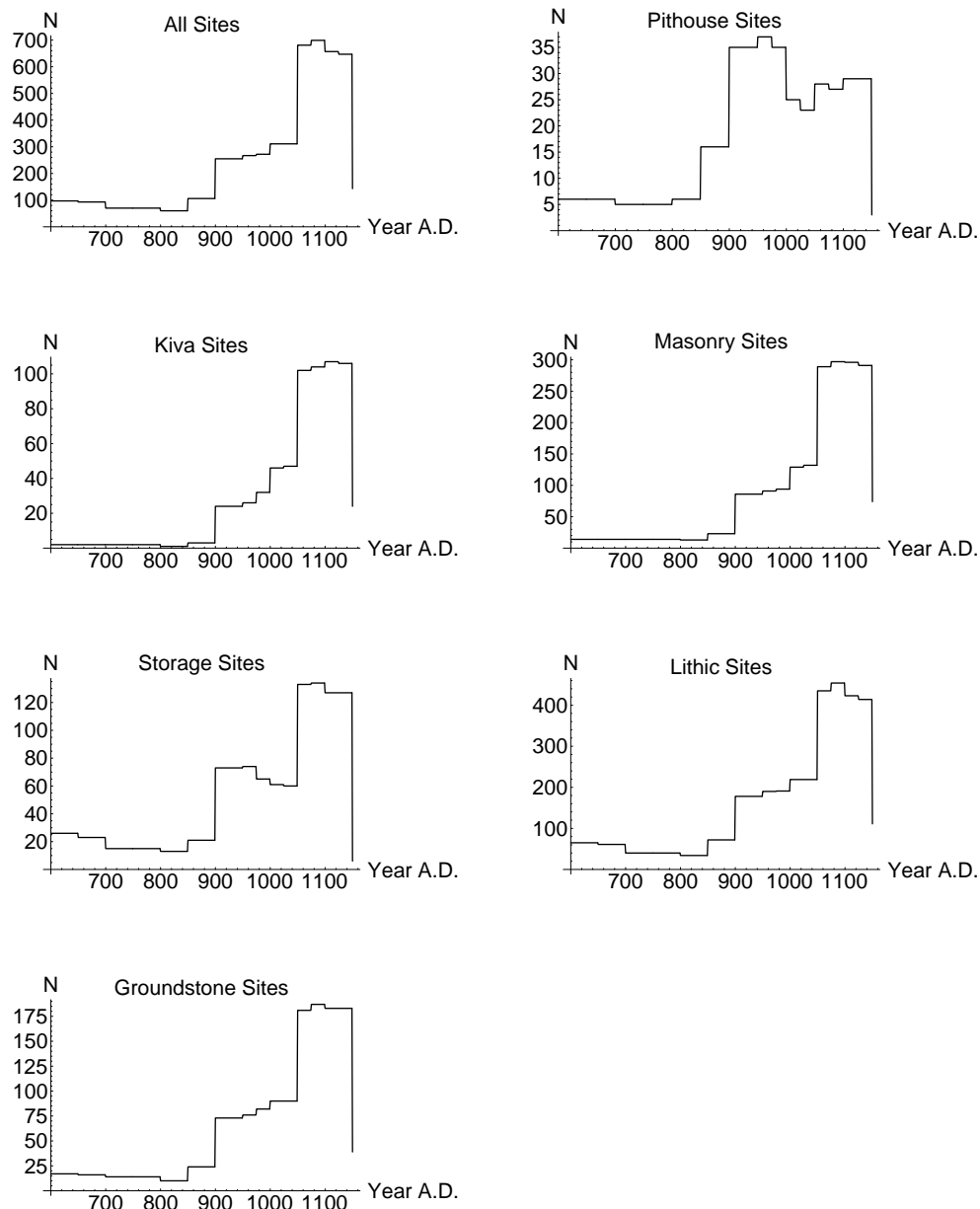


Figure 6.1: Analysis Sample Sizes.

provides a reasonable proxy for vegetative productivity (Webb, et al. 1983)[Burns, 1983 *3955, and through the analysis area precipitation variance model a proxy for predictability of localized productivity. Because the emphasis of this analysis is locational response to subsistence risk, the discussion will focus on the interpretation of the precipitation analysis and to a lesser extent the temperature reconstruction.

The second section of the results discussion focusses on the analyses of the other environmental factors examined in the analysis. Overall, these analyses provide a broader interpretive context for the observed locational trends, and allow for a more integrative explanation of the observed patterns beyond those that relate to locational response to risk. The environmental attributes included in this section relate directly to the commonly referenced influential factors of elevation (the Upland-Lowland pattern of occupation), availability of water (here represented by the smoothed flow-accumulation data), and plant community (both as an indicator of available wild plant and animal species and as an indicator of areas with agricultural potential).

Overall, the analysis of activity location patterning relative to mapped precipitation variance indicates that there are trends in the occupation data that relate to, and reflect trends in local population, a pattern of association that is discussed in the context of behavioral ecological models of risk response. These results add locational response to risk to the suite of other environmental factors, such as vegetation community and availability of water, found to influence activity location.

6.1 Interpretive Framework - the Z-score Model

Because the primary focus of this analysis is response to subsistence risk, a model of risk-response is required, and one has been adopted for this project. The model used is a subsistence shortfall model that defines risk as the likelihood of failing to obtain sufficient food resources to meet survival needs. More specifically, it is the z-score model – a model that predicts the risk profile of foragers based upon the relative values of subsistence requirements and mean foraging productivity. In particular, the z-score model predicts two primary risk-response scenarios (Stephens and Krebs 1986:138-139):

1. Under conditions where the mean harvest rate (of wild and cultivated resources in

the case of this analysis) falls below the requirement for survival, individuals are expected to be risk seeking – adopting behaviors that increase the harvest variance.

2. Under conditions where the mean harvest rate is above the requirement for survival, individuals will be risk averse – adopting behaviors that decrease harvest variance.

The characteristics of the z-score model are illustrated in Figure 6.2. This figure depicts the continuum of harvest rates falling below the survival requirement to those falling above it. The survival requirement is the midpoint on the horizontal axis with the “value” (labelled “Utility”) of a given harvest amount depicted on the vertical axis. The heavy curved line crossing from the lower left corner of the plot to the upper right is a sample (one not uncommon in animal studies) utility curve that exhibits increasing utility (value) as the mean harvest rate increases towards the survival requirement. After reaching the survival requirement the utility curve is concave-down, indicating decreasing value as greater harvest levels above the survival requirement are achieved. The two symmetric probability distributions in the figure (labelled #1 and #2) illustrate the logic behind the z-score model – that when the mean harvest is less than the survival requirement (#1 in the figure), increased variance yields a larger gain than loss (the “Gain” and “Loss” values in the lower half of the vertical axis). Similarly, when the mean harvest rate is greater than the requirement (#2 in the figure), increased variance yields a larger loss than gain (the “Gain” and “Loss” values in the upper half of the vertical axis).

The z-score model presented thus far is based upon a scenario where survival is predicated only upon the resources harvested during the current time-step (annual in the case of this analysis) — it assumes no carry-over from one time-step to the next. The availability and use of storage to carry-over surplus from one year to the next creates what Stephens and Krebs (Stephens and Krebs 1986:143) refer to as the “achieved mean effect”. The achieved mean effect results in a scenario in which foragers will be risk-seeking when the mean harvest rate equals the requirement, since the likelihood of failure remains the same (50%), but if the achieved harvest rate is greater than the requirement, the surplus may be stored and carried over, increasing the likelihood of meeting the next time step's requirement. A second implication of the achieved mean effect is that if the mean harvest is larger than the requirement by only a small amount,

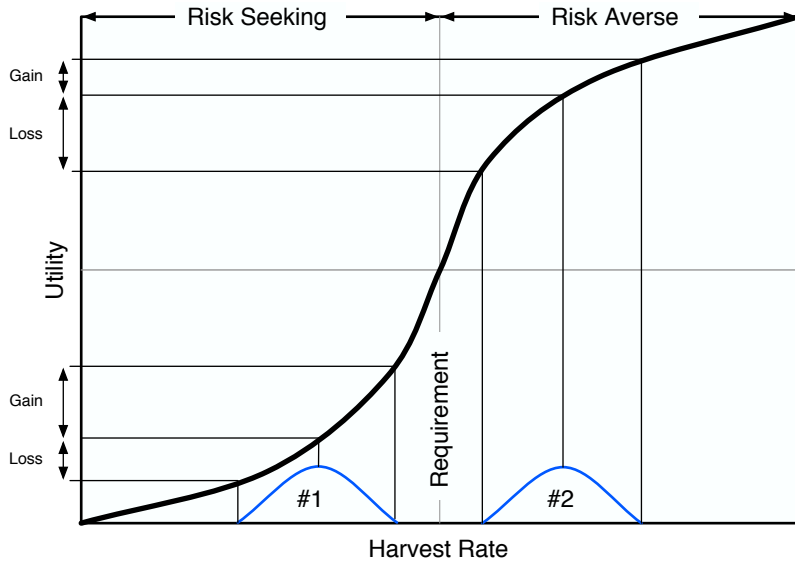


Figure 6.2: z-score Model Characteristics. See text for explanation.

and the forager is offered only large variances (therefore yielding a significant likelihood of failure), the carry-over provided by the achieved mean effect may lead to the selection of high-variance options. In situations where only small variances are offered the standard z-score expectation of small variance selection will hold (Stephens and Krebs 1986:142-144).

These general characteristics of the z-score model translate into specific implications for locational behavior. Specifically, under conditions where the mean harvest rate is above survival requirements and variance is low, harvest variance reduction will be the goal. This variance reduction goal is expected to be reflected in locational behavior through the selection of locations with low precipitation variance. In instances where there is evidence that mean harvest rates have fallen below survival requirements, or when variance is very high, differential selection of locations of high variation is the expected pattern. In the context of this analysis, it is assumed that when local population is increasing mean harvest rates are above the levels required for survival. This basic assumption is founded upon the basic fact that under starvation conditions the likelihood of successful reproduction and survival are reduced, necessitating increasingly expensive and inclusive responses to reduce food stress (Minnis 1985). The first analysis presented below tests these expectations through reference to changes in locational behavior within

the analysis region relative to patterns of precipitation variance.

6.2 Analysis Results

6.2.1 Analyses of Temporally Aggregated Climate Data

The precipitation and temperature data employed in this analysis provide a detailed diachronic record of temporal and spatial variation in climate. The Gaussian smoothed precipitation reconstruction provides a reconstruction that varies both spatially and temporally, yielding variation in both the local mean and local variance through time. The linear regression model used to estimate temperature provides high resolution temperature reconstructions that vary through time, but with uniform variance across space. This characteristic makes an analysis of locational response to temperature variance impossible. The following sections present the results of three analyses: locational response to local 30-year moving average precipitation, local 30-year moving precipitation variance, and local 30-year moving average temperature.

Precipitation Analysis

The presentation of the precipitation analysis results begins with a detailed discussion of the trends observed when all archaeological sites are combined. After outlining the associations between all sites and precipitation trends, deviations from those general trends by subsets of sites (e.g. pithouse sites, sites containing ground stone) are highlighted. The precipitation analysis for all sites is summarized in Figure 6.3, while Figures H.3, H.8, H.13, H.18, H.23, H.28, H.33 (in Appendix H) present the analysis results for all site types. Figure 6.3 presents the following data:

- *Local Precipitation Variance* : the weighted mean 30-year precipitation moving variance for the sample of random locations within the project area. Scaled from 0 – 1, with 0 representing the lowest weighted mean variance and 1 representing the highest weighted mean variance.
- *Local Precipitation Mean* : the weighted mean 30-year moving average precipitation for the random locations within the project area. Scaled from 0 – 1, with 0

representing the lowest weighted mean moving average precipitation value and 1 representing the highest weighted mean moving average precipitation value.

- *Mean P-value* : the percentile location of the observed weighted mean 30-year moving average precipitation when compared with the simulated distribution of randomly generated weighted mean 30-year moving average values for the analysis area. Scaled from 0 – 1, with 0 representing an observed value less than or equal to the lowest simulated value, and 1 representing an observed value greater than or equal to the greatest simulated value. The gray lines in Figure 6.3 forming the upper and lower boundaries of the plot represent the upper and lower 2.5 percentile ranges, indicating the region where a statistically significant ($\alpha = 0.05$) deviation from the simulated distribution of weighted average values for the randomly selected locations. Locations in the plot where the annual value falls into the lower or upper gray band indicate a significant *annual* deviation from the simulated values.
- *Variance P-value* : the percentile location of the observed weighted mean 30-year moving precipitation variance when compared with the simulated distribution of randomly generated weighted mean 30-year moving average values for the analysis area. Scaled from 0 – 1, with 0 representing an observed value less than or equal to the lowest simulated value, and 1 representing an observed value greater than or equal to the greatest simulated value. The gray lines in Figure 6.3 forming the upper and lower boundaries of the plot represent the upper and lower 2.5 percentile ranges, indicating the region where a statistically significant ($\alpha = 0.05$) deviation from the simulated distribution of weighted average values for the randomly selected locations. Locations in the plot where the annual value falls into the lower or upper gray band indicate a significant *annual* deviation from the simulated values.
- *Black Mesa Population* : The Black Mesa population curve (see Section 4.9 for a discussion of the derivation of the curve), standardized to a scale of 0 – 1, with 0 representing the minimum population for the time series, and 1 representing the maximum population for the time series.
- *Long House Valley Population* : The Long House Valley population curve (see

Section 4.9 for a discussion of the derivation of the curve), standardized to a scale of 0 – 1, with 0 representing the minimum population for the time series, and 1 representing the maximum population for the time series.

- *Kayenta Region Population* : The Kayenta region population curve (see Section 4.9 for a discussion of the derivation of the curve), standardized to a scale of 0 – 1, with 0 representing the minimum population for the time series, and 1 representing the maximum population for the time series.

Examination of Figure 6.3 results in the identification of two major regions, and several smaller subregions within the plot worthy of delineation and discussion.

First, the patterns observed for the first three hundred years of the analysis period (A.D. 600–900) are dominated by the local pattern of occupation within Long House Valley. The broad time ranges to which Black Mesa sites are assigned during this period result in low annual weights being applied to these sites in all years, except those where the numbers of Long House Valley sites decline (i.e. at A.D. 700, compare Figures 6.4, 6.5, and 6.6). Keeping this broad distribution pattern in mind, the following observations can be made:

1. Sites are associated with locations of higher mean precipitation than the study area as a whole. Considering the dominance of Long House Valley sites during this period, this is not surprising, because there is a consistent gradient in mean precipitation from southeast to northwest, with higher precipitation values in the northwest portion of the analysis region (see Appendix I for the annual mean precipitation plots).
2. The broad reversals in precipitation variance p-values at A.D. 607, 650, 690, 694, and 733 can be ascribed to variations in the regional variance gradient across the analysis area (see Appendix J for plots of the annual precipitation variance gradients).

Overall, the A.D. 600–900 period represents a time of low population density throughout the entire study area, with the bulk of the study area population occupying Long House Valley. The fact that Long House Valley is not representative of the study area as a whole

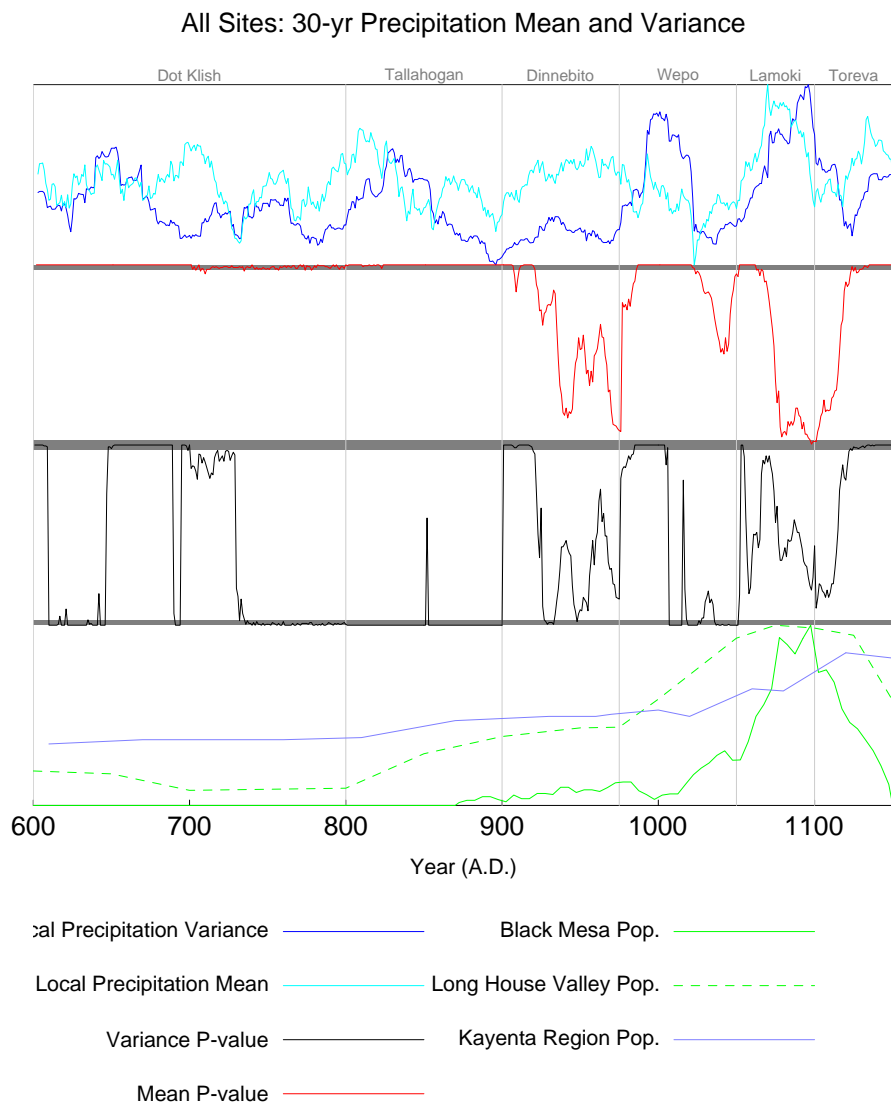


Figure 6.3: Analysis Results: Precipitation Mean and Variance, A.D. 600-1150. Note: all lines are standardized to a linear scale of 0 – 1, with 0 representing the lowest value for the time series and 1 representing the highest value of the time series.

(both precipitation mean and variance exhibit gradients that tend to differentiate Long House Valley from northern Black Mesa), in combination with the low resolution temporal data for this time period, makes the observed patterns difficult to assess relative to the z-score model outlined above. The following 250 years provide a much more detailed picture of locational response to precipitation variance.

The onset of the Black Mesa population reconstruction in A.D. 875 marks the beginning of the period for which there are more detailed population data for use in the analysis, while A.D. 900 marks the starting point for the availability of more detailed chronological assignment data for both Black Mesa and Long House Valley. This is reflected in the shorter segments in the Long House Valley population curve, and the shorter period designations used in the Black Mesa site classification system. These more refined chronological data result in a much more detailed pattern of variation in the relationship between location and precipitation variance.

Beginning in A.D. 900, greater numbers of sites appear on northern Black Mesa (Figure 6.7), though the relative population (as indicated by the Black Mesa population curve) remains low and variable. Also at roughly A.D. 900, the analysis area precipitation variance reaches the minimum for the entire analysis and remains at consistently low values for the next 75 years. The first 20 years of this time span coincides with a reversal in the variance p-value, with site locations occurring in locations with significantly greater variance values than the simulated analysis area variance. The remaining 55 years are a period of varying variance p-values that, with the exception of a single spike between A.D. 960 and 970, remain below the 50th percentile for the distribution of simulated variance p-values. During this 55-year period the first deviation from consistent high p-values for mean precipitation appears, exhibiting p-values near or below the 50th percentile for the simulated mean precipitation distribution until A.D. 975, the time at which both p-value distributions rapidly increase to at or near 100 percent.

A.D. 975 marks the beginning of a period of accelerating increases in the number of sites in Long House Valley and a 25-year period of population decline on northern Black Mesa (Figure 6.8). Climatically, A.D. 975 marks the beginning of a rapid increase in precipitation variance and the beginning of a decline towards the minimum precipitation mean for the analysis period. These deteriorating climatic conditions are associated with

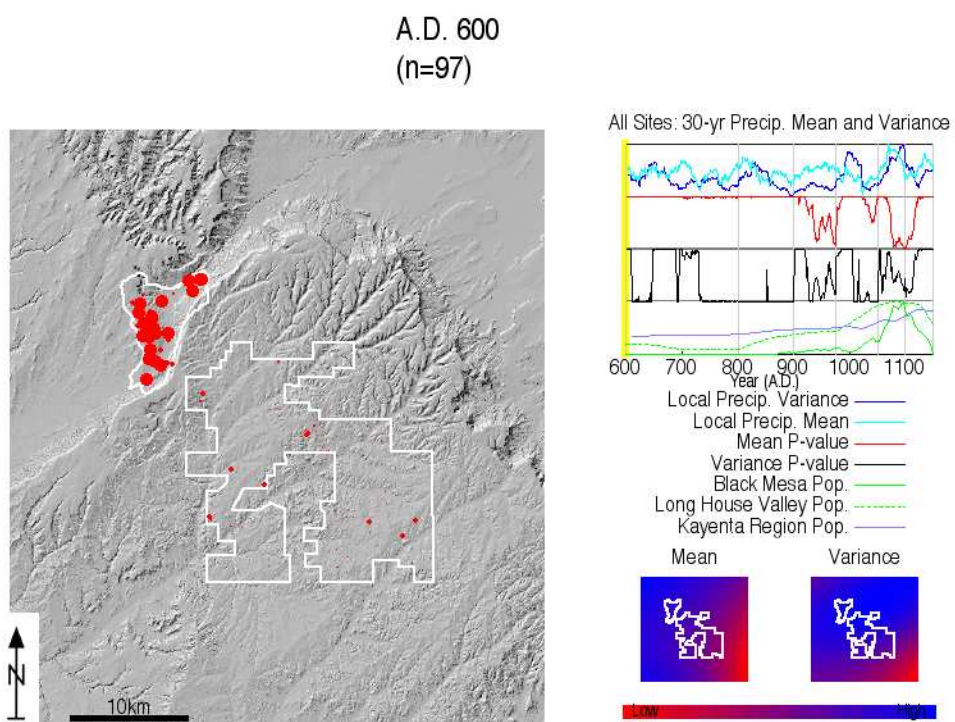


Figure 6.4: Analysis Results: Precipitation Mean and Variance, Site Distribution, and Result Plot, A.D. 600. Site location markers (red disks) vary in size according to weighting of location value in the current year's analysis.

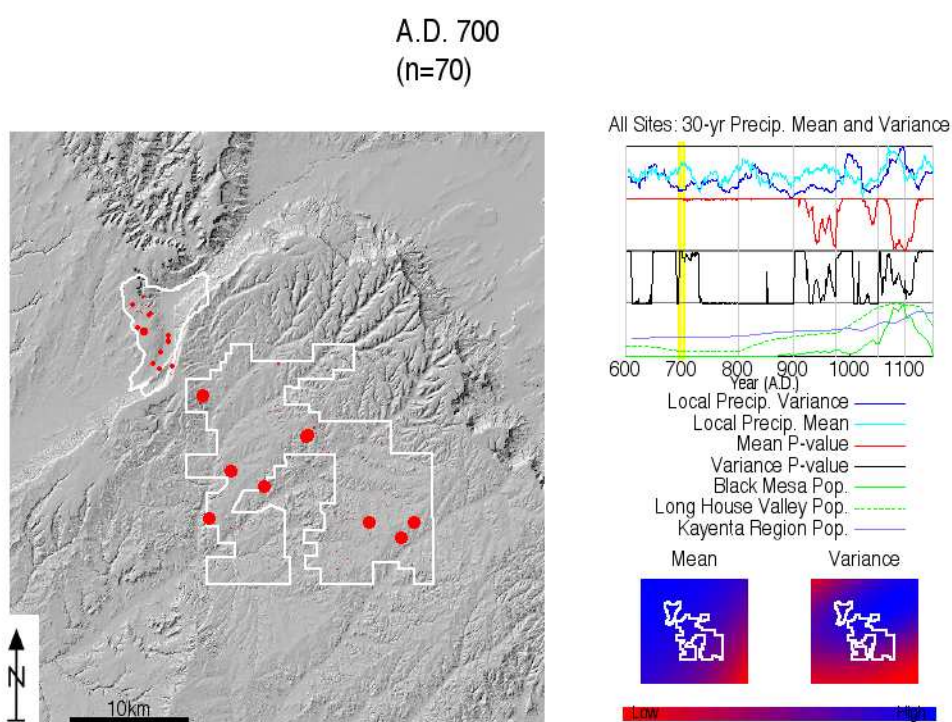


Figure 6.5: Analysis Results: Precipitation Mean and Variance, Site Distribution, and Result Plot, A.D. 700. Site location markers (red disks) vary in size according to weighting of location value in the current year's analysis.

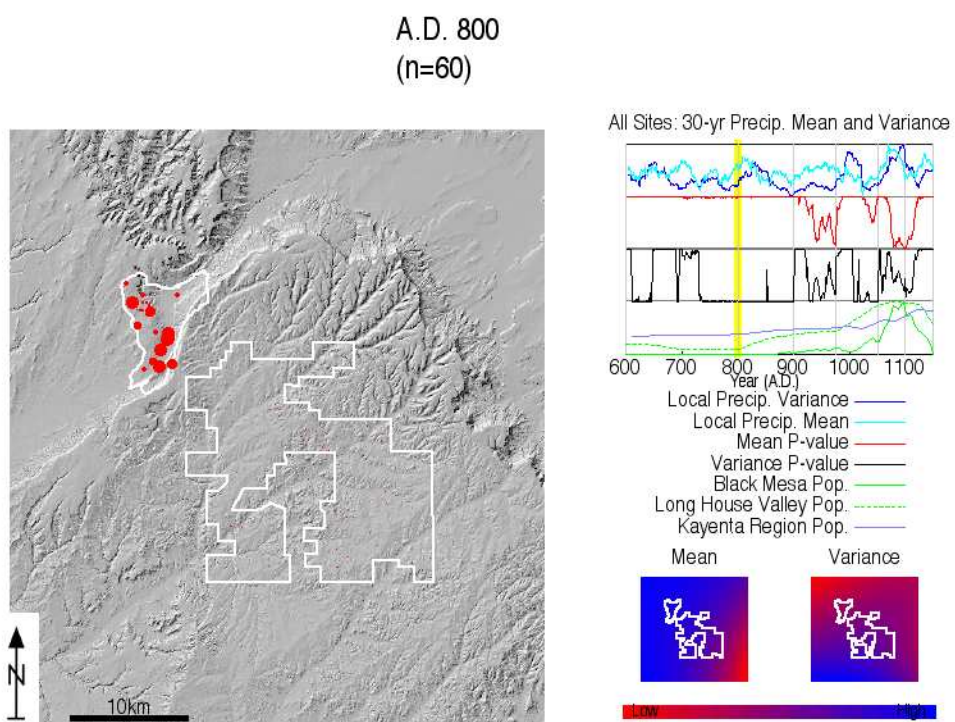


Figure 6.6: Analysis Results: Precipitation Mean and Variance, Site Distribution, and Result Plot, A.D. 800. Site location markers (red disks) vary in size according to weighting of location value in the current year's analysis.

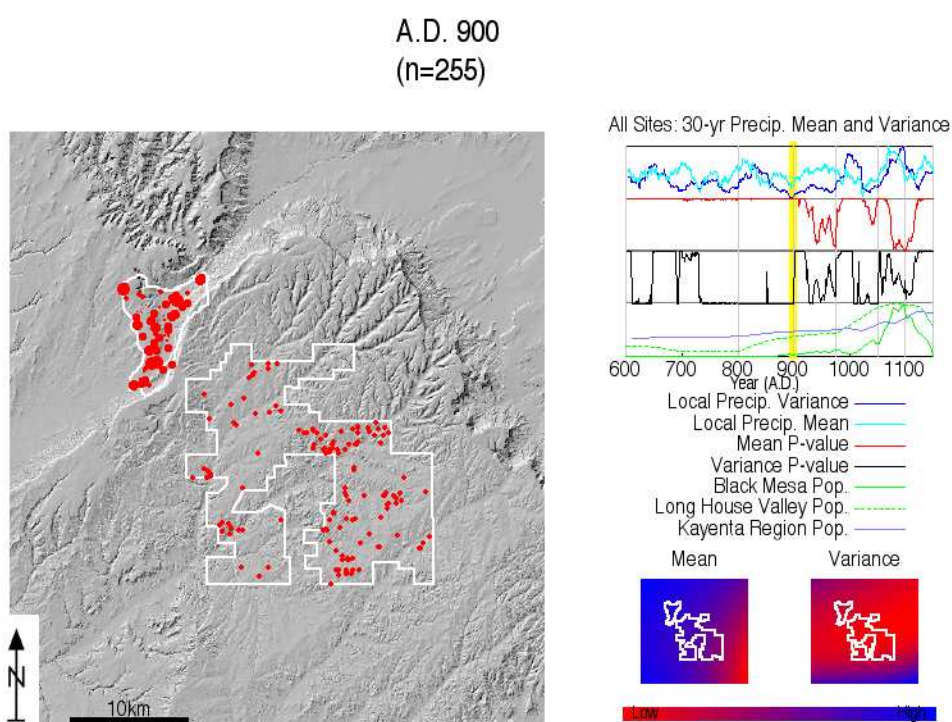


Figure 6.7: Analysis Results: Precipitation Mean and Variance, Site Distribution, and Result Plot, A.D. 900. Site location markers (red disks) vary in size according to weighting of location value in the current year's analysis.

a major reversal in the p-value trends for both precipitation mean and variance, with both approaching 100 percent by A.D. 985. This trend does not reverse for variance p-values until roughly A.D. 1000, the point at which the analysis area precipitation variance peaks and the Black Mesa population decline reverses and begins a steady upward climb. Precipitation variance p-values rapidly decline to near 0 by A.D. 1010, and remain at or near 0 (with the exception of a single very sharp spike at A.D. 1018) until A.D. 1050. The p-value trend for precipitation mean remains near 100 percent until roughly A.D. 1025, the point at which the analysis area mean precipitation reaches the low point for the analysis period, and begins a rapid trend towards the maximum mean precipitation value for the analysis period. Between A.D. 1025 and 1050 the mean precipitation p-value decreases to near the 50th percentile before reversing direction and returning to 100 percent by A.D. 1050.

Both precipitation mean and variance begin a rapid climb towards their maximum values at roughly A.D. 1050. This period of improving conditions (at least in terms of mean precipitation) is marked by a slow down in the rate of increase in the number of sites in Long House Valley and by a brief decline then rapid increase in the population of northern Black Mesa (Figure 6.9). These climatic and demographic changes are accompanied by a spike in the precipitation variance p-value at the low point in the small Black Mesa population dip at A.D. 1050, fluctuating variance p-values through roughly A.D. 1087, when there is a substantial drop in the variance p-value that lasts until roughly A.D. 1115. The precipitation mean p-value remains near 100 percent through A.D. 1075, when analysis area precipitation reaches its maximum for the analysis period and begins a decline towards more moderate values. Following the peak in A.D. 1075, the precipitation mean p-value declines rapidly to well below the 25th percentile, where it remains until after A.D. 1100.

A.D. 1100 marks the beginning of the 50-year period of population decline and ultimately the abandonment of the Black Mesa analysis area and a period of population aggregation in Long House Valley and a corresponding decline in the number of sites within the Long House Valley analysis area (Figure 6.10). This period corresponds with a time of moderate local mean precipitation and rapidly declining precipitation variance. Precipitation mean and variance p-values exhibit rapid increases towards 100 percent as

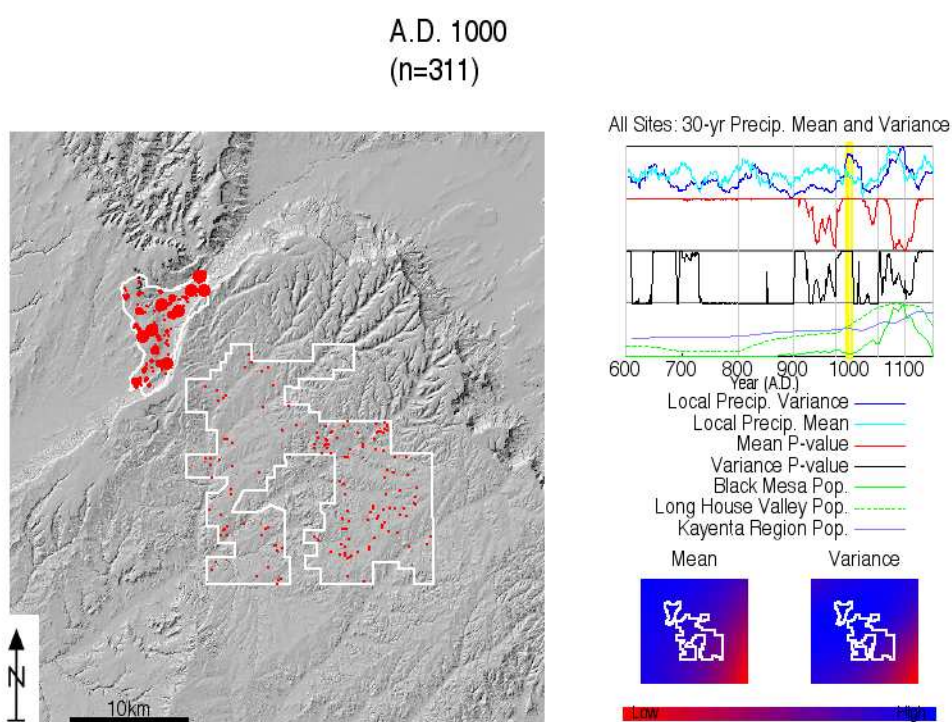


Figure 6.8: Analysis Results: Precipitation Mean and Variance, Site Distribution, and Result Plot, A.D. 1000. Site location markers (red disks) vary in size according to weighting of location value in the current year's analysis.

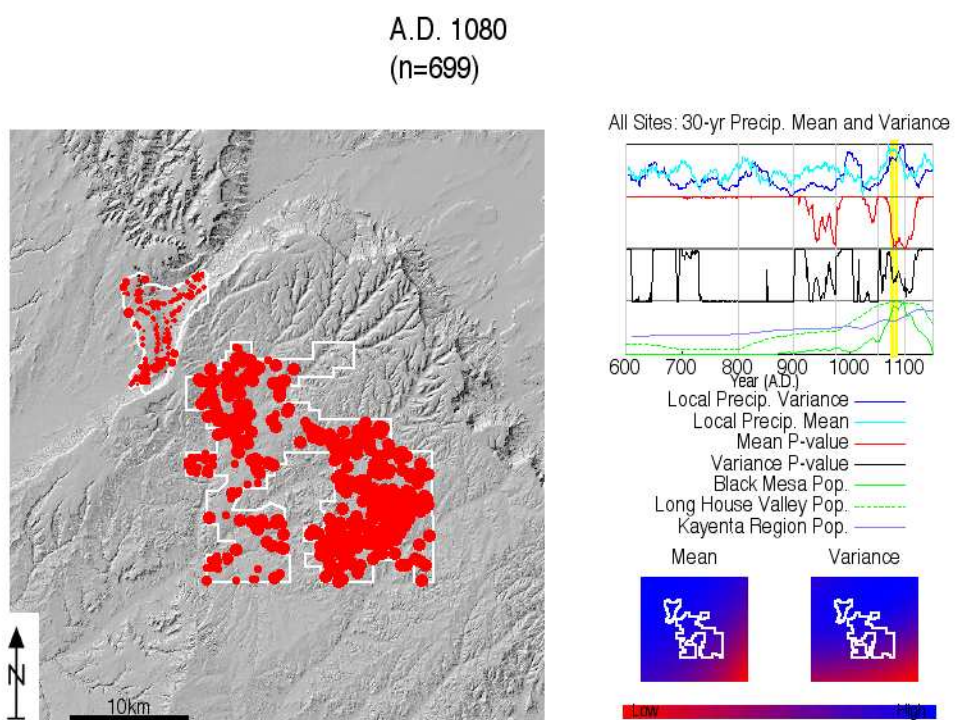


Figure 6.9: Analysis Results: Precipitation Mean and Variance, Site Distribution, and Result Plot, A.D. 1080. Site location markers (red disks) vary in size according to weighting of location value in the current year's analysis.

the population of Black Mesa declines, with both reaching 100 percent by A.D. 1130 and remaining there until the end of the analysis period.

The preceding summary of the trends exhibited in the precipitation mean and variance p-values for all site locations provides information important in linking general locational behavior to the z-score model of risk response outlined above. The following discussion links the trends identified above with expectations derived from the z-score model and integrates the results of analyses performed on subset of sites containing the feature and artifact classes listed above.

The trends described above agree with the expectations of the z-score model in several areas. Two complimentary assumptions regarding the relationship between mean harvest rate and requirements are made in the following analysis. First, that periods of population growth in both parts of the analysis area are indicative of a situation in which the mean harvest rate is greater than the requirement. Second, periods of population decline possibly indicate that mean harvest rates have fallen below the requirement level. With these assumptions in mind the following observations can be made regarding the relationship between the model expectations and the observed trends:

- Each period of population decline on Black Mesa is accompanied by a shift from low variance locations to higher variance locations, even when those declines are small and brief (e.g. the small declines just following A.D. 900, and at A.D. 1050). This pattern of association is consistent with the expectation of movement to high-variance locations when mean harvest rates fall below the requirement. This overall pattern manifests itself variably for subclasses of sites, with the following patterns of association:
 - Pithouse sites (Figure H.8) lack the rapid p-value fluctuations seen in the all-sites analysis.
 - Masonry sites (Figure H.13) show less extreme p-value variations between 0 percent and 100 percent.
 - Kiva sites (Figure H.18) exhibit a weaker association with this trend, but still have upward spikes in variance p-values associated with the population declines at A.D. 1000, 1050, and 1100.

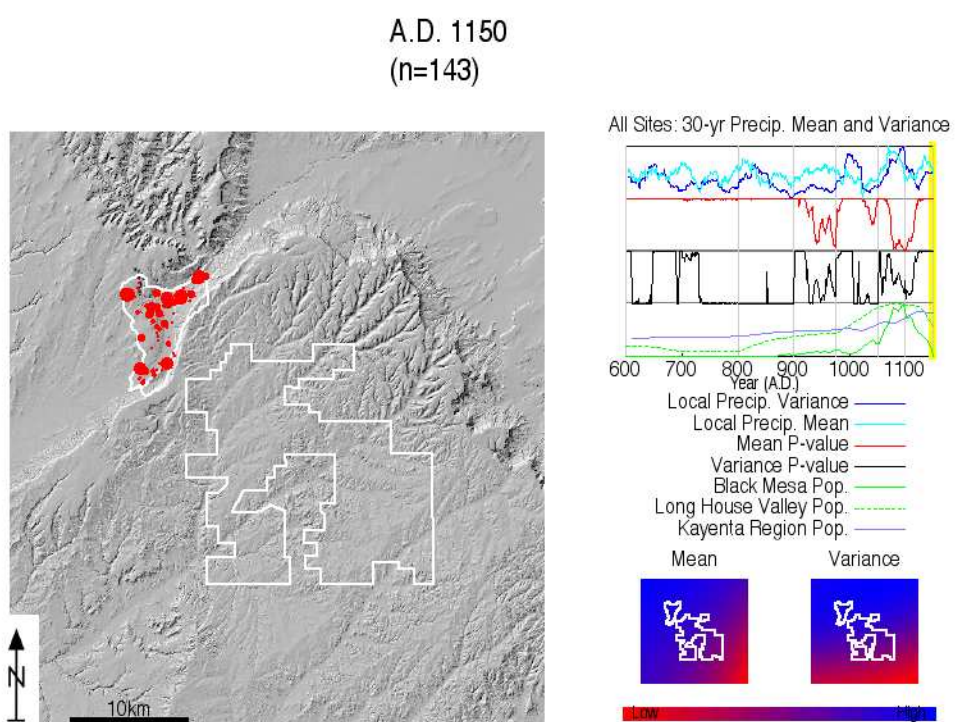


Figure 6.10: Analysis Results: Precipitation Mean and Variance, Site Distribution, and Result Plot, A.D. 1150. Site location markers (red disks) vary in size according to weighting of location value in the current year's analysis.

- Storage site variance p-values (Figure H.23) are consistent with this observation, though the shift to high-variance locations associated with the abandonment of northern Black Mesa occurs only at the very end of the analysis period.
 - Lithic sites (Figure H.28) match the trends observed in the all-sites analysis very closely.
 - Ground stone sites (Figure H.33) match the trends observed in the all-sites analysis very closely.
- Each period of consistent population growth in both Long House Valley and Black Mesa is accompanied by movement to low-variance locations within the analysis area. This is consistent with the z-score model expectation that when mean harvest rates exceed requirements, activity locations will move towards low-variance locations. This pattern is reflected in the site subclasses, with the following exception:
 - Kiva sites (Figure H.18) exhibit relatively high variance p-values throughout the tenth century while the all-sites analysis has relatively low p-values for the latter 80 years of the century.
- Two broad periods of relatively high variance are identifiable within the precipitation record: around A.D. 1000 and roughly A.D. 1070 – 1100. The bulk of these periods are associated with declines in Black Mesa population. Only a brief spike in precipitation variance at around A.D. 1075 shows the possibility of a corroboration of the achieved mean expectation of movement to locations of high variance when variance is high and mean harvest rates are above the requirements. This spike appears in the variance p-value distributions of several site sub-classes, including masonry, kiva, lithic and ground stone sites.

In summary, the observed trends in the precipitation analysis lend strong support to the expectations of the z-score model. In instances where population is in decline, locational decision-making shifts from a risk-averse to risk-seeking mode, yielding increasing variance p-value scores for each year. Conversely, when population is increasing, locational decision-making reflects a risk-averse pattern, with preferential selection of

low-variance locations. Though variable, this pattern is consistent across all site classes, regardless of feature or artifact composition.

Temperature Analysis

The distribution of sites relative to 30-year mean annual mean daily maximum temperature (MDMT) provides insights into how local temperature conditions influence the selection of activity locations, and how that influence may change through time. The presentation of the temperature analysis results begins with an overview of the trends observed when all archaeological sites are combined. After outlining the associations between all sites and temperature trends, deviations from those general trends by subsets of sites (e.g. pithouse sites, sites containing ground stone) are highlighted. The resulting plots for the all-sites analysis are presented in Figure 6.11, while Figures H.4, H.9, H.14, H.19, H.24, H.29, H.34 (in Appendix H) present the analysis results for all site types. Figure 6.11 presents the following data:

- *Local Mean Temperature* : the weighted mean 30-year moving average temperature for the random locations within the project area. Scaled from 0 – 1, with 0 representing the lowest weighted mean moving average temperature value and 1 representing the highest weighted mean moving average temperature value.
- *Mean P-value* : the percentile location of the observed weighted mean 30-year moving average temperature when compared with the simulated distribution of randomly generated weighted mean 30-year moving average values for the analysis area. Scaled from 0 – 1, with 0 representing an observed value less than or equal to the lowest simulated value, and 1 representing an observed value greater than or equal to the greatest simulated value. The gray lines forming the upper and lower boundaries of the plot in Figure 6.11 represent the upper and lower 2.5 percentile ranges, indicating the region where a statistically significant ($\alpha = 0.05$) deviation from the simulated distribution of weighted average values for the randomly selected locations. Locations in the plot where the annual value falls into the lower or upper gray band indicate a significant *annual* deviation from the simulated values.

- *Black Mesa Population* : The Black Mesa population curve (see Section 4.9 for a discussion of the derivation of the curve), standardized to a scale of 0 – 1, with 0 representing the minimum population for the time series, and 1 representing the maximum population for the time series.
- *Long House Valley Population* : The Long House Valley population curve (see Section 4.9 for a discussion of the derivation of the curve), standardized to a scale of 0 – 1, with 0 representing the minimum population for the time series, and 1 representing the maximum population for the time series.
- *Kayenta Region Population* : The Kayenta region population curve (see Section 4.9 for a discussion of the derivation of the curve), standardized to a scale of 0 – 1, with 0 representing the minimum population for the time series, and 1 representing the maximum population for the time series.

The relationship between MDMT and location selection for all sites in the analysis generally exhibits a preference for below average temperature locations on the landscape, with all years but the last 50 (from A.D. 1100–1150) showing an association with locations at or below the 50th percentile. This preference translates into the selection of locations on the landscape that are higher in elevation and/or receive less incoming solar radiation, since both of these factors contribute to the local temperature calculation. While this trend holds when all sites are considered, different patterns emerge when examining the individual site classes.

- Pithouse sites (Figure H.9) locations relative to temperature show variability through time. From A.D. 850 through 975 pithouse site locations appear relatively insensitive to temperature, appearing in locations that are at or just below the 50th percentile for temperature. At A.D. 975 pithouse sites appear in cooler locations, but begin to occupy increasingly warm locations as the Black Mesa population increases, a trend that reverses when the Black Mesa population decline begins in A.D. 1100.
- Storage site (Figure H.24) locations exhibit two primary trends in the analysis. First, prior to A.D. 900, they appear in significantly cooler locations. Second,

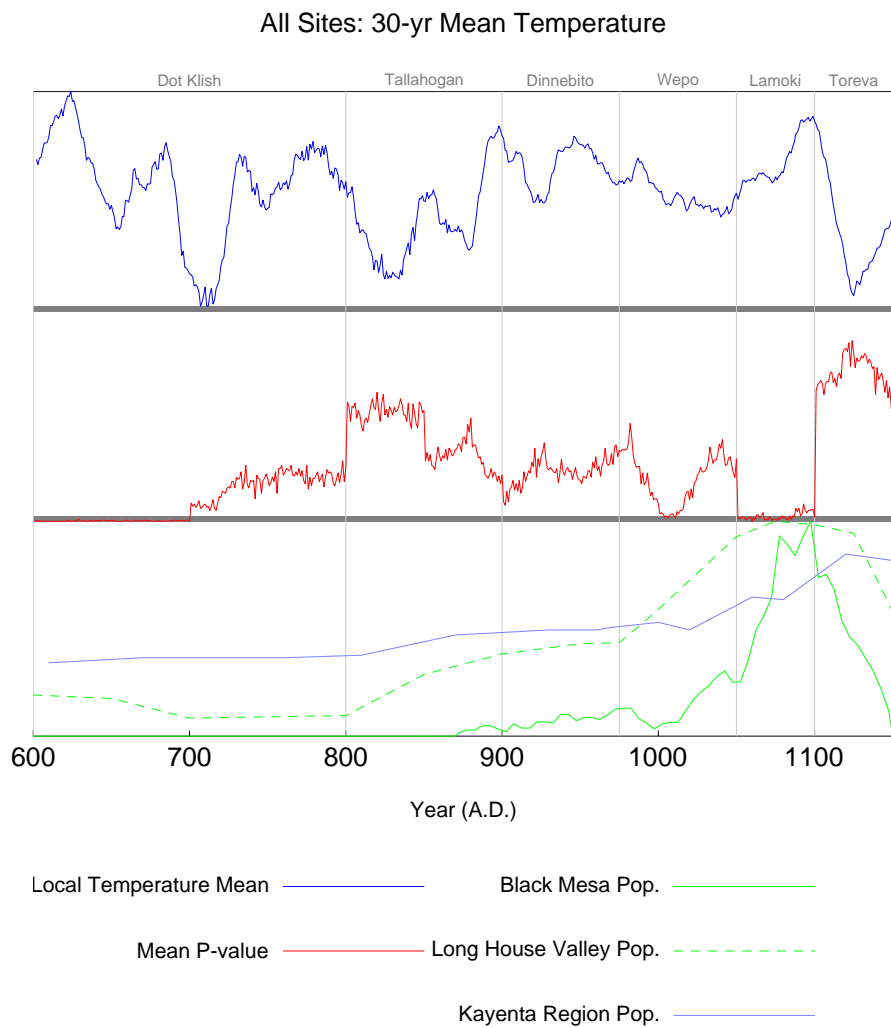


Figure 6.11: Analysis Results: Mean Annual Mean Daily Maximum Temperature, A.D. 600-1150. Note: all lines are standardized to a linear scale of 0 – 1, with 0 representing the lowest value for the time series and 1 representing the highest value of the time series.

after A.D. 900 they appear to be relatively insensitive to temperature, appearing in locations that fluctuate around the 50th percentile.

- Ignoring the period of A.D. 600–899 because of small sample sizes, kiva sites (Figure H.19) exhibit an association with above average temperature locations from A.D. 900–975, after which they shift to below average temperature locations. They remain in these locations until A.D. 1050, when they rapidly increase towards the 50th percentile and continue trending upward until A.D. 1100 when they are, and remain associated with high temperature locations again.
- Masonry sites (Figure H.14) exhibit a three-part association with temperature throughout the analysis period. Prior to A.D. 800 they are found in locations of significantly lower than average temperature. Between A.D. 800 and 850 they are associated with locations that are not significantly different from the values for the analysis area as a whole. At A.D. 850 the temperature p-values for masonry sites spike upward and remain high until A.D. 900 when they begin to trend downward towards the 50th percentile. At A.D. 1000 they abruptly decrease to well below the 50th percentile and begin a steady rise back towards the 50th percentile by A.D. 1050. Following a spike upwards at A.D. 1050, masonry site locations tend towards the 50th percentile, spiking up again at A.D. 1100 to near 100 percent, where they remain for the balance of the analysis period.
- Ground stone sites (Figure H.34) exhibit a trend line that begins at low temperature locations from A.D. 600–800, and then convert to high-temperature locations, where they remain until A.D. 1000. Afterword they dip briefly and rise back to the general location of the 75th percentile. A.D. 1050–1100 marks an abrupt change to slightly lower than average temperature locations, a trend that reversed in A.D. 1100 when ground stone sites again appear at higher than average temperature locations.
- Lithic sites (Figure H.29) are associated with lower than average temperature locations throughout the entire analysis period, fluctuating around the 25th percentile from A.D. 700–850. Between A.D. 850 and 925 there is a period of greater varia-

tion followed by an additional 75 years of relative stability near the 25th percentile which ends at A.D. 975 with a sudden drop to near 0. The trend line remains near 0 until A.D. 1100 when there is a small upturn and downturn in temperature p-values during the final 50 years of the Black Mesa occupation.

Overall, with the exception of lithic sites, none of the site subsets exhibit a clear and consistent association with a particular temperature p-value range — often exhibiting extreme variations that do not seem linked to the trends in the mean temperature data. One feature that is common in five of the six records (lithic sites do not show this association) is a major change in the p-value trend line at A.D. 1000 and A.D. 1100, both occasions when there were significant declines in Black Mesa population. This phenomenon is consistent with the major relocation of population that would have taken place during each of these depopulation events on northern Black Mesa.

6.2.2 Analyses of Environmental Data Treated as Temporally Invariate

The previous section outlined the results of analyses performed using data that varied throughout the period of analysis, essentially creating an analysis environment in which two analysis variables are changing simultaneously – activity locations and the local climatic conditions within which those activity locations are selected. This section presents the results of three analyses in which the environmental variables are held constant throughout the analysis, and only activity locations change. Like the analyses in the previous section, the discussion of each analysis will begin with a summary of the analytic results for all sites combined and will conclude with a discussion of how the subsets of sites defined using feature and artifact classes relate to the overall trends observed in the all-sites analysis.

Vegetation Analysis

The vegetation community analysis proceeded in a slightly different manner than that for the other analyses because the plant community classes are qualitative as opposed to quantitative values. Because of this difference, weighted proportions as opposed to

weighted average values were used. More specifically, for each year of the analysis the weights associated with all of the sites falling within each of the six mapped vegetation categories mapped by the GAP project within the analysis area are summed and divided by the sum of weights for all sites. This calculation results in a proportion of sites falling within each vegetation class that reflects the weights assigned to each site location. These weighted proportions for each year are plotted relative to the proportions obtained through the simulation of random locations and calculation of the weighted proportions employing the same weights as used in the calculation of the observed weighted proportion (the p-value).

The vegetation classes included in the analysis include six GAP classes that fall within the analysis area (with GAP class codes provided for reference to Table 2.1): Pinyon-Juniper (1122.I0a0), Mixed Scrub (1152.I0a5), Saltbush (1152.I0a6), and Shrub-Grass Disclimax (1142.j0a4), in addition to Agriculture and Water (refer to Section 2.2.1 and Table 2.1 for a detailed discussion of these plant communities).

The results of the analysis of all sites are presented in Figure 6.12, and the results plots for all vegetation analyses are provided in Figures H.5, H.10, H.15, H.20, H.25, H.30, H.35 (in Appendix H). Each plot consists of seven separate plot regions. The first six regions provide the weighted proportion p-value for each of the above listed vegetation communities (scaled from 0 to 1); the seventh region provides the three reference human population curves for the area (standardized to a scale of 0 to 1, with 0 representing the minimum population and 1 representing the maximum population).

In the analysis of all sites, two vegetation communities stand out as having more high weighted proportion p-values than low for much of the analysis period: the Pinyon-Juniper (PJ) and Mixed Scrub (MS) communities. Two communities exhibit highly variable weighted proportion p-value trends that tend to draw down the p-values for PJ and MS when they increase: Saltbush (SB) and Agriculture (AG). The Shrub-Grass Disclimax (SG) exhibits generally low and relatively steady values throughout the analysis period. With the initiation of increased occupation of northern Black Mesa in A.D. 900, there is a marked increase in the p-values associated with both AG and SB, bringing both distributions well above the 50th percentile. This increase in weighted proportions for AG and SB is reflected in a substantial drop in the p-values of PJ and MS communities,

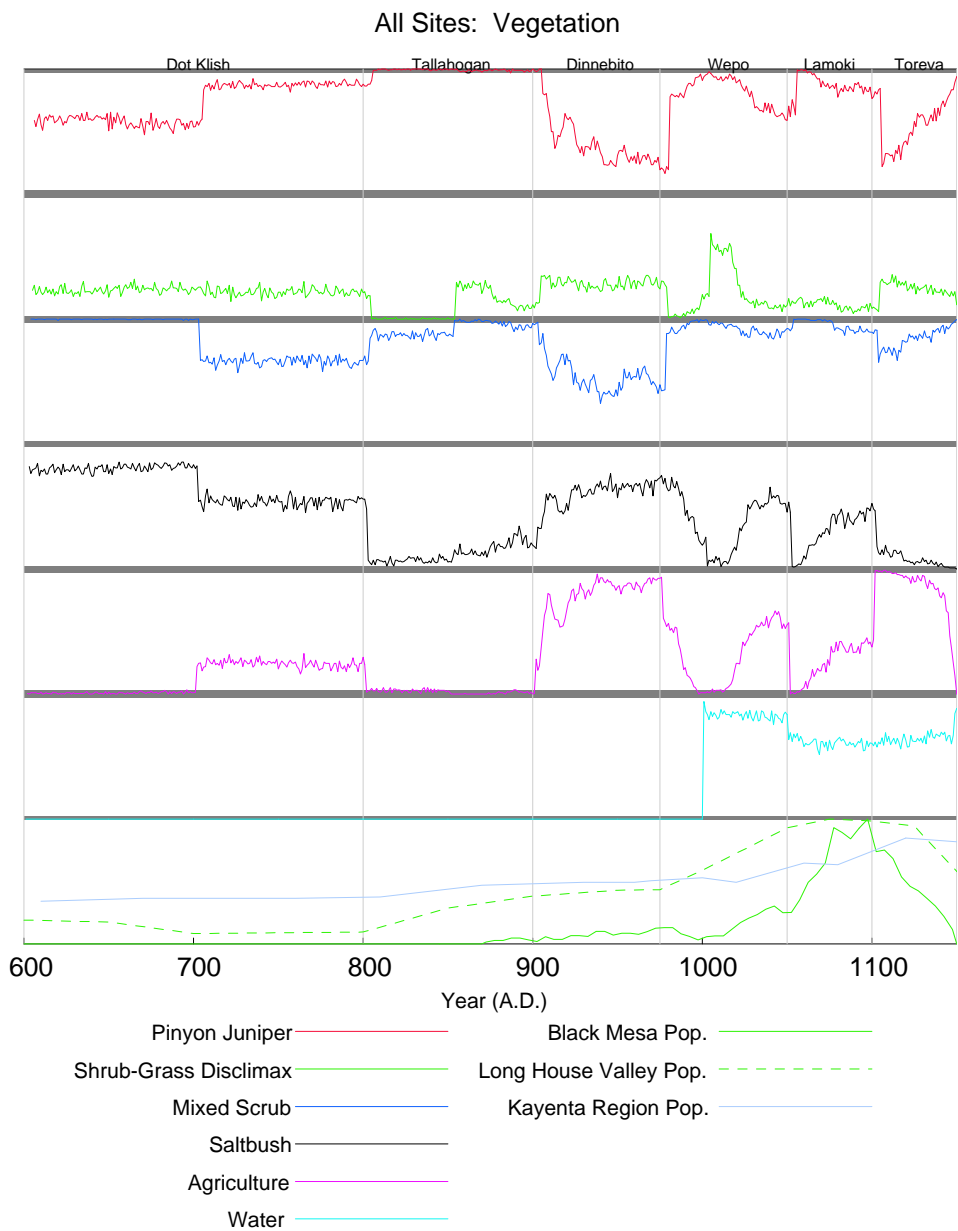


Figure 6.12: Analysis Results: Vegetation Community Proportion P-Values, A.D. 600–1150. Note: all lines are standardized to a linear scale of 0 – 1, with 0 representing the lowest value for the time series and 1 representing the highest value of the time series. Refer to Section 2.2.1 and Table 2.1 for descriptions of the vegetation communities.

placing them at or below the 50th percentile for most of the tenth century A.D. Both the PJ and MS communities rebound to their characteristically high p-values shortly after A.D. 975 while simultaneously the AG and SB communities drop back to near-zero values. Following A.D. 975 the MS community remains at near 100 percent levels throughout the remainder of the analysis period. The trend observed for PJ reflects a potential trade-off between PJ and the combination of AG and SB, with PJ exhibiting several downturns that mirror increases in AG and SB. The patterns observed for different site classes differ markedly from those observed in the all-sites analysis.

Examination of the result plots (Figures H.5, H.10, H.15, H.20, H.25, H.30, H.35) for the individual site subsets suggests a complex and variable pattern of association between particular feature and artifact classes and vegetation communities, with no class exhibiting a clear pattern of preference or avoidance throughout the analysis period. Instead, each site class exhibits variable patterns of association that change through time, with the major temporal subdivisions providing a useful framework for summarizing the observed patterns. Tables 6.1, 6.2, 6.3 summarize the trends for each site class for each of the vegetation communities, with one table for each of the broad chronological subdivisions outlined in Chapter 4 (BMIII, PI, and PII).

The more patterned trends observable in Table 6.1 are likely to have been created by the relatively small number of sites located within the northern Black Mesa analysis area, biasing the distribution of sites towards the vegetation communities that dominate Long House Valley (Figure 2.17). Each site type seems to be preferentially located within specific communities: storage sites within the SB community, Masonry sites within the SG disclimax, Lithic sites within the SB community, and ground stone sites within the PJ community.

Table 6.1: Basketmaker III Vegetation Association P-Value Trends

	Pithouse	Storage	Masonry	Kiva	Lithic	Ground stone
Pinyon-Juniper (1122.I0a0)	—	↔	↔	—	↔	↑
Mixed Scrub (1152.I0a5)	—	↓	↓	—	↔	↓
Saltbush (1152.I0a6)	—	↑	↔	—	↑	↔
Shrub-Grass Disclimax (1142.j0a4)	—	↔	↑	—	↓	↓
Agriculture	—	↓	↓	—	↔	↔
Water	—	↓	↓	—	↓	↓

(continued on next page)

Table 6.1: Basketmaker III Vegetation Association P-Value Trends (*continued*)

Pithouse	Storage	Masonry	Kiva	Lithic	Ground stone
↑: higher than average, ↓: lower than average, ↔: no clear trend high or low, —: sample size too small					

The patterns of association become much less clear in PI times (Table 6.2), with most cells in the table reflecting no clear trends towards preference or avoidance, with the exception of pithouse and ground stone sites, both of which exhibit more clear positive or negative associations than the other site classes. Pithouse sites appear to be preferentially located within MS and SG disclimax communities while avoiding the SB, and AG communities. Ground stone sites are preferentially located within the MS and SB communities while avoiding the SG disclimax community. Lithic sites show an association with MS communities with no clear association with any other communities, while masonry sites exhibit an association with SB communities. An important characteristic of the PI distribution of associations, is that in each instance where a positive or negative association is observed during PI, that association is absent or the opposite from the association observed in BMIII. This pattern continues in PII, with little continuity in the pattern of association.

Table 6.2: Pueblo I Vegetation Association P-Value Trends

	Pithouse	Storage	Masonry	Kiva	Lithic	Ground stone
Pinyon-Juniper (1122.I0a0)	↔	↔	↔	↔	↔	↔
Mixed Scrub (1152.I0a5)	↑	↔	↔	↓	↑	↑
Saltbush (1152.I0a6)	↓	↔	↑	↔	↔	↑
Shrub-Grass Disclimax (1142.j0a4)	↑	↔	↔	↔	↔	↓
Agriculture	↓	↔	↔	↔	↔	↔
Water	↓	↓	↓	↓	↓	↓

↑: higher than average, ↓: lower than average,
↔: no clear trend high or low, —: sample size too small

The patterns of association in PII (Table 6.3) are no more clear than those observed in PI, and only in two instances is there consistency in the associations observed between site classes and vegetation communities. Specifically, ground stone sites show continuity in their avoidance of SG disclimax community locations and pithouse sites continue their avoidance of SB community locations. New patterns of association that appear during

PII include: the association of pithouse and lithic sites with the PJ community; and the association of storage, masonry, and lithic sites with areas mapped as AG.

Table 6.3: Pueblo II Vegetation Association P-Value Trends

	Pithouse	Storage	Masonry	Kiva	Lithic	Ground stone
Pinyon-Juniper (1122.I0a0)	↑	↓	↔	↔	↑	↔
Mixed Scrub (1152.I0a5)	↔	↔	↔	↔	↔	↔
Saltbush (1152.I0a6)	↓	↔	↔	↔	↔	↔
Shrub-Grass Disclimax (1142.j0a4)	↔	↔	↔	↔	↓	↓
Agriculture	↔	↑	↑	↔	↑	↔
Water	↓	↓	↓	↓	↑	↑

↑: higher than average, ↓: lower than average,
 ↔: no clear trend high or low, —: sample size too small

Overall, the patterns of association observed in the analysis reflect a changing site selection process through time that is likely to reflect multiple criteria. The fact that the patterns of association become less clear through PI and PII may be partially explained by the wide dispersal of sites throughout these periods (particularly PII), with criteria other than vegetation community (i.e. existing occupation, availability of water, presence of a suitable location for constructing a habitation, availability of fuel and construction materials, etc.) contributing to the ultimate selection of site location.

Elevation Analysis

The analysis of site location provides an opportunity to examine the upland/lowland occupational trends described in Chapter 4. In particular, it allows a comparative assessment of elevational movement of activity locations through time.

The analysis follows the same procedure as the outlined above for the climate variables, with one significant difference: elevation is static throughout the study period, leading to the calculation of weighted average elevation values for each analysis year solely upon the site location weighting for each year. Following the analysis procedure used in the preceding analyses, a weighted average elevation is calculated for each analysis year and plotted against a simulated distribution of weighted average values for that year, with the resulting plot providing a graphic representation of the relationship between the observed and simulated elevation for random locations within the analysis area. The

results of the analysis for all sites are presented in Figure 6.13, and the results plots for all elevation analyses are provided in Figures H.1, H.6, H.11, H.16, H.21, H.26, H.31 (in Appendix H).

The data in the plots fall into three display areas. The top area depicts the mean elevation trend as calculated using the simulation approach. This line provides a representation of what the elevation trend line for each analysis would look like if each year's site sample were drawn from locations independent of elevation. The second plot area (in the middle of the figure) represents the relationship between the observed weighted mean and the distribution of weighted mean values obtained through simulation. The lower half of the plot area represents observed elevations lower than the analysis area average while the upper half represents observed elevations higher than the average for the analysis region. The gray bands bordering the top and bottom of the central plot area represent the upper and lower 2.5 percent regions that signify a significant ($\alpha = 0.05$) annual deviation from the distribution weighted average elevations derived from the randomly selected points. The lower portion of the plot represents the three reference human population curves used in the analysis: Long House Valley, Black Mesa, and the Kayenta Region. The plotted lines in the upper and lower plot region are scaled from 0 to 1, with 0 representing the lowest value in the time series and 1 representing the highest value.

An examination of Figure 6.13 suggests that there is an overall tendency for activity locations to be preferentially located at low elevations except during three distinct periods when there are observable deviations from this pattern. First, between A.D. 700 and 800 there is an increase in weighted mean elevation p-values to roughly 35 percent, still indicating a bias towards low elevation sites, but not showing as strong a preference as observed before and after this period. There is a minor deviation from the strong preference for low elevation locations between A.D. 940 and 975. The third and most significant deviation from the strong pattern of locational association with low elevations occurs between A.D. 1060 and 1120, the period of most rapid population growth within the Black Mesa analysis area. While this trend line shows a strong overall preference for low elevation locations, the trend lines for individual site classes show differential preferences regarding elevation.

- Pithouse sites (Figure H.6) show a very strong association with low elevation loca-

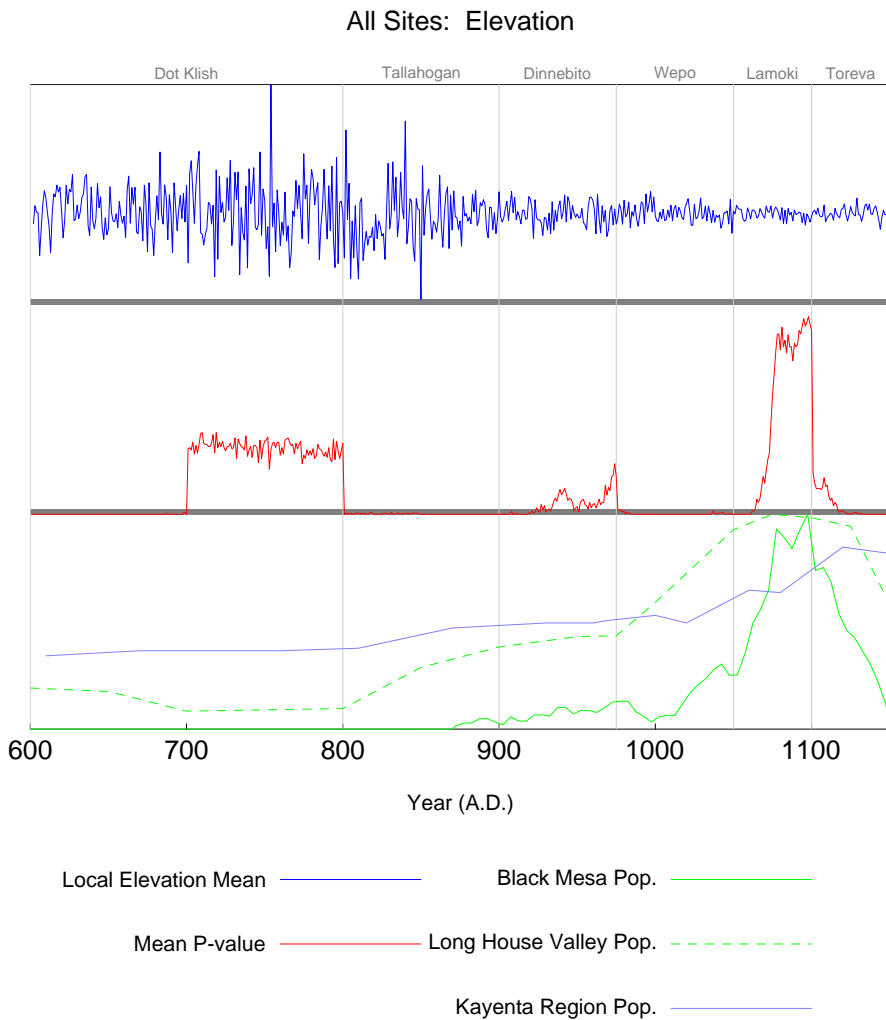


Figure 6.13: Analysis Results: Elevation Distribution of Activity Locations, A.D. 600–1150. Note: all lines are standardized to a linear scale of 0 – 1, with 0 representing the lowest value for the time series and 1 representing the highest value of the time series.

tions throughout the analysis period until A.D. 1100, when there is a rapid increase in the weighted average elevation p-value from near 0 to over the 50th percentile. The p-value for pithouse sites then declines back to 0 by A.D. 1150.

- Kiva sites (ignoring the period of A.D. 600-849 due to small sample size, Figure H.16) exhibit a markedly variable relationship with elevation. Until A.D. 975, kiva sites are associated with low elevation locations. Beginning at A.D. 975 there appear three distinct upward fluctuations in the weighted average elevation p-value, with the first reaching above the 80th percentile before rapidly declining back to below the 10th percentile. The second upward spike in p-values occurs at roughly A.D. 1010, with the maximum p-value reaching the 60th percentile before decreasing back to 0 at A.D. 1050. The third and final increase in p-values begins just after A.D. 1050 and only reaches a moderate value of roughly 30 percent before declining at A.D. 1100.
- Masonry site (Figure H.11) locations appear to be significantly associated with low elevation throughout the analysis period following A.D. 800, prior to which there is an observed association with higher elevation locations that may be attributable to the limited sample size for masonry sites prior to A.D. 849. There are two minor deviations from p-values near 0, one between A.D. 900 and 975, and the second between A.D. 1075 and 1100. Both of these deviations fail to increase above the 25th percentile and neither signal a serious deviation from a preference for low elevation locations for masonry sites.
- Storage sites (Figure H.21) exhibit a very different pattern than the site classes already discussed. Although storage sites begin the analysis period with a general association with low elevation locations, this pattern changes dramatically following the Black Mesa population decline around A.D. 1000. Specifically, beginning at about A.D. 1010 the weighted average elevation p-value for storage sites begins to increase rapidly towards a plateau of values at or above the 90th percentile by A.D. 1055. This high value is maintained through the rest of the analysis period until A.D. 1150 when Black Mesa is abandoned.

- Ground stone (Figure H.31) and lithic sites (Figure H.26) both exhibit patterns similar to those already described for the all sites analysis. These include a period of elevated p-values between A.D. 700 and 800, a long term association with low elevation sites beginning at A.D. 800 and continuing, with some fluctuations, until there appear rapid increases that correlate with the rapid growth of population on northern Black Mesa between A.D. 1050 and 1100. Following these rapid increases in weighted average elevation p-values there is a rapid decline between A.D. 1100 and 1150, corresponding with the rapid decline in northern Black Mesa population during this period.

In total, the elevation analysis suggests that there was a strong locational preference for low elevation except when population levels increased rapidly, perhaps indicating that the availability of preferred low-elevation locations was limited. The deviation from this general pattern by storage sites, specifically through the maintenance of a preference for high elevation locations late in the analysis period, potentially indicates an increasing need for storage at these locations as mean precipitation declined and variation peaked in the late 11th and early 12th centuries.

Flow Accumulation Analysis

The final analysis examining the relationship between activity location and local environmental conditions looks at the local water availability potential as reflected by the maximum flow-accumulation within a square catchment, 250m across, surrounding each site location. Flow-accumulation represents the number of upslope pixels contributing to flow through a given analysis pixel, and provides a reasonable proxy for the potential water flow through a given location on the landscape (see Figure 2.16). Flow accumulation represents potential *surface flow* and does not reflect potential subsurface water sources like the springs located along the western edge of Long House Valley.

The analysis itself follows the same procedure as the outlined above for elevation. Following this analysis procedure, a weighted average maximum flow accumulation is calculated for each analysis year and plotted against a simulated distribution of weighted average values for that year, with the resulting plot providing a graphic representation

of the relationship between the observed and simulated flow accumulation for random locations within the analysis area. The results of the analysis for all sites are presented in Figure 6.14, and the results plots for all elevation analyses are provided in Figures H.2, H.7, H.12, H.17, H.22, H.27, H.32 (in Appendix H).

The data in the plots are displayed in three areas. The top area depicts the mean maximum flow accumulation trend as calculated using the simulation approach. This line provides a reference of what the flow accumulation trend line for each analysis would look like if each year's site sample were drawn from locations independent of flow accumulation. The second plot area (in the middle of the plot) represents the relationship between the observed weighted mean and the distribution of weighted mean values obtained through simulation. The lower half of the central plot area represents observed flow accumulations lower than the analysis area average while the upper half represents observed flow accumulations higher than the average for the analysis region. The gray bands bordering the top and bottom of the central plot area represent the upper and lower 2.5 percent regions that signify a significant ($\alpha = 0.05$) annual deviation from the distribution weighted average flow accumulations derived from the randomly selected points. The lower portion of the plot represents the three reference human population curves used in the analysis: Long House Valley, Black Mesa, and the Kayenta Region. The plotted lines in the upper and lower plot region are scaled from 0 to 1, with 0 representing the lowest value in the time series and 1 representing the highest value.

Examination of Figure 6.14 suggests two trends in the pattern of association between all sites locations and local maximum flow accumulation. First, prior to A.D. 900, there is a variable association between local flow accumulation and activity location. Specifically, between A.D. 600 and 700 there is no clear association between location and flow accumulation. Between A.D. 700 and 800 there is an avoidance of locations of high flow accumulation. The ninth century A.D. exhibits a mixed pattern of no significant association during the first half of the century, and a strong avoidance in the second half of the century. This pattern changes dramatically in A.D. 900, when sites begin to appear at locations with significantly high flow accumulation, with this pattern of association continuing until very late in the abandonment of the Black Mesa analysis area.

These patterns relate to the patterns of drainage aggradation and degradation (Figure

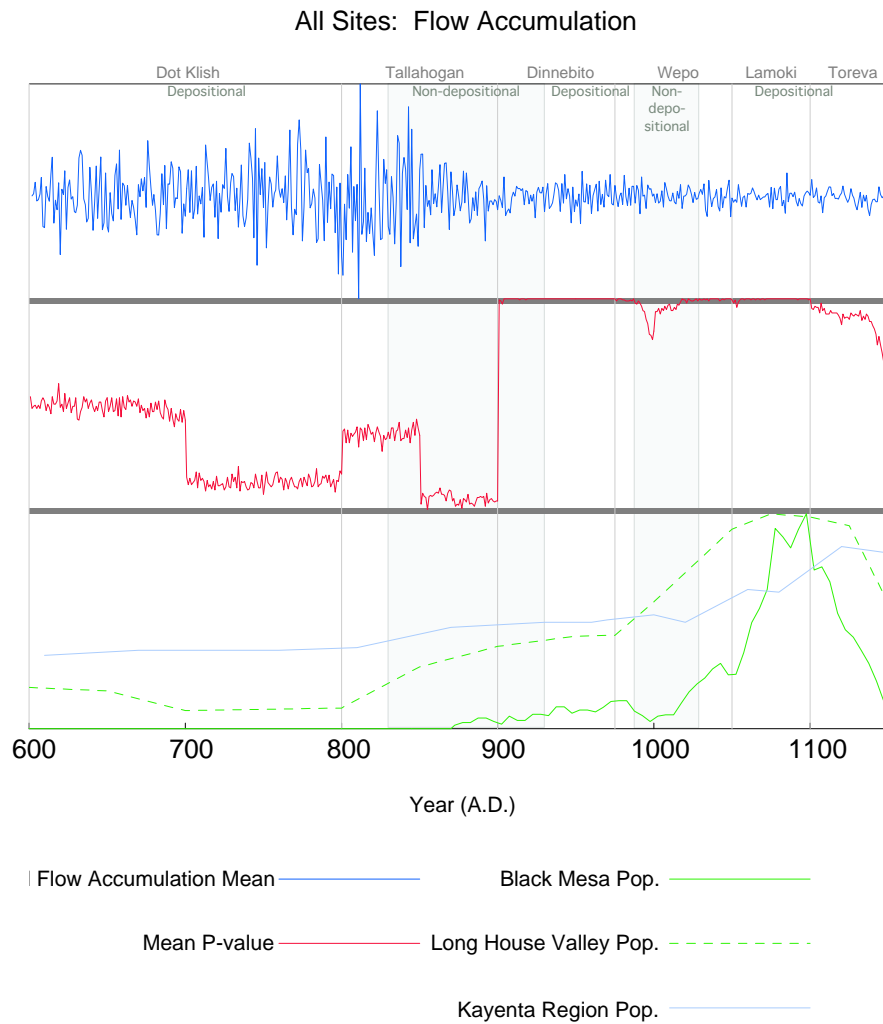


Figure 6.14: Analysis Results: Maximum Flow Accumulation for Activity Locations, A.D. 600-1150. Note: all lines are standardized to a linear scale of 0 – 1, with 0 representing the lowest value for the time series and 1 representing the highest value of the time series. Alternating white and gray regions across figure represent depositional and non-depositional periods from Plog et al. (1988: Fig. 8.1-A)

3.1 D.1, D.2; Figure 6.14) in two ways. First, early in the analysis period there is little clear association between flow accumulation, site location and depositional or non-depositional conditions. There are periods of both 50th percentile and below 20th percentile p-values during both depositional regimes prior to A.D. 900. Beginning in A.D. 900 the very strong pattern of high p-values for site locations is associated with the end of a non-depositional period and continues until the period of abandonment of northern Black Mesa. The only deviation in this trend for p-values at or near the 100th percentile is during the brief non-depositional period that began just before A.D. 1000 and continued into the early 11th century. There is a distinct decrease in the site-location p-values near the onset of this period, a phenomenon consistent with a brief, and minor, shift away from a settlement pattern focussed on high flow-accumulation locations.

The patterns exhibited by the different site classes in the analysis tend to follow these trends, with the exception of pithouse and kiva sites which show some significant deviations.

- Pithouse sites exhibit a different pattern of association between local maximum flow accumulation and location. Specifically (ignoring the period before A.D. 849 because of small sample sizes), pithouse sites show the same association with low flow accumulation locations between A.D. 850 and 900, and high flow accumulation locations between A.D. 900 and 975 as exhibited by all sites, but following A.D. 975 reflects a major change in association. Between A.D. 975 and 1050 pithouse sites exhibit highly variable associations with both high and low flow accumulation locations. Following A.D. 1050 pithouse sites are associated with low flow accumulation locations.
- Kiva sites (ignoring the trend line prior to A.D. 899 due to small sample size) exhibit highly variable patterns of association with flow accumulation. Between A.D. 900 and 975 kiva sites are significantly associated with high flow accumulation locations. Between A.D. 975 and 1050 the reverse pattern holds, with kiva site locations occurring in low flow accumulation locations. Finally, following A.D. 1050, kiva sites are again associated with high flow accumulation locations.
- Masonry sites exhibit a pattern quite similar to that for all sites, particularly after

A.D. 900. Prior to A.D. 900, masonry sites demonstrate a weak association with high flow accumulation sites, with p-values ranging from roughly 50 percent to 85 percent. Following A.D. 900, masonry sites show a strong association with high flow accumulation sites, with this trend only changing after A.D. 1100 when the flow accumulation p-values begin a decline to the 50th percentile by A.D. 1150.

- Storage sites are also similar to all sites in their pattern of association between flow accumulation and site location. Between A.D. 600 and 850 storage sites tend to be associated with higher flow accumulation locations, with the flow accumulation p-values ranging from 70 percent to 90 percent. Following A.D. 850 there is a 50 year period of association with low flow accumulation locations. Beginning at A.D. 900 there is a long period of consistent association with high flow accumulation locations that only tapers slightly between A.D. 1100 and 1150.
- Lithic sites exhibit a pattern that very closely matches the pattern of association described above for all sites. The one exception to this similarity is a rapid decrease in associated flow accumulation between A.D. 975 and 1050, with the bulk of the decrease being associated with the downturn in Black Mesa population that occurs between A.D. 980 and 1010.
- Ground stone sites also exhibit a pattern of association between site location and low flow accumulation with the minor difference of reflecting higher flow accumulation p-values for the period of A.D. 600 to 850.

In summary, the flow accumulation analysis reflects the importance of water availability in locational decision making, but also highlights the limitations in concentrating on surface water when assessing location choice and water availability. Periods of aggradation and degradation also appear to be related to the pattern of association between drainages (locations of high flow accumulation) and site locations with the strong association slightly weakened during periods of degradation, an unsurprising, but important pattern of behavior. Additionally, it must be remembered that two different water provision scenarios exist within the analysis area: surface flow and local accumulation within drainage bottoms on northern Black Mesa, and more limited surface flow and more sig-

nificant contribution from springs along the western margin of Long House Valley. This pattern of differential importance of local flow accumulation is reflected in the lower flow accumulation p-values encountered during those times when Black Mesa's population was low or declining while Long House Valley's population was steady or increasing. This is because more of Long House Valley's water needs are met through springs than through surface flow.

6.3 Relationship of Analysis Methods and Results to Previous Analyses

This analysis and results build upon and complements previous regional research programs in several respects. It builds upon previous work by combining the results of diverse long-term research programs into a unified analytic framework that employs current statistical, geospatial, and simulation methods in a quantitative evaluating the relationship between environmental parameters and the loci of archaeologically observable past human behavior. This analysis complements previous regional research by addressing questions of localized spatial decision-making, an analytic question generally defined at lower spatial resolutions than employed here.

One key analysis that this analytic effort relates to is that completed by Plog and Hantman (1990), in which they statistically evaluate the relationship between the high-resolution population reconstruction for northern Black Mesa (the reconstruction used in this analysis, S. Plog 1986b; S. Plog and Hantman 1990) and four precipitation parameters. These parameters include

- a) decadal departures for the dendroclimatic station closest to the study area;
- b) the standard deviation at that station of the departures for the decade in question and the preceding two decades (a measure of temporal variability);
- c) the average of the decadal departures for the four stations within a 94 km (60 mi.) radius of the study area; and d) the standard deviation of the departures at those four stations (a measure of spatial variability). (S. Plog and Hantman 1990:449)

A critical distinction between these precipitation parameters and the precipitation model used in this analysis is that each of the four variables used in Plog and Hantman's analysis

is a single value for each analysis year (A.D. 870-1150) while the precipitation model used in this analysis provides a raster of precipitation values across the analysis region. This contrast in used climate data directly relates to the difference between Plog and Hantman's analyses and that presented above – Plog and Hantman's analysis concentrates on assessing the relationship between regional population and climate, while this analysis examines local locational behavior relative to mapped risk as quantified by climate variation. Stated another way, Plog and Hantman's analysis seeks to assess the linkage between climate and regional population trends proposed by Dean, Euler and others (Dean, et al. 1985; Euler, et al. 1979), while this analysis treats population as an independent variable used only to determine the statistical weights given to site locations used in the analysis. In this context, the results of this analysis neither support nor conflict with the conclusions reached by Plog and Hantman that there are no statistically significant relationships between their high-resolution population reconstruction for northern Black Mesa and the temporal and spatial summaries of annual precipitation data for the surrounding region (S. Plog and Hantman 1990:449).

Similarly, the methods employed and results obtained in this analysis are qualitatively different from those obtained by Plog, Dean, and others (Dean, et al. 1985; Euler, et al. 1979; F. Plog, et al. 1988). Specifically, this analysis quantitatively tests the relationship between site location and risk within the analysis area while the climate/settlement behavior/social interaction/subsistence practice/territoriality hypothesis tests performed by Plog et al. (1988) are qualitative, and generally performed at a regional scale (e.g. Black Mesa, Chaco Canyon, Long House Valley, etc.). The results of this analysis provide a high-resolution evaluation of site location selection *within* the project area while the Plog et al.'s analyses collapse much variation within project areas into single or binary characteristics for qualitative comparison with paleoclimate records.

When comparing the results obtained in this analysis with those presented by Plog et al. (F. Plog, et al. 1988:252-253), the only area where there is direct overlap between the analyses is in the context of upland-lowland movement. This analysis interprets patterns in upland-lowland movement in reference to population trends while Plog et al. explore these trends in reference to drainage aggradation and degradation and high and low effective moisture estimates. These contrasting comparisons highlight the multivariate nature

of settlement pattern analyses in which multiple explanatory variables may contribute to the development of increasingly inclusive explanations for prehistoric locational behavior.

Finally, when compared to the work of Van West and Kohler (Kohler and Van West 1996; Kohler, et al. 1996b; Van West 1994) for Mesa Verde, this analysis provides additional parameters that may be used in their agent based modeling efforts (Kohler, et al. 1996b) to simulate spatial patterning of archaeological sites resulting from household-level decision making. Specifically, the meteorological interpolation methods employed in this analysis may be used to refine the localized PDSI estimates generated by Van West (1994), while the general concept of locational response to localized variation in climate would also complement their population aggregation and food storage modeling components. The other major contrast with the work of Van West and Kohler is based upon the limited availability of detailed soil data like that used by Van West (1994) in her development of the localized PDSI and agricultural productivity maps for the Mesa Verde region. The high resolution soil data used by Van West are not yet available for this analysis area, limiting the applicability of Van West's analytic approach to this study. The absence of detailed soil data for the study area results in a requirement to employ other approximation methods for localized productivity, local precipitation estimates in the case of this analysis.

In summary, this analysis builds upon the long record of research in the northern Southwest by combining the outputs of multiple archaeological, paleoclimatic, and meteorological data collection programs into an analytic framework that allows for the assessment of localized variation in prehistoric proxy climate measurements. This framework provides a means for mapping local mean and variance in climate against which hypotheses relating locational decision making may be tested. The results obtained herein complement the efforts of researchers in the region by examining how households position themselves on the landscape relative to mapped precipitation mean and variance in addition to other environmental variables. The observed general preference for low variance locations except during periods of sub-regional population decline suggests that this parameter is an important element in locational decision making and analyses that seek to model or explain site patterning should consider localized climate variation in their explanations.

6.4 Analysis Summary and Conclusions

The unique diachronic perspective that archaeological analysis brings to the evaluation of models of human decision-making provides a powerful tool for evaluating and refining those models. This analysis provides just such an assessment of the z-score model, a model that predicts the conditions under which foragers will adopt risk-averse or risk-seeking modes of risk response.

Key to the success of the analysis is the integration of multiple datasets in the development of diachronic models of localized environment, population, and activity location. Once developed, these models provide the framework for testing hypotheses derived from the z-score model. As a complement to the z-score model evaluation component of the analysis, the same data are applied to the assessment of the relationships between activity location and environmental characteristics that are assumed to have remained constant throughout the analysis period.

The analysis provides the following outcomes:

1. A weighted regression based precipitation interpolation method for estimating local precipitation from a network of remote precipitation measurement locations was developed, tested, and found to be able to reasonably estimate precipitation over the study region when using a network of 18 long-term historic climate stations.
2. This weighted regression precipitation method was determined to be unable to reasonably reconstruct prehistoric precipitation from a network of six paleoclimate locations surrounding the analysis area. This failure is likely a result of the small number of locations used in the modeling effort and the limited elevation range represented by the locations.
3. An interpolated annual precipitation surface was generated using data from the six prehistoric precipitation locations using a Gaussian smoothing filter. This smoothed precipitation surface was then used to calculate 30-year moving average and variance values for the period of A.D. 600 to 1150.
4. The generated moving average and variance records for precipitation provide both spatial and temporal patterning useful in testing hypotheses relating locational

decision-making and risk response. The results of this hypothesis testing are:

- Under conditions where mean harvest rates are above requirements (as indicated by growing populations in Long House Valley and Black Mesa) a pattern of risk-aversion is apparent in the relationship between activity location and precipitation variance.
 - Under conditions where mean harvest rates are below requirements (as indicated by declining populations on northern Black Mesa) a pattern of risk-seeking is apparent in the relationship between activity location and precipitation variance.
 - There is a single instance in the analysis where there is support for the hypothesis of adopting a risk-seeking position under conditions of high variance.
 - These patterns are apparent across all site classes.
5. A regression model for temperature extrapolation from the San Francisco Peaks prehistoric temperature reconstruction was successfully developed and tested using historic temperature data from 18 long-term records and solar radiation calculations for each location.
 6. This temperature reconstruction was applied to the project area, generating an annual record of temperature variation across the analysis area.
 7. An analysis of patterns of association between local temperature and site location found no clear and significant patterns of association, either when all sites are analyzed as a group or when considered as separate site classes defined by the presence of specific feature or artifact classes.
 8. Analyses of patterns of association between activity location and vegetation community, elevation, and flow accumulation provided patterns of association between site location and these variables. These patterns include:
 - Location of sites relative to vegetation communities reflects a complex pattern of changing association without clear and consistent linkages between particular vegetation communities and site classes.

- Location of sites relative to elevation suggests that there is a strong preference for low elevation locations except under conditions of high and growing population. This pattern holds true for all site types, with the exception of storage sites which exhibit a strong and continuing association with high elevation sites during the period of population growth on northern Black Mesa
- Flow accumulation, as a proxy for surface water availability, shows a strong association with all site types for much of the analysis period. The exceptions to this pattern are generally associated with periods of population decline on Black Mesa. This results in a greater influence of Long House Valley sites in the analysis, reducing the importance of surface water because of the availability of springs in Long House Valley.

The central goal of this analysis has been to develop and test hypotheses relating locational decision making to subsistence risk. A strong pattern of association between site locations and mapped precipitation variance has been found that suggests two distinct modes: one of a strong positive association one of a strong negative association. These two modes are not randomly distributed through time, but instead are clearly associated with specific upward and downward trends in the high resolution Black Mesa population curve. Specifically, periods of population growth on northern Black Mesa are associated with periods where there is a strong association between site locations and locations of low precipitation variance. In contrast, periods of population decline on northern Black Mesa are associated with periods where there is a strong association between site locations and locations of high precipitation variance. These results are consistent with the general expectations, derived from the z-score model, that under conditions where mean productivity exceeds household requirements individuals will be risk-averse, and under conditions where mean productivity is less than household requirements individuals will be risk seeking.

These results are compelling, but without quantitative harvest rates (such as those developed by Van West for Mesa Verde) the exact points in the local archaeological record when harvest rates cross the requirement threshold for households remain undefined. The proposed linkage between population trends on northern Black Mesa and localized harvest

rates is tentative, but provides a strong candidate explanation for the patterning observed in site locations relative to mapped variation. Ultimately further research will aid in the final assessment of the conclusions reached here.

Further research that would enhance the hypothesis tests developed here includes:

- The application of the meteorological interpolation methods to the historic climate data used to generate paleoclimate reconstructions, providing the potential for the development of localized paleoclimate reconstructions useful in the modeling of remote local climates.
- The utilization of more detailed soil data (when they become available) to produce estimated wild and domesticated plant yields from which mean and variance maps may be developed, allowing for a similar analysis using actual crop yields as opposed to the precipitation proxy.
- The development of a high resolution population curve for Long House Valley that is comparable in temporal sensitivity to that for northern Black Mesa.
- The use of long term remote sensing datasets (i.e. Landsat TM/ETM) for developing high resolution models of spatial variation in vegetation growth in response to meterological and climatic variation.

Overall, each of these areas of research relates to the further refinement of models and methods for estimating localized plant productivity from the climatic and environmental data available for prehistoric analyses. As the spatial resolution of these models and data improves, the ability to develop and test models of localized decision making will improve, ultimately allowing for the development of multivariate models that integrate multiple explanatory variables (i.e. mean productivity, productivity variation, availability of water, proximity of neighboring settlements, localized environmental degradation, defensibility, settlement aggregation, etc.) in location selection.

The potential for applying the methods employed in this analysis to other study areas is high, and is the other major contribution of this study. The use of commonly available environmental data (GAP vegetation data, USGS Digital Elevation Data, USHCN climate data) in combination with generally applicable spatial modeling methods simplifies

implementation where these or similar data are available. Overall, the spatial association tests developed herein are generally applicable to questions relating archaeological site locations to any other mapped parameters, including other site locations.

In total, the analyses presented above combine numerous datasets in an integrated analysis environment that includes powerful data management tools, geographic information systems, and innovative statistical approaches. This environment provides a powerful combination of data, method, visualization, and interpretation that enables the archaeologist to develop and test hypotheses with increased spatial and temporal resolution while also providing greater flexibility in the questions that may be asked of and answered with the data.

Appendices

Appendix A

USGS Quads Used in the Analyses

A.1 7.5 Minute: 1:24,000

Table A.1: 7.5' USGS Quads

Quad Name	USGS Quad Identifier
Cliff Rose Hill	36110D2
Yucca Hill	36110D3
Great Spring	36110D4
Black Mesa Wash NE	36110D5
Owl Spring	36110E2
Marsh Pass SE	36110E3
Long House Valley	36110E4
Shonto SE	36110E5
Kayenta East	36110F2
Kayenta West	36110F3
Marsh Pass	36110F4
Betatakin Ruin	36110F5

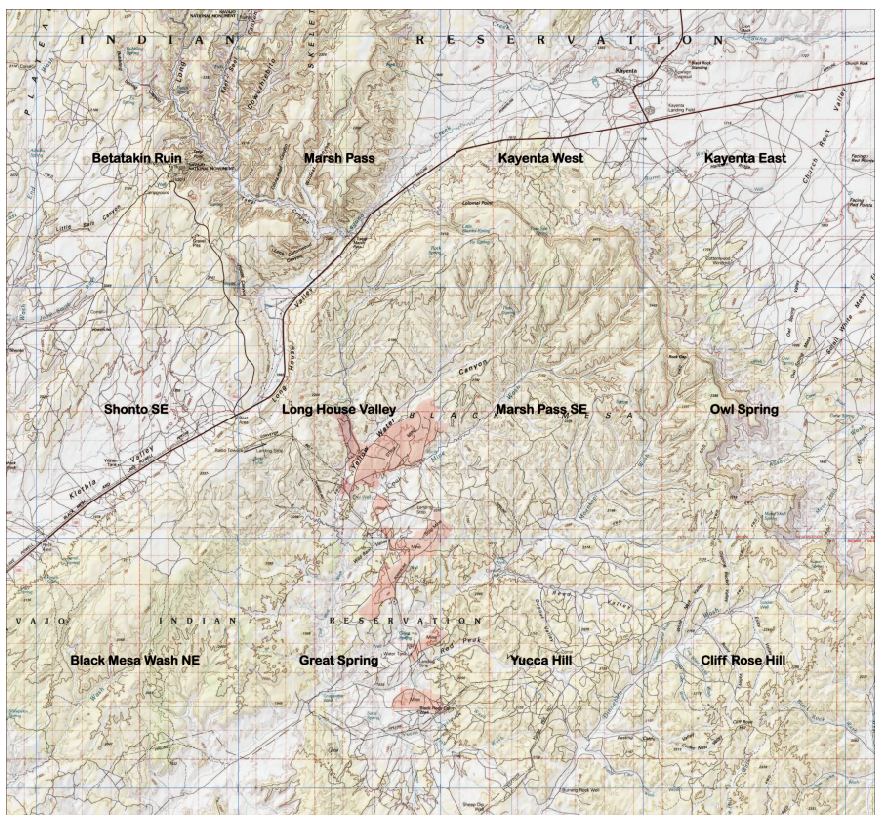


Figure A.1: 7.5' USGS Quads

A.2 1x2 Degree: 1:250,000

Table A.2: 1:250000 USGS Quads

Quad Name			
Ajo	Albuquerque	Aztec	Brigham City
Brownfield	Caliente	Carlsbad	Cedar City
Cheyenne	Clifton	Clovis	Cortez
Craig	Dalhart	Delta	Denver
Douglas	Durango	El Centro	El Paso
Elko	Ely	Escalante	Flagstaff
Fort Sumner	Gallup	Grand Canyon	Grand Junction
Greeley	Hobbs	Holbrook	Kingman
La Junta	Lamar	Las Cruces	Las Vegas
Leadville	Limon	Lukeville	Lund
Marble Canyon	Mesa	Moab	Montrose
Needles	Nogales	Ogden	Phoenix
Prescott	Price	Pueblo	Raton
Rawlins	Richfield	Rock Springs	Roswell
Saint Johns	Salina	Salt Lake City	Salton Sea
Santa Fe	Scottsbluff	Shiprock	Silver City
Socorro	Sterling	Tooele	Trinidad
Tucson	Tucumcari	Tularosa	Vernal
Wells	Williams		

Appendix B

Sampling ArcGIS ASCII Grid Files and Statistical Comparison Between the Project Area and the Colorado Plateau

Significance tests performed using SPSS ver. 10.0, Kolmogorov-Smirnov non-parametric test of correlation between samples. The samples were at 0.01% sample of all calculated (non-missing) values for both the Colorado Plateau and the project area, as extracted from ArcGIS Grids exported as ASCII text files, and sampled using a custom procedure developed in Mathematica 3.0. The developed procedure generates a random number ranging in value from 0-1 for each non-missing value. If the random number is less than the sample threshold (0.0001 in this case) the value is included in the analysis. The sample sizes for the comparisons are as follows:

Table B.1: Physiographic Attributes Sample Sizes

Attribute	Colorado Plateau	Project Area
Elevation	52926	3028
Aspect (only for non-flat locations)	43658	2890

(continued on next page)

Table B.1: Physiographic Attributes Sample Sizes

Attribute	Colorado Plateau	Project Area
Lapse Rate	52999	53
Slope	52957	3111

Appendix C

Plant Species Associated With Mapped Biotic Communities

The tables provided in this Appendix list the plant species associated with the biotic communities present within and surrounding the project area (D. E. Brown 1994a).

Table C.1: Great Basin Conifer Woodland

Scientific Name	Common Name
<i>Agropyron smithii</i>	Western Wheatgrass
<i>Amelanchier alnifolia</i>	Saskatoon Serviceberry
<i>Artemisia arbuscula</i> spp. nova	Black Sagebrush
<i>A. ludoviciana</i>	Louisiana Sagebrush
<i>Atriplex canescens</i>	Fourwing Saltbush
<i>A. confertifolia</i>	Shadscale
<i>Berberis fremontii</i>	Fremont Mahonia, Barberry
<i>B. haematocarpa</i>	Red Mahonia
<i>Bouteloua gracilis</i>	Blue Grama
<i>Bromus</i> spp.	brome grasses
<i>Calochortus nuttallii</i>	Sego-lily
<i>Canotia holocantha</i>	Crucifixion Thorn, Canotia

(continued on next page)

Table C.1: Great Basin Conifer Woodland (*continued*)

Scientific Name	Common Name
<i>Ceratoides lanata</i>	Winterfat
<i>Cercocarpus intricatus</i>	Littleleaf Mountain-mahogany
<i>C. ledifolius</i>	Curileaf Mountain-mahogany
<i>C. montanus</i>	Alderleaf Mountain-mahogany
<i>Chaemaebara millifolium</i>	Fernbush, Desert Sweet
<i>Chrysothamnus</i> spp.	rabbitbrushes
<i>Coleogyne ramosissima</i>	Blackbrush
<i>Coryphantha vivipara</i> var. <i>arizonica</i>	—
<i>C. missouriensis</i>	—
<i>Cowania mexicana</i>	Cliff rose
<i>Echinocereus engelmannii</i> var. <i>variegatus</i>	Hedgehog Cactus
<i>E fendleri</i>	—
<i>E triglochidiatus</i> var. <i>melanacanthus</i>	Red Hedgehog Cactus
<i>Ephedra viridis</i>	Mountain Joint-fir
<i>Eriogonum</i> spp.	buckwheats
<i>Fallugia paradoxa</i>	Apache Plume
<i>Garrya wrightii</i>	Wright Silktassel
<i>Gilia</i> spp.	gillas
<i>Gutierrezia sarothrae</i>	Broom Snakeweed
<i>Hilaria jamesii</i>	Galleta
<i>Juniperus californica</i>	California Juniper
<i>J. monosperma</i>	One-seed Juniper
<i>J. osteosperma</i>	Utah Juniper
<i>J. scopulorum</i>	Rocky Mountain Juniper

(continued on next page)

Table C.1: Great Basin Conifer Woodland (*continued*)

Scientific Name	Common Name
<i>Koeleria cristata</i>	Prairie Junegrass
<i>Lupinus</i> spp.	lupines
<i>Mammillaria wrightii</i>	Wright Pincushion
<i>Muhlenbergia</i> spp.	muhlies
<i>Opuntia basilaris</i> var. aurea	Yellow Beavertail
<i>O. erinacea</i>	Mohave Prickly Pear
<i>O. fragilis</i>	Little Prickly Pear
<i>O. imbricata</i>	Tree Cholla
<i>O. macrorhiza</i>	Plains Prickly Pear
<i>O. phaeacantha</i>	Engelmann Prickly Pear
<i>O. polycantha</i>	Plains Prickly Pear
<i>O. whipplei</i>	Whipple Cholla
<i>Oryzopsis hymenoides</i>	Indian Ricegrass
<i>Pediocactus papyracanthus</i>	Grama Grass Cactus
<i>P. simpsonii</i>	—
<i>Penstemon</i> spp.	penstemons, beardtongues
<i>Pinus cembroides</i>	Mexican Pinyon
<i>P. edulis</i>	Rocky Mountain Pinyon
<i>P. monophylla</i>	Singleleaf Pinyon, One-needle
<i>P. quadrifolia</i>	Parry Pinyon
<i>Purshia tridentata</i>	Antelope Bitterbrush
<i>Quercus arizonica</i>	Arizona White Oak
<i>Q. emoryi</i>	Emory Oak
<i>Q. gambelii</i>	Gambel Oak
<i>Q. grisea</i>	Gray Oak
<i>Q. turbinella</i>	Shrub Live Oak

(continued on next page)

Table C.1: Great Basin Conifer Woodland (*continued*)

Scientific Name	Common Name
<i>Rhamnus crocea</i>	Hollyleaf Buckthorn
<i>Rhus triobata</i>	Squawbush, Skunkbush
	Sumac
<i>Ribes</i> spp.	currants
<i>Scierocactus whipplei</i> var. <i>intermedius</i>	—
<i>Senecio longilobus</i>	Threadleaf Groundsel
<i>Shepherdia</i> spp.	buffaloberries
<i>Sphaeralcea coccinea</i>	Scarlet Globe Mallow
<i>S. digitata</i>	Juniper Globe Mallow
<i>S. marginata</i>	—
<i>Sporobolus</i> spp.	dropseeds
<i>Symphoricarpos</i> spp.	snowberries
<i>Yucca baccata</i>	Banana Yucca, Datil
<i>Y. glauca</i>	Small Soapweed

Table C.2: Great Basin Desertsrub

Scientific Name	Common Name
<i>Artemisia arbuscula</i> ssp. <i>nova</i>	Black Sagebrush
<i>A. bigelovii</i>	Bigelow Sagebrush
<i>A. filifolia</i>	Sand Sagebrush
<i>A. parryi</i>	Parry Sagebrush
<i>A. spinescens</i>	Bud Sagebrush
<i>A. tridentata</i>	Big Sagebrush
<i>Atriplex canescens</i>	Fourwing Saltbush

(*continued on next page*)

Table C.2: Great Basin Desertscrub (*continued*)

Scientific Name	Common Name
<i>A. confertifolia</i>	Shadscale
<i>A. gardneri</i>	Gardner Saltbush
<i>A. nuttallii</i>	Nuttall Saltbush
<i>Bassia hyssopifolia</i>	Fivehook Bassia
<i>Bouteloua</i> spp.	grama grasses
<i>Bromus rubens</i>	Red Brome, Foxtail Chess
<i>B. tectorum</i>	Downy Chess, Cheatgrass Brome
<i>Ceratoides lanata</i>	Winterfat
<i>Chrysothamnus</i> spp.	rabbitbrushes
<i>C. greenei</i>	Greene Rabbitbrush
<i>C. nauseosus</i>	Rubber Rabbitbrush
<i>Coleogyne ramosissima</i>	Blackbrush
<i>Descurainia pinnata</i>	Tansy Mustard
<i>Distichlis spicata</i> var. <i>stricta</i>	Desert Saltgrass
<i>Echinocactus polycephalus</i> var. <i>xeranthe-</i> <i>moides</i>	Manyheaded Barrel Cactus
<i>Echinocereus fendleri</i> var. <i>fendleri</i>	Fendler Hedgehog
<i>E. triglochidiatus</i> var. <i>melanacanthus</i>	Red-flowered Hedgehog
<i>Elaeagnus angustifolia</i>	Russian Olive
<i>Ephedra nevadensis</i>	Rough Joint-fir
<i>E. torreyana</i>	Torrey Joint-fir
<i>Eriogonum fasciculatum</i>	Bush Buckwheat
<i>Erodium cicutarium</i>	Filaree, Heron's Bill
<i>Forestiera neomexicana</i>	Tanglebrush, Adelia
<i>Grayia spinosa</i>	Spiny Hopsage

(continued on next page)

Table C.2: Great Basin Desertsrub (*continued*)

Scientific Name	Common Name
<i>Gutierrezia microcephala</i>	Three-leaved Snakeweed
<i>C. sarothrae</i>	Broom Snakeweed
<i>Hilaria jamesii</i>	Galleta
<i>Opuntia erinacea</i>	Mohave Prickly Pear
<i>O. gracilis</i>	Narrow Cholla
<i>O. polyacantha</i>	Plains Prickly Pear
<i>O. pulchella</i>	Sand Cholla
<i>O. ramosissima</i>	Diamond Cholla
<i>O. whipplei</i>	Whipple Cholla
<i>Oryzopsis hymenoides</i>	Indian Rice Grass
<i>Pediocactus</i> spp.	—
<i>Salsola iberica</i>	Russian Thistle
<i>S. kali</i>	Russian Thistle, Tumbleweed
<i>S. paulsenii</i>	—
<i>Sarcobatus vermiculatus</i>	Black Greasewood
<i>Sclerocactus</i> spp.	—
<i>Sisymbrium altissimum</i>	Tumble Mustard
<i>Sitanion hystrix</i>	Bottlebrush Squirretail
<i>Sporobolus airoides</i>	Alkali Sacaton
<i>Stenopsis linearifolius</i>	—
<i>Stipa speciosa</i>	Desert Needlegrass
<i>Suaeda</i> spp.	seep weeds, sea blights
<i>S. fruticosa</i>	Seep Weed
<i>Tamarix chinensis</i>	Salt Cedar
<i>Tetradymia canescens</i>	Gray Horsebrush

Table C.3: Plains and Great Basin Grassland

Scientific Name	Common Name
<i>Agropyron smithii</i>	Western Wheatgrass
<i>Andropogon gerardi</i>	Big Bluestem
<i>A. gerardi</i> var. <i>paucipilus</i>	Sand Bluestem
<i>Argemone</i> spp.	prickly poppies
<i>Aristida longiseta</i>	Red Three-awn
<i>Artemisia</i> spp.	sagebrushes
<i>A. filifolia</i>	Sand Sagebrush
<i>A. tridentata</i>	Big sagebrush
<i>Aster</i> spp.	asters
<i>Atriplex canescens</i>	Fourwing Saltbush
<i>Bahia</i> spp.	bahias
<i>Bouteloua chondrosioides</i>	Sprucetop Grama
<i>B. curtipendula</i>	Sideoats Grama
<i>B. eriopoda</i>	Black Grama
<i>B. gracilis</i>	Blue Grama
<i>B. hirsuta</i>	Hairy Grama
<i>Brickellia</i> spp.	bricklebushes
<i>Buchloe dactyloides</i>	Buffalo Grass
<i>Ceratoides lanata</i>	Winterfat
<i>Chrysothamnus</i> spp.	rabbitbrushes
<i>Cirsium</i> spp.	thistles
<i>Cleome</i> spp.	spiderflowers
<i>Echinocereus engelmannii</i> var. <i>variegatus</i>	Hedgehog Cactus
<i>E fendleri</i>	Fendler Hedgehog
<i>Eragrosti intermedia</i>	Plains Lovegrass
<i>Festuca arizonica</i>	Arizona Fescue

(continued on next page)

Table C.3: Plains and Great Basin Grassland (*continued*)

Scientific Name	Common Name
<i>Gaura</i> spp.	gauras
<i>Gutierrezia</i> spp.	snakeweeds
<i>G sarothrae</i>	Broom Snakeweed
<i>Helianthus</i> spp.	sunflowers
<i>Hilaria jamesii</i>	Galleta
<i>Juniperus monosperma</i>	One-seed Juniper
<i>j. osteosperma</i>	Utah Juniper
<i>j. scopulorum</i>	Rocky Mountain Juniper
<i>Koeleria cristata</i>	Prairie Junegrass
<i>Lycurus phleoides</i>	Wolf tail, Texas Timothy
<i>Mammillaria wrightii</i>	Wright Pincushion
<i>Mirabilis</i> spp.	four oclocks
<i>Oenothera</i> spp.	primroses
<i>Opuntia</i> spp.	prickly pears, chollas
<i>O. arbuscula</i>	Pencil Cholla
<i>O. clavata</i>	Club Cholla
<i>O. imbricata</i>	Tree Cholla
<i>O. macrorhiza</i>	Plains Prickly Pear
<i>O. phaeacantha</i>	Engelmann Prickly Pear
<i>O. polycantha</i>	Plains Prickly Pear
<i>O. whipplei</i>	Whipple Cholla
<i>Oryzopsis hymenoides</i>	Indian Ricegrass
<i>Panicum obtusum</i>	Vine Mesquite Grass
<i>P virgatum</i>	Switchgrass
<i>Pediocactus papyracanthus</i>	Grama Grass Cactus
<i>Prosopis glandulosa</i>	Honey Mesquite

(continued on next page)

Table C.3: Plains and Great Basin Grassland (*continued*)

Scientific Name	Common Name
<i>Psoralea</i> spp.	scurf-peas
<i>Quercus havardii</i>	Shinnery Oak, Midget Oak
<i>Ratibida</i> spp.	coneflowers, Mexican hats
<i>Rhus copallina</i> var. lanceolata	Prairie Sumac
<i>Rosa</i> spp.	wild roses
<i>Schizachyrium scoparium</i>	Little Bluestem
<i>Senecio</i> spp.	groundsels
<i>Setaria macrostachya</i>	Plains Bristlegrass
<i>Sorghastrum nutans</i>	Indian Grass
<i>Sphaeralcea</i> spp.	mallows
<i>Sporobolus airoides</i>	Alkali Sacaton
<i>S. cryptandrus</i>	Sand Dropseed
<i>Stipa comata</i>	Needle and Thread Grass
<i>Viguiera</i> spp.	Goldeneye
<i>Yucca glauca</i>	Soapweed

Appendix D

Summary Statistics for USHCN Monthly Climate Values

The following tables present summary statistics for each of the eighteen USHCN stations that were used in the characterization of the regional climate surrounding the project area. The statistics were calculated for the entire available record for each station, with each summary statistic representing the mean, standard deviation, and sample size for monthly statistics for each station. Only those stations with monthly values calculated from all days in each month are included in each summary.

Following the tables are three figures that illustrate the interannual variation for each of the 18 USHCN stations for each month of the year. These figures provide a large-scale overview of the variation for each station through the presentation of similarly scaled small plots for each stations and month combination. The plots with a wide interannual variation are depicted with a broad range of low and high values while low interannual variation is depicted by narrow bands of variation for the presented annual values.

The summary statistics represent the following values:

- Precipitation Data: summed daily precipitation for each day of each month
- Daily minimum and maximum temperature: mean value for each month based upon daily observations over the entire month.

D.1 Precipitation Data (hundredths of an inch)

Table D.1: Station 2432 Precipitation

Month	Mean	Standard Deviation	n
Jan.	157.967	145.21	92
Feb.	147.75	119.752	92
Mar.	168.589	125.453	90
Apr.	139.264	104.124	91
May	111.066	83.5041	91
Jun.	78.8352	87.4331	91
Jul.	191.292	110.461	89
Aug.	232.066	133.57	91
Sep.	178.989	122.791	91
Oct.	184.567	178.677	90
Nov.	135.319	110.775	91
Dec.	171.571	138.713	91

Table D.2: Station 2592 Precipitation

Month	Mean	Standard Deviation	n
Jan.	99.3068	93.6775	88
Feb.	78.2184	71.1001	87
Mar.	86.8333	81.7908	84
Apr.	54.8953	64.9758	86
May	59.7143	67.0226	91
Jun.	46.1136	58.9945	88
Jul.	121.708	103.419	89
Aug.	176.621	118.115	87
Sep.	115.6	112.126	90

(continued on next page)

Table D.2: Station 2592 Precipitation (*continued*)

Month	Mean	Standard Deviation	n
Oct.	101.556	114.281	90
Nov.	67.6477	75.7499	88
Dec.	84.4091	90.105	88

Table D.3: Station 3160 Precipitation

Month	Mean	Standard Deviation	n
Jan.	223.795	185.418	88
Feb.	213.352	157.571	88
Mar.	222.333	171.039	87
Apr.	142.739	122.386	88
May	81.573	83.4677	89
Jun.	58.4773	72.2585	88
Jul.	296.315	166.001	89
Aug.	326.393	161.502	89
Sep.	193.705	171.02	88
Oct.	155.236	149.997	89
Nov.	142.136	130.476	88
Dec.	198.584	154.254	89

Table D.4: Station 3611 Precipitation

Month	Mean	Standard Deviation	n
Jan.	39.3878	45.9673	49
Feb.	22.2083	17.768	48
Mar.	45.8163	47.8669	49
Apr.	40.9388	49.0151	49

(*continued on next page*)

Table D.4: Station 3611 Precipitation (*continued*)

Month	Mean	Standard Deviation	n
May	46.7755	50.4621	49
Jun.	26.3061	36.0481	49
Jul.	49.8367	51.4969	49
Aug.	74.72	70.4015	50
Sep.	67.74	62.3459	50
Oct.	64.898	66.9002	49
Nov.	36.2245	38.6449	49
Dec.	29.06	34.5037	50

Table D.5: Station 4089 Precipitation

Month	Mean	Standard Deviation	n
Jan.	58.1122	59.2289	98
Feb.	54.3402	57.0111	97
Mar.	54.802	51.1867	101
Apr.	42.9109	42.3056	101
May	30.7245	39.3516	98
Jun.	31.1	56.34	100
Jul.	137.99	120.809	101
Aug.	149.818	106.977	99
Sep.	102.961	88.5085	102
Oct.	77.13	84.1398	100
Nov.	59.8687	71.8819	99
Dec.	57.7755	59.3027	98

Table D.6: Station 4508 Precipitation

Month	Mean	Standard Deviation	n
Jan.	177.959	178.515	49
Feb.	138.816	128.427	49
Mar.	153.796	140.066	49
Apr.	85.7551	88.1801	49
May	69.7755	71.1472	49
Jun.	41.4694	47.3872	49
Jul.	93.54	80.4407	50
Aug.	149.94	103.408	50
Sep.	107.72	147.603	50
Oct.	102.1	94.9389	50
Nov.	111.44	99.1787	50
Dec.	121.8	122.279	50

Table D.7: Station 4849 Precipitation

Month	Mean	Standard Deviation	n
Jan.	42.0286	46.7451	70
Feb.	43.2286	41.4138	70
Mar.	49.5286	42.7194	70
Apr.	37.4571	46.5598	70
May	31.5942	35.7027	69
Jun.	19.3239	32.7212	71
Jul.	76.875	63.5102	72
Aug.	103.542	74.2028	72
Sep.	50.0556	49.562	72
Oct.	61.863	70.5959	73
Nov.	43.4167	44.4426	72

(continued on next page)

Table D.7: Station 4849 Precipitation (*continued*)

Month	Mean	Standard Deviation	n
Dec.	44.2029	39.759	69

Table D.8: Station 5148 Precipitation

Month	Mean	Standard Deviation	n
Jan.	42.5652	43.3941	46
Feb.	29.3043	30.8854	46
Mar.	52.8182	46.7518	44
Apr.	41.9545	43.761	44
May	72.25	52.034	44
Jun.	48.2667	45.5204	45
Jul.	103.404	65.1212	47
Aug.	131.413	95.3722	46
Sep.	86.913	71.7805	46
Oct.	65.8936	54.3016	47
Nov.	39.413	36.9964	46
Dec.	35.1591	27.8283	44

Table D.9: Station 5733 Precipitation

Month	Mean	Standard Deviation	n
Jan.	58.5217	52.003	69
Feb.	55.7313	42.784	67
Mar.	76.1471	58.9918	68
Apr.	85.058	61.7961	69
May	72.7246	63.3816	69
Jun.	42.4853	52.2541	68

(*continued on next page*)

Table D.9: Station 5733 Precipitation (*continued*)

Month	Mean	Standard Deviation	n
Jul.	68.5147	75.0748	68
Aug.	88.5588	62.1112	68
Sep.	77.5735	77.6166	68
Oct.	106.647	100.482	68
Nov.	71.1176	51.8202	68
Dec.	63.5362	47.6225	69

Table D.10: Station 6601 Precipitation

Month	Mean	Standard Deviation	n
Jan.	56.2917	49.0475	48
Feb.	58.8542	55.8006	48
Mar.	73.5306	58.3153	49
Apr.	58.8333	46.994	48
May	76.0638	61.5059	47
Jun.	55.8298	55.3304	47
Jul.	136.551	79.1344	49
Aug.	172.917	121.447	48
Sep.	96.2857	105.993	49
Oct.	76.6531	86.7714	49
Nov.	73.2979	68.0645	47
Dec.	51.5417	46.9032	48

Table D.11: Station 6686 Precipitation

Month	Mean	Standard Deviation	n
Jan.	94.7755	73.0902	49

(*continued on next page*)

Table D.11: Station 6686 Precipitation (*continued*)

Month	Mean	Standard Deviation	n
Feb.	108.041	62.9672	49
Mar.	146.917	89.2255	48
Apr.	125.083	77.0868	48
May	95.8163	62.939	49
Jun.	52.0816	50.6663	49
Jul.	116.76	89.4125	50
Aug.	141.98	99.3829	50
Sep.	86.44	79.4363	50
Oct.	102.9	83.2837	50
Nov.	105.06	74.3007	50
Dec.	91.12	60.3762	50

Table D.12: Station 692 Precipitation

Month	Mean	Standard Deviation	n
Jan.	91.62	76.2389	50
Feb.	71.5	57.7568	50
Mar.	81.98	71.5118	50
Apr.	68.2	62.3794	50
May	61.34	57.928	50
Jun.	41.3	50.4507	50
Jul.	90.96	79.5736	50
Aug.	127.429	79.2341	49
Sep.	94.2	72.665	50
Oct.	112.76	104.308	50
Nov.	77.56	68.4905	50
Dec.	82.66	64.1343	50

Table D.13: Station 738 Precipitation

Month	Mean	Standard Deviation	n
Jan.	137.079	119.462	89
Feb.	117.91	92.5797	89
Mar.	101.708	79.4179	89
Apr.	86.0667	80.5547	90
May	73.5604	61.3127	91
Jun.	46.4222	62.5162	90
Jul.	118.611	84.5093	90
Aug.	140.478	107.164	90
Sep.	126.934	99.6422	91
Oct.	143.462	136.44	91
Nov.	104.418	89.2287	91
Dec.	137.12	127.151	92

Table D.14: Station 7435 Precipitation

Month	Mean	Standard Deviation	n
Jan.	70.6897	63.4281	87
Feb.	60.3182	53.3433	88
Mar.	74.1264	61.898	87
Apr.	50.1591	46.7859	88
May	46.3371	54.1702	89
Jun.	51.2759	65.0942	87
Jul.	205.586	119.457	87
Aug.	218.077	129.459	91
Sep.	134.626	106.038	91
Oct.	89.7692	85.2677	91
Nov.	56.8864	50.9883	88

(continued on next page)

Table D.14: Station 7435 Precipitation (*continued*)

Month	Mean	Standard Deviation	n
Dec.	74.1778	58.1568	90

Table D.15: Station 788 Precipitation

Month	Mean	Standard Deviation	n
Jan.	72.5316	72.2178	79
Feb.	70.8481	58.5625	79
Mar.	61.5833	59.4992	84
Apr.	50.2875	53.4065	80
May	42.5802	43.4658	81
Jun.	24.3	34.8088	80
Jul.	69.8214	76.3532	84
Aug.	75.8452	79.7729	84
Sep.	77.3855	69.5838	83
Oct.	89.5854	94.0286	82
Nov.	57.8519	53.7694	81
Dec.	74.0759	59.1271	79

Table D.16: Station 86 Precipitation

Month	Mean	Standard Deviation	n
Jan.	182.929	175.745	70
Feb.	174.686	157.356	70
Mar.	160.	131.582	69
Apr.	104.129	86.4871	70
May	87.7429	70.2215	70
Jun.	56.6429	59.674	70

(*continued on next page*)

Table D.16: Station 86 Precipitation (*continued*)

Month	Mean	Standard Deviation	n
Jul.	139.5	87.8825	70
Aug.	172.643	116.826	70
Sep.	147.629	144.947	70
Oct.	127.086	113.844	70
Nov.	125.471	125.33	70
Dec.	156.594	134.874	69

Table D.17: Station 9359 Precipitation

Month	Mean	Standard Deviation	n
Jan.	209.903	171.932	93
Feb.	216.793	191.008	92
Mar.	206.129	173.763	93
Apr.	130.495	129.395	95
May	75.6702	81.1438	94
Jun.	45.8404	60.0556	94
Jul.	286.221	175.686	95
Aug.	317.298	176.772	94
Sep.	169.269	143.093	93
Oct.	143.383	164.107	94
Nov.	159.168	185.867	95
Dec.	209.742	173.36	93

Table D.18: Station 9717 Precipitation

Month	Mean	Standard Deviation	n
Jan.	168.517	147.716	89

(*continued on next page*)

Table D.18: Station 9717 Precipitation (*continued*)

Month	Mean	Standard Deviation	n
Feb.	170.822	141.93	90
Mar.	190.659	156.044	91
Apr.	119.023	112.125	88
May	79.4432	72.0546	88
Jun.	41.2717	65.3732	92
Jul.	105.053	94.2798	94
Aug.	154.837	111.63	92
Sep.	111.413	114.663	92
Oct.	109.292	103.035	89
Nov.	119.33	96.1715	88
Dec.	138.629	107.267	89

D.2 Daily Minimum Temperature (°F)

Table D.19: Station 2432 Min. Temp.

Month	Mean	Standard Deviation	n
Jan.	10.3552	4.75873	92
Feb.	15.8874	4.85847	92
Mar.	22.4875	3.31807	91
Apr.	29.0436	2.9697	91
May	35.2746	2.44752	91
Jun.	41.7188	2.96172	91
Jul.	49.8962	2.19277	90
Aug.	48.8516	2.55247	91
Sep.	40.7608	2.90545	91
Oct.	31.1296	2.34334	90

(*continued on next page*)

Table D.19: Station 2432 Min. Temp. (*continued*)

Month	Mean	Standard Deviation	n
Nov.	21.2633	2.93885	91
Dec.	12.8501	3.88304	91

Table D.20: Station 2592 Min. Temp.

Month	Mean	Standard Deviation	n
Jan.	13.4598	5.66972	88
Feb.	19.9625	4.99341	88
Mar.	25.9895	3.22078	84
Apr.	32.3173	2.922	85
May	39.6633	2.7119	91
Jun.	46.8299	2.82309	87
Jul.	53.9196	2.14736	88
Aug.	52.3373	2.77839	85
Sep.	43.9461	3.26109	91
Oct.	34.5673	2.69211	90
Nov.	24.0489	2.88867	88
Dec.	16.0823	4.60673	88

Table D.21: Station 3160 Min. Temp.

Month	Mean	Standard Deviation	n
Jan.	9.61209	4.68522	88
Feb.	12.8924	5.18805	87
Mar.	17.6303	3.85244	87
Apr.	23.2927	2.70305	89
May	28.3865	2.60641	89

(*continued on next page*)

Table D.21: Station 3160 Min. Temp.(*continued*)

Month	Mean	Standard Deviation	n
Jun.	35.0796	3.25992	89
Jul.	44.7939	2.65165	89
Aug.	44.4563	3.05796	89
Sep.	36.7901	3.14702	87
Oct.	26.4735	2.66442	89
Nov.	17.8703	3.23416	88
Dec.	11.4476	4.47614	89

Table D.22: Station 3611 Min. Temp.

Month	Mean	Standard Deviation	n
Jan.	11.2379	6.9693	49
Feb.	19.1276	6.14977	48
Mar.	28.0718	3.03552	49
Apr.	36.5297	2.63558	49
May	45.625	2.51648	49
Jun.	53.9952	2.75059	49
Jul.	60.8275	2.7845	49
Aug.	58.9845	3.10711	50
Sep.	49.0547	3.26024	50
Oct.	36.4668	3.41362	49
Nov.	23.5682	3.70779	49
Dec.	14.6665	4.26265	50

Table D.23: Station 4089 Min. Temp

Month	Mean	Standard Deviation	n
Jan.	18.2603	5.49453	97
Feb.	23.4536	4.21534	97
Mar.	28.3444	3.72307	98
Apr.	35.1623	3.9086	100
May	42.4315	3.35465	97
Jun.	50.7967	3.15086	99
Jul.	59.8243	3.47817	100
Aug.	58.7585	3.38158	99
Sep.	50.4148	3.17205	102
Oct.	37.8452	3.63987	99
Nov.	26.0671	3.48775	97
Dec.	19.5221	4.33082	98

Table D.24: Station 4508 Min. Temp.

Month	Mean	Standard Deviation	n
Jan.	22.5882	4.02467	49
Feb.	26.4158	4.14647	49
Mar.	30.4081	2.79247	49
Apr.	36.1551	2.72421	49
May	43.4086	2.207	48
Jun.	51.2585	2.54373	48
Jul.	58.4906	2.18028	50
Aug.	57.3593	2.36218	50
Sep.	50.4018	2.55079	50
Oct.	40.4115	2.54616	50
Nov.	30.3128	2.25315	50

(continued on next page)

Table D.24: Station 4508 Min. Temp. (*continued*)

Month	Mean	Standard Deviation	n
Dec.	23.8311	3.25088	50

Table D.25: Station 4849 Min. Temp.

Month	Mean	Standard Deviation	n
Jan.	26.3219	3.91128	69
Feb.	32.2224	3.68088	68
Mar.	39.1101	2.73754	68
Apr.	47.4117	2.93795	69
May	55.3881	7.36195	67
Jun.	63.8751	8.23869	70
Jul.	71.1591	8.80885	70
Aug.	68.7626	8.65952	70
Sep.	60.2218	7.67335	69
Oct.	48.0571	6.40958	70
Nov.	35.1284	5.44705	69
Dec.	27.2539	4.73227	67

Table D.26: Station 5148 Min. Temp.

Month	Mean	Standard Deviation	n
Jan.	7.35367	4.79177	46
Feb.	12.2519	4.56082	46
Mar.	18.6404	3.84516	44
Apr.	25.1395	3.09057	44
May	33.0062	2.308	44
Jun.	40.1269	2.68948	45

(*continued on next page*)

Table D.26: Station 5148 Min. Temp. (*continued*)

Month	Mean	Standard Deviation	n
Jul.	46.9409	1.94398	47
Aug.	45.1505	3.07172	46
Sep.	37.0089	2.7961	47
Oct.	27.0771	2.43707	47
Nov.	16.7836	3.72191	46
Dec.	9.00591	4.00622	45

Table D.27: Station 5733 Min. Temp.

Month	Mean	Standard Deviation	n
Jan.	18.299	5.36596	69
Feb.	24.7909	5.36615	67
Mar.	33.33	3.30507	68
Apr.	41.3122	2.66356	69
May	49.3856	2.83938	69
Jun.	57.0165	3.12536	68
Jul.	63.3765	2.33352	68
Aug.	61.8787	2.99768	68
Sep.	52.3245	3.00193	68
Oct.	40.1847	2.95939	68
Nov.	28.5016	3.37444	68
Dec.	20.9527	3.62304	69

Table D.28: Station 6601 Min. Temp.

Month	Mean	Standard Deviation	n
Jan.	7.86672	5.10215	48

(*continued on next page*)

Table D.28: Station 6601 Min. Temp. (*continued*)

Month	Mean	Standard Deviation	n
Feb.	12.6562	4.81482	47
Mar.	19.0197	3.42265	48
Apr.	24.4439	2.35872	47
May	31.7338	2.13535	47
Jun.	38.2721	2.3448	47
Jul.	45.7125	2.27785	48
Aug.	44.1873	3.08845	48
Sep.	35.6809	3.2781	49
Oct.	25.6625	2.54373	49
Nov.	16.7754	3.33296	48
Dec.	9.1784	4.47306	48

Table D.29: Station 6686 Min. Temp.

Month	Mean	Standard Deviation	n
Jan.	15.2551	4.96365	49
Feb.	19.5756	4.95501	49
Mar.	25.2358	3.0543	48
Apr.	32.0644	3.06849	48
May	40.0602	2.73718	49
Jun.	48.09	2.50206	49
Jul.	55.1752	2.01423	50
Aug.	53.3991	2.31655	50
Sep.	45.	2.84336	50
Oct.	34.3796	3.00684	50
Nov.	24.0111	3.22155	50
Dec.	16.8555	4.03559	50

Table D.30: Station 692 Min. Temp.

Month	Mean	Standard Deviation	n
Jan.	15.313	5.08963	50
Feb.	20.6717	3.89207	50
Mar.	25.2609	3.15266	50
Apr.	31.7528	2.57408	50
May	40.2343	2.80255	50
Jun.	48.7061	2.74383	50
Jul.	56.4615	2.41403	50
Aug.	55.3327	3.04288	49
Sep.	46.8691	2.97604	50
Oct.	36.018	2.77764	50
Nov.	24.5406	3.26724	50
Dec.	16.7932	4.51547	50

Table D.31: Station 738 Min. Temp.

Month	Mean	Standard Deviation	n
Jan.	16.3588	5.08694	89
Feb.	21.9055	4.95303	89
Mar.	27.4061	3.05488	89
Apr.	34.1575	3.49149	90
May	41.7163	3.00106	91
Jun.	50.3554	3.18276	90
Jul.	57.4728	1.9689	90
Aug.	55.8195	2.43825	90
Sep.	47.9104	3.04365	91
Oct.	37.5724	3.22996	90
Nov.	26.357	3.36917	91

(continued on next page)

Table D.31: Station 738 Min. Temp. (*continued*)

Month	Mean	Standard Deviation	n
Dec.	18.7817	4.29197	92

Table D.32: Station 7435 Min. Temp.

Month	Mean	Standard Deviation	n
Jan.	17.0039	5.30034	86
Feb.	21.5754	4.06966	88
Mar.	26.8307	3.49	86
Apr.	33.593	3.22238	88
May	41.0142	3.14337	89
Jun.	49.1302	3.07877	86
Jul.	56.944	2.36041	85
Aug.	55.4121	2.24075	90
Sep.	47.8126	3.39472	91
Oct.	35.4849	3.10469	91
Nov.	24.2718	3.62588	87
Dec.	17.615	4.25403	89

Table D.33: Station 788 Min. Temp.

Month	Mean	Standard Deviation	n
Jan.	17.6993	5.74455	76
Feb.	24.391	4.58445	79
Mar.	30.5756	3.22322	84
Apr.	38.1	3.47351	81
May	46.614	3.42318	82
Jun.	54.184	4.54685	81

(*continued on next page*)

Table D.33: Station 788 Min. Temp. (*continued*)

Month	Mean	Standard Deviation	n
Jul.	61.9413	3.883	84
Aug.	60.4539	4.49459	85
Sep.	50.8473	5.62062	84
Oct.	37.8016	4.78852	81
Nov.	26.6552	4.50414	81
Dec.	18.6921	4.91523	79

Table D.34: Station 86 Min. Temp.

Month	Mean	Standard Deviation	n
Jan.	14.6471	4.01846	70
Feb.	17.2557	4.7243	70
Mar.	21.5289	3.33699	69
Apr.	27.9291	2.85624	70
May	34.7223	2.41408	69
Jun.	41.997	2.34274	70
Jul.	49.6805	2.01705	70
Aug.	48.8706	2.23251	70
Sep.	41.6642	2.68761	70
Oct.	32.9246	2.32818	70
Nov.	22.8852	2.62694	70
Dec.	16.7311	3.71777	69

Table D.35: Station 9359 Min. Temp.

Month	Mean	Standard Deviation	n
Jan.	19.033	5.77725	91

(*continued on next page*)

Table D.35: Station 9359 Min. Temp. (*continued*)

Month	Mean	Standard Deviation	n
Feb.	21.3608	5.09071	91
Mar.	25.2339	3.74812	94
Apr.	31.2464	3.58986	95
May	38.0415	3.73323	95
Jun.	45.9056	4.28286	94
Jul.	52.8035	2.93731	94
Aug.	51.7576	2.9482	94
Sep.	45.6099	3.77878	93
Oct.	35.2212	4.47575	94
Nov.	25.852	4.6305	95
Dec.	20.4074	5.02524	92

Table D.36: Station 9717 Min. Temp.

Month	Mean	Standard Deviation	n
Jan.	27.65	5.35964	92
Feb.	32.5617	4.91772	91
Mar.	36.6692	3.68849	91
Apr.	43.1403	3.33391	88
May	51.4564	3.31754	89
Jun.	61.0208	3.29006	92
Jul.	67.8749	2.81732	94
Aug.	66.1188	3.62501	91
Sep.	59.3503	3.36804	93
Oct.	48.5441	4.44524	91
Nov.	36.0224	4.42373	89
Dec.	29.3321	4.52256	89

D.3 Maximum Daily Temperature ($^{\circ}\text{F}$)

Table D.37: Station 2432 Max. Temp.

Month	Mean	Standard Deviation	n
Jan.	39.5147	4.28631	92
Feb.	44.7261	4.6668	92
Mar..	51.8689	4.43199	91
Apr.	61.1672	3.98784	91
May	70.2257	3.81775	91
Jun.	80.6865	3.31438	91
Jul.	85.0522	3.0877	90
Aug.	83.0946	2.73636	91
Sep.	76.5347	3.39661	91
Oct.	65.7385	4.23754	90
Nov.	52.082	4.62401	91
Dec.	41.4028	5.06846	91

Table D.38: Station 2592 Max. Temp.

Month	Mean	Standard Deviation	n
Jan.	39.8484	4.83333	87
Feb.	45.3998	5.6754	87
Mar.	54.0465	4.77463	84
Apr.	63.0645	4.19509	85
May	72.3413	4.07558	91
Jun.	83.14	3.60593	87
Jul.	88.2176	2.91309	88
Aug.	85.3335	2.93004	85
Sep.	78.0632	3.28425	91

(continued on next page)

Table D.38: Station 2592 Max. Temp. (*continued*)

Month	Mean	Standard Deviation	n
Oct.	66.4901	3.87573	90
Nov.	52.5556	4.3905	88
Dec.	41.9936	4.94695	88

Table D.39: Station 3160 Max. Temp.

Month	Mean	Standard Deviation	n
Jan.	41.2389	3.93519	88
Feb.	43.5893	4.32058	87
Mar.	48.1883	4.6646	87
Apr.	56.7347	4.43364	89
May	66.1891	4.07172	89
Jun.	76.8693	3.43842	89
Jul.	80.0875	2.94089	89
Aug.	77.4468	2.51872	89
Sep.	72.7735	3.08296	87
Oct.	62.8669	4.25309	89
Nov.	51.2995	4.20024	88
Dec.	43.1942	4.29081	89

Table D.40: Station 3611 Max. Temp.

Month	Mean	Standard Deviation	n
Jan.	40.1587	6.0552	49
Feb.	49.2157	5.95706	48
Mar.	59.8492	4.51028	49
Apr.	69.9844	4.24698	49

(*continued on next page*)

Table D.40: Station 3611 Max. Temp. (*continued*)

Month	Mean	Standard Deviation	n
May	80.7364	3.67081	49
Jun.	92.249	4.06732	49
Jul.	98.2585	2.52965	49
Aug.	95.0445	2.71653	50
Sep.	85.8373	3.3058	50
Oct.	71.7334	4.26431	49
Nov.	54.5106	4.1185	49
Dec.	42.6743	4.60924	50

Table D.41: Station 4089 Max. Temp.

Month	Mean	Standard Deviation	n
Jan.	47.7353	6.33407	97
Feb.	55.6747	6.48538	99
Mar.	62.7337	4.11585	100
Apr.	71.4938	3.67204	100
May	80.5617	3.33409	98
Jun.	90.8003	2.81256	99
Jul.	93.9912	2.19248	100
Aug.	91.3901	2.3183	99
Sep.	85.3342	2.89106	102
Oct.	74.0167	3.55554	99
Nov.	60.3527	4.54156	98
Dec.	48.6652	6.35972	98

Table D.42: Station 4508 Max. Temp.

Month	Mean	Standard Deviation	n
Jan.	47.6106	4.71544	49
Feb.	53.3814	4.70535	49
Mar.	59.1222	4.48774	49
Apr.	67.946	4.29126	49
May	77.129	3.43433	48
Jun.	87.9286	3.26664	48
Jul.	93.0913	2.25567	50
Aug.	90.4172	2.10723	50
Sep.	83.9167	3.16182	50
Oct.	73.0909	4.20991	50
Nov.	58.8997	3.97873	50
Dec.	49.5864	4.70631	50

Table D.43: Station 4849 Max. Temp.

Month	Mean	Standard Deviation	n
Jan.	48.0173	4.75179	69
Feb.	56.9595	4.47862	68
Mar.	66.5335	4.00193	68
Apr.	77.2407	3.93906	69
May	86.993	3.297	66
Jun.	98.0521	3.18026	69
Jul.	103.096	1.96297	69
Aug.	99.8529	2.33122	69
Sep.	92.5498	2.98234	68
Oct.	78.2689	3.62156	69
Nov.	60.9574	3.28353	68

(continued on next page)

Table D.43: Station 4849 Max. Temp. (*continued*)

Month	Mean	Standard Deviation	n
Dec.	49.1178	4.34971	66

Table D.44: Station 5148 Max. Temp.

Month	Mean	Standard Deviation	n
Jan.	39.0818	4.53072	46
Feb.	42.9801	4.2642	46
Mar.	49.1105	4.07786	44
Apr.	57.8276	4.35052	44
May	67.2294	3.31164	44
Jun.	77.4117	3.54073	45
Jul.	82.3297	1.8515	47
Aug.	79.8437	2.06168	46
Sep.	73.5979	2.82047	47
Oct.	63.107	4.60766	47
Nov.	49.4621	4.56559	46
Dec.	40.6631	4.70087	45

Table D.45: Station 5733 Max. Temp.

Month	Mean	Standard Deviation	n
Jan.	42.4397	5.59915	69
Feb.	51.0972	5.68373	67
Mar.	62.2732	4.55411	68
Apr.	72.4523	4.11113	69
May	82.4999	3.40855	69
Jun.	92.9126	3.46959	68

(*continued on next page*)

Table D.45: Station 5733 Max. Temp. (*continued*)

Month	Mean	Standard Deviation	n
Jul.	99.0543	2.10934	68
Aug.	96.2749	2.50413	68
Step	87.634	3.5188	68
Oct.	74.4439	4.24961	68
Nov.	57.0359	3.78849	68
Dec.	45.2226	4.35016	69

Table D.46: Station 6601 Max. Temp.

Month	Mean	Standard Deviation	n
Jan.	40.0626	4.74313	48
Feb.	44.2298	4.76809	47
Mar.	51.1319	4.73611	48
Apr.	60.8081	4.14124	47
May	69.8406	3.37093	47
Jun.	80.0179	3.17989	47
Jul.	85.4113	2.28468	48
Aug.	82.8201	2.39521	48
Step	76.534	2.78939	49
Oct.	66.3074	4.05181	49
Nov.	51.3661	4.89363	48
Dec.	41.8595	4.80567	48

Table D.47: Station 6686 Max. Temp.

Month	Mean	Standard Deviation	n
Jan.	42.0888	4.39581	49

(*continued on next page*)

Table D.47: Station 6686 Max. Temp. (*continued*)

Month	Mean	Standard Deviation	n
Feb.	46.5054	4.24854	49
Mar.	52.4514	4.32647	48
Apr.	60.9819	4.18674	48
May	70.6865	4.02625	49
Jun.	81.5436	3.21155	49
Jul.	87.5239	2.14753	50
Aug.	85.3426	2.16979	50
Step	78.6523	2.96608	50
Oct.	67.3738	4.35092	50
Nov.	52.9678	4.62214	50
Dec.	43.8994	4.45049	50

Table D.48: Station 692 Max. Temp.

Month	Mean	Standard Deviation	n
Jan.	42.7775	4.27339	50
Feb.	49.8909	4.18925	50
Mar.	58.3347	3.96934	50
Apr.	68.1097	3.52947	50
May	77.3602	3.07291	50
Jun.	87.3374	2.93702	50
Jul.	91.8178	2.27177	50
Aug.	89.0117	2.1825	49
Step	82.1465	2.82074	50
Oct.	70.4036	3.68479	50
Nov.	54.8855	3.8303	50
Dec.	44.053	4.31049	50

Table D.49: Station 738 Max. Temp.

Month	Mean	Standard Deviation	n
Jan.	38.6036	4.5322	89
Feb.	44.6222	4.81752	89
Mar.	52.3703	4.34697	89
Apr.	61.98	4.19637	90
May	71.7795	3.92345	91
Jun.	82.9799	3.54548	90
Jul.	88.288	3.16135	90
Aug.	85.9375	2.89318	89
Step	78.0395	3.3405	91
Oct.	65.7901	4.10371	90
Nov.	51.311	3.6516	90
Dec.	40.7276	4.51399	92

Table D.50: Station 7435 Max. Temp.

Month	Mean	Standard Deviation	n
Jan.	48.0314	5.17073	86
Feb.	54.6341	4.03888	87
Mar.	60.8888	4.10212	86
Apr.	69.9253	3.73346	88
May	78.2546	3.43465	89
Jun.	88.1136	2.6819	87
Jul.	90.0786	2.43294	86
Aug.	87.6245	2.38133	91
Step	82.679	2.76768	91
Oct.	72.6796	3.36021	91
Nov.	59.6987	3.99699	88

(continued on next page)

Table D.50: Station 7435 Max. Temp. (*continued*)

Month	Mean	Standard Deviation	n
Dec.	49.2224	4.92205	90

Table D.51: Station 788 Max. Temp.

Month	Mean	Standard Deviation	n
Jan.	41.9828	5.54171	77
Feb.	51.1893	5.16546	79
Mar.	61.3056	4.36241	84
Apr.	70.7122	3.6662	81
May	80.186	3.47169	82
Jun.	90.8078	2.97964	82
Jul.	95.5668	2.6799	85
Aug.	92.956	2.70304	85
Sept.	85.0992	3.26796	84
Oct.	71.9886	3.76877	81
Nov.	56.1381	3.92846	81
Dec.	43.5972	5.47771	80

Table D.52: Station 86 Max. Temp.

Month	Mean	Standard Deviation	n
Jan.	39.1736	4.67715	70
Feb.	42.0791	5.03173	70
Mar.	47.4413	4.92266	69
Apr.	57.5093	4.36177	70
May	66.7782	4.11394	69
Jun.	76.4535	3.59209	70

(*continued on next page*)

Table D.52: Station 86 Max. Temp. (*continued*)

Month	Mean	Standard Deviation	n
Jul.	82.3127	2.76471	70
Aug.	80.1652	2.66719	70
Step	73.6737	2.98184	70
Oct.	62.9427	4.13441	70
Nov.	49.9896	4.47369	70
Dec.	41.7952	4.81516	69

Table D.53: Station 9359 Max. Temp.

Month	Mean	Standard Deviation	n
Jan.	44.8791	4.11714	91
Feb.	47.3425	4.49493	91
Mar.	52.3527	4.60259	94
Apr.	61.0449	3.94842	95
May	69.7635	4.08779	95
Jun.	80.3075	3.1914	94
Jul.	83.6195	2.59343	94
Aug.	80.8888	2.58151	94
Step	75.9258	2.91733	93
Oct.	66.3365	4.14371	94
Nov.	55.1115	4.59594	94
Dec.	47.0118	4.31759	92

Table D.54: Station 9717 Max. Temp.

Month	Mean	Standard Deviation	n
Jan.	51.6828	4.97483	92

(*continued on next page*)

Table D.54: Station 9717 Max. Temp. (*continued*)

Month	Mean	Standard Deviation	n
Feb.	57.1733	5.11474	91
Mar.	63.6364	4.33	91
Apr.	72.1138	4.70361	88
May	81.7892	4.89183	89
Jun.	93.0164	3.55777	92
Jul.	98.4927	3.62086	94
Aug.	95.9639	3.87292	92
Sept.	89.1797	3.94143	93
Oct.	77.4732	4.50955	91
Nov.	62.9989	3.87724	89
Dec.	53.2384	4.404	90

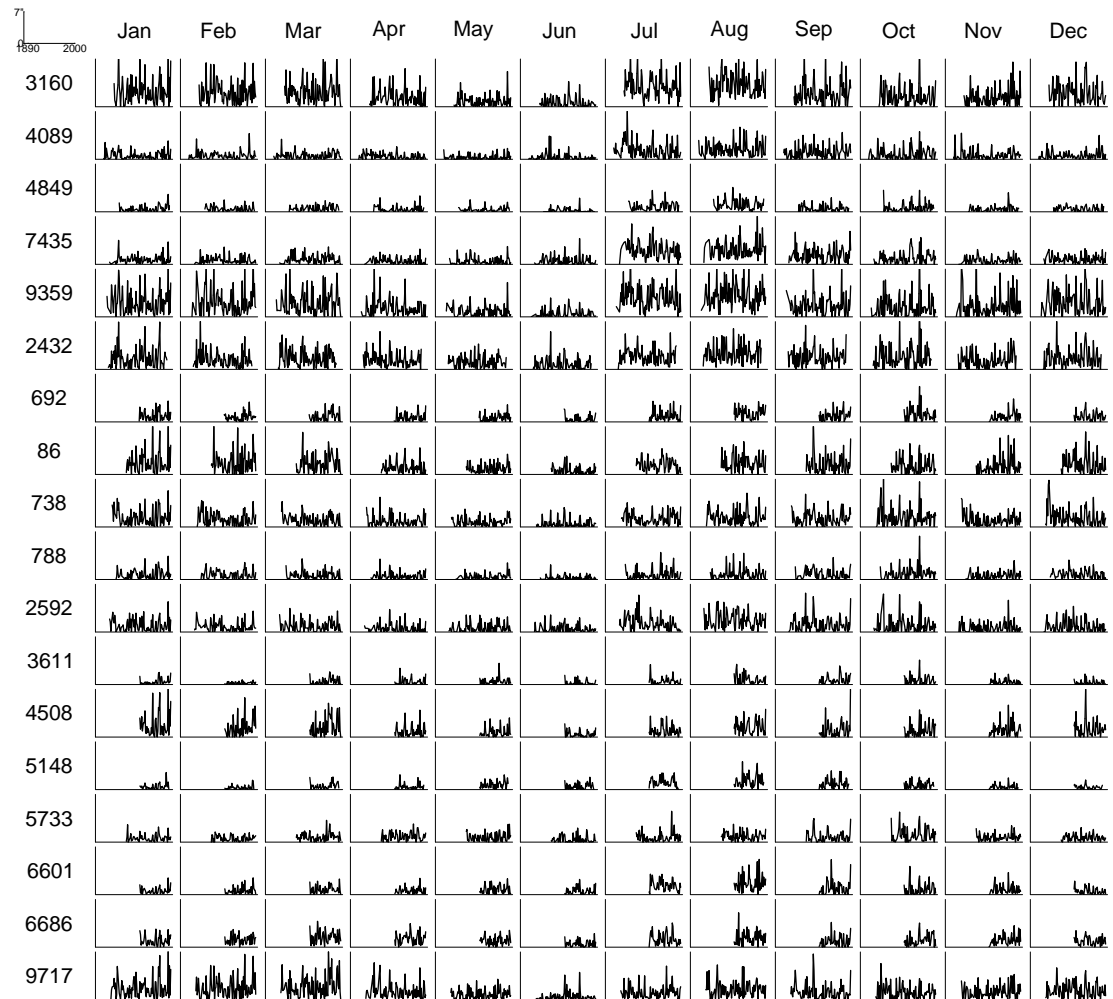


Figure D.1: Interannual Variation in Precipitation for 18 USHCN Stations Within 250 km of the Project Area

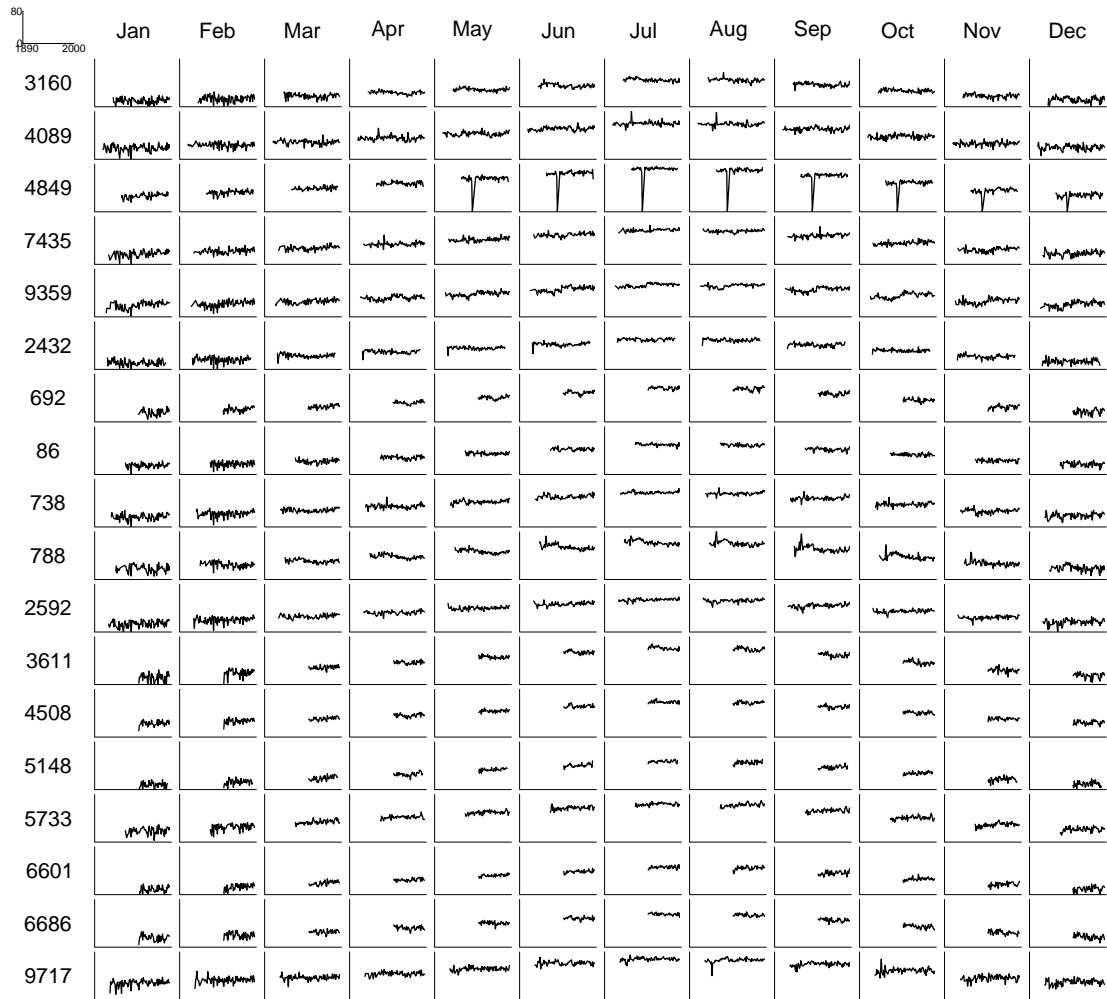


Figure D.2: Interannual Variation in Average Minimum Daily Temperature for 18 USHCN Stations Within 250 km of the Project Area

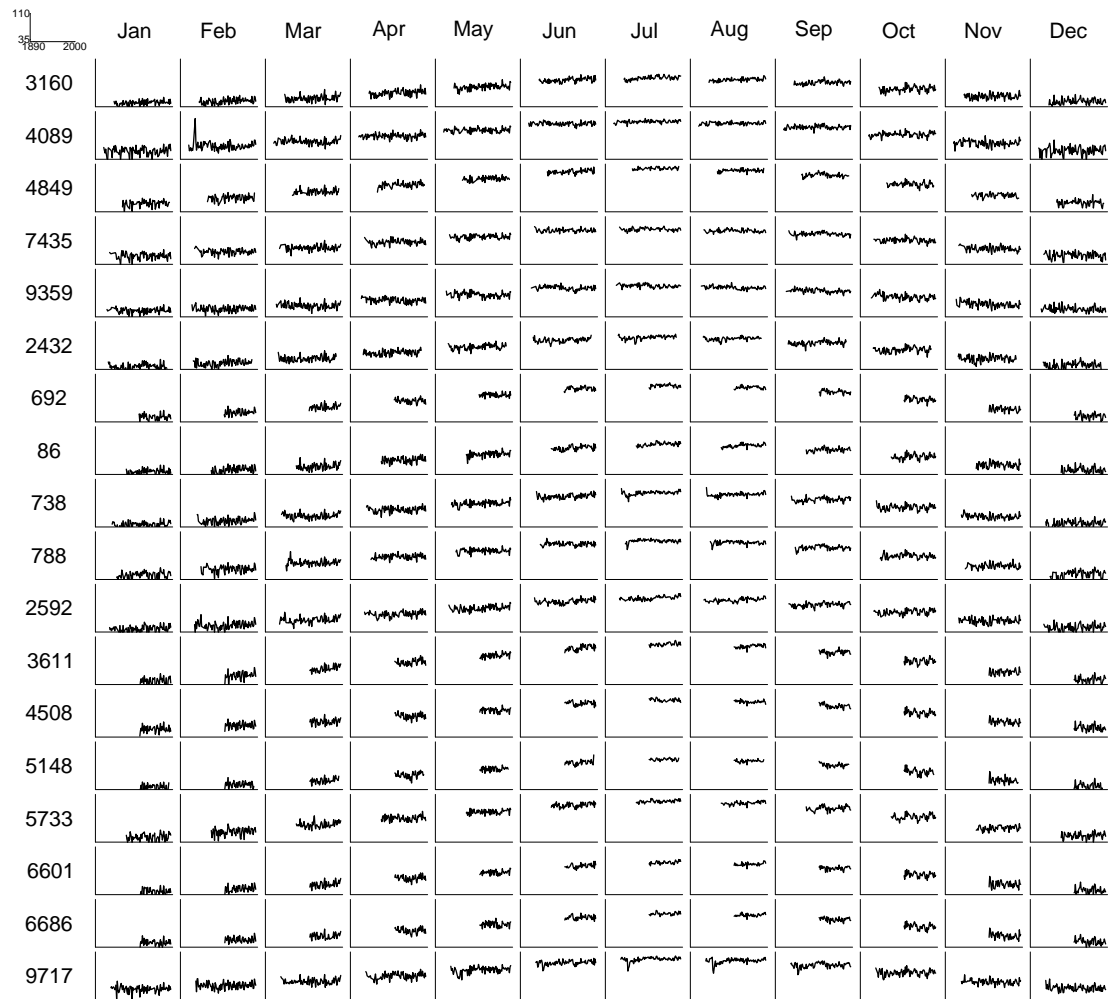


Figure D.3: Interannual Variation in Average Maximum Daily Temperature for 18 USHCN Stations Within 250 km of the Project Area

Appendix E

Regression models for the prediction of temperature or precipitation values from latitude and elevation.

The regression models developed for this analysis are of the general form:

$$\theta = \beta_0 + \beta_1\Omega + \beta_2\Phi + \epsilon \quad (\text{E.1})$$

where,

θ = Climate variable (Precipitation or Temperature [max or min])

β_0 = Intercept (constant)

β_1 = Latitude Weighting Parameter

β_2 = Elevation Weighting Parameter

Ω = Latitude

Φ = Elevation

ϵ = Error Term

In total 54 regression models were developed and assessed in terms of their ability to resolve the influence of latitude and elevation on mean monthly precipitation, and

mean daily minimum and maximum temperature by month. A separate regression model was developed for each month's values from data available for the 18 USHCN stations (Easterling, et al. 1999) described in Section 2.3 starting on page 78. The following table presents the parameters and associated significance levels, R^2 values, and p-values for each regression model. The significance levels for each parameter represent the results of a hypothesis test that the given parameter is 0, indicating that it does not make a statistically significant contribution to a particular model. The significance levels provided for the R^2 values represent a test of the hypothesis that the full model predicts values no better than a model where the predicted values are randomly selected from a normally distributed collection of climate values with a mean and variance equal to those determined from the observed values. The p-values presented in the last column of each table are for the entire model and are the values used in the significance level assignments for the R^2 values.

The significance levels are represented using a standardized symbology (with P representing the p-value for the specific significance test Sokal and Rohlf 1995:172):

- * = $0.05 \geq P > 0.01$
- ** = $0.01 \geq P > 0.001$
- *** = $P \leq 0.001$

Table E.1: Monthly Precipitation Regression Models

Month	β_0	β_1	β_2	R^2	Model p-value
Jan.	472.18	-12.87	0.0205	0.2666	0.0977
Feb.	374.03	-9.83	0.0157	0.1570	0.3025
Mar.	535.32	-13.30	0.0124	0.1660	0.3074
Apr.	214.00	-4.29	0.0051	0.0545	0.7144
May.	10.62	0.42	0.0083	0.2665	0.1818
Jun.	90.79	-2.47	0.0087**	0.5211*	0.0252

(continued on next page)

Table E.1: Monthly Precipitation Regression Models (*continued*)

Month	β_0	β_1	β_2	R^2	Model p-value
Jul.	485.24	-12.99	0.0192**	0.6658**	0.0072
Aug.	1279.68	-33.39	0.0212*	0.6016*	0.0252
Sep.	917.34*	-22.70	0.0068	0.4586	0.1168
Oct.	587.66	-12.42	-0.0052	0.3255	0.3069
Nov.	1817.84	-45.19*	-0.0052	0.7069*	0.0465
Dec.	2356.64*	-58.84*	-0.0096	0.8253*	0.0305

Table E.2: Average Daily Minimum Temperature Regression Models

Month	β_0	β_1	β_2	R^2	Model p-value
Jan.	96.06**	-1.62*	-0.0036***	0.6199***	0.0007
Feb.	95.06**	-1.39**	-0.0040*	0.7634***	< 0.0001
Mar.	90.80***	-1.04	-0.0045***	0.8917***	< 0.0001
Apr.	90.36***	-0.82	-0.0047***	0.8791***	< 0.0001
May.	108.18**	-1.01	-0.0052***	0.9132***	< 0.0001
Jun.	114.19*	-0.89	-0.0057***	0.8856***	< 0.0001
Jul.	148.52*	-1.64	-0.0055***	0.8874***	0.0001
Aug.	165.28*	-2.14	-0.0054***	0.8906***	0.0001
Sep.	195.04*	-3.16	-0.0054***	0.8472**	0.0014
Oct.	192.35	-3.46	-0.0048**	0.8161**	0.0062
Nov.	248.85*	-5.30*	-0.0043**	0.8863**	0.0044
Dec.	280.28*	-6.33	-0.0043*	0.8628*	0.0188

Table E.3: Average Daily Maximum Temperature Regression Models

Month	β_0	β_1	β_2	R^2	Model p-value
Jan.	130.3209***	-2.0346***	-0.0021***	0.6930***	0.0001

(continued on next page)

Table E.3: Average Daily Maximum Temperature Regression Models (*continued*)

Month	β_0	β_1	β_2	R^2	Model p-value
Feb.	149.7175***	-2.1849***	-0.0035***	0.9161***	< 0.0001
Mar.	138.2848***	-1.5209***	-0.0046***	0.9617***	< 0.0001
Apr.	144.2711***	-1.3989**	-0.0048***	0.9449***	< 0.0001
May.	120.8938***	-0.5046	-0.0049***	0.9633***	< 0.0001
Jun.	132.2925***	-0.487	-0.0052***	0.9724***	< 0.0001
Jul.	114.6908***	0.1419	-0.0053***	0.9779***	< 0.0001
Aug.	94.9101***	0.5759	-0.0052***	0.9895***	< 0.0001
Sep.	120.3142**	-0.3744	-0.0046***	0.9725***	< 0.0001
Oct.	146.1977*	-1.5139	-0.0036***	0.9038***	0.0009
Nov.	214.5175**	-3.7993*	-0.0029**	0.9183**	0.0019
Dec.	253.4651**	-5.2099*	-0.002*	0.8871*	0.0127

Appendix F

Merged Master Site List Used in the Analysis.

The following table provides the merged attributes from the Long House Valley Archaeological Project SARG database (Gaines 1978, n.d.) and the Black Mesa Archaeological Project archaeological site compliance status report (Robison 1984). The contents of this table are based upon the results of the execution of the SQL script presented in Appendix G.

Table F.1: Analysis Site List

Project Area	Site Number	Date (A.D.)	Range	LIT	GDS	CER	PIT	MAS	KIV	STO
bm	70105	50-350		•	•	○	○	○	○	○
bm	70151	50-350		•	○	○	○	○	○	○
bm	70152	50-350		•	○	○	○	●	○	○
bm	70153	50-350		•	—	○	○	○	○	○
bm	70207	50-350		•	○	○	○	○	○	○
bm	70236	50-350		•	○	○	○	○	○	●
bm	70239	50-350		•	•	●	●	○	○	○
bm	70310	50-350		•	●	○	○	○	○	○
bm	70447	50-350		•	●	○	○	○	○	○
bm	70451	50-350		•	○	○	○	○	○	○
bm	70500	50-350		•	○	○	○	○	○	○
bm	70513	50-350		○	○	●	○	○	○	○
bm	70515	50-350		•	○	●	○	○	○	○

● = Present, ○ = Absent, — = Unknown, bm = Black Mesa, lhv = Long House Valley

LIT = Lithics, GDS = Groundstone, CER = Ceramics, PIT = Pithouse, MAS = Masonry, KIV = Kiva

(continued on next page)

Table F.1: Analysis Site List (*continued*)

Project Area	Site Number	Date (A.D.)	Range	LIT	GDS	CER	PIT	MAS	KIV	STO
bm	70536	50-350		●	●	●	○	○	○	○
bm	70540	50-350		●	●	○	○	○	○	●
bm	70540	50-350		●	●	○	○	○	○	●
bm	70713	50-350		●	○	○	○	○	○	○
bm	71110	50-350		●	○	○	○	○	○	○
bm	72012	50-350		●	●	○	○	○	○	○
bm	72043	50-350		●	○	○	○	○	○	○
bm	72100	50-350		●	○	●	○	○	○	○
bm	73013	50-350		●	○	○	○	○	○	○
bm	73017	50-350		●	●	○	○	○	○	○
bm	73030	50-350		●	○	○	○	○	○	○
bm	73032	50-350		●	○	○	○	○	○	○
bm	73037	50-350		●	○	○	○	○	○	○
bm	73043	50-350		●	○	○	○	○	○	○
bm	73045	50-350		●	○	○	○	○	○	○
bm	73049	50-350		●	○	○	○	○	○	○
bm	73107	50-350		○	●	○	○	○	○	●
bm	73110	50-350		●	○	○	○	○	○	○
bm	73114	50-350		●	○	○	○	○	○	○
bm	73119	50-350		●	○	○	○	○	○	○
bm	73130	50-350		●	○	○	○	○	○	○
bm	73141	50-350		●	○	○	○	○	○	●
bm	73144	50-350		●	●	○	○	○	○	●
bm	73173	50-350		●	○	○	○	○	○	○
bm	73195	50-350		●	○	●	○	○	○	○
bm	73201	50-350		●	○	○	○	○	○	●
bm	110042	50-350		●	○	○	○	○	○	○
bm	110244	50-350		●	●	○	○	○	○	●
bm	110246	50-350		●	●	●	○	○	○	○
bm	110449	50-350		●	○	●	○	○	○	○
bm	110651	50-350		●	○	●	○	○	○	○
bm	110886	50-350		●	●	○	○	●	○	○
bm	110896	50-350		●	—	●	○	●	○	○
bm	110899	50-350		●	●	○	○	○	○	○
bm	110912	50-350		●	○	○	○	○	○	○
bm	110924	50-350		●	○	○	○	○	○	○
bm	111014	50-350		●	○	●	●	○	○	●
bm	111043	50-350		●	○	○	○	○	○	○

● = Present, ○ = Absent, — = Unknown, bm = Black Mesa, lhv = Long House Valley

LIT = Lithics, GDS = Groundstone, CER = Ceramics, PIT = Pithouse, MAS = Masonry, KIV = Kiva

(continued on next page)

Table F.1: Analysis Site List (*continued*)

Project Area	Site Number	Date (A.D.)	Range	LIT	GDS	CER	PIT	MAS	KIV	STO
bm	111059	50-350		●	○	○	○	○	○	○
bm	111090	50-350		●	○	●	○	○	○	○
bm	111124	50-350		—	○	●	○	○	○	○
bm	111153	50-350		●	●	●	○	○	○	○
bm	111161	50-350		●	○	●	○	○	○	○
bm	111162	50-350		●	○	●	○	○	○	●
bm	111171	50-350		●	●	●	●	○	○	●
bm	111176	50-350		●	○	●	○	○	○	○
bm	111291	50-350		●	○	○	○	○	○	●
bm	111294	50-350		●	○	○	○	○	○	○
bm	111296	50-350		●	●	●	○	○	○	●
bm	111410	50-350		●	●	○	○	○	○	●
bm	111411	50-350		●	●	○	○	●	○	○
bm	111504	50-350		●	○	○	○	○	○	○
bm	111505	50-350		●	●	○	○	○	○	○
bm	111513	50-350		●	○	○	○	○	○	○
bm	112045	50-350		●	○	○	○	○	○	●
bm	112058	50-350		●	○	○	○	○	○	○
bm	112059	50-350		●	○	○	○	○	○	○
bm	112063	50-350		●	●	○	○	●	○	○
bm	112076	50-350		●	○	○	○	○	○	○
bm	112126	50-350		●	●	○	○	○	○	○
bm	112127	50-350		●	○	○	○	○	○	●
bm	112135	50-350		●	○	○	○	○	○	○
bm	112137	50-350		●	○	○	○	○	○	○
bm	112138	50-350		●	○	○	○	○	○	○
bm	112151	50-350		●	●	○	○	○	○	○
bm	112152	50-350		●	○	○	○	○	○	○
bm	112158	50-350		●	○	○	○	○	○	○
bm	112161	50-350		●	○	○	○	○	○	○
bm	112163	50-350		●	○	○	○	○	○	○
bm	112166	50-350		●	○	○	○	○	○	○
bm	112172	50-350		●	○	○	○	○	○	○
bm	112175	50-350		●	○	○	●	○	●	●
bm	112177	50-350		●	●	●	○	○	○	●
bm	112184	50-350		●	●	○	○	○	○	○
bm	112187	50-350		●	○	○	○	○	○	○
bm	112190	50-350		●	●	○	○	○	○	○

● = Present, ○ = Absent, — = Unknown, bm = Black Mesa, lhv = Long House Valley

LIT = Lithics, GDS = Groundstone, CER = Ceramics, PIT = Pithouse, MAS = Masonry, KIV = Kiva

(continued on next page)

Table F.1: Analysis Site List (*continued*)

Project Area	Site Number	Date (A.D.)	Range	LIT	GDS	CER	PIT	MAS	KIV	STO
bm	112196	50-350		○	○	●	○	○	○	○
bm	112197	50-350		●	●	○	○	○	○	○
bm	113002	50-350		●	○	○	○	○	○	○
bm	113032	50-350		●	○	○	○	○	○	○
bm	113036	50-350		●	●	○	○	○	○	○
bm	113063	50-350		●	○	○	○	○	○	●
bm	113074	50-350		●	○	○	○	○	○	○
bm	113078	50-350		●	○	○	○	○	○	○
bm	113080	50-350		●	○	○	○	○	○	○
bm	113094	50-350		●	○	○	○	○	○	○
bm	113101	50-350		●	○	○	○	○	○	○
bm	113104	50-350		●	○	○	●	●	○	●
bm	113127	50-350		●	○	●	○	○	○	○
bm	113128	50-350		●	○	●	○	○	○	●
bm	113130	50-350		●	●	●	○	○	○	●
bm	113130	50-350		●	●	●	○	○	○	●
bm	113131	50-350		●	●	●	○	○	○	○
bm	113132	50-350		●	●	○	○	○	○	○
bm	113133	50-350		●	●	○	○	○	○	○
bm	113135	50-350		●	●	○	○	○	○	○
bm	113139	50-350		●	○	○	○	○	○	○
bm	113167	50-350		●	○	○	○	○	○	●
bm	113170	50-350		●	○	○	○	○	○	○
bm	113172	50-350		●	○	○	○	○	○	●
bm	113182	50-350		●	○	○	○	○	○	○
bm	113197	50-350		●	○	○	○	○	○	○
bm	114086	50-350		●	●	○	○	○	○	○
bm	120302	50-350		●	○	●	○	○	○	○
bm	120317	50-350		○	○	●	○	○	○	○
bm	120320	50-350		●	●	●	○	○	○	○
bm	70473	50-800		●	○	●	○	○	○	○
bm	71120	50-800		○	○	●	○	○	○	○
bm	72078	50-800		●	○	●	○	○	○	○
bm	112038	50-800		●	○	●	○	○	○	●
bm	112067	50-800		●	○	○	○	○	○	○
bm	112067	50-800		●	○	○	○	○	○	○
bm	70483	600-800		●	○	○	○	○	○	○
bm	70484	600-800		○	●	○	○	○	○	○

● = Present, ○ = Absent, — = Unknown, bm = Black Mesa, Ihv = Long House Valley

LIT = Lithics, GDS = Groundstone, CER = Ceramics, PIT = Pithouse, MAS = Masonry, KIV = Kiva

(continued on next page)

Table F.1: Analysis Site List (*continued*)

Project Area	Site Number	Date (A.D.)	Range	LIT	GDS	CER	PIT	MAS	KIV	STO
bm	71118	600-800		o	o	•	o	•	o	o
bm	110113	600-800		—	—	•	•	—	—	—
bm	111262	600-800		•	o	•	o	o	o	o
bm	111370	600-800		•	•	•	o	o	o	o
bm	111393	600-800		•	•	•	o	•	•	o
bm	113076	600-800		•	o	o	o	o	o	o
bm	113095	600-800		•	•	•	o	o	o	o
bm	70094	600-975		o	o	•	o	o	o	o
bm	70211	600-975		o	o	•	o	o	o	o
bm	70254	600-975		•	o	•	o	•	o	•
bm	70416	600-975		o	o	•	o	o	o	o
bm	70419	600-975		o	o	•	o	o	o	o
bm	70428	600-975		•	o	•	o	o	o	o
bm	70482	600-975		o	o	•	o	o	o	o
bm	70482	600-975		o	o	•	o	o	o	o
bm	70487	600-975		•	o	•	o	o	o	o
bm	70496	600-975		o	o	•	o	o	o	o
bm	70507	600-975		o	o	•	o	o	o	o
bm	72027	600-975		•	•	•	o	•	o	o
bm	73055	600-975		o	o	•	o	o	o	o
bm	73057	600-975		•	•	•	o	•	o	o
bm	73194	600-975		•	o	•	o	o	o	o
bm	110057	600-975		•	•	•	o	•	o	o
bm	110114	600-975		o	o	•	o	o	o	•
bm	110255	600-975		•	o	•	o	•	o	•
bm	110456	600-975		•	o	•	o	o	o	•
bm	110482	600-975		o	•	•	o	•	o	o
bm	110521	600-975		•	•	•	o	o	o	•
bm	110522	600-975		•	o	•	o	•	o	•
bm	110534	600-975		•	•	•	o	•	o	•
bm	110543	600-975		•	o	•	o	•	o	•
bm	110612	600-975		o	o	•	o	o	o	•
bm	111071	600-975		o	o	•	o	o	o	o
bm	111076	600-975		o	•	•	o	o	o	o
bm	111145	600-975		•	o	•	o	•	o	o
bm	111146	600-975		•	o	•	o	o	o	o
bm	111158	600-975		•	o	•	o	o	o	o
bm	111190	600-975		•	o	•	o	o	o	•

• = Present, o = Absent, — = Unknown, bm = Black Mesa, lhv = Long House Valley

LIT = Lithics, GDS = Groundstone, CER = Ceramics, PIT = Pithouse, MAS = Masonry, KIV = Kiva

(continued on next page)

Table F.1: Analysis Site List (*continued*)

Project Area	Site Number	Date (A.D.)	Range	LIT	GDS	CER	PIT	MAS	KIV	STO
bm	111222	600-975		○	●	●	○	○	○	○
bm	111230	600-975		●	○	●	○	○	○	○
bm	111273	600-975		○	○	●	○	○	○	○
bm	111332	600-975		●	○	●	○	○	○	○
bm	112023	600-975		●	○	●	○	●	●	○
bm	112025	600-975		●	●	●	○	○	○	●
bm	112065	600-975		●	●	●	○	○	○	○
bm	112153	600-975		●	○	●	●	●	○	●
bm	112160	600-975		●	●	●	○	○	○	●
bm	112168	600-975		●	●	●	○	○	○	●
bm	70025	900-975		●	○	●	○	●	●	●
bm	70051	900-975		●	●	●	○	○	○	●
bm	70134	900-975		●	—	●	○	●	●	○
bm	70137	900-975		●	●	●	○	●	○	●
bm	70154	900-975		●	○	●	○	○	○	○
bm	70202	900-975		●	●	●	○	●	●	●
bm	70214	900-975		●	●	●	○	●	○	○
bm	70223	900-975		●	○	●	○	●	●	●
bm	70224	900-975		●	○	●	○	●	○	●
bm	70232	900-975		●	○	●	○	●	●	○
bm	70232	900-975		●	○	●	○	●	●	○
bm	70233	900-975		○	○	●	○	●	○	○
bm	70234	900-975		●	●	●	●	●	●	○
bm	70238	900-975		○	○	●	●	●	○	○
bm	70259	900-975		●	○	●	●	●	●	○
bm	70263	900-975		●	●	●	○	●	○	●
bm	70265	900-975		●	●	●	○	●	●	●
bm	70271	900-975		●	○	●	○	●	○	●
bm	70274	900-975		●	●	●	○	●	○	○
bm	70278	900-975		●	●	●	○	●	●	●
bm	70280	900-975		●	○	●	○	●	●	●
bm	70409	900-975		●	●	●	○	○	○	○
bm	70410	900-975		○	○	●	○	○	○	○
bm	70414	900-975		○	○	●	○	○	○	○
bm	70420	900-975		●	○	●	○	○	○	○
bm	70442	900-975		○	○	●	○	○	○	○
bm	70449	900-975		●	○	●	○	○	○	○
bm	70457	900-975		○	○	●	○	○	○	○

● = Present, ○ = Absent, — = Unknown, bm = Black Mesa, Ihv = Long House Valley

LIT = Lithics, GDS = Groundstone, CER = Ceramics, PIT = Pithouse, MAS = Masonry, KIV = Kiva

(continued on next page)

Table F.1: Analysis Site List (*continued*)

Project Area	Site Number	Date (A.D.)	Range	LIT	GDS	CER	PIT	MAS	KIV	STO
bm	70468	900-975		o	o	•	o	o	o	o
bm	70469	900-975		o	o	•	o	o	o	o
bm	70481	900-975		o	o	•	o	o	o	o
bm	70486	900-975		o	o	•	o	o	o	o
bm	70490	900-975		o	•	•	o	o	o	o
bm	70491	900-975		o	o	•	o	o	o	o
bm	70502	900-975		o	o	•	o	o	o	o
bm	70509	900-975		•	o	•	o	o	o	o
bm	72013	900-975		•	o	•	•	•	•	o
bm	72064	900-975		•	•	•	o	•	o	•
bm	72077	900-975		•	•	•	o	•	o	•
bm	72099	900-975		•	•	•	o	•	o	•
bm	73011	900-975		o	o	•	o	o	o	o
bm	73021	900-975		•	o	•	o	o	o	o
bm	73111	900-975		•	o	•	o	•	o	o
bm	73112	900-975		•	•	•	o	o	o	o
bm	73191	900-975		•	•	•	o	o	o	•
bm	73196	900-975		•	o	•	o	•	o	o
bm	110031	900-975		o	o	•	•	o	o	•
bm	110037	900-975		•	•	•	—	•	—	o
bm	110073	900-975		•	o	•	o	•	o	o
bm	110117	900-975		•	o	•	o	o	o	o
bm	110231	900-975		•	•	•	o	•	o	—
bm	110254	900-975		•	•	•	o	•	o	o
bm	110256	900-975		•	o	•	•	•	o	o
bm	110320	900-975		•	•	•	o	•	o	•
bm	110338	900-975		•	o	•	o	•	o	•
bm	110381	900-975		•	o	•	o	•	o	o
bm	110394	900-975		•	o	•	•	•	•	o
bm	110397	900-975		•	•	•	o	•	o	o
bm	110444	900-975		•	o	•	o	o	o	•
bm	110445	900-975		•	o	•	o	•	o	o
bm	110459	900-975		•	•	•	o	•	o	o
bm	110468	900-975		•	•	•	o	•	o	•
bm	110485	900-975		•	o	•	o	o	o	•
bm	110494	900-975		•	•	•	•	•	•	•
bm	110527	900-975		•	•	•	o	•	o	•
bm	110539	900-975		•	o	•	o	•	•	o

• = Present, o = Absent, — = Unknown, bm = Black Mesa, lhv = Long House Valley

LIT = Lithics, GDS = Groundstone, CER = Ceramics, PIT = Pithouse, MAS = Masonry, KIV = Kiva

(continued on next page)

Table F.1: Analysis Site List (*continued*)

Project Area	Site Number	Date (A.D.)	Range	LIT	GDS	CER	PIT	MAS	KIV	STO
bm	110655	900-975		●	●	●	●	○	○	●
bm	110866	900-975		○	○	●	○	●	○	○
bm	110889	900-975		●	●	●	○	●	○	○
bm	110893	900-975		●	○	●	○	○	○	●
bm	111032	900-975		○	○	●	○	○	○	○
bm	111040	900-975		○	○	●	○	○	○	○
bm	111053	900-975		○	○	●	○	○	○	○
bm	111062	900-975		●	○	●	○	○	○	○
bm	111063	900-975		○	○	●	○	○	○	○
bm	111070	900-975		○	○	●	○	○	○	○
bm	111072	900-975		●	○	●	○	○	○	○
bm	111075	900-975		●	○	●	○	○	○	●
bm	111088	900-975		●	○	●	○	○	○	○
bm	111113	900-975		○	○	●	○	○	○	○
bm	111131	900-975		●	●	●	○	●	○	●
bm	111143	900-975		●	○	●	○	○	○	○
bm	111149	900-975		●	●	●	○	●	○	○
bm	111191	900-975		●	○	●	○	○	○	○
bm	111203	900-975		●	●	●	○	●	○	○
bm	111210	900-975		●	●	●	○	○	○	●
bm	111216	900-975		○	○	●	○	○	○	○
bm	111219	900-975		○	○	●	○	○	○	○
bm	111226	900-975		○	○	●	○	○	○	○
bm	111247	900-975		●	○	●	○	○	○	●
bm	111253	900-975		●	○	●	○	○	○	○
bm	111334	900-975		●	○	●	○	○	○	○
bm	111387	900-975	—	○	●	●	○	○	○	○
bm	112018	900-975		○	○	●	○	○	○	●
bm	112024	900-975		○	○	●	○	○	○	●
bm	112026	900-975		●	●	●	●	○	○	●
bm	112030	900-975		●	●	●	●	●	●	●
bm	112040	900-975		●	●	●	○	●	●	●
bm	112060	900-975		●	●	●	○	○	○	●
bm	112061	900-975		●	●	●	○	○	○	●
bm	112062	900-975		●	●	●	○	●	○	●
bm	112069	900-975		●	○	●	○	●	●	●
bm	112070	900-975		●	○	●	○	●	○	○
bm	112145	900-975		●	●	●	○	○	○	●

● = Present, ○ = Absent, — = Unknown, bm = Black Mesa, lhv = Long House Valley

LIT = Lithics, GDS = Groundstone, CER = Ceramics, PIT = Pithouse, MAS = Masonry, KIV = Kiva

(continued on next page)

Table F.1: Analysis Site List (*continued*)

Project Area	Site Number	Date (A.D.)	Range	LIT	GDS	CER	PIT	MAS	KIV	STO
bm	112154	900-975		•	•	•	•	○	○	○
bm	112167	900-975		•	•	•	○	○	○	•
bm	113011	900-975		•	•	•	○	•	○	○
bm	113041	900-975		○	○	•	○	○	○	○
bm	113052	900-975		•	○	•	○	○	○	○
bm	113061	900-975		○	•	•	○	○	○	•
bm	113093	900-975		○	○	•	○	○	○	○
bm	113158	900-975		○	○	•	○	○	○	○
bm	113164	900-975		•	•	•	○	○	○	•
bm	113179	900-975		•	○	○	○	○	○	○
bm	113183	900-975		•	•	•	○	○	○	○
bm	113184	900-975		•	○	•	○	○	○	•
bm	113185	900-975		○	○	•	○	○	○	○
bm	113188	900-975		•	○	•	○	○	○	○
bm	120245	900-975		•	•	•	○	•	○	•
bm	120249	900-975		•	•	•	○	○	○	•
bm	120304	900-975		•	○	•	○	○	○	○
bm	120321	900-975		•	•	•	○	○	○	•
bm	120324	900-975		○	○	•	○	○	○	○
bm	70424	900-1050		○	○	•	○	○	○	○
bm	72024	900-1050		•	•	•	○	•	•	•
bm	72065	900-1050		•	•	•	○	○	○	○
bm	72067	900-1050		•	•	•	○	•	•	○
bm	72090	900-1050		•	•	•	○	•	○	•
bm	73051	900-1050		○	○	•	○	○	○	○
bm	73053	900-1050		•	○	•	○	○	○	•
bm	73193	900-1050		•	○	•	○	○	○	○
bm	111506	900-1050		○	○	•	○	○	○	○
bm	112010	900-1050		•	•	•	○	○	○	•
bm	112027	900-1050		•	○	•	○	•	•	○
bm	112028	900-1050		○	○	•	○	•	○	○
bm	112029	900-1050		•	•	•	○	○	○	•
bm	112143	900-1050		•	•	•	•	•	○	•
bm	112144	900-1050		•	•	•	•	•	○	○
bm	112185	900-1050		•	•	•	○	•	○	•
bm	112194	900-1050		•	○	•	○	•	○	•
bm	113017	900-1050		○	○	•	○	○	○	•
bm	113035	900-1050		○	○	•	○	○	○	○

• = Present, ○ = Absent, - = Unknown, bm = Black Mesa, lhv = Long House Valley

LIT = Lithics, GDS = Groundstone, CER = Ceramics, PIT = Pithouse, MAS = Masonry, KIV = Kiva

(continued on next page)

Table F.1: Analysis Site List (*continued*)

Project Area	Site Number	Date (A.D.)	Range	LIT	GDS	CER	PIT	MAS	KIV	STO
bm	113040	900-1050		o	o	•	o	•	o	o
bm	113042	900-1050		o	o	•	o	o	o	o
bm	113049	900-1050		•	o	•	o	o	o	o
bm	113059	900-1050		o	o	•	o	o	o	o
bm	70097	975-1050		—	—	—	—	—	—	—
bm	70135	975-1050		•	—	•	o	o	o	•
bm	70203	975-1050		•	•	•	o	•	o	o
bm	70205	975-1050		•	•	•	o	•	•	o
bm	70212	975-1050		•	o	•	o	•	•	o
bm	70213	975-1050		•	•	•	o	•	o	o
bm	70216	975-1050		•	o	•	o	•	•	o
bm	70217	975-1050		o	•	•	o	•	o	o
bm	70218	975-1050		•	o	•	o	•	o	o
bm	70226	975-1050		o	•	•	o	o	o	•
bm	70240	975-1050		•	•	•	o	•	o	•
bm	70264	975-1050		•	•	•	o	•	•	o
bm	70266	975-1050		•	•	•	o	•	o	•
bm	70312	975-1050		•	•	•	o	•	o	o
bm	70316	975-1050		o	•	•	o	o	o	o
bm	70323	975-1050		•	•	•	o	•	o	o
bm	70413	975-1050		o	o	•	o	o	o	o
bm	70415	975-1050		•	o	•	o	o	o	o
bm	70425	975-1050		o	o	•	o	o	o	o
bm	70429	975-1050		•	o	•	o	o	o	o
bm	70459	975-1050		o	o	•	o	o	o	o
bm	70460	975-1050		o	o	•	o	o	o	o
bm	70467	975-1050		•	o	•	o	o	o	o
bm	70470	975-1050		o	o	•	o	o	o	o
bm	70471	975-1050		o	o	•	o	o	o	o
bm	70478	975-1050		•	o	•	o	o	o	o
bm	70493	975-1050		o	o	•	o	o	o	o
bm	70501	975-1050		•	o	•	o	o	o	o
bm	70506	975-1050		o	o	•	o	o	o	o
bm	70510	975-1050		•	o	•	o	o	o	o
bm	70511	975-1050		•	o	•	o	o	o	o
bm	70535	975-1050		o	o	•	o	•	o	o
bm	70542	975-1050		o	o	•	o	o	o	o
bm	70711	975-1050		o	o	•	o	•	o	o

• = Present, o = Absent, — = Unknown, bm = Black Mesa, lhv = Long House Valley

LIT = Lithics, GDS = Groundstone, CER = Ceramics, PIT = Pithouse, MAS = Masonry, KIV = Kiva

(continued on next page)

Table F.1: Analysis Site List (*continued*)

Project Area	Site Number	Date (A.D.)	Range	LIT	GDS	CER	PIT	MAS	KIV	STO
bm	70714	975-1050		●	○	●	○	○	○	○
bm	70716	975-1050		●	○	●	●	○	○	○
bm	71109	975-1050		●	○	●	○	○	○	○
bm	71130	975-1050		○	●	●	○	○	○	●
bm	72066	975-1050		●	○	●	●	●	○	●
bm	72070	975-1050		●	●	●	○	●	○	○
bm	72091	975-1050		●	●	●	○	●	●	●
bm	73004	975-1050		○	○	●	○	○	○	○
bm	73022	975-1050		○	○	●	○	○	○	○
bm	73039	975-1050		○	○	●	○	○	○	○
bm	73048	975-1050		○	○	●	○	○	○	○
bm	73212	975-1050		○	○	●	○	○	○	○
bm	73213	975-1050		○	○	●	○	○	○	○
bm	110003	975-1050		○	○	●	○	●	●	○
bm	110018	975-1050		○	—	●	○	●	●	○
bm	110027	975-1050		○	○	●	○	●	○	○
bm	110120	975-1050		○	○	●	●	●	○	○
bm	110204	975-1050		●	○	●	○	●	○	●
bm	110216	975-1050		●	○	●	○	●	○	○
bm	110217	975-1050		●	○	●	●	●	○	●
bm	110236	975-1050		●	●	●	○	●	●	○
bm	110240	975-1050		●	●	●	○	○	○	●
bm	110308	975-1050		●	●	●	○	○	○	○
bm	110329	975-1050		●	○	●	○	●	○	●
bm	110390	975-1050		●	○	●	○	●	●	●
bm	110404	975-1050		●	●	●	○	●	○	○
bm	110406	975-1050		●	○	●	○	○	○	●
bm	110416	975-1050		●	●	●	○	○	○	○
bm	110448	975-1050		●	●	●	○	○	○	○
bm	110453	975-1050		●	●	●	○	●	○	●
bm	110473	975-1050		●	●	●	○	○	○	●
bm	110474	975-1050		●	○	●	○	●	●	○
bm	110478	975-1050		●	●	●	○	●	●	○
bm	110516	975-1050		●	○	●	○	●	●	●
bm	110520	975-1050		●	●	●	○	○	●	○
bm	110552	975-1050		○	●	●	○	●	○	●
bm	110569	975-1050		●	●	●	○	●	●	●
bm	110572	975-1050		●	●	●	○	●	○	○

● = Present, ○ = Absent, — = Unknown, bm = Black Mesa, lhv = Long House Valley

LIT = Lithics, GDS = Groundstone, CER = Ceramics, PIT = Pithouse, MAS = Masonry, KIV = Kiva

(continued on next page)

Table F.1: Analysis Site List (*continued*)

Project Area	Site Number	Date (A.D.)	Range	LIT	GDS	CER	PIT	MAS	KIV	STO
bm	110586	975-1050		●	●	●	○	○	○	○
bm	110589	975-1050		●	○	●	○	○	●	○
bm	110603	975-1050		●	○	●	●	●	○	●
bm	110622	975-1050		●	●	●	○	●	○	●
bm	110633	975-1050		●	●	●	○	○	●	○
bm	110638	975-1050		●	●	●	○	●	○	●
bm	110665	975-1050		●	●	●	○	●	○	○
bm	110676	975-1050		○	○	●	○	●	●	●
bm	110700	975-1050		●	●	●	○	●	○	○
bm	110707	975-1050		●	●	●	○	●	●	●
bm	110814	975-1050		●	○	●	○	●	●	○
bm	110943	975-1050		●	—	●	○	○	○	○
bm	111018	975-1050		○	○	●	○	○	○	○
bm	111050	975-1050		○	○	●	○	●	○	○
bm	111058	975-1050		○	○	●	○	○	○	○
bm	111081	975-1050		●	○	●	○	○	○	●
bm	111084	975-1050		●	●	●	○	○	○	○
bm	111100	975-1050		●	○	●	○	○	○	○
bm	111101	975-1050		●	○	●	○	○	○	○
bm	111103	975-1050		○	○	●	○	○	○	○
bm	111119	975-1050		●	●	●	○	○	○	○
bm	111128	975-1050		●	○	●	○	○	○	○
bm	111152	975-1050		○	○	●	○	○	○	○
bm	111154	975-1050		○	●	●	○	○	○	○
bm	111170	975-1050		○	●	●	○	●	○	○
bm	111183	975-1050		○	○	●	○	○	○	○
bm	111187	975-1050		○	○	●	○	○	○	●
bm	111204	975-1050		●	○	●	○	●	○	●
bm	111206	975-1050		●	○	●	○	●	○	○
bm	111212	975-1050		○	○	●	○	●	○	●
bm	111223	975-1050		●	○	●	○	○	○	○
bm	111232	975-1050		○	○	●	○	○	○	○
bm	111242	975-1050		○	○	●	○	●	○	○
bm	111248	975-1050		●	○	●	○	○	○	●
bm	111264	975-1050		●	●	●	○	○	○	○
bm	111271	975-1050		●	○	●	○	○	○	○
bm	111309	975-1050		●	○	●	○	○	○	○
bm	111324	975-1050		●	○	●	○	○	○	○

● = Present, ○ = Absent, — = Unknown, bm = Black Mesa, lhv = Long House Valley

LIT = Lithics, GDS = Groundstone, CER = Ceramics, PIT = Pithouse, MAS = Masonry, KIV = Kiva

(continued on next page)

Table F.1: Analysis Site List (*continued*)

Project Area	Site Number	Date (A.D.)	Range	LIT	GDS	CER	PIT	MAS	KIV	STO
bm	111333	975-1050		o	o	•	o	o	o	o
bm	111337	975-1050		o	o	•	o	o	o	•
bm	111340	975-1050		•	o	•	o	o	o	o
bm	111364	975-1050		•	o	•	o	o	o	o
bm	112005	975-1050		•	•	•	o	•	o	•
bm	112007	975-1050		•	o	•	o	o	o	•
bm	112009	975-1050		•	•	•	o	•	•	•
bm	112015	975-1050		•	•	•	•	•	o	o
bm	112032	975-1050		•	•	•	o	o	o	o
bm	112034	975-1050		•	•	•	•	•	o	•
bm	112052	975-1050		•	o	•	o	•	•	•
bm	112053	975-1050		•	•	•	o	•	•	o
bm	112071	975-1050		•	•	•	o	•	o	•
bm	112072	975-1050		•	•	•	o	•	•	o
bm	112074	975-1050		•	o	•	o	•	o	•
bm	112109	975-1050		•	•	•	o	•	•	o
bm	112111	975-1050		•	•	•	o	•	o	o
bm	112114	975-1050		•	•	•	o	•	o	•
bm	112115	975-1050		•	•	•	o	o	o	•
bm	112134	975-1050		•	o	•	o	o	o	o
bm	112170	975-1050		•	o	•	o	o	o	o
bm	113001	975-1050		•	o	•	o	o	o	•
bm	113013	975-1050		o	o	•	o	o	o	o
bm	113021	975-1050		o	o	•	o	o	o	•
bm	113022	975-1050		•	•	•	o	o	o	o
bm	113136	975-1050		•	•	•	o	•	o	o
bm	113140	975-1050		o	o	•	o	o	o	o
bm	113150	975-1050		•	•	•	o	o	o	o
bm	113186	975-1050		o	o	•	o	o	o	o
bm	113196	975-1050		o	o	•	o	o	o	o
bm	120248	975-1050		•	o	•	•	•	o	o
bm	120324	975-1050		•	•	•	•	•	o	o
bm	70277	975-1100		•	•	•	o	•	o	o
bm	70505	975-1100		•	•	•	o	o	o	•
bm	72025	975-1100		•	•	•	o	•	o	o
bm	110009	975-1100		•	o	•	o	o	o	o
bm	110222	975-1100		•	•	•	o	•	•	•
bm	110287	975-1100		o	o	•	o	o	o	•

• = Present, o = Absent, - = Unknown, bm = Black Mesa, lhv = Long House Valley

LIT = Lithics, GDS = Groundstone, CER = Ceramics, PIT = Pithouse, MAS = Masonry, KIV = Kiva

(continued on next page)

Table F.1: Analysis Site List (*continued*)

Project Area	Site Number	Date (A.D.)	Range	LIT	GDS	CER	PIT	MAS	KIV	STO
bm	110290	975-1100		●	●	●	○	●	●	○
bm	111123	975-1100		○	○	●	○	○	○	○
bm	112008	975-1100		●	○	●	○	●	●	●
bm	112043	975-1100		●	○	●	○	●	○	●
bm	112051	975-1100		●	●	●	○	●	○	●
bm	112106	975-1100		●	●	●	○	●	●	●
bm	112107	975-1100		●	○	●	○	○	○	○
bm	112173	975-1100		●	○	●	○	●	●	●
bm	112179	975-1100		●	○	●	○	●	○	●
bm	113029	975-1100		○	○	●	○	○	○	●
bm	113055	975-1100		○	○	●	○	○	○	○
bm	113056	975-1100		●	●	●	○	○	○	○
bm	113057	975-1100		●	●	●	○	○	○	○
bm	113071	975-1100		○	○	●	○	○	○	○
bm	113089	975-1100		○	○	●	○	○	○	○
bm	113138	975-1100		○	○	●	○	○	○	○
bm	113153	975-1100		●	○	●	○	○	○	○
bm	113160	975-1100		○	○	●	○	○	○	○
bm	70018	1050-1100		●	—	●	●	●	●	○
bm	70024	1050-1100		●	○	●	●	●	○	●
bm	70035	1050-1100		○	○	●	○	○	○	○
bm	70042	1050-1100		○	○	●	○	○	○	○
bm	70045	1050-1100		○	●	●	●	○	○	○
bm	70069	1050-1100		○	○	●	○	○	○	○
bm	70074	1050-1100		○	●	●	○	●	●	○
bm	70087	1050-1100		○	○	●	○	○	○	○
bm	70108	1050-1100		○	○	●	○	○	○	○
bm	70109	1050-1100		○	●	●	○	●	●	○
bm	70117	1050-1100		○	○	●	○	○	○	○
bm	70144	1050-1100		○	○	●	○	●	○	○
bm	70204	1050-1100		●	●	●	○	●	●	○
bm	70215	1050-1100		○	○	●	○	●	○	○
bm	70231	1050-1100		●	○	●	○	●	●	○
bm	70237	1050-1100		●	○	●	○	●	○	—
bm	70255	1050-1100		●	●	●	○	○	○	●
bm	70256	1050-1100		●	○	●	○	○	○	●
bm	70258	1050-1100		●	●	●	○	●	●	●
bm	70306	1050-1100		●	○	●	○	●	○	○

● = Present, ○ = Absent, — = Unknown, bm = Black Mesa, lhv = Long House Valley

LIT = Lithics, GDS = Groundstone, CER = Ceramics, PIT = Pithouse, MAS = Masonry, KIV = Kiva

(continued on next page)

Table F.1: Analysis Site List (*continued*)

Project Area	Site Number	Date (A.D.)	Range	LIT	GDS	CER	PIT	MAS	KIV	STO
bm	70309	1050-1100		•	•	•	○	•	•	○
bm	70311	1050-1100		•	•	•	○	•	○	•
bm	70314	1050-1100		•	•	•	○	○	○	•
bm	70411	1050-1100		•	○	•	○	○	○	○
bm	70412	1050-1100		○	○	•	○	○	○	○
bm	70421	1050-1100		○	○	•	○	○	○	○
bm	70430	1050-1100		•	○	•	○	○	○	○
bm	70441	1050-1100		•	○	•	○	○	○	○
bm	70443	1050-1100		○	○	•	○	○	○	○
bm	70446	1050-1100		○	○	•	○	○	○	○
bm	70448	1050-1100		•	○	•	○	○	○	○
bm	70450	1050-1100		•	○	•	○	○	○	○
bm	70454	1050-1100		○	○	•	○	○	○	○
bm	70466	1050-1100		•	○	•	○	○	○	○
bm	70474	1050-1100		•	○	•	○	○	○	○
bm	70475	1050-1100		•	○	•	○	○	○	○
bm	70476	1050-1100		○	○	•	○	○	○	○
bm	70477	1050-1100		○	○	•	○	○	○	○
bm	70479	1050-1100		○	○	•	○	○	○	○
bm	70480	1050-1100		○	○	•	○	○	○	○
bm	70485	1050-1100		○	○	•	○	○	○	○
bm	70494	1050-1100		○	○	•	○	●	○	○
bm	70495	1050-1100		○	○	•	○	○	○	○
bm	70499	1050-1100		○	○	•	○	○	○	○
bm	70508	1050-1100		•	○	•	○	○	○	○
bm	70512	1050-1100		○	○	•	○	○	○	○
bm	70537	1050-1100		○	○	•	○	○	○	○
bm	70543	1050-1100		•	●	•	○	○	○	○
bm	70544	1050-1100		○	○	•	○	○	○	○
bm	70719	1050-1100		•	○	•	○	●	○	○
bm	71122	1050-1100		○	○	•	○	○	○	○
bm	71125	1050-1100		○	○	•	○	○	○	○
bm	71131	1050-1100		○	○	•	○	○	○	○
bm	71133	1050-1100		○	○	•	○	○	○	○
bm	71135	1050-1100		○	○	•	○	○	○	○
bm	71136	1050-1100		○	○	•	○	○	○	○
bm	71137	1050-1100		○	○	•	○	○	○	○
bm	71141	1050-1100		○	●	●	○	●	○	○

● = Present, ○ = Absent, - = Unknown, bm = Black Mesa, lhv = Long House Valley

LIT = Lithics, GDS = Groundstone, CER = Ceramics, PIT = Pithouse, MAS = Masonry, KIV = Kiva

(continued on next page)

Table F.1: Analysis Site List (*continued*)

Project Area	Site Number	Date (A.D.)	Range	LIT	GDS	CER	PIT	MAS	KIV	STO
bm	71142	1050-1100		●	●	●	○	○	○	○
bm	71144	1050-1100		○	○	●	○	○	○	○
bm	71145	1050-1100		○	○	●	○	○	○	○
bm	72001	1050-1100		●	○	●	○	●	○	●
bm	72002	1050-1100		●	○	●	○	●	○	●
bm	72003	1050-1100		○	○	●	○	●	○	●
bm	72004	1050-1100		●	●	●	○	●	●	○
bm	72005	1050-1100		●	●	●	○	●	○	●
bm	72006	1050-1100		○	●	●	○	●	○	○
bm	72007	1050-1100		○	○	●	○	○	○	○
bm	72008	1050-1100		○	●	●	○	●	○	●
bm	72009	1050-1100		○	●	●	○	●	●	○
bm	72010	1050-1100		●	●	●	○	●	○	●
bm	72011	1050-1100		●	●	●	○	○	○	○
bm	72014	1050-1100		●	○	●	●	●	●	○
bm	72015	1050-1100		○	●	●	○	○	○	○
bm	72016	1050-1100		●	○	●	○	○	○	●
bm	72017	1050-1100		○	●	●	○	●	●	○
bm	72018	1050-1100		○	●	●	○	●	●	○
bm	72019	1050-1100		●	○	●	○	○	○	○
bm	72020	1050-1100		○	●	●	○	●	○	●
bm	72021	1050-1100		○	●	●	○	●	○	○
bm	72022	1050-1100		●	—	●	○	●	○	○
bm	72045	1050-1100		●	●	●	○	●	●	●
bm	72068	1050-1100		●	●	●	○	●	●	●
bm	72086	1050-1100		●	●	●	○	●	●	●
bm	72092	1050-1100		●	●	●	○	○	○	●
bm	73002	1050-1100		●	○	●	○	○	○	○
bm	73005	1050-1100		○	○	●	○	○	○	○
bm	73007	1050-1100		●	○	●	○	○	○	○
bm	73008	1050-1100		●	○	●	○	○	○	○
bm	73009	1050-1100		●	○	●	○	○	○	●
bm	73012	1050-1100		○	○	●	○	○	○	○
bm	73014	1050-1100		○	○	●	○	○	○	○
bm	73023	1050-1100		○	○	●	○	○	○	○
bm	73026	1050-1100		○	○	●	○	○	○	○
bm	73028	1050-1100		○	○	●	○	○	○	○
bm	73029	1050-1100		○	○	●	○	○	○	○

● = Present, ○ = Absent, — = Unknown, bm = Black Mesa, lhv = Long House Valley

LIT = Lithics, GDS = Groundstone, CER = Ceramics, PIT = Pithouse, MAS = Masonry, KIV = Kiva

(continued on next page)

Table F.1: Analysis Site List (*continued*)

Project Area	Site Number	Date (A.D.)	Range	LIT	GDS	CER	PIT	MAS	KIV	STO
bm	73031	1050-1100		●	○	●	○	○	○	○
bm	73033	1050-1100		●	○	●	○	○	○	○
bm	73034	1050-1100		○	○	●	○	○	○	○
bm	73035	1050-1100		○	○	●	○	○	○	○
bm	73036	1050-1100		○	○	●	○	○	○	○
bm	73038	1050-1100		○	●	●	○	●	○	○
bm	73041	1050-1100		●	○	●	○	○	○	○
bm	73042	1050-1100		○	○	●	○	○	○	○
bm	73044	1050-1100		●	●	●	○	●	○	○
bm	73050	1050-1100		○	○	●	○	○	○	○
bm	73056	1050-1100		○	○	●	○	○	○	○
bm	73086	1050-1100		○	○	●	○	○	○	●
bm	73117	1050-1100		●	○	●	○	○	○	●
bm	73120	1050-1100		○	○	●	○	○	○	○
bm	73175	1050-1100		○	○	●	○	○	○	○
bm	73190	1050-1100		○	○	●	○	○	○	○
bm	110015	1050-1100		●	○	●	○	●	○	○
bm	110016	1050-1100		○	○	●	○	●	○	○
bm	110017	1050-1100		○	○	●	○	○	○	○
bm	110085	1050-1100		○	○	●	○	○	○	○
bm	110086	1050-1100		●	○	●	●	○	○	○
bm	110129	1050-1100		●	○	●	○	○	○	●
bm	110134	1050-1100		○	○	●	○	●	○	○
bm	110211	1050-1100		●	○	●	○	○	○	○
bm	110215	1050-1100		●	○	●	○	●	○	○
bm	110230	1050-1100		●	●	●	○	●	○	●
bm	110239	1050-1100		●	○	●	○	○	○	○
bm	110273	1050-1100		●	●	●	○	●	○	○
bm	110275	1050-1100		●	○	●	○	●	●	○
bm	110279	1050-1100		●	●	●	○	●	○	○
bm	110297	1050-1100		●	●	●	○	●	●	●
bm	110299	1050-1100		●	●	●	○	●	○	●
bm	110300	1050-1100		●	○	●	○	●	●	○
bm	110306	1050-1100		●	●	●	○	○	○	●
bm	110316	1050-1100		●	●	●	○	○	○	●
bm	110318	1050-1100		●	●	●	●	●	○	●
bm	110326	1050-1100		●	○	●	○	○	○	●
bm	110328	1050-1100		●	●	●	○	●	○	●

● = Present, ○ = Absent, - = Unknown, bm = Black Mesa, lhv = Long House Valley

LIT = Lithics, GDS = Groundstone, CER = Ceramics, PIT = Pithouse, MAS = Masonry, KIV = Kiva

(continued on next page)

Table F.1: Analysis Site List (*continued*)

Project Area	Site Number	Date (A.D.)	Range	LIT	GDS	CER	PIT	MAS	KIV	STO
bm	110330	1050-1100		•	•	•	○	•	○	○
bm	110332	1050-1100		•	○	•	○	•	○	•
bm	110336	1050-1100		•	○	•	○	•	•	•
bm	110339	1050-1100		•	•	•	○	•	○	•
bm	110342	1050-1100		•	•	•	○	•	○	○
bm	110346	1050-1100		•	•	•	○	•	•	○
bm	110347	1050-1100		•	○	•	○	•	○	•
bm	110349	1050-1100		•	•	•	○	○	○	○
bm	110352	1050-1100		•	•	•	○	•	•	•
bm	110353	1050-1100		•	○	•	○	○	○	○
bm	110354	1050-1100		•	○	•	○	○	○	○
bm	110360	1050-1100		•	•	•	○	•	•	○
bm	110366	1050-1100		•	○	•	○	•	•	○
bm	110373	1050-1100		•	○	•	•	•	○	•
bm	110374	1050-1100		•	•	•	○	•	○	○
bm	110385	1050-1100		•	•	•	○	○	○	•
bm	110387	1050-1100		•	•	•	○	•	•	○
bm	110391	1050-1100		•	○	•	○	○	○	○
bm	110402	1050-1100		•	○	•	○	•	○	○
bm	110403	1050-1100		•	○	•	○	○	○	○
bm	110407	1050-1100		•	○	•	○	•	○	○
bm	110409	1050-1100		•	○	•	○	•	○	○
bm	110410	1050-1100		•	•	•	○	•	•	•
bm	110413	1050-1100		•	•	•	○	•	○	○
bm	110414	1050-1100		•	○	•	○	•	•	○
bm	110418	1050-1100		•	○	•	○	•	•	○
bm	110426	1050-1100		•	•	•	•	•	•	•
bm	110438	1050-1100		•	○	•	○	•	○	•
bm	110442	1050-1100		•	•	•	○	○	○	•
bm	110450	1050-1100		•	○	•	○	•	○	•
bm	110458	1050-1100		•	•	•	○	•	•	○
bm	110460	1050-1100		•	•	•	○	○	○	○
bm	110466	1050-1100		•	•	•	○	•	•	○
bm	110472	1050-1100		•	•	•	○	•	•	•
bm	110475	1050-1100		•	•	•	○	•	○	•
bm	110477	1050-1100		•	•	•	○	•	•	•
bm	110481	1050-1100		•	•	•	○	•	○	○
bm	110489	1050-1100		•	•	•	○	•	•	○

• = Present, ○ = Absent, — = Unknown, bm = Black Mesa, lhv = Long House Valley

LIT = Lithics, GDS = Groundstone, CER = Ceramics, PIT = Pithouse, MAS = Masonry, KIV = Kiva

(continued on next page)

Table F.1: Analysis Site List (*continued*)

Project Area	Site Number	Date (A.D.)	Range	LIT	GDS	CER	PIT	MAS	KIV	STO
bm	110491	1050-1100		•	•	•	○	•	•	•
bm	110493	1050-1100		•	•	•	○	○	○	○
bm	110496	1050-1100		•	•	•	○	○	○	○
bm	110498	1050-1100		•	•	•	•	○	○	○
bm	110499	1050-1100		○	○	•	○	○	○	•
bm	110500	1050-1100		•	•	•	○	•	•	○
bm	110503	1050-1100		•	•	•	•	•	•	○
bm	110505	1050-1100		•	•	•	○	○	○	○
bm	110508	1050-1100		•	○	•	○	•	○	○
bm	110528	1050-1100		•	○	•	○	•	•	•
bm	110538	1050-1100		•	○	•	○	•	•	•
bm	110546	1050-1100		•	○	•	○	○	○	•
bm	110550	1050-1100		•	•	•	○	•	•	•
bm	110563	1050-1100		•	○	•	○	○	○	•
bm	110565	1050-1100		•	○	•	○	○	○	•
bm	110568	1050-1100		•	○	•	○	•	•	•
bm	110570	1050-1100		•	•	•	○	•	•	○
bm	110574	1050-1100		•	•	•	○	○	○	○
bm	110579	1050-1100		•	•	•	○	•	○	•
bm	110602	1050-1100		•	○	•	○	○	○	○
bm	110604	1050-1100		•	○	•	○	•	•	○
bm	110606	1050-1100		•	•	•	○	○	○	○
bm	110624	1050-1100		•	○	•	○	•	○	•
bm	110625	1050-1100		○	•	•	○	•	○	•
bm	110626	1050-1100		•	○	•	○	•	○	○
bm	110627	1050-1100		•	•	•	○	•	○	○
bm	110628	1050-1100		•	•	•	•	•	○	○
bm	110630	1050-1100		•	•	•	○	•	○	○
bm	110632	1050-1100		•	•	•	•	○	•	•
bm	110637	1050-1100		•	•	•	○	•	○	•
bm	110643	1050-1100		○	○	•	○	○	○	○
bm	110644	1050-1100		•	•	•	○	•	○	•
bm	110646	1050-1100		•	○	•	○	○	○	○
bm	110657	1050-1100		•	•	•	○	•	○	•
bm	110664	1050-1100		•	•	•	○	•	○	○
bm	110677	1050-1100		•	○	•	○	○	•	•
bm	110690	1050-1100		•	•	•	○	•	•	•
bm	110701	1050-1100		○	○	•	○	○	○	○

• = Present, ○ = Absent, - = Unknown, bm = Black Mesa, lhv = Long House Valley

LIT = Lithics, GDS = Groundstone, CER = Ceramics, PIT = Pithouse, MAS = Masonry, KIV = Kiva

(continued on next page)

Table F.1: Analysis Site List (*continued*)

Project Area	Site Number	Date (A.D.)	Range	LIT	GDS	CER	PIT	MAS	KIV	STO
bm	110703	1050-1100		●	●	●	○	●	●	○
bm	110704	1050-1100		●	●	●	○	○	○	○
bm	110705	1050-1100		●	○	●	○	○	○	○
bm	110706	1050-1100		●	●	●	○	●	●	●
bm	110877	1050-1100		○	○	●	○	○	○	○
bm	110894	1050-1100		●	○	●	○	●	○	○
bm	110897	1050-1100		●	○	●	○	●	○	○
bm	110903	1050-1100		○	○	●	○	○	○	○
bm	110905	1050-1100		●	○	●	○	○	○	○
bm	110908	1050-1100		○	○	●	○	○	○	○
bm	110911	1050-1100		●	○	●	○	○	○	○
bm	110914	1050-1100		○	○	●	○	○	○	○
bm	110916	1050-1100		○	○	●	○	○	○	○
bm	110918	1050-1100		●	○	●	○	○	○	○
bm	110919	1050-1100		●	○	●	○	●	○	○
bm	110920	1050-1100		○	○	●	○	○	○	○
bm	111009	1050-1100		●	○	●	○	○	○	○
bm	111010	1050-1100		●	○	●	○	○	○	●
bm	111012	1050-1100		●	○	●	○	○	○	○
bm	111013	1050-1100		○	○	●	○	○	○	○
bm	111015	1050-1100		●	○	●	○	●	○	○
bm	111017	1050-1100		○	○	●	○	○	○	○
bm	111027	1050-1100		●	○	●	○	○	○	○
bm	111033	1050-1100		○	○	●	○	○	○	○
bm	111039	1050-1100		○	○	●	○	○	○	○
bm	111046	1050-1100		○	○	●	○	○	○	○
bm	111048	1050-1100		○	○	●	○	○	○	○
bm	111051	1050-1100		○	○	●	○	○	○	○
bm	111052	1050-1100		○	○	●	○	○	○	○
bm	111055	1050-1100		○	●	●	○	○	○	○
bm	111061	1050-1100		○	○	●	○	○	○	○
bm	111064	1050-1100		○	○	●	○	○	○	○
bm	111067	1050-1100		●	○	●	○	○	○	○
bm	111068	1050-1100		○	○	●	○	○	○	○
bm	111069	1050-1100		○	○	●	○	○	○	○
bm	111074	1050-1100		●	○	●	○	○	○	●
bm	111077	1050-1100		●	○	●	○	○	○	○
bm	111082	1050-1100		●	●	●	○	●	○	○

● = Present, ○ = Absent, — = Unknown, bm = Black Mesa, lhv = Long House Valley

LIT = Lithics, GDS = Groundstone, CER = Ceramics, PIT = Pithouse, MAS = Masonry, KIV = Kiva

(continued on next page)

Table F.1: Analysis Site List (*continued*)

Project Area	Site Number	Date (A.D.)	Range	LIT	GDS	CER	PIT	MAS	KIV	STO
bm	111091	1050-1100		•	○	•	○	○	○	○
bm	111092	1050-1100		○	○	•	○	○	○	○
bm	111093	1050-1100		○	○	•	○	○	○	○
bm	111094	1050-1100		○	○	•	○	●	○	●
bm	111095	1050-1100		○	○	•	○	○	○	○
bm	111105	1050-1100		•	○	•	○	○	○	○
bm	111108	1050-1100		○	○	•	○	○	○	○
bm	111115	1050-1100		○	○	•	○	○	○	○
bm	111117	1050-1100		○	○	•	○	○	○	○
bm	111120	1050-1100		•	●	•	○	○	○	○
bm	111121	1050-1100		•	○	•	○	●	○	○
bm	111130	1050-1100		○	○	•	○	●	○	●
bm	111136	1050-1100		•	○	•	○	○	○	●
bm	111142	1050-1100		•	○	•	○	○	○	○
bm	111144	1050-1100		•	○	•	○	○	○	○
bm	111147	1050-1100		○	○	•	○	○	○	○
bm	111148	1050-1100		○	○	•	○	○	○	○
bm	111150	1050-1100		○	○	•	○	○	○	○
bm	111151	1050-1100		○	○	•	○	○	○	○
bm	111156	1050-1100		○	○	•	○	●	○	○
bm	111157	1050-1100		○	○	•	○	○	○	○
bm	111168	1050-1100		•	○	•	○	○	○	●
bm	111172	1050-1100		○	○	•	○	○	○	○
bm	111179	1050-1100		•	○	•	○	○	○	○
bm	111180	1050-1100		•	○	•	○	○	○	○
bm	111186	1050-1100		•	○	•	○	○	○	●
bm	111192	1050-1100		○	●	•	○	○	○	●
bm	111198	1050-1100		○	○	•	○	○	○	○
bm	111202	1050-1100		○	○	•	○	○	○	○
bm	111205	1050-1100		•	○	•	○	●	○	○
bm	111208	1050-1100		•	○	•	○	●	○	○
bm	111214	1050-1100		•	○	•	○	○	○	○
bm	111215	1050-1100		•	○	•	○	●	○	●
bm	111218	1050-1100		•	●	•	○	●	○	○
bm	111227	1050-1100		•	○	•	○	○	○	○
bm	111228	1050-1100		•	○	•	○	○	○	○
bm	111237	1050-1100		○	○	•	○	●	○	○
bm	111249	1050-1100		○	○	•	○	○	○	○

● = Present, ○ = Absent, - = Unknown, bm = Black Mesa, lhv = Long House Valley

LIT = Lithics, GDS = Groundstone, CER = Ceramics, PIT = Pithouse, MAS = Masonry, KIV = Kiva

(continued on next page)

Table F.1: Analysis Site List (*continued*)

Project Area	Site Number	Date (A.D.)	Range	LIT	GDS	CER	PIT	MAS	KIV	STO
bm	111251	1050-1100		●	○	●	○	○	○	○
bm	111254	1050-1100		●	○	●	○	○	○	●
bm	111255	1050-1100		●	○	●	○	●	○	○
bm	111256	1050-1100		●	●	●	○	●	○	○
bm	111258	1050-1100		○	○	●	○	○	○	●
bm	111269	1050-1100		●	○	●	○	●	○	○
bm	111270	1050-1100		○	○	●	○	○	○	○
bm	111270	1050-1100		○	○	●	○	○	○	○
bm	111272	1050-1100		○	○	●	○	○	○	○
bm	111276	1050-1100		●	●	●	○	○	○	○
bm	111280	1050-1100		○	○	●	○	○	○	○
bm	111282	1050-1100		○	○	●	○	○	○	●
bm	111283	1050-1100		●	●	●	○	○	○	●
bm	111285	1050-1100		○	○	●	○	●	○	●
bm	111292	1050-1100		○	○	●	○	○	○	○
bm	111301	1050-1100		●	●	●	○	○	○	●
bm	111302	1050-1100		●	●	●	○	○	○	○
bm	111303	1050-1100		●	○	●	○	○	○	○
bm	111304	1050-1100		○	○	●	○	○	○	○
bm	111306	1050-1100		○	○	●	○	○	○	○
bm	111308	1050-1100		○	○	●	○	○	○	○
bm	111326	1050-1100		●	○	●	○	○	○	○
bm	111327	1050-1100		○	○	●	○	○	○	○
bm	111328	1050-1100		●	○	●	○	○	○	○
bm	111329	1050-1100		●	○	●	○	○	○	●
bm	111346	1050-1100		○	○	●	○	○	○	○
bm	111358	1050-1100		○	○	●	○	○	○	○
bm	111359	1050-1100		○	○	●	○	○	○	○
bm	111360	1050-1100		○	○	●	○	○	○	○
bm	111361	1050-1100		●	○	●	○	○	○	○
bm	111383	1050-1100		○	○	●	○	○	○	○
bm	111384	1050-1100		●	○	●	○	○	○	○
bm	111392	1050-1100		○	○	●	○	○	○	○
bm	111398	1050-1100		○	○	●	○	○	○	○
bm	111412	1050-1100		○	●	●	○	●	○	○
bm	111413	1050-1100		○	○	●	○	○	○	○
bm	111507	1050-1100		○	○	●	○	○	○	○
bm	112001	1050-1100		○	○	●	○	○	○	○

● = Present, ○ = Absent, — = Unknown, bm = Black Mesa, lhv = Long House Valley

LIT = Lithics, GDS = Groundstone, CER = Ceramics, PIT = Pithouse, MAS = Masonry, KIV = Kiva

(continued on next page)

Table F.1: Analysis Site List (*continued*)

Project Area	Site Number	Date (A.D.)	Range	LIT	GDS	CER	PIT	MAS	KIV	STO
bm	112002	1050-1100		o	—	•	—	o	•	o
bm	112003	1050-1100		•	o	•	o	o	o	•
bm	112006	1050-1100		o	o	•	o	o	o	o
bm	112014	1050-1100		o	o	•	•	•	•	•
bm	112017	1050-1100		•	•	•	o	o	o	•
bm	112020	1050-1100		•	o	•	•	•	•	o
bm	112022	1050-1100		•	•	•	o	•	•	o
bm	112064	1050-1100		o	o	•	o	o	o	o
bm	112073	1050-1100		•	•	•	•	o	o	•
bm	112195	1050-1100		•	o	•	o	•	o	o
bm	113003	1050-1100		o	o	•	o	o	o	o
bm	113004	1050-1100		o	o	•	o	o	o	o
bm	113005	1050-1100		o	o	•	o	o	o	o
bm	113023	1050-1100		o	o	•	o	o	o	o
bm	113030	1050-1100		•	•	•	o	o	o	•
bm	113034	1050-1100		•	o	•	o	o	o	o
bm	113053	1050-1100		•	o	•	o	o	o	•
bm	113075	1050-1100		•	o	•	o	o	o	o
bm	113085	1050-1100		•	o	•	o	•	o	o
bm	113086	1050-1100		o	o	•	o	o	o	o
bm	113088	1050-1100		•	o	•	o	o	o	o
bm	113091	1050-1100		o	o	•	o	•	o	o
bm	113103	1050-1100		o	o	•	o	o	o	o
bm	113187	1050-1100		o	o	•	o	o	o	•
bm	113189	1050-1100		•	o	•	o	o	o	o
bm	113192	1050-1100		o	o	•	o	o	o	o
bm	113207	1050-1100		o	o	•	o	o	o	o
bm	120206	1050-1100		•	o	•	o	•	o	o
bm	120217	1050-1100		•	•	•	o	o	o	o
bm	120219	1050-1100		•	•	•	o	•	o	•
bm	120238	1050-1100		•	•	•	o	•	•	•
bm	120246	1050-1100		•	•	•	o	•	o	•
bm	120252	1050-1100		•	o	•	o	o	o	o
bm	120261	1050-1100		•	•	•	o	o	o	o
bm	120307	1050-1100		•	o	•	o	o	o	•
bm	120310	1050-1100		•	o	•	o	o	o	o
bm	120312	1050-1100		•	•	•	o	o	o	•
bm	120315	1050-1100		•	o	•	o	o	o	o

• = Present, o = Absent, — = Unknown, bm = Black Mesa, Ihv = Long House Valley

LIT = Lithics, GDS = Groundstone, CER = Ceramics, PIT = Pithouse, MAS = Masonry, KIV = Kiva

(continued on next page)

Table F.1: Analysis Site List (*continued*)

Project Area	Site Number	Date (A.D.)	Range	LIT	GDS	CER	PIT	MAS	KIV	STO
bm	120333	1050-1100		o	o	•	o	o	o	o
bm	120334	1050-1100		•	o	•	o	o	o	o
bm	120341	1050-1100		o	o	•	o	•	o	o
bm	70020	1050-1150		o	o	•	o	•	•	o
bm	70031	1050-1150		•	•	•	o	•	o	o
bm	70039	1050-1150		o	o	•	•	•	o	o
bm	70725	1050-1150		•	•	•	•	•	•	•
bm	70732	1050-1150		•	•	•	o	•	o	•
bm	71134	1050-1150		o	o	•	o	o	o	o
bm	72023	1050-1150		o	o	•	o	•	o	o
bm	72028	1050-1150		•	•	•	o	o	o	o
bm	72029	1050-1150		•	•	•	o	•	•	•
bm	72046	1050-1150		o	o	•	o	•	•	o
bm	72047	1050-1150		•	•	•	o	•	o	•
bm	72087	1050-1150		•	o	•	o	•	o	•
bm	72088	1050-1150		o	•	•	o	•	o	•
bm	72089	1050-1150		•	o	•	o	•	o	•
bm	72093	1050-1150		•	•	•	o	•	o	o
bm	72095	1050-1150		•	•	•	o	•	o	o
bm	72096	1050-1150		•	o	•	o	o	o	•
bm	72097	1050-1150		•	•	•	o	•	o	•
bm	72098	1050-1150		•	•	•	o	•	o	o
bm	72101	1050-1150		•	•	•	o	•	•	•
bm	72102	1050-1150		•	•	•	o	•	•	o
bm	72104	1050-1150		•	•	•	o	•	o	•
bm	73088	1050-1150		o	o	•	o	o	o	o
bm	73113	1050-1150		o	o	•	o	o	o	o
bm	73121	1050-1150		o	o	•	o	o	o	o
bm	73128	1050-1150		•	•	•	o	•	o	•
bm	73133	1050-1150		•	o	•	o	o	o	•
bm	73134	1050-1150		o	o	•	o	o	o	•
bm	73135	1050-1150		o	o	•	o	o	o	o
bm	73136	1050-1150		o	o	•	o	o	o	o
bm	73138	1050-1150		o	o	•	o	o	o	o
bm	73139	1050-1150		o	o	•	o	o	o	o
bm	73139	1050-1150		o	o	•	o	o	o	o
bm	73146	1050-1150		o	o	•	o	o	o	o
bm	73148	1050-1150		o	o	•	o	o	o	o

• = Present, o = Absent, — = Unknown, bm = Black Mesa, Ihv = Long House Valley

LIT = Lithics, GDS = Groundstone, CER = Ceramics, PIT = Pithouse, MAS = Masonry, KIV = Kiva

(continued on next page)

Table F.1: Analysis Site List (*continued*)

Project Area	Site Number	Date (A.D.)	Range	LIT	GDS	CER	PIT	MAS	KIV	STO
bm	73153	1050-1150		o	o	•	o	o	o	o
bm	73156	1050-1150		o	o	•	o	•	o	o
bm	73170	1050-1150		o	o	•	o	o	o	o
bm	73171	1050-1150		•	o	•	o	o	o	o
bm	73174	1050-1150		o	o	•	o	o	o	o
bm	73176	1050-1150		o	o	•	o	o	o	o
bm	73178	1050-1150		o	o	•	o	o	o	o
bm	73182	1050-1150		o	o	•	o	o	o	o
bm	73185	1050-1150		o	o	•	o	o	o	o
bm	73188	1050-1150		•	o	•	o	o	o	•
bm	73189	1050-1150		o	o	•	o	o	o	o
bm	73198	1050-1150		o	o	•	o	o	o	o
bm	73202	1050-1150		o	o	•	o	o	o	o
bm	73211	1050-1150		o	o	•	o	o	o	o
bm	110224	1050-1150		o	•	•	o	•	•	•
bm	110233	1050-1150		•	o	•	o	•	o	•
bm	110851	1050-1150		•	o	•	o	o	o	o
bm	110856	1050-1150		—	•	•	o	•	o	•
bm	110860	1050-1150		•	o	•	o	o	o	o
bm	110861	1050-1150		o	o	•	o	o	o	o
bm	110864	1050-1150		o	o	•	o	•	o	o
bm	111502	1050-1150		o	o	•	o	o	o	o
bm	112004	1050-1150		•	•	•	o	•	o	•
bm	112016	1050-1150		•	o	•	o	•	o	•
bm	112019	1050-1150		•	•	•	o	•	•	•
bm	112021	1050-1150		•	o	•	o	•	o	o
bm	112036	1050-1150		•	o	•	•	•	•	o
bm	112041	1050-1150		o	o	•	o	o	o	o
bm	112044	1050-1150		•	•	•	o	•	•	o
bm	112046	1050-1150		•	•	•	o	o	o	o
bm	112047	1050-1150		•	•	•	o	•	o	o
bm	112048	1050-1150		•	•	•	o	o	o	o
bm	112049	1050-1150		•	•	•	o	o	•	o
bm	112050	1050-1150		•	•	•	o	•	•	o
bm	112054	1050-1150		•	•	•	o	o	o	•
bm	112055	1050-1150		•	•	•	o	•	•	•
bm	112056	1050-1150		•	•	•	o	o	•	•
bm	112057	1050-1150		•	•	•	o	o	o	o

• = Present, o = Absent, — = Unknown, bm = Black Mesa, lhv = Long House Valley

LIT = Lithics, GDS = Groundstone, CER = Ceramics, PIT = Pithouse, MAS = Masonry, KIV = Kiva

(continued on next page)

Table F.1: Analysis Site List (*continued*)

Project Area	Site Number	Date (A.D.)	Range	LIT	GDS	CER	PIT	MAS	KIV	STO
bm	112077	1050-1150		•	•	•	○	•	•	•
bm	112108	1050-1150		•	•	•	○	•	•	○
bm	112110	1050-1150		•	•	•	○	•	•	○
bm	112113	1050-1150		•	○	•	○	•	•	•
bm	112128	1050-1150		•	•	•	○	○	○	○
bm	112129	1050-1150		•	•	•	○	○	○	•
bm	112132	1050-1150		•	•	•	○	•	○	○
bm	112133	1050-1150		○	○	•	○	○	○	○
bm	112142	1050-1150		•	•	•	○	•	•	•
bm	112147	1050-1150		•	•	•	○	•	○	•
bm	112149	1050-1150		•	•	•	○	•	•	•
bm	112171	1050-1150		•	○	•	○	•	•	•
bm	112176	1050-1150		•	○	•	○	○	○	○
bm	112183	1050-1150		•	○	•	○	○	○	○
bm	112193	1050-1150		•	○	•	○	○	○	•
bm	113031	1050-1150		○	○	•	○	○	○	○
bm	113054	1050-1150		•	•	•	○	○	○	○
bm	113058	1050-1150		○	○	•	○	○	○	○
bm	113062	1050-1150		○	○	•	○	○	○	○
bm	113065	1050-1150		○	○	•	○	•	○	○
bm	113066	1050-1150		○	○	•	○	○	○	○
bm	113068	1050-1150		○	○	•	○	○	○	○
bm	113070	1050-1150		•	○	•	○	○	○	○
bm	113081	1050-1150		○	○	•	○	○	○	○
bm	113082	1050-1150		○	○	•	○	○	○	○
bm	113137	1050-1150		○	•	•	○	•	○	○
bm	113148	1050-1150		○	○	•	○	○	○	○
bm	113152	1050-1150		○	○	•	○	○	○	○
bm	113154	1050-1150		•	○	•	○	○	○	•
bm	113156	1050-1150		○	○	•	○	○	○	○
bm	113159	1050-1150		○	○	•	○	○	○	○
bm	113161	1050-1150		○	○	•	○	○	○	•
bm	113162	1050-1150		•	○	•	○	○	○	○
bm	113163	1050-1150		•	○	•	○	○	○	○
bm	113173	1050-1150		○	○	•	○	○	○	•
bm	113174	1050-1150		○	○	•	○	○	○	○
bm	113175	1050-1150		○	○	•	○	○	○	•
bm	113194	1050-1150		○	○	•	○	○	○	○

• = Present, ○ = Absent, — = Unknown, bm = Black Mesa, lhv = Long House Valley

LIT = Lithics, GDS = Groundstone, CER = Ceramics, PIT = Pithouse, MAS = Masonry, KIV = Kiva

(continued on next page)

Table F.1: Analysis Site List (*continued*)

Project Area	Site Number	Date (A.D.)	Range	LIT	GDS	CER	PIT	MAS	KIV	STO
bm	113205	1050-1150		o	o	•	o	o	o	o
bm	113215	1050-1150		o	o	•	o	o	o	o
bm	70014	1100-1150		—	—	•	o	•	o	o
bm	70015	1100-1150		•	o	•	o	•	•	o
bm	70016	1100-1150		o	•	•	o	•	o	o
bm	70019	1100-1150		o	•	•	o	•	•	o
bm	70022	1100-1150		o	o	•	o	•	•	o
bm	70023	1100-1150		o	o	•	o	•	•	o
bm	70026	1100-1150		•	o	•	o	•	o	•
bm	70027	1100-1150		o	o	•	o	•	•	o
bm	70028	1100-1150		o	o	•	o	o	o	o
bm	70030	1100-1150		•	•	•	o	•	•	o
bm	70032	1100-1150		o	o	•	o	•	•	o
bm	70040	1100-1150		•	—	•	o	o	o	o
bm	70041	1100-1150		•	o	•	•	•	o	o
bm	70043	1100-1150		•	—	—	•	•	•	o
bm	70044	1100-1150		o	•	•	•	•	•	o
bm	70050	1100-1150		o	o	•	o	o	o	o
bm	70052	1100-1150		o	o	•	o	•	o	o
bm	70053	1100-1150		o	o	•	•	o	o	o
bm	70054	1100-1150		•	—	•	o	•	o	o
bm	70058	1100-1150		o	o	•	•	•	o	o
bm	70064	1100-1150		•	•	•	o	o	o	o
bm	70068	1100-1150		o	•	•	o	o	o	o
bm	70070	1100-1150		o	o	•	o	o	o	o
bm	70072	1100-1150		o	o	•	o	o	o	o
bm	70073	1100-1150		o	o	•	o	o	o	o
bm	70075	1100-1150		o	o	•	o	o	o	o
bm	70085	1100-1150		o	o	•	o	•	o	•
bm	70088	1100-1150		o	o	•	o	o	o	o
bm	70089	1100-1150		•	•	•	o	•	•	o
bm	70111	1100-1150		o	o	•	o	•	•	o
bm	70121	1100-1150		—	—	—	—	—	—	—
bm	70133	1100-1150		•	—	•	o	o	o	•
bm	70140	1100-1150		o	—	•	o	•	o	o
bm	70143	1100-1150		o	o	•	o	•	o	o
bm	70146	1100-1150		o	o	•	o	o	o	•
bm	70149	1100-1150		o	o	•	o	o	o	o

• = Present, o = Absent, — = Unknown, bm = Black Mesa, Ihv = Long House Valley

LIT = Lithics, GDS = Groundstone, CER = Ceramics, PIT = Pithouse, MAS = Masonry, KIV = Kiva

(continued on next page)

Table F.1: Analysis Site List (*continued*)

Project Area	Site Number	Date (A.D.)	Range	LIT	GDS	CER	PIT	MAS	KIV	STO
bm	70201	1100-1150		o	o	•	o	o	o	o
bm	70209	1100-1150		•	•	•	o	•	•	•
bm	70219	1100-1150		•	•	•	o	•	o	•
bm	70220	1100-1150		•	•	•	•	•	•	o
bm	70222	1100-1150		•	•	•	o	o	o	•
bm	70235	1100-1150		•	o	•	o	•	•	o
bm	70257	1100-1150		•	o	•	o	•	o	o
bm	70324	1100-1150		•	•	•	o	•	o	•
bm	70324	1100-1150		•	•	•	o	•	o	•
bm	70405	1100-1150		o	o	•	o	o	o	o
bm	70422	1100-1150		o	o	•	o	o	o	o
bm	70445	1100-1150		•	o	•	o	o	o	o
bm	70514	1100-1150		o	o	•	o	•	o	o
bm	70704	1100-1150		•	o	•	o	•	•	•
bm	70710	1100-1150		•	o	•	o	o	o	•
bm	70730	1100-1150		o	—	•	o	o	o	o
bm	71103	1100-1150		•	o	•	o	o	o	•
bm	71104	1100-1150		o	o	•	o	o	o	o
bm	71114	1100-1150		o	o	•	o	o	o	o
bm	71117	1100-1150		o	o	•	o	o	o	o
bm	71143	1100-1150		o	o	•	o	o	o	o
bm	71147	1100-1150		•	•	•	o	o	o	o
bm	72026	1100-1150		•	•	•	o	•	•	o
bm	72044	1100-1150		•	o	•	o	•	o	•
bm	72072	1100-1150		•	•	•	o	•	o	•
bm	72073	1100-1150		•	o	•	o	•	o	•
bm	72074	1100-1150		•	•	•	o	•	o	•
bm	72075	1100-1150		•	•	•	o	o	o	•
bm	72106	1100-1150		•	•	•	o	•	o	•
bm	73018	1100-1150		o	o	•	o	o	o	•
bm	73047	1100-1150		•	o	•	o	o	o	o
bm	73054	1100-1150		o	o	•	o	o	o	o
bm	73108	1100-1150		•	o	•	o	•	o	o
bm	73109	1100-1150		•	o	•	o	•	o	•
bm	73116	1100-1150		o	o	•	o	o	o	o
bm	73122	1100-1150		o	o	•	o	o	o	o
bm	73132	1100-1150		o	o	•	o	o	o	o

• = Present, o = Absent, — = Unknown, bm = Black Mesa, lhv = Long House Valley

LIT = Lithics, GDS = Groundstone, CER = Ceramics, PIT = Pithouse, MAS = Masonry, KIV = Kiva

(continued on next page)

Table F.1: Analysis Site List (*continued*)

Project Area	Site Number	Date (A.D.)	Range	LIT	GDS	CER	PIT	MAS	KIV	STO
bm	73149	1100-1150		o	o	•	o	o	o	o
bm	73150	1100-1150		o	o	•	o	o	o	o
bm	73151	1100-1150		•	o	•	o	o	o	o
bm	73152	1100-1150		o	o	•	o	o	o	o
bm	73154	1100-1150		o	o	•	o	o	o	o
bm	73155	1100-1150		o	o	•	o	o	o	o
bm	73203	1100-1150		o	o	•	o	o	o	o
bm	73204	1100-1150		o	o	•	o	o	o	o
bm	73214	1100-1150		o	o	•	o	o	o	o
bm	73215	1100-1150		•	o	•	o	o	o	o
bm	73216	1100-1150		o	o	•	o	o	o	o
bm	110002	1100-1150		o	o	•	o	•	o	o
bm	110008	1100-1150		o	o	•	o	•	o	o
bm	110011	1100-1150		o	o	•	•	o	o	o
bm	110012	1100-1150		o	o	•	o	•	•	o
bm	110013	1100-1150		o	o	•	o	•	o	o
bm	110014	1100-1150		o	o	•	o	•	o	o
bm	110020	1100-1150		o	o	•	•	o	o	o
bm	110021	1100-1150		o	•	•	o	o	o	o
bm	110022	1100-1150		o	o	•	o	•	o	o
bm	110023	1100-1150		o	o	•	o	o	o	o
bm	110024	1100-1150		o	o	•	o	•	•	o
bm	110029	1100-1150		o	o	•	o	o	o	o
bm	110030	1100-1150		o	•	•	o	o	o	o
bm	110033	1100-1150		o	o	•	o	o	•	o
bm	110035	1100-1150		o	o	•	o	o	o	•
bm	110038	1100-1150		•	•	•	o	•	o	o
bm	110042	1100-1150		o	o	•	o	o	o	o
bm	110043	1100-1150		o	o	•	o	o	o	o
bm	110044	1100-1150		o	•	•	o	o	o	o
bm	110045	1100-1150		•	•	•	o	o	o	o
bm	110045	1100-1150		•	•	•	o	o	o	o
bm	110047	1100-1150		•	o	•	o	o	o	o
bm	110050	1100-1150		o	o	•	o	o	o	o
bm	110051	1100-1150		o	o	•	o	o	o	o
bm	110075	1100-1150		o	o	•	o	o	o	•
bm	110076	1100-1150		o	•	•	o	•	•	o
bm	110077	1100-1150		•	•	•	o	•	o	o

• = Present, o = Absent, - = Unknown, bm = Black Mesa, Ihv = Long House Valley

LIT = Lithics, GDS = Groundstone, CER = Ceramics, PIT = Pithouse, MAS = Masonry, KIV = Kiva

(continued on next page)

Table F.1: Analysis Site List (*continued*)

Project Area	Site Number	Date (A.D.)	Range	LIT	GDS	CER	PIT	MAS	KIV	STO
bm	110078	1100-1150	—	—	●	○	●	●	○	
bm	110079	1100-1150	○	●	●	○	●	●	○	
bm	110079	1100-1150	○	●	●	○	●	●	○	
bm	110081	1100-1150	○	●	●	○	●	●	○	
bm	110084	1100-1150	○	—	●	○	○	○	○	
bm	110092	1100-1150	○	○	●	○	○	○	○	●
bm	110093	1100-1150	—	●	●	○	●	●	●	
bm	110094	1100-1150	○	○	●	○	○	○	○	
bm	110095	1100-1150	○	○	●	○	○	○	○	
bm	110096	1100-1150	○	●	●	○	○	○	○	
bm	110102	1100-1150	○	○	●	○	●	●	●	○
bm	110103	1100-1150	○	○	●	○	●	●	●	○
bm	110104	1100-1150	○	○	●	○	●	●	●	○
bm	110105	1100-1150	○	○	●	○	○	○	○	
bm	110106	1100-1150	●	●	●	○	●	●	○	
bm	110107	1100-1150	—	—	●	○	○	○	○	
bm	110108	1100-1150	●	—	●	○	○	○	○	
bm	110109	1100-1150	○	○	●	○	○	○	○	
bm	110110	1100-1150	○	○	●	○	●	●	○	
bm	110111	1100-1150	●	—	●	○	●	●	○	
bm	110112	1100-1150	○	○	●	○	●	●	○	
bm	110118	1100-1150	○	●	●	—	—	—	—	
bm	110121	1100-1150	○	●	●	○	○	○	○	
bm	110201	1100-1150	○	●	●	○	○	○	○	
bm	110207	1100-1150	●	○	●	○	●	●	●	
bm	110209	1100-1150	○	○	●	●	●	●	●	
bm	110214	1100-1150	●	●	●	○	●	●	●	
bm	110219	1100-1150	●	○	●	○	○	○	○	
bm	110221	1100-1150	●	○	●	○	●	●	○	
bm	110225	1100-1150	○	○	●	○	●	●	○	●
bm	110226	1100-1150	○	●	●	○	●	●	○	
bm	110238	1100-1150	●	●	●	○	●	●	○	—
bm	110249	1100-1150	●	○	●	○	○	○	○	
bm	110253	1100-1150	●	●	●	○	○	○	○	
bm	110260	1100-1150	●	●	●	○	●	●	—	
bm	110261	1100-1150	○	○	●	○	○	○	○	
bm	110262	1100-1150	●	○	●	●	●	○	●	
bm	110265	1100-1150	●	○	●	○	●	●	●	○

● = Present, ○ = Absent, — = Unknown, bm = Black Mesa, Ihv = Long House Valley

LIT = Lithics, GDS = Groundstone, CER = Ceramics, PIT = Pithouse, MAS = Masonry, KIV = Kiva

(continued on next page)

Table F.1: Analysis Site List (*continued*)

Project Area	Site Number	Date (A.D.)	Range	LIT	GDS	CER	PIT	MAS	KIV	STO
bm	110266	1100-1150		•	○	•	○	○	○	○
bm	110270	1100-1150		•	○	•	○	○	○	•
bm	110272	1100-1150		•	○	•	○	•	○	○
bm	110274	1100-1150		•	○	•	○	•	○	•
bm	110276	1100-1150		•	○	•	○	○	○	•
bm	110277	1100-1150		•	•	•	○	○	○	•
bm	110280	1100-1150		•	○	•	○	•	○	○
bm	110288	1100-1150		•	○	•	○	○	○	○
bm	110289	1100-1150		•	•	•	•	•	•	•
bm	110295	1100-1150		•	•	•	○	○	○	○
bm	110296	1100-1150		○	•	•	○	•	○	○
bm	110298	1100-1150		•	○	•	○	○	○	•
bm	110302	1100-1150		•	•	•	○	○	○	•
bm	110303	1100-1150		○	•	•	○	○	○	○
bm	110309	1100-1150		•	○	•	○	•	•	○
bm	110314	1100-1150		•	○	•	○	•	○	○
bm	110322	1100-1150		•	•	•	○	○	○	○
bm	110323	1100-1150		•	○	•	○	○	○	•
bm	110324	1100-1150		○	○	•	○	•	○	•
bm	110325	1100-1150		○	○	•	○	○	○	•
bm	110331	1100-1150		•	•	•	•	•	○	•
bm	110334	1100-1150		○	○	•	○	○	○	○
bm	110335	1100-1150		•	○	•	○	•	○	•
bm	110344	1100-1150		○	○	•	○	○	○	•
bm	110348	1100-1150		•	○	•	○	○	•	○
bm	110350	1100-1150		•	•	•	○	•	○	○
bm	110355	1100-1150		•	•	•	○	○	○	○
bm	110358	1100-1150		•	○	•	○	•	○	•
bm	110359	1100-1150		•	•	•	○	○	○	○
bm	110362	1100-1150		•	•	•	○	•	○	•
bm	110368	1100-1150		•	•	•	○	•	○	•
bm	110368	1100-1150		•	•	•	○	•	○	•
bm	110375	1100-1150		•	○	•	○	•	•	•
bm	110376	1100-1150		•	○	•	•	•	○	○
bm	110379	1100-1150		•	○	•	○	•	•	•
bm	110389	1100-1150		•	•	•	○	○	○	○
bm	110392	1100-1150		•	•	•	○	○	○	•
bm	110393	1100-1150		•	•	•	○	•	○	○

• = Present, ○ = Absent, - = Unknown, bm = Black Mesa, lhv = Long House Valley

LIT = Lithics, GDS = Groundstone, CER = Ceramics, PIT = Pithouse, MAS = Masonry, KIV = Kiva

(continued on next page)

Table F.1: Analysis Site List (*continued*)

Project Area	Site Number	Date (A.D.)	Range	LIT	GDS	CER	PIT	MAS	KIV	STO
bm	110396	1100-1150		•	○	•	○	•	○	○
bm	110400	1100-1150		•	•	•	○	•	○	○
bm	110401	1100-1150		•	○	•	○	•	○	○
bm	110411	1100-1150		•	•	•	○	•	○	○
bm	110415	1100-1150		•	○	•	○	•	○	○
bm	110417	1100-1150		•	•	•	○	•	•	○
bm	110419	1100-1150		•	•	•	○	•	•	○
bm	110425	1100-1150		•	•	•	○	•	•	•
bm	110429	1100-1150		•	○	•	○	•	•	○
bm	110429	1100-1150		•	○	•	○	•	•	○
bm	110446	1100-1150		•	•	•	○	○	○	•
bm	110452	1100-1150		•	○	•	○	•	○	•
bm	110454	1100-1150		•	○	•	○	•	○	•
bm	110457	1100-1150		•	•	•	○	○	○	○
bm	110462	1100-1150		•	•	•	○	•	•	•
bm	110463	1100-1150		•	○	•	○	•	•	•
bm	110464	1100-1150		•	•	•	○	○	•	•
bm	110469	1100-1150		•	•	•	○	○	•	•
bm	110479	1100-1150		•	•	•	○	•	○	○
bm	110480	1100-1150		•	•	•	○	•	•	○
bm	110483	1100-1150		•	○	•	○	•	○	•
bm	110488	1100-1150		•	•	•	○	•	○	○
bm	110490	1100-1150		•	•	•	○	•	○	○
bm	110501	1100-1150		•	•	•	○	○	○	○
bm	110510	1100-1150		•	○	•	○	•	•	○
bm	110513	1100-1150		•	•	•	○	•	○	○
bm	110515	1100-1150		•	○	•	○	○	○	○
bm	110517	1100-1150		•	•	•	○	•	•	○
bm	110518	1100-1150		•	○	•	○	•	○	○
bm	110524	1100-1150		•	•	•	○	•	○	•
bm	110526	1100-1150		•	•	•	○	○	○	•
bm	110531	1100-1150		•	○	•	○	•	•	○
bm	110548	1100-1150		•	○	•	○	○	○	○
bm	110551	1100-1150		•	•	•	○	•	•	•
bm	110554	1100-1150		•	•	•	○	○	○	•
bm	110560	1100-1150		○	○	•	○	•	○	○
bm	110566	1100-1150		•	○	•	○	○	○	•
bm	110567	1100-1150		•	•	•	○	•	○	•

• = Present, ○ = Absent, — = Unknown, bm = Black Mesa, lhv = Long House Valley

LIT = Lithics, GDS = Groundstone, CER = Ceramics, PIT = Pithouse, MAS = Masonry, KIV = Kiva

(continued on next page)

Table F.1: Analysis Site List (*continued*)

Project Area	Site Number	Date (A.D.)	Range	LIT	GDS	CER	PIT	MAS	KIV	STO
bm	110576	1100-1150		•	•	•	○	•	•	•
bm	110577	1100-1150		•	•	•	•	•	•	•
bm	110580	1100-1150		•	•	•	○	•	○	•
bm	110581	1100-1150		•	○	•	○	○	○	•
bm	110582	1100-1150		•	•	•	○	○	○	•
bm	110591	1100-1150		•	•	•	○	○	○	○
bm	110610	1100-1150		•	○	•	○	•	○	○
bm	110621	1100-1150		•	○	•	○	○	○	•
bm	110623	1100-1150		•	•	•	○	•	○	•
bm	110645	1100-1150		•	○	•	○	○	○	○
bm	110649	1100-1150		•	○	•	○	•	○	○
bm	110654	1100-1150		•	•	•	○	○	○	•
bm	110659	1100-1150		○	○	•	○	•	○	○
bm	110666	1100-1150		•	•	•	○	•	•	•
bm	110681	1100-1150		○	○	•	○	•	○	○
bm	110686	1100-1150		•	•	•	•	•	○	○
bm	110687	1100-1150		•	•	•	•	•	•	•
bm	110702	1100-1150		•	•	•	○	•	•	○
bm	110875	1100-1150		•	—	•	○	•	•	•
bm	110876	1100-1150		•	•	•	○	○	○	•
bm	110878	1100-1150		•	○	•	○	○	○	○
bm	110879	1100-1150		•	•	•	○	○	○	•
bm	110880	1100-1150		•	○	•	○	○	○	○
bm	110883	1100-1150		•	○	•	○	○	○	○
bm	110885	1100-1150		•	—	•	—	•	—	—
bm	110887	1100-1150		•	•	•	○	○	○	○
bm	110890	1100-1150		•	○	•	○	○	○	○
bm	110910	1100-1150		○	○	•	○	○	○	○
bm	110923	1100-1150		•	○	•	○	•	○	○
bm	110930	1100-1150		○	○	•	○	○	○	○
bm	110932	1100-1150		•	○	•	○	•	•	•
bm	110935	1100-1150		○	○	•	○	○	○	○
bm	110938	1100-1150		•	○	•	○	•	•	○
bm	110939	1100-1150		○	○	•	○	○	○	○
bm	110940	1100-1150		○	○	•	○	○	○	○
bm	111001	1100-1150		•	○	•	○	○	○	○
bm	111002	1100-1150		•	○	•	○	○	○	○
bm	111004	1100-1150		•	○	•	○	○	○	○

• = Present, ○ = Absent, — = Unknown, bm = Black Mesa, lhv = Long House Valley

LIT = Lithics, GDS = Groundstone, CER = Ceramics, PIT = Pithouse, MAS = Masonry, KIV = Kiva

(continued on next page)

Table F.1: Analysis Site List (*continued*)

Project Area	Site Number	Date (A.D.)	Range	LIT	GDS	CER	PIT	MAS	KIV	STO
bm	111005	1100-1150		○	○	●	○	○	○	○
bm	111011	1100-1150		●	○	●	○	○	○	○
bm	111025	1100-1150		●	○	●	○	○	○	○
bm	111031	1100-1150		●	○	●	○	○	○	○
bm	111034	1100-1150		○	○	●	○	○	○	○
bm	111049	1100-1150		○	○	●	○	○	○	○
bm	111054	1100-1150		○	○	●	○	○	○	○
bm	111056	1100-1150		○	○	●	○	○	○	○
bm	111060	1100-1150		○	○	●	○	○	○	○
bm	111083	1100-1150		●	○	●	○	○	○	○
bm	111085	1100-1150		○	○	●	○	○	○	○
bm	111086	1100-1150		○	○	●	○	○	○	○
bm	111097	1100-1150		●	○	○	○	○	○	○
bm	111104	1100-1150		●	○	●	○	○	○	○
bm	111109	1100-1150		●	○	●	○	○	○	○
bm	111112	1100-1150		●	○	●	○	○	○	○
bm	111129	1100-1150		●	○	●	○	○	○	○
bm	111138	1100-1150		○	○	●	○	●	○	○
bm	111163	1100-1150		○	○	●	○	○	○	○
bm	111164	1100-1150		●	○	●	○	○	○	○
bm	111165	1100-1150		●	○	●	○	○	○	○
bm	111167	1100-1150		○	○	●	○	○	○	○
bm	111169	1100-1150		●	○	●	○	○	○	●
bm	111173	1100-1150		●	○	●	○	○	○	○
bm	111174	1100-1150		●	○	●	○	●	○	○
bm	111177	1100-1150		○	○	●	○	○	○	○
bm	111189	1100-1150		●	○	●	○	○	○	○
bm	111199	1100-1150		○	○	●	○	○	○	○
bm	111207	1100-1150		●	●	●	○	●	○	○
bm	111209	1100-1150		●	○	●	○	●	○	●
bm	111213	1100-1150		●	●	●	○	●	○	○
bm	111217	1100-1150		○	○	●	○	○	○	○
bm	111220	1100-1150		○	○	●	○	○	○	○
bm	111233	1100-1150		○	○	●	○	○	○	●
bm	111234	1100-1150		○	○	●	○	○	○	○
bm	111236	1100-1150		○	○	●	○	○	○	○
bm	111238	1100-1150		○	○	●	○	○	○	○
bm	111244	1100-1150		●	○	●	○	○	○	○

● = Present, ○ = Absent, — = Unknown, bm = Black Mesa, lhv = Long House Valley

LIT = Lithics, GDS = Groundstone, CER = Ceramics, PIT = Pithouse, MAS = Masonry, KIV = Kiva

(continued on next page)

Table F.1: Analysis Site List (*continued*)

Project Area	Site Number	Date (A.D.)	Range	LIT	GDS	CER	PIT	MAS	KIV	STO
bm	111252	1100-1150		•	•	•	○	○	○	•
bm	111260	1100-1150		○	○	•	○	○	○	○
bm	111265	1100-1150		•	•	•	○	●	○	○
bm	111268	1100-1150		•	○	•	○	○	○	○
bm	111278	1100-1150		•	○	•	○	○	○	○
bm	111279	1100-1150		•	○	•	○	○	○	○
bm	111284	1100-1150		•	○	•	○	○	○	○
bm	111322	1100-1150		•	•	•	○	○	○	○
bm	111330	1100-1150		•	○	•	○	○	○	•
bm	111339	1100-1150		○	○	•	○	○	○	○
bm	111342	1100-1150		•	○	•	○	○	○	○
bm	111351	1100-1150		○	○	•	○	○	○	○
bm	111355	1100-1150		○	○	•	○	○	○	○
bm	111362	1100-1150		•	○	•	○	○	○	○
bm	111363	1100-1150		•	○	•	○	○	○	○
bm	111366	1100-1150		•	○	•	○	○	○	○
bm	111367	1100-1150		•	○	•	○	○	○	○
bm	111381	1100-1150		•	○	•	○	○	○	○
bm	111389	1100-1150		○	○	•	○	○	○	○
bm	111390	1100-1150		○	○	•	○	○	○	○
bm	111500	1100-1150		•	—	•	○	○	○	○
bm	111511	1100-1150		○	○	•	○	○	○	○
bm	112012	1100-1150		•	•	•	○	○	●	●
bm	112013	1100-1150		•	•	•	○	●	●	●
bm	112031	1100-1150		•	•	•	○	○	○	○
bm	112033	1100-1150		•	•	•	○	○	○	●
bm	112035	1100-1150		•	•	•	○	○	○	●
bm	112042	1100-1150		•	•	•	○	○	○	●
bm	112075	1100-1150		•	○	•	○	●	●	●
bm	112112	1100-1150		•	○	•	○	○	●	○
bm	112130	1100-1150		•	•	•	○	●	●	●
bm	112141	1100-1150		•	•	•	○	●	●	●
bm	112148	1100-1150		•	○	•	○	●	●	○
bm	112150	1100-1150		•	○	•	○	●	○	○
bm	112155	1100-1150		•	○	•	○	○	●	○
bm	112156	1100-1150		•	•	•	○	●	●	○
bm	112162	1100-1150		•	○	•	○	●	●	●
bm	112164	1100-1150		•	•	•	○	○	○	●

• = Present, ○ = Absent, — = Unknown, bm = Black Mesa, lhv = Long House Valley

LIT = Lithics, GDS = Groundstone, CER = Ceramics, PIT = Pithouse, MAS = Masonry, KIV = Kiva

(continued on next page)

Table F.1: Analysis Site List (*continued*)

Project Area	Site Number	Date (A.D.)	Range	LIT	GDS	CER	PIT	MAS	KIV	STO
bm	112169	1100-1150		●	●	●	○	○	○	○
bm	112174	1100-1150		●	○	●	○	○	○	○
bm	112178	1100-1150		●	○	●	○	○	●	○
bm	112180	1100-1150		●	○	●	○	○	○	●
bm	112181	1100-1150		●	●	●	○	●	●	●
bm	112186	1100-1150		○	○	●	○	○	○	○
bm	112192	1100-1150		●	○	●	○	○	○	○
bm	113011	1100-1150		○	○	●	○	○	○	○
bm	113020	1100-1150		○	○	●	○	○	○	○
bm	113044	1100-1150		○	○	●	○	●	○	○
bm	113047	1100-1150		○	●	●	○	○	○	●
bm	113064	1100-1150		●	●	●	○	○	○	●
bm	113079	1100-1150		○	○	●	○	○	○	●
bm	113155	1100-1150		●	●	●	○	○	○	○
bm	113169	1100-1150		○	○	●	○	○	○	○
bm	113171	1100-1150		○	●	●	○	○	○	○
bm	113176	1100-1150		○	○	●	○	○	○	○
bm	113180	1100-1150		●	○	●	○	○	○	○
bm	113195	1100-1150		○	○	●	○	○	○	○
bm	113226	1100-1150		○	○	●	○	○	○	○
bm	120203	1100-1150		●	●	●	○	●	○	●
bm	120218	1100-1150		●	●	●	○	●	○	○
bm	120220	1100-1150		●	○	●	○	●	○	○
bm	120231	1100-1150		○	●	●	○	●	●	○
bm	120242	1100-1150		●	●	●	○	●	●	○
bm	120306	1100-1150		●	○	●	○	○	○	○
bm	120309	1100-1150		○	○	●	○	○	○	○
bm	120311	1100-1150		○	●	●	○	○	○	○
bm	120318	1100-1150		○	○	●	○	○	○	○
bm	120332	1100-1150		○	○	●	○	○	○	○
bm	70029	(null)		○	●	●	○	○	○	○
bm	70268	(null)		○	○	●	○	●	○	○
bm	73016	(null)		●	●	●	○	●	○	○
bm	73046	(null)		○	○	●	○	○	○	○
bm	73087	(null)		●	○	●	○	○	○	○
bm	73106	(null)		○	○	●	○	○	○	○
bm	73131	(null)		○	○	●	○	○	○	○
bm	73184	(null)		○	○	●	○	○	○	○

● = Present, ○ = Absent, — = Unknown, bm = Black Mesa, lhv = Long House Valley

LIT = Lithics, GDS = Groundstone, CER = Ceramics, PIT = Pithouse, MAS = Masonry, KIV = Kiva

(continued on next page)

Table F.1: Analysis Site List (*continued*)

Project Area	Site Number	Date (A.D.)	Range	LIT	GDS	CER	PIT	MAS	KIV	STO
bm	73186	(null)		o	o	●	o	o	o	o
bm	73187	(null)		●	o	●	o	o	o	●
bm	73192	(null)		o	o	●	o	o	o	o
bm	111201	(null)		o	o	●	o	o	o	o
bm	112146	(null)		o	●	●	o	●	o	●
bm	113201	(null)		●	●	●	o	o	o	o
bm	113210	(null)		o	●	●	o	o	o	o
bm	113220	(null)		o	o	●	o	o	o	o
bm	70086	(null)		o	●	●	●	●	o	o
bm	70112	(null)		o	—	●	o	●	o	●
bm	70406	(null)		o	o	●	o	o	o	o
bm	70423	(null)		o	o	●	o	o	o	o
bm	71102	(null)		o	o	●	o	o	o	o
bm	71115	(null)		o	o	●	o	o	o	o
bm	71139	(null)		●	o	●	o	o	o	●
bm	71148	(null)		o	o	●	o	o	o	o
bm	72069	(null)		●	o	●	o	●	●	o
bm	72107	(null)		●	●	●	o	●	o	o
bm	73010	(null)		o	o	●	o	o	o	o
bm	73115	(null)		●	o	●	o	o	o	o
bm	73127	(null)		o	o	●	o	o	o	o
bm	73129	(null)		●	o	●	o	●	o	o
bm	73132	(null)		o	o	●	o	o	o	o
bm	73137	(null)		o	o	●	o	o	o	o
bm	73140	(null)		o	o	●	o	o	o	o
bm	73142	(null)		o	o	●	o	o	o	o
bm	73143	(null)		o	o	●	o	o	o	o
bm	73145	(null)		o	o	●	o	o	o	●
bm	73147	(null)		o	o	●	o	o	o	o
bm	73159	(null)		o	o	●	o	o	o	o
bm	73160	(null)		o	o	●	o	o	o	o
bm	73160	(null)		o	o	●	o	o	o	o
bm	73172	(null)		o	o	●	o	o	o	o
bm	73177	(null)		o	o	●	o	o	o	o
bm	73179	(null)		o	o	●	o	o	o	o
bm	73180	(null)		o	o	●	o	o	o	o
bm	73181	(null)		o	o	●	o	o	o	o
bm	73183	(null)		o	o	●	o	o	o	o

● = Present, o = Absent, — = Unknown, bm = Black Mesa, lhv = Long House Valley

LIT = Lithics, GDS = Groundstone, CER = Ceramics, PIT = Pithouse, MAS = Masonry, KIV = Kiva

(continued on next page)

Table F.1: Analysis Site List (*continued*)

Project Area	Site Number	Date (A.D.)	Range	LIT	GDS	CER	PIT	MAS	KIV	STO
bm	73197	(null)		o	o	●	o	o	o	o
bm	110210	(null)		●	o	●	o	o	o	o
bm	110223	(null)		o	o	●	o	o	o	o
bm	110821	(null)		●	o	●	o	o	o	o
bm	110853	(null)		o	o	●	o	o	o	o
bm	110858	(null)		o	o	●	o	o	o	o
bm	110884	(null)		o	●	●	o	●	o	o
bm	110902	(null)		o	o	●	o	o	o	o
bm	110907	(null)		o	o	●	o	o	o	o
bm	110931	(null)		●	●	●	o	●	●	o
bm	111007	(null)		o	o	o	o	o	o	o
bm	111036	(null)		o	o	●	o	o	o	●
bm	111066	(null)		o	o	●	o	o	o	o
bm	111087	(null)		o	o	●	o	o	o	o
bm	111096	(null)		o	o	●	o	o	o	o
bm	111099	(null)		o	—	●	—	o	—	—
bm	111102	(null)		o	o	●	o	o	o	o
bm	111114	(null)		o	o	●	o	o	o	o
bm	111141	(null)		o	o	●	o	o	o	o
bm	111155	(null)		o	o	●	o	o	o	o
bm	111159	(null)		o	o	●	o	o	o	o
bm	111160	(null)		o	o	●	o	o	o	o
bm	111166	(null)		●	o	●	o	o	o	o
bm	111175	(null)		o	o	●	o	o	o	o
bm	111178	(null)		o	o	●	o	o	o	o
bm	111185	(null)		●	o	●	o	o	o	●
bm	111221	(null)		o	o	●	o	o	o	●
bm	111225	(null)		o	o	●	o	o	o	o
bm	111229	(null)		o	o	●	o	o	o	o
bm	111231	(null)		o	o	●	o	o	o	o
bm	111235	(null)		o	o	●	o	o	o	o
bm	111250	(null)		●	o	●	o	o	o	o
bm	111257	(null)		●	o	●	o	o	o	o
bm	111287	(null)		o	o	●	o	●	o	●
bm	111299	(null)		●	o	●	o	o	o	●
bm	111325	(null)		o	o	●	o	o	o	o
bm	111335	(null)		●	o	●	o	o	o	o
bm	111336	(null)		o	o	●	o	o	o	●

● = Present, o = Absent, — = Unknown, bm = Black Mesa, lhv = Long House Valley

LIT = Lithics, GDS = Groundstone, CER = Ceramics, PIT = Pithouse, MAS = Masonry, KIV = Kiva

(continued on next page)

Table F.1: Analysis Site List (*continued*)

Project Area	Site Number	Date (A.D.)	Range	LIT	GDS	CER	PIT	MAS	KIV	STO
bm	111344	(null)		o	o	●	o	o	o	o
bm	111350	(null)		o	o	●	o	o	o	o
bm	111353	(null)		o	o	●	o	o	o	o
bm	111356	(null)		●	o	●	o	o	o	o
bm	111365	(null)		●	o	●	o	o	o	o
bm	111369	(null)		o	o	●	o	o	o	o
bm	111382	(null)		o	o	●	o	o	o	o
bm	111385	(null)		o	o	●	o	o	o	o
bm	111394	(null)		o	o	●	o	o	o	o
bm	111397	(null)		●	o	●	o	o	o	o
bm	111508	(null)		●	—	—	o	o	o	o
bm	111509	(null)		o	o	●	o	o	o	o
bm	111512	(null)		o	o	●	o	o	o	o
bm	112066	(null)		●	o	●	o	o	o	●
bm	112139	(null)		●	●	●	o	●	●	●
bm	112140	(null)		o	●	●	o	o	o	o
bm	112157	(null)		●	●	●	●	o	o	o
bm	112165	(null)		●	o	●	o	●	o	o
bm	112189	(null)		o	●	●	o	o	o	o
bm	113009	(null)		o	o	●	o	o	o	o
bm	113010	(null)		o	o	●	o	o	o	●
bm	113014	(null)		o	o	●	o	o	o	o
bm	113015	(null)		o	o	●	o	o	o	o
bm	113016	(null)		o	o	●	o	o	o	o
bm	113024	(null)		o	o	●	o	o	o	o
bm	113025	(null)		o	o	●	o	o	o	o
bm	113027	(null)		o	o	●	o	o	o	o
bm	113028	(null)		o	o	●	o	o	o	o
bm	113033	(null)		o	o	●	o	o	o	o
bm	113037	(null)		o	o	●	o	o	o	o
bm	113038	(null)		o	o	●	o	●	o	o
bm	113039	(null)		o	o	●	o	o	o	o
bm	113045	(null)		o	o	●	o	o	o	o
bm	113048	(null)		o	o	●	o	o	o	o
bm	113067	(null)		o	o	●	o	o	o	o
bm	113069	(null)		o	o	●	o	o	o	o
bm	113072	(null)		o	o	●	o	o	o	o
bm	113092	(null)		o	●	●	o	o	o	●

● = Present, o = Absent, — = Unknown, bm = Black Mesa, lhv = Long House Valley

LIT = Lithics, GDS = Groundstone, CER = Ceramics, PIT = Pithouse, MAS = Masonry, KIV = Kiva

(continued on next page)

Table F.1: Analysis Site List (*continued*)

Project Area	Site Number	Date (A.D.)	Range	LIT	GDS	CER	PIT	MAS	KIV	STO
bm	113149	(null)		○	○	●	○	○	○	○
bm	113166	(null)		●	●	●	○	○	○	●
bm	113168	(null)		○	○	●	○	○	○	○
bm	113199	(null)		○	○	●	○	○	○	○
bm	113202	(null)		●	○	●	○	○	○	○
bm	113203	(null)		○	○	●	○	○	○	○
bm	113204	(null)		○	○	●	○	○	○	○
bm	113208	(null)		●	○	●	○	○	○	○
bm	113209	(null)		●	○	●	○	○	○	○
bm	113211	(null)		○	○	●	○	○	○	○
bm	113211	(null)		○	○	●	○	○	○	●
bm	113214	(null)		○	○	●	○	○	○	○
bm	113216	(null)		○	○	●	○	○	○	○
bm	113217	(null)		○	○	●	○	○	○	○
bm	113217	(null)		○	●	○	○	●	○	○
bm	113219	(null)		○	○	●	○	○	○	○
bm	113221	(null)		○	○	●	○	○	○	○
bm	113222	(null)		●	●	●	○	○	○	○
bm	113223	(null)		○	○	●	○	○	○	○
bm	113225	(null)		○	○	●	○	○	○	○
bm	120251	(null)		○	○	●	○	○	○	○
bm	120301	(null)		○	○	●	○	○	○	○
bm	120313	(null)		○	○	●	○	○	○	○
bm	111354	(null)		●	○	●	○	○	○	●
bm	112039	(null)		●	○	●	○	○	○	○
bm	112136	(null)		●	○	○	○	○	○	○
bm	113050	(null)		●	○	○	○	○	○	○
bm	113206	(null)		●	○	○	○	○	○	○
bm	70136	(null)		●	—	●	○	○	○	○
bm	70262	(null)		●	●	●	●	●	●	○
bm	70303	(null)		●	●	●	○	●	○	○
bm	70707	(null)		●	●	●	○	●	○	●
bm	71108	(null)		●	○	●	○	○	○	○
bm	72094	(null)		●	●	●	○	○	○	○
bm	72103	(null)		●	●	●	○	●	○	○
bm	73003	(null)		●	○	●	○	○	○	○
bm	73003	(null)		●	○	●	○	○	○	○
bm	110202	(null)		●	○	●	○	●	○	●

● = Present, ○ = Absent, — = Unknown, bm = Black Mesa, lhv = Long House Valley

LIT = Lithics, GDS = Groundstone, CER = Ceramics, PIT = Pithouse, MAS = Masonry, KIV = Kiva

(continued on next page)

Table F.1: Analysis Site List (*continued*)

Project Area	Site Number	Date (A.D.)	Range	LIT	GDS	CER	PIT	MAS	KIV	STO
bm	110218	(null)		●	●	●	○	●	○	●
bm	110942	(null)		●	—	●	○	●	○	●
bm	111016	(null)		○	○	●	○	○	○	○
bm	112011	(null)		●	○	●	○	○	○	○
bm	112037	(null)		●	●	●	●	○	○	●
bm	112159	(null)		●	●	●	●	○	○	○
bm	70106	(null)		●	●	○	○	○	○	○
bm	70107	(null)		●	●	○	○	○	○	○
bm	70128	(null)		●	○	○	○	○	○	○
bm	70145	(null)		●	○	○	○	○	○	○
bm	70444	(null)		○	○	○	○	○	○	○
bm	70538	(null)		○	○	○	○	○	●	○
bm	70539	(null)		○	○	○	●	○	○	○
bm	73006	(null)		●	○	○	○	○	○	○
bm	73200	(null)		●	○	○	○	○	○	○
bm	110945	(null)		○	○	○	○	○	○	○
bm	111139	(null)		○	○	○	○	●	○	○
bm	111246	(null)		○	○	○	○	○	○	○
bm	113006	(null)		●	○	○	○	○	○	○
bm	113007	(null)		●	○	○	○	○	○	○
bm	113018	(null)		○	○	○	○	●	○	○
bm	113043	(null)		○	○	○	○	○	○	○
bm	113051	(null)		○	○	○	○	○	○	○
bm	113087	(null)		○	○	○	○	○	○	○
bm	113102	(null)		○	○	○	○	○	○	○
bm	113190	(null)		○	○	○	○	○	○	○
bm	113191	(null)		○	●	○	●	○	○	○
bm	113213	(null)		○	○	○	○	○	○	○
bm	113224	(null)		○	●	○	○	○	○	○
bm	113227	(null)		○	○	○	○	○	○	●
bm	115001	(null)		●	—	○	○	○	○	○
bm	70038	(null)		○	●	●	○	○	○	○
bm	70046	(null)		○	○	●	○	○	○	○
bm	70049	(null)		○	○	●	○	○	○	○
bm	70091	(null)		●	○	●	●	○	○	○
bm	70104	(null)		●	—	●	○	●	●	○
bm	70113	(null)		○	○	●	○	○	○	○
bm	70115	(null)		○	○	●	○	○	○	○

● = Present, ○ = Absent, — = Unknown, bm = Black Mesa, lhv = Long House Valley

LIT = Lithics, GDS = Groundstone, CER = Ceramics, PIT = Pithouse, MAS = Masonry, KIV = Kiva

(continued on next page)

Table F.1: Analysis Site List (*continued*)

Project Area	Site Number	Date (A.D.)	Range	LIT	GDS	CER	PIT	MAS	KIV	STO
bm	70125	(null)		o	o	●	o	o	o	o
bm	70129	(null)		o	o	●	o	●	o	o
bm	70452	(null)		●	o	●	o	o	o	o
bm	70708	(null)		●	o	—	o	●	o	o
bm	70723	(null)		o	o	●	o	o	o	o
bm	71105	(null)		o	o	●	o	o	o	o
bm	71112	(null)		o	o	●	o	o	o	o
bm	71116	(null)		o	o	●	o	o	o	o
bm	71129	(null)		o	o	o	o	o	o	●
bm	71140	(null)		●	o	●	o	●	o	o
bm	73015	(null)		o	o	●	o	o	o	o
bm	73019	(null)		o	o	●	o	o	o	●
bm	73020	(null)		o	o	●	o	o	o	o
bm	73027	(null)		o	●	●	o	o	o	o
bm	73040	(null)		o	o	●	o	o	o	●
bm	73052	(null)		o	o	●	o	o	o	o
bm	73158	(null)		o	o	●	o	o	o	o
bm	73158	(null)		o	o	●	o	o	o	o
bm	73199	(null)		●	●	●	o	o	o	o
bm	110055	(null)		o	●	●	o	o	o	o
bm	110689	(null)		●	●	●	o	o	o	●
bm	110867	(null)		o	o	●	o	o	o	o
bm	110882	(null)		●	●	●	o	o	o	o
bm	110947	(null)		o	o	●	o	o	o	●
bm	111073	(null)		o	o	●	o	o	o	o
bm	111078	(null)		o	o	●	o	o	o	o
bm	111118	(null)		o	o	●	o	o	o	o
bm	111137	(null)		o	o	●	o	●	o	●
bm	111140	(null)		o	o	●	o	o	o	o
bm	111197	(null)		●	●	●	o	●	o	●
bm	111200	(null)		o	o	●	o	o	o	o
bm	111259	(null)		o	o	●	o	o	o	o
bm	111293	(null)		o	o	●	o	o	o	o
bm	111310	(null)		●	o	●	o	o	o	●
bm	111321	(null)		●	o	●	o	o	o	o
bm	111323	(null)		o	o	●	o	o	o	●
bm	111343	(null)		●	o	●	o	o	o	o
bm	112131	(null)		●	o	●	o	o	o	o

● = Present, o = Absent, — = Unknown, bm = Black Mesa, lhv = Long House Valley

LIT = Lithics, GDS = Groundstone, CER = Ceramics, PIT = Pithouse, MAS = Masonry, KIV = Kiva

(continued on next page)

Table F.1: Analysis Site List (*continued*)

Project Area	Site Number	Date (A.D.)	Range	LIT	GDS	CER	PIT	MAS	KIV	STO
bm	112182	(null)		●	○	●	○	○	○	○
bm	112188	(null)		●	●	●	○	○	○	○
bm	113008	(null)		○	●	○	○	○	○	○
bm	113019	(null)		○	○	●	○	○	○	○
bm	113026	(null)		○	○	●	○	○	○	○
bm	113046	(null)		○	●	○	○	○	○	○
bm	113060	(null)		●	○	●	○	○	○	○
bm	113073	(null)		●	○	○	○	○	○	○
bm	113077	(null)		○	●	○	○	○	○	○
bm	113084	(null)		○	○	●	○	○	○	○
bm	113134	(null)		○	○	●	○	○	○	○
bm	113151	(null)		○	○	○	○	●	○	○
bm	113157	(null)		○	○	●	○	○	○	○
bm	113165	(null)		●	○	●	○	○	○	●
bm	113177	(null)		○	○	○	○	○	○	○
bm	113178	(null)		○	○	○	○	○	○	○
bm	113181	(null)		○	○	○	○	○	○	○
bm	113193	(null)		○	○	●	○	○	○	○
bm	113198	(null)		●	○	●	○	○	○	○
bm	113200	(null)		○	○	●	○	○	○	○
bm	120305	(null)		○	○	●	○	○	○	○
bm	112191	(null)		●	●	○	○	○	○	○
lhv	2000	1000-1100		○	●	●	—	○	○	○
lhv	2001	1050-1150		●	●	●	—	●	○	○
lhv	2002	1200-1350		●	●	●	—	○	○	○
lhv	2003	1050-1150		●	●	●	●	●	○	●
lhv	2004	1050-1150		●	—	●	—	●	○	○
lhv	2005	1000-1300		●	●	●	—	●	●	○
lhv	2006	1175-1300		●	—	●	—	●	○	○
lhv	2007	1250-1300		●	—	●	—	●	—	○
lhv	2008	1225-1300		●	—	●	○	●	—	○
lhv	2009	1225-1300		●	—	●	○	●	—	○
lhv	2010	1000-1150		●	●	●	—	○	○	○
lhv	2011	1250-1300		●	●	●	○	●	—	○
lhv	2012	1150-1300		●	●	●	—	●	●	●
lhv	2013	1050-1150		●	○	●	○	●	○	○
lhv	2014	1150-1300		●	●	●	○	●	●	○
lhv	2015	850-1000		●	●	●	—	—	○	—

● = Present, ○ = Absent, — = Unknown, bm = Black Mesa, lhv = Long House Valley

LIT = Lithics, GDS = Groundstone, CER = Ceramics, PIT = Pithouse, MAS = Masonry, KIV = Kiva

(continued on next page)

Table F.1: Analysis Site List (*continued*)

Project Area	Site Number	Date (A.D.)	Range	LIT	GDS	CER	PIT	MAS	KIV	STO
Ihv	2016	1150-1300		●	●	●	○	●	●	○
Ihv	2017	1150-1200		●	●	●	○	●	○	○
Ihv	2018	1200-1250		●	○	●	○	○	○	○
Ihv	2019	800-1000		●	—	●	●	○	○	—
Ihv	2020	1200-1250		●	—	●	—	●	●	○
Ihv	2021	850-1250		●	●	●	○	●	○	○
Ihv	2022	1100-1300		○	○	○	○	○	○	○
Ihv	2023	1200-1250		●	●	●	○	●	●	●
Ihv	2024	1200-1300		●	—	●	○	●	○	○
Ihv	2025	1050-1150		●	○	●	○	○	○	○
Ihv	2026	1075-1300		●	●	●	○	●	—	○
Ihv	2027	1075-1300		●	●	●	○	●	●	○
Ihv	2028	1200-1250		●	—	●	○	●	○	○
Ihv	2029	1225-1300		●	—	●	—	●	●	○
Ihv	2030	1250-1300		●	—	●	○	●	○	○
Ihv	2031	1000-1150		●	—	●	—	●	○	○
Ihv	2032	850-1200		●	●	●	—	●	●	○
Ihv	2033	1050-1150		●	—	●	—	●	○	○
Ihv	2034	1200-1300		●	—	●	—	●	○	○
Ihv	2035	850-950		●	—	●	—	●	○	○
Ihv	2036	1050-1150		●	—	●	—	●	○	○
Ihv	2037	1150-1225		●	—	●	—	○	○	○
Ihv	2038	1200-1300		●	○	●	—	●	●	○
Ihv	2039	0-650		●	●	○	—	○	○	●
Ihv	2040	1225-1300		○	○	●	○	○	○	○
Ihv	2041	1150-1300		●	—	●	○	○	○	○
Ihv	2042	1200-1300		●	○	●	—	●	●	○
Ihv	2043	1250-1300		●	—	●	—	●	●	○
Ihv	2044	1050-1150		●	●	●	—	●	●	○
Ihv	2045	1150-1225		●	—	●	—	●	○	○
Ihv	2046	1200-1250		●	—	●	—	●	—	○
Ihv	2047	1050-1150		●	—	●	—	●	—	○
Ihv	2048	1050-1150		●	●	●	—	●	—	○
Ihv	2049	1250-1300		●	—	●	—	●	●	○
Ihv	2050	1100-1300		○	○	○	○	○	○	○
Ihv	2051	1000-1150		○	—	●	—	●	○	○
Ihv	2052	950-1125		○	○	●	○	●	○	○
Ihv	2053	900-1025		●	—	●	●	○	○	●

● = Present, ○ = Absent, — = Unknown, bm = Black Mesa, Ihv = Long House Valley

LIT = Lithics, GDS = Groundstone, CER = Ceramics, PIT = Pithouse, MAS = Masonry, KIV = Kiva

(continued on next page)

Table F.1: Analysis Site List (*continued*)

Project Area	Site Number	Date (A.D.)	Range	LIT	GDS	CER	PIT	MAS	KIV	STO
Ihv	2054	1150-1200		•	—	•	—	•	○	○
Ihv	2055	1150-1250		•	—	•	—	○	—	•
Ihv	2056	1150-1250		○	○	•	○	•	○	○
Ihv	2057	1050-1150		•	—	•	•	•	○	○
Ihv	2058	1200-1270		•	○	•	○	•	•	○
Ihv	2059	1050-1150		•	—	•	○	•	○	○
Ihv	2060	1200-1300		•	•	•	—	•	•	○
Ihv	2061	1150-1250		•	—	•	—	•	—	○
Ihv	2062	850-1050		•	—	•	—	○	○	○
Ihv	2063	1100-1300		•	—	•	○	○	○	•
Ihv	2064	1050-1250		○	○	•	—	•	•	○
Ihv	2065	1150-1250		•	—	•	—	•	○	○
Ihv	2066	900-1100		•	—	•	—	•	○	○
Ihv	2067	1000-1225		•	○	•	—	•	○	○
Ihv	2068	1000-1250		•	•	•	—	•	•	○
Ihv	2069	1150-1250		•	—	•	—	•	—	○
Ihv	2070	1150-1250		•	—	•	—	•	—	○
Ihv	2071	1200-1250		•	—	•	○	•	○	○
Ihv	2072	-1550-0		•	•	○	○	○	○	○
Ihv	2073	1100-1300		○	○	•	○	•	○	○
Ihv	2074	900-1050		○	○	•	○	•	○	○
Ihv	2075	850-1000		•	•	•	—	○	○	○
Ihv	2076	1200-1250		•	•	•	—	○	○	○
Ihv	2077	1200-1250		•	○	•	○	○	○	○
Ihv	2078	1250-1300		•	—	•	—	•	—	○
Ihv	2079	1250-1300		•	—	•	○	•	•	○
Ihv	2080	1075-1200		•	—	•	—	•	—	○
Ihv	2081	1050-1150		•	—	•	—	○	○	○
Ihv	2082	1075-1300		•	—	•	—	•	○	○
Ihv	2083	1150-1300		•	—	•	—	•	—	○
Ihv	2084	1050-1200		•	○	•	—	•	—	○
Ihv	2085	850-1300		○	○	•	—	○	○	○
Ihv	2086	1250-1300		•	•	•	—	—	—	○
Ihv	2087	-1550-0		•	○	•	•	○	○	○
Ihv	2088	1000-1125		•	—	•	○	•	○	○
Ihv	2089	850-1300		•	—	•	○	○	○	○
Ihv	2090	600-700		•	○	•	○	○	○	○
Ihv	2091	1075-1200		•	—	•	○	○	○	•

• = Present, ○ = Absent, — = Unknown, bm = Black Mesa, Ihv = Long House Valley

LIT = Lithics, GDS = Groundstone, CER = Ceramics, PIT = Pithouse, MAS = Masonry, KIV = Kiva

(continued on next page)

Table F.1: Analysis Site List (*continued*)

Project Area	Site Number	Date (A.D.)	Range	LIT	GDS	CER	PIT	MAS	KIV	STO
Ihv	2092	1000-1050		•	—	•	○	•	○	○
Ihv	2093	850-1300		○	○	•	○	○	○	○
Ihv	2094	1025-1225		•	—	•	—	•	—	○
Ihv	2095	850-1075		•	—	•	—	○	○	○
Ihv	2096	1200-1250		•	—	•	—	•	—	○
Ihv	2097	1000-1125		•	—	•	—	•	○	○
Ihv	2098	1050-1250		•	○	•	—	•	—	○
Ihv	2099	1250-1300		•	○	•	○	○	○	○
Ihv	2100	1000-1300		○	○	•	○	○	○	○
Ihv	2101	1050-1300		•	—	•	—	•	•	○
Ihv	2102	1150-1250		•	—	•	○	•	○	○
Ihv	2103	1225-1300		•	—	•	○	•	—	○
Ihv	2104	1050-1150		•	—	•	○	○	○	○
Ihv	2105	1250-1300		•	—	•	○	•	•	○
Ihv	2106	1075-1150		•	—	•	—	○	○	○
Ihv	2107	1050-1250		•	○	•	—	○	○	○
Ihv	2108	600-950		•	—	•	—	○	○	—
Ihv	2109	600-700		•	—	•	—	○	○	—
Ihv	2110	1075-1150		•	—	•	—	○	○	○
Ihv	2111	1200-1250		•	○	•	○	○	○	○
Ihv	2112	1000-1250		•	—	•	○	○	○	○
Ihv	2113	1000-1250		•	○	•	○	•	•	○
Ihv	2114	600-1300		○	○	•	○	○	○	•
Ihv	2115	1100-1300		•	•	•	—	•	•	○
Ihv	2116	1075-1150		•	—	•	○	○	○	•
Ihv	2117	1050-1150		○	○	•	○	○	○	○
Ihv	2118	1150-1250		•	—	•	○	•	•	○
Ihv	2119	400-1300		○	○	○	○	○	○	○
Ihv	2120	1000-1150		•	•	•	—	—	—	—
Ihv	2121	1150-1300		•	•	•	—	•	—	○
Ihv	2122	0-1300		•	○	○	○	○	○	○
Ihv	2123	600-1300		○	○	○	○	○	○	○
Ihv	2124	1150-1250		•	•	•	—	•	—	—
Ihv	2125	900-1250		•	•	•	—	○	○	○
Ihv	2126	1075-1250		•	○	•	○	○	○	○
Ihv	2127	1150-1250		•	—	•	○	○	○	○
Ihv	2128	1075-1250		•	•	•	—	•	•	○
Ihv	2129	400-600		•	○	○	•	○	○	•

• = Present, ○ = Absent, — = Unknown, bm = Black Mesa, Ihv = Long House Valley

LIT = Lithics, GDS = Groundstone, CER = Ceramics, PIT = Pithouse, MAS = Masonry, KIV = Kiva

(continued on next page)

Table F.1: Analysis Site List (*continued*)

Project Area	Site Number	Date (A.D.)	Range	LIT	GDS	CER	PIT	MAS	KIV	STO
Ihv	2130	1050-1150		o	o	•	o	o	o	o
Ihv	2131	1000-1100		•	o	•	o	o	o	o
Ihv	2132	400-1300		o	o	o	o	o	o	o
Ihv	2133	400-1300		o	o	o	o	o	o	o
Ihv	2134	950-1150		•	o	•	—	•	o	o
Ihv	2135	1000-1075		•	o	•	o	o	o	o
Ihv	2136	1250-1300		•	•	•	—	—	—	—
Ihv	2137	1200-1250		o	—	•	o	o	o	o
Ihv	2138	1250-1300		o	o	•	—	o	o	o
Ihv	2139	1225-1270		•	o	•	—	o	o	o
Ihv	2140	0-600		•	o	•	o	o	o	•
Ihv	2141	1225-1300		•	o	•	o	o	o	o
Ihv	2142	1050-1250		o	—	•	—	o	o	o
Ihv	2143	0-600		•	•	o	o	o	o	•
Ihv	2144	0-600		•	o	o	o	o	o	•
Ihv	2145	600-850		•	—	•	o	o	o	•
Ihv	2146	1100-1300		•	•	•	o	•	•	o
Ihv	2147	0-600		•	o	o	o	o	o	•
Ihv	2148	0-600		•	—	o	o	o	o	•
Ihv	2149	50-450		o	•	o	o	o	o	•
Ihv	2150	0-600		•	o	o	o	o	o	o
Ihv	2151	0-600		•	•	o	o	o	o	•
Ihv	2152	1150-1300		•	•	•	o	•	o	o
Ihv	2153	1100-1300		•	•	•	o	o	o	o
Ihv	2154	1050-1150		•	—	•	—	—	o	—
Ihv	2155	0-600		•	•	o	o	o	o	o
Ihv	2156	550-850		•	—	•	—	o	o	—
Ihv	2157	600-900		•	•	•	o	o	o	o
Ihv	2158	1150-1225		•	—	•	o	o	o	o
Ihv	2159	1050-1150		•	o	•	o	•	o	o
Ihv	2160	1100-1270		o	o	•	—	•	—	o
Ihv	2161	0-650		•	o	o	o	o	o	o
Ihv	2162	0-600		•	—	o	o	o	o	•
Ihv	2163	850-1000		•	•	•	—	•	—	o
Ihv	2164	600-700		•	o	•	—	o	o	•
Ihv	2165	0-700		•	—	•	—	o	o	•
Ihv	2166	850-1000		•	•	•	—	•	—	o
Ihv	2167	0-600		•	—	o	—	o	o	•

• = Present, o = Absent, — = Unknown, bm = Black Mesa, Ihv = Long House Valley

LIT = Lithics, GDS = Groundstone, CER = Ceramics, PIT = Pithouse, MAS = Masonry, KIV = Kiva

(continued on next page)

Table F.1: Analysis Site List (*continued*)

Project Area	Site Number	Date (A.D.)	Range	LIT	GDS	CER	PIT	MAS	KIV	STO
Ihv	2168	1000-1100		•	○	•	○	○	○	○
Ihv	2169	900-1000		•	—	•	○	○	○	○
Ihv	2170	1250-1300		•	•	•	—	•	•	○
Ihv	2171	1250-1300		•	○	•	—	•	○	○
Ihv	2172	1150-1300		•	•	•	—	•	○	○
Ihv	2173	1075-1300		•	•	•	—	•	○	○
Ihv	2174	1250-1300		○	○	•	—	•	—	○
Ihv	2175	1000-1300		•	—	•	—	○	○	○
Ihv	2176	1250-1300		•	—	•	—	•	—	○
Ihv	2177	900-1300		•	•	•	—	•	•	○
Ihv	2178	900-1000		•	○	•	—	○	○	•
Ihv	2179	950-1150		•	•	•	—	○	○	○
Ihv	2180	1250-1300		•	•	•	—	•	•	○
Ihv	2181	1250-1300		•	•	•	—	•	—	○
Ihv	2182	950-1300		•	—	•	○	○	○	○
Ihv	2183	600-700		•	○	•	○	○	○	○
Ihv	2184	900-1300		•	○	•	○	○	○	○
Ihv	2185	0-600		•	•	○	○	○	○	○
Ihv	2186	600-700		•	○	○	○	○	○	○
Ihv	2187	600-700		•	○	•	○	○	○	•
Ihv	2188	1000-1100		•	—	•	○	•	○	○
Ihv	2189	600-900		•	—	•	—	○	○	○
Ihv	2190	0-600		•	○	○	○	○	○	○
Ihv	2191	1000-1125		•	○	•	—	•	•	○
Ihv	2192	0-600		•	○	○	○	○	○	○
Ihv	2193	600-800		•	○	•	○	○	○	•
Ihv	2194	1000-1150		•	—	•	—	○	○	○
Ihv	2195	1150-1300		•	—	•	—	○	○	○
Ihv	2196	1050-1150		•	—	•	—	•	•	○
Ihv	2197	0-600		•	○	○	○	○	○	•
Ihv	2198	1025-1150		•	—	•	—	•	○	○
Ihv	2199	1000-1050		•	○	○	○	○	○	○
Ihv	2200	1000-1150		•	—	•	—	•	•	○
Ihv	2201	1075-1300		•	—	•	—	•	—	○
Ihv	2202	1200-1300		•	○	•	•	•	○	•
Ihv	2203	1000-1150		•	—	•	—	○	○	○
Ihv	2204	900-1100		•	•	•	—	•	○	○
Ihv	2205	850-1100		•	○	•	—	•	—	○

• = Present, ○ = Absent, — = Unknown, bm = Black Mesa, Ihv = Long House Valley

LIT = Lithics, GDS = Groundstone, CER = Ceramics, PIT = Pithouse, MAS = Masonry, KIV = Kiva

(continued on next page)

Table F.1: Analysis Site List (*continued*)

Project Area	Site Number	Date (A.D.)	Range	LIT	GDS	CER	PIT	MAS	KIV	STO
Ihv	2206	1050-1150		o	o	•	o	o	o	o
Ihv	2207	1050-1225		•	•	•	—	o	o	o
Ihv	2208	800-1000		•	—	•	—	o	o	o
Ihv	2209	600-700		•	—	•	—	o	o	o
Ihv	2210	600-700		•	o	•	o	o	o	o
Ihv	2211	1000-1300		•	—	•	—	•	—	o
Ihv	2212	0-600		•	•	o	—	o	o	o
Ihv	2213	900-1050		•	•	•	—	•	—	o
Ihv	2214	0-600		•	—	o	o	o	o	o
Ihv	2215	600-700		•	o	•	—	o	o	•
Ihv	2216	1050-1150		•	o	•	—	o	o	o
Ihv	2217	0-600		•	o	o	o	o	o	o
Ihv	2218	1000-1150		•	o	•	—	•	—	o
Ihv	2219	1000-1100		•	—	•	—	•	•	o
Ihv	2220	900-1050		•	—	•	—	—	—	o
Ihv	2221	850-1000		•	o	•	—	o	o	o
Ihv	2222	1050-1150		•	—	•	—	•	—	o
Ihv	2223	1000-1150		o	o	•	—	o	o	o
Ihv	2224	0-600		•	•	o	—	o	o	o
Ihv	2225	850-1000		•	—	•	•	o	o	•
Ihv	2226	1100-1300		•	•	•	—	o	o	o
Ihv	2227	850-1000		•	o	•	—	o	o	—
Ihv	2228	950-1025		•	—	•	—	o	o	o
Ihv	2229	1150-1250		•	o	•	—	o	o	o
Ihv	2230	600-700		•	•	•	—	o	o	o
Ihv	2231	0-600		•	o	o	o	o	o	•
Ihv	2232	1050-1150		•	—	•	—	•	o	•
Ihv	2233	1050-1150		•	o	•	—	•	o	o
Ihv	2234	1000-1150		•	—	•	—	o	o	•
Ihv	2235	1050-1150		•	o	•	—	•	—	o
Ihv	2236	1050-1150		•	o	•	—	o	o	o
Ihv	2237	0-600		•	o	o	o	o	o	o
Ihv	2238	1150-1200		•	—	•	—	o	o	o
Ihv	2239	600-700		•	o	•	o	o	o	o
Ihv	2240	1000-1200		•	•	•	—	•	•	o
Ihv	2241	0-600		•	o	o	o	o	o	•
Ihv	2242	950-1150		•	—	•	•	o	o	o
Ihv	2243	0-600		•	o	o	o	o	o	o

• = Present, o = Absent, — = Unknown, bm = Black Mesa, Ihv = Long House Valley

LIT = Lithics, GDS = Groundstone, CER = Ceramics, PIT = Pithouse, MAS = Masonry, KIV = Kiva

(continued on next page)

Table F.1: Analysis Site List (*continued*)

Project Area	Site Number	Date (A.D.)	Range	LIT	GDS	CER	PIT	MAS	KIV	STO
Ihv	2244	950-1150		●	○	●	—	○	○	○
Ihv	2245	900-1050		●	○	○	○	○	○	○
Ihv	2246	1050-1150		●	○	○	○	○	○	○
Ihv	2247	950-1125		●	○	●	—	○	○	○
Ihv	2248	1050-1150		●	○	●	○	○	○	○
Ihv	2249	1050-1150		●	—	●	—	●	●	○
Ihv	2250	1200-1270		●	—	●	○	●	○	○
Ihv	2251	1050-1250		●	○	●	○	○	○	○
Ihv	2252	1050-1150		○	—	●	—	●	—	○
Ihv	2253	1000-1175		●	●	●	●	●	●	○
Ihv	2254	1050-1175		●	●	●	—	●	●	○
Ihv	2255	1050-1150		○	○	●	—	●	○	○
Ihv	2256	1050-1300		○	—	●	—	●	○	○
Ihv	2257	800-1050		●	—	●	—	●	○	○
Ihv	2258	1050-1100		○	○	●	—	○	○	○
Ihv	2259	1050-1200		●	—	●	—	●	—	○
Ihv	2260	1050-1150		○	—	●	—	●	○	○
Ihv	2261	0-600		●	○	●	—	○	○	○
Ihv	2262	0-600		●	—	○	○	○	○	○
Ihv	2263	1200-1300		●	○	●	—	●	○	○
Ihv	2264	1200-1250		●	○	●	—	○	○	●
Ihv	2265	900-1000		●	○	●	●	○	○	●
Ihv	2266	600-900		●	○	●	—	●	○	○
Ihv	2267	850-950		○	○	●	●	○	○	○
Ihv	2268	900-1050		●	—	●	●	●	○	○
Ihv	2269	1150-1200		○	○	●	○	○	○	○
Ihv	2270	900-1075		●	—	●	●	○	—	●
Ihv	2271	0-600		●	●	○	○	○	○	●
Ihv	2272	900-1000		●	—	●	●	○	○	○
Ihv	2273	600-700		●	○	●	—	○	○	○
Ihv	2274	600-700		●	—	●	—	○	○	●
Ihv	2275	950-1050		●	—	●	●	●	●	○
Ihv	2276	1050-1150		●	●	●	—	●	—	○
Ihv	2277	1050-1150		●	—	●	—	●	○	○
Ihv	2278	850-1200		○	○	●	●	○	○	○
Ihv	2279	900-1100		●	○	●	—	●	○	○
Ihv	2280	1050-1150		●	○	●	○	○	○	●
Ihv	2281	900-1100		●	—	●	—	●	○	○

● = Present, ○ = Absent, — = Unknown, bm = Black Mesa, Ihv = Long House Valley

LIT = Lithics, GDS = Groundstone, CER = Ceramics, PIT = Pithouse, MAS = Masonry, KIV = Kiva

(continued on next page)

Table F.1: Analysis Site List (*continued*)

Project Area	Site Number	Date (A.D.)	Range	LIT	GDS	CER	PIT	MAS	KIV	STO
Ihv	2282	1050-1150		•	—	•	—	•	•	○
Ihv	2283	1050-1150		•	○	•	—	—	—	○
Ihv	2284	1050-1150		•	—	•	—	•	—	○
Ihv	2285	600-700		○	○	•	—	○	○	●
Ihv	2286	600-850		○	—	•	●	○	○	○
Ihv	2287	900-1100		•	—	•	—	○	○	●
Ihv	2288	1100-1200		•	—	•	○	●	○	○
Ihv	2289	1050-1150		•	—	•	—	•	●	○
Ihv	2290	1050-1150		•	—	•	●	○	—	○
Ihv	2291	1000-1075		•	—	•	—	•	○	○
Ihv	2292	950-1050		•	—	•	●	○	○	○
Ihv	2293	1050-1150		•	○	•	—	○	○	○
Ihv	2294	1050-1150		•	—	•	—	—	—	—
Ihv	2295	1050-1150		•	●	•	○	●	●	●
Ihv	2296	1050-1150		•	—	•	—	—	○	—
Ihv	2297	900-1000		•	—	•	—	○	○	○
Ihv	2298	850-1050		○	—	•	—	○	○	○
Ihv	2299	1000-1150		•	○	•	—	●	○	●
Ihv	2300	1000-1150		•	—	•	—	—	—	—
Ihv	2301	0-600		○	—	○	○	○	○	○
Ihv	2302	1000-1100		○	○	•	—	—	—	○
Ihv	2303	600-700		○	○	•	○	○	○	●
Ihv	2304	850-1000		•	○	•	●	○	○	○
Ihv	2305	1000-1150		•	—	•	●	●	—	○
Ihv	2306	1050-1150		○	○	•	—	●	○	○
Ihv	2307	1050-1100		○	○	•	○	○	○	○
Ihv	2308	1050-1150		•	—	•	○	●	○	○
Ihv	2309	850-1000		•	○	•	●	○	○	○
Ihv	2310	850-1000		•	—	•	—	—	○	○
Ihv	2311	850-1000		•	—	•	—	○	○	○
Ihv	2312	1050-1150		•	—	•	—	●	—	○
Ihv	2313	900-1150		○	○	•	○	○	○	○
Ihv	2314	0-600		•	○	○	○	○	○	○
Ihv	2315	0-600		•	—	○	○	○	○	○
Ihv	2316	900-1050		•	—	•	●	○	○	○
Ihv	2317	1000-1150		•	—	•	●	○	○	○
Ihv	2318	1000-1150		○	○	•	—	●	○	○
Ihv	2319	1200-1270		○	○	•	—	—	○	○

● = Present, ○ = Absent, — = Unknown, bm = Black Mesa, Ihv = Long House Valley

LIT = Lithics, GDS = Groundstone, CER = Ceramics, PIT = Pithouse, MAS = Masonry, KIV = Kiva

(continued on next page)

Table F.1: Analysis Site List (*continued*)

Project Area	Site Number	Date (A.D.)	Range	LIT	GDS	CER	PIT	MAS	KIV	STO
Ihv	2320	1050-1150		○	—	●	—	○	○	○
Ihv	2321	1100-1150		○	—	●	○	●	○	○
Ihv	2322	850-1000		●	—	●	—	○	○	○
Ihv	2323	1050-1225		○	○	●	—	○	○	○
Ihv	2324	1000-1200		●	—	●	—	●	—	○
Ihv	2325	1000-1150		○	○	●	○	○	○	○
Ihv	2326	1100-1250		○	—	●	—	●	○	○
Ihv	2327	1050-1150		○	○	●	○	●	○	○
Ihv	2328	1100-1200		○	—	●	●	○	○	○
Ihv	2329	600-850		●	○	●	●	○	○	○
Ihv	2330	600-850		○	—	●	●	○	○	○
Ihv	2331	900-1150		○	○	●	○	○	○	●
Ihv	2332	1050-1150		●	○	●	○	●	○	○
Ihv	2333	850-1250		○	○	●	—	●	●	○
Ihv	2334	0-600		●	—	●	●	○	○	○
Ihv	2335	1050-1150		●	—	●	—	●	—	○
Ihv	2336	600-700		●	—	●	●	○	○	○
Ihv	2337	850-1150		●	●	●	—	○	—	○
Ihv	2338	600-850		●	○	●	●	○	○	○
Ihv	2339	1050-1150		●	○	●	—	●	○	○
Ihv	2340	1200-1250		●	—	●	—	●	○	○
Ihv	2341	1000-1100		○	○	●	—	○	○	○
Ihv	2342	850-1000		○	○	○	○	○	○	○
Ihv	2343	850-1000		●	—	●	●	○	○	○
Ihv	2344	1200-1300		●	—	●	○	●	●	○
Ihv	2345	1250-1300		●	—	●	○	●	—	○
Ihv	2346	1050-1150		●	—	●	—	●	●	○
Ihv	2347	1100-1150		●	—	●	—	●	○	●
Ihv	2348	1050-1200		●	—	●	—	—	—	○
Ihv	2349	850-1000		○	—	●	—	○	○	○
Ihv	2350	1100-1150		○	—	●	—	●	○	○
Ihv	2351	1000-1200		●	●	●	—	●	●	○
Ihv	2352	850-1000		●	—	●	●	○	○	○
Ihv	2353	1050-1150		●	—	●	○	○	○	○
Ihv	2354	1050-1150		●	●	●	—	●	—	○
Ihv	2355	850-1050		●	○	●	—	○	○	●
Ihv	2356	850-1000		●	—	●	●	○	○	○
Ihv	2357	850-1000		●	●	●	●	○	○	○

● = Present, ○ = Absent, — = Unknown, bm = Black Mesa, Ihv = Long House Valley

LIT = Lithics, GDS = Groundstone, CER = Ceramics, PIT = Pithouse, MAS = Masonry, KIV = Kiva

(continued on next page)

Table F.1: Analysis Site List (*continued*)

Project Area	Site Number	Date (A.D.)	Range	LIT	GDS	CER	PIT	MAS	KIV	STO
Ihv	2358	1050-1150		•	—	•	—	•	○	○
Ihv	2359	1050-1200		•	—	•	—	•	—	○
Ihv	2360	0-600		○	○	○	○	○	○	●
Ihv	2361	1050-1150		•	—	•	—	•	—	○
Ihv	2362	1050-1150		○	—	•	—	•	○	○
Ihv	2363	1000-1050		○	—	•	●	○	○	○
Ihv	2364	1200-1250		○	○	•	—	•	○	○
Ihv	2365	1050-1150		•	—	•	—	•	●	○
Ihv	2366	850-1000		○	○	•	—	○	○	○
Ihv	2367	900-1100		•	○	•	—	•	○	○
Ihv	2368	1200-1250		○	—	•	—	•	—	○
Ihv	2369	850-1200		•	—	•	—	•	—	●
Ihv	2370	850-1000		•	—	•	●	○	○	○
Ihv	2371	1200-1275		•	○	•	—	•	○	○
Ihv	2372	1050-1200		○	—	•	—	•	—	○
Ihv	2373	1050-1150		○	○	•	—	•	—	○
Ihv	2374	0-600		○	○	○	○	○	○	○
Ihv	2375	0-600		•	—	○	—	○	○	●
Ihv	2376	1050-1150		○	○	•	—	•	○	○
Ihv	2377	1000-1250		○	○	•	—	○	○	○
Ihv	2378	1000-1050		○	—	•	—	—	—	○
Ihv	2379	1250-1300		○	○	•	—	○	○	○
Ihv	2380	0-600		•	○	○	○	○	○	○
Ihv	2381	1050-1150		•	○	•	—	•	—	○
Ihv	2382	0-600		•	—	•	●	○	○	○
Ihv	2383	0-600		•	○	○	○	○	○	○
Ihv	2384	0-600		•	●	○	○	○	○	○
Ihv	2385	1075-1275		•	—	•	—	○	○	○
Ihv	2386	0-600		•	○	○	○	○	○	○
Ihv	2387	1050-1150		•	—	•	—	•	—	○
Ihv	2388	1050-1150		○	○	•	—	•	—	○
Ihv	2389	1000-1100		○	—	•	—	•	—	○
Ihv	2390	0-650		•	—	○	○	○	○	●
Ihv	2391	0-600		•	—	○	○	○	○	●
Ihv	2392	0-600		•	—	○	○	○	○	○
Ihv	2393	1150-1250		•	○	•	—	•	—	○
Ihv	2394	1000-1150		•	—	•	—	•	●	○
Ihv	2395	950-1050		○	○	•	—	○	○	●

• = Present, ○ = Absent, — = Unknown, bm = Black Mesa, Ihv = Long House Valley

LIT = Lithics, GDS = Groundstone, CER = Ceramics, PIT = Pithouse, MAS = Masonry, KIV = Kiva

(continued on next page)

Table F.1: Analysis Site List (*continued*)

Project Area	Site Number	Date (A.D.)	Range	LIT	GDS	CER	PIT	MAS	KIV	STO
Ihv	2396	1000-1100		•	•	•	—	•	•	•
Ihv	2397	850-1050		•	•	•	—	○	○	○
Ihv	2398	1025-1075		○	○	•	○	○	○	○
Ihv	2399	1000-1050		•	—	•	—	•	—	○
Ihv	2400	900-1100		•	—	•	•	•	•	○
Ihv	2401	1000-1050		•	—	•	—	•	—	•
Ihv	2402	0-600		•	—	○	—	○	○	•
Ihv	2403	1150-1300		•	•	•	—	•	—	○
Ihv	2404	1025-1250		•	—	•	—	○	○	○
Ihv	2405	900-1025		•	—	•	•	○	○	•
Ihv	2406	1000-1150		•	—	•	—	•	•	○
Ihv	2407	1000-1150		•	○	•	—	○	○	○
Ihv	2408	850-1000		•	—	•	•	○	○	•
Ihv	2409	1000-1150		•	—	•	○	○	○	○
Ihv	2410	850-1000		•	○	•	•	○	○	•
Ihv	2411	850-1000		•	—	•	•	○	○	•
Ihv	2412	900-1000		•	—	•	—	○	○	○
Ihv	2413	600-700		•	—	•	—	○	○	•
Ihv	2414	600-700		•	○	•	—	○	○	○
Ihv	2415	1050-1150		○	—	•	○	○	○	○
Ihv	2416	1000-1100		•	—	•	—	○	○	○
Ihv	2417	1050-1300		○	○	•	○	○	○	○
Ihv	2418	0-600		•	—	•	•	○	○	•
Ihv	2419	600-700		•	○	•	○	○	○	○
Ihv	2420	1050-1150		•	○	•	—	•	—	○
Ihv	2421	1050-1150		•	○	•	—	•	•	○
Ihv	2422	1000-1100		•	—	•	—	•	•	○
Ihv	2423	1200-1300		○	○	•	—	•	—	○
Ihv	2424	850-1150		•	○	•	○	○	○	•
Ihv	2425	1050-1150		•	—	•	—	•	—	•
Ihv	2426	1150-1300		•	—	•	—	•	•	○
Ihv	2427	1200-1300		•	—	•	—	•	•	○
Ihv	2428	1150-1250		•	—	•	—	•	•	○
Ihv	2429	950-1100		•	—	•	—	•	—	○
Ihv	2430	1025-1100		•	—	•	—	•	•	•
Ihv	2431	1000-1050		•	○	•	○	○	○	○
Ihv	2432	1000-1100		—	•	•	—	•	○	○
Ihv	2433	0-1300		○	○	○	○	○	○	○

• = Present, ○ = Absent, — = Unknown, bm = Black Mesa, Ihv = Long House Valley

LIT = Lithics, GDS = Groundstone, CER = Ceramics, PIT = Pithouse, MAS = Masonry, KIV = Kiva

(continued on next page)

Table F.1: Analysis Site List (*continued*)

Project Area	Site Number	Date (A.D.)	Range	LIT	GDS	CER	PIT	MAS	KIV	STO
Ihv	2434	850-1000		●	●	●	—	○	○	○
Ihv	2435	0-600		●	—	○	—	○	○	○
Ihv	2436	600-700		●	○	○	○	○	○	○
Ihv	2437	0-600		●	—	○	○	○	○	●
Ihv	2438	0-600		●	○	○	○	○	○	○
Ihv	2439	1050-1100		●	●	●	●	○	●	○
Ihv	2440	1050-1175		●	—	●	—	●	—	○
Ihv	2441	1050-1200		●	—	●	—	●	—	○
Ihv	2442	1050-1200		●	—	●	—	●	—	○
Ihv	2443	1050-1200		●	—	●	—	●	○	○
Ihv	2444	1050-1200		●	—	●	—	—	○	○
Ihv	2445	1050-1200		●	—	●	—	●	○	○
Ihv	2446	1050-1200		●	—	●	—	○	○	○
Ihv	2447	1050-1300		○	○	●	○	○	○	○
Ihv	2448	1050-1300		○	○	●	○	○	○	○
Ihv	2449	1050-1300		○	○	○	○	○	○	○
Ihv	2450	1050-1300		○	○	○	○	○	○	○
Ihv	2451	850-1050		●	●	●	—	●	—	○
Ihv	2452	1025-1100		●	●	●	○	○	○	○
Ihv	2453	1250-1300		●	●	●	○	○	○	○
Ihv	2454	1100-1250		●	●	●	○	●	—	○
Ihv	2455	1150-1250		●	●	●	○	●	—	○
Ihv	2456	1100-1200		●	●	●	○	○	—	○
Ihv	2457	1250-1300		●	●	●	—	○	○	○
Ihv	2458	1100-1200		●	●	●	—	●	—	○
Ihv	2459	1150-1200		●	●	●	—	●	●	○
Ihv	2460	1150-1200		●	●	●	—	●	—	○
Ihv	2461	1200-1300		●	●	●	—	●	●	○
Ihv	2462	1200-1300		●	●	●	—	●	●	○
Ihv	2463	1000-1150		●	●	●	○	●	○	○
Ihv	2464	1100-1250		●	○	●	○	○	○	○
Ihv	2465	1050-1200		●	●	●	●	○	○	○
Ihv	2466	850-950		●	○	●	○	○	○	○
Ihv	2467	1075-1150		●	○	●	○	○	○	○
Ihv	2468	1000-1150		●	○	●	●	○	○	○
Ihv	2469	1150-1200		●	○	●	○	○	○	○
Ihv	2470	1100-1150		●	●	●	○	●	●	○
Ihv	2471	1150-1200		●	●	●	○	○	○	○

● = Present, ○ = Absent, — = Unknown, bm = Black Mesa, Ihv = Long House Valley

LIT = Lithics, GDS = Groundstone, CER = Ceramics, PIT = Pithouse, MAS = Masonry, KIV = Kiva

(continued on next page)

Table F.1: Analysis Site List (*continued*)

Project Area	Site Number	Date (A.D.)	Range	LIT	GDS	CER	PIT	MAS	KIV	STO
Ihv	2472	850-1025		●	○	●	○	○	○	○
Ihv	2473	1100-1150		●	○	●	○	○	○	○
Ihv	2474	950-1100		●	●	●	○	○	○	○
Ihv	2475	1000-1150		●	○	●	○	○	○	○
Ihv	2476	1000-1100		●	○	●	○	○	○	○
Ihv	2477	1150-1200		●	○	●	○	○	○	○
Ihv	2478	800-1000		●	○	●	●	○	○	○
Ihv	2479	1075-1150		●	○	●	○	○	○	○
Ihv	2480	1000-1150		●	●	●	○	●	●	○
Ihv	2481	0-550		●	○	○	○	○	○	○
Ihv	2482	1000-1300		●	○	●	○	○	○	○
Ihv	2483	1000-1175		●	●	●	○	○	○	○
Ihv	2484	0-550		●	○	○	○	○	○	○
Ihv	2485	1050-1300		●	○	●	○	○	○	○
Ihv	2486	0-550		●	○	○	○	○	○	●
Ihv	2487	1100-1270		●	●	●	○	○	○	○
Ihv	2488	1075-1150		●	○	●	○	○	○	○
Ihv	2489	1100-1150		●	●	●	○	○	○	○
Ihv	2490	0-1300		○	○	○	○	○	○	○
Ihv	2491	550-700		●	○	●	○	○	○	○
Ihv	2492	1050-1270		●	○	●	○	●	○	○
Ihv	2493	950-1075		●	○	●	○	●	○	○
Ihv	2494	1100-1300		○	○	●	○	○	○	○
Ihv	2495	1000-1150		●	●	●	○	○	○	○
Ihv	2496	1075-1150		●	○	●	○	●	○	○
Ihv	2497	850-1000		●	○	●	○	○	○	●
Ihv	2498	1200-1300		●	○	●	○	○	○	○
Ihv	2499	1075-1200		●	○	●	○	●	○	○
Ihv	2500	1075-1250		●	○	●	○	○	○	○
Ihv	2501	1050-1150		●	○	●	○	○	○	○
Ihv	2502	1000-1300		●	○	●	○	○	○	○
Ihv	2503	1000-1250		○	○	●	○	○	○	○
Ihv	2504	1000-1150		●	○	●	○	●	—	○
Ihv	2505	850-1000		●	○	●	○	○	○	○
Ihv	2506	1075-1150		●	○	●	○	●	○	○
Ihv	2507	1025-1300		●	○	●	○	○	○	○
Ihv	2508	550-850		●	○	●	○	○	○	○
Ihv	2509	1000-1150		●	○	●	○	●	—	○

● = Present, ○ = Absent, — = Unknown, bm = Black Mesa, Ihv = Long House Valley

LIT = Lithics, GDS = Groundstone, CER = Ceramics, PIT = Pithouse, MAS = Masonry, KIV = Kiva

(continued on next page)

Table F.1: Analysis Site List (*continued*)

Project Area	Site Number	Date (A.D.)	Range	LIT	GDS	CER	PIT	MAS	KIV	STO
Ihv	2510	1000-1125		•	○	•	○	•	○	○
Ihv	2511	1075-1150		•	○	•	—	—	—	○
Ihv	2512	1150-1200		•	○	•	○	•	○	○
Ihv	2513	850-1150		•	○	•	○	•	—	○
Ihv	2514	500-650		•	○	•	○	○	○	•
Ihv	2515	1000-1150		○	○	•	○	○	○	○
Ihv	2516	975-1150		•	○	•	○	—	—	○
Ihv	2517	1075-1150		•	•	•	○	○	○	○
Ihv	2518	850-1000		•	•	•	—	○	○	•
Ihv	2519	0-550		•	•	○	○	○	○	○
Ihv	2520	850-1025		•	•	•	○	○	○	○
Ihv	2521	950-1175		•	○	•	○	•	•	○
Ihv	2522	1000-1150		•	○	•	○	•	—	○
Ihv	2523	850-1100		•	○	•	•	○	○	○
Ihv	2524	0-550		•	○	○	○	○	○	○
Ihv	2525	950-1025		•	○	•	○	○	○	○
Ihv	2526	1050-1150		•	○	•	○	•	○	○
Ihv	2527	1050-1150		•	○	•	○	○	○	•
Ihv	2528	1000-1075		•	○	•	○	○	○	○
Ihv	2529	1225-1300		•	○	•	○	○	○	○
Ihv	2530	1050-1175		•	○	•	○	○	○	○
Ihv	2531	1050-1125		•	○	•	○	○	○	○
Ihv	2532	1050-1150		•	○	•	○	○	○	○
Ihv	2533	950-1150		•	•	•	○	○	○	○
Ihv	2534	850-1150		•	•	•	○	○	○	○
Ihv	2535	1000-1300		•	○	•	○	○	○	○
Ihv	2536	1075-1125		•	○	•	○	○	○	○
Ihv	2537	1075-1200		•	•	•	○	○	○	○
Ihv	2538	1075-1125		•	○	•	○	○	○	○
Ihv	2539	1100-1200		•	○	•	○	○	○	○
Ihv	2540	850-950		○	○	•	○	○	○	○
Ihv	2541	600-850		○	○	•	○	○	○	○
Ihv	2542	1175-1300		○	○	•	○	○	○	○
Ihv	2543	1075-1175		•	•	•	○	○	○	○
Ihv	2544	850-1000		○	○	•	○	○	○	○
Ihv	2545	850-1025		○	○	•	○	○	○	○
Ihv	2546	1000-1075		•	•	•	○	○	○	○
Ihv	2547	1000-1125		•	○	•	○	○	○	○

• = Present, ○ = Absent, — = Unknown, bm = Black Mesa, Ihv = Long House Valley

LIT = Lithics, GDS = Groundstone, CER = Ceramics, PIT = Pithouse, MAS = Masonry, KIV = Kiva

(continued on next page)

Table F.1: Analysis Site List (*continued*)

Project Area	Site Number	Date Range (A.D.)	LIT	GDS	CER	PIT	MAS	KIV	STO
Ihv	2548	850-1300	•	○	•	○	○	○	○
Ihv	2549	600-700	•	•	•	○	○	○	○
Ihv	2550	1150-1225	•	○	•	○	•	○	○

• = Present, ○ = Absent, — = Unknown, bm = Black Mesa, Ihv = Long House Valley
 LIT = Lithics, GDS = Groundstone, CER = Ceramics, PIT = Pithouse, MAS = Masonry, KIV = Kiva

Appendix G

SQL Expression for Merging Black Mesa and Long House Valley Archaeological Data Tables.

The following SQL code creates a temporary table within PostgreSQL that contains the combined archeological attribute data for the Long House Valley and Black Mesa site tables.

```
drop table all_sites;

create temporary table all_sites
as
(select
    'bm' as proj_area,
    bm_sites.siteno,
    utm_zone,
    utm_northing,
    utm_easting,
    date_initial,
    date_terminal,
    case      when lithics = 0 then 0
               when lithics >= 1 then 1
               else -999
    end as lithics,
    case      when manos = 0 and metates = 0 then 0
               when manos >= 1 or metates >= 1 then 1
               else -999
    end as manos,
    case      when lithics = 0 then 0
               when lithics >= 1 then 1
               else -999
    end as metates)
```

```

        end as groundstone,
        case      when redware = 0 and grayware = 0 and whiteware = 0 then 0
                  when redware >= 1 or grayware >= 1 or whiteware >= 1 then 1
                  else -999
        end as ceramics,
        case      when pithouse_depressions = 0 then 0
                  when pithouse_depressions >= 1 then 1
                  else -999
        end as pithouse,
        case      when rubble_mounds = 0 then 0
                  when rubble_mounds >= 1 then 1
                  else -999
        end as masonry,
        case      when kiva_depressions = 0 then 0
                  when kiva_depressions >= 1 then 1
                  else -999
        end as kiva,
        case      when slab_lined = 0 then 0
                  when slab_lined >= 1 then 1
                  else -999
        end as store,
        1 as bm_count,
        0 as lhv_count
      from
        bm_sites,
        bm_periods,
        bm_site_coords
      where
        phase = period_code and
        bm_sites.siteno = bm_site_coords.siteno
    );
  insert into all_sites
  (
  select
    'lhv' as proj_area,
    siteno,
    utmzone as utm_zone,
    northing as utm_northing,
    easting as utm_easting,
    1950 - date_initial as date_initial,
    1950 - date_terminal as date_terminal,
    case      when chipped_stone = 0 then 0
              when chipped_stone >= 1 then 1
              else -999

```

```

end as lithics,
case      when ground_stone = 0 then 0
            when ground_stone >= 1 then 1
            else -999
end as groundstone,
case      when ceramics = 0 then 0
            when ceramics >= 1 then 1
            else -999
end as ceramics,
case      when pithouse = 0 then 0
            when pithouse >= 1 then 1
            else -999
end as pithouse,
case      when rooms_masonry = 0 then 0
            when rooms_masonry >= 1 then 1
            else -999
end as masonry,
case      when great_kiva = 0 and kiva = 0 then 0
            when great_kiva >= 1 or kiva >= 1 then 1
            else -999
end as kiva,
case      when cist = 0 then 0
            when cist >= 1 then 1
            else -999
end as store,
0 as bm_count,
1 as lhv_count
from lhv_sites
);

```

Appendix H

Result Plots for All 42 Archaeological – Environmental Analyses

H.1 All Sites

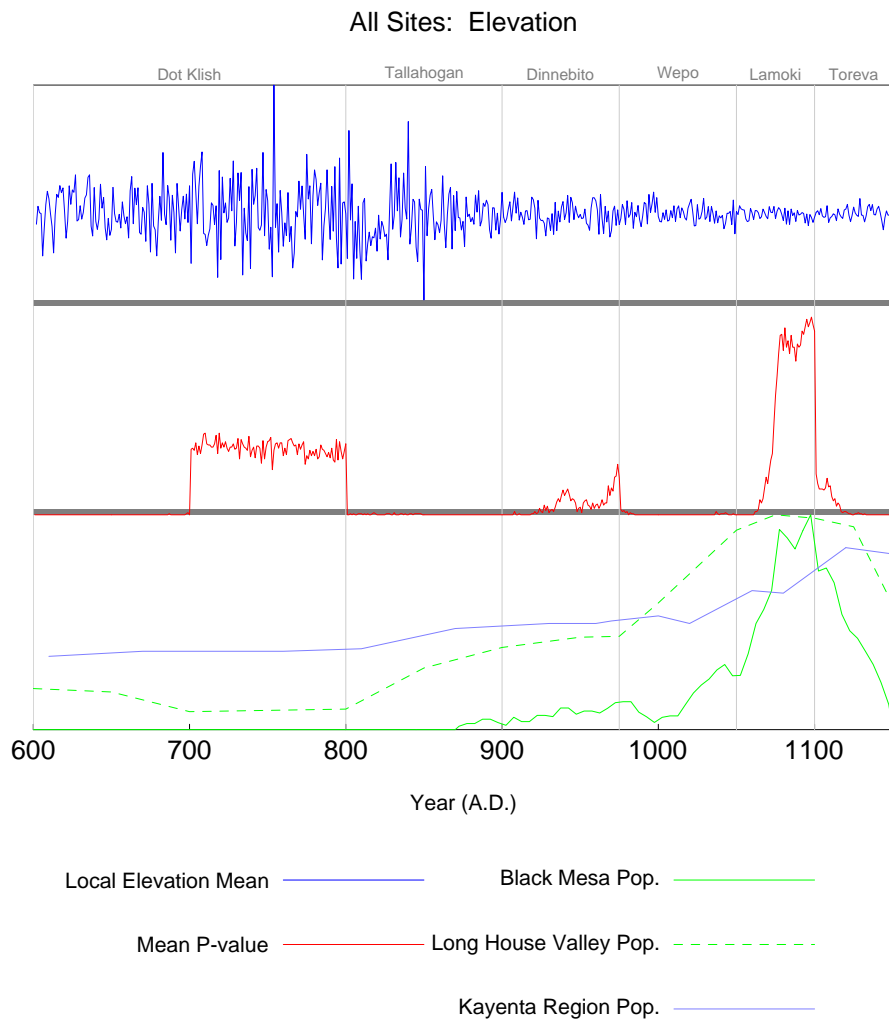


Figure H.1: Elevation Data Analysis for All Sites

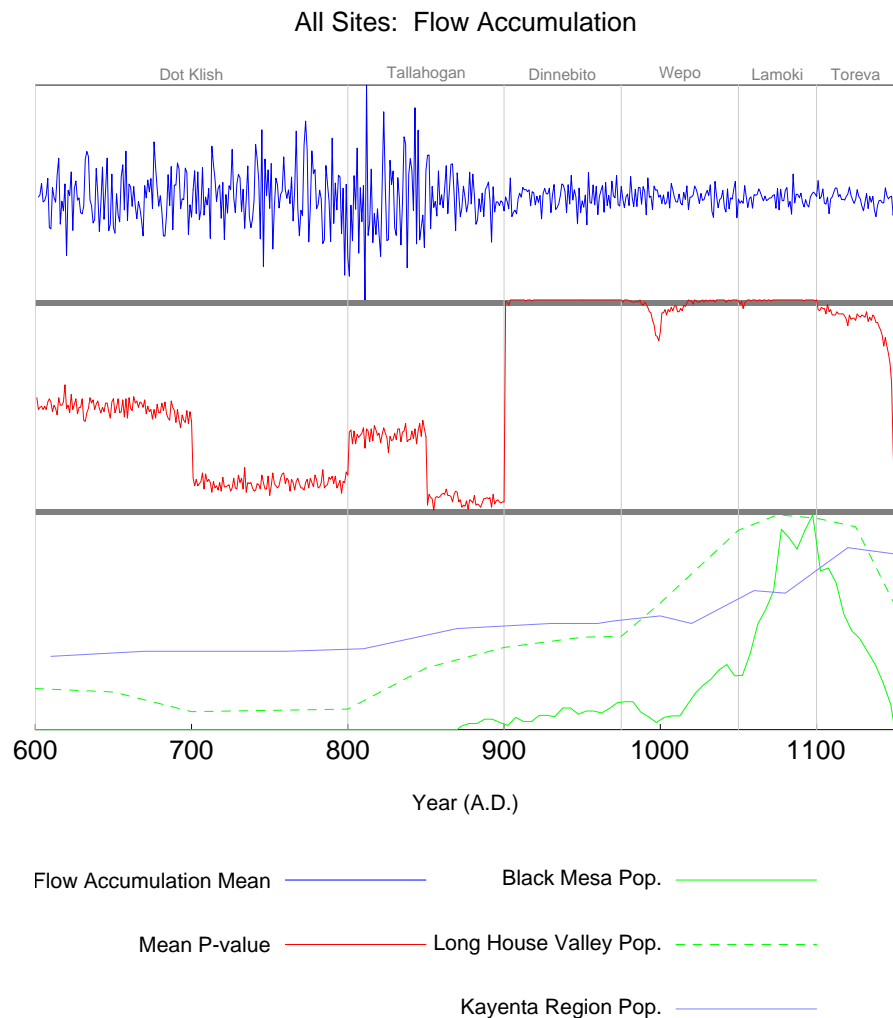


Figure H.2: Flow Accumulation Data Analysis for All Sites

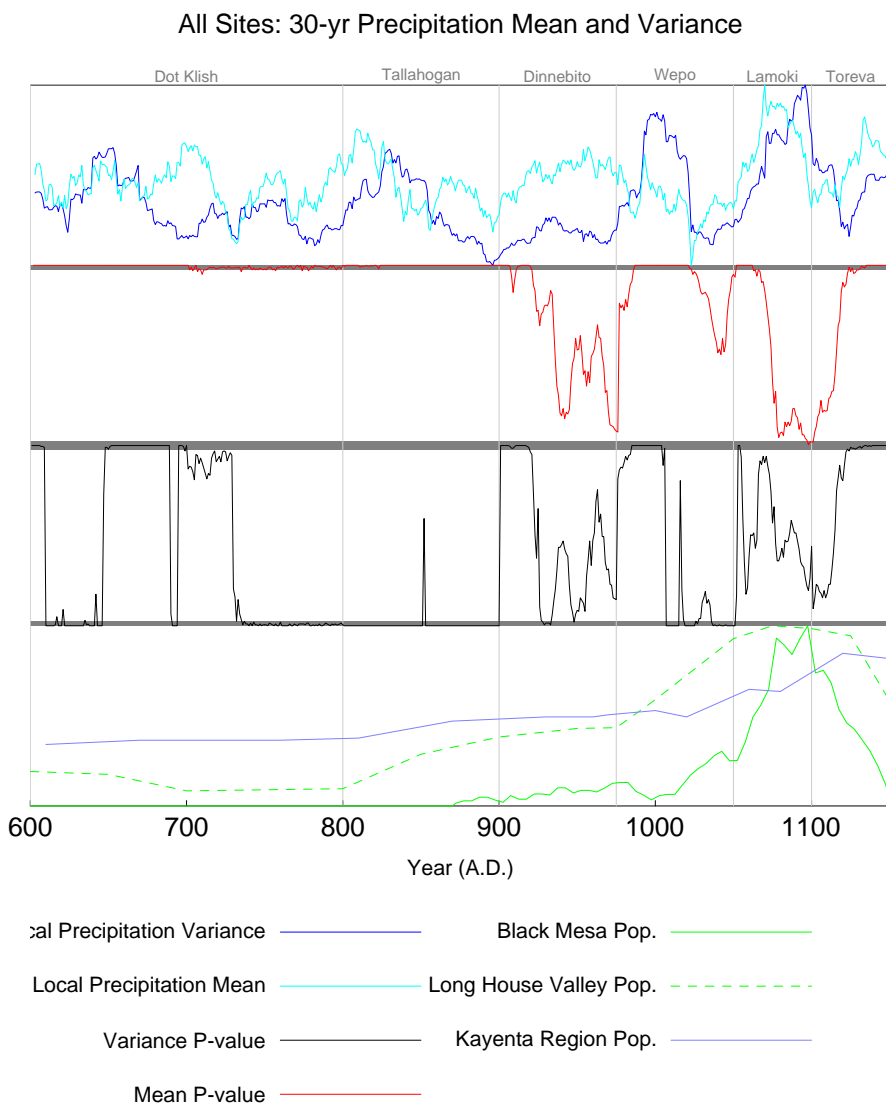


Figure H.3: Precipitation Data Analysis for All Sites

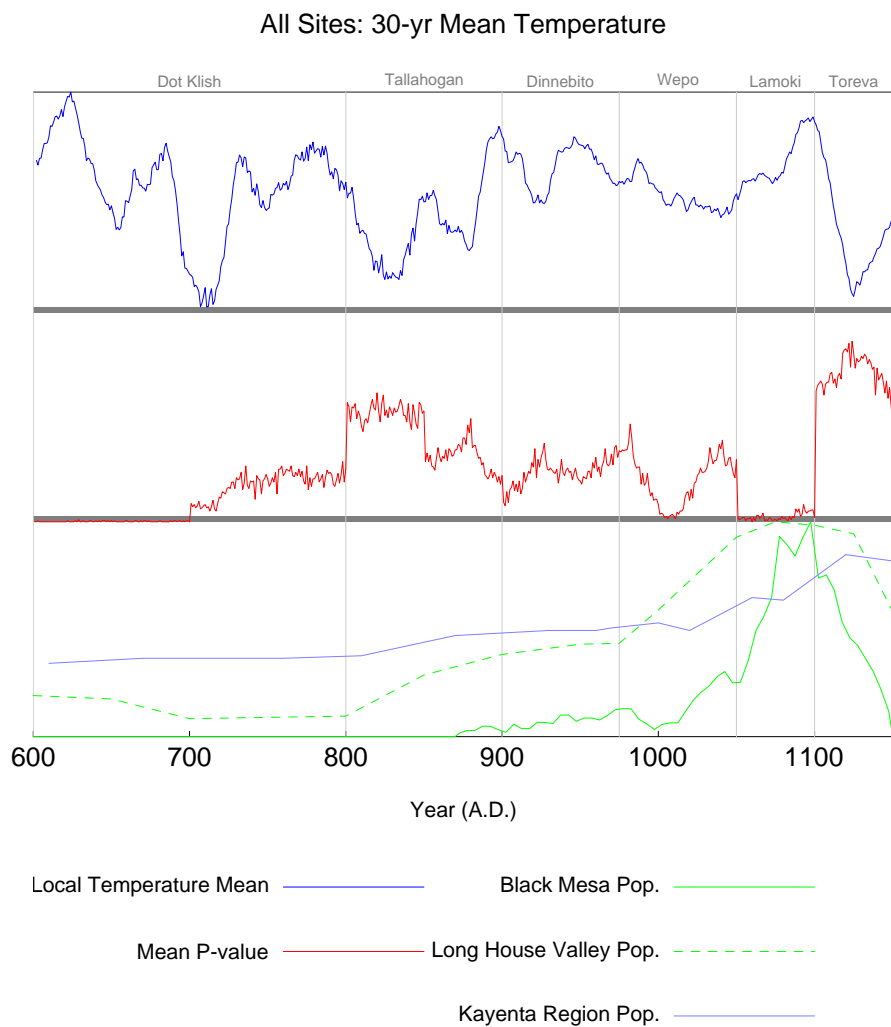


Figure H.4: Temperature Data Analysis for All Sites

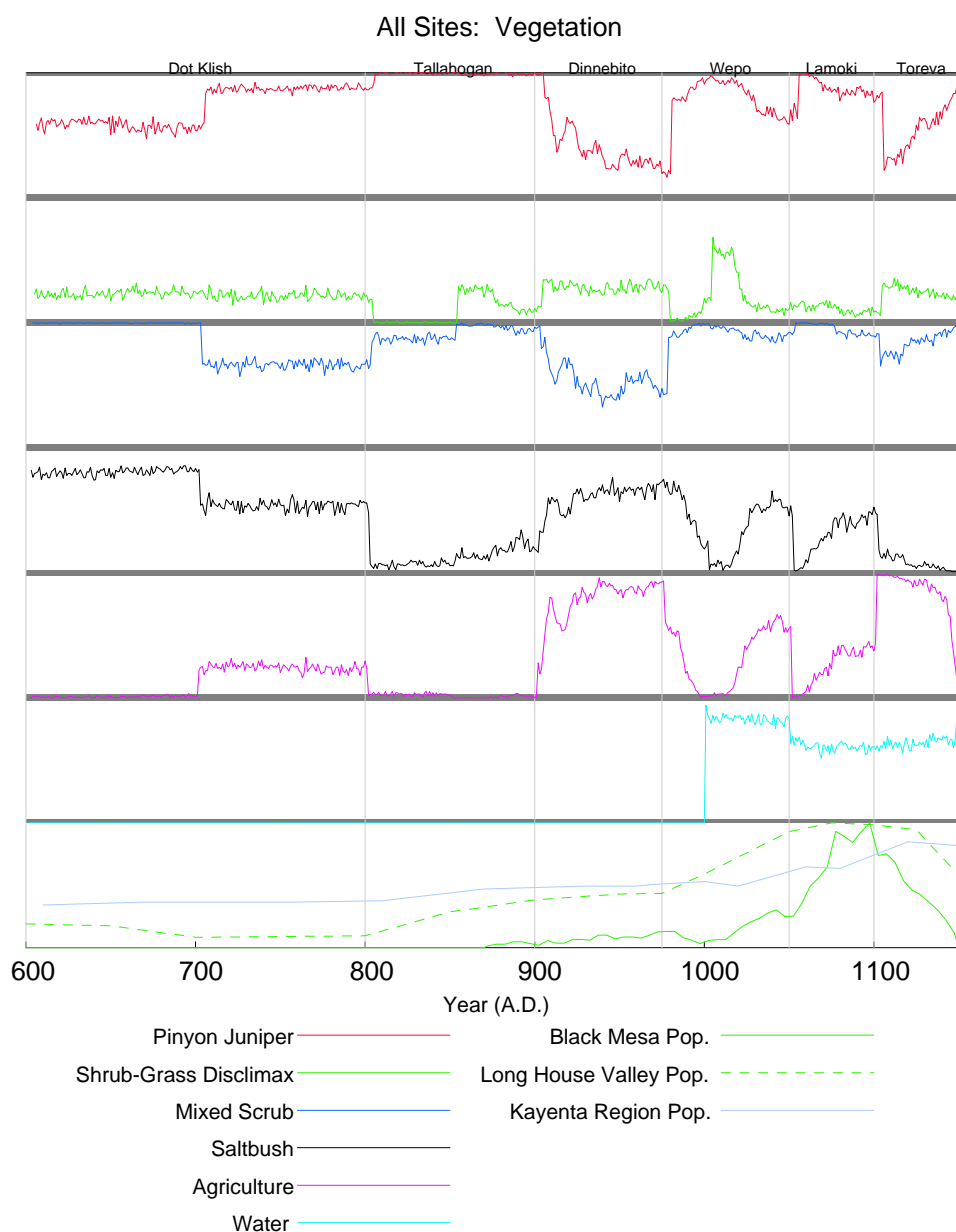


Figure H.5: Vegetation Data Analysis for All Sites

H.2 Pithouse Sites

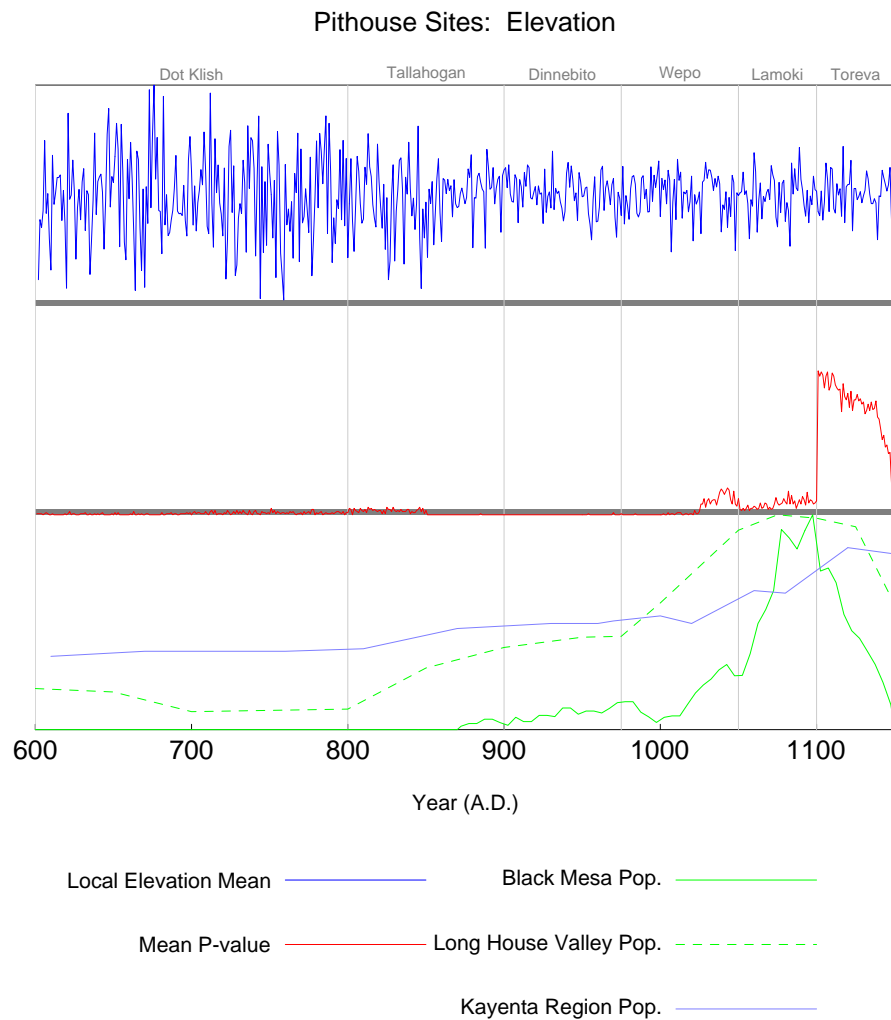


Figure H.6: Elevation Data Analysis for Pithouse Sites

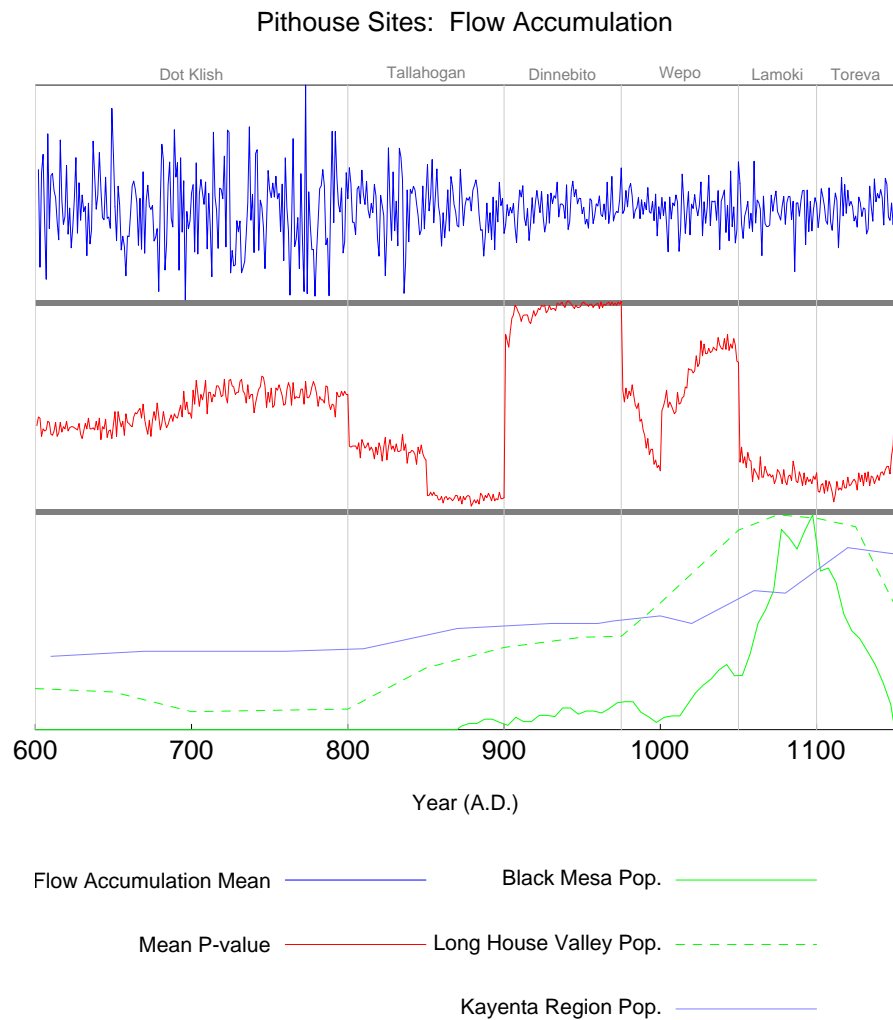


Figure H.7: Flow Accumulation Data Analysis for Pithouse Sites

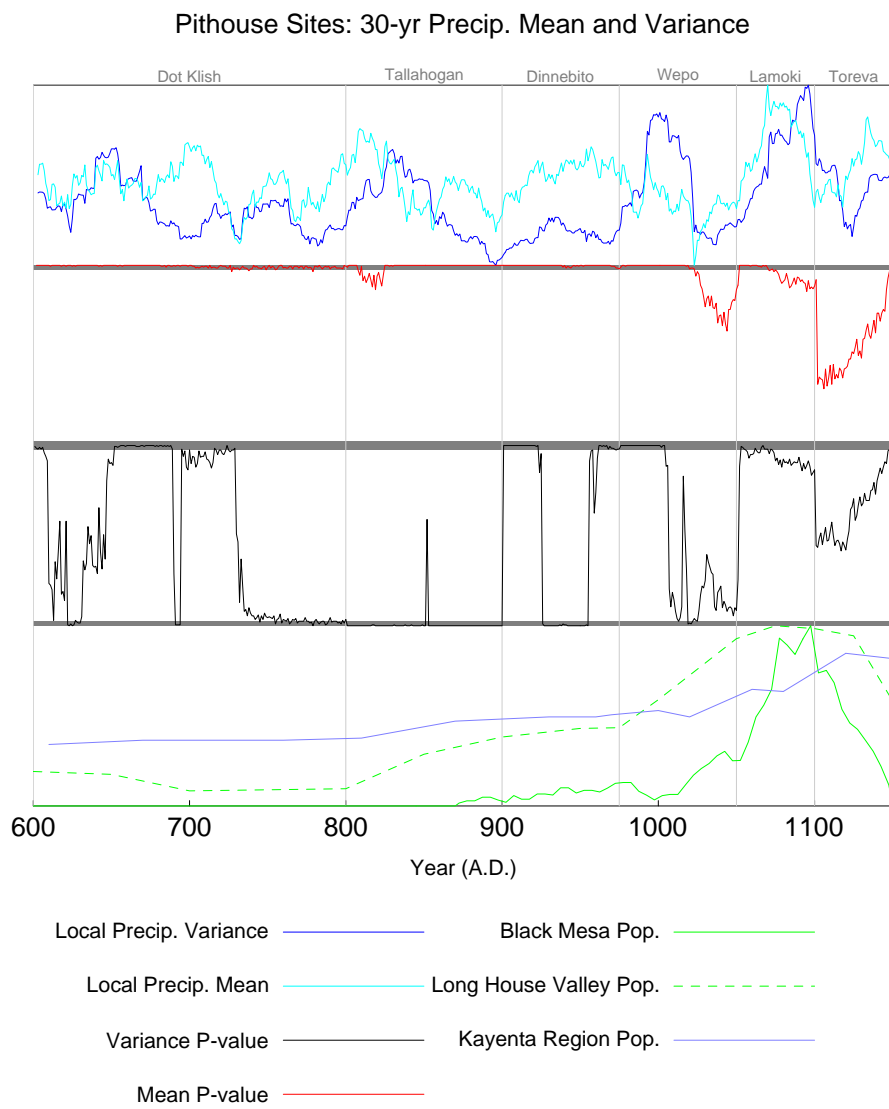


Figure H.8: Precipitation Data Analysis for Pithouse Sites

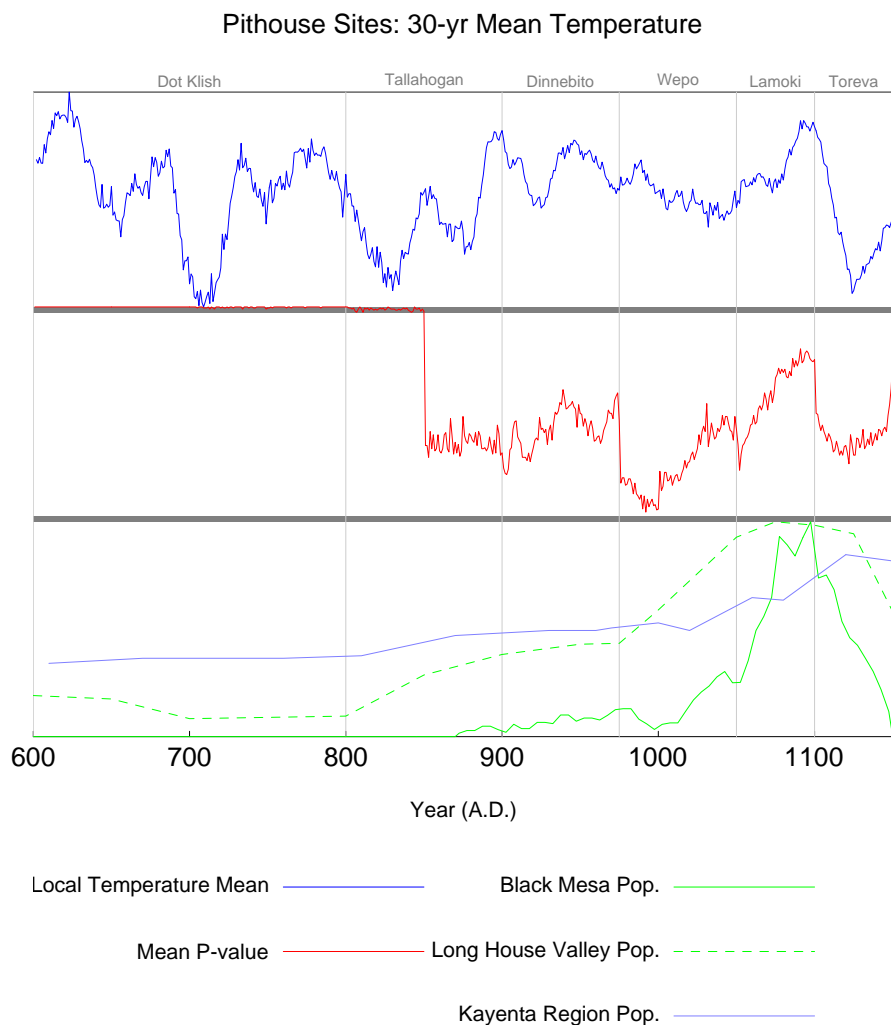


Figure H.9: Temperature Data Analysis for Pithouse Sites

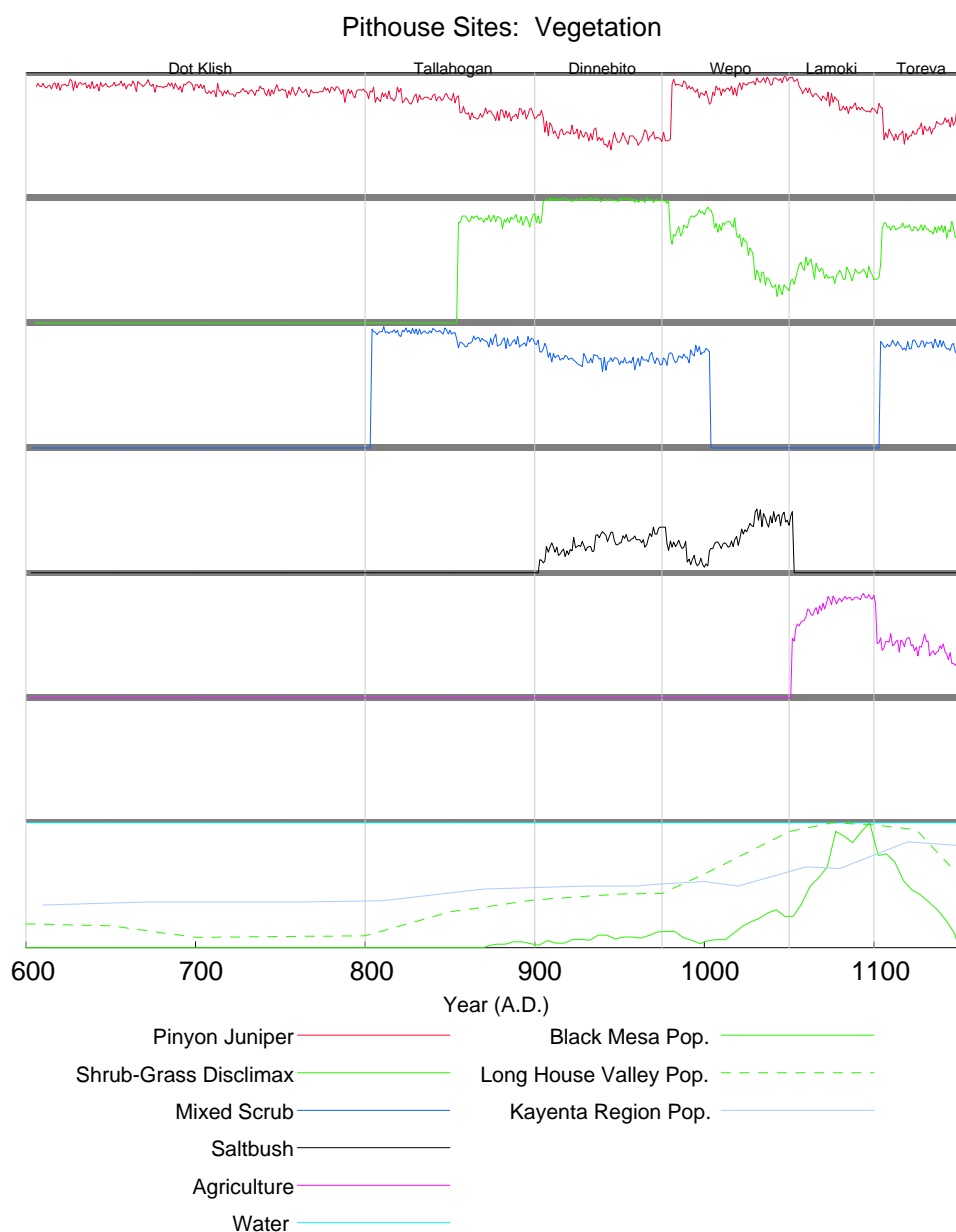


Figure H.10: Vegetation Data Analysis for Pithouse Sites

H.3 Masonry Sites

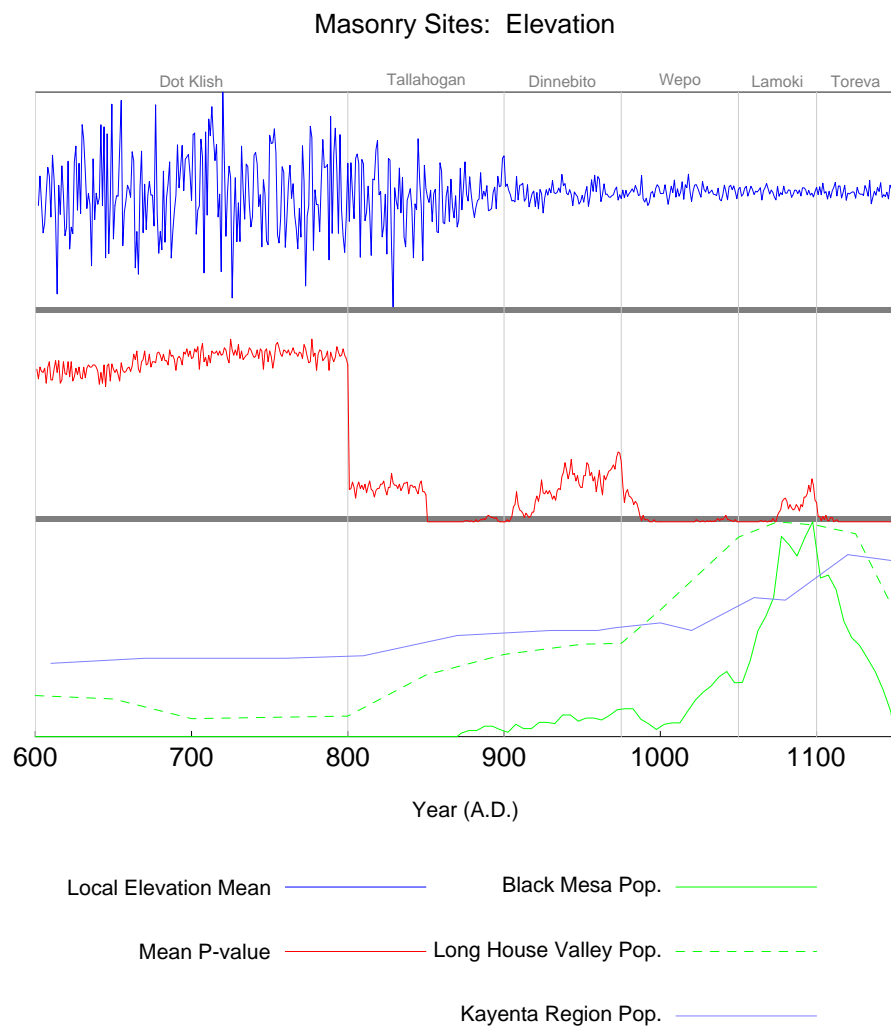


Figure H.11: Elevation Data Analysis for Masonry Sites

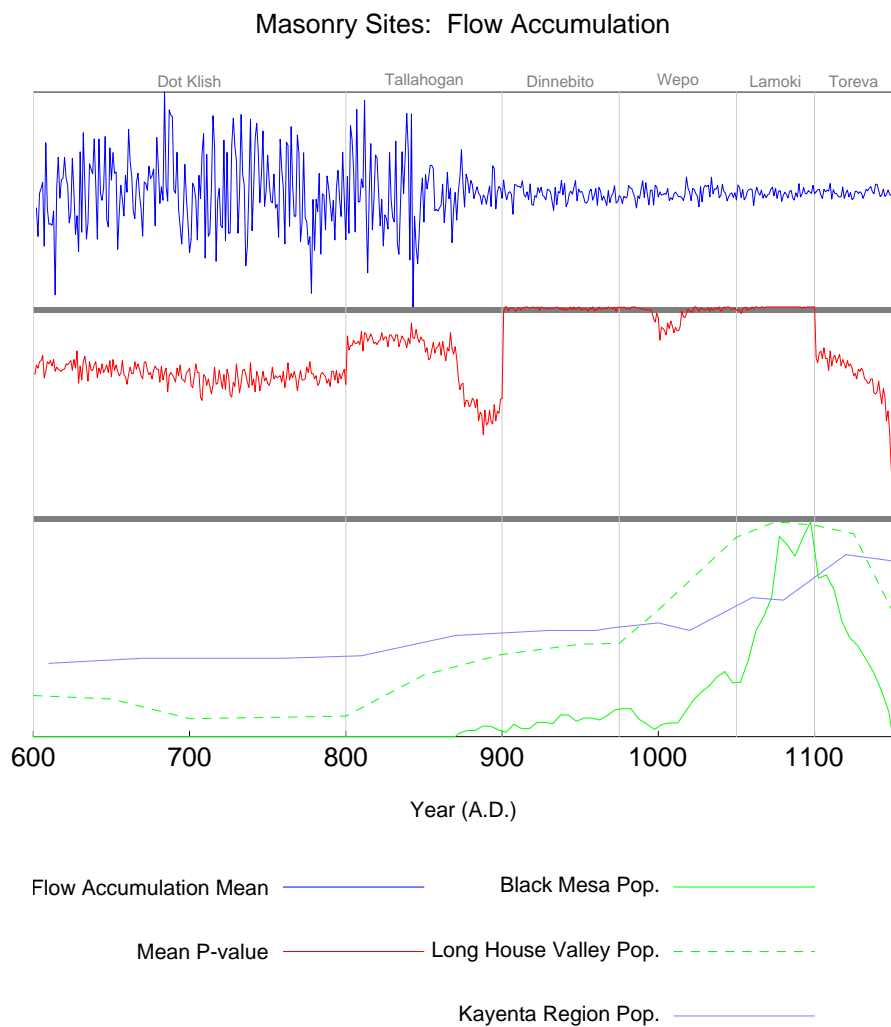


Figure H.12: Flow Accumulation Data Analysis for Masonry Sites

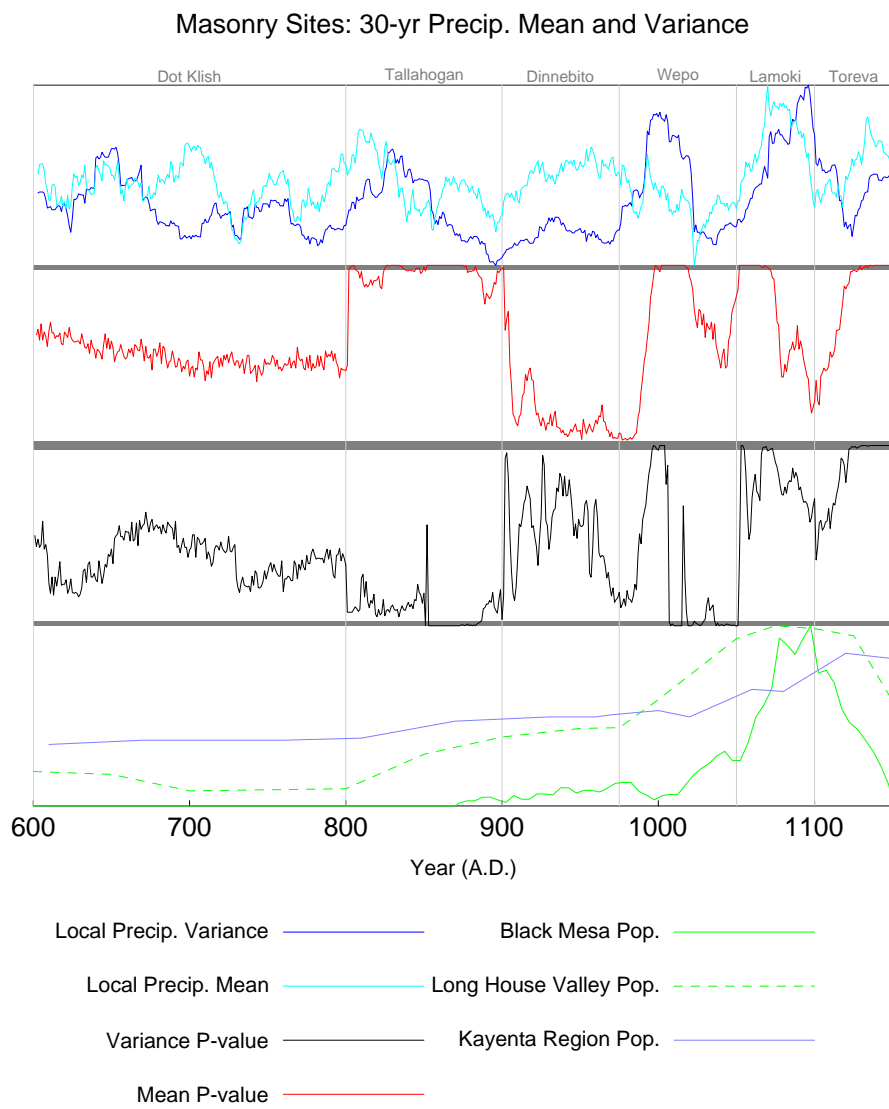


Figure H.13: Precipitation Data Analysis for Masonry Sites

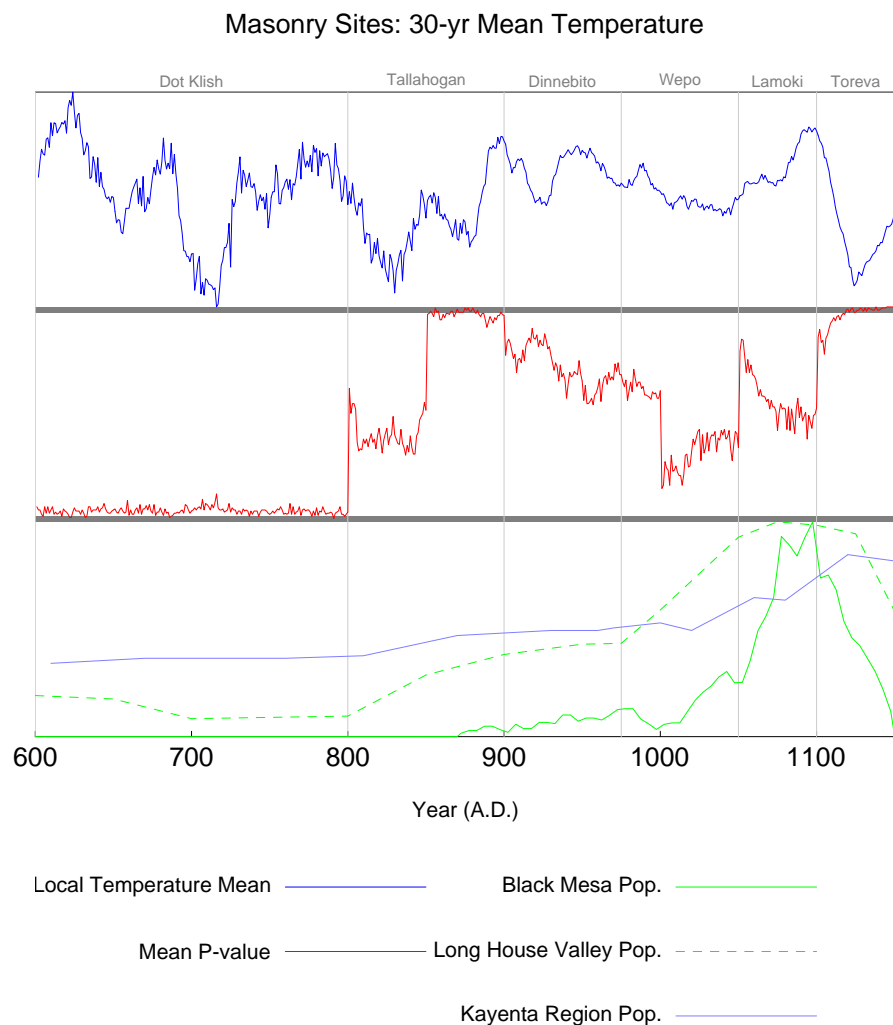


Figure H.14: Temperature Data Analysis for Masonry Sites

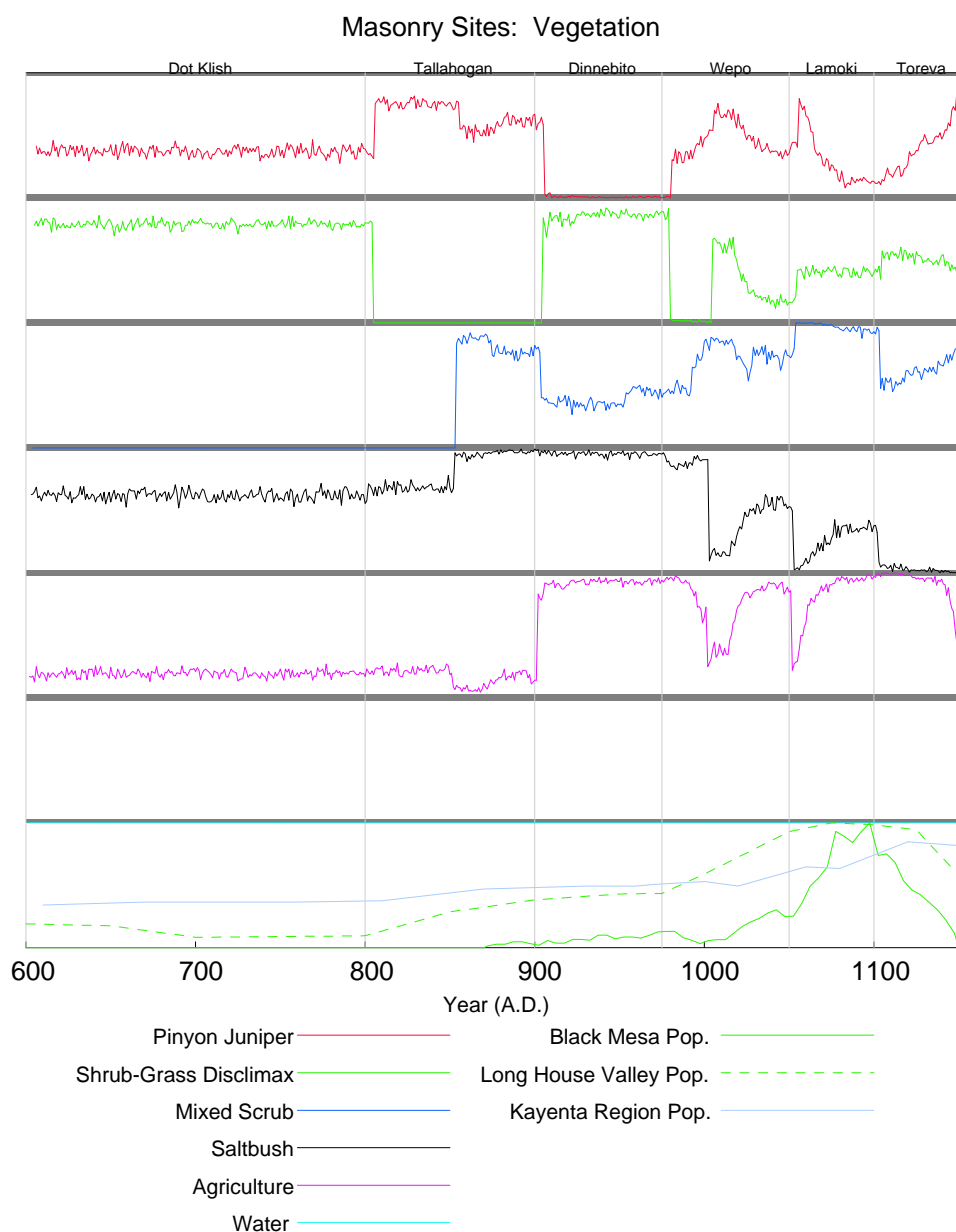


Figure H.15: Vegetation Data Analysis for Masonry Sites

H.4 Kiva Sites

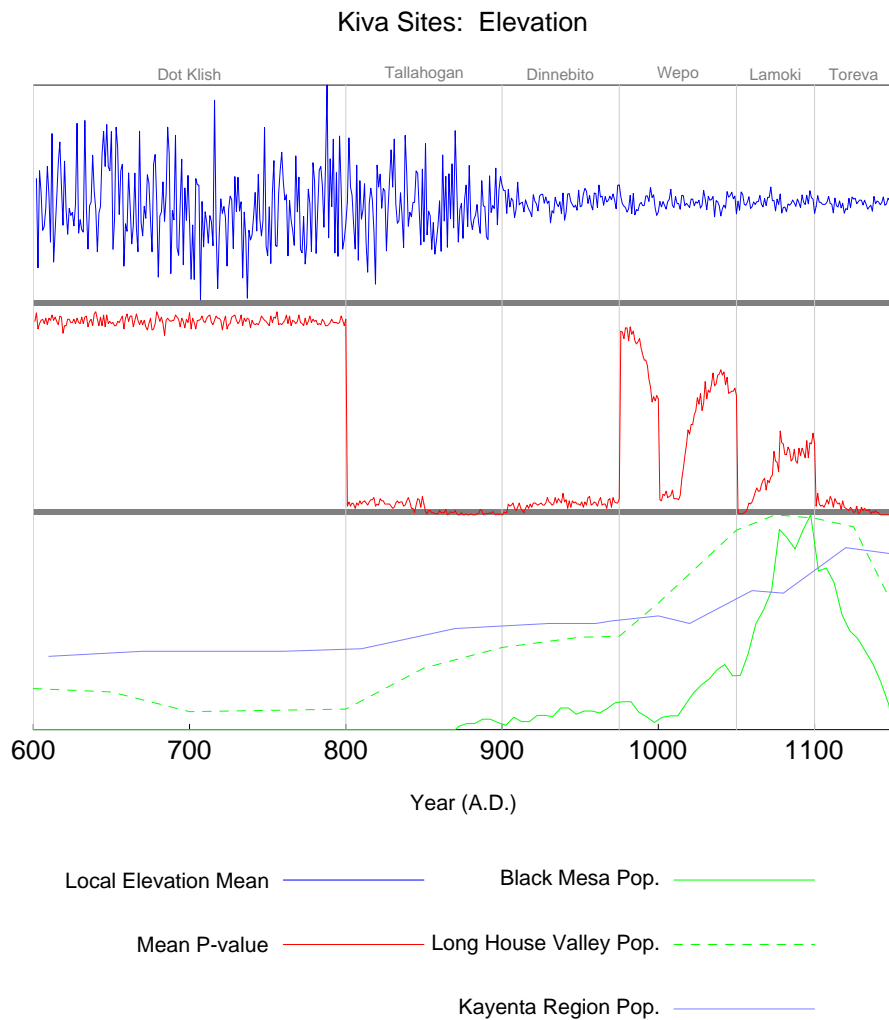


Figure H.16: Elevation Data Analysis for Kiva Sites

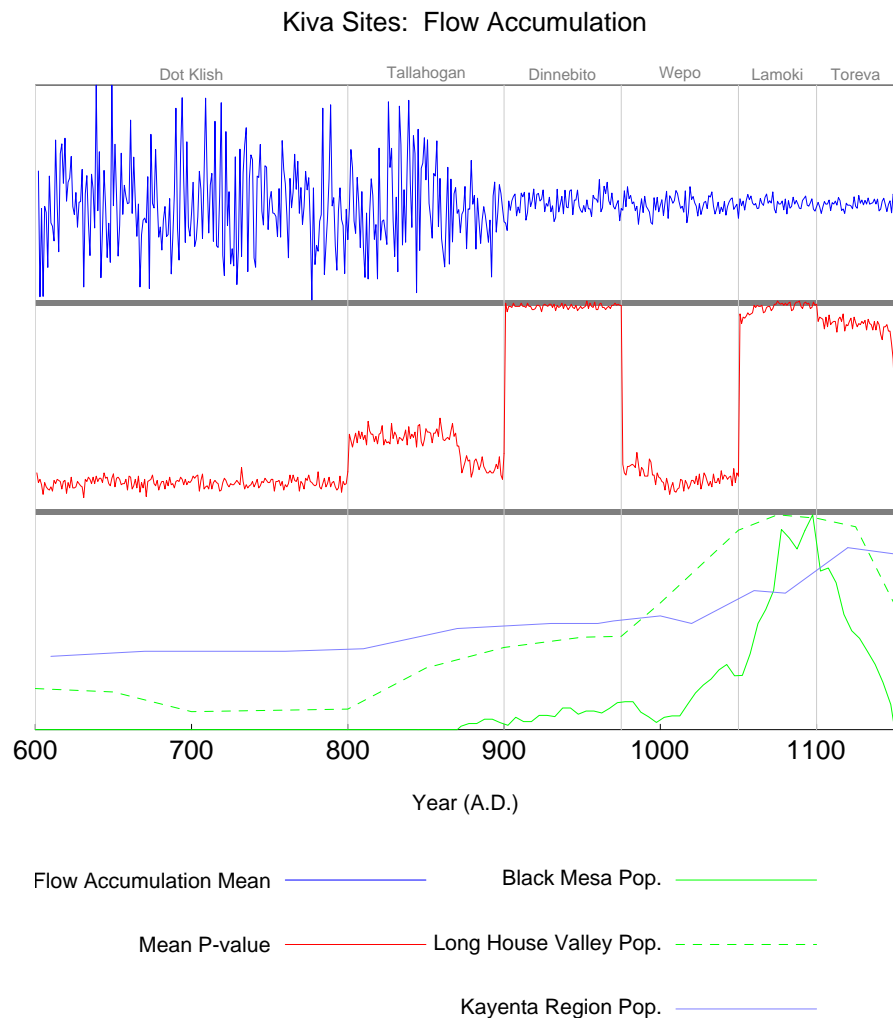


Figure H.17: Flow Accumulation Data Analysis for Kiva Sites

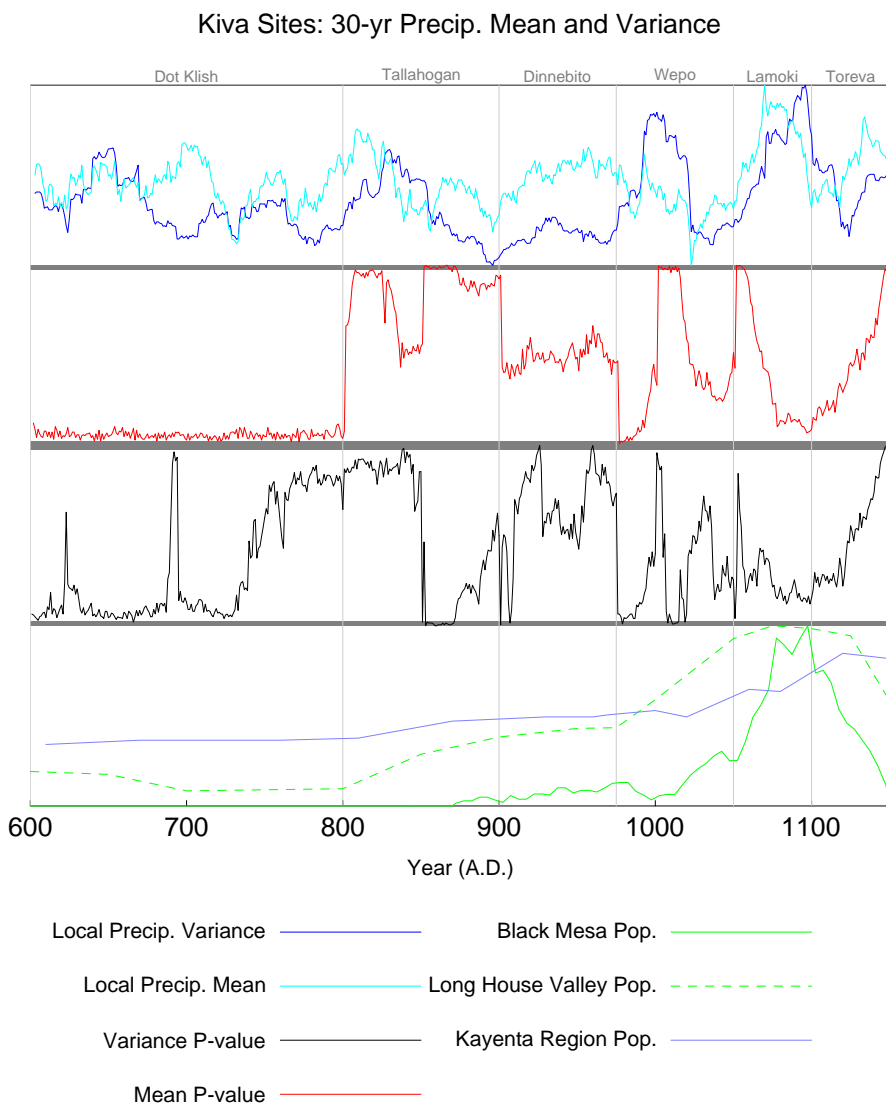


Figure H.18: Precipitation Data Analysis for Kiva Sites

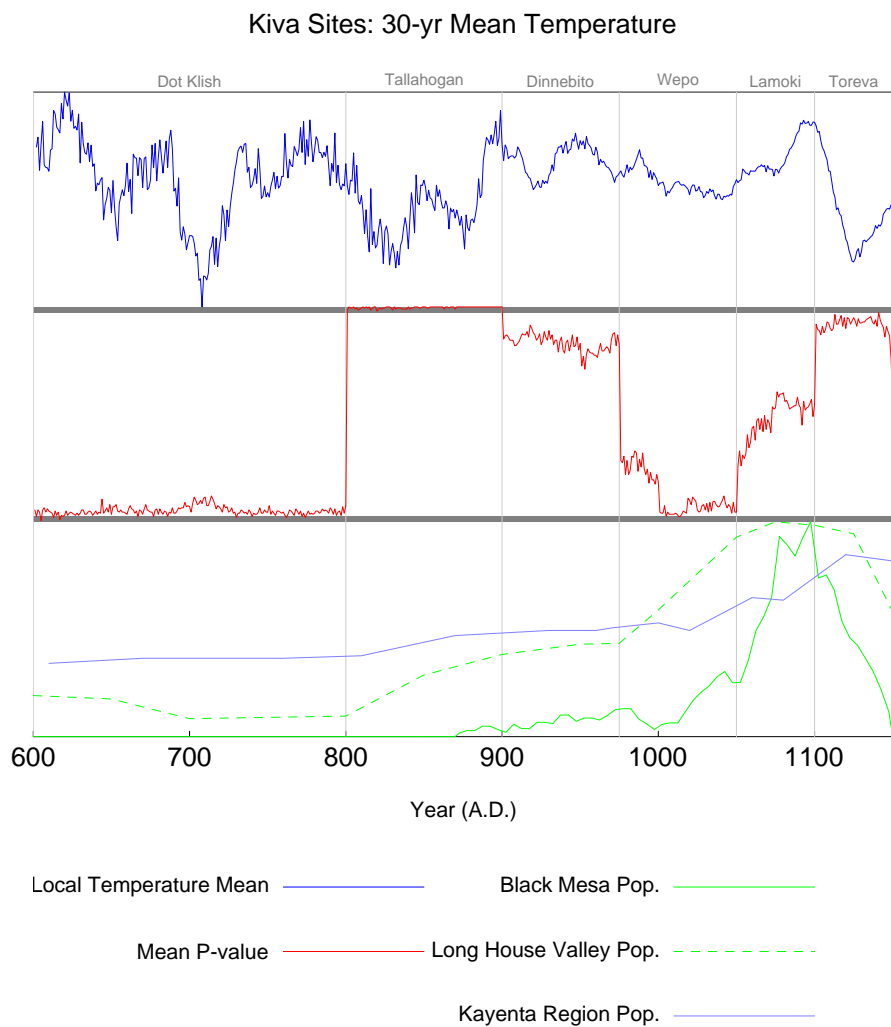


Figure H.19: Temperature Data Analysis for Kiva Sites

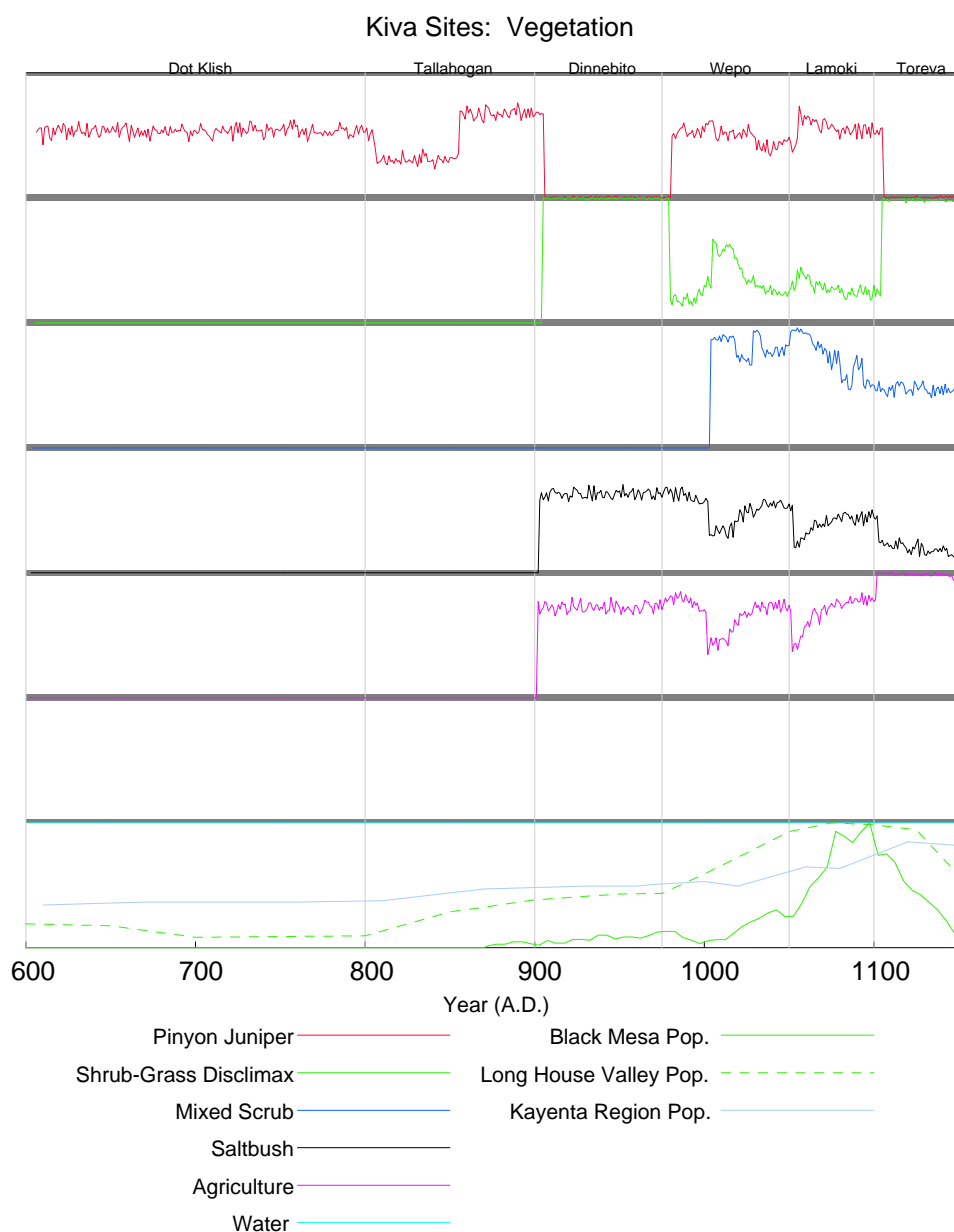


Figure H.20: Vegetation Data Analysis for Kiva Sites

H.5 Sites with Storage

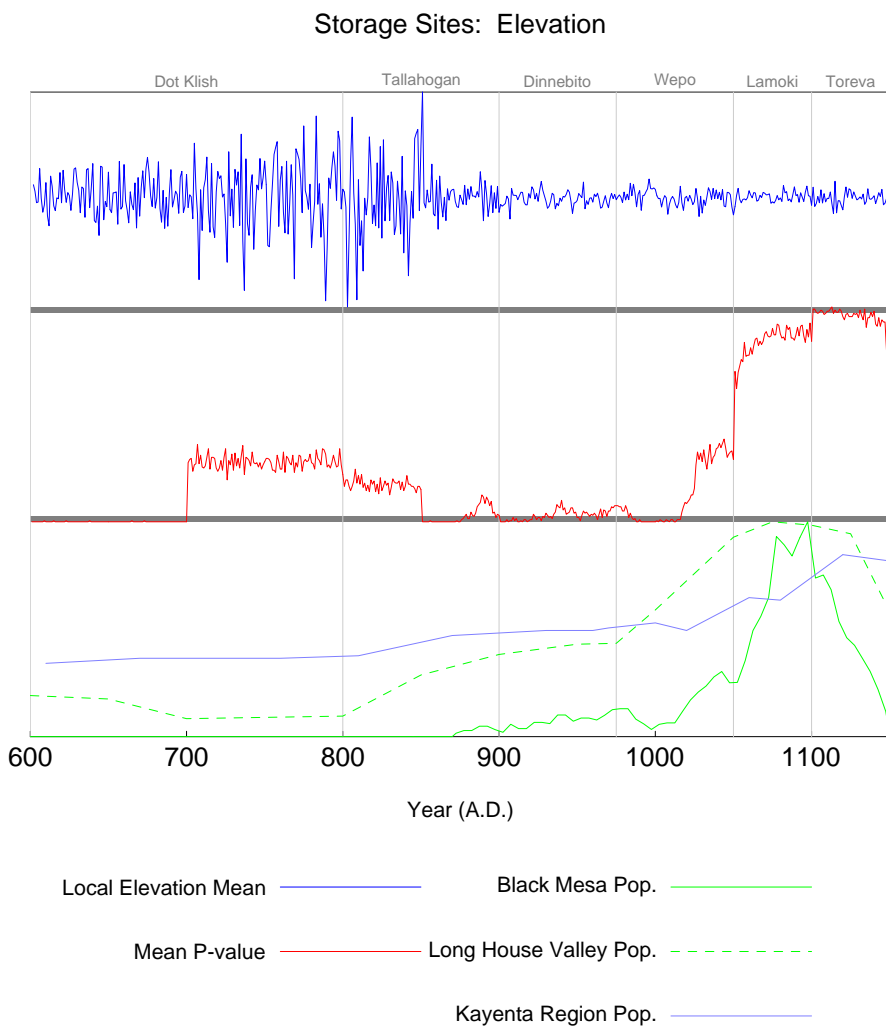


Figure H.21: Elevation Data Analysis for Storage Sites

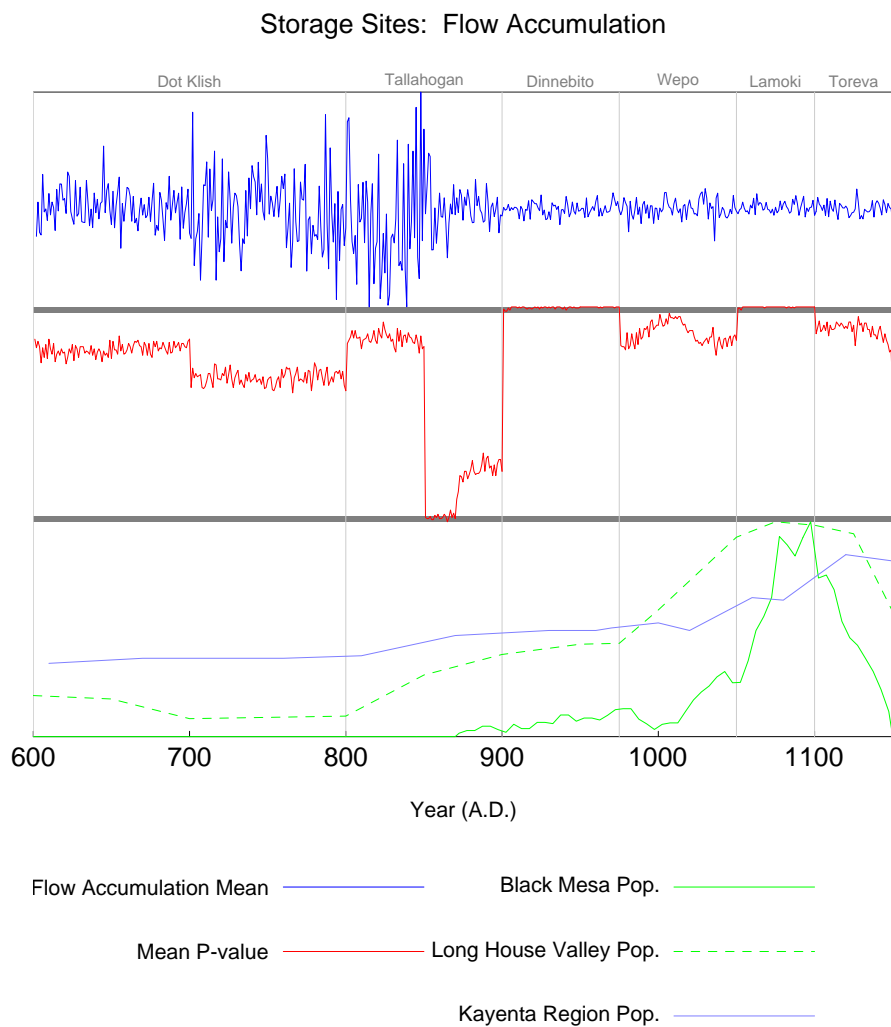


Figure H.22: Flow Accumulation Data Analysis for Storage Sites

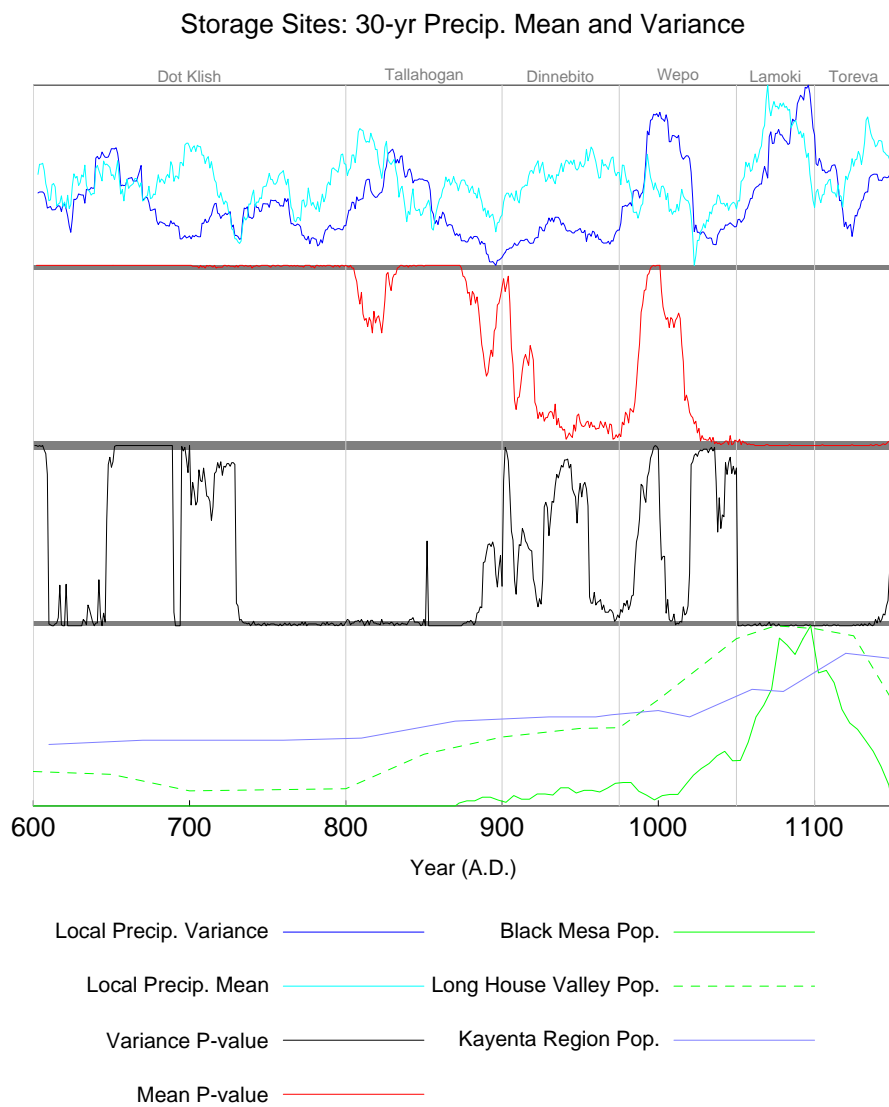


Figure H.23: Precipitation Data Analysis for Storage Sites

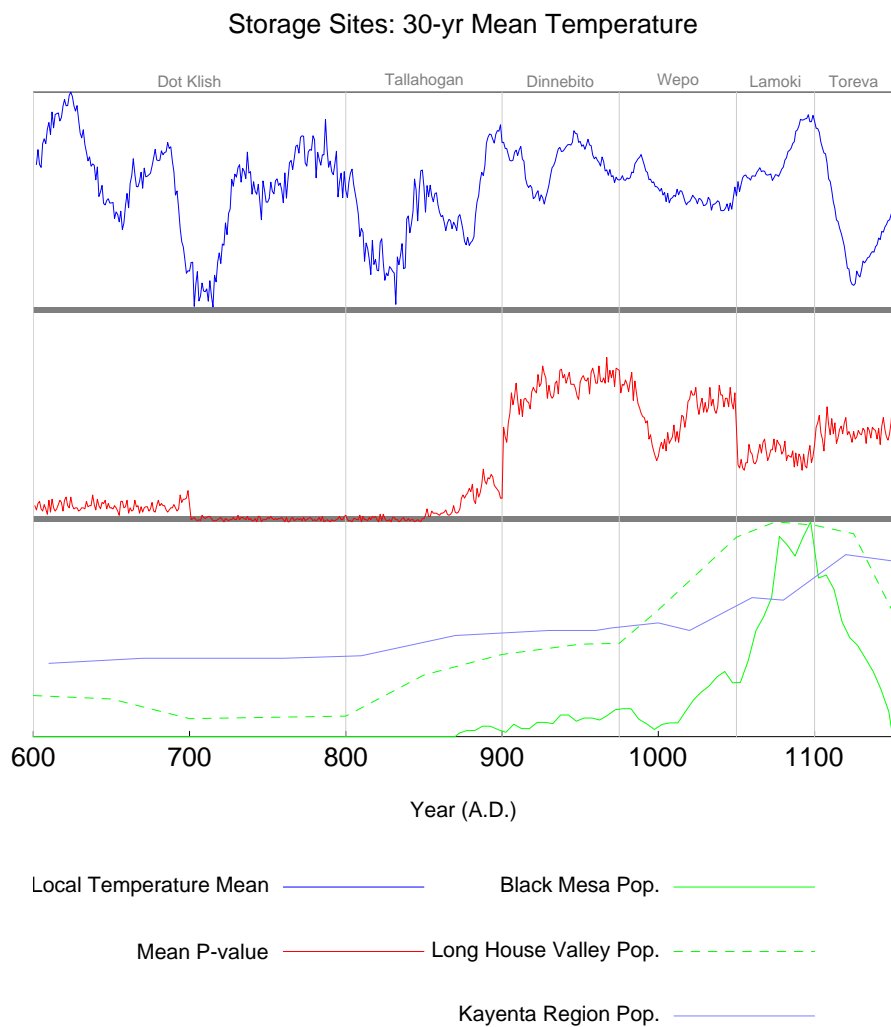


Figure H.24: Temperature Data Analysis for Storage Sites

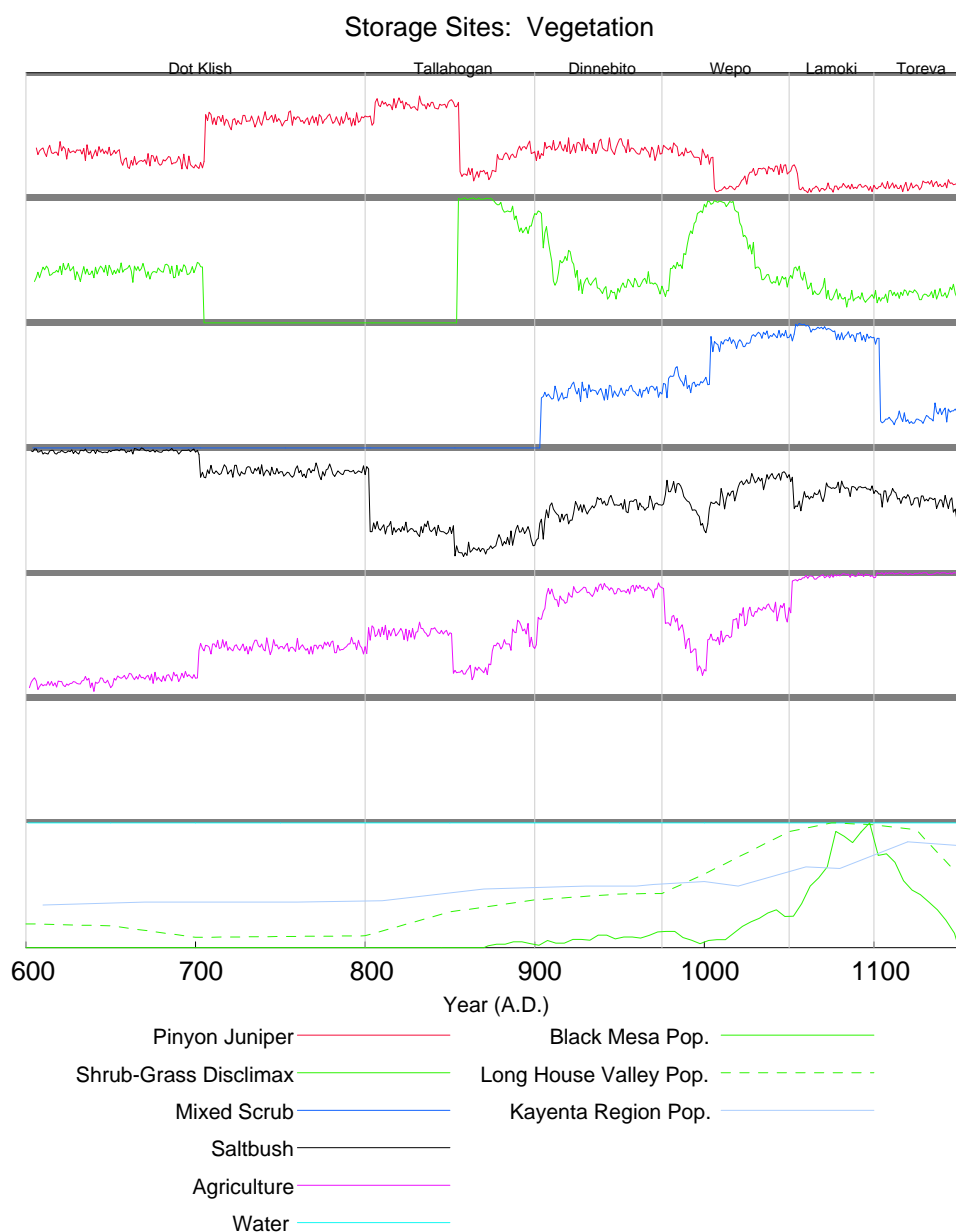


Figure H.25: Vegetation Data Analysis for Storage Sites

H.6 Lithic Sites

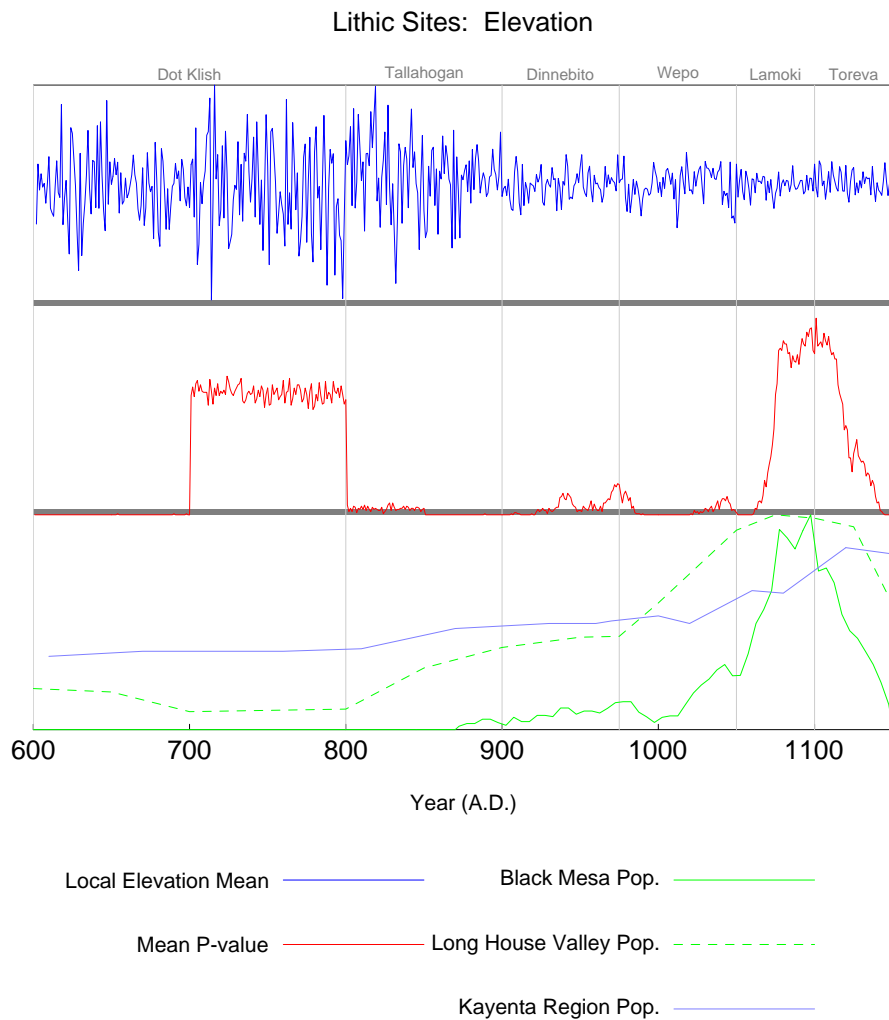


Figure H.26: Elevation Data Analysis for Lithic Sites

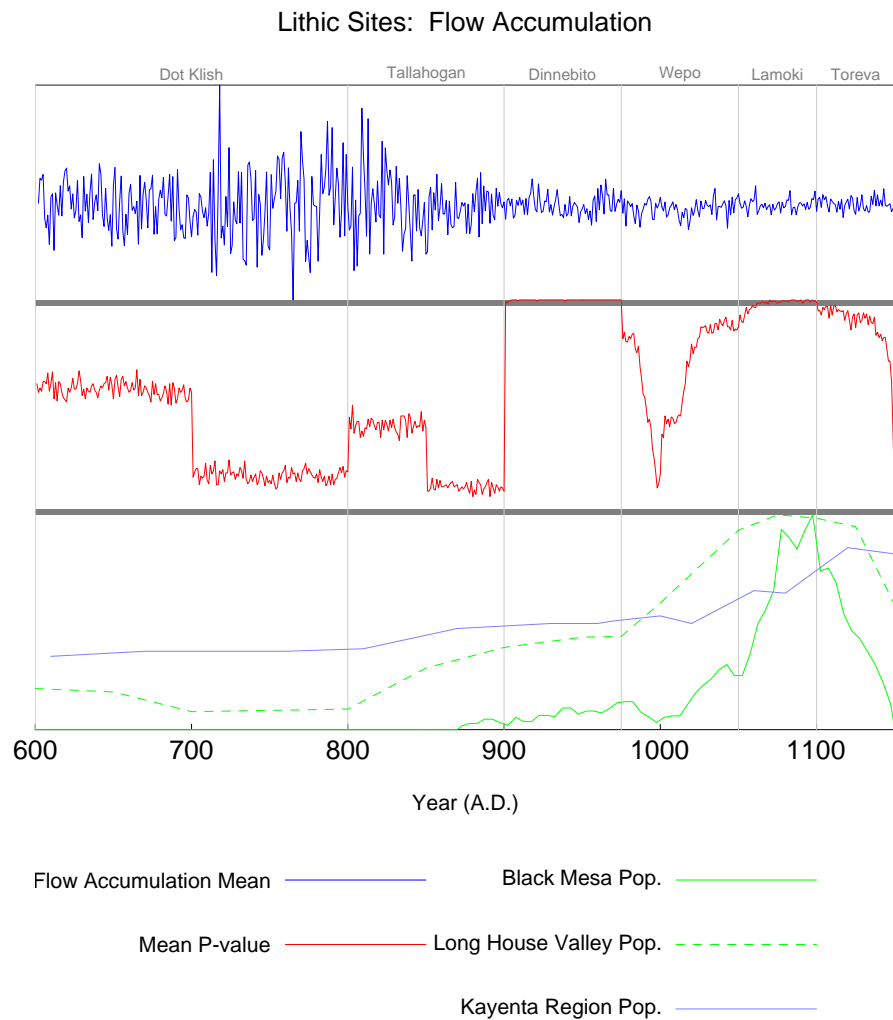


Figure H.27: Flow Accumulation Data Analysis for Lithic Sites

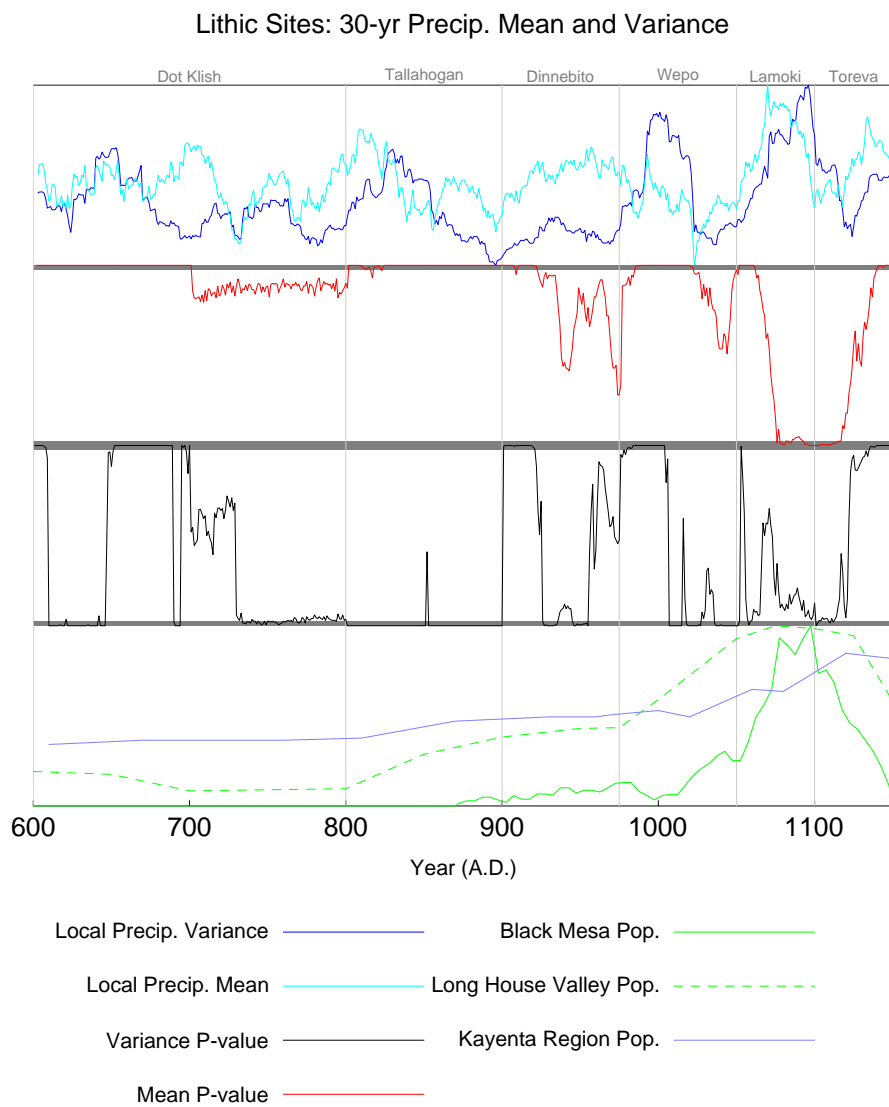


Figure H.28: Precipitation Data Analysis for Lithic Sites

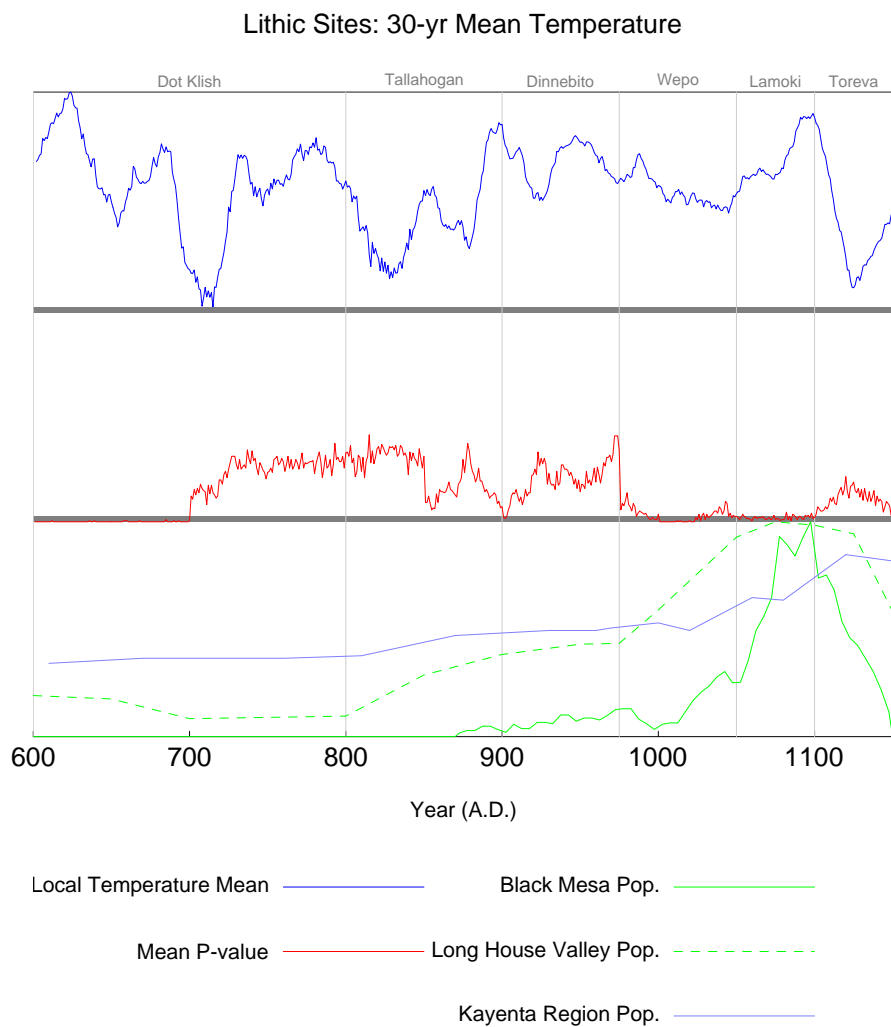


Figure H.29: Temperature Data Analysis for Lithic Sites

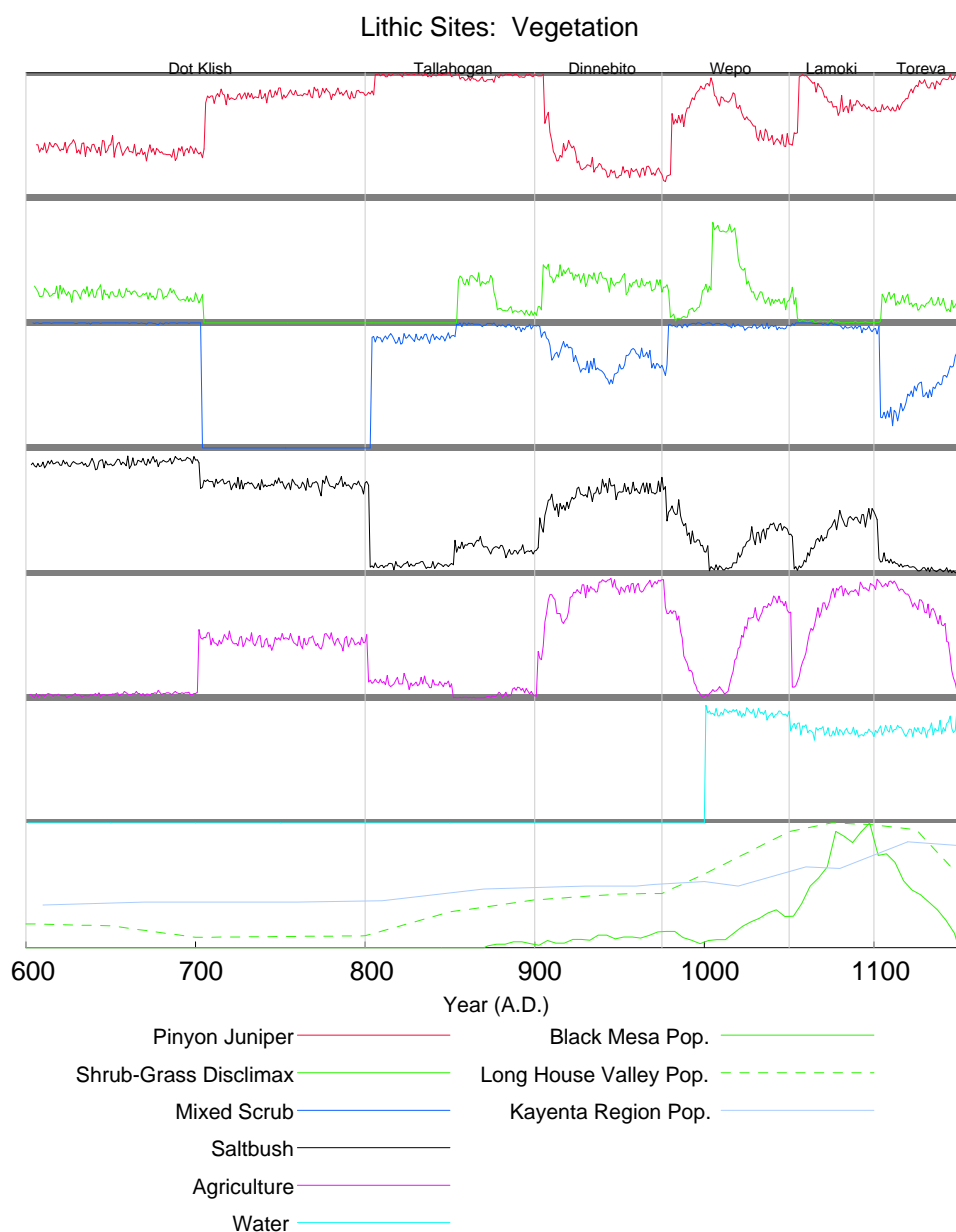


Figure H.30: Vegetation Data Analysis for Lithic Sites

H.7 Groundstone Sites

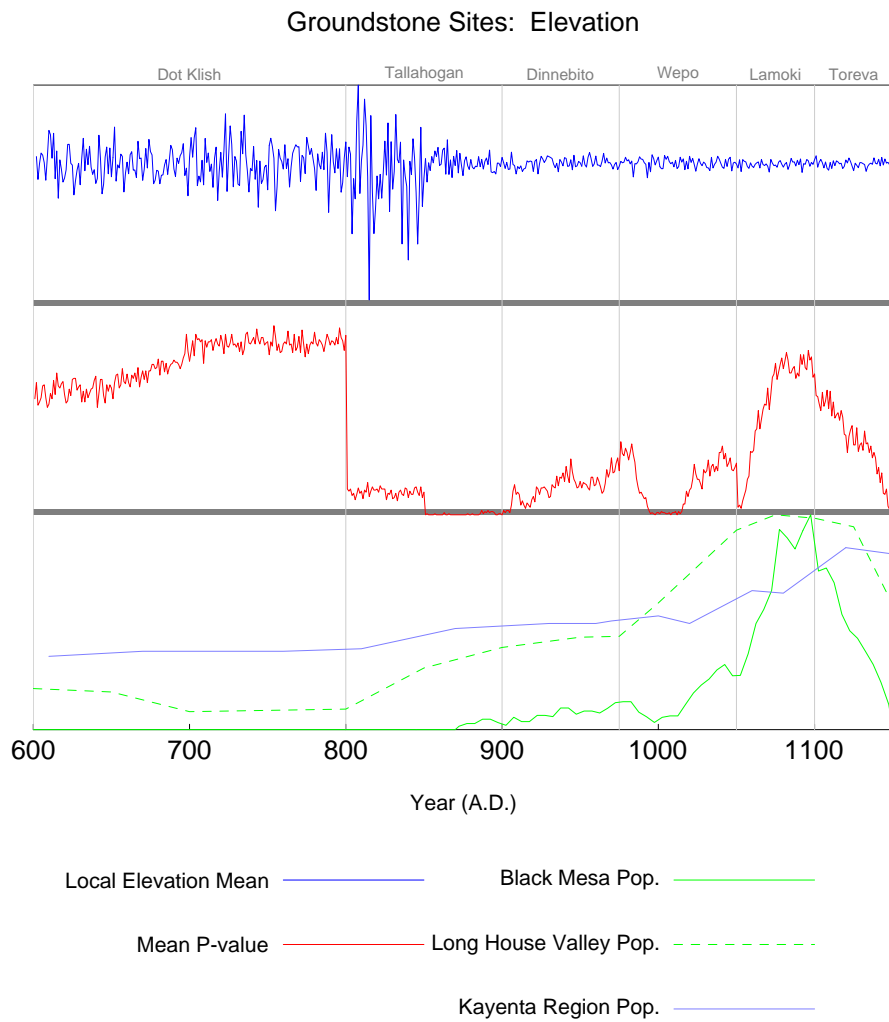


Figure H.31: Elevation Data Analysis for Groundstone Sites

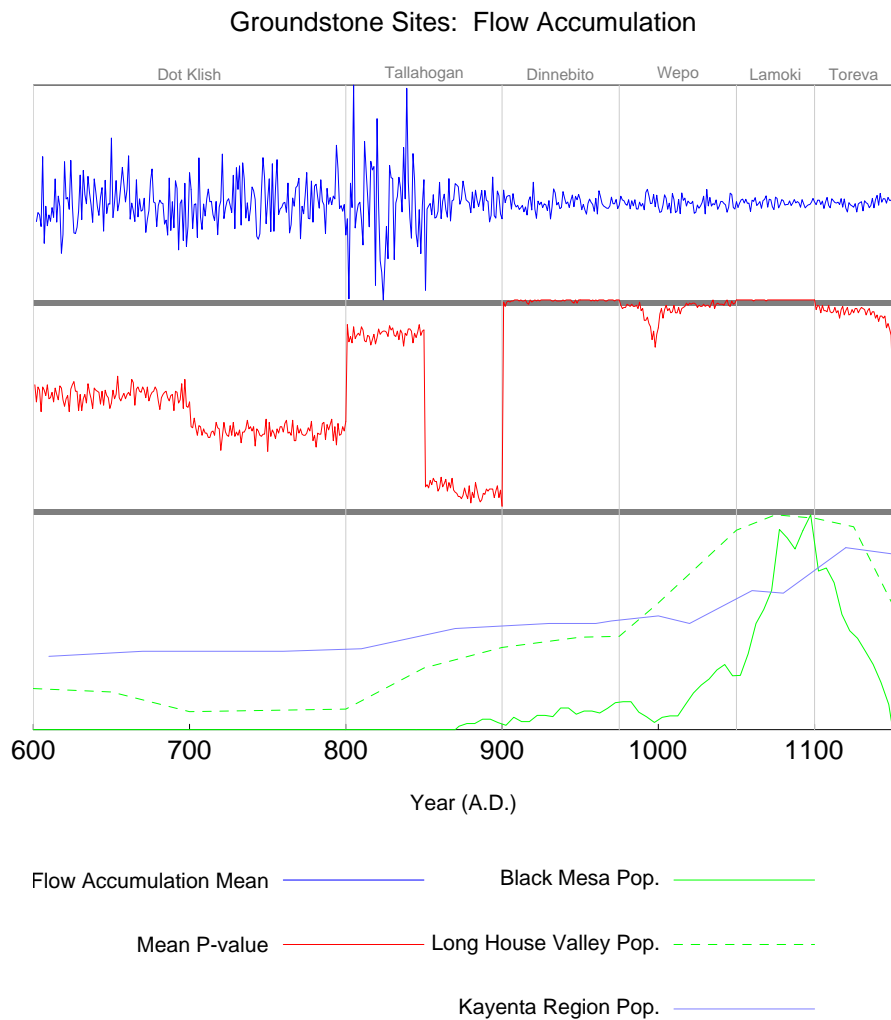


Figure H.32: Flow Accumulation Data Analysis for Groundstone Sites

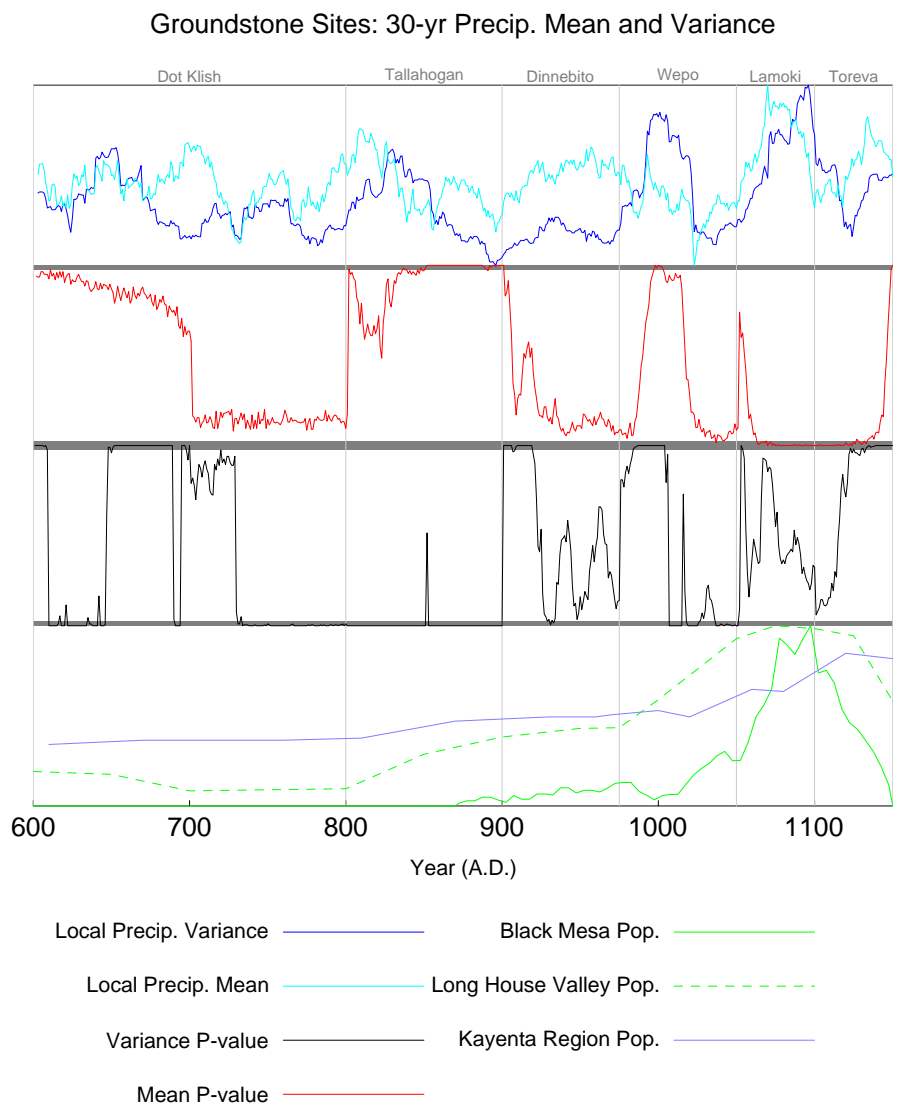


Figure H.33: Precipitation Data Analysis for Groundstone Sites

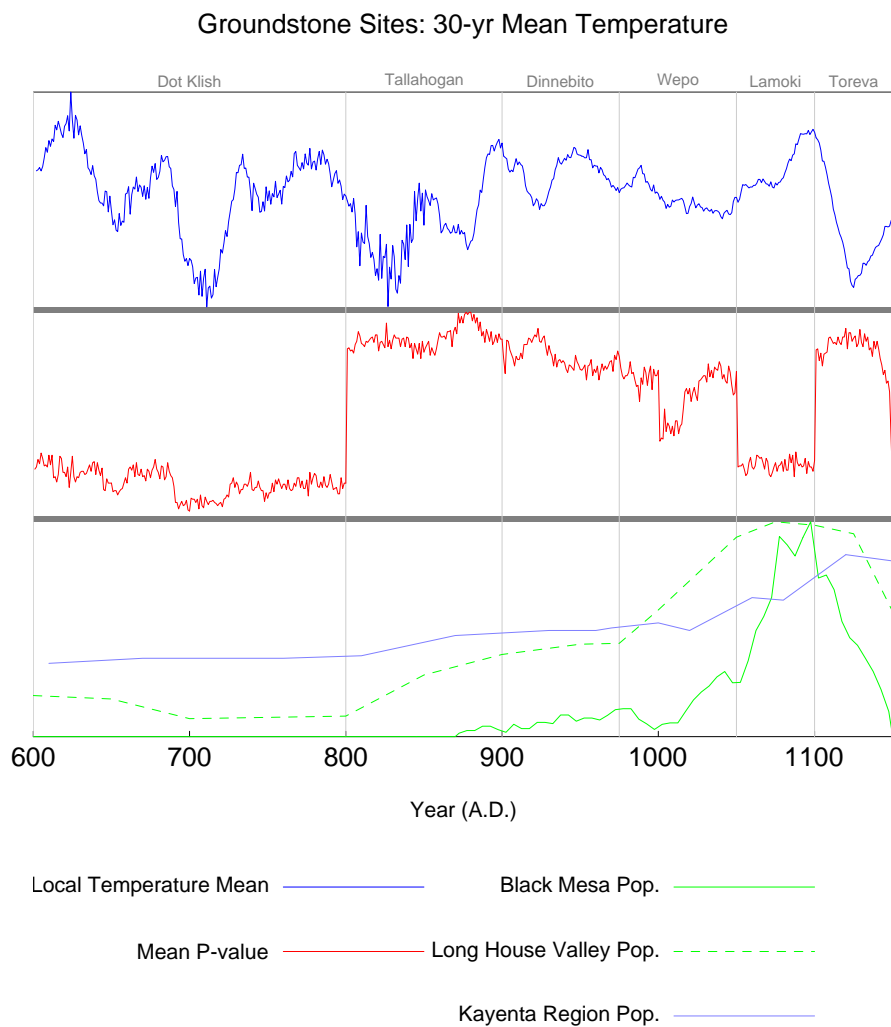


Figure H.34: Temperature Data Analysis for Groundstone Sites

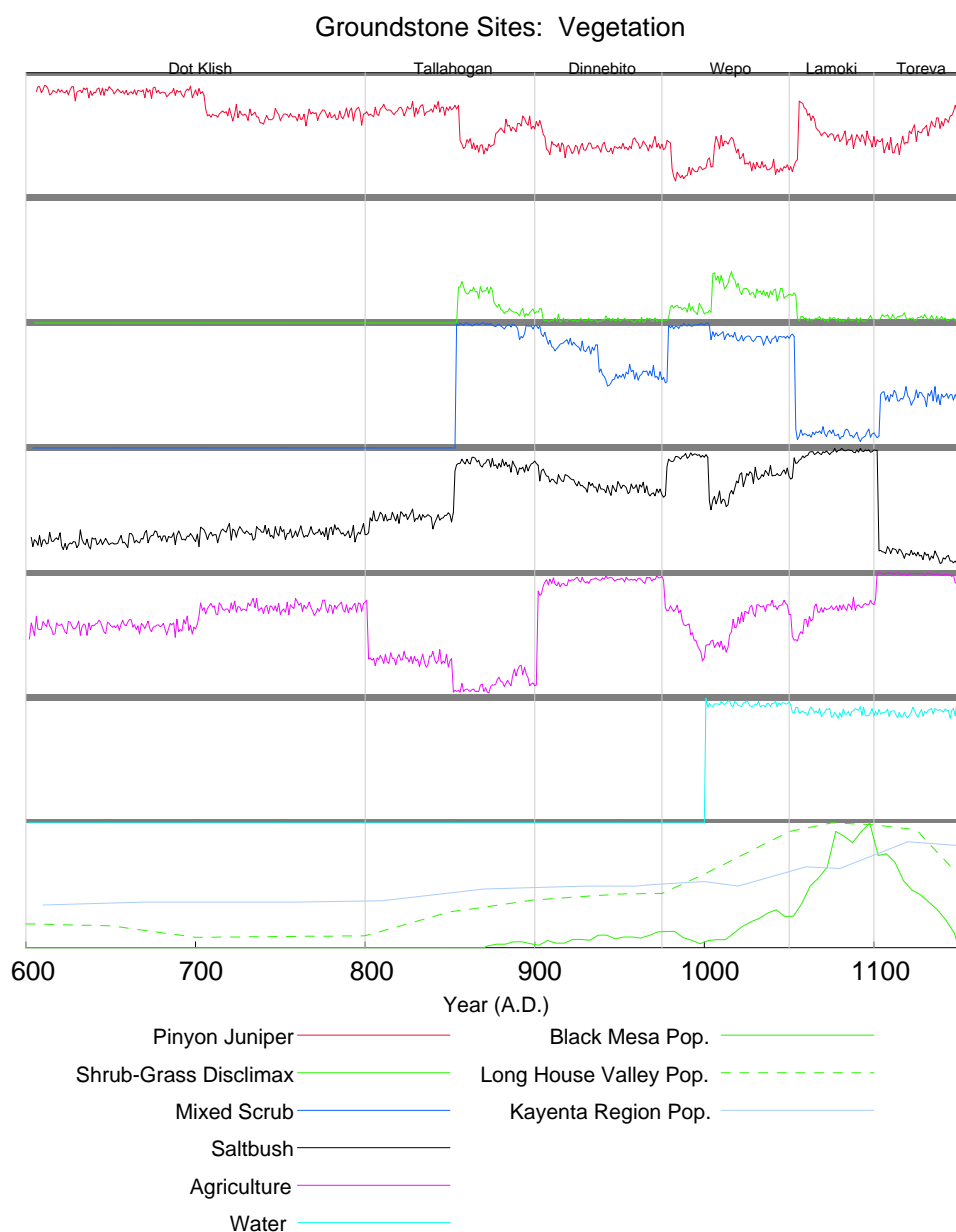


Figure H.35: Vegetation Data Analysis for Groundstone Sites

Appendix I

Mean Precipitation Plots

The plots presented in the following figures represent annual 30-year moving mean values for precipitation over the analysis region. The color gradient in each plot ranges from low (red) to high (blue), with the range standardized *within* each plot to the range of values *for that year*. This scaling of values is intended to emphasize the spatial gradient of average precipitation for each year independent of absolute value. For plots representing the local average 30-year moving average, refer to the plots in Appendix H.

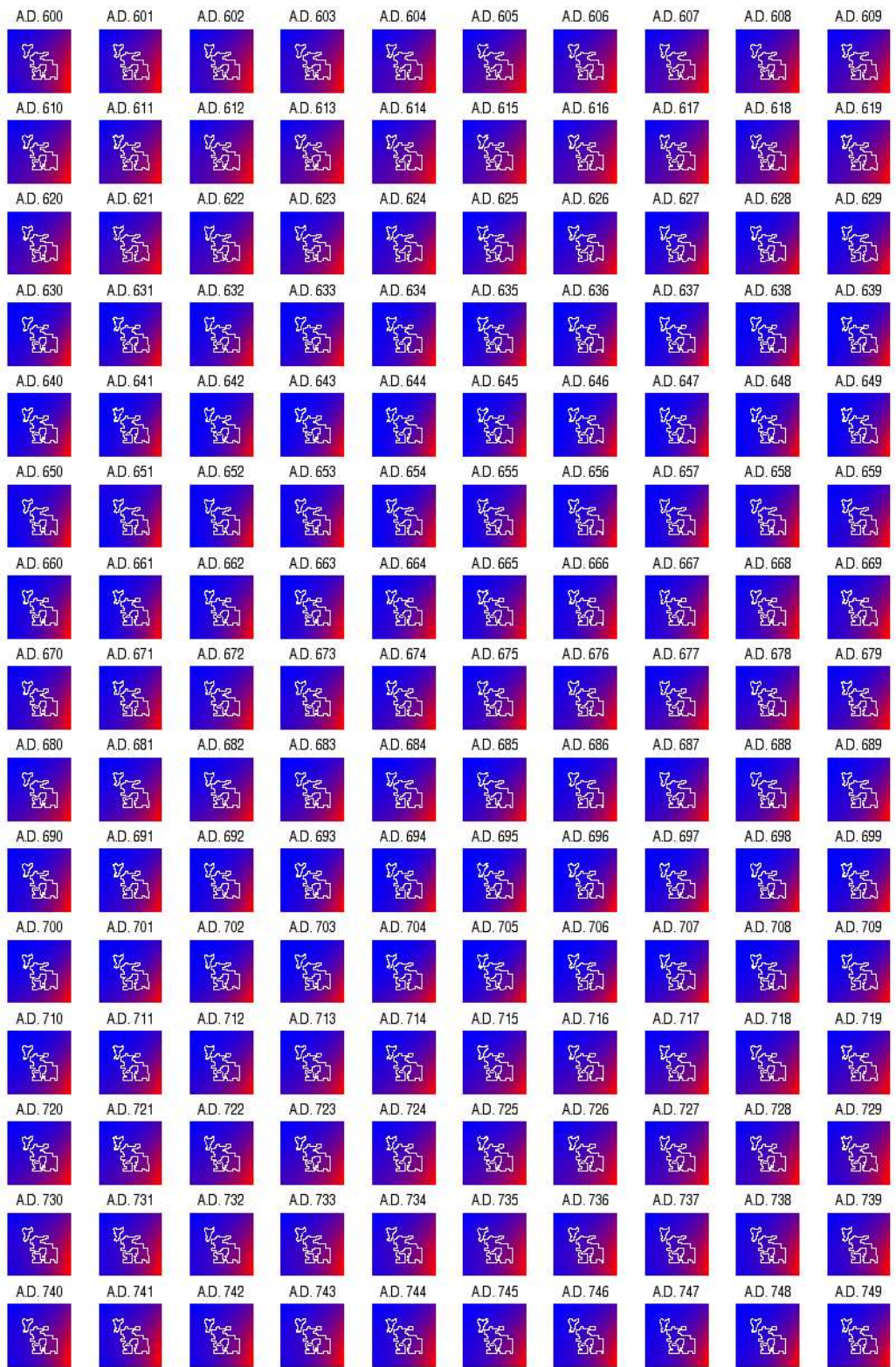


Figure I.1: Analysis Area Mean Precipitation: A.D. 600 – 749

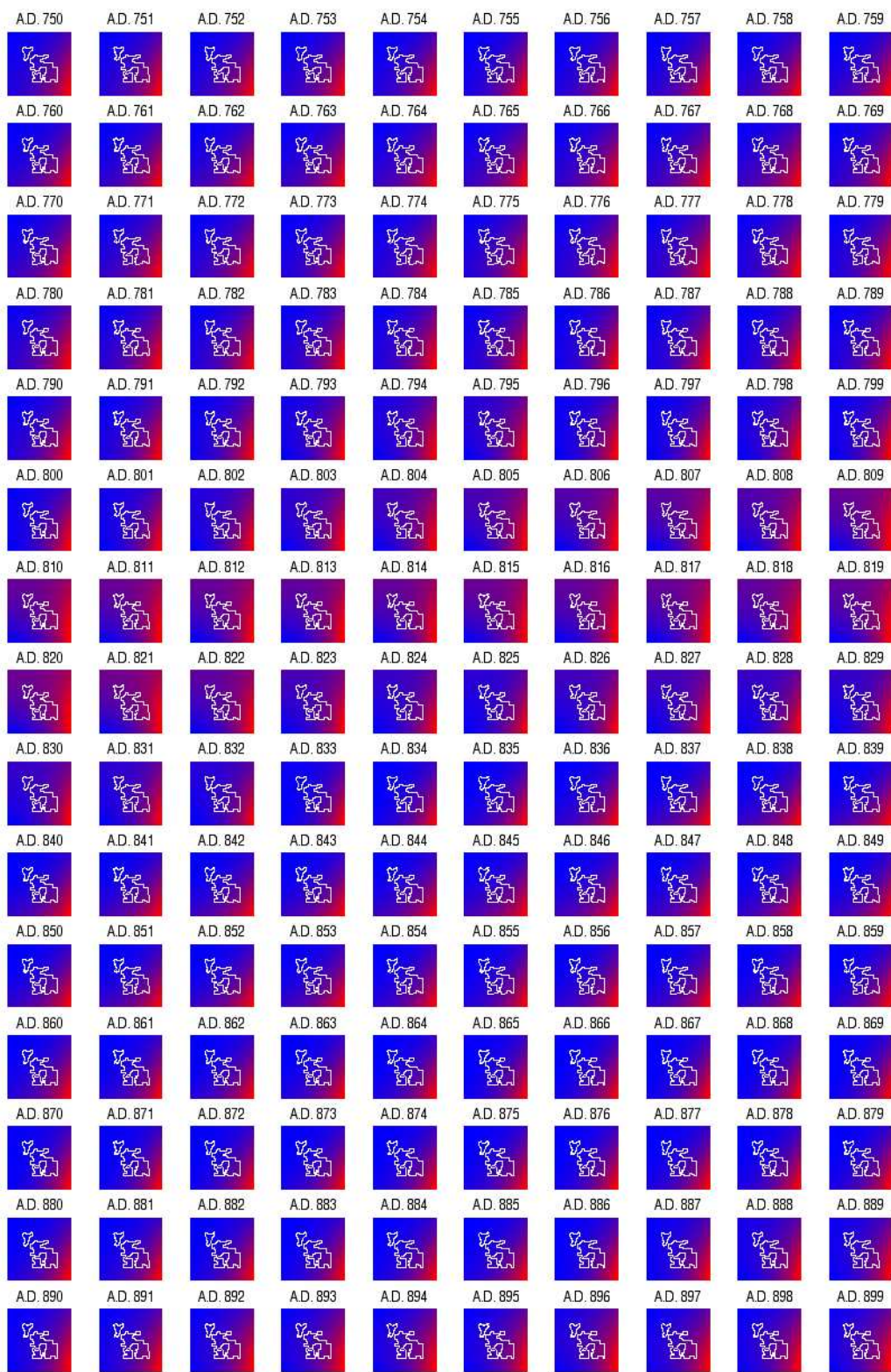


Figure I.2: Analysis Area Mean Precipitation: A.D. 750 – 899

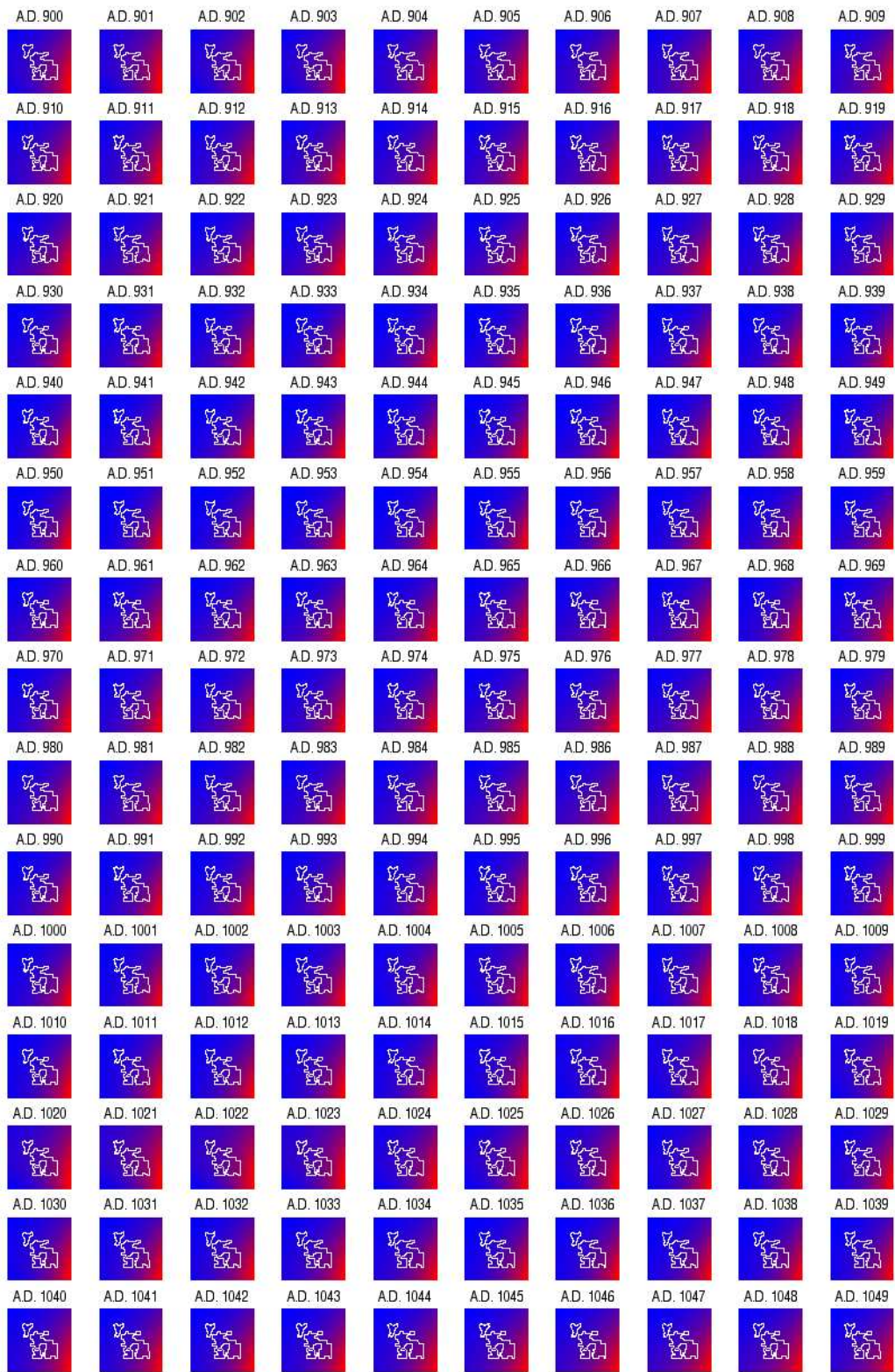


Figure I.3: Analysis Area Mean Precipitation: A.D. 900 – 1049

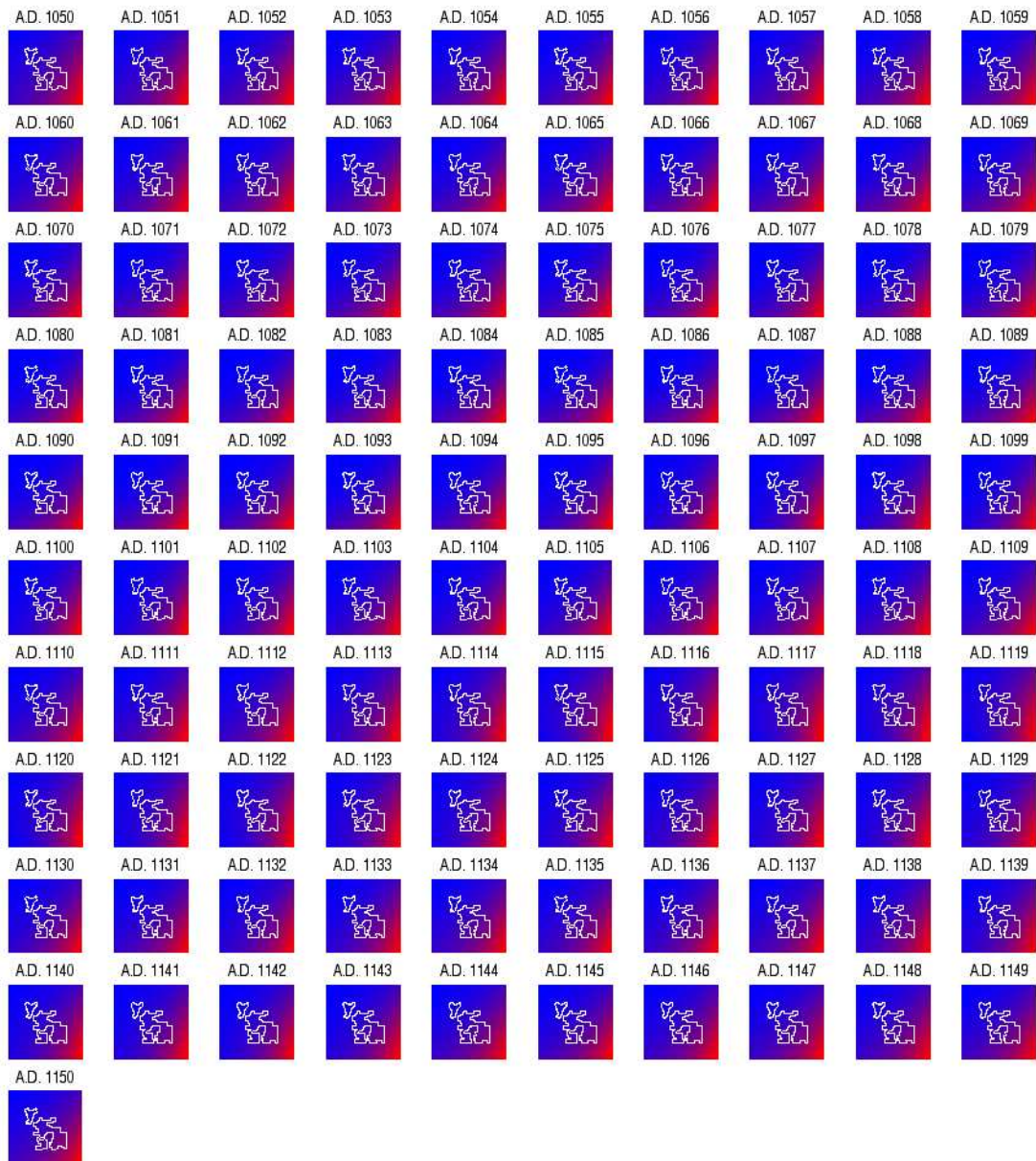


Figure I.4: Analysis Area Mean Precipitation: A.D. 1050 – 1150

Appendix J

Precipitation Variance Plots

The plots presented in the following figures represent annual 30-year moving variance values for precipitation over the analysis region. The color gradient in each plot ranges from low (red) to high (blue), with the range standardized *within* each plot to the range of values *for that year*. This scaling of values is intended to emphasize the spatial gradient of variance for each year independent of absolute value. For plots representing the local average 30-year moving variance, refer to the plots in Appendix H.

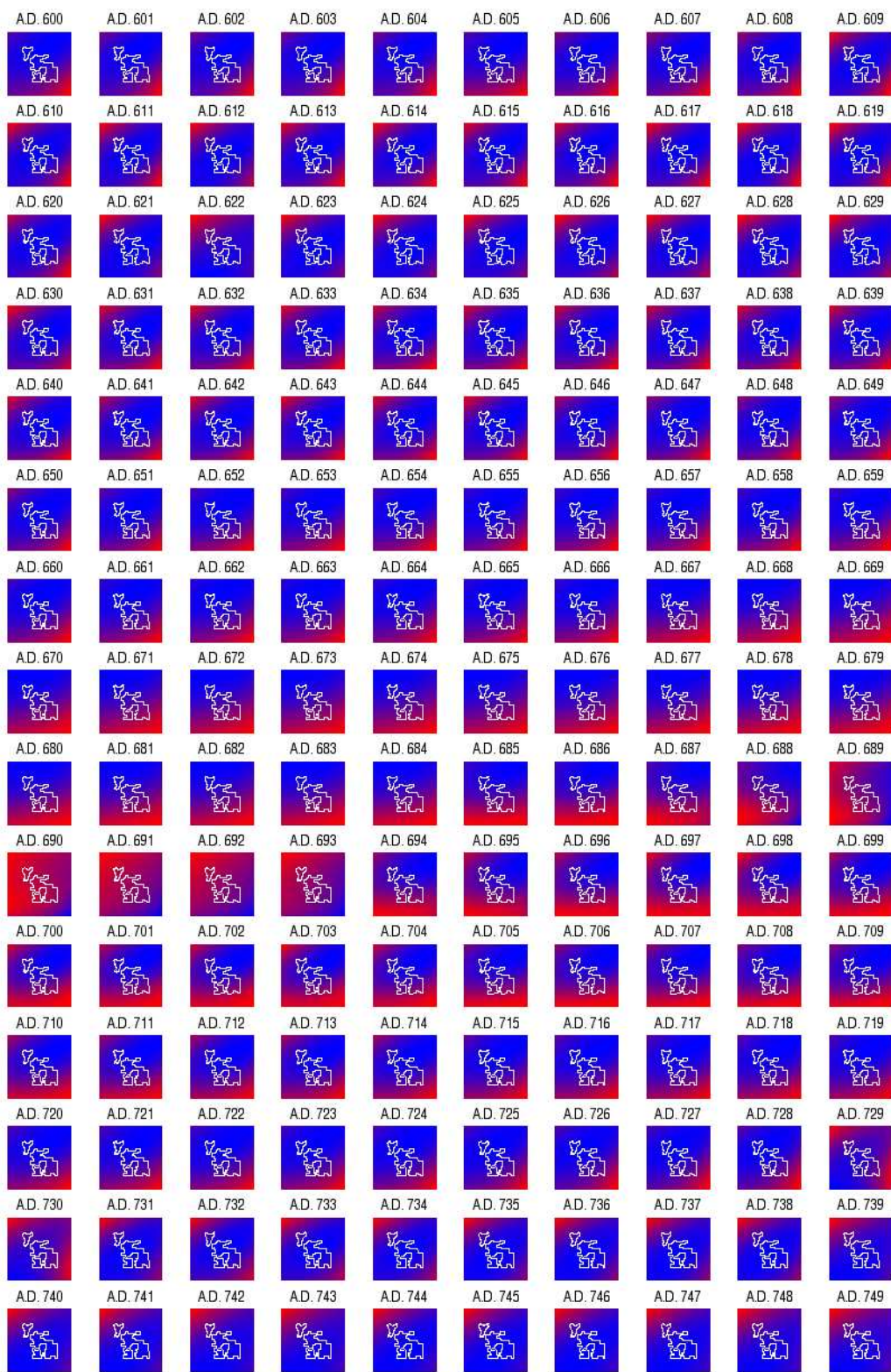


Figure J.1: Analysis Area Precipitation Variance: A.D. 600 – 749

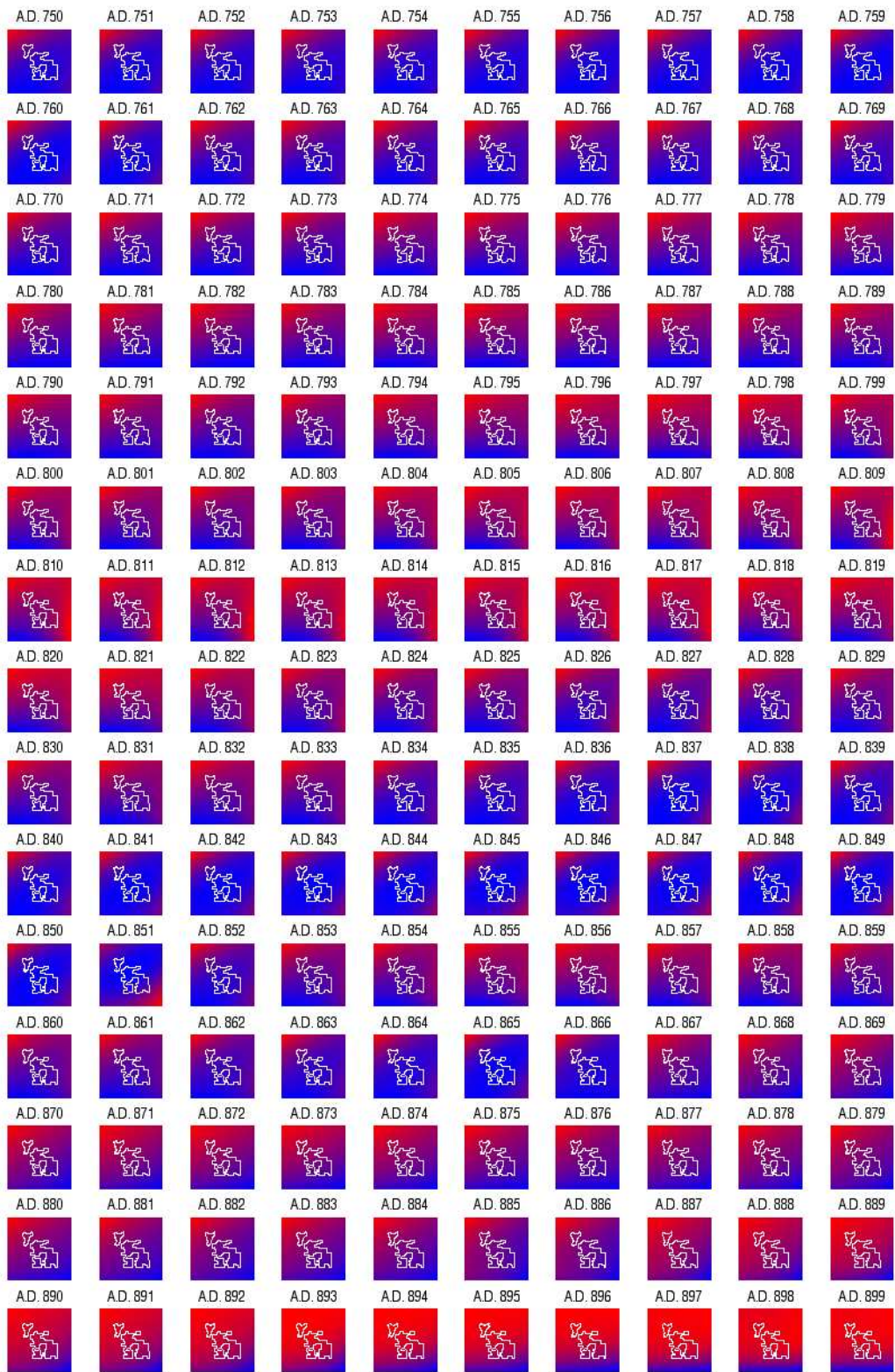


Figure J.2: Analysis Area Precipitation Variance: A.D. 750 – 899

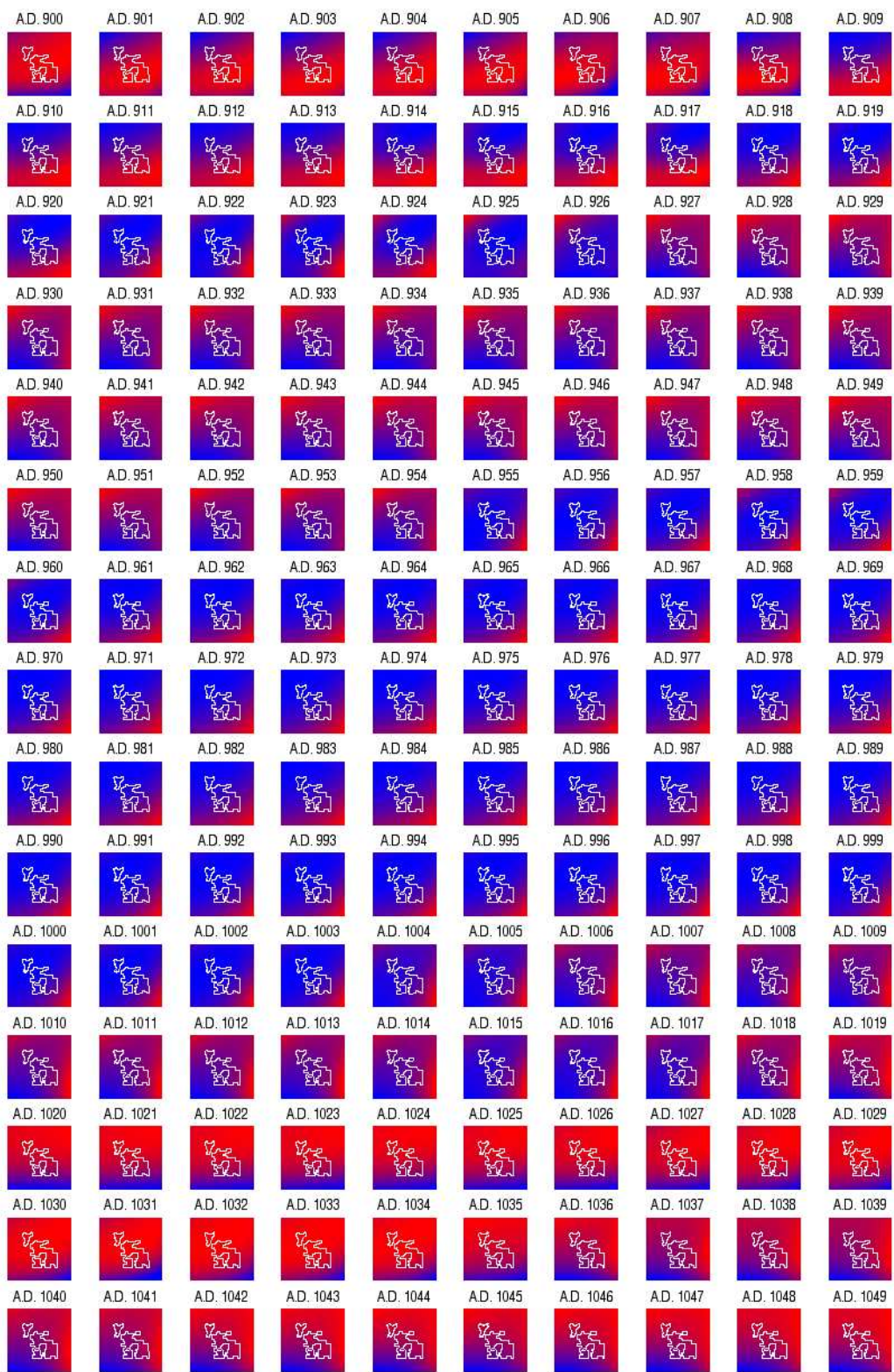


Figure J.3: Analysis Area Precipitation Variance: A.D. 900 – 1049

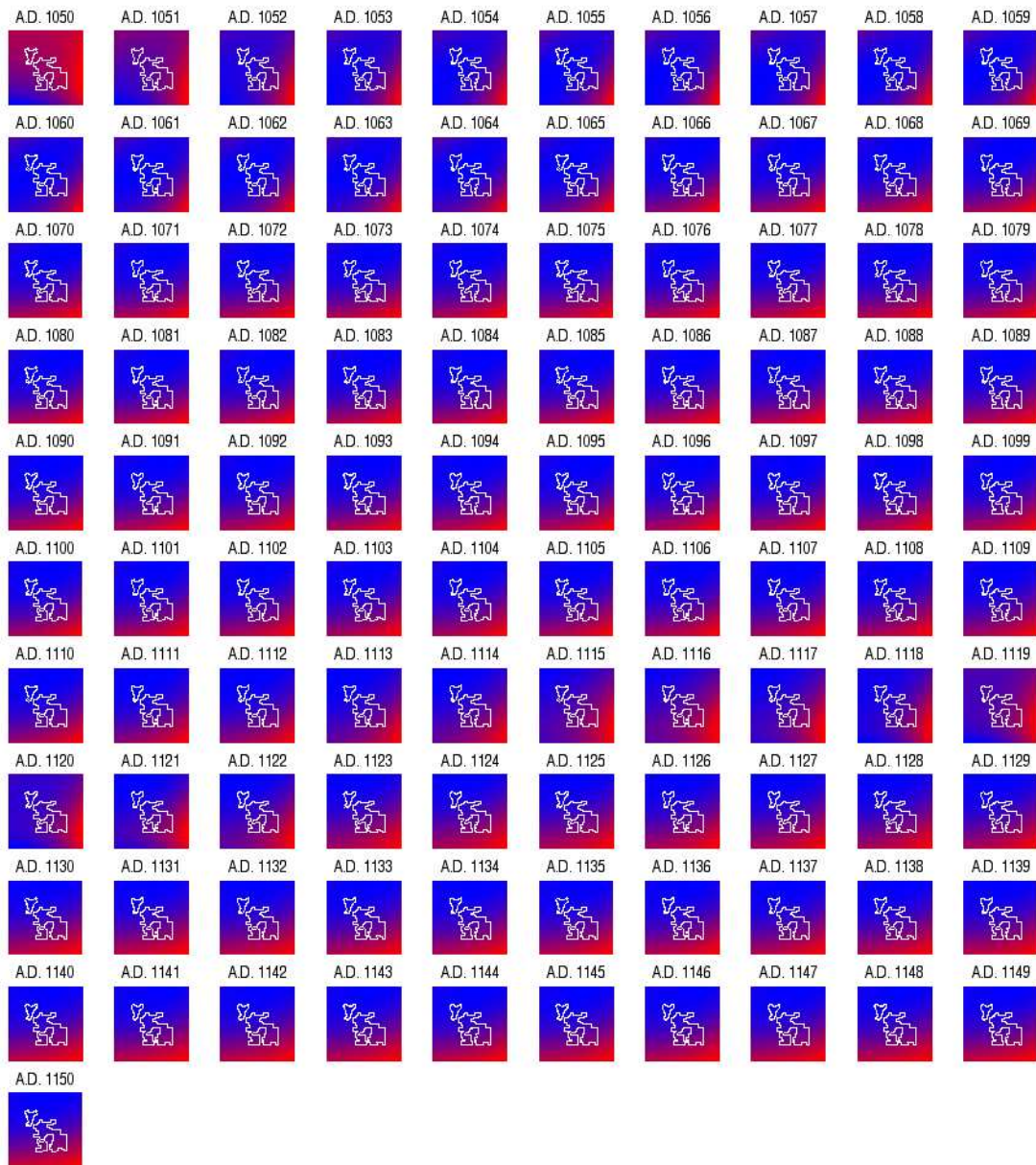


Figure J.4: Analysis Area Precipitation Variance: A.D. 1050 – 1150

References Cited

- Andrews, P. P.
1982 Research and Culture History. In *Excavation on Black Mesa, 1980: a Descriptive Report*, edited by P. P. Andrews, R. Layhe and D. L. Nichols, pp. 39-54. Research Paper. vol. 24. Center for Archaeological Investigations, Southern Illinois University, Carbondale, Carbondale, IL.
- Ayres, J. E.
1966 A Clovis Fluted Point from the Kayenta, Arizona Area. *Plateau* 38:76-78.
- Baars, D. L.
1983 *The Colorado Plateau, a Geologic History*. University of New Mexico Press, Albuquerque.
- Bailey, T. C. and A. C. Gatrell
1995 *Interactive Spatial Data Analysis*. Longman Scientific & Technical, Essex, England.
- Bannister, B., J. S. Dean and E. A. M. Gell
1966 *Tree-Ring Dates from Arizona E, Chinle-De Chelly-Red Rock Area*. Laboratory of Tree-Ring Research, University of Arizona, Tucson, Arizona.
- Bannister, B., J. S. Dean and W. J. Robinson
1968 *Tree-Ring Dates from Arizona C-D, Eastern Grand Canyon-Tsegi Canyon-Kayenta Area*. Laboratory of Tree-Ring Research, University of Arizona, Tucson, Arizona.
- 1969 *Tree-Ring Dates from Utah S-W, Southern Utah Area*. Laboratory of Tree-Ring Research, University of Arizona, Tucson, Arizona.
- Barry, R. G.
1992 *Mountain Weather and Climate*. 2nd ed. Routledge, New York.

- Beaumont, E. C. and G. H. Dixon
1965 *Geology of the Kayenta and Chilchinbito Quadrangles, Navajo County, Arizona*. Contributions to Economic Geology, Geological Survey Bulletin 1202-A. US Department of Interior, Geological Survey, US Government Printing Office, Washington D. C.
- Bell, S. B. M., A. R. Chadwick, P. R. Cooper, M. D. C, M. O'Connell and P. A. V. Young
1990 Handling four Dimensional Geo-Coded Data. Paper presented at the Proceedings of the 4th International Symposium on Spatial Data Handling, Zurich, Switzerland.
- Berry, C. F. and M. S. Berry
1986 Chronological and Conceptual Models of the Southwestern Archaic. In *Anthropology of the Desert West: Essays in Honor of Jesse D. Jennings*, edited by C. J. Condie and D. D. Fowler, pp. 252-327. Anthropological Papers. vol. 110. University of Utah Press, Salt Lake City, UT.
- Binford, L.
1980 Willow Smoke and Dog's Tails: Hunter-Gatherer Settlement Systems and Archaeological Site Formation. *American Antiquity* 45:4-20.
- Black Mesa Archaeological Project
1977 Vegetation Transect Field Notes, Original field notes on file at the Center for Archaeological Investigations, SIU Carbondale.
- 1978 Vegetation Transect Field Notes, Original field notes on file at the Center for Archaeological Investigations, SIU Carbondale.
- 1980 Vegetation Transect Field Notes, Original field notes on file at the Center for Archaeological Investigations, SIU Carbondale.
- 1981 Vegetation Transect Field Notes, Original field notes on file at the Center for Archaeological Investigations, SIU Carbondale.
- 1982 Vegetation Transect Field Notes, Original field notes on file at the Center for Archaeological Investigations, SIU Carbondale.
- 1983 Vegetation Transect Field Notes, Original field notes on file at the Center for Archaeological Investigations, SIU Carbondale.
- Boughey, A. S.
1973 *Ecology of Populations*. 2nd ed. Collier-Macmillan Publishers, London.
- Bradfield, M.
1971 *The Changing Pattern of Hopi Agriculture*. Royal Anthropological Institute of Great Britain and Ireland, London.

Brannon, P. A., B. Cummings, F.-C. Cole, J. A. MacLean, C. R. Keyes, W. B. Hinsdale, W. M. Babcock, L. Bloom, A. C. Parker, W. C. Mills, J. B. Thoburn, F. Dorrance, W. H. Over, P. E. Cox, J. E. Pearce, A. A. Kerr, C. E. Brown, H. I. Smith, C. Wissler, R. H. Lowie, M. E. Ashley, G. G. Heye, M. M. Judd, C. C. Willoughby, F. G. Speck, H. S. Colton, W. K. Moorehead, W. Bradfield, H. S. Gladwin, V. J. Smith, J. W. Fewkes and A. V. Kidder

1927 Archaeological Field Work in North America During 1926. *American Anthropologist* 29(2):313-337.

Braun, D. P. and S. Plog

1982 Evolution of "Tribal" Social Networks: Theory and Prehistoric North American Evidence. *American Antiquity* 47(3):504-527.[10pt]

Brown, D. E.

1994a Appendix II. Scientific and Equivalent Common Names of Plants and Animals Arranged by Biomes. In *Biotic Communities of the Southwestern United States and Northwestern Mexico*, edited by D. E. Brown, pp. 316-342. University of Utah Press, Salt Lake City.

1994b *Biotic Communities, Southwestern United States and Northwestern Mexico*. University of Utah Press, Salt Lake City.

1994c Grasslands. In *Biotic Communities of the Southwestern United States and Northwestern Mexico*., edited by D. E. Brown, pp. 107-142. University of Utah Press, Salt Lake City.

1994d Great Basin Conifer Woodland. In *Biotic Communities of the Southwestern United States and Northwestern Mexico*., edited by D. E. Brown, pp. 52-57. University of Utah Press, Salt Lake City.

Brown, D. E. and C. H. Lowe

1994a *Biotic Communities of the Southwest*. University of Utah Press, Salt Lake City.

1994b *Biotic Communities of the Southwest - GIS Coverage Created by the Arizona Game and Fish Department*. University of Utah Press, Salt Lake City.

Brown, D. E., C. H. Lowe and C. P. Pase

1979 A Digitized Classification System for the Biotic Communities of North America, With Community (Series) and Association Examples for the Southwest. *Journal of the Arizona-Nevada Academy of Science* 14 (Suppl. 1):1-16.

Brown, J. H.

1995 *Macroecology*. University of Chicago Press, Chicago.

- Bryan, K.
- 1925 Date of Channel Trenching (Arroyo Cutting) in the Arid Southwest. *Science* 62(1607):338-344.
- 1929 Flood-water Farming. *Geographical Review* 19(3):444-456.
- 1941 Pre-Columbian Agriculture in the Southwest as Conditioned by Periods of Alluviation. *Annals of the Association of American Geographers* XXXI(4):219-242.
- Burns, B. T.
- 1983 *Simulated Anasazi Storage Behavior Using Crop Yields Reconstructed from Tree Rings: A.D. 652-1968*. Ph.D., University of Arizona.
- Cayan, D. R. and R. H. Webb
- 1992 El Nio/Southern Oscillation and Streamflow in the Western United States. In *El Nio, Historical and Paleoclimatic Aspects of the Southern Oscillation*, edited by H. F. Diaz and V. Markgraf, pp. 29-68. Cambridge University Press, Cambridge.
- Chisholm, B. and R. G. Matson
- 1994 Carbon and Nitrogen Isotopic Evidence on Basketmaker II Diet at Cedar Mesa, Utah. *Kiva* 60(2):239-255.
- Christenson, A. L.
- 1980 Change in the Human Food Niche in Response to Population Growth. In *Modeling Change in Prehistoric Subsistence Economies*, edited by T. K. Earle and A. L. Christenson, pp. 30-78. Academic Press, New York.
- 1983 Comments on Smith (1983): Anthropological Applications of Optimal Foraging Theory: A Critical Review. *Current Anthropology* 24:643-644.
- Collins, F. C. and P. V. Bolstad
- 1996 A Comparison of Spatial Interpolation Techniques in Temperature Estimation. Paper presented at the Third International Conference/Workshop on Integrating Geographic Information Systems and Environmental Modeling, Santa Fe, New Mexico.
- Cordell, L. S.
- 1997 *Archaeology of the Southwest*. Second ed. Academic Press, San Diego.
- Cowan, C. W.
- 1978 Appendix I: A Preliminary Analysis of Paleoethnobotanical Remains from Black Mesa Arizona: 1977 Season. In *Excavation on Black Mesa, 1977: a Preliminary Report*, edited by A. L. Klesert, pp. 137-156. Research Paper. vol. 1. Center for Archaeological Investigations, Southern Illinois University, Carbondale, IL.

- Csuti, B.
1996 Mapping Animal Distribution Areas for GAP Analysis. In *Gap Analysis, A Landscape Approach to Biodiversity Planning*, edited by J. M. Scott, T. H. Tear and F. W. Davis, pp. 135-145. American Society for Photogrammetry and Remote Sensing, Bethesda, Maryland.
- Csuti, B. and P. Crist
n.d. Methods for Assessing Accuracy of Animal Distribution Maps. In, Gap Analysis Handbook (Digital Manuscript). vol. 2002. Gap Analysis Project, Idaho Cooperative Fish and Wildlife Research Unit, Department of Fish and Wildlife, University of Idaho, Moscow, ID.
- Cummings, L. S.
1995 Agriculture and the Mesa Verde Area Anasazi Diet: Description and Nutritional Analysis. In *Soil, Water, Biology and Belief in Prehistoric and Traditional Southwestern Agriculture*, edited by H. W. Toll, pp. 335-352. New Mexico Archaeological Council Special Publication. vol. 2. New Mexico Archaeological Council, Albuquerque.
- Danson, E. B.
1961 Early Man Points from the Vicinity of Sanders, Arizona. *Plateau* 34(2):67-68.
- Davey, C. A. and R. A. Pielke Sr.
n.d. Microclimate Exposures of Surface-Based Weather Stations - Implications for the Assessment of Long-Term Temperature Trends, Fort Collins, CO.
- Davis, W. E.
1985 The Montgomery Folsom Site. *Current Research in the Pleistocene* 2:11-12.
1986 The Montgomery Folsom Site. *Utah Archaeology* 24(2):14-18.
- Davis, W. E. and G. M. Brown
1986a The Lime Ridge Clovis Site. *Current Research in the Pleistocene* 3:1-3.
1986b The Lime Ridge Clovis Site. *Utah Archaeology* 24(2):14-18.
- Davison, A. C. and D. V. Hinkley
1997 *Bootstrap Methods and Their Application*. Cambridge Series on Statistical and Probabilistic Mathematics. Cambridge University Press, Cambridge.
- Dean, J. S.
1982 Dendroclimatic Variability on Black Mesa, A.D. 385 to 1970, Paper Presented at the 47th Annual Meeting of the Society for American Archaeology, Minneapolis, MN.
1986 Environmental context of Food Production on Black Mesa, Northeastern Arizona, Paper Presented at the 51st Annual Meeting of the Society for American Archaeology, New Orleans, LA.

- 1988a Dendrochronology and Paleoenvironmental Reconstruction on the Colorado Plateaus. In *The Anasazi in a Changing Environment*, edited by G. J. Gumerman, pp. 119-167. Cambridge University Press, Cambridge.
- 1988b A Model of Anasazi Behavioral Adaptation. In *The Anasazi in a Changing Environment*, edited by G. J. Gumerman, pp. 25-44. Cambridge University Press, Cambridge.
- 1990 Intensive Archaeological Survey of Long House Valley, Northeastern Arizona. In *The Archaeology of Regions, A Case for Full-Coverage Survey*, edited by S. K. Fish and S. A. Kowalewski, pp. 173-188. Smithsonian Institution Press, Washington, D.C.
- 1996a Demography, Environment, and Subsistence Stress. In *Evolving Complexity and Environmental Risk in the Prehistoric Southwest. Proceedings of the Workshop "Resource Stress, Economic Uncertainty, and Human Response in the Prehistoric Southwest"*, held February 25-29, 1992 in Santa Fe, NM, edited by J. Tainter and B. B. Tainter, pp. 25-56. Addison-Wesley, Reading, MA.
- 1996b Kayenta Anasazi Settlement Transformation in Northeastern Arizona, A.D. 1150 to 1350. In *The Prehistoric Pueblo World, A.D. 1150-1350*, edited by M. A. Adler, pp. 29-47. The University of Arizona, Tucson.
- 1999 Precipitation reconstructions (June PDSI, August-July Precipitation) for six dendroclimatic stations: Tsegi Canyon, Hopi Mesas, Flagstaff, Canyon de Chelly, Mesa Verde, and Navajo Mountain. Southwest Paleoclimate Project of the Laboratory of Tree Ring Research, University of Arizona.
- 2002 Late Pueblo II-Pueblo III in Kayenta-Branch Prehistory. In *Prehistoric Culture Change on the Colorado Plateau, Ten Thousand Years on Black Mesa*, edited by S. Powell and F. E. Smiley, pp. 121-158. The University of Arizona Press, Tucson.
- Dean, J. S., W. H. Doelle and J. D. Orcutt
- 1994 Adaptive Stress, Environment, and Demography. In *Themes in Southwest Prehistory*, edited by G. J. Gumerman, pp. 53-86. School of American Research Advanced Seminar Series, J. K. O'Donnell, general editor. School of American Research Press, Santa Fe, New Mexico.
- Dean, J. S., R. C. Euler, G. J. Gumerman, F. Plog, R. H. Hevly and T. N. V. Karlstrom
1985 Human Behavior, Demography, and Paleoenvironment on the Colorado Plateaus. *American Antiquity* 50(3):537-554.

- Dean, J. S., A. J. Lindsay Jr. and W. J. Robinson
1978 Prehistoric Settlement in Long House Valley, Northeastern Arizona. In *Investigations of the Southwestern Anthropological Research Group: an Experiment in Archaeological Cooperation: The Proceedings of the 1976 Conference.*, edited by R. C. Euler and G. J. Gumerman, pp. 25-44. Museum of Northern Arizona, Flagstaff.
- Dean, J. S. and W. J. Robinson
1969 *Tree-ring Evidence for Climatic Changes in the Prehistoric Southwest from A.D. 1000 to 1200*. Laboratory of Tree-ring Research, University of Arizona, Tucson, Arizona.
- 1977 *Dendroclimatic Variability in the American Southwest A.D. 680 to 1970*. Laboratory of Tree-Ring Research, The University of Arizona. Submitted to Final Report to the National Park Service, Dept. of Interior.
- 1978 *Expanded Tree-Ring Chronologies for the Southwestern United States*. Laboratory of Tree-Ring Research Chronology Series 3. Laboratory of Tree-Ring Research, University of Arizona, Tucson, Arizona.
- Diaz, H. F. and G. N. Kiladis
1992 Atmospheric Teleconnections Associated with the Extreme phases of the Southern Oscillation. In *El Niño, Historical and Paleoclimatic Aspects of the Southern Oscillation*, edited by H. F. Diaz and V. Markgraf, pp. 7-28. Cambridge University Press, Cambridge.
- Dunmire, W. W. and G. D. Tierney
1997 *Wild Plants and Native Peoples of the Four Corners*. Museum of New Mexico Press, Santa Fe.
- Easterling, D. R., T. R. Karl, J. H. Lawrimore and S. A. Del Greco
1999 United States Historical Climatology Network Daily Temperature, Precipitation, and Snow Data for 1871-1997. ORNL/CDIAC-118, NDP-070. May 1999 ed. vol. 2000. Carbon Dioxide Information Analysis Center, Oak Ridge National Laboratory, Oak Ridge Tennessee.
- Eckles, D.
1984 Intersite Variation in Faunal Remains on Black Mesa. In *Papers on the Archaeology of Black Mesa, Arizona, Volume II*, edited by S. Plog and S. Powell, pp. 158-172. Southern Illinois University Press, Carbondale.
- Edwards, T. C., E. T. Deshler, D. Foster and G. G. Moisen
1996 Adequacy of Wildlife Habitat Relation Models for Estimating Spatial Distributions of Terrestrial Vertebrates. *Conservation Biology* 10(1):263-270.
- Efron, B. and R. J. Tibshirani
1993 *An Introduction to the Bootstrap*. Chapman & Hall, New York.

Espey Huston and Associates Inc.

1980 *Vegetation and Wildlife Resources of the Black Mesa and Kayenta Mine Site*. Espey, Huston, and Associates, Inc. Copies available from Espey, Huston, and Associates, Inc.: Document No. 8071, EH and A Job No. 0748.

Euler, R. C.

1988 Demography and Cultural Dynamics on the Colorado Plateaus. In *The Anasazi in a Changing Environment*, edited by G. J. Gumerman, pp. 192-229. Cambridge University Press, Cambridge.

Euler, R. C. and G. J. Gumerman

1974 A Resume of the Archaeology of Northern Arizona. In *Geology of Northern Arizona, with Notes on Archaeology and Paleoclimate, Part I, Regional Studies*, edited by T. N. V. Karlstrom, G. A. Swann and R. Eastwood, pp. 296-315. Rocky Mountain Section Meeting, Flagstaff, Arizona. Geological Society of America, Flagstaff, Arizona.

Euler, R. C., G. J. Gumerman, T. N. V. Karlstrom, J. S. Dean and R. H. Hevly

1979 The Colorado Plateaus: Cultural Dynamics and Paleoenvironment. *Science* 205 (4411): 1089-1101.

Evenden, G. I.

1995a Cartographic Projection Procedures, Release 4, Second Interim Report, pp. 21.

1995b Cartographic Projection Procedures for the UNIX Environment: A User's Manual, pp. 68.

Fish, S. K. and S. A. Kowalewski (editors)

1990 *The Archaeology of Regions, A Case for Full-Coverage Survey*. Smithsonian Institution Press, Washington, D.C.

Ford, R., I.

1984 Ecological Consequences of Early Agriculture in the Southwest. In *Papers on the Archaeology of Black Mesa, Arizona, Volume II*, edited by S. Plog and S. Powell, pp. 127-139. Southern Illinois University Press, Carbondale.

Ford, R., I., J. French, J. Stock, T. Smart, G. Hazen and D. Jessup

1983 Appendix VIII, 1981 Ethnobotanical Recovery: Summary of Analysis and Frequency Table. In *Excavations on Black Mesa, 1981. A Descriptive Report*, edited by F. E. Smiley, D. L. Nichols and P. P. Andrews, pp. 461-480. Research Paper. vol. 36. Center for Archaeological Investigations, Southern Illinois University, Carbondale.

- Ford, R., I. P. Vander Werf, C. Goland and H. B. Trigg
1985 Paleoethnobotany of Anasazi Sites. In *Excavations on Black Mesa, 1983. A Descriptive Report*, edited by A. L. Christenson and W. Parry, pp. 473-487. Research Paper. vol. 46. Center for Archaeological Investigations, University of Southern Illinois at Carbondale, Carbondale.
- Fritts, H.
1974 Relationship of Ring Widths in Arid-Site Conifers to Variations in Monthly Temperature and Precipitation. *Ecological Monographs* 44(4):411-440.
- Fritts, H. C.
1965 Tree-Ring Evidence for Climatic Changes in Western North America. *Monthly Weather Review* 93:421-443.
1976 *Tree Rings and Climate*. Academic Press, London.
1991 *Reconstructing Large-Scale Climatic Patterns from Tree-Ring Data, a Diagnostic Analysis*. University of Arizona Press, Tucson.
- Fritts, H. C., G. R. Lofgren and G. A. Gordon
1979 Variations in Climate since 1602 as Reconstructed from Tree Rings. *Quaternary Research* 12:18-46.
- Gaines, S. W.
1978 Computer Application of SARG Data: An Evaluation. In *Investigations of the Southwestern Anthropological Research Group: an Experiment in Archaeological Cooperation: The Proceedings of the 1976 Conference*, edited by R. C. Euler and G. J. Gumerman, pp. 119-138. Museum of Northern Arizona, Flagstaff.
- n.d. SARG Database for the Long House Valley Archaeological Project, pp. SPSS data file provided by Sylvia Gaines containing the SARG data collected as part of the Long House Valley Archaeological Project.
- Garrett, E. M.
1986 A Petrographic Analysis of Black Mesa Ceramics. In *Spatial Organization and Exchange, Archaeological Survey on Northern Black Mesa*, edited by S. Plog, pp. 114-142. Publications in Archaeology, D. P. Braun, general editor. Southern Illinois University Press, Carbondale.
- Geib, P. R. and M. M. Callahan
1987 Ceramic Exchange Within the Kayenta Anasazi Region: Volcanic Ash-Tempered Tusayan White Ware. *Kiva* 52(2):95-113.

- Geib, P. R. and K. Spurr
2000 The Basketmaker II-III Transition on the Rainbow Plateau. In *Foundations of Anasazi Culture: the Basketmaker to Pueblo Transition*, edited by P. F. Reed, pp. 175-202. University of Utah Press, Salt Lake City, UT.
- Gilpin, D.
1994 Lukachukai and Salina Springs: Late Archaic/ Early Basketmaker Habitation Sites in the Chinle Valley, Northeastern New Mexico. *Kiva* 60(2):203-218.
- Glassy, J. M. and S. W. Running
1994 Validating Diurnal Climatology Logic of the MT-CLIM Model Across a Climatic Gradient in Oregon. *Ecological Applications* 4(2):248-257.
- Graham, L. A.
1995 Arizona Natural Vegetation, as Mapped for the Arizona GAP Analysis Program. School of Renewable Natural Resources, University of Arizona, Tucson.
- Green, M.
1985 *Chipped Stone Raw Materials and the Study of Interaction on Black Mesa, Arizona*. Occasional Paper 11. Center for Archaeological Investigations, Southern Illinois University at Carbondale, Carbondale.
- 1986 The Distribution of Chipped Stone Raw Materials at Functionally Nonequivalent Sites. In *Spatial Organization and Exchange, Archaeological Survey on Northern Black Mesa*, edited by S. Plog, pp. 143-168. Publications in Archaeology, D. P. Braun, general editor. Southern Illinois University Press, Carbondale.
- Gregory, H. E.
1916 *The Navajo Country: A Geographic and Hydrographic Reconnaissance of Parts of Arizona, New Mexico, and Utah*. Water Supply Paper 380. Department of the Interior, Geological Survey, Washington D. C.
- Grissino-Mayer, H. D.
1995 *Tree-Ring Reconstructions of Climate and Fire History at El Malpais National Monument, New Mexico*. Ph.D., University of Arizona.
- Guernsey, S. J.
1931 *Explorations in Northeastern Arizona: Report on the Archaeological Fieldwork of 1920-1923*. Papers of the Peabody Museum of American Archaeology and Ethnology, Harvard University 12. The Museum, Cambridge, MA.

- Guernsey, S. J. and A. V. Kidder
1921 *Basket-maker caves of northeastern Arizona; report on the explorations, 1916-1917.*
Papers of the Peabody Museum of Archaeology and Ethnology, Harvard University 8(2).
The Museum, Cambridge, Mass.,.
- Gumerman, G.
1998 Personal communication.
- Gumerman, G. and S. Powell
1981 Anasazi Cultural Developments and Paleoenvironmental Correlates, Unpublished
manuscript on file at the Center for Archaeological Investigations, SIU Carbondale.
- Gumerman, G. J.
1966 A Folsom Point from the Area of Mishongnovi, Arizona. *Plateau* 38:79-80.
1988 *The Anasazi in a Changing Environment.* Cambridge University Press, Cambridge.
- Gumerman, G. J. and J. S. Dean
1989 Prehistoric Cooperation and Competition in the Western Anasazi Area. In *Dynamics of Southwest Prehistory*, edited by L. S. Cordell and G. J. Gumerman, pp. 99-148.
Smithsonian Institution Press, Washington, D.C.
- Gumerman, G. J. and R. C. Euler
1976 Black Mesa: Retrospect and Prospect. In *Papers on the Archaeology of Black Mesa, Arizona*, edited by G. J. Gumerman and R. C. Euler, pp. 165-170. Southern Illinois University Press, Carbondale, IL.
- Gunn, J. D.
1994 Global Climate and Regional Biocultural Diversity. In *Historical Ecology*, edited by C. L. Crumley, pp. 67-97. School of American Research Press, Santa Fe.
- Haas, J. and W. Creamer
1996 The Role of Warfare in the Pueblo III Period. In *The Prehistoric Pueblo World, A.D. 1150-1350*, edited by M. A. Adler, pp. 205-213. The University of Arizona, Tucson.
- Hack, J. T.
1942 *The Changing Physical Environment of the Hopi Indians of Arizona.* Peabody Museum Papers XXXV, no. 1. Peabody Museum, Harvard University, Cambridge.
- Harshbarger, J. W., C. A. Repenning and R. L. Jackson
1957 *Stratigraphy of the Uppermost Triassic and the Jurassic Rocks of the Navajo Country [Colorado Plateau].* Professional Paper 291. US Geological Survey, US Government Printing Office, Washington, D. C.

- Hegmon, M.
- 1989 Risk Reduction and Variation in Agricultural Economies: A Computer Simulation of Hopi Agriculture. In *Research in Economic Anthropology*, edited by B. L. Isaac, pp. 89-121. Research in Economic Anthropology, a Research Annual. vol. 11. JAI Press, Greenwich, CT.
- 1996 Variability in Food Production, Strategies of Storage and Sharing, and the Pithouse-to-Pueblo Transition in the Northern Southwest. In *Evolving Complexity and Environmental Risk in the Prehistoric Southwest. Proceedings of the Workshop "Resource Stress, Economic Uncertainty, and Human Response in the Prehistoric Southwest", held February 25-29, 1992 in Santa Fe, NM*, edited by J. Tainter and B. B. Tainter, pp. 223-250. Addison-Wesley, Reading, MA.
- Hevly, R. H.
- 1988 Prehistoric Vegetation and Paleoclimates on the Colorado Plateaus. In *The Anasazi in a Changing Environment*, edited by G. J. Gumerman, pp. 92-118. Cambridge University Press, Cambridge.
- Hevly, R. H. and T. N. V. Karlstrom
- 1974 Southwest Paleoclimate and Continental Correlations. In *Geology of Northern Arizona, with Notes on Archaeology and Paleoclimate, Part I, Regional Studies*, edited by T. N. V. Karlstrom, G. A. Swann and R. Eastwood, pp. 257-295. Rocky Mountain Section Meeting, Flagstaff, Arizona. Geological Society of America, Flagstaff, Arizona.
- Hill, D. V.
- 1994 Technological Analysis: Making and Using Ceramics on Black Mesa. In *Function and Technology of Anasazi Ceramics from Black Mesa, Arizona*, edited by M. F. Smith Jr., pp. 23-53. Occasional Paper. vol. 15. Southern Illinois University, Center for Archaeological Investigations, Carbondale.
- Huckell, B.
- 1982 *The Distribution of Fluted Points in Arizona: A Review and Update*. Arizona State Museum Archaeological Series 145. University of Arizona, Arizona State Museum, Tucson.
- Huckell, B. B.
- 1977 *The Hastqin Site: A Multicomponent Site Near Ganado, Arizona*. Arizona State Museum Contribution to Highway Salvage Archaeology in Arizona 61. University of Arizona Press, Tucson.

Hungerford, R. D., R. R. Nemani, S. W. Running and J. C. Coughlan
1989 *MTCLIM: A Mountain Microclimate Simulation Model*. US Dept. of Agriculture,
Forest Service, Intermountain Research Station. Submitted to Research Paper. Copies
available from INT-414.

Hunt, A. P. and D. Tanner

1960 Early Man Sites Near Moab, Utah. *American Antiquity* 26:110-117.

Jennings, M. D.

1996 Mapping Units: Their Classification and Nomenclature for Gap Analysis Land Cover
Data. In *Gap Analysis, A Landscape Approach to Biodiversity Planning*, edited by J. M.
Scott, T. H. Tear and F. W. Davis, pp. 71-78. American Society for Photogrammetry
and Remote Sensing, Bethesda, Maryland.

Jones, H. G.

1992 *Plants and Microclimate, A Quantitative Approach to Environmental Plant Physi-
ology*. Cambridge University Press, Cambridge.

Karlstrom, T. N. V.

1988 Alluvial Chronology and Hydrologic Change of Black Mesa and Nearby Regions. In
The Anasazi in a Changing Environment, edited by G. J. Gumerman, pp. 45-91. Cam-
bridge University Press, Cambridge.

Karlstrom, T. N. V., G. J. Gumerman and R. Euler

1976 Paleoenvironmental and Cultural Correlates in the Black Mesa Region. In *Papers
on the Archaeology of Black Mesa, Arizona*, edited by G. J. Gumerman and R. C. Euler,
pp. 149-161. Southern Illinois University Press, Carbondale.

Karlstrom, T. N. V., G. J. Gumerman and R. C. Euler

1974 Paleoenvironmental and Cultural Changes in the Black Mesa Region, Northeastern
Arizona. In *Geology of Northern Arizona with Notes on Archaeology and Paleoclimate*,
edited by T. N. V. Karlstrom, G. A. Swann and R. L. Eastwood, pp. 768-792. vol. Part
II - Area Studies and Field Guides. Geological Society of America, Flagstaff, Arizona.

Kelly, R. L. and L. C. Todd

1988 Coming into the Country: Early Paleoindian Hunting and Mobility. *American An-
tiquity* 53(2):231-244.

Kidder, A. V. and S. J. Guernsey

1919 *Archeological Explorations in Northeastern Arizona*. Smithsonian Institution, Bu-
reau of American Ethnology Bulletin 65. Government Printing Office, Washington, DC.

1921 Peabody Museum Arizona Exploration, 1920. *Proceedings of the National Academy
of Sciences of the United States of America* 7(3):69-71.

Kimball, J., S. W. Running and R. Nemani
1995 An Improved Method for Estimating Surface Humidity from Daily Minimum Temperature. *Submitted to Agricultural and Forest Meteorology*.

Kohler, T. A. and C. R. Van West
1996 The Calculus of Self-Interest in the Development of Cooperation: Sociopolitical Development and Risk Among the Northern Anasazi. In *Evolving Complexity and Environmental Risk in the Prehistoric Southwest. Proceedings of the Workshop "Resource Stress, Economic Uncertainty, and Human Response in the Prehistoric Southwest"*, held February 25-29, 1992 in Santa Fe, NM, edited by J. Tainter and B. B. Tainter, pp. 169-196. Addison-Wesley, Reading, MA.

Kohler, T. A., C. R. Van West, E. P. Carr and C. Langton
1996a Agent-Based Modeling of Prehistoric Settlement Systems in the Northern American Southwest. Paper presented at the Third International Conference/Workshop on Integrating GIS and Environmental Modeling, Santa Fe, NM.

Kohler, T. A., C. R. Van West, E. P. Carr and C. G. Langton
1996b Agent-Based Modeling of Prehistoric Settlement Systems in the Northern American Southwest. In *Proceedings of the Third International Conference/Workshop on Integrating GIS and Environmental Modeling (Web Publication)*. vol. 1998. NCGIA, Santa Fe, NM.

Krebs, J. R. and N. B. Davies
1993 *An Introduction to Behavioral Ecology*. Third ed. Blackwell Scientific Publications, Oxford.

Krohn, W. B.
1996 Predicted Vertebrate Distributions from Gap Analysis: Considerations in the Design of Statewide Accuracy Assessments. In *Gap Analysis, A Landscape Approach to Biodiversity Planning*, edited by J. M. Scott, T. H. Tear and F. W. Davis, pp. 147-162. American Society for Photogrammetry and Remote Sensing, Bethesda, Maryland.

Larson, D. O., H. Neff, D. A. Graybill, J. Michaelsen and E. Ambos
1996 Risk, Climatic Variability, and the Study of Southwestern Prehistory: An Evolutionary Perspective. *American Antiquity* 61(2):217-241.

Lebo, C. J.
1991 *Anasazi Harvests: Agroclimate, Harvest Variability, and Agricultural Strategies on Prehistoric Black Mesa, Northeastern Arizona*. Ph.D., Indiana University.

- Leonard, R. D.
1989 *Anasazi Faunal Exploitation: Prehistoric Subsistence on Northern Black Mesa, Arizona*. Occasional Paper 13. Center for Archaeological Investigations, Southern Illinois University at Carbondale, Carbondale.
- Levitt, J.
1980 *Responses of Plants to Environmental Stresses*. 2nd ed. Physiological Ecology 1, Chilling, Freezing, and High Temperature Stresses. 2 vols. Academic Press, New York.
- Lowe, C. H. and D. E. Brown
1994 Introduction. In *Biotic Communities of the Southwestern United States and Northwestern Mexico*, edited by D. E. Brown, pp. 8-16. University of Utah Press, Salt Lake City.
- Martin, D. L., A. H. Goodman, G. J. Armelagos and A. L. Magennis
1991 *Black Mesa Anasazi Health: Reconstructing Life from Patterns of Death and Disease*. Occasional Paper 14. Center for Archaeological Investigations, Southern Illinois University at Carbondale, Carbondale.
- Matson, R. G.
1991 *The Origins of Southwestern Agriculture*. University of Arizona Press, Tucson, Arizona.
1994 Anomalous Basketmaker II Sites on Cedar Mesa: Not So Anomalous After All. *Kiva* 60(2):219-237.
- Matson, R. G. and B. Chisholm
1991 Basketmaker II Subsistence: Carbon Isotopes and Other Dietary Indicators from Cedar Mesa, Utah. *American Antiquity* 56(3).
- McCarthy, S. B., J. Mangiameli, M. R. Kunzmann and W. L. Halvorson
1998 GIS and Vertebrate Species Richness Models for Arizona GAP. Paper presented at the Eighteenth Annual ESRI International User Conference, San Diego.
- McGavock, E. H. and G. W. Levings
1974 Ground Water in the Navajo Sandstone in the Black Mesa Area, Arizona. In *Geology of Northern Arizona, with Notes on Archaeology and Paleoclimate, Part I, Regional Studies*, edited by T. N. V. Karlstrom, G. A. Swann and R. Eastwood, pp. 757-767. Rocky Mountain Section Meeting, Flagstaff, Arizona. Geological Society of America, Flagstaff, Arizona.
- Meltzer, D. J.
1995 Clocking the First Americans. *Annual Review of Anthropology* 24:21-45.

Merrill, E. H., T. W. Kohley, M. E. Herdendorf, W. A. Reiners, K. L. Driese, R. W. Marrs and S. H. Anderson

1996 *Wyoming Gap Analysis Project Final Report*. Department of Zoology and Physiology, Department of Botany, and Wyoming Cooperative Fish and Wildlife Research Unit, USGS Biological Resources Division, University of Wyoming.

Minnis, P. E.

1985 *Social Adaptation to Food Stress, a Prehistoric Southwestern Example*. Prehistoric Archaeology and Ecology. University of Chicago Press, Chicago.

Moore, J.

1979 1978 Ethnobotanical and Ecological Research , Black Mesa. In *Excavations on Black Mesa, 1978, A Descriptive Report*, edited by A. L. Klesert and S. Powell, pp. 179-215. Research Papers. vol. 8. Southern Illinois University at Carbondale, Center for Archaeological Investigations, Carbondale.

Morss, N.

1927 *Archaeological Explorations in the Middle Chinlee, 1925*. Memoirs of the American Anthropological Association 34. American Anthropological Association, Menasha, WI.

Muenchrath, D. A. and R. J. Salvador

1995 Maize Productivity and Agroecology: Effects of Environment and Agricultural Practices on the Biology of Maize. In *Soil, Water, Biology and Belief in Prehistoric and Traditional Southwestern Agriculture*, edited by H. W. Toll, pp. 303-333. New Mexico Archaeological Council Special Publication. vol. 2. New Mexico Archaeological Council, Albuquerque.

National Research Council Committee on State Archaeological Surveys

1922 Notes on State Archaeological Surveys. *American Anthropologist* 24(2):233-242.

Nichols, D. L.

2002 Basketmaker III: Early Ceramic-Period Villages in the Kayenta Region. In *Prehistoric Culture Change on the Colorado Plateau, Ten Thousand Years on Black Mesa*, edited by S. Powell and F. E. Smiley, pp. 66-76. The University of Arizona Press, Tucson.

Nichols, D. L. and F. E. Smiley

1985 An Overview of Northern Black Mesa Archaeology. In *Excavations on Black Mesa, 1983, A Descriptive Report*, edited by A. L. Christenson and W. J. Parry, pp. 47-82. Research Paper. vol. 46. Center for Archaeological Investigations, Southern Illinois University, Carbondale, IL.

NOAA, National Climate Data Center
2002 NOAA/NWS Cooperative Observer Network. vol. 2002. NOAA, National Climate Data Center.

Oke, T. R.
1978 *Boundary Layer Climates*. 2nd (1987) ed. Routledge, London.

Olberding, S. D.
2000 Fort Valley, the Beginnings of Forest Research. *Forest History Today* Spring, 2000:9-15.

Parry, W. J.
1987 Sources of Chipped Stone Materials. In *Prehistoric Stone Technology on Northern Black Mesa, Arizona*, edited by W. J. Parry and A. L. Christenson, pp. 21-42. Occasional Paper. vol. 12. Center for Archaeological Investigations, Southern Illinois University at Carbondale, Carbondale.

Parry, W. J. and F. E. Smiley
1990 Hunter-Gatherer Archaeology in Northeastern Arizona and Southeastern Utah. In *Perspectives on Southwestern Prehistory*, edited by P. E. Minis and C. L. Redman, pp. 47-56. Westview Press, Boulder, Colorado.

Parry, W. J., F. E. Smiley and G. R. Burgett
1994 The Archaic Occupation of Black Mesa, Arizona. In *Archaic Hunter-Gatherer Archaeology in the American Southwest*, edited by B. Vierra, pp. 185-230. Eastern New Mexico Contributions in Anthropology. vol. 13.

Plog, F.
1979 Prehistory: Western Anasazi. In *Handbook of North American Indians: Southwest*, edited by A. Ortiz, pp. 108-130. vol. 9, W. C. Sturtevant, general editor. Smithsonian Institution, Washington, D.C.

Plog, F., G. J. Gumerman, R. C. Euler, J. S. Dean, R. H. Hevly and T. N. V. Karlstrom
1988 Anasazi Adaptive Strategies: The Model, Predictions, and Results. In *The Anasazi in a Changing Environment*, edited by G. J. Gumerman, pp. 192-229. Cambridge University Press, Cambridge.

Plog, S.
1986a Chronology and Culture History. In *Spatial Organization and Exchange, Archaeological Survey of Northern Black Mesa*, edited by S. Plog, pp. 50-86. Southern Illinois University Press, Carbondale.

1986b The Environment: Present and Past. In *Spatial Organization and Exchange, Archaeological Survey of Northern Black Mesa*, edited by S. Plog, pp. 17-31. Southern Illinois University Press, Carbondale.

1986a Group Mobility and Locational Strategies: Tests of Some Settlement Hypotheses. In *Spatial Organization and Exchange, Archaeological Survey on Northern Black Mesa*, edited by S. Plog, pp. 187-223. Southern Illinois University Press, Carbondale.

1986c Models and Methods in Southwestern Research. In *Spatial Organization and Exchange, Archaeological Survey of Northern Black Mesa*, edited by S. Plog, pp. 1-16. Southern Illinois University Press, Carbondale.

1986b Patterns of Demographic Growth and Decline. In *Spatial Organization and Exchange, Archaeological Survey on Northern Black Mesa*, edited by S. Plog, pp. 224-255. Southern Illinois University Press, Carbondale.

1986d The Survey Strategy. In *Spatial Organization and Exchange, Archaeological Survey of Northern Black Mesa*, edited by S. Plog, pp. 32-49. Southern Illinois University Press, Carbondale.

Plog, S. and J. L. Hantman

1986 Multiple Regression Analysis as a Dating Method in the American Southwest. In *Spatial Organization and Change, Archaeological Survey of Northern Black Mesa*, edited by S. Plog, pp. 87-113. Southern Illinois University Press, Carbondale.

1990 Chronology Construction and the Study of Prehistoric Culture Change. *Journal of Field Archaeology* 17(4):439-456.

Powell, S.

1983 *Mobility and Adaptation, the Anasazi of Black Mesa, Arizona*. Center for Archaeological Investigations, Southern Illinois University Press, Carbondale.

2002 The Puebloan Florescence and Dispersion: Dinnebito and Beyond, A.D. 800-1150. In *Prehistoric Culture Change on the Colorado Plateau, Ten Thousand Years on Black Mesa*, edited by S. Powell and F. E. Smiley, pp. 79-118. The University of Arizona Press, Tucson.

Reed, L. S., C. D. Wilson and K. A. Hays-Gilpin

2000 From Brown to Gray, The Origins of Ceramic Technology in the Northern Southwest. In *Foundations of Anasazi Culture: the Basketmaker to Pueblo Transition*, edited by P. F. Reed, pp. 203-229. University of Utah Press, Salt Lake City, UT.

Reed, P. F.

2000 Fundamental Issues in Basketmaker Archaeology. In *Foundations of Anasazi Culture: the Basketmaker to Pueblo Transition*, edited by P. F. Reed, pp. 3-18. University of Utah Press, Salt Lake City, UT.

Reynolds, S. J.

1988 Geologic Map of Arizona. Arizona Geological Survey.

- Rindos, D.
1980 Symbiosis, Instability and the Origins and Spread of Agriculture: A New Model. *Current Anthropology* 21:751-772.
- 1984 *The Origins of Agriculture, an Evolutionary Perspective*. Academic Press, New York.
- Robison, C. A.
1984 Summary of Archaeological and Compliance Information on Archaeological Sites in the Peabody Coal Company's Leasehold on Black Mesa, Navajo County, Arizona, pp. 176, Carbondale, IL.
- Rose, M. R., J. S. Dean and W. J. Robinson
1981 *The Past Climate of Arroyo Hondo, New Mexico, Reconstructed from Tree Rings*. Arroyo Hondo Archaeological Series 4. School of American Research Press, Santa Fe, New Mexico.
- Running, S. W. and J. Coughlan
1988 A General Model of Forest Ecosystem Processes for Regional Applications. I. Hydrologic Balance, Canopy Gas Exchange and Primary Production Processes. *Ecological Modelling* 42:125-154.
- Running, S. W. and S. T. Gower
1991 FOREST-BGC, A General Model of Forest Ecosystem Processes for Regional Applications. II. Dynamic Carbon Allocation and Nitrogen Budgets. *Tree Physiology* 9:147-157.
- Running, S. W. and E. Raymond Hunt Jr.
1993 Generalization of a Forest Ecosystem Process Model for Other Biomes, BIOME-BGC, and an Application for Global-Scale Models. In *Scaling Physiological Processes, Leaf to Globe*, edited by J. R. Ehleringer and C. B. Field, pp. 141-158. Academic Press, San Diego.
- Running, S. W., R. R. Nemani and R. D. Hungerford
1987 Extrapolation of Synoptic Meteorological Data in Mountainous Terrain and Its Use for Simulating Forest Evapotranspiration and Photosynthesis. *Canadian Journal of Forest Research* 17:472-483.
- Ruppé, P. A.
1985 A Long Pollen Record from Tsosie Shelter, Black Mesa, Arizona. In *Excavations on Black Mesa, 1983, A Descriptive Report*, edited by A. L. Christenson and W. J. Parry, pp. 513-530. Southern Illinois University at Carbondale Center for Archaeological Investigations, Research Paper. vol. 46. Southern Illinois University Press, Carbondale.

- Salzer, M. W.
2000 *Dendroclimatology in the San Francisco Peaks Region of Northern Arizona, USA*.
Ph.D. Dissertation, University of Arizona.
- Schneider, H. K.
1974 *Economic Man, the Anthropology of Economies*. Sheffield Publishing Company,
Salem, Wisconsin.
- Schroedl, A. R.
1977 The Paleoindian Period on the Colorado Plateau. *Southwestern Lore* 43(3):1-9.
- Schwarz, G. E. and R. B. Alexander
1995 State Soil Geographic (STATSGO) Data Base for the Conterminous United States.
1.1 ed. vol. 2002. U. S. Geological Survey.
- Semé, M.
1984 The Effects of Agricultural Fields on Faunal Assemblage Variation. In *Papers on the Archaeology of Black Mesa, Arizona, Volume II*, edited by S. Plog and S. Powell, pp. 139-157. Southern Illinois University Press, Carbondale.
- Sink, C., L. Nelson, p. Danlavey, C. Prowse, G. Reed, M. Sant and J. T. Balsitis
1985 Black Mesa Archaeological Project, Base Anasazi Site Map with Mining Areas Corrected 8-14-1985, Compliance Status & Excavated Sites, pp. Mylar original map. Original map on file at the Center for Archaeological Investigations, Southern Illinois University, Carbondale.
- Smiley, F. E.
1985 *The Chronometrics of Early Agricultural Sites in Northeastern Arizona: Approaches to the Interpretation of Radiocarbon Dates*. Ph.D., University of Michigan.
- 1994 The Agricultural Transition in the Northern Southwest: Patterns in the Current Chronometric Data. *Kiva* 60(2):165-189.
- 1998a Chapter 2, Black Mesa: Time, Place, and Chronometry. In *Archaeological Chronometry, Radiocarbon and Tree-Ring Models and Applications from Black Mesa, Arizona*, edited by F. E. Smiley and R. V. N. Ahlstrom, pp. 13-24. Occasional Paper. vol. 16. Southern Illinois University, Center for Archaeological Investigations, Carbondale.
- 1998b Chapter 5, Wood Age and Site Age: An Ethnoarchaeological Approach. In *Archaeological Chronometry, Radiocarbon and Tree-Ring Models and Applications from Black Mesa, Arizona*, edited by F. E. Smiley and R. V. N. Ahlstrom, pp. 65-82. Occasional Paper. vol. 16. Southern Illinois University, Center for Archaeological Investigations, Carbondale.

1998c Chapter 6, Old Wood and Natural Process: A Simulation Approach to Site Age Determination. In *Archaeological Chronometry, Radiocarbon and Tree-Ring Models and Applications from Black Mesa, Arizona*, edited by F. E. Smiley and R. V. N. Ahlstrom, pp. 83-97. Occasional Paper. vol. 16. Southern Illinois University, Center for Archaeological Investigations, Carbondale.

1998d Chapter 7, Applying Radiocarbon Models: Lolomai Phase Chronometry on Black Mesa. In *Archaeological Chronometry, Radiocarbon and Tree-Ring Models and Applications from Black Mesa, Arizona*, edited by F. E. Smiley and R. V. N. Ahlstrom, pp. 99-135. Occasional Paper. vol. 16. Southern Illinois University, Center for Archaeological Investigations, Carbondale.

2002a Black Mesa Before Agriculture: Paleoindian and Archaic Evidence. In *Prehistoric Culture Change on the Colorado Plateau, Ten Thousand Years on Black Mesa*, edited by S. Powell and F. E. Smiley, pp. 15-34. The University of Arizona Press, Tucson.

2002b The First Black Mesa Farmers: The White Dog and Lolomai Phases. In *Prehistoric Culture Change on the Colorado Plateau, Ten Thousand Years on Black Mesa*, edited by S. Powell and F. E. Smiley, pp. 37-65. The University of Arizona Press, Tucson.

Smiley, F. E. and R. V. N. Ahlstrom

1998a *Archaeological Chronometry, Radiocarbon and Tree-Ring Models and Applications from Black Mesa, Arizona*. Occasional Paper 16. Southern Illinois University, Center for Archaeological Investigations, Carbondale.

1998b Chapter 13, Assessing Black Mesa Chronometry and Chronology. In *Archaeological Chronometry, Radiocarbon and Tree-Ring Models and Applications from Black Mesa, Arizona*, edited by F. E. Smiley and R. V. N. Ahlstrom, pp. 217-222. Occasional Paper. vol. 16. Southern Illinois University, Center for Archaeological Investigations, Carbondale.

Smith, E. A.

1983 Anthropological Applications of Optimal Foraging Theory: A Critical Review. *Current Anthropology* 24(5):625-651.

1987 Optimization Theory in Anthropology: Applications and Critiques. In *The Latest and the Best: Essays on Evolution and Optimality*, edited by J. Dupré, pp. 201-249. Bradford Books, MIT Press, Cambridge, Mass.

1991 Risk and Uncertainty in the 'Original Affluent Society': Evolutionary Ecology of Resource-Sharing and Land Tenure. In *Hunters and Gatherers 1: History, Evolution and Social Change*, edited by T. Ingold, D. Riches and J. Woodburn, pp. 222-251. St. Martin's Press, New York.

- Smith, E. A. and B. Winterhalder
1992 Natural Selection and Decision Making: Some Fundamental Principles. In *Evolutionary Ecology and Human Behavior*, edited by E. A. Smith and B. Winterhalder, pp. 25-60. Aldine de Gruyter, New York.
- Smith, M. F. (editor)
1994a *Function and Technology of Anasazi Ceramics from Black Mesa, Arizona*. 15. Center for Archaeological Investigations, Southern Illinois University at Carbondale, Carbondale.
- 1994b Introduction and Background for Ceramic Studies. In *Function and Technology of Anasazi Ceramics from Black Mesa, Arizona*, edited by M. F. Smith Jr., pp. 1-10. Occasional Paper. vol. 15. Southern Illinois University, Center for Archaeological Investigations, Carbondale.
- Sokal, R. R. and F. J. Rohlf
1995 *Biometry, the Principles and Practice of Statistics in Biological Research*. Third ed. W. H. Freeman and Company, New York.
- Southwest Paleoclimate Project of the Laboratory of Tree-Ring Research, U. o. A.
1999a Dendroclimatic Reconstructions for Canyon de Chelly.
- 1999b Dendroclimatic Reconstructions for Flagstaff.
- 1999c Dendroclimatic Reconstructions for Hopi Mesas.
- 1999d Dendroclimatic Reconstructions for Mesa Verde.
- 1999e Dendroclimatic Reconstructions for Navajo Mountain.
- 1999f Dendroclimatic Reconstructions for Tsegi Canyon.
- Stephens, D. W. and J. R. Krebs
1986 *Foraging Theory*. Princeton University Press, Princeton, New Jersey.
- Thomas, K.
1997 Arizona Gap Analysis Program Land Cover Map Accuracy Assessment Field Data - Metadata Record. U.S. Geological Survey, Forest and Rangeland Ecosystem Science Center (FRESC), Colorado Plateau Field Station.
- Thompson, B. C., P. J. Crist, J. S. Prior-Magee, R. A. Deitner, D. L. Garber and M. A. Hughes
1996 *Gap Analysis of Biological Diversity Conservation in New Mexico Using Geographic Information Systems*. New Mexico Cooperative Fish and Wildlife Research Unit, USGS Biological Resources Division, New Mexico State University, Las Cruces.

Thornton, P. E., S. W. Running and M. A. White
1997 Generating Surfaces of Daily Meteorological Variables Over Large Regions of Complex Terrain. *Journal of Hydrology* 190:214-251.

Trigg, H. B.
1985 Ethnobotanical Analysis of D:7:2085. In *Excavations on Black Mesa, 1983, A Descriptive Report*, edited by A. L. Christenson and W. J. Parry, pp. 489-512. Southern Illinois University at Carbondale Center for Archaeological Investigations, Research Paper. vol. 46. Southern Illinois University Press, Carbondale.

Trigger, B. G.
1989 *A History of Archaeological Thought*. Cambridge University Press, Cambridge.

Turner, R. M.
1994 Great Basin Desertsrub. In *Biotic Communities of the Southwestern United States and Northwestern Mexico*, edited by D. E. Brown, pp. 145-155. University of Utah Press, Salt Lake City.

U.S. Geological Survey
2003 Geographic Names Information System (GNIS). vol. 2003.

Van West, C. R.
1994 *Modeling Prehistoric Agricultural Productivity in Southwestern Colorado: A GIS Approach*. Washington State University Department of Anthropology, Reports of Investigations 67. Washington State University Department of Anthropology and Crow Canyon Archaeological Center, Cortez, Colo., Pullman, Wash.

Wagner, G., T. Smart, R. Ford, I. and H. B. Trigg
1984 Appendix G: Ethnobotanical Recovery, 1982: Summary of Analysis and Frequency Tables. In *Excavations on Black Mesa, 1982, A Descriptive Report*, edited by D. L. Nichols and F. E. Smiley, pp. 613-632. Research Paper. vol. 39. SIU Carbondale, Center for Archaeological Investigations, Carbondale.

Waguespack, N. M. and T. A. Surovell
2003 Clovis Hunting Strategies, Or How to Make Out on Plentiful Resources. *American Antiquity* 68(2):333-352.

Webb, W. L., W. K. Lauenroth, S. R. Szarek and R. S. Kinerson
1983 Primary Production and Abiotic Controls in Forests, Grasslands, and Desert Ecosystems in the United States. *Ecology* 64(1):134-151.

Western Regional Climate Center
2003a 30 Year Daily Temperature and Precipitation Summary, Betatakin, Arizona. Western Regional Climate Center.

2003b 30 Year Daily Temperature and Precipitation Summary, Lukachukai, Arizona. Western Regional Climate Center.

Whiting, A. F.

1939 *Ethnobotany of the Hopi*. Museum of Northern Arizona, Bulletin 15. Northern Arizona Society of Science and Art, Flagstaff, AZ.

Willey, G. R. and J. A. Sabloff

1974 *A History of American Archaeology*. Thames and Hudson Ltd., London.

Wills, W. H.

1988 *Early Prehistoric Agriculture in the American Southwest*. School of American Research Press, Santa Fe, New Mexico.

1992 Plant Cultivation and the Evolution of Risk-Prone Economies in the Prehistoric American Southwest. In *Transitions to Agriculture in Prehistory*, edited by A. B. Gebauer and T. D. Price, pp. 153-176. Prehistory Press, Madison.

Wilson, R. F.

1974 Mesozoic Stratigraphy of Northeastern Arizona. In *Geology of Northern Arizona with Notes on Archaeology and Paleoclimate*, edited by T. N. V. Karlstrom, G. A. Swann and R. L. Eastwood, pp. 192-207. vol. Part 1 - Regional Studies. Geological Society of America, Flagstaff, Arizona.

Winterhalder, B.

1986 Diet Choice, Risk, and Food Sharing in a Stochastic Environment. *Journal of Anthropological Archaeology* 5:369-392.

1990 Open Field, Common Pot: Harvest Variability and Risk Avoidance in Agricultural and Foraging Societies. In *Risk and Uncertainty in Tribal and Peasant Economies*, edited by E. Cashdan, pp. 67-88. Westview Press, Boulder, CO.

Winterhalder, B. and C. Goland

1993 On Population, Foraging Efficiency, and Plant Domestication. *Current Anthropology* 34(5).

1997 An Evolutionary Ecology Perspective on Diet Choice, Risk, and Plant Domestication. In *People, Plants, and Landscapes*, edited by K. J. Gremillion, pp. 123-160. University of Alabama Press, Tuscaloosa.

Wolfe, J. A.

1992 *An Analysis of Present-Day Terrestrial Lapse Rates in the Western Coterminal United States and Their Significance to Paleoaltitudinal Estimates*. U.S. Geological Survey Bulletin 1964. United States Government Printing Office, Washington, D.C.

- Woodbury, R. B.
1954 *Prehistoric Stone Implements of Northeastern Arizona*. Papers of the Peabody Museum of American Archaeology and Ethnology 34. Peabody Museum of American Archaeology and Ethnology, Cambridge.
- Woodward, F. I.
1987 *Climate and Plant Distribution*. Cambridge Studies in Ecology. Cambridge University Press, Cambridge.
- Yoshino, M. M.
1975 *Climate in a Small Area, an Introduction to Local Meteorology*. University of Tokyo Press, Tokyo.